

ÉCOLE DOCTORALE DE PHYSIQUE ET CHIMIE-PHYSIQUE
ICPEES – UMR 7515

THÈSE présentée par :

Lisa SOUGRATI

soutenue le : **03 Octobre 2024**

pour obtenir le grade de : **Docteur de l'université de Strasbourg**

Discipline/ Spécialité : Chimie des Polymères

**Développement de nouveaux réseaux
covalents adaptables biosourcés et
aromatiques à partir de lignines**

THÈSE dirigée par :

Pr. AVÉROUS Luc

Professeur, Université de Strasbourg

RAPPORTEURS :

Dr CAILLOL Sylvain

Pr. GRELIER Stéphane

Directeur de recherche, Université de Montpellier

Professeur, Université de Bordeaux

AUTRES MEMBRES DU JURY :

Pr. BISTAC-BROGLY Sophie

Professeure, Université de Haute Alsace

MEMBRE INVITÉ :

Dr DUVAL Antoine

Responsable R&D Chimie Verte, Soprema, France

REMERCIEMENTS

REMERCIEMENTS

Je souhaite tout d'abord remercier le Pr. Luc Avérous, mon directeur de thèse et le directeur de la Bioteam au sein de l'Institut de Chimie et Procédés pour l'Energie, l'Environnement et la Santé (ICPEES-UMR 7515), de m'avoir donné l'opportunité de pouvoir effectuer mes travaux de recherche. Je le remercie profondément pour la confiance qu'il m'a accordé pendant ces trois années de collaboration. Je suis sincèrement reconnaissante de nos échanges, qui, je le pense, ont permis de bâtir des fondations solides qui me permettront d'exercer une recherche rigoureuse et critique dans le reste de ma carrière. Je tiens à le remercier chaleureusement pour sa grande disponibilité pour les relectures et corrections de mes articles et de mon manuscrit qui m'a permis d'appréhender et d'effectuer la rédaction de ce manuscrit avec sérénité. Enfin, je suis reconnaissante pour ses conseils lors des situations de doute qui m'ont permis d'appréhender certains challenges de ma thèse plus aisément.

Je désire également remercier chaleureusement le Dr Antoine Duval, responsable R&D Chimie Verte de SOPREMA, pour son encadrement. Je le remercie d'avoir pris le temps de partager ses connaissances scientifiques pointues, notamment dans le domaine de la lignine, qui m'ont permises d'aborder au mieux les challenges de cette thèse. Je le remercie pour ses conseils toujours avisés. Enfin, je suis reconnaissante de ses nombreuses relectures et corrections qui ont permis d'approfondir mes travaux doctoraux.

J'adresse tous mes remerciements au Monsieur Sylvain Caillol, Directeur de recherche au CNRS de Montpellier, ainsi qu'au Monsieur Stéphane Grelier, Professeur à l'Université de Bordeaux, d'avoir accepté d'être rapporteurs de cette thèse. J'exprime également ma gratitude à Madame Sophie Bistac-Brogly, Professeure à l'Université de Haute Alsace, d'avoir accepté d'être examinatrice de mes travaux de thèse.

Je tiens à remercier les membres de l'entreprise SOPREMA avec lesquels j'ai eu la chance de collaborer dans le cadre du laboratoire commun Mutaxio. Un grand merci à Rémi Perrin, Directeur R&D, pour son accueil, sa bonne humeur, ses conseils et son expertise dans le domaine des matériaux. Je remercie également Monsieur Alexandru Sarbu, Directeur R&D Chimie des Matériaux, pour sa gentillesse et ses conseils.

Mes remerciements vont également à Monsieur Eric Pollet, Maître de Conférences à l'Université de Strasbourg, pour nos échanges lors des réunions d'équipe.

Je tiens également à remercier tous mes collègues de travail au sein de la Bioteam pour leur bonne humeur, soutien et entraide au cours de ces trois années. Leur soutien et leur gentillesse ont largement contribué au bon déroulement de ma thèse. Je souhaite adresser mes plus sincères remerciements à Sophie de m'avoir communiqué son enthousiasme pour la recherche lors de mon stage M2 qui m'a inspiré à poursuivre une thèse dans l'équipe. Mille mercis pour sa bienveillance, ses conseils, et son soutien sans faille pendant cette aventure. Je remercie particulièrement Alexis et Agathe pour tous les bons moments passés au laboratoire et nos nombreux vortex. Des fous-rires aux nervous breakdowns, je suis très reconnaissante d'avoir pu travailler et apprendre à leurs côtés. Leur soutien moral quotidien et leur bonne humeur m'ont permis de surmonter les moments difficiles avec le sourire. Merci également pour tous les moments hors du laboratoire, pour tous les festivals, les bbq, les apéros et les soirées gin to'. Je remercie également Nathan et Théo pour leur bonne humeur et leur soutien moral indéfectibles dans ma dernière année de thèse. Je les remercie d'avoir été présent dans les moments de doutes et de m'avoir conseillé avec sagesse. Je remercie également Kim et Alfred pour leur accueil et leur gentillesse qui ont contribué à ma bonne intégration dans l'équipe. Ma thèse n'aurait pas été une aussi belle aventure sans les innombrables qualités humaines de mes collègues et amis précédemment cités. Je remercie également tous les collègues que j'ai pu rencontrer pendant ces trois

REMERCIEMENTS

années, Grégoire, William, Maria, et Audrey, sans oublier les collègues de Polyfun, pour tous les bons moments passés ensemble qui ont contribué au bon déroulement de ma thèse.

Je remercie Christophe S. pour toutes nos discussions quotidiennes qui n'ont cessé d'égailler mes journées. Je le remercie de s'être toujours rendu disponible pour m'aider, même en périodes très chargées, et d'avoir été d'un soutien précieux dans les moments compliqués. Je souhaite également remercier Christophe M. pour sa sympathie et sa grande disponibilité, surtout quand le rhéomètre ou la presse étaient capricieux. Je remercie également Céline, Emeric, Thierry D. et Alexandre pour leur aide technique. Un grand merci à Catherine pour sa sympathie et son aide administrative. Je souhaite remercier chaleureusement l'équipe administrative, Michèle, Kevin, Julien, Cuong et Agnès pour avoir toujours été très réactifs et m'avoir aidé à trouver mon chemin dans les méandres de l'administration.

Je souhaite à remercier tous les copains de Crossfit Strasbourg pour m'avoir permis de devenir une femme plus forte. En me donnant de nouveaux objectifs, ils ont contribué au maintien de ma santé physique et mentale. Un merci particulier à Yoann, Geoffroy et la team de 18 h.

Je tiens à remercier tous mes amis. Merci pour tous les instants partagés et leur bienveillance au cours et ces trois ans. Merci à Jérôme, Chloë et Adrien, la meilleure des familles de l'ECPM, pour votre folie et pour nos week-ends endiablés aux quatre coins de la France qui m'ont fait un grand bien. Un grand merci à Laurie, Claire, et Flore, qui malgré la distance et les longs mois sans se voir m'ont fait preuve de leur amitié pendant ces trois années. Mille merci à Kim, Lazare et Mozza pour tous les instants passés ensemble et leur amitié, qui m'ont été d'un incroyable soutien. Je souhaite également remercier Océane et Hélène, mon crew de Louisiane, pour tous les bons moments partagés ensemble remplis de brunchs, de visites, de karaokés et de films des années 2000. Merci à Elise pour tous les instants hors du temps passés ensemble. Merci pour toutes nos discussions, tous les festivals, pour tous les apéros, pour toutes les soirées jeux, films d'horreurs et les soirées à endiabler le dancefloor qui ont été une vraie bouffée d'air frais. Merci au GRC, Sophie (qui mérite un double remerciement en tant que mentor scientifique et amie très chère), Antho, Céssou, Concordel, Emma, Fab, Flavie, Hugo, Sam, Jérém, Léa, Mag, Duj, Maude, Romain, Romane, Simon et Thib, pour votre incroyable bonne humeur. Merci pour les week-ends passés ensembles qui m'ont permis de déconnecter et de souffler l'espace d'un moment pendant la thèse. Je remercie également Juliette, pour son amitié et son soutien inconditionnel depuis toutes ces années.

Je remercie ma famille du plus profond de mon cœur pour son soutien et son amour sans faille. Un merci infini à mes parents, Claudie et Philippe, de m'avoir donné les moyens de faire ma thèse. Je les remercie d'avoir toujours été présents, dans les bons moments et ceux plus difficiles où ma motivation était au plus bas. Merci d'avoir toujours cru en moi. Merci de m'avoir rappelée, en boucle parfois quand je n'arrivais pas à l'entendre, que j'en étais capable. Ma thèse n'aurait pas été possible sans votre soutien et votre amour. Je vous en serai éternellement reconnaissante. Je remercie également ma sœur, Anna, qui a toujours trouvé les mots justes pour me rebooster. Merci de m'avoir changé les idées avec ta bonne humeur et ta folie. Mille mercis de m'avoir aidé à prendre du recul et m'avoir encouragée. Merci d'avoir été ma meilleure cheerleader.

Enfin, je souhaite remercier de tout mon cœur Rodolphe d'avoir été à mes côtés pendant ces trois années. Merci infiniment de m'avoir écoutée, comprise, rassurée, encouragée, et motivée à toujours me surpasser. Je suis profondément reconnaissante d'avoir pu partager cette expérience qu'est la thèse à tes côtés. Je te remercie pour ta patience et ton amour sans faille, sans lesquels rien de tout ça n'aurait été possible. J'ai si hâte de commencer ce nouveau chapitre de vie, le plus joyeux, à tes côtés. Tout simplement, merci.

NOTA BENE

NOTA BENE

Les chapitres de ce manuscrit de thèse sont rédigés en grande partie sous la forme d'articles qui ont été, ou vont prochainement être, soumis à des revues à comité de relecture. Afin de rester fidèle au texte, ces articles sont rédigés en anglais et le reste du manuscrit est rédigé en français. Nous vous prions de bien vouloir être indulgents au regard du changement de langue et des répétitions que ce type de format pourrait engendrer.

COMMUNICATIONS LIÉES AUX TRAVAUX DE THÈSE

Article publié

Sougrati, L., Duval, A., Avérous, L., 2023. From Lignins to Renewable Aromatic Vitrimers based on Vinylogous Urethane. **ChemSusChem** 16, e202300792.
<https://doi.org/10.1002/cssc.202300792>

Articles soumis ou prochainement soumis

Sougrati, L., Duval, A., Avérous, L. Biobased and Aromatic Covalent Adaptable Networks: when Architectures meet Properties, within the Framework of a Circular Bioeconomy. *Soumis dans Materials Science and Engineering: R :Reports*

Sougrati, L., Duval, A., Avérous, L. Sustainable Lignin-based Vinylogous Urethane Vitrimers: "Structural Design-Properties" Relationships Analysis. *Prochainement soumis dans un journal à comité de relecture.*

Sougrati, L., Duval, A., Avérous, L. Phenol-yne Chemistry for the Design of Lignin-based Vitrimers: Towards Sustainable and Recyclable Materials. *Prochainement soumis dans un journal à comité de relecture.*

Communication orale

Sougrati, L., Duval, A., Avérous, L., 2023. From Lignins to Renewable Aromatic Vitrimers. **ESBP 2023**, Brno (République Tchèque). 13 – 15 Sept. 2023.

LISTE DES ABRÉVIATIONS

LISTE DES ABREVIATIONS

2,5-DMF	2,5-Dimethylfuran
2 θ	Scattering angle
3,4-DHBA	3,4-Dihydroxybenzaldehyde
3,4-DHBAC	3,4-Dihydroxybenzoic acid
4-HBA	4-Hydroxybenzaldehyde
AA	Acetic acid
AA	Anarcadic acid
ACV	Analyse de cycle de vie
Al-OH	Aliphatic hydroxyl
Al-VE	Aliphatic vinyl ether
Al-VU	<i>tert</i> -butyl (Z)-3-(benzylamino)but-2-enoate
ATR	Attenuated Total Reflectance
BA	Benzylamine
BHMF	2,5-Bis(hydroxymethyl)furan
BTX	Benzène, Toluène, Xylène
CA	Caffeic acid
CA	Citric acid
CAGR	Compound annual growth rate
CANs	Covalent adaptable networks
CDCl ₃	Deuterated chloroform
CI-TMDP	4,4,5,5-tetramethyl-1,3,2-dioxaphospholane
CMR	Agents chimiques cancérogènes, mutagènes ou toxiques pour la reproduction
CNCs	Cellulose nanocrystals
CNSL	Cashew nutshell liquid
CNTS	Carbon nanotubes
COOH	Carboxylic acid
Đ	Dispersity
D	Real-space distance
DA	Diels-Alder
DBTL	Dibutyltin dilaurate
DBU	1,8-Diazabicyclo[5.4.0]undec-7-ene
DFT	Density functional theory
DGEBA	Diglycidyl ether bisphenol A
DHB	2,5-diamino-1,4-benzenedithiol hydrochloride
DL	Dealkaline lignin
DMA	Dynamic Mechanical Analysis
DMF	<i>N,N</i> -dimethylformamide
DMSO- <i>d</i> ₆	Deuterated dimethyl sulfoxide
DMSO	Dimethyl sulfoxide
DoD	Debonding-on-demand
DOPO	9,10-Dihydro-9-oxa-10-phosphaphenanthrene-10-oxide
DOSL	Partially depolymerized organosolv lignin
DRIFT	Diffuse Reflectance Fourier Transform Infrared
DSC	Differential Scanning Calorimetry
DVA	Divanillic acid
E	Young's modulus
E _a	Activation energy
EC	Ethylene carbonate
EN	European Standards
EP	Ethyl propiolate
ESO	Epoxidized soybean oil
FA	Ferulic acid
FA	Furfuryl alcohol

LISTE DES ABRÉVIATIONS

FBA	Formylboronic acids
FDC	2,5-Furandicarboxaldehyde
FDCA	2,5-Furandicarboxylic acid
FEHBP	FA-based hyperbranched epoxy resin
FEP	FA-derived epoxy resin
FR	Flame retardant
FT-IR	Fourier Transform Infrared
G-VE	Ethyl-3-(2-methoxy-4-methylphenoxy)acrylate
G'	Storage modulus
$G'_{23\text{ °C}}$	Storage modulus at 23 °C
GF	Gel fraction
HDPE	High-density polyethylene
HMBC	Heteronuclear Multiple Bond Correlation
HMDA	Hexamethylene diamine
HMF	5-hydroxymethylfurfural
HPAMAM	Hyperbranched polyamidoamine
HSQC	Heteronuclear Single Quantum Coherence
IS	Internal standard
J ₂₀₀₀	PPG diamine of molar mass 2000 g mol ⁻¹
J ₄₀₀	PPG diamine of molar mass 400 g mol ⁻¹
J ₆₀₀	PPG/PEG diamine of molar mass 600 g mol ⁻¹
J ₉₀₀	PPG/PEG diamine of molar mass 900 g mol ⁻¹
K	Equilibration constant
KL	Kraft lignin
KWW	Kohraush-William-Watts
LOI	Limiting oxygen index
LTECV	Loi de Transition Énergétique pour la Croissance Verte
<i>m</i> -CPBA	Meta-chloroperbenzoic acid
M _c	Molar mass between crosslinks
MDMP	Methyl-2,6-dimethoxyphenol
M _n	Number-average molar mass
Mt	Million Tons
M _w	Weight-average molar mass
NCO	Isocyanate
NIPTU	Non-isocyanate polythiourethane
NIPU	Non-isocyanate PU
NMR	Nuclear Magnetic Resonance
OH	Hydroxyl
OIT	Oxidation induction time
OL-AC	Acetoacetylated lignin
OL	OSL-based polyol
<i>p</i> -H	Hydrogen <i>para</i> -substituent
<i>p</i> -Me	Methyl <i>para</i> -substituent
P(ImA)	Poly(imine acetal)
PC	Polycarbonate
PEG-DA	Poly(ethylene) glycol dialkyne
PEG	Poly(ethylene) glycol
PET	Polyethylene terephthalate
Ph-OH	phenolic hydroxyl
Ph-VE	Phenyl vinyl ether
Ph-VU	2,6-dimethoxy-4-methylphenyl (Z)-3-(benzylamino)but-2-enoate
Ph-VU _N	<i>N</i> -benzyl-3-(benzylamino)but-2-enamide
PHU	Polyhydroxyurethane
PP	Polypropylene
PPG diamine	Poly(propylene glycol) bis(2-aminopropyl ether)

LISTE DES ABRÉVIATIONS

PPG	Poly(propylene) glycol
PPG/PEG diamines	O,O'-Bis(2-aminopropyl) polypropylene glycol-block-polyethylene glycol-block-polypropylene glycol
ppm	Part-per-million
PS	Polystyrene
<i>p</i> TsOH	<i>p</i> -Toluene sulphonic acid
PU _s	polyurethane
PY	Phenol-yne
q	Scattering vector
R	Molar gas constant
RAFT	Reversible addition/fragmentation chain transfer
RID	Refractive Index Detection
S-VE	Ethyl-3-(2,6-dimethoxy-4-methylphenoxy)acrylate
SAOS	Small amplitude oscillatory shear
SBR	Styrene-butadiene rubber
SEC	Size-exclusion Chromatography
SI	Appendices
SL	Soda lignin
SR	Swelling ratio
<i>t</i> -BuOH	<i>tert</i> -butanol
TA	Tannic acid
<i>T</i> _{amb}	Ambient temperature
TBAA	<i>tert</i> -butyl acetoacetate
TBD	Triazabicyclodecene
TCP	3,4,5-trichloropyridine
<i>T</i> _{deg}	Temperature of maximal mass loss rate
<i>T</i> _{d5%}	Temperature at 5% mass loss
TEG	Triethylene glycol
<i>T</i> _g	Glass transition temperature
TGA	Thermogravimetric Analysis
THF	Tetrahydrofuran
TMDO	2,2,6-trimethyl-4H-1,3-dioxin-4-one
TOB	Tobramycin
TREN	Tris(2-aminoethyl) amine
TRL	Technology Readiness Level
<i>T</i> _v	Topological freezing temperature
USA	United States of America
UV	Ultra-violet
VE	Vinyl ether
VU	Vinylogous urethane
VU _N	Vinylogous urea
WAXS	Wide Angle X-Ray Scattering
WCA	Water Contact Angle
WLF	Williams–Landel–Ferry
wt%	Weight percent
β	Exponent indicating the distribution of relaxation times
ε	Elongation at break
λ	X-rays wavelength
ρ	Density
σ	Maximal stress at break
τ*	Characteristic relaxation time
<i>v</i>	Crosslinking density

SOMMAIRE

Communications liées aux travaux de thèse	I
Liste des abréviations	II
Sommaire	V
Liste des figures.....	VIII
Liste des tableaux	XIV

INTRODUCTION GÉNÉRALE 1

Références	6
------------------	---

CHAPITRE 1. Réseaux covalents adaptables biosourcés et aromatiques : quand les architectures rencontrent les propriétés, dans le cadre d'une bioéconomie circulaire 9

Introduction du chapitre 1	10
1. Abstract	12
2. Introduction	12
3. Generalities.....	14
3.1. Introduction to CANs	14
3.2. Dynamic bond chemistries	16
3.2.1. Systems based on transesterification.....	17
3.2.2. Boronic esters and boroxines-based systems	17
3.2.3. Imine-based systems	17
3.2.4. Urethane-based systems.....	18
3.2.5. Systems based on vinylogous urethane.....	19
3.2.6. Acetal-based systems	19
3.2.7. Systems based on Michael reaction	19
3.2.8. Systems based on Diels-Alder	20
3.2.9. Systems based on disulfide exchange	20
3.2.10. Systems based on [2 + 2] cycloaddition.....	20
3.2.11. Systems based on siloxane exchange.....	20
4. Biobased aromatic CANs	21
4.1. Sources of renewable aromatic structures	21
4.1.1. Lignins and derivatives	21
4.1.2. Tannins and derivatives	22
4.1.3. Cashew nutshell liquid.....	23
4.1.4. Furan and derivatives	24
4.1.5. Other phenolic building blocks	25
4.2. Aromatic building blocks in CANs	26
4.2.1. Lignins and lignin-derived monomers	26
4.2.2. Tannins and derived building blocks	39
4.2.3. Cashew nutshell liquid and its derivatives	45
4.2.4. Furan and derivatives	48
4.2.5. Other aromatic building blocks.....	51
5. Applications of biobased and aromatic CANs	56
5.1. Biomedical applications.....	56
5.1.1. Wound sealants	56
5.1.2. Implants and tissue engineering.....	57
5.1.3. Drug release	57
5.2. Flame retardant applications.....	57
5.3. Coatings applications.....	58

SOMMAIRE

5.4. Adhesive applications.....	59
5.5. Other applications.....	60
6. Conclusions and outlooks.....	61
7. References.....	63
Conclusion du chapitre 1.....	84

CHAPITRE 2. Des lignines aux vitrimères aromatiques renouvelables à base d'uréthane vinylogues 85

Introduction du chapitre 2.....	86
1. Abstract.....	88
2. Introduction.....	88
3. Experimental section.....	90
3.1. Materials.....	90
3.2. Synthesis of lignin-based liquid polyols.....	91
3.3. Synthesis of lignin-based polyacetoacetate.....	91
3.4. Synthesis of VU networks.....	91
3.5. Materials designation.....	91
3.6. Reprocessing study of VU networks.....	91
3.7. Characterization techniques.....	92
4. Results and discussion.....	94
4.1. Polyacetoacetates from OSL.....	94
4.2. VU networks.....	96
5. Conclusion.....	102
6. References.....	102
7. Appendices (SI).....	107
Conclusion du chapitre 2.....	128

CHAPITRE 3. Vitrimères uréthane vinylogues durables à partir de lignine : analyse des relations « conception structurelle-propriétés » 129

Introduction du chapitre 3.....	130
1. Abstract.....	132
2. Introduction.....	132
3. Experimental section.....	133
3.1. Materials.....	133
3.2. Synthesis of acetoacetylated lignin (OL-AC).....	134
3.3. Model reaction of OL-AC with benzylamine.....	134
3.4. Model compound synthesis.....	134
3.4.1. Synthesis of 2,6-dimethoxy-4-methylphenyl (Z)-3-(benzylamino)but-2-enoate (Ph-VU).....	134
3.4.2. Synthesis of <i>tert</i> -butyl (Z)-3-(benzylamino)but-2-enoate (Al-VU).....	134
3.4.3. Synthesis of <i>N</i> -benzyl-3-(benzylamino)but-2-enamide (Ph-VU _N).....	135
3.5. Synthesis of lignin-based VU networks.....	135
3.6. Physical and chemical recycling studies of VU networks.....	135
3.7. Characterization techniques.....	135
4. Results and discussion.....	137
4.1. Analysis of lignin acetoacetylation.....	137
4.2. Analysis of the reaction of aromatic acetoacetate with amines.....	140
4.3. Analysis of the obtained aromatic VU networks.....	143
4.3.1. Results from FT-IR characterizations.....	143
4.3.2. Results from the thermal characterizations by TGA and DSC.....	144
4.3.3. Results from the morphological characterizations using X-ray scattering.....	144

SOMMAIRE

4.3.4.	Results from the rheological characterizations by DMA and stress relaxation ...	146
4.3.5.	Results from the mechanical characterizations by uniaxial tensile tests.....	149
4.3.6.	Results from the structural characterizations	150
4.3.7.	Results from the physical and chemical recycling study	150
5.	Conclusion.....	153
6.	References	154
7.	Appendices (SI).....	159
	Conclusion du chapitre 3.....	172

CHAPITRE 4. Chimie phénol-yné pour la conception de vitrimères à base de lignine : vers des matériaux durables et recyclables..... 173

	Introduction du chapitre 4	174
1.	Abstract	176
2.	Introduction	176
3.	Experimental section	178
3.1.	Materials	178
3.2.	Synthesis of aromatic model compounds	179
3.3.	Vinyl ether model exchange reactions.....	179
3.4.	Click-addition kinetics study on aliphatic and phenolic models	180
3.5.	Lignin modification with ethyl propiolate.....	180
3.6.	Synthesis of PEG dialkyne crosslinker (PEG-DA).....	180
3.7.	Synthesis of lignin-based phenol-yné materials	180
3.8.	Physical and chemical recycling studies of phenol-yné materials.....	180
3.9.	Characterization techniques.....	181
4.	Results and discussion.....	183
4.1.	Analysis of the vinyl ether rearrangements: model study on mono- and di-substituted phenols	183
4.2.	Kinetic study on aliphatic and phenolic alcohols: from models to lignins	186
4.3.	Analysis of the lignin-derived CANs based on phenol-yné	187
4.3.1.	Analysis of the synthesis of PEG-DA crosslinker	187
4.3.2.	Analysis of the synthesis and the structural characterization of lignin-based phenol-yné materials	189
4.3.3.	Analysis of the thermal, rheological, and mechanical behaviors of the materials	194
4.3.4.	Analysis of the physical recycling	199
4.3.5.	Analysis of the chemical recycling	201
5.	Conclusion.....	204
6.	References	205
7.	Appendices (SI).....	209
	Conclusion du chapitre 4.....	235

CONCLUSION GÉNÉRALE ET PERSPECTIVES..... 237

	Références associées à la conclusion générale.....	244
--	--	-----

LISTE COMPLÈTE DES RÉFÉRENCES BIBLIOGRAPHIQUES..... 245

LISTE DES FIGURES

INTRODUCTION GÉNÉRALE

Figure 0-1. Modèle structurel de lignine issue de bois de feuillus.	3
Figure 0-2. Gestion des déchets plastiques post-consommation en Europe en 2020 (adapté de Plastics Europe 2022).	3
Figure 0-3. Mécanismes de réarrangement dissociatifs et associatifs des réseaux moléculaires.	4
Figure 0-4. Schéma récapitulatif de l'organisation du mémoire de doctorat.	5

CHAPITRE 1

Figure 1-1. Different types of molecular network rearrangements within covalent networks.	15
Figure 1-2. A) Plot of $\ln(\eta)$ versus temperature of an amorphous vitrimer in which the topology freezing transition temperature, T_v , is greater than the glass transition temperature, T_g . B) Plot of $\ln(\eta)$ versus temperature of a semi-crystalline vitrimer in which T_v is greater than the melting temperature, T_m . C) Plot of $\ln(\eta)$ versus temperature for a vitrimer that features a T_g that is greater than its T_v . Reprinted from Ref.(Van Zee and Nicolaÿ, 2020) Copyright 2020, with permission from Elsevier.	15
Figure 1-3. Dynamic covalent chemistries used in the elaboration of biobased aromatic CANs. A = associative mechanism. D = dissociative mechanism.	18
Figure 1-4. From top to bottom: A structural model of hardwood lignin and some aromatic compounds derived from lignins.	22
Figure 1-5. Some aromatic compounds derived from condensed or hydrolysable tannins.	23
Figure 1-6. Chemical structures and composition of CNSL.	24
Figure 1-7. Some furan-derived building blocks for the synthesis of CANs.	25
Figure 1-8. Structures of other biobased phenolic building blocks.	25
Figure 1-9. Presentation of most lignin chemical modifications into precursors used in the synthesis of various types of CANs. With DA= Diels-Alder, VU= vinylogous urethane, PU= polyurethane, AC= acetal, S-S= disulfide.	28
Figure 1-10. Vanillin as a chemical platform for the preparation of different poly(epoxy imine) networks.	31
Figure 1-11. Vanillin chemical modifications into precursors for the synthesis of acetal, ester, and imine-based CANs.	33
Figure 1-12. Vanillin derivatives as precursors for the synthesis of CANs.	34
Figure 1-13. 4-hydroxybenzaldehyde as platform chemical for the synthesis of imine-containing monomers.	35
Figure 1-14. 3,4-dihydroxybenzaldehyde and 3,4-dihydroxybenzoic acid as precursors for the synthesis of epoxy building blocks.	36
Figure 1-15. Guaiacol and 4-methyl guaiacol as precursors for the preparation of different CANs.	37
Figure 1-16. Tannic acid as curing agent for the preparation of dynamic epoxy networks. Refs. (Yizhen Chen et al., 2023; Feng et al., 2020).	40
Figure 1-17. Tannic acid as precursor for the preparation of CANs.	40
Figure 1-18. Catechol-derived structures as precursors for the preparation of CANs.	41
Figure 1-19. Epigallocatechin gallate as precursor for the preparation of CANs.	42
Figure 1-20. Gallic acid as precursor for the preparation of CANs.	43
Figure 1-21. Resorcinol and resorcinol diglycidyl ether as CANs precursors.	43
Figure 1-22. Chemical pathways for the synthesis of cardanol-derived benzoxazines.	46
Figure 1-23. Cardanol as precursor for the preparation of CANs.	47
Figure 1-24. 2,5-furandicarboxaldehyde as a precursor for the preparation of CANs.	49
Figure 1-25. 5-(hydroxymethyl)furfural as precursor for the preparation of CANs.	49
Figure 1-26. Different Eugenol chemical modifications into precursors for the synthesis of ester, disulfide, and urethane-based CANs.	52

LISTE DES FIGURES

Figure 1-27. Reversible crosslinking by [2 + 2] photocycloaddition of TPU prepared from EC-diol..	54
Figure 1-28. Synthetic pathways for the preparation of biobased benzoxazine precursors from phloretic acid and tyrosol.	55

CHAPITRE 2

Figure 2-1. Synthetic pathways for the preparation of a) polyols, b) polyacetoacetate, and c) VU networks from OSL.	90
Figure 2-2. Stacked ³¹ P NMR of OSL, OL-30-300 and AC-30-300 with details of (A) phenolic hydroxyls conversion after the OL-30-300 synthesis, and (B) aliphatic hydroxyls conversion after AC-30-300 synthesis; IS = Internal standard.	94
Figure 2-3. FT-IR spectra with some examples of lignin-based polyol, polyacetoacetate and VU network, from top to bottom.	96
Figure 2-4. Flow behavior of VU-40-300 with a) stress relaxation curves from 100 to 140°C, and b) Arrhenius plot.	98
Figure 2-5. Uniaxial tensile tests of vitrimer series.	99
Figure 2-6. a) Swelling ratios and b) gel fractions of the vitrimer series.	99
Figure 2-7. Reprocessing study. a) Thermomechanical reprocessing of VU-40-400, b) FT-IR analysis, and c) uniaxial tensile tests after each reprocessing cycle.	100
Figure 2-8. Study of transamination reactions: a) VU in DMF, b) VU in DMF after heating at 100°C, c) VU in DMF after heating with an excess of n-octylamine, and d) VU in DMF after heating, with an excess of ethyl acetoacetate.	101
Figure 2-9. Transamination reaction between VU networks and n-octylamine in DMF.	102
Figure S2-10. ³¹ P NMR of OL-30-300.	108
Figure S2-11. ³¹ P NMR of OL-40-300.	108
Figure S2-12. ³¹ P NMR of OL-50-300.	109
Figure S2-13. ³¹ P NMR of OL-40-400.	109
Figure S2-14. ³¹ P NMR of OL-40-150.	110
Figure S2-15. Stacked FT-IR spectra of the different polyols, with a) OSL, b) OL-30-300, c) OL-40-300, d) OL-50-300, e) OL-40-400, and f) OL-40-150.	110
Figure S2-16. ³¹ P NMR of AC-30-300.	111
Figure S2-17. ³¹ P NMR of AC-40-300.	111
Figure S2-18. ³¹ P NMR of AC-50-300.	112
Figure S2-19. ³¹ P NMR of AC-40-400.	112
Figure S2-20. ³¹ P NMR of AC-40-150.	113
Figure S2-21. Potential reaction of TBAA with Cl-TMDP.	113
Figure S2-22. ³¹ P NMR of TBAA.	114
Figure S2-23. ¹ H NMR of AC-30-300 in CDCl ₃	114
Figure S2-24. ¹ H NMR of AC-40-300 in CDCl ₃	115
Figure S2-25. ¹ H NMR of AC-50-300 in CDCl ₃	115
Figure S2-26. ¹ H NMR of AC-40-400 in CDCl ₃	116
Figure S2-27. ¹ H NMR of AC-40-150 in CDCl ₃	116
Figure S2-28. SEC curves of polyacetoacetates (RID detection, THF as eluent, calibration with PS standards).	117
Figure S2-29. Stacked FT-IR spectra of a) VU-30-300, b) VU-40-300, c) VU-50-300, d) VU-40-400, and e) VU-40-150.	117
Figure S2-30. TGA curves of the different final materials.	118
Figure S2-31. DSC curves of the series of materials.	118
Figure S2-32. DSC curve of TEG.	119
Figure S2-33. DSC curve of PEG ₃₀₀	119
Figure S2-34. DSC curve of PEG ₄₀₀	119
Figure S2-35. DMA curves of the different final VU.	120

LISTE DES FIGURES

Figure S2-36. Stress relaxation curves of VU-30-300.	120
Figure S2-37. Arrhenius relationship of VU-30-300.	121
Figure S2-38. Stress relaxation curves of VU-50-300.	121
Figure S2-39. Arrhenius relationship of VU-50-300.	121
Figure S2-40. Stress relaxation curves of VU-40-400.	122
Figure S2-41. Arrhenius relationship of VU-40-400.	122
Figure S2-42. Stress-relaxation curves of VU-40-150.	122
Figure S2-43. Arrhenius relationship of VU-40-150.	123
Figure S2-44. Plot of E_a as a function of a) lignin content, b) PEG molar mass, and c) crosslinking density.	123
Figure S2-45. Swelling kinetics study of VU-40-400 in acetone and water.	125
Figure S2-46. DMA curves of unrecycled and recycled VU-40-400.	125
Figure S2-47. OIT curve of original VU-40-400.	126
Figure S2-48. OIT curve of VU-40-400 after 1 st recycling.	126
Figure S2-49. OIT curve of VU-40-400 after 2 nd recycling.	126
Figure S2-50. OIT curve of VU-40-400 after 3 rd recycling.	127
Figure S2-51. Images of self-healed samples after 0, 2 and 6 h at 140 °C.	127

CHAPITRE 3

Figure 3-1. Synthetic pathway for the preparation of a) acetoacetylated lignin, and b) VU networks from OSL.	138
Figure 3-2. Stacked ³¹ P NMR of OSL and OL-AC. IS= Internal standard.	139
Figure 3-3. FT-IR spectra of OSL and OL-AC from top to bottom. Right spectra are magnifications of the left spectra, between 2000 and 1000 cm ⁻¹	140
Figure 3-4. Two potential mechanistic pathways for the reaction of aromatic acetoacetates with an excess amine groups forming 1) vinylogous urethanes, and 2) vinylogous ureas. Adapted from Ref (Haida et al., 2022).	140
Figure 3-5. SEC curves in THF of OL-AC and the products of the formation of vinylogous urethanes and ureas.	142
Figure 3-6. ¹ H- ¹⁵ N HMBC spectra of a) Ph-VU-L, b) Al-VU, c) Ph-VU, and d) Ph-VU _N	142
Figure 3-7. Stacked FT-IR spectra of OL-AC and Ph-VU-400, Ph-VU-600, Ph-VU-900, and Ph-VU-2000, from top to bottom. Right spectra are magnifications of the left spectra, between 1800 and 1400 cm ⁻¹	143
Figure 3-8. WAXS curves and corresponding deconvolutions of a) OSL, b) OL-AC, c) Ph-VU-400, d) Ph-VU-600, e) Ph-VU-900, and f) Ph-VU-2000.	145
Figure 3-9. Physical interaction proportions as a function of crosslinking density.	147
Figure 3-10. a) Stress relaxation curves of Ph-VU-400 with temperature variations between 160 and 200 °C, and b) Arrhenius plots of the different vitrimers.	148
Figure 3-11. Variation of the Young's modulus and stress at break with lignin content.	149
Figure 3-12. a) Swelling ratio and b) gel fraction of VU networks in acetone and water.	150
Figure 3-13. FT-IR of Ph-VU-600 upon three physical recycling cycles.	151
Figure 3-14. Depolymerization assays of Ph-VU-600 in a) 1M HCl, b) 1M AA, and c) aqueous solution of AA (9:1) before heating, and d) 1M HCl, e) 1M AA, and f) aqueous solution of AA (9:1) after heating at 90 °C for 24 h.	152
Figure 3-15. Study of acid-catalyzed depolymerization of VU networks: a) VU in H ₂ O, b) VU in acetic acid, c) VU in H ₂ O after heating at 100 °C for 48h, and d) VU in acetic acid after heating at 110 °C for 48h.	152
Figure 3-16. Hypothesized acid hydrolysis of VU.	152
Figure 3-17. Stacked FT-IR spectra of pristine Ph-VU-600 and chemically recycled Ph-VU-600, from top to bottom. Right spectra are magnifications of the left spectra, between 2000 and 1200 cm ⁻¹	153
Figure S3-18. ¹ H NMR of OSL in DMSO- <i>d</i> ₆	159

LISTE DES FIGURES

Figure S3-19. ^1H NMR of OL-AC in CDCl_3	160
Figure S3-20. ^1H NMR Ph-VU-L in CDCl_3	160
Figure S3-21. ^1H NMR Ph-VU in CDCl_3	161
Figure S3-22. ^1H NMR of Al-VU in CDCl_3	161
Figure S3-23. ^1H NMR of Ph-VU _N in CDCl_3	162
Figure S3-24. a) Production of a reactive acetylketene and acetone from TMDO via retro-Diels-Alder reaction, and b) acetoacetylation reactions between the formed acetylketene and nucleophile hydroxyls.	162
Figure S3-25. SEC curves of OSL and OL-AC in THF.....	163
Figure S3-26. ^{31}P NMR of Ph-VU-01.	163
Figure S3-27. ^{31}P NMR of Ph-VU-02.	164
Figure S3-28. ^{31}P NMR of Ph-VU-03.	164
Figure S3-29. ^{31}P NMR of Ph-VU-L.....	165
Figure S3-30. TGA curves of lignin-based VU networks.....	165
Figure S3-31. DSC curve of OL-AC.....	165
Figure S3-32. DSC curves of the diamines.	166
Figure S3-33. DSC curves of different Ph-VU materials.....	166
Figure S3-34. Evolutions of T_g and T_α with lignin content.	167
Figure S3-35. Evolutions of physical interaction proportions as a function of lignin content.	167
Figure S3-36. DMA curves of the Ph-VU materials.	168
Figure S3-37. Stress relaxation curves of Ph-VU-600 at different temperatures.	168
Figure S3-38. Stress relaxation curves of Ph-VU-900 at different temperatures.	169
Figure S3-39. Stress relaxation oh Ph-VU-2000 at different temperatures.....	169
Figure S3-40. Stress-strain curves of the vitrimer series.....	170
Figure S3-41. Uniaxial stress-strain curves of Ph-VU-600 upon three physical recycling cycles.	170
Figure S3-42. DMA curves of pristine and physically recycled Ph-VU-600 after different cycles... ..	171
Figure S3-43. DMA of chemically recycled Ph-VU-600.....	171

CHAPITRE 4

Figure 4-1. Extraction processes to separate lignin from lignocellulosic biomass for the production of technical lignins. Adapted from (Laurichesse and Avérous, 2014).....	177
Figure 4-2. Synthetic pathway for the preparation of a) PEG dialkyne crosslinker (PEG-DA), and b) phenol-yne (PY) networks from KL, OSL, and DOSL.	178
Figure 4-3. Mechanistic pathway for the exchange of phenyl vinyl ether dynamic bonds.	183
Figure 4-4. Exchange reactions GG', SS', GS', and SG' conditions and equilibrium constants. For clarity purpose only <i>E</i> -isomers were represented.....	184
Figure 4-5. a) Illustration of the dynamic exchange of substituted phenols, b) kinetics of the exchange reaction with K_2CO_3 at 120 °C with a zoom on molar ratios from 0 to 0.15, and c) stacked ^1H NMR sequence of the exchange reaction at different times.....	185
Figure 4-6. Kinetic monitoring of the conversion of vinyl ether aliphatic (Al-VE) and aromatic (Ph-VE) adducts.....	186
Figure 4-7. a) Stacked ^1H RMN in $\text{DMSO}-d_6$ and b) FT-IR spectra of PEG ₄₀₀ and PEG-DA.....	188
Figure 4-8. SEC curves of PEG ₄₀₀ and PEG-DA in THF.....	189
Figure 4-9. Evolution of the normalized absorbance of alkyne signal at 2111 cm^{-1} as a function of time, at 80 and 120°C.	190
Figure 4-10. Stress relaxation curves obtained at 190 °C on materials synthesized with different experimental conditions: varying the amount of free Ph-OH (from 0.2 to 0.4 equivalents), and the catalyst equivalents (from 0.05 to 0.2).	190
Figure 4-11. Stacked FT-IR spectra of KL, PEG-DA, and the series of materials.....	191
Figure 4-12. a) Swelling ratio, and b) gel fraction of the lignin-based CANs.	192
Figure 4-13. WCA of the series of material.	192

LISTE DES FIGURES

Figure 4-14. WAXS curves and deconvolutions of a) KL-PY, b) OSL-PY, and c) DOSL-PY.....	193
Figure 4-15. Evolution of the crosslinking density as a function of Ph-OH content.....	195
Figure 4-16. Stress relaxation curves of KL-PY, OSL-PY and DOSL-PY, and Arrhenius plots of the networks.....	196
Figure 4-17. Evolution of the relaxation time at 200 °C with lignin molar mass.....	197
Figure 4-18. Evolution of E_a of the vitrimers with a) the crosslinking density, and b) the Ph-OH content.	198
Figure 4-19. Stress-strain curves of the series of CANs.....	198
Figure 4-20. FT-IR spectra of pristine and recycled KL-PY.....	199
Figure 4-21. Stress-strain curves of a) pristine and recycled KL-PY, and b) pristine and recycled DOSL-PY.....	200
Figure 4-22. Full life cycle of PY material from a) the synthesis to b) the depolymerization, and c) the recovery of lignin.....	201
Figure 4-23. Acid-catalyzed hydrolysis of KL-PY vinyl ether and ester groups.....	202
Figure 4-24. Stacked ^{31}P NMR of pristine and chemically recovered KL.....	202
Figure 4-25. 2D HSQC of a) KL, b) KL-EP, and c) recovered KL.....	203
Figure 4-26. SEC curves of pristine and recovered KL.....	204
Figure S4-27. ^{31}P NMR spectra of KL, OSL, and DOSL.....	209
Figure S4-28. SEC curves of KL, OSL, and DOSL in THF.....	210
Figure S4-29. Synthesis of G-VE and S-VE model compounds by click-addition.....	210
Figure S4-30. ^1H NMR of G-VE in CDCl_3	211
Figure S4-31. ^1H NMR of S-VE in CDCl_3	211
Figure S4-32. 2D HSQC spectra of a) KL, b) KL-EP, c) OSL, and d) OSL-EP in $\text{DMSO}-d_6$	212
Figure S4-33. ^{31}P NMR spectra of OSL-80 in $\text{DMSO}-d_6$	213
Figure S4-34. ^{31}P NMR spectra of KL-80 in $\text{DMSO}-d_6$	214
Figure S4-35. ^{31}P NMR spectra of KL-120 in $\text{DMSO}-d_6$	214
Figure S4-36. ^{31}P NMR spectra of OSL-DMSO in $\text{DMSO}-d_6$	215
Figure S4-37. ^1H NMR spectra of PEG-DA in $\text{DMSO}-d_6$	215
Figure S4-38. Markovnikov and anti-Markovnikov addition of ethyl propiolate and phenols.....	216
Figure S4-39. ^1H NMR sequence of GG' exchange reaction between G-VE and G in CDCl_3	216
Figure S4-40. ^1H NMR sequence of SS' exchange reaction between S-VE and S' in CDCl_3	217
Figure S4-41. Kinetics of SS' exchange reaction between S-VE and S' at 120 °C.....	218
Figure S4-42. ^1H NMR sequence of GS' exchange reaction between G-VE and S' in CDCl_3	219
Figure S4-43. Kinetics of GS' exchange reaction between G-VE and S' at 120 °C, with zoom on molar ratios from 0 to 0.2.....	219
Figure S4-44. ^1H NMR sequence of SG' exchange reaction between S-VE and G' in CDCl_3	220
Figure S4-45. Kinetics of SG' exchange reaction between S-VE and G' at 120 °C, with zoom on molar ratios from 0 to 0.2.....	221
Figure S4-46. ^1H NMR sequence of GSB exchange reaction between G-VE and S in CDCl_3	222
Figure S4-47. Kinetics of GSB exchange reaction between G-VE and S at 120 °C, with zoom on molar ratios from 0 to 0.2.....	222
Figure S4-48. ^1H NMR of the reaction of benzyl alcohol with ethyl propiolate at 120 °C in CDCl_3 and proposition for the attribution of possible product from click-addition and transesterification reactions.	223
Figure S4-49. ^1H NMR sequence of Al-OH/G exchange reaction between Benz-VE and G in CDCl_3	224
Figure S4-50. ^1H NMR sequence of G/Al-OH exchange reaction between G-VE and benzyl alcohol in CDCl_3	224
Figure S4-51. Stacked ^1H NMR spectra in CDCl_3 of S, ethyl propiolate and S-VE, from top to bottom.* = solvent.....	225
Figure S4-52. ^1H NMR of the reaction of 1-butanol with ethyl propiolate at 120 °C in CDCl_3 and proposition for the attribution of possible product from click-addition and transesterification reactions.	225

LISTE DES FIGURES

Figure S4-53. Representation of dynamic and non-dynamic vinyl ether adducts on lignin.....	226
Figure S4-54. 3D view of the kinetic monitoring of the click addition by FT-IR at a) 120 °C and b) 80 °C.....	226
Figure S4-55. Evolution of swelling ratios in water with Al-OH content.....	227
Figure S4-56. Evolution of the WCA with water GF.....	227
Figure S4-57. TGA curves of the materials.....	228
Figure S4-58. DSC curves of the different lignins: KL (red), OSL (light blue), and DOSL (dark blue).	228
Figure S4-59. DSC curves of the series of materials.....	229
Figure S4-60. DMA curves of the materials.	229
Figure S4-61. Stacked FT-IR spectra of aliphatic vinyl ethers (Benz-VE and Al-VE) and phenyl vinyl ethers (G-VE and S-VE).....	230
Figure S4-62. Curve of KL-PY thermal degradation under an isotherm at 160 °C for 4 h.....	230
Figure S4-63. FT-IR spectra of pristine KL-PY and KL-PY after thermal treatment at 160 °C for 30 minutes.	231
Figure S4-64. DMA curves of pristine and recycled KL-PY.....	231
Figure S4-65. FT-IR spectra of pristine and recycled DOSL-PY.	232
Figure S4-66. DMA curves of pristine and recycled DOSL-PY.....	232
Figure S4-67. Pictures of the tested depolymerizations.	233
Figure S4-68. ³¹ P NMR of PEG ₄₀₀	234
Figure S4-69. Stacked FT-IR spectra of KL-PY, pristine KL, and recovered KL.....	234

CONCLUSION GÉNÉRALE ET PERSPECTIVES

Figure 5-0-1. Structure globale de la thèse de doctorat et attribution de TRL à chaque chapitre.	238
Figure 5-0-2. Récapitulatif des propriétés mécaniques obtenues dans les différents travaux de thèse et comparaison avec les CANs à partir de lignine rapportés dans la littérature. 1 = (Thys et al., 2021), 2 = (Zhang et al., 2018), 3 = (Xue et al., 2021), 4 = (Duval et al., 2024), 5 = (Liu et al., 2024), 6 = (Ma et al., 2023a), 7 = (Ma et al., 2023b), and 8 = (Moreno et al., 2021).	241
Figure 5-0-3. Récapitulatif des propriétés rhéologiques obtenues dans les différents travaux de thèse et comparaison avec les CANs à partir de lignines rapportés dans la littérature. 1 = (Thys et al., 2021), 2 = (Zhang et al., 2018), 3 = (Hao et al., 2019), 4 = (Xue et al., 2021), 5 = (Du et al., 2022), 6 = (Song et al., 2023), 7 = (Adjaoud et al., 2023), 8 = (Duval et al., 2024), 9 = (Liu et al., 2024), 10 = (Liu et al., 2019), 11 = (Ma et al., 2023a), 12 = (Ma et al., 2023b), 13 = (Moreno et al., 2021), and 14 = (Liu et al., 2020).	241

LISTE DES TABLEAUX

LISTE DES TABLEAUX

CHAPITRE 1

Table 1-1. Main stress-relaxation, physical and chemical recycling parameters of lignin-based CANs.	29
Table 1-2. Main stress-relaxation, physical and chemical recycling parameters of CANs from lignin-derived precursors.	38
Table 1-3. Main stress-relaxation, physical and chemical recycling parameters of tannin-derived CANs.	45
Table 1-4. Main stress-relaxation, physical and chemical recycling parameters of CNSL-derived CANs.	47
Table 1-5. Main stress-relaxation, physical and chemical recycling parameters of furan-derived CANs.	51
Table 1-6. Main stress-relaxation, physical and chemical recycling parameters of eugenol, hydroxycinnamic acids, urushiol, phloretic acid, and tyrosol-derived CANs.	56

CHAPITRE 2

Table 2-1. Main physico-chemical properties of the polyols.	95
Table 2-2. Thermal and physico-chemical properties of the VU networks.	97
Table 2-3. Main stress relaxation parameters.	98
Table S2-4. Detailed values used for density calculations of each material.	107
Table S2-5. Main physico-chemical properties of polyacetoacetates.	117
Table S2-6. Parameters used for T_v calculation of each vitrimers.	124
Table S2-7. Swelling ratio and gel fraction data.	124
Table S2-8. DMA measurements on original and recycled VU-40-400.	125

CHAPITRE 3

Table 3-1. Acetoacetylation conditions optimization from OSL.	138
Table 3-2. Conditions and corresponding parameters obtained from the formation of vinylogous urethanes and ureas.	141
Table 3-3. Thermal and rheological properties of the aromatic VU networks.	144
Table 3-4. WAXS parameters and interaction proportions for OSL, OL-AC, and the series of materials.	146
Table 3-5. Main stress-relaxation parameters.	148
Table 3-6. Mechanical properties of the series of vitrimers.	149
Table 3-7. Mechanical and rheological properties of pristine, physically, and chemically recycled Ph-VU-600.	151
Table S3-8. SEC results of OSL and OL-AC.	163
Table S3-9. Parameters used for T_v calculation of each vitrimers.	169
Table S3-10. Swelling ratios (SR) and gels fractions (GF) in acetone and water of the vitrimer series.	170

CHAPITRE 4

Table 4-1. Main chemical and physicochemical parameters of KL, OSL, and DOSL.	179
Table 4-2. Determination of dynamic and non-dynamic bonds contents, from the click-addition of a monoalkyne with different lignins and in different conditions.	187
Table 4-3. Physicochemical values of PEG ₄₀₀ and PEG-DA.	189

LISTE DES TABLEAUX

Table 4-4. WAXS parameters and interaction proportions for KL, OSL, DOSL, and the series of materials.	194
Table 4-5. Thermal and rheological properties of the PY-based networks.	195
Table 4-6. Main stress relaxation parameters.	197
Table 4-7. Mechanical properties of the series of CANs.	199
Table 4-8. Mechanical and rheological properties of pristine and physically recycled KL-PY and DOSL-PY.	201
Table S4-9. Vinyl ether model exchange reactions conditions.	212
Table S4-10. Reactional conditions of lignin modification with ethyl propiolate (EP) and conversion of Ph-OH and Al-OH.	213
Table S4-11. Synthesis condition of lignin-based materials.	216
Table S4-12. Parameters used for K_{GG} calculation.	217
Table S4-13. Parameters used for K_{SS} calculation.	218
Table S4-14. Parameters used for K_{GS} calculation.	220
Table S4-15. Parameters used for K_{SG} calculation.	221
Table S4-16. Parameters used for K_{GSB} calculation.	223
Table S4-17. Relaxation parameters obtained at 190 °C varying the amount of free Ph-OH and the catalyst equivalents.	226
Table S4-18. Swelling, gel fraction and WCA values of the materials.	226
Table S4-19. Parameters used for T_v calculation of each vitrimers.	230
Table S4-20. Depolymerization tested conditions on OSL.	233
Table S4-21. Physicochemical properties of pristine and recovered KL.	233

CONCLUSION GÉNÉRALE ET PERSPECTIVES

Tableau 5-1. Évaluation des principes de chimie verte des différents chapitres.	240
Tableau 5-2. Description de l'échelle TRL. Adaptée de (Beims et al., 2019).	242

INTRODUCTION GÉNÉRALE

INTRODUCTION GÉNÉRALE

Les plastiques sont des matériaux constitués d'un polymère auquel des additifs ou d'autres substances ont pu être ajoutés, capable de servir de principal composant structurel de matériaux et d'objets finaux (European Commission, 2011). Le marché de ces matériaux n'a cessé d'augmenter depuis les années 50, atteignant une production mondiale de 390 million de tonnes (Mt) en 2021 (Plastics Europe, 2022). Du fait de leurs propriétés attractives, ces matériaux sont particulièrement présents dans le domaine du packaging, du bâtiment, de l'automobile, de l'électronique, ou de l'agriculture. En raison de leur légèreté, la consommation d'énergie et les émissions de gaz à effet de serres liées à leur production et leur transport sont inférieures par rapport à d'autres matériaux tels que le bois ou le métal. Cependant, leur impact environnemental reste important sur plusieurs aspects de leur production et de leur fin de vie, entraînant une pollution environnementale considérable.

L'impact environnemental des plastiques peut être amélioré en adoptant une stratégie de bioéconomie circulaire qui combine deux approches : la valorisation de la biomasse et la recyclabilité. Il est ici question de prendre en compte l'entièreté du cycle de vie du matériau en adoptant une philosophie du berceau au berceau, en opposition au fonctionnement de l'économie actuelle basée du berceau à la tombe. L'objectif de cette stratégie est de créer un cercle vertueux à l'impact positif en améliorant la manière de produire les matières plastiques.

Les matières biosourcés sont définies par Citeo comme étant toutes les matières d'origine biologique à l'exclusion des matières intégrées dans des formations géologiques ou fossilisées (Citeo, 2020). Les plastiques biosourcés représentaient en 2021 1,5 % de la production mondiale de plastiques, soit environ 5,8 Mt (Plastics Europe, 2022). Bien qu'ils constituent une part marginale de la production mondiale, ces matériaux alternatifs sont appelés à se développer en France, notamment depuis la promulgation en 2015 de la Loi de Transition Energétique pour la Croissance Verte (LTECV) (ADEME, 2016).

Dans ce contexte, les synthons biosourcés sont une alternative intéressante à leurs homologues issus de ressources fossiles car ils s'inscrivent dans une dynamique renouvelable et d'économie circulaire. Ils permettent également de palier à la raréfaction de certaines structure et/ou d'en obtenir de nouvelles conférant des propriétés innovantes et ainsi permettant de satisfaire de nouvelles fonctionnalités. Par la grande variété de structures aliphatiques, cycloaliphatiques et aromatiques disponibles, les synthons biosourcés contribuent à la synthèse de polymères aux propriétés polyvalentes.

Les composés aromatiques confèrent des propriétés intéressantes aux polymères telles que la rigidité, la résistance thermique, l'hydrophobie et les propriétés barrières (Llevot et al., 2016). En outre, grâce aux interactions π - π entre les cycles aromatiques, les propriétés mécaniques des polymères aromatiques sont supérieures à leurs équivalents aliphatiques. En raison de leurs applications étendues dans l'industrie chimique, les molécules aromatiques tels que le benzène, le toluène ou le xylène (BTX) ont une valeur importante. Traditionnellement, ces aromatiques sont produits en plusieurs étapes à partir de ressources fossiles tels que le naphta, le charbon ou le gaz naturel. Or, ces ressources sont beaucoup plus rapidement consommées qu'elles ne sont produites, engendrant la raréfaction et l'augmentation du prix de certaines fractions (Wegelin and Meier, 2024). La substitution de ces ressources fossiles pour des ressources renouvelable à l'approvisionnement plus fiable présente un intérêt économique et environnemental majeur.

La biomasse lignocellulosique représente la plus grande source de structures aromatiques biosourcés. Parmi les nombreux composés issus de cette ressource, la lignine s'impose comme une source intéressante de phénols pour la synthèse de polymères durables (Laurichesse and Avérous, 2014). La structure de ce polyphénol, particulièrement présent dans le bois, dépend fortement de son origine botanique et de son procédé d'extraction (Tribot et al., 2019). Son architecture moléculaire amorphe et complexe résulte de la polymérisation de trois précurseurs aromatiques appelés monolignols : l'alcool p-coumarylique, l'alcool coniférylique et l'alcool sinapylique. Les principaux procédés d'extraction sont les procédés sulfite produisant les lignosulfonates, kraft, soda et organosolv. Ces différentes

INTRODUCTION GÉNÉRALE

méthodes consistent à solubiliser la lignine en la fragmentant en résidus de plus faible masse molaires qui peuvent ensuite se recombinaer. Elle est généralement récupérée par précipitation et filtration. Cet oligomère polyfonctionnel comporte une teneur élevée en hydroxyles aliphatiques et phénoliques, ainsi que quelques groupements acides carboxyliques offrant de nombreuses possibilités de modifications chimiques (Figure 0-1).

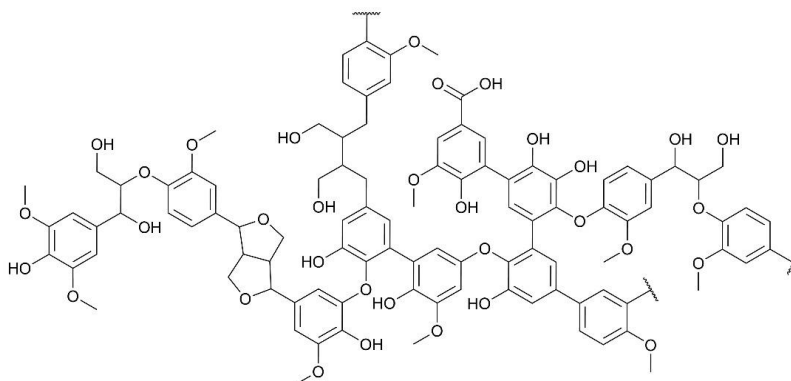


Figure 0-1. Modèle structurel de lignine issue de bois de feuillus.

Du fait de son importante fonctionnalité, la lignine est très largement utilisée pour préparer des thermdurcissables, notamment des polyesters, des polyuréthanes (PU) ainsi que des résines époxy et phénoliques (Upton and Kasko, 2016; Lawoko and Samec, 2023). Cette structure réticulée confère une excellente résistance thermique et mécanique, mais limite considérablement le potentiel de recyclabilité des matériaux.

Dans une stratégie de bioéconomie circulaire, et pour limiter l'impact environnemental des plastiques, le développement de matériaux réutilisables, recyclables ou recyclés est un enjeu majeur de la recherche actuelle. En Europe en 2020, 35% des 29,5 Mt de déchets plastiques post-consommation étaient recyclés (Figure 0-2), le reste étant valorisé énergétiquement ou disposé en décharge. Bien que les quantités de plastiques recyclés aient augmenté de +69% entre 2006 et 2020 (Plastics Europe, 2022), des limitations relatives aux filières de tri mais également à la production de ces matériaux persistent. Il est maintenant primordial de penser la fin de vie des polymères dès leur conception.

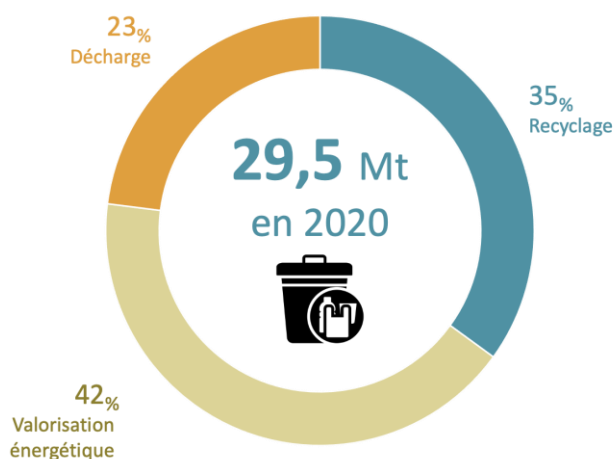


Figure 0-2. Gestion des déchets plastiques post-consommation en Europe en 2020 (adapté de Plastics Europe 2022).

INTRODUCTION GÉNÉRALE

C'est dans ce contexte que les réseaux covalents adaptables (CANs) se sont révélés comme une alternative plus durable aux polymères conventionnels. Cette nouvelle catégorie de polymère regroupe les avantages des thermoplastiques et des thermodurcissables en combinant d'excellentes propriétés thermiques et mécaniques, et recyclabilité. Il s'agit de réseaux réticulés dans lesquels sont incorporées des liaisons dynamiques qui peuvent se réarranger en réponse à un ou plusieurs stimuli, tel que la température, la lumière, ou le pH par exemple, entraînant un écoulement du matériau (Kloxin et al., 2010). Les CANs sont classés en deux catégories, en fonction de leur mécanisme de réarrangement (Figure 0-3). Pour les CANs dits dissociatifs, la liaison initiale est rompue avant la formation d'une nouvelle, entraînant une diminution de la densité de réticulation du matériau et dans certains cas sa dépolymérisation. Les CANs dits associatifs sont quant à eux caractérisés par la formation d'une nouvelle liaison avant la rupture de la liaison initiale, maintenant la densité de réticulation constante au sein du réseau. Les matériaux présentant ce mécanisme ont été nommés « vitrimères » en 2011 par Leibler (Montarnal et al., 2011). De nombreuses chimies dynamiques peuvent être utilisées pour la préparation de CANs. Les polyoléfines, polyesters, PU ou polyimines par exemple, qui représentent les familles de polymères les plus produites, sont au cœur de la recherche pour le développement de matériaux dynamiques (Hassanian-Moghaddam et al., 2023; Tao et al., 2023; Van Zee and Nicolay, 2020).

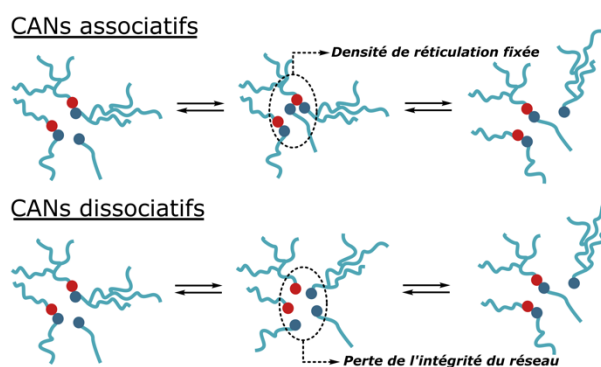


Figure 0-3. Mécanismes de réarrangement dissociatifs et associatifs des réseaux moléculaires.

Le développement de CANs biosourcés permet d'améliorer l'impact environnemental des matériaux en prenant en compte l'intégralité de leur cycle de vie : de la production à la fin de vie. De nombreux synthons biosourcés ont pu être combinés avec des chimies dynamiques pour la préparation notamment de réseaux époxy (Zhao et al., 2022), polyesters (Kumar and Connal, 2023), ou polyimines (Liguori and Hakkarainen, 2022).

L'importante fonctionnalité de la lignine est compatible avec une multitude de chimies dynamiques pour la synthèse de CANs biosourcés. L'intégration de liaisons Diels-Alder au sein de réseaux à base de lignine a premièrement été rapporté (Duval et al., 2015; Buono et al., 2017). Par la suite, la conceptualisation de réseaux polyesters (Zhang et al., 2018; Adjaoud et al., 2023), PU (Liu et al., 2019; Ma et al., 2023), ou polyacétal (Moreno et al., 2021) dynamiques à partir de lignine ont fait l'objet de plusieurs publications, révélant l'engouement de la communauté scientifique pour cette thématique.

Cette thèse a été financée par la fondation Jean-Marie Lehn (projet LigniCAN). Elle a été dirigée par le Pr. Luc Avérous et co-encadrée par le Dr Antoine Duval. Les travaux de recherches ont été effectués dans l'équipe BioTeam au sein de l'Institut de Chimie et Procédé pour l'Énergie, l'Environnement et la Santé (ICPEES-UMR 7515).

Ce projet s'inscrit dans la continuité des travaux de recherche effectués dans la BioTeam portant sur la valorisation de la lignine pour la synthèse de matériaux performants. Depuis plus d'une décennie, la modification chimique de lignine a largement été explorée. La méthylation avec du phosphate de

INTRODUCTION GÉNÉRALE

triméthyl, l'oxyalkylation avec du carbonate d'éthylène, et le greffage de groupement vinyles avec du carbonate de vinyle éthylène ont par exemple été réalisés avec succès sur plusieurs lignines organosolv (Duval and Avérous, 2020; Duval et al., 2021). Les lignines modifiées par diverses voies de synthèses ont pu être utilisées pour préparer des réseaux Diels-Alder (Buono et al., 2017) et PU (Laurichesse et al., 2014). Récemment, des mousses PU ont été développées à partir de polyols liquides de faible viscosités composés de lignine et de polyéthylène glycol (Duval et al., 2022).

En parallèle, toujours dans l'objectif de développer des matériaux durables, la thématique des CANs a également fait l'objet de multiples recherches au sein de la BioTeam. Plusieurs études récentes ont développé de nouveaux réseaux polyimines (Dhers et al., 2019; Hajj et al., 2020; Lucherelli et al., 2023) et polyuréthanes dynamiques (Tremblay-Parrado and Avérous, 2020; Tremblay-Parrado et al., 2020; Duval and Avérous, 2023). Ces différents travaux ont mis en avant le potentiel de synthons biosourcés aliphatiques (acides gras issus d'huiles végétales) et aromatiques (dérivés furaniques et acides p-hydroxycinnamiques) pour la synthèse de polymères plus durables. Fort de cette double expertise, l'ensemble de ces travaux a ouvert la voie vers l'utilisation de lignine, composé abondant et relativement économique, pour la synthèse de matériaux recyclables.

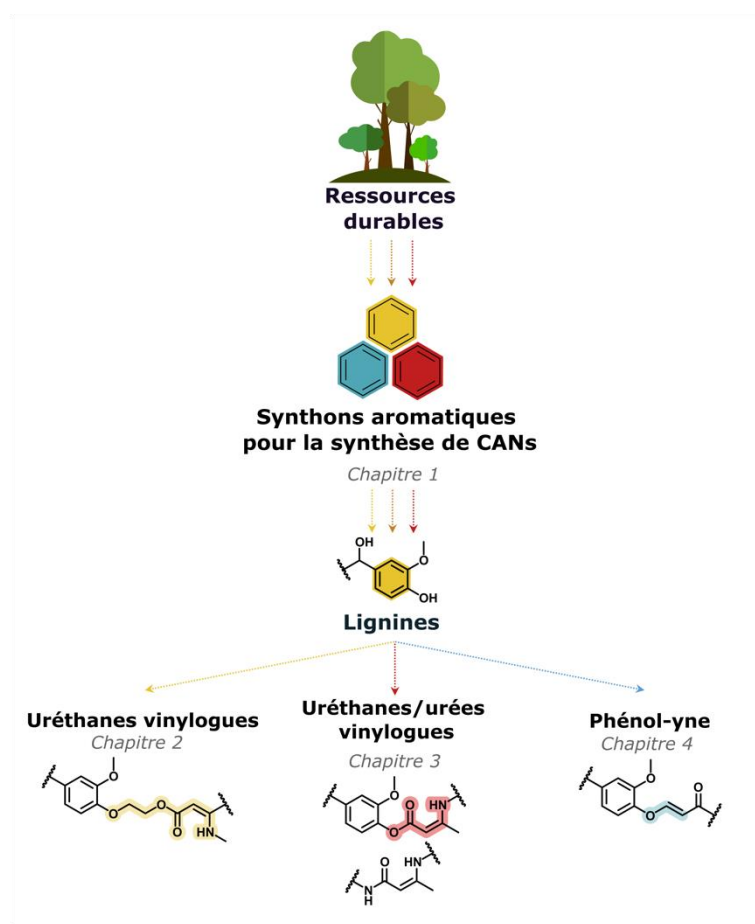


Figure 0-4. Schéma récapitulatif de l'organisation du mémoire de doctorat.

L'objectif de cette thèse est de développer de nouvelles architectures macromoléculaires aromatique et biosourcés durables à partir de lignine en prenant en compte l'entièreté du cycle de vie du matériau, et adoptant ainsi une philosophie du berceau au berceau. Ces travaux de recherche ont l'ambition de développer des CANs à base de lignine, alliant des propriétés thermiques et mécaniques intéressantes, et recyclabilité. Ce manuscrit est organisé en 4 chapitres constitués d'articles scientifiques,

INTRODUCTION GÉNÉRALE

déjà publiés ou prochainement soumis, encadrés par des introductions et conclusions rédigées en français (Figure 0-4).

Le **premier chapitre** de ce manuscrit propose un état de l'art sur les réseaux covalents adaptables biosourcés et aromatiques. Il se présente sous la forme d'une revue bibliographique intitulée «*Biobased and Aromatic Covalent Adaptable Networks: when architectures meet properties, within the framework of a circular bioeconomy*». Il discute des différentes voies de préparation de CANs à partir de synthons aromatiques issus de diverses sources botaniques, ainsi que l'influence de l'aromaticité pour l'obtention de propriétés spécifiques. Il met également en lumière les différents domaines d'applications de ces matériaux durables. Ce chapitre permet ainsi de mieux appréhender la synthèse et les propriétés rhéologiques de CANs, à partir de molécules aromatiques.

Le **second chapitre** amorce la partie expérimentale de cette thèse en s'intéressant à la synthèse d'uréthanes vinylogues à partir de lignine organosolv. Dans un premier temps la lignine est modifiée chimiquement pour la rendre réactive pour la synthèse de matériaux. Cette lignine modifiée est ensuite utilisée dans la synthèse d'une gamme de matériaux caractérisée chimiquement, mécaniquement et rhéologiquement. Les propriétés finales des matériaux sont discutées et le potentiel de recyclabilité est mis en évidence par recyclage physique. Ce chapitre fait l'objet d'un article scientifique intitulé «*From Lignins to Renewable Aromatic Vitrimers based on Vinylogous Urethane* », publié dans *ChemSusChem* (Sougrati et al., 2023).

Le **troisième chapitre** porte également sur la synthèse d'uréthanes vinylogues à partir de lignines organosolv. La préparation de matériaux à forte teneur en lignine est proposée, en accord avec les principes de chimie verte. Une voie de synthèse permettant de modifier les différents groupements réactifs de la lignine en une étape a été développée. La réaction de condensation de la lignine modifiée avec des amines a été examinée, notamment pour appréhender la réactivité des acétoacétates aromatiques pouvant former simultanément des groupements uréthanes et des urées vinylogues. La relation structure-propriétés de la série de vitrimères a été étudiée, avec une attention particulière sur l'influence de la structure des agents de réticulation sur les propriétés mécaniques et rhéologiques des matériaux.

Enfin, le **quatrième chapitre** est une ouverture sur le développement de matériaux recyclables par voie physique et chimique en utilisant une chimie dynamique émergente, la phénol-yne. Dans un premier temps, le potentiel de réarrangement des liaisons éthers d'énol en présence de phénols mono- et di-substitués en positions *ortho* a été étudié. Ensuite, une étude cinétique de réactivité a été effectuée sur des composés modèles pour examiner les différences de réactivité entre les différents groupements réactifs de la lignine. Fort de ces observations, une gamme de matériaux a été synthétisée à partir de lignines de structures distinctes issues de différents procédés d'extraction (lignine Kraft, lignine organosolv et lignine organosolv dépolymérisée). Ces matériaux ont été caractérisés structurellement, mécaniquement et rhéologiquement. Enfin, le potentiel de recyclabilité a été exploré par recyclage physique, via remise en forme thermomécanique, ainsi que par recyclage chimique, via hydrolyse acide.

REFERENCES

- ADEME, 2016. Plastiques biosourcés (Les). Libr. ADEME. URL <https://librairie.ademe.fr/produire-autrement/3063-plastiques-biosources-les.html> (accessed 4.29.24).
- Adjaoud, A., Puchot, L., Federico, C.E., Das, R., Verge, P., 2023. Lignin-based benzoxazines: A tunable key-precursor for the design of hydrophobic coatings, fire resistant materials and catalyst-free vitrimers. *Chem. Eng. J.* 453, 139895. <https://doi.org/10.1016/j.cej.2022.139895>

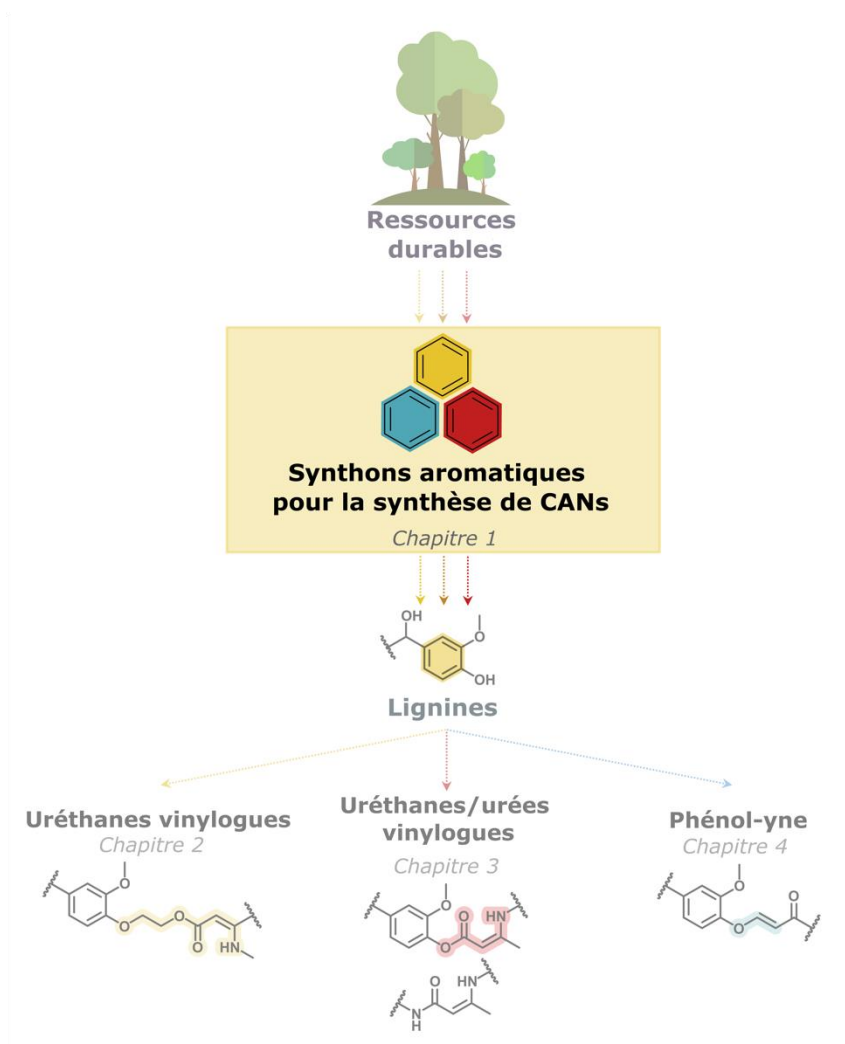
INTRODUCTION GÉNÉRALE

- Buono, P., Duval, A., Averous, L., Habibi, Y., 2017. Thermally healable and remendable lignin-based materials through Diels – Alder click polymerization. *Polymer* 133, 78–88. <https://doi.org/10.1016/j.polymer.2017.11.022>
- Citeo, 2020. Citeo Prospective - Note réglementation plastiques compostables et biosourcés. URL <https://bo.citeo.com/sites/default/files/2020-06/Citeo%20Prospective%20-%20Note%20r%C3%A9glementation%20plastiques%20compostables%20et%20biosourc%C3%A9s.pdf> (accessed 4.29.24).
- Dhers, S., Vantomme, G., Avérous, L., 2019. A fully bio-based polyimine vitrimer derived from fructose. *Green Chem.* 21, 1596–1601. <https://doi.org/10.1039/C9GC00540D>
- Duval, A., Avérous, L., 2023. From thermoplastic polyurethane to covalent adaptable network via reversible photo-crosslinking of a biobased chain extender synthesized from caffeic acid. *Polym. Chem.* 14, 2685–2696. <https://doi.org/10.1039/D3PY00162H>
- Duval, A., Avérous, L., 2020. Mild and controlled lignin methylation with trimethyl phosphate: towards a precise control of lignin functionality. *Green Chem.* 22, 1671–1680. <https://doi.org/10.1039/C9GC03890F>
- Duval, A., Lange, H., Lawoko, M., Crestini, C., 2015. Reversible crosslinking of lignin via the furan–maleimide Diels–Alder reaction. *Green Chem.* 17, 4991–5000. <https://doi.org/10.1039/C5GC01319D>
- Duval, A., Layrac, G., van Zomeren, A., Smit, A.T., Pollet, E., Avérous, L., 2021. Isolation of Low Dispersity Fractions of Acetone Organosolv Lignins to Understand their Reactivity: Towards Aromatic Building Blocks for Polymers Synthesis. *ChemSusChem* 14, 387–397. <https://doi.org/10.1002/cssc.202001976>
- Duval, A., Vidal, D., Sarbu, A., René, W., Avérous, L., 2022. Scalable single-step synthesis of lignin-based liquid polyols with ethylene carbonate for polyurethane foams. *Mater. Today Chem.* 24, 100793. <https://doi.org/10.1016/j.mtchem.2022.100793>
- European Commission, 2011. Règlement (UE) no 10/2011 de la Commission du 14 janvier 2011 concernant les matériaux et objets en matière plastique destinés à entrer en contact avec des denrées alimentaires. URL <https://eur-lex.europa.eu/LexUriServ/LexUriServ.do?uri=OJ:L:2011:012:0001:0089:fr:PDF> (accessed 5.2.24).
- Hajj, R., Duval, A., Dhers, S., Avérous, L., 2020. Network Design to Control Polyimine Vitrimer Properties: Physical Versus Chemical Approach. *Macromolecules* 53, 3796–3805. <https://doi.org/10.1021/acs.macromol.0c00453>
- Hassanian-Moghaddam, D., Asghari, N., Ahmadi, M., 2023. Circular Polyolefins: Advances toward a Sustainable Future. *Macromolecules* 56, 5679–5697. <https://doi.org/10.1021/acs.macromol.3c00872>
- Kloxin, C.J., Scott, T.F., Adzima, B.J., Bowman, C.N., 2010. Covalent Adaptable Networks (CANs): A Unique Paradigm in Cross-Linked Polymers. *Macromolecules* 43, 2643–2653. <https://doi.org/10.1021/ma902596s>
- Kumar, A., Connal, L.A., 2023. Biobased Transesterification Vitrimers. *Macromol. Rapid Commun.* 44, 2200892. <https://doi.org/10.1002/marc.202200892>
- Laurichesse, S., Avérous, L., 2014. Chemical modification of lignins: Towards biobased polymers. *Prog. Polym. Sci.* 39, 1266–1290. <https://doi.org/10.1016/j.progpolymsci.2013.11.004>
- Laurichesse, S., Huillet, C., Avérous, L., 2014. Original polyols based on organosolv lignin and fatty acids: new bio-based building blocks for segmented polyurethane synthesis. *Green Chem.* 16, 3958–3970. <https://doi.org/10.1039/C4GC00596A>
- Lawoko, M., Samec, J.S.M., 2023. Kraft lignin valorization: Biofuels and thermoset materials in focus. *Curr. Opin. Green Sustain. Chem.* 40, 100738. <https://doi.org/10.1016/j.cogsc.2022.100738>
- Liguori, A., Hakkarainen, M., 2022. Designed from Biobased Materials for Recycling: Imine-Based Covalent Adaptable Networks. *Macromol. Rapid Commun.* 43, 2100816. <https://doi.org/10.1002/marc.202100816>

INTRODUCTION GÉNÉRALE

- Liu, W., Fang, C., Wang, S., Huang, J., Qiu, X., 2019. High-Performance Lignin-Containing Polyurethane Elastomers with Dynamic Covalent Polymer Networks. *Macromolecules* 52, 6474–6484. <https://doi.org/10.1021/acs.macromol.9b01413>
- Llevot, A., Grau, E., Carlotti, S., Grelier, S., Cramail, H., 2016. From Lignin-derived Aromatic Compounds to Novel Biobased Polymers. *Macromol. Rapid Commun.* 37, 9–28. <https://doi.org/10.1002/marc.201500474>
- Lucherelli, M.A., Duval, A., Averous, L., 2023. Combining Associative and Dissociative Dynamic Linkages in Covalent Adaptable Networks from Biobased 2,5-Furandicarboxaldehyde. *ACS Sustain. Chem. Eng.* 11, 2334–2344. <https://doi.org/10.1021/acssuschemeng.2c05956>
- Ma, X., Li, S., Wang, F., Wu, J., Chao, Y., Chen, X., Chen, P., Zhu, J., Yan, N., Chen, J., 2023. Catalyst-Free Synthesis of Covalent Adaptable Network (CAN) Polyurethanes from Lignin with Editable Shape Memory Properties. *ChemSusChem* 16, e202202071. <https://doi.org/10.1002/cssc.202202071>
- Montarnal, D., Capelot, M., Tournilhac, F., Leibler, L., 2011. Silica-Like Malleable Materials from Permanent Organic Networks. *Science* 334, 965–968. <https://doi.org/10.1126/science.1212648>
- Moreno, A., Morsali, M., Sipponen, M.H., 2021. Catalyst-Free Synthesis of Lignin Vitrimers with Tunable Mechanical Properties: Circular Polymers and Recoverable Adhesives. *ACS Appl. Mater. Interfaces* 13, 57952–57961. <https://doi.org/10.1021/acsami.1c17412>
- Plastics Europe, 2022. *Plastics - the facts 2022*. *Plast. Eur. FR.* URL <https://plasticseurope.org/fr/knowledge-hub/plastics-the-facts-2022/> (accessed 4.23.24).
- Sougrati, L., Duval, A., Avérous, L., 2023. From Lignins to Renewable Aromatic Vitrimers based on Vinylogous Urethane. *ChemSusChem* 16, e202300792. <https://doi.org/10.1002/cssc.202300792>
- Tao, Y., Liang, X., Zhang, J., Lei, I.M., Liu, J., 2023. Polyurethane vitrimers: Chemistry, properties and applications. *J. Polym. Sci.* 61, 2233–2253. <https://doi.org/10.1002/pol.20220625>
- Tremblay-Parrado, K.-K., Avérous, L., 2020. Renewable Responsive Systems Based on Original Click and Polyurethane Cross-Linked Architectures with Advanced Properties. *ChemSusChem* 13, 238–251. <https://doi.org/10.1002/cssc.201901991>
- Tremblay-Parrado, K.-K., Bordin, C., Nicholls, S., Heinrich, B., Donnio, B., Avérous, L., 2020. Renewable and Responsive Cross-Linked Systems Based on Polyurethane Backbones from Clickable Biobased Bismaleimide Architecture. *Macromolecules* 53, 5869–5880. <https://doi.org/10.1021/acs.macromol.0c01115>
- Tribot, A., Amer, G., Abdou Alio, M., De Baynast, H., Delattre, C., Pons, A., Mathias, J.-D., Callois, J.-M., Vial, C., Michaud, P., Dussap, C.-G., 2019. Wood-lignin: Supply, extraction processes and use as bio-based material. *Eur. Polym. J.* 112, 228–240. <https://doi.org/10.1016/j.eurpolymj.2019.01.007>
- Upton, B.M., Kasko, A.M., 2016. Strategies for the Conversion of Lignin to High-Value Polymeric Materials: Review and Perspective. *Chem. Rev.* 116, 2275–2306. <https://doi.org/10.1021/acs.chemrev.5b00345>
- Van Zee, N.J., Nicolaÿ, R., 2020. Vitrimers: Permanently crosslinked polymers with dynamic network topology. *Prog. Polym. Sci.* 104, 101233. <https://doi.org/10.1016/j.progpolymsci.2020.101233>
- Wegelin, S., Meier, M.A.R., 2024. Biobased aromatics for chemicals and materials: Advances in renewable drop-in and functional alternatives. *Curr. Opin. Green Sustain. Chem.* 100931. <https://doi.org/10.1016/j.cogsc.2024.100931>
- Zhang, S., Liu, T., Hao, C., Wang, L., Han, J., Liu, H., Zhang, J., 2018. Preparation of a lignin-based vitrimer material and its potential use for recoverable adhesives. *Green Chem.* 20, 2995–3000. <https://doi.org/10.1039/C8GC01299G>
- Zhao, X.-L., Li, Y.-D., Zeng, J.-B., 2022. Progress in the design and synthesis of biobased epoxy covalent adaptable networks. *Polym. Chem.* 13, 6573–6588. <https://doi.org/10.1039/D2PY01167K>

CHAPITRE 1. RESEAUX COVALENTS ADAPTABLES BIOSOURCES ET AROMATIQUES : QUAND LES ARCHITECTURES RENCONTRENT LES PROPRIETES, DANS LE CADRE D'UNE BIOECONOMIE CIRCULAIRE



INTRODUCTION DU CHAPITRE 1

L'étude bibliographique présentée dans ce premier chapitre vise à exposer les plus récentes avancées et résultats dans la synthèse de réseaux covalents adaptables à partir de synthons aromatiques issus de ressources renouvelables. Cet état de l'art se présente sous la forme d'une revue de littérature intitulée «Biobased and Aromatic Covalent Adaptable Networks: when architectures meet properties, within the framework of a circular bioeconomy», soumise dans *Materials Science and Engineering: R: Reports*.

La première partie introduit brièvement les CANs et leurs principales caractéristiques. Les différentes chimies covalentes dynamiques utilisées pour la synthèse de CANs aromatiques et biosourcés sont décrites. La deuxième partie s'intéresse à l'identification des principaux composés aromatiques issus de ressources renouvelables, telles que la biomasse lignocellulosique et les polysaccharides. Les origines botaniques, processus d'extractions et aspects structurels de molécules plateformes aromatiques d'intérêt, telles que la vanilline, le syringaldéhyde, le 4-hydroxybenzaldéhyde, le 3,4-dihydroxybenzaldéhyde, l'acide tannique, le resvératrol, le cardanol, l'eugénol ou des dérivés furaniques, sont décrits. Les CANs préparés à partir de ces molécules, n'ayant pour la majeure partie jamais fait l'objet de revue de littérature, sont largement rapportés. L'influence des structures utilisées, en combinaison avec différentes chimies covalentes dynamiques, sur leurs propriétés est étudiée. Un accent est particulièrement mis sur les propriétés rhéologiques finales ainsi que les potentiels de recyclage physique et chimique de ces matériaux. Une dernière partie porte sur l'étude des propriétés des CANs aromatiques et biosourcés en réponse à des spécifications particulières pour des applications ciblées, telles que les capteurs, les matériaux conducteurs, les adhésifs, les retardateurs de flamme, les dispositifs médicaux et les revêtements. Enfin, des conclusions souligneront les défis qui restent à relever et les perspectives dans ce domaine d'avenir, pour le développement de polymères plus durables dans une approche de bioéconomie circulaire. Ces conclusions et cet ensemble permettront d'ouvrir les perspectives et orientations de ce travail de doctorat.

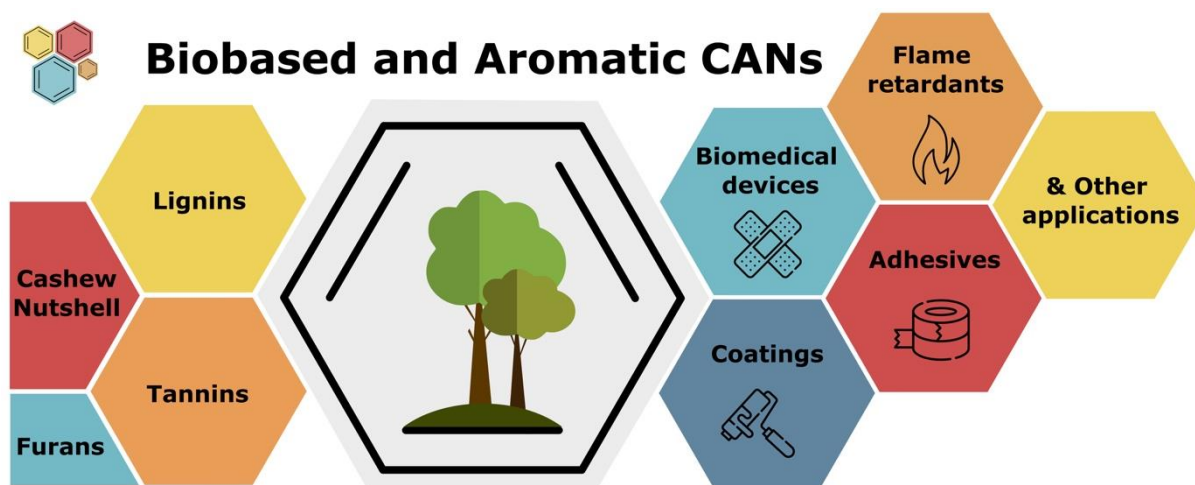
BIOBASED AND AROMATIC COVALENT ADAPTABLE NETWORKS: WHEN ARCHITECTURES MEET PROPERTIES, WITHIN THE FRAMEWORK OF A CIRCULAR BIOECONOMY

Lisa Sougrati ^a, Antoine Duval ^{a, b, *}, Luc Avérous ^{a, *}

^a BioTeam/ICPEES-ECPM, UMR CNRS 7515, Université de Strasbourg, 25 rue Becquerel, 67087 Strasbourg, Cedex 2, France

^b Soprema, 15 rue de Saint Nazaire, 67100, Strasbourg, France

*Corresponding authors.



1. ABSTRACT

In the current context of environmental emergency, the need for sustainable materials with controlled end-of-life is paramount. Covalent adaptable networks (CANs) are a novel class of polymers offering a unique solution by combining the main advantages of thermosets and thermoplastics such as high mechanical performance and recyclability. Sustainable feedstock, such as biobased compounds from biomass represent nowadays prime alternatives to fossil-based chemicals. Consequently, aromatic-rich renewable resources, owing to their abundances and structural variety, are feedstocks of choice in the design of materials combining performance, sustainability, and circularity. Then, the substitution of fossil-based raw materials with biobased compounds for the preparation of CANs is improving, among which aromatic structures, such as lignins, tannins, cashew nutshell liquid or furan, provide unprecedented features and properties. After a description of CANs general features and the presentation of available biobased aromatic feedstocks, an overview of recent advances in the synthesis of biobased and aromatic networks is presented. An emphasis is placed on the opportunity offered by the aromatic building blocks functional groups to implement dynamic covalent chemistries. Subsequently, an understanding on the benefits of aromaticity on specific properties required for targeted applications, including sensors, adhesives, flame retardants, biomedical devices, or coatings, is proposed. All these proving the design of biobased and aromatic CANs to be a considerable step towards for a more sustainable future in the frame of a circular bioeconomy.

2. INTRODUCTION

Polymers are widely used nowadays owing to their unprecedented features such as inexpensive production, lightweight, and durability fitting a wide range of applications in many technological fields (Dorigato, 2021). Till today, although the production of polymer materials is continuously increasing, around 10% of produced materials are recycled annually, while 8% are incinerated, and the remaining is being landfilled (Organization for Economic Co-operation and Development, 2022; Naderi Kalali et al., 2023). The implementation of efficient collection and waste management systems is a priority for governments to divert waste plastics from landfills or littering (Hopewell et al., 2009). However, the recycling is subjected to several increasing challenges. For instance, amongst solid waste streams, multilayer films or polymer blends present additional difficulties related to the association of different constituents that can be hard to separate for recycling (Morinval and Averous, 2022). Current European standardization define mechanical recycling as a process not (intentionally) changing the chemical structure of the material in opposition to chemical recycling technologies altering the polymer chains chemical structure (ISO 15270, 2008). Following this definition and to avoid confusions, the term ‘physical recycling’ was introduced to encompass mechanical and solvent-based recycling, neither processes changing the structure of the polymers. Chemical recycling category includes depolymerization, pyrolysis, and gasification techniques (Ragaert et al., 2023).

Thermoplastics represent approximately 80% of plastics production (Fortman et al., 2018). Due to their solubility and viscoelastic liquid behavior upon heating, they are suitable for various processing techniques and can be recycled via chemical and physical pathways (Biron, 2018; Emblem, 2012; Košir and Slavič, 2023; Rosato and Rosato, 2012; Thomas and Yang, 2009). In contrast, thermosetting matrices employed in high-performance industrial applications (Mahajan et al., 2020; Raquez et al., 2010) and elastomers cannot be recovered through physical processes because of their crosslinked nature endowing a viscoelastic solid behavior, which makes them less adequate to meet current environmental challenges (Post et al., 2020). In this frame, covalent adaptable networks (CANs) are a novel class of polymers aiming to combine advantages of thermoplastics and thermosets. By incorporating dynamic covalent bonds within a crosslinked macromolecular architecture, flow is induced through network rearrangements. In response to one or several stimuli including the temperature, pH, or light, bonds can break and reform leading to a novel topological structure of the network. Over the last decade, this blooming realm is extensively explored to gain a comprehensive understanding of the mechanistic pathways and rheological profiles occurring during exchange reactions. Two main rearrangements

mechanisms are distinguished: dissociative and associative pathways. Associative mechanisms give rise to the so-called vitrimers, mainly introduced by Leibler and co-workers (Montarnal et al., 2011) in 2011. CANs dynamic chemistries are implemented to all the major polymer families, such as polyolefins (Ahmadi et al., 2022; Caffy and Nicolaÿ, 2019; Ricarte et al., 2020; Tellers et al., 2019), polyesters (M. Chen et al., 2021; Cuminet et al., 2022; Debnath et al., 2020), polyurethanes (PUs) (Debnath et al., 2021; Tao et al., 2023; Yan et al., 2017), polyimines (K. Schoustra et al., 2021; Liguori and Hakkarainen, 2022), or polysiloxanes, among others (Nishimura et al., 2017; Tretbar et al., 2019). Indeed, the great array of covalent dynamic chemistries makes them facile to integrate within a polymer network. Numerous chemistries proved to impart crosslinked materials with high recyclability, as boronic esters (Zhang et al., 2020), vinylogous urethanes (Denissen et al., 2015), acetal (Yu et al., 2020), Diels-Alder (Tremblay-Parrado and Avérous, 2020a), aza and thiol-Michael (Berne et al., 2022b, 2022c), disulfide (L. Li et al., 2020), or [2 + 2] cycloaddition (Duval and Avérous, 2023). These chemistries offer built-in reprocessability, closed-loop recycling (Hong et al., 2023; Ye et al., 2021), and upcycling approaches (H. Zhang et al., 2022; Britt et al., 2019; Jehanno et al., 2022; Korley et al., 2021; Qiu et al., 2021; H. Li et al., 2022).

The development of biobased CANs provides an opportunity to improve the environmental impact of polymer materials by embracing a circular bioeconomy philosophy and considering their entire life cycle, from production to end-of-life (Chandel et al., 2020; D'Adamo et al., 2022). In the European Union, the share of organic chemicals produced from biobased feedstock is estimated around 10%, corresponding to approximately 7.8 Mt per year (Popp et al., 2021). For instance, 1.6 million Tons (Mt) of starch and sugar, 1.6 Mt of vegetable oils, and 0.6 Mt bioethanol and natural rubbers are employed for chemical production. The use of biobased feedstock is expected to increase by 25% by 2030.

Large array of renewable structures can be obtained including aliphatic (e.g. triglycerides and fatty acids derivatives, or natural rubbers), cycloaliphatic (e.g. terpenes, or cholesterol), and aromatic (e.g. lignins, tannins, furan and derivatives) precursors (Buono et al., 2018; Sardon et al., 2021; Liu et al., 2014; Zia et al., 2016; Beller et al., 2015; van Es, 2013). Among the variety of biobased structures, aromatic compounds are extremely abundant in nature through lignocellulosic biomass with particularly the lignins (Souto and Calado, 2022), tannins (Arbenz and Avérous, 2015), cashew nutshell liquid (CNSL) and all their derivatives (Decostanzi et al., 2019; Lochab et al., 2014; C. Zhang et al., 2022; Sarika et al., 2020). Besides these structures naturally occurring in biomass, furans are formed by chemical modifications of renewable (poly)saccharides (Gandini and Belgacem, 1997). The extraction, depolymerization or chemical treatments lead to platform chemicals of major interest, such as vanillin, syringaldehyde, 4-hydroxybenzaldehyde, 3,4-dihydroxybenzaldehyde, tannic acid, resveratrol, cardanol, 2,5-furandicarboxaldehyde, or eugenol. Thanks to their multiple functional sites, renewable aromatic building blocks can be easily integrated into dynamic networks, mostly polyesters, polyimines, polyurethanes, and polyacetals, through straightforward, atom-efficient, and innovative synthetic pathways following green chemistry principles. Those principles are founded on prevention, atom-economy, the use of renewable feedstocks, less hazardous chemicals and solvents, and the design of safer and degradable products while reducing the formation of byproducts and the processes energy consumption (Anastas and Eghbali, 2010). In polymers, aromatic compounds provide interesting properties including stiffness, thermal resistance, hydrophobicity, and barrier properties (Llevot et al., 2016). Owing to π - π interactions between aromatic rings, glass transition temperature (T_g), and mechanical behavior of aromatic polymers are increased as compared to aliphatic ones.

This review aims to present the state-of-the-art advances in the synthesis of CANs from biobased aromatic precursors. Following a brief introduction on CANs and their main characteristics, an overview of the dynamic covalent chemistries used in the literature for the synthesis of biobased and aromatic CANs is presented. The main biobased and aromatic building blocks in the toolboxes of today's chemists to develop high-performance and innovative materials are identified, with an emphasis on their botanical origins, extraction processes and structural aspects. CANs prepared from these precursors are surveyed, with a specific focus on their rheological parameters as well as their recycling abilities. Subsequently,

the properties according to specific requirements are investigated, for targeted applications including sensors, conductive materials, adhesives, flame retardants, biomedical devices, and coatings. Finally, concluding remarks will draw attention to the remaining challenges and future perspectives in this dynamic field.

3. GENERALITIES

3.1. Introduction to CANs

Reversible covalent bonds are well-known in organic chemistry. In response to a trigger, which can be temperature or UV-light for instance, bonds can break and reform. Such chemistries have been exploited in polymer matrix for a long time (Leibler et al., 1991; Rubinstein and Semenov, 1998; Semenov and Rubinstein, 1998; Stadler, 1988). Wudl and co-workers (Chen et al., 2002) pioneered the field of self-healing materials by exploiting thermally reversible Diels-Alder reaction in a polymer matrix. The concept of CANs was introduced by Bowman in 2010, revolutionizing crosslinked polymers recycling (Bowman and Kloxin, 2012; J. Kloxin and N. Bowman, 2013; Kloxin et al., 2010). By incorporating stimuli-responsive bonds within crosslinked networks, materials exhibit unique attributes such as recyclability, repairability, self-healing, adaptability and shape memory. Since then, extensive research has been carried out on the development of these performing adaptable materials, with increased lifecycle, controlled end-of-life and recyclability.

CANs are classified into two major groups based on the bond exchange reaction mechanism and materials behavior: dissociative and associative, as illustrated in Figure 1-1 (McBride et al., 2019; Winne et al., 2019). Detailed discussion on the mechanistic perspectives distinguished concerted mechanism from associative and dissociative stepwise bond exchanges (Winne et al., 2019). Dissociative rearrangements rely on the prior dissociation of the initial bond through an endothermic transition state, followed by the formation of a new bond from the free reactive end chains. The crosslinking density and thus the viscosity are dependent on the temperature that can shift the reaction equilibrium to the associated or dissociated state. Diels-Alder chemistry is a well-known example of dissociative crosslink (Gandini, 2013). The links become reversible upon heating, increasing the rate of bond breaking and forming, whereas when cooled down the network regains its connectivity and topology. Thermoset properties are re-established, such as dimensional stability and creep/chemical resistance. In associative CANs, a short-lived intermediate is formed by the reaction of a free reactive chain end on the initial bond, increasing the connectivity. The crosslinking density is maintained through the network rearrangement. The viscosity is mainly controlled by the rate of chemical exchange reactions. The first associative CANs, based on photo-induced allyl sulfides exchange, were introduced by Scott *et al.* (Scott et al., 2005) in 2005. However these materials were later designated as vitrimers by analogy with vitreous silica, which viscosity decreases progressively with temperature following an Arrhenius law (Montarnal et al., 2011). Although the Arrhenius-temperature dependence was first seen as a characteristic feature of associative CANs, some dissociative bond exchanges also exhibit such a behavior, reducing the frontier between associative and dissociative CANs (Elling and Dichtel, 2020; W.-X. Liu et al., 2017; Zhang and Rowan, 2017). Rearrangement mechanisms can be complex to be precisely identified. Some chemical systems have proven to rearrange following distinct mechanistic pathways depending on the conditions, such as the temperature, humidity, catalyst type and content along with neighboring group participation and internal catalysis (Cuminet et al., 2021; Van Lijsebetten et al., 2020).

CHAPITRE 1

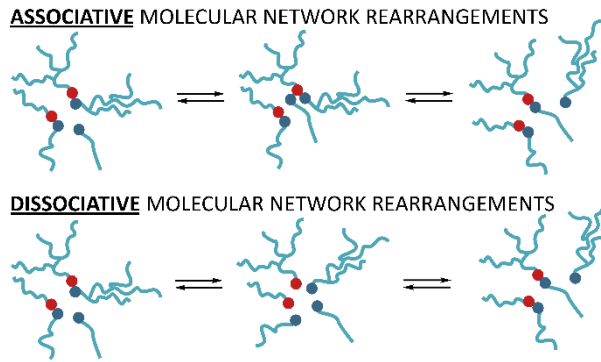


Figure 1-1. Different types of molecular network rearrangements within covalent networks.

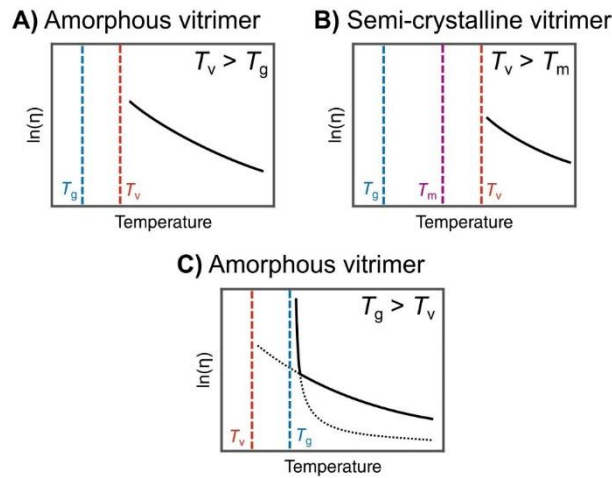


Figure 1-2. A) Plot of $\ln(\eta)$ versus temperature of an amorphous vitrimer in which the topology freezing transition temperature, T_v , is greater than the glass transition temperature, T_g . B) Plot of $\ln(\eta)$ versus temperature of a semi-crystalline vitrimer in which T_v is greater than the melting temperature, T_m . C) Plot of $\ln(\eta)$ versus temperature for a vitrimer that features a T_g that is greater than its T_v . Reprinted from Ref.(Van Zee and Nicolaÿ, 2020) Copyright 2020, with permission from Elsevier.

Upon heating, the dynamic linkages can be redistributed within the network. The temperature above which a macroscopic flow can be achieved via dynamic exchange (transition from elastic solid to viscoelastic liquid) was defined as the topological freezing temperature (T_v). Above T_v , bond rearrangements are fast enough to endow a viscous flow. Whereas below T_v , the network dynamics is considered as frozen resulting in a conventional thermoset-like behavior (Denissen et al., 2016). By convention, T_v is determined by extrapolation of the Arrhenius plot to a viscosity of 10^{12} Pa s (Brutman et al., 2014; Lessard et al., 2019). Several viscosity profiles are distinguished depending on the position of the T_v value with respect to the T_g (Figure 1-2) (Van Zee and Nicolaÿ, 2020). When $T_v < T_g$, bond exchange reactions are first limited by the rigidity of the network. Whereas when $T_v > T_g$ the flow is mainly controlled by the bond exchange kinetic (Denissen et al., 2016). The viscoelastic behavior is in most case determined via network stress-relaxation. Maxwell Equation (1) is very often used to model the stress-relaxation data.

$$\frac{G(t)}{G_0} = \exp \left\{ -\left(\frac{t}{\tau^*} \right) \right\} \quad (1)$$

$G(t)/G_0$ is the normalized stress at relaxation time t and τ^* is a characteristic relaxation time. In this case, the relaxation time τ^* is taken for $G/G_0 = 1/e$. However, many studies showed that the Maxwell model is often inadequate to fit the stress-relaxation behavior of complex vitrimer systems (Martins et

al., 2023; Porath and Evans, 2021). Other models are more appropriate, such as generic Kohlraush-William-Watts (KWW) stretch exponential decay, which is now widespread, particularly for networks dissipating stress through plural relaxation modes. This model introduces an exponent β ($0 < \beta < 1$), indicating the distribution of relaxation times, a decreasing β value corresponding to a broader distribution (Li et al., 2018). For $\beta = 1$, KWW model reduces to a Maxwell model. In addition, this model can also be extended to take into consideration the presence of permanent (non-dynamic) linkages in mixed networks, by introducing the parameter G_{perm} , leading to the general Equation (2).

$$\frac{G(t)}{G_0} = \frac{G_{perm}}{G_0} + \left(1 - \frac{G_{perm}}{G_0}\right) \exp\left\{-\left(t/\tau^*\right)^\beta\right\} \quad (2)$$

For $G_{perm} = G_0$, the network is only composed of permanent linkages, whereas for $G_{perm} = 0$ it only contains dynamic bonds. τ^* and β are determined by fitting the experimental data. For KWW relaxation, the average relaxation time $\langle \tau \rangle$ is obtained by Equation (3).

$$\langle \tau \rangle = \frac{\tau^* \Gamma\left(\frac{1}{\beta}\right)}{\beta} \quad (3)$$

Other fitting models have also been introduced such as mono-exponential and delayed exponential evolutions (Jourdain et al., 2020). Moreover, Du Prez *et al.* (Lijsebetten et al., 2022) proposed a generalized Maxwell model to examine the contribution of distinct segments types as a separate Maxwell element following a single exponential decay.

However, many studies still determine τ^* as the time for which $G/G_0 = 1/e$, without ensuring that a Maxwell model adequately fit the data. It can lead to wrong estimates of time scales and incorrect values of the energy barrier for bond dissociation, as discussed recently (Martins et al., 2023). Small amplitude oscillatory shear (SAOS), eventually combined with time-temperature superpositions, can also be used to characterize the viscoelastic properties of CANs, and is particularly useful in the determination of short relaxation times (Taplan et al., 2020; Zhou et al., 2017).

The activation energy (E_a) required for macroscopic flow is calculated according to the Arrhenius Equation (4) by plotting $\ln \langle \tau \rangle = f(1000/T)$. Arrhenius behavior is observed for $T > T_v$, otherwise when $T < T_v$, the plot follows the Williams–Landel–Ferry’s (WLF), as for thermoset materials (Ferry, 1980; Perego et al., 2022).

$$\langle \tau \rangle = A \exp\left(\frac{-E_a}{RT}\right) \quad (4)$$

Although these models are principally applied to networks harboring associative bond exchanges, dissociative CANs have also been reported to exhibit similar stress relaxation processes (Konuray et al., 2023).

3.2. Dynamic bond chemistries

Chemical systems inducing these exceptional thermal behaviors were extensively explored in the last decade. Recent overviews focused on the diversity of dynamic chemistries, exploring the exchange reactions and their mechanistic profiles (Denissen et al., 2016; Zou et al., 2017; Chakma and Konkolewicz, 2019; Huang et al., 2020; Krishnakumar et al., 2020). This section is then limited to an examination and brief presentation of the dynamic covalent bonds employed in biobased aromatic CANs (Figure 1-3).

3.2.1. Systems based on transesterification

Since the pioneering work of Montarnal *et al.* (Hoppe *et al.*, 2005; Montarnal *et al.*, 2011), transesterification reactions have been extensively used in CANs architectures (Figure 1-3.1). The concept was demonstrated on networks formed by stoichiometric reaction between epoxies and carboxylic acids, in the presence of a transesterification catalyst. The resulting β -hydroxy ester bonds can rearrange thanks to the reaction between free hydroxyl groups and ester moieties. Other chemical routes can be considered to form ester bonds, such as epoxy/anhydride or hydroxyl/carboxylic acid, though the stoichiometry has to be adapted to ensure that free hydroxyl groups remain accessible in the network (Capelot *et al.*, 2012; Dusek and Matejka, 1984). Thermo-reversibility of the networks, governed by associative bond exchange reactions, is highly dependent on the temperature and catalyst (Lewis acids or bases such as triazabicyclodecene (TBD), 1,8-diazabicyclo[5.4.0]undec-7-ene (DBU), or tertiary amines) (Capelot *et al.*, 2012; Pan *et al.*, 2011). Stress-relaxations are generally investigated between 160 and 200 °C, and subsequent activation energies can vary from 25 to 155 kJ mol⁻¹ (Kumar and Connal, 2023).

The considerable diversity of available building blocks and the facile synthetic pathways make this chemistry appropriate for industrial applications. Thus, transesterifications are widely used in the preparation of vitrimers, as recently reviewed for biobased systems (Kumar and Connal, 2023).

3.2.2. Boronic esters and boroxines-based systems

Boron-based compounds can be employed to prepare different dynamic-covalent assemblies (Bapat *et al.*, 2011; Cromwell *et al.*, 2015). Boronic acids self-condensation can reversibly form dynamic six-membered boroxines (Figure 1-3.2. i) (Nishiyabu *et al.*, 2011). The equilibrium is then controlled by addition of water, catalysis of Lewis bases and temperature. Condensation of boronic acids with 1,2-diols in basic aqueous or in anhydrous organic media enable the formation of five-membered boronic esters, also called dioxaborolanes (Cash *et al.*, 2015). The synthesis of six-membered ring is also possible, although less stable, through the use of 1,3-diols. Different mechanistic profiles were described, mainly impacted by stoichiometry but also by environmental conditions such as humidity, pH and temperature (Kuhl *et al.*, 2015). Boronic esters undergo transesterification reactions in the presence of an excess of diols (Figure 1-3.2 ii). Metathesis reaction of dioxaborolanes in absence of free diols or water in the material is also possible, avoiding potential side reactions (Figure 1-3.2 iii) (Caffy and Nicolaÿ, 2019; Röttger *et al.*, 2017). Finally, linear boronic esters can be formed from the reaction of boric or boronic acids with alcohols (Figure 1-3.2. iv) (Porath *et al.*, 2022; Porath and Evans, 2021).

3.2.3. Imine-based systems

Imine dynamic chemistry is widely used in the synthesis of thermo-responsive materials. Imines are also referred as “Schiff bases” (Belowich and Stoddart, 2012). Three mechanisms of imine rearrangement were reported (Ciaccia and Stefano, 2014). Firstly, hydrolysis leads to the reversion of imine bond to the precursors amine and carbonyl groups (Figure 1-3.3. i). Secondly, transamination is reported in presence of an excess of amine moieties (Figure 1-3.3. ii). Finally, imine metathesis is observed between two imines (Figure 1-3.3. iii). Thus, by adjusting the structure of imine-based networks, materials can undergo swift bond exchange reactions at moderate temperatures and without catalyst. Fast relaxation and wide range of activation energies, from 10 to 130 kJ mol⁻¹, can easily be achieved (X.-L. Zhao *et al.*, 2022). Imines can also be triggered by UV light, enabling the photo-isomerization, and used as photo-switch in a polymer matrix (Vantomme and Lehn, 2014).

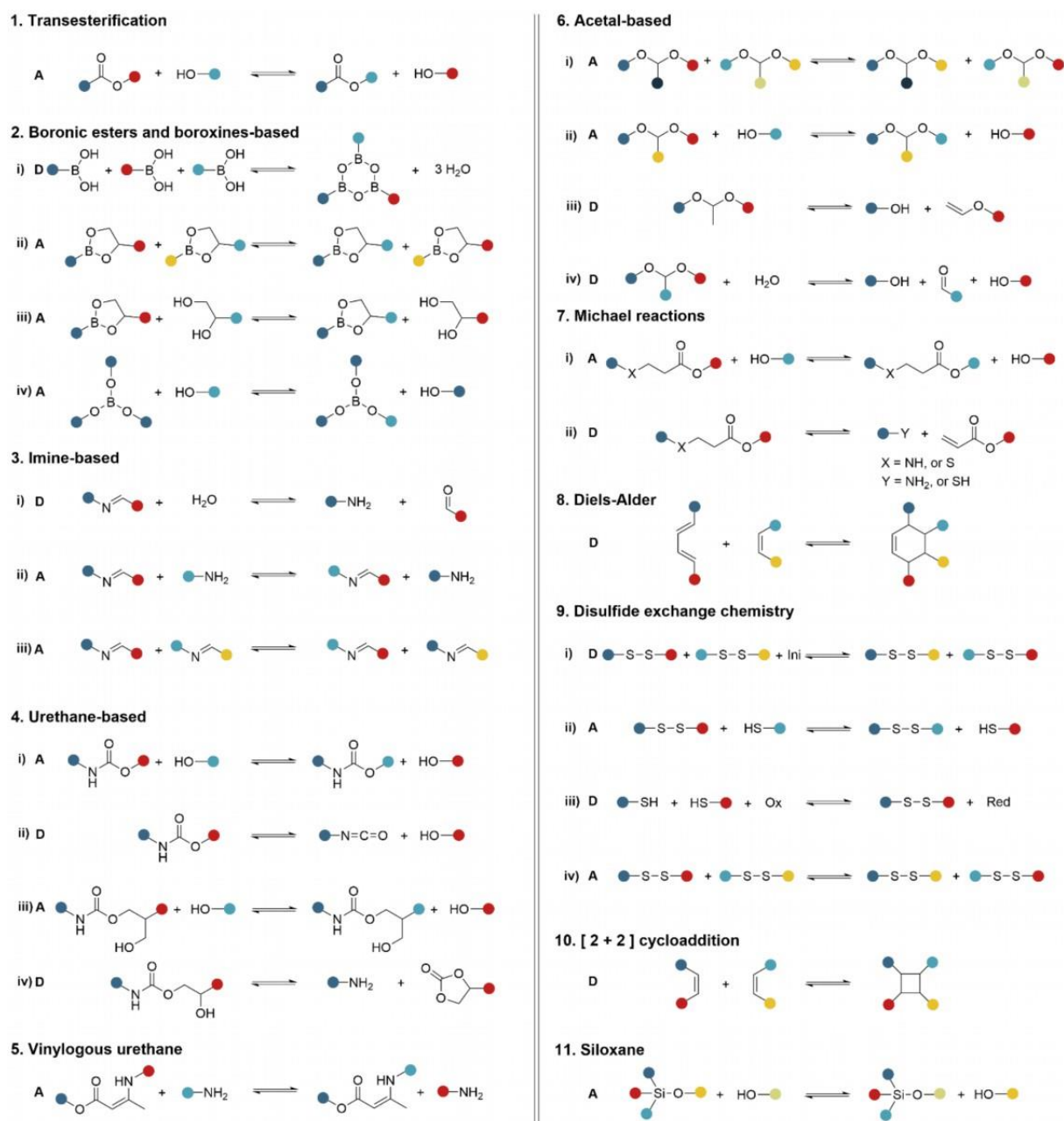


Figure 1-3. Dynamic covalent chemistries used in the elaboration of biobased aromatic CANs. A = associative mechanism. D = dissociative mechanism.

3.2.4. Urethane-based systems

Urethane-based polymers are traditionally obtained by polyaddition between polyols and polyisocyanates (Mouren and Avérous, 2023). Although stress-relaxation of crosslinked PU was already reported by Tobolsky (Offenbach and Tobolsky, 1956), thermo-reversibility of PU networks is very limited due to the sluggishness of transcarbamoylation reaction (Figure 1-3.4 i). On the other hand, the dissociative reaction of carbamate to alcohol and isocyanate can generate nocuous side reactions (Figure 1-3.4 ii). In average, dynamicity of the networks occurs over long stimulation periods and requires high temperatures (> 160 °C) as well as catalysts such as dibutyltin dilaurate (DBTL) (W. Liu et al., 2022). However, aromatic hydroxyls do favor the reversibility of urethane bonds. According to reactivity classification, thermal dissociation occurs at different temperature according to the chemical structures, such as alkyl-NCO/alkyl-OH (250 °C), aryl-NCO/alkyl-OH (200 °C), alkyl-NCO/aryl-OH (180 °C) and

aryl-NCO/aryl-OH (120 °C) (Simon et al., 1988). Phenol-carbamate are stable at room temperature but exhibit faster bond exchanges than aliphatic alcohol-based urethane, owing to electron delocalization (Nasar et al., 2004; Shi et al., 2019). Furthermore, transcarbamoylation reactions were found to be favored by the addition of nucleophilic hydroxyl groups to the carbamate moieties, through the development of polyhydroxyurethane (PHU) vitrimers derived from the reaction between cyclocarbonate and amines (Figure 1-3.4 iii) (Fortman et al., 2015). Dissociative network rearrangement can also occur through reversible cyclic carbonate aminolysis (Figure 1-3.4 iv) (Chen et al., 2017).

3.2.5. Systems based on vinylogous urethane

Denissen *et al.* (Denissen et al., 2015) recently introduced vitrimers based on vinylogous urethane (VU) chemistry as an alternative to transesterification reactions (Figure 1-3.5). Resulting from the condensation of acetoacetate and amine moieties, such networks undergo rearrangements through transamination reactions, with an excess of amines. Fast exchange rates are achieved in catalyst-free conditions, from 100 °C. The network dynamicity can be further accelerated under acidic conditions with the addition of small amount of *p*-toluene sulphonic acid (*p*TsOH), sulphuric acid (H₂SO₄) or DBTL, resulting in a shifted activation energy (Denissen et al., 2017). Several mechanistic profiles are involved. In neutral or slightly acidic condition, a protic iminium-pathway was found, involving an activated iminium intermediate with an activation barrier circa 70 kJ mol⁻¹. Whereas an aprotic Michael-type pathway occurs in presence of strong bases, leading to higher enthalpic barriers of about 100 to 140 kJ mol⁻¹ (Guerre et al., 2018). As an alternative to conventional acetoacetate-amine condensation, polyaddition reaction of alkyne esters and amines was demonstrated (Spiesschaert et al., 2021). This water-free pathway lessen the formation of defects induced by the formation of bubbles in cured samples (Guo et al., 2021).

3.2.6. Acetal-based systems

Reversible acetal chemistry is well-known by organic chemists, who took advantage of this dynamicity by using cyclic acetals as protecting groups in multi-steps syntheses (Brachvogel and von Delius, 2016). Acetal are commonly synthesized by acid-catalyzed reaction of hydroxyl groups with aldehydes, through the formation of a hemiacetal intermediate and release of water. They can also be prepared by water-free acid-catalyzed “click” addition between hydroxyl groups and vinyl-ether moieties (Li et al., 2019). Two bond exchange mechanisms are involved. An acetal metathesis is observed after introduction of a second acetal (Figure 1-3.6 i), and transacetalization is reported by introduction of free hydroxyl groups within the network (Figure 1-3.6 ii) (Cacciapaglia et al., 2005; Pemba and Miller, 2019). A dissociative mechanistic pathway of aromatic substituted acetal consisting of the cleavage of acetal into phenolic hydroxyl and vinyl ether was also reported (Figure 1-3.6 iii) (Q. Li et al., 2020). Finally, the dissociative acid-catalyzed hydrolysis of acetal into a hydroxyl and a formyl group is known for decades (Figure 1-3.6 iv) (Li et al., 2019; Cordes and Bull, 1974).

3.2.7. Systems based on Michael reaction

The Michael reaction alludes to the base-catalyzed addition of a nucleophile called Michael donor, to an activated α,β -unsaturated carbonyl-containing compound referred as Michael acceptor (Mather et al., 2006). The literature counts various types of Michael click additions, among which thiol-Michael and aza-Michael additions, revealed to be reversible. Thiol-Michael thermal reversibility was very early reported on adducts formed by the addition of mercaptans to conjugated systems of double bonds present in ketones, esters, and the like (Allen et al., 1964). Adducts can also be triggered in response to a pH stimulus (Shi and Greaney, 2005). Although aza-Michael adducts in bulk polymer systems were commonly considered not reversible, Du Prez and co-workers (Holloway et al., 2022; Stricker et al., 2022; Taplan et al., 2021) recently demonstrated the dynamic nature of this linkage through the preparation of β -amino esters. Materials synthesized from the reaction between acrylic and amine functionalities have demonstrated to combine both associative and dissociative rearrangement

mechanisms through transesterification (Figure 1-3.7 i) and retro aza-Michael reactions (Figure 1-3.7 ii), respectively (Berne et al., 2022a). The dual mechanisms impart attractive and robust properties to the networks, as well as a remarkable creep resistance.

3.2.8. Systems based on Diels-Alder

Diels-Alder (DA) is an old and ubiquitous reaction occurring between an electron-deficient dienophile and an electron-rich conjugated diene to form a cyclohexene adduct (Figure 1-3.8). The reaction is defined as “click” [4 + 2] cycloaddition in virtue of its outstanding efficiency at moderate temperatures (below 90 °C) and selectivity. The retro-DA essentially takes place between 110 and 130 °C (Boul et al., 2005). Since the pioneering work of Wudl and co-workers (Chen et al., 2002), who demonstrated the self-healing ability of polymers based on reversible DA, the dissociative bond was integrated in a plethora of polymer matrices, mostly using the furan/maleimide reaction (Gandini, 2013), such as for instance PUs (Tremblay-Parrado et al., 2020; Tremblay-Parrado and Avérous, 2020b), polyesters (Sridhar et al., 2020; Zeng et al., 2013), and polymethacrylates (García-Astrain et al., 2013).

3.2.9. Systems based on disulfide exchange

Disulfide linkage was extensively studied by the scientific community for decades (Takahashi and Tobolsky, 1971; Tobolsky et al., 1964), and its reversible character was already exploited in epoxy resins in the early 1990s (Sastri and Tesoro, 1990; Tesoro and Sastri, 1990). Since then, a lot of research has been conducted to understand the complex mechanisms involved in disulfide exchange, governed by the reaction conditions. Depending on the stimulus, such as temperature, UV-light and pH, four chemical pathways are invoked. Radical pathway is induced by homolytic cleavage of S–S bond by a sulfur containing radical generated by light or by the addition of a radical initiator, followed by radical transfer and crossovers (Figure 1-3.9 i) (Banchereau et al., 1995; Fairbanks et al., 2011). Anionic pathway occurs in basic conditions, a generated thiolate anion attacks and cleaves heterolytically the disulfide bond, releasing a thiolate from the original disulfide bond (Figure 1-3.9 ii) (Black et al., 2014). Reduction-oxidation pathway results from the oxidation of thiols into disulfide using weak oxidants such as Fe³⁺, salts, atmospheric oxygen, or halogens, which can be subsequently reduced again (Figure 1-3.9 iii) (Sastri and Tesoro, 1990). Finally, disulfide metathesis is observed upon introduction of a second disulfide (Figure 1-3.9 iv) (Rekondo et al., 2014). Disulfide bond exchange is one of the most used chemistry in the preparation of self-healing materials by virtue of its swift exchanges in the network in mild conditions and even at room temperature with aromatic disulfide (Rekondo et al., 2014).

3.2.10. Systems based on [2 + 2] cycloaddition

Photo-dimerization occurring through a [2 + 2] cycloaddition is a reversible mechanism triggered under thermal, photochemical and microwave induced conditions. Starting from alkenes or alkynes, cyclobutane and cyclobutene skeletons dimer are formed in a single step (Figure 1-3.10). [2 + 2] cycloaddition induced by UV light under exposure to a certain wavelength is widely used in the synthesis of photo-crosslinkable and shape memory polymers (Kaur et al., 2014; Li et al., 2012). Although the efficiency of these systems as CANs is sometimes questioned due to limited penetration depth of the UV radiation in the materials leading to restrained recovery, this approach interestingly follows green chemistry principles by allowing crosslinking in bulk, without catalyst and solvents.

3.2.11. Systems based on siloxane exchange

The first report of siloxane dynamic chemistry was published in the 1950s by Grubb and co-workers (Osthoft et al., 1954), demonstrated with the relaxation of silicone rubbers. Later Si–O exchanges were reintroduced for the design of self-healing silicone rubber (Zheng and McCarthy, 2012). Exchange reactions can be catalyzed by acids or bases (Figure 1-3.11). Although mechanistic pathways still remain unclear and require further investigations, base-catalyzed rearrangements are supposed to

undergo an associative trans-siloxanation mechanism (Schmolke et al., 2015), whereas acid-catalyzed mechanistic pathway was hypothesized to involve silyl ether metathesis (Tretbar et al., 2019).

4. BIOBASED AROMATIC CANS

4.1. Sources of renewable aromatic structures

This section identifies the main biobased and aromatic building blocks in the toolboxes of today's chemists to develop high-performance and innovative materials integrated into a circular bioeconomy. An overview of the availability, chemical structures of the different aromatic renewable architectures is provided.

4.1.1. Lignins and derivatives

Lignins are the second most abundant renewable resources on Earth and constitute the first sources of renewable aromatic units (Laurichesse and Avérous, 2014). They are a fraction of lignocellulosic biomass, with cellulose and hemicellulose, and represent up to 40% of the dry weight of feedstock. Lignin is mainly found in the cell walls, adding structure and protection against chemical and biological stresses. Nowadays, it is essentially a by-product of pulp and paper industry as well as second-generation bioethanol production. Lignin is naturally present in lignocellulosic plants amounts to 300,000 Mt with a compound annual growth rate (CAGR) around 7% (Dessbesell et al., 2020). The annual worldwide production of technical lignin, defined as lignin isolated after a series of biomass processing steps in industrial conditions (Souto and Calado, 2022), was estimated around 100 Mt in 2015, with a CAGR expected to reach 2.2% by 2025 (Bajwa et al., 2019).

The structure of lignin is highly depend on the botanical origin and the extraction process (Tribot et al., 2019). The complex amorphous structure of lignins results from the polymerization of three main aromatic alcohols precursors called monolignols: coniferyl alcohol (G), sinapyl alcohol (S), and p-coumaryl alcohol (H). Other aromatic compounds, such as flavonoids, hydroxystilbenes, and hydroxycinnamic amides, can also be encountered as minor lignin monomers in some plants (del Río et al., 2020). Lignification, the biosynthesis of lignin, relies on the oxidative combinatorial-like coupling reactions between monolignols, via peroxidase and/or laccase generated radicals (Ralph et al., 2004; Vanholme et al., 2010). Lignin monomers are combined through numerous characteristic inter-units linkages: ether bonds (β -O-4, α -O-4, 4-O-5), carbon-carbon bonds (β - β , β -5, β -1) and other complex structures connecting three monomeric units (dibenzodioxocin) (Duval and Lawoko, 2014). Lignin presents various reactive functional sites, including hydroxyl, methoxyl, carbonyl, and carboxyl groups, offering plenty of opportunities for chemical modifications (Laurichesse and Avérous, 2014).

Lignin can be recovered from lignocellulosic biomass through different isolation processes. Chemical isolation methods rely on the solubilization of lignin, through its fragmentation into lower molar mass residues, which can however recombine later. Lignin is usually recovered by precipitation and filtration. The main processes for lignin isolation are sulfite (leading to lignosulfonates), Kraft (sodium hydroxide (NaOH) and sodium sulfide), Soda (NaOH) and Organosolv (aqueous organic solvents, usually catalyzed by acids). Lignin can also be recovered from physical, physico-chemical, and biological treatments (Eraghi Kazzaz and Fatehi, 2020).

Depolymerization of isolated lignin enables the formation of a wide variety of low molar mass high-value phenolic compounds, which can easily be integrated in the preparation of performing polymers. Several depolymerization methods have been developed, such as oxidation, hydrogenation, microbial conversion, pyrolysis, gasification, and hydrolysis. However, for most methods relying on the cleavage of inter-unit ether bonds, the yield of aromatic monomers is directly correlated to the content of β -O-4 bonds of isolated lignin. The extent of depolymerization is thus limited by the fractionation

method employed and its severity, as well as the biomass feedstock (Schutyser et al., 2018; Sun et al., 2018).

To overcome these limitations, alternative biorefinery processes are being developed to isolate lignin with high β -O-4 content, or to combine lignin isolation and depolymerization in a single step. In contrast to the carbohydrate-oriented traditional lignocellulosic biorefinery, “lignin-first” fractionation is an emerging paradigm regarding lignin as one of the primary targets (Renders et al., 2017).

Many aromatic compounds can be obtained from lignin depolymerization, among which 4-hydroxybenzaldehyde, syringic and vanillic acids, guaiacol or phenol (Ludmila et al., 2015; Wahyudiono et al., 2008), as recently reviewed (Sun et al., 2018). The vanillin case is particular. Although it can be produced by oxidation of liginosulfonates, mostly commercialized by Borregaard (Fache et al., 2015), 85 to 90% of the synthetic vanillin used today is derived from fossil-based intermediates (Hocking, 1997; Rinaldi et al., 2016; Rodrigues Pinto et al., 2012). The production of vanillin from lignin was extensively discussed in a review (Fache et al., 2016). Example of lignin structure as well as lignin-based phenolic monomers used in the preparation of CANs are illustrated in Figure 1-4.

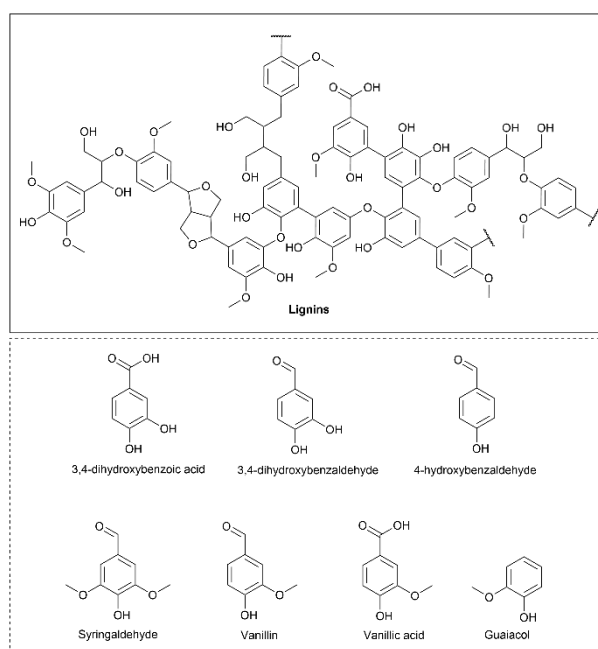


Figure 1-4. From top to bottom: A structural model of hardwood lignin and some aromatic compounds derived from lignins.

4.1.2. Tannins and derivatives

After lignins, tannins are the second most abundant renewable aromatic compounds. In 2017, worldwide market was estimated to 1.1 Mt, with a CAGR of 6.7 % by 2025 (Pagliaro et al., 2021). Tannins are widely distributed in plants. Their abundance and structure varies depending on the botanical origin, environment and seasonal variations, or position in the plant (Frutos et al., 2004). Nowadays, tannins are described as water-soluble polyphenols of average molar masses between 500 and 3000 g mol⁻¹ (Arbenz and Avérous, 2015). These phenolic compounds are classified as hydrolysable or condensed tannins depending on their chemical structures. Hydrolysable tannins, often called tannic acid, include gallotannins and ellagitannins resulting from the esterification reaction between a phenolic acid or polyphenolic acid and a polyol, typically a carbohydrate. After acid hydrolysis, gallic acid, digallic acid and derivatives or ellagic acid can be recovered (Frutos et al., 2004). Condensed tannins on the other hand are stable towards hydrolysis. They are derived from the oligomerization of 3 to 8

CHAPITRE 1

flavonoid units (flavan-3-ol, flavan-3,4-diol, and other analogues). The non-phenolic part is composed of carbohydrates, imino acids, and amino acids (Pizzi, 2019).

Finally, complex tannins are a mixture of monomeric units of hydrolysable and condensed tannins (Hatano et al., 1991). From condensed tannins, high-value aromatic chemicals can be extracted or generated for instance by pyrolysis, such as catechol (Pinto et al., 2018). Flavonoids (Yazaki, 2015), phloroglucinol (Ford et al., 2019; Shrestha et al., 2021), and resorcinol are structures of interest in tannins (Pizzi and Daling, 1980). The main structures derived from tannins are illustrated in Figure 1-5.

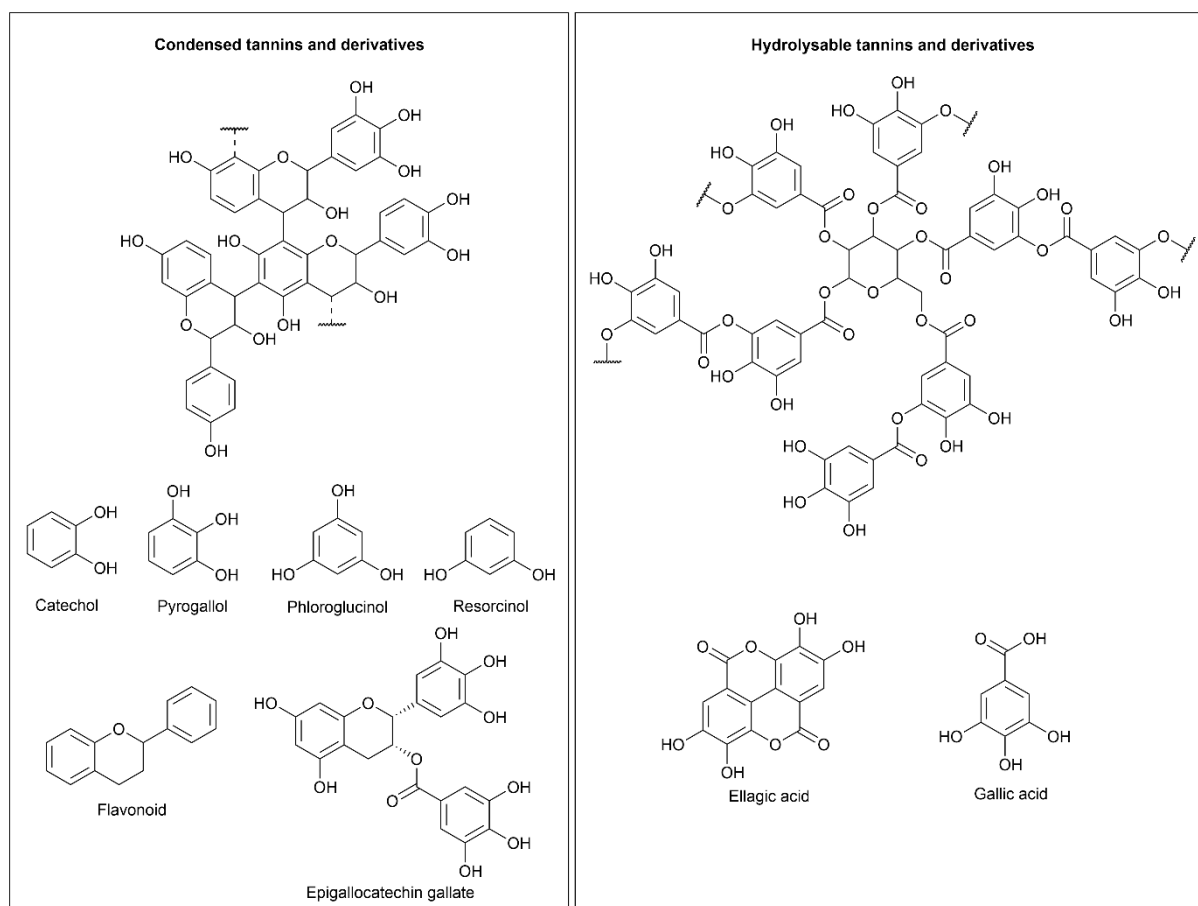


Figure 1-5. Some aromatic compounds derived from condensed or hydrolysable tannins.

Some reviews bring complementary information on the chemical structures and modifications, extraction processes, and valorization into biobased macromolecular architectures (Arbenz and Avérous, 2015; de Hoyos-Martínez et al., 2019).

4.1.3. Cashew nutshell liquid

Cashew (*Anacardium occidentale L.*) is a tropical evergreen tree, essentially cultivated in Africa, Asia and South America (Candolle, 1885). Cashew tree produce an edible pseudocarp also called “apple” and a fruit, cashew nut, representing the commercial product of the plantation. Cashew nuts are composed of 35 to 45 %wt of kernel and 55 to 65 %wt of shells. The shells, which constitute a considerable amount of agro-wastes (Statista, 2021), contain 30 to 35% of a brownish liquid commonly named cashew nutshell liquid (CNSL) (Mubofu and Mgaya, 2018). CNSL is composed of anacardic acid, cardanol, cardol and 2-methylcardol, which proportions vary depending on the extraction process (Figure 1-6) (Gedam and Sampathkumaran, 1986). Natural and technical CNSL can be distinguished.

CHAPITRE 1

The former is extracted either with cold solvents or by mechanical extraction and contains 60 to 65% of anacardic acid, 15 to 20% of cardol, around 10% of cardanol and some traces of 2-methylcardol. Upon heating, anacardic acid is decarboxylated resulting in technical CNSL essentially composed of 60 to 65% of cardanol, 15 to 20% of cardol, 10% of polymeric material, and traces of 2-methylcardol (Phani Kumar et al., 2002).

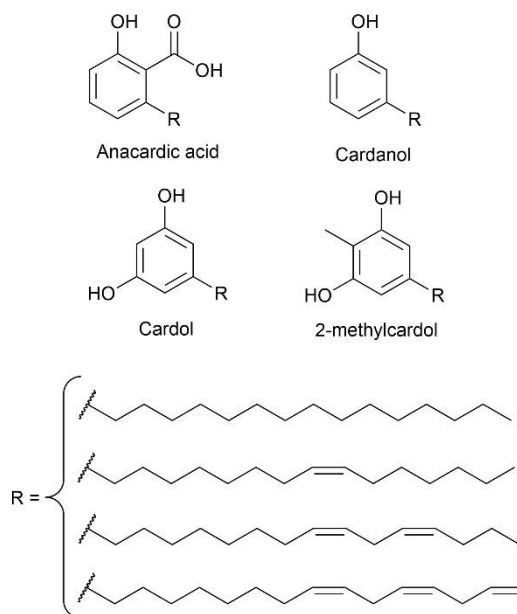


Figure 1-6. Chemical structures and composition of CNSL.

Cardanol is the most valorized compound extracted from CNSL. Its C15 hydrocarbon chains contain up to three double bonds per molecule, with approximately 8% of saturated chains, 47% monoene, 16% of diene, and 29% of triene (Sultania et al., 2011). Its various reactive sites makes it a suitable building block for several chemical modifications and polymerization (Caillol, 2023, 2018). For a more in-depth discussion on CNSL extraction processes and valorization, the readers can refer to a recent review (Mgaya et al., 2019).

4.1.4. Furan and derivatives

Furan and derivatives are attractive platform molecules for the preparation of high-value biobased aromatic polymers, biofuels or solvents (Figure 1-7) (Moreau et al., 2004; Xu et al., 2016). Furans are obtained through the catalytic transformation of sugars, typically pentoses and hexoses. For instance, D-fructose and glucose are economical and easily accessible renewable resources, thus suitable candidates as chemical feedstocks. Modification of carbohydrates into furans occurs through numerous steps: dehydration, hydrolysis, isomerization, reforming, aldol condensation, hydrogenation and oxidation (Tong et al., 2010). Numerous monomers of interest can be obtained, such as furfural, 5-(hydroxymethyl)furfural (HMF), 2,5-furandicarboxylic acid (FDCA), or 2,5-dimethylfuran (2,5-DMF). Among these structures, furfural and HMF are industrial commodities capable of being converted into a vast array of useful monomers (John et al., 2019). HMF is often regarded as one of the most promising biobased platform molecule (Galkin and Ananikov, 2019; van Putten et al., 2013). Its controlled oxidation can lead to 2,5 furandicarboxyaldehyde (Chatterjee et al., 2017; Jiang et al., 2019; Kisszekelyi et al., 2020; Nie et al., 2013), while FDCA and 2,5-bis(hydroxymethyl)furan are obtained respectively by oxidation and hydrogenation.

Biocatalysis has also proven to be efficient and environmentally friendly alternative in the production of furans, with milder synthesis conditions and excellent selectivity (Lalanne et al., 2021).

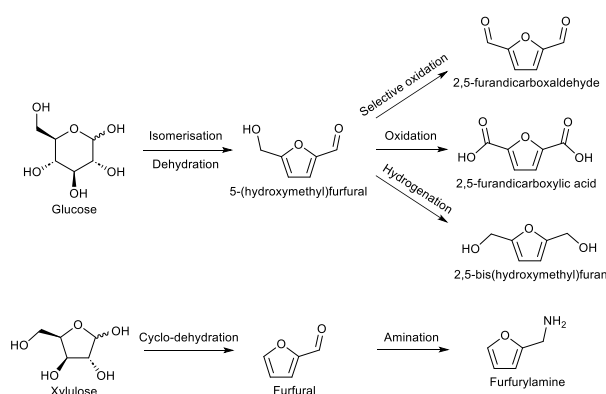


Figure 1-7. Some furan-derived building blocks for the synthesis of CANs.

4.1.5. Other phenolic building blocks

All the structures of the phenolic compounds mentioned in this chapter are displayed in Figure 1-8. Eugenol is a phytochemical bioactive compound. It was first extracted from leaves, buds and stems of cloves (*Eugenia caryophyllata*) essential oils containing from 70 to 90% eugenol, but is also present in nutmeg oil, cinnamon extract and other plants (Ahmed Khalil et al., 2017). Annually, approximately 6000 tons of clove essential oil are extracted (Danthu et al., 2020), and its CAGR is expected to reach 8% growth by 2025 (Lucintel, 2021). Numerous extraction processes can be employed, including solvent extraction, hydro-distillation, micro-wave assisted extraction, supercritical CO₂ extraction and ultrasound-based extraction. Eugenol can also be recovered from depolymerization of lignin (Molina-Gutiérrez et al., 2019). Its structure present four reactive sites, including an aromatic ring, phenolic hydroxyl group, allylic double bond and methoxy group, providing various functional modifications sites and possible polymerization reactions (Morales-Cerrada et al., 2021).

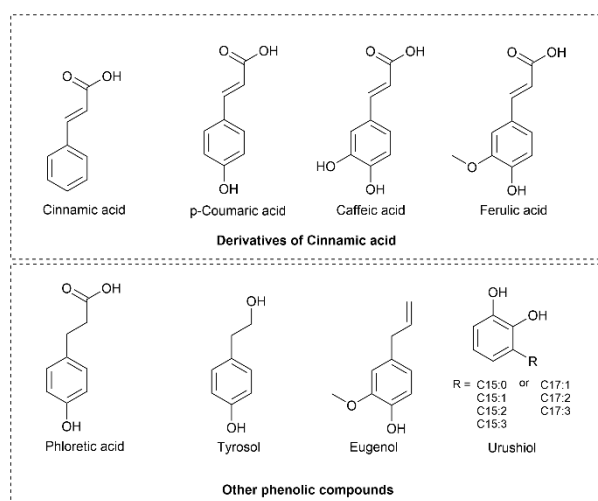


Figure 1-8. Structures of other biobased phenolic building blocks.

p-Hydroxycinnamic acid derivatives such as coumaric, ferulic and caffeic acids are naturally occurring phenolic compounds involved in the biosynthesis of lignin (Emiliani et al., 2009). Their corresponding esters are produced by plants, to connect hemicellulose with lignin in the cell wall, providing them resistance, and protection against oxidative stresses and solar radiations. Hydroxycinnamic acid have been reported to have therapeutic properties such as anticancer (Rocha et al., 2012), antidiabetic (Adisakwattana et al., 2008), anti-inflammatory activities (Nagasaka et al., 2007), and other properties making them compounds of interest in cosmeceutical fields (Taofiq et al., 2017).

They can be extracted from agricultural byproducts, such as mustard seeds, mostly using water/alcohol extractions. Production by microorganisms engineering is currently being developed, although modest caffeic and ferulic acids productivities were reported (Flourat et al., 2021). It is worth mentioning that biobased vanillin can be produced via the conversion of ferulic acid through fermentation, increasing the demand for this compound.

Other phenolic compounds are widely produced from annual plants such as tyrosol in olive leaves (Romero and Brenes, 2012; Ruiz et al., 2017), phloretic acid in apple tree leaves (Picinelli et al., 1995), and resveratrol in several parts of the vine and in wine (Celotti et al., 1996). Urushiol is an abundant natural catechol derivative mainly present in lacquer tree, poison ivy or poison oak (Fan et al., 2020; Symes and Dawson, 1954). Its structure presents long unsaturated alkyl side chains with catechol chain end (Symes and Dawson, 1953). However, urushiol is well-known for its allergen and skin sensitizing properties which have been extensively documented for decades (Murphy et al., 1983).

4.2. Aromatic building blocks in CANs

This section surveys the integration of biobased and aromatic architectures within CANs. For each chemical structures and the corresponding macromolecular architectures, a table summarizing the main stress-relaxation parameters, physical and chemical recycling conditions is proposed.

4.2.1. Lignins and lignin-derived monomers

Lignins

Almost a decade ago, Duval *et al.* (Duval et al., 2015) pioneered the field of lignin-based CANs by leveraging of the dissociative furan-maleimide Diels-Alder reaction (Table 1-1 and Figure 1-9). Two kraft lignin (KL) derived precursors were synthesized. Maleimide moieties were incorporated via esterification of aliphatic and phenolic hydroxyls with 6-maleimidoheptanoic acid (Figure 1-9a), while furan groups were introduced by glycidylation of phenolic hydroxyls with furfuryl glycidyl ether (Figure 1-9b). Both functionalized lignins were combined to prepare a crosslinked adduct reversible upon heating at 120 °C, highlighting the potential of this chemistry for the development of recyclable lignin-based networks. Subsequently, this concept was further studied through the preparation of thermo-reversible materials from maleimide-functionalized soda lignin (SL) (Figure 1-9a) and furan bearing crosslinkers obtained by the reaction between furfuryl glycidyl ether and thiols (Buono et al., 2017). Thermo-mechanical properties were adjusted by varying the functionality of both precursors. Through retro Diels-Alder reaction, the network was successfully reprocessed via compression molding. The recovery of mechanical properties through several reprocessing cycles of a Diels-Alder network prepared from furan-bearing lignin (Figure 1-9b) and furan functional polyether with a bismaleimide was investigated (Thys et al., 2021). The networks with lignin contents up to 29 wt % showed excellent properties recovery, with reprocessing efficiencies of 100%. Recently, the preparation of reversible elastomers (up to 28.7 wt% lignin content) containing Diels-Alder bonds from fractionated and partially modified KL with furan groups was reported (Thys et al., 2023b, 2023a). The system could be used as a >90% biobased, nontoxic, and easy to apply superglue.

Zhang *et al.* (Zhang et al., 2018) synthesized the very first lignin-based vitrimer, based on epoxy chemistry. KL was modified by ozonation to introduce carboxylic acid moieties (Figure 1-9c) that were further reacted with a sebacic acid-derived diepoxy monomer in the presence of zinc acetylacetonate hydrate to obtain high T_g materials (95 to 133 °C). Since then, the search for lignin-based recyclable alternatives to epoxy resins continued to arouse interest. Similarly, carboxylic acid functionalized lignins (Figure 1-9c and d) were reacted, in presence of a zinc catalyst with poly(ethylene glycol) (PEG) diglycidyl ether to prepare high-lignin content epoxy vitrimers (>47 wt%, and <50 wt% in the two respective studies) (Hao et al., 2019; More et al., 2023). The reverse strategy for the design of epoxy vitrimers with up to 70 wt% of lignin content consists of introducing epoxy groups on lignin via reaction

with epichlorohydrin and reacting this precursor with a dicarboxylic acid such as sebacic acid (Tang et al., 2022). The reaction of a mixture of lignin-epoxy macromonomer (Figure 1-9e) with diglycidyl ether bisphenol A and dodecanedioic acid or 1,2,3-propanetricarboxylic acid was also reported (Xue et al., 2021), as well as the blending with PEG bis(carboxymethyl) ether (Zheng et al., 2023). The combination of epoxy functionalized (Figure 1-9e) and carboxylic acid functionalized lignin-derived precursors (Figure 1-9f) was considered as well (Du et al., 2022; Song et al., 2023). To provide the network with flexible chains, PEG 400 was added to the synthesis.

Shape memory materials containing dynamic ester bonds were prepared in one-step from unmodified enzymatic hydrolysis lignin (20 to 40 wt%), itaconic acid and 1,12-dodecanediol (X. Jin et al., 2023). T_g between 21.2 and 157.3 °C were observed. Maximum tensile strength of 46.9 MPa was achieved for the material containing 30 wt% of lignin whereas a maximal elongation a break of 93.7% was obtained for 20 wt% of lignin. Although the vitrimer behavior was not examined, it is worth mentioning the straightforward and facile synthesis, and the recycling potential of the materials presented in this work. Based on transesterification exchanges, the synthesis of CANs from methacrylated dealkaline lignin (DL) (Figure 1-9g) and vanillin, epoxidized soybean oil and PEG dithiol in the presence of a zinc catalyst was reported (Johnson et al., 2023). The series of materials with 70 wt% biobased content exhibited self-healing when subjected to a scratch. Benzoxazine precursors were prepared through esterification of soda lignin with 3-(p-Hydroxyphenyl)propionic acid, also known as phloretic acid, followed by the Mannich-like ring closure reaction with a primary amine (Figure 1-9h) (Adjaoud et al., 2023). The selection of the primary amine structure enabled fine tuning of the features of the benzoxazine precursors. Only the network prepared with mono-ethanolamine presented a vitrimer behavior, owing to the simultaneous presence of free OH groups, esters and tertiary amines moieties. Mechanical properties were retained after five physical recycling steps. Besides, chemical recycling was successfully demonstrated after immersion in 1 M NaOH due to saponification of the ester bond.

Sougrati *et al.* (Sougrati et al., 2023) recently developed vinylogous urethane-based vitrimers from lignin using green chemistry and solvent-free approach. Liquid polyols were synthesized by oxyalkylation with ethylene carbonate of organosolv lignin in the presence of PEGs of different chain length. The polyols were then acetoacetylated using *tert*-butyl acetoacetate yielding low viscosity polyacetoacetates (Figure 1-9i). The series of macromonomers were cured with hexamethylene diamine to obtain the final vitrimers. Networks exhibited fast relaxation and activation energies values in accordance with the previously reported values for vinylogous urethane CANs. No major loss of mechanical properties was observed after the second reprocessing step, while chemical recycling potential and healing ability were successfully demonstrated after immersion in *n*-octylamine. Subsequently, the direct modification of soda lignin with *tert*-butyl acetoacetate (Figure 1-9i) which was condensed with a mixture of 1,10-diaminodecane and of a branched diamine derived from fatty acid dimer (Priamine™ 1075, a registered trademark of Croda) was reported (Liu et al., 2024).

Dynamic PU elastomers undergoing transcarbamoylation rearrangements, in combination with hydrogen bonding, were prepared from enzymatic hydrolysis lignin (Figure 1-9j) (Liu et al., 2019). Isocyanate-terminated prepolymers were synthesized from the addition reaction of polytetramethylene ether glycol with hexamethylene diisocyanate in presence of dibutyltin dilaurate, then lignin was added with molar ratio of NCO/OH kept at 1.2. The introduction of lignin in higher content significantly improved the strength and toughness of the elastomers, but on the other hand slowed down the relaxation process. Moreover, owing to the hydrogen bonds between lignin and the PU matrix, orientation of the chain segments resulting in strain-induced crystallization was observed. The authors mention transcarbamoylation reactions to drive the materials dynamicity. However, with the NCO/OH used, there should not be free OH groups in the network. Besides, the dynamicity is suspected to rather result from dissociative mechanisms involving the cleavage of the phenyl-carbamate bonds into phenols and isocyanates. PU-based CANs containing up to 50% of lignin content using a similar synthetic pathway (Figure 1-9j) were reported (Ma et al., 2023a, 2023b). However, in this case the low NCO/OH ratio (NCO/OH < 1.0) ensures the presence of free hydroxyls in the network, which can induce associative

exchange via transcarbamylation. Free hydroxyls also participated in the formation of coordination sacrificial bonds dissipating energy induced by applying external forces, resulting in significantly improved mechanical properties of the materials (Ma et al., 2023a). Thus, in a second study, low isocyanate index were used in the synthetic pathway to increase the properties while maintaining good reprocessing ability. Closed-loop recycling was successfully achieved through dissolution of the CANs in ethanol, recovery of the precursor after ethanol evaporation, followed by a final hot-press remolding step.

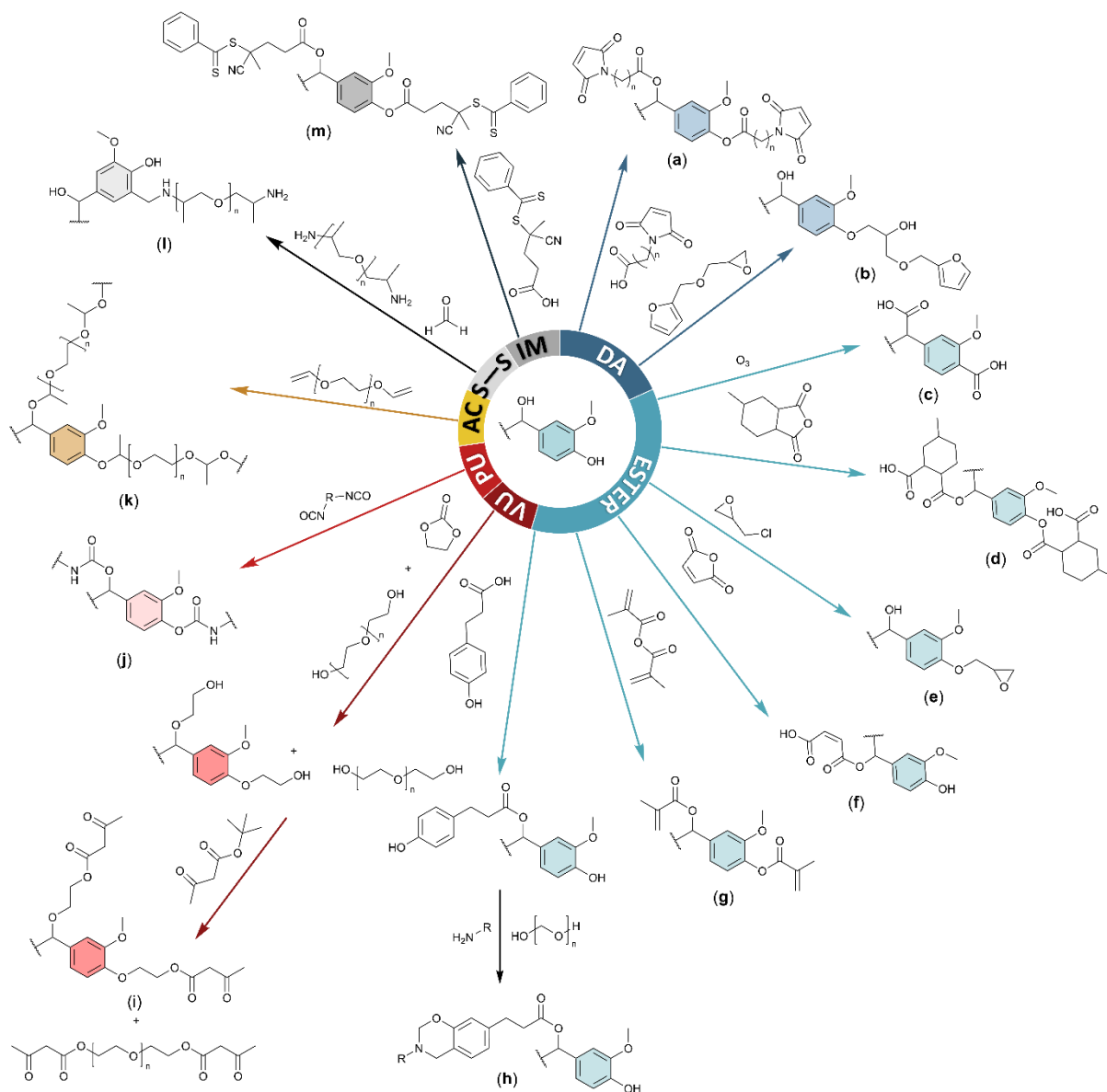


Figure 1-9. Presentation of most lignin chemical modifications into precursors used in the synthesis of various types of CANs. With DA= Diels-Alder, VU= vinylogous urethane, PU= polyurethane, AC= acetal, S-S= disulfide.

Acetal lignin-based vitrimer were prepared through the one-pot and catalyst free “click” addition of softwood kraft lignin to PEG divinyl ether (Figure 1-9k) (Moreno et al., 2021). The atom-efficient and easily scalable synthetic pathway enables facile tuning of the mechanical properties. Moreover, it was found that increasing the lignin content from 28 to 50 wt % enabled faster stress-relaxation (from

CHAPITRE 1

2500 s to 77 s) owing to a higher concentration of free hydroxyl groups promoting the transacetalization mechanism.

Polyurea self-healing network containing disulfide reversible bonds were also synthesized. An isocyanate-terminated prepolymer was prepared from polyetheramine and isophorone diisocyanate (W. Liu et al., 2020). The prepolymer was mixed with a disulfide-containing chain extender and lignin previously grafted with polyetheramine via Mannich reaction (Figure 1-9l). Excellent self-healing originating from the aromatic disulfide bonds exchanges enabled the recovery of 78.2% of the pristine tensile strength after 60 minutes at room temperature.

Grafting-from reversible addition-fragmentation chain-transfer (RAFT) polymerization was used as a complement of imine condensation for the synthesis of lignin-based self-healing, antifungal and conductive adhesives (Gao et al., 2020). Lignin-based macroinitiator was prepared by esterification with the carboxylic acid groups of the RAFT agent (Figure 1-9m), and was reacted with vanillin methacrylate and lauryl methacrylate through RAFT polymerization. Then, structurally modified lignin was cured with different diamine crosslinkers, to obtain the final dual networks. Reprocessing was performed using mild conditions (80 °C and 1 MPa) and after the fifth cycle up to 78.7% and 48.7% of the modulus and tensile strength were recovered, reaching around 2.4 and 1.0 MPa.

Table 1-1. Main stress-relaxation, physical and chemical recycling parameters of lignin-based CANs.

Biomass	Dynamic linkage	E_a (kJ mol ⁻¹)	τ	Physical recycling conditions ^a	Chemical recycling conditions	Ref.
KL	Diels-Alder	n/a	n/a	n/a	120 °C, 6 h	(Duval et al., 2015)
SL	Diels-Alder	n/a	n/a	130 °C, 7 metric tons, 30 min	n/a	(Buono et al., 2017)
KL	Diels-Alder	n/a	20 – 70 s at 90 °C ^b	120 °C, –, 45 min	CHCl ₃ , 55 °C, 5 days	(Thys et al., 2021)
KL	Ester	n/a	81 – 1290 s at 200 °C	190 °C, –, 2 h	n/a	(Zhang et al., 2018)
KL	Ester	54.4	720 – 2000 s at 200 °C	n/a	n/a	(Hao et al., 2019)
KL	Ester	n/a	<0.1 s at RT ^b	n/a	n/a	(More et al., 2023)
EL	Ester	n/a	n/a	160 °C, 5 MPa, 24 h	n/a	(Tang et al., 2022)
EL	Ester	n/a	1570 – 4374 s at 160 °C	160 °C, 10 MPa, 1 h	n/a	(Xue et al., 2021)
KL	Ester	n/a	n/a	150 °C, –, 2 h	n/a	(Zheng et al., 2023)
EL	Ester	18.1	>1000 s at 220 °C ^b	160 °C, 4 MPa, 15 min	Excess ethylene glycol, 190 °C, 12 h	(Du et al., 2022)
EL	Ester	97.2	>1000 s at 220 °C ^b	180 °C, no pressure, –	n/a	(Song et al., 2023)
DL	Ester	n/a	n/a	140 °C, 2 metric tons, 4 h	n/a	(Johnson et al., 2023)
SL	Ester	181.0	233 s at 200 °C	175 °C, <10 Pa, 1 h	1 M NaOH, 25 °C, 2 h	(Adjaoud et al., 2023)
OSL	Vinylogous urethane	51.0 – 114.0	39 – 488 s at 140 °C	140 °C, 16 MPa, 20 min	Excess n-octylamine in DMF, 100 °C, 1 h	(Sougrati et al., 2023)
SL	Vinylogous urethane	133.5	104 s at 150 °C	170 °C, 40 bar, 30 min	n/a	(Liu et al., 2024)
EL	Urethane + hydrogen bonds	n/a	~5 s – 500 s at 160 °C ^b	160 °C, 5 MPa, 5 min	n/a	(Liu et al., 2019)
EL	Urethane	90.5 – 124.2	4.1 – 10.5 min at 180 °C	180 °C, 10 MPa, 1 h	n/a	(Ma et al., 2023a)
EL	Urethane	65.2 – 96.6	~5 – 50 s at 130 °C ^b	120 °C, 10 MPa, 10 min	Ethanol, 60 °C, 2 h	(Ma et al., 2023b)
KL	Acetal	77.0 – 204.0	77 – 2500 s at 180 °C	150 °C, –, 2 h	n/a	(Moreno et al., 2021)
EL	Disulfide	n/a	<5 s at 60 °C	170 °C, 0.17 MPa, 10 min	Ethanol, 25 °C, 3 h	(W. Liu et al., 2020)
EL	Imine	n/a	n/a	80 °C, 1 MPa, 10 min	n/a	(Gao et al., 2020)

^a conditions of physical recycling are given as follow: temperature, time, applied pressure or force. ^b graphical values.

To outline the current trends in the field of lignin-based dynamic networks, previously mentioned chemical modifications of lignin are illustrated in Figure 1-9. This compendium clearly highlights that lignin has proven to be a suitable building block for the preparation of CANs. Owing to the reactivity of its hydroxyl groups, ester-containing networks are easily prepared following one step chemical modification to graft reactive carboxylic acid or epoxy moieties. As summarized in Table 1-1, some studies achieved low relaxation times at 200 °C (81 or 233 s) (Adjaoud et al., 2023; Zhang et al., 2018), however relaxation times reported are often of 1000 s or more (Du et al., 2022; Song et al., 2023; Xue et al., 2021). Subsequently, temperatures between 140 and 180 °C are usually applied for several hours in order to physically recycle the materials. Given the relatively low thermal stability of lignin, such long exposure to high temperature is likely to generate side reactions, such as lignin condensations, which might limit the dynamic character of the materials by creating permanent carbon-carbon linkages.

Directly benefiting from the reactive phenolic hydroxyls of lignin, urethane-based networks do not require any lignin chemical modification, which can be advantageous for industrial scale-up for instance (Liu et al., 2019; Ma et al., 2023a, 2023b). However, the low reactivity of phenols with isocyanates imposes relatively long processing time for the network synthesis. In addition, the use of nocuous isocyanates is a drawback because of the health and safety issues during both the virgin material synthesis and the recycling step (dissociative reaction of carbamate to alcohol and isocyanate). This issue can be limited by tuning the NCO/OH ratio to have an excess of hydroxyls and favoring the transcaramoylation associative rearrangements. This way, relaxation times as low as 5 to 50 s can be achieved allowing reprocessing in mild conditions (10 min at 120 °C) (Ma et al., 2023b). Acetal chemistry revealed to be a relevant dynamic bond for valorization of lignin without prior chemical modification. Moreover, the facile one-pot synthetic pathway enabled easy tuning of the mechanical and rheological properties, making it one of the most straightforward and interesting approach (Moreno et al., 2021). A strategy to completely overcome the use of solvents in the synthesis of lignin-based VU networks was also proposed through the synthesis of liquid polyacetoacetates from lignin. With this approach, large-scale synthesis of the materials could be performed in a solvent-free process by employing mechanical stirring, owing to the low viscosity of the precursors (Sougrati et al., 2023). Fastest relaxations were achieved using DA (20 s at 90 °C) and disulfide (5 s at 50 °C) chemistries, allowing physical recycling at low temperatures (120-130 °C) (Buono et al., 2017; W. Liu et al., 2020; Thys et al., 2021). However, relaxation at low temperatures can be a disadvantage if rearrangement occur at room temperature, which could lead to materials creeping during their use. CANs are more prone to creep compared to traditional thermosets. In addition to being susceptible to primary creep associated to segmental chain mobility, dynamic networks are inclined to secondary creep arising from chain mobilization and network rearrangements, and tertiary creep associated with errors in bond exchanges creating permanent non-dynamic linkages, which is catalyst and temperature dependent (Hubbard et al., 2022b). To achieve highly dynamic but creep resistant materials chemical reactivity in low and high temperature regimes must be disconnected. A strategy is therefore to aim for a high activation energy.

A current shortcoming in the field is the lack of studies on chemical recycling, which could further upgrade the sustainability of lignin-based CANs by offering an alternative to thermomechanical recycling.

Vanillin

Owing to its high availability and chemical structure, extensive research was conducted on vanillin. Its aldehyde, phenol and methoxy reactive groups enable its integration into various dynamic networks (Table 1-2, Figure 1-10, Figure 1-11, and Figure 1-12). For concision purpose, this section on a very active field only discusses recent advances in vanillin-derived CANs over the last years. For an overview of older works, readers can refer to the following reviews providing a critical examination of vanillin-based CANs (Krishnakumar et al., 2022; Kumar and Connal, 2023; Lucherelli et al., 2022; Muhammad Abdur Rashid et al., 2023b; Vidil and Llevot, 2022).

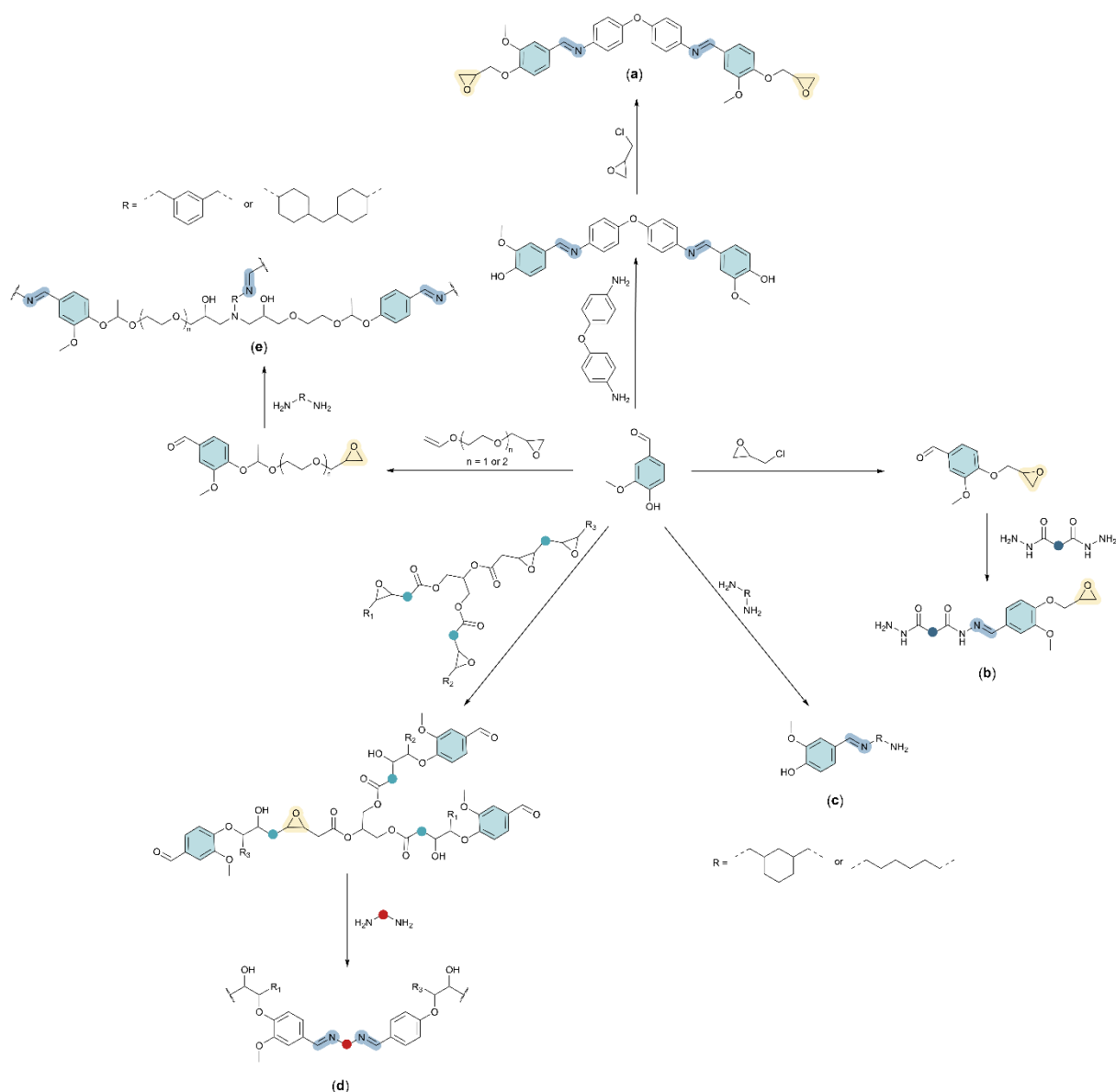


Figure 1-10. Vanillin as a chemical platform for the preparation of different poly(epoxy imine) networks.

In the context of substituting bisphenol A, an endocrine disrupting chemical widely used in the synthesis of epoxy resins (Czarny-Krzyminska et al., 2023), epoxy-amine networks derived from vanillin represent a significant area of research in the realm of CANs (Figure 1-10). Particularly, the preparation of epoxy-amine resins containing imine bonds was reported. Imine epoxy monomer was synthesized by condensation of vanillin with 4,4'-oxydianiline and further glycidylation with epichlorohydrin (Figure 1-10a), then cured with three polyether amines, produced under the commercial name of Jeffamine® by Huntsman (Roig et al., 2022a). Poly(acylhydrazone) vitrimers were developed in two sequential steps by condensing the aldehyde group of epoxydized vanillin with dihydrazide monomers at low temperature (Figure 1-10b), followed by the reaction of remaining hydrazine with epoxide (Roig et al., 2022b). Hardeners to cure epoxy resins of bisphenol-F and neopentyl glycol diglycidyl ether were synthesized from vanillin and syringaldehyde through condensation with bis-aminomethyl cyclohexane (Figure 1-10c) (Muhammad A. Rashid et al., 2023b). High T_g of 82 and 92 °C were obtained for the syringaldehyde and vanillin-based materials. This study was completed with the addition of a low viscosity co-curing agent (4-methyl-1,3-cyclohexendiamine) to the vanillin-derived imine containing hardener to avoid the use of solvent in the preparation of fully biobased and

high T_g materials (around 100 °C) (Muhammad Abdur Rashid et al., 2023a; Muhammad A. Rashid et al., 2023a). The reaction of vanillin with epoxidized soybean oil (ESO) to generate aldehyde-terminated ESO monomer (Figure 1-10d) was reported (F. Zhao et al., 2022). Through imine condensation of the monomer with aliphatic and aromatic diamines, a series of polyimine networks was prepared exhibiting physical and chemical recyclability, and weldability. Acetal containing poly(epoxy imine) networks were prepared from the reaction of vanillin with vinyl ethers, followed by oxirane opening of epoxy monomers with diamines (Figure 1-10e) (Türel and Tomović, 2023). Acid depolymerization of acetal and imines allowed the recovery of 92% of the vanillin, which was employed in the preparation of a new generation of epoxy networks, while the residual polyols generated from depolymerization were upcycled into PUs. Abetz and co-workers (Klein et al., 2023) expanded the knowledge of imine-containing vanillin vitrimers by examining the influence of the network design and composition on the resulting properties. Tough materials to highly flexible and elastomeric behaviors were obtained by increasing the chain length of the polyether di- and triamines used to cure two vanillin-based dialdehyde of different alkyl chain spacer. Topology rearrangement of the network could be accelerated without addition of catalyst, by simply varying the ratio of aldehyde to amine groups.

The incorporation within materials of imine bonds capable of hydrolytic cleavage into aldehyde and amine is an efficient strategy to prepare chemically recyclable networks (Figure 1-11). In this context, closed-loop recyclability of polyimine networks, synthesized from vanillin-based di- and trialdehyde with diamines (Figure 1-11a and b), was achieved within only 3 min of immersion into a 0.1 M hydrochloric acid (HCl) solution (Hong et al., 2022). Recyclable-by-design concept enabling the closed-loop recycling of poly(imine acetal) (P(ImA)) network through depolymerization and selective extraction (Figure 1-11c) was reported (Saito et al., 2023). P(ImA) was obtained by condensation of a mixture of commercial di- and triamines with a di-vanillin acetal monomer synthesized using catalyst-free click addition reaction between vanillin and di-vinyl ether. The combination of imine and acetal hydrolysable bonds promoted the depolymerization into primary building blocks (neat vanillin, diethylene glycol, polyamine, and acetaldehyde). The depolymerization of P(ImA) network is also effective when mixed with plastic wastes including polyethylene terephthalate (PET), high-density polyethylene (HDPE), polycarbonate (PC), and polypropylene (PP). An analogous strategy of closed-loop recycling of poly(imine carbonate) derived from PC wastes consists of the selective depolymerization through transesterification reactions using a vanillin derivative (Saito et al., 2022). From the subsequent di-vanillin carbonate monomer (Figure 1-11d), a library of poly(imine carbonate)s were prepared by reaction with various amines. Under acidic conditions, the novel networks display good chemical recyclability, allowing the recovery of high purity monomers which are reusable for the synthesis of next generation networks, even mixed with other commodity plastics. Polycarbonate waste were also upcycled into poly(imine carbonate) networks employing vanillin-derived aldehyde followed by a reaction with two aromatic diamines (Figure 1-11e) (Reddy et al., 2023). Surprisingly, networks exhibited unprecedented acid hydrolysis resistance as imines usually cleaves in acidic media. Chemical recycling was however achieved by carbonate aminolysis and imine transamination with hexylamine.

Vanillin-based water-borne polyimine vitrimer were synthesized through RAFT-controlled radical polymerization of vanillin-derived monomer (Figure 1-11f) followed by the copolymerization with 2-octylacrylate either in solution or in emulsion employing a water-borne macro-RAFT agent (Stouten et al., 2023). Aldehyde groups of resulting polymers were further condensed with the trifunctional tris(2-aminoethyl) amine (TREN). Fully biobased and dual networks combining imine and ester dynamic linkages were prepared with dialdehyde monomer synthesized from vanillin, 2,5-furandicarboxylic acid, and succinic acid (Figure 1-11g) (Jiang et al., 2023). Monomers were cured with the biobased dimer diamine (Priamine™ 1071 from Croda). Cleavage of imine moieties in acidic conditions and of esters in alkaline media enabled specific chemical recycling. Two-functional imine modifier prepared via one-pot imine condensation of vanillin with a dimer diamine (Priamine™ 1074 from Croda) (Figure 1-11h) were cured with hexamethylene diisocyanate trimer as crosslinker and isophorone diisocyanate as chain extender, to form imine-containing PU networks with about 70% biomass content (H. Wang et al., 2023). The rigidity of vanillin aromatic structure and urethane bonds

combined with the flexible branched chain provided the vitrimers with moderates strength and excellent ductility. Besides, they show fast network rearrangement with relaxation times reaching 377 s at 100 °C.

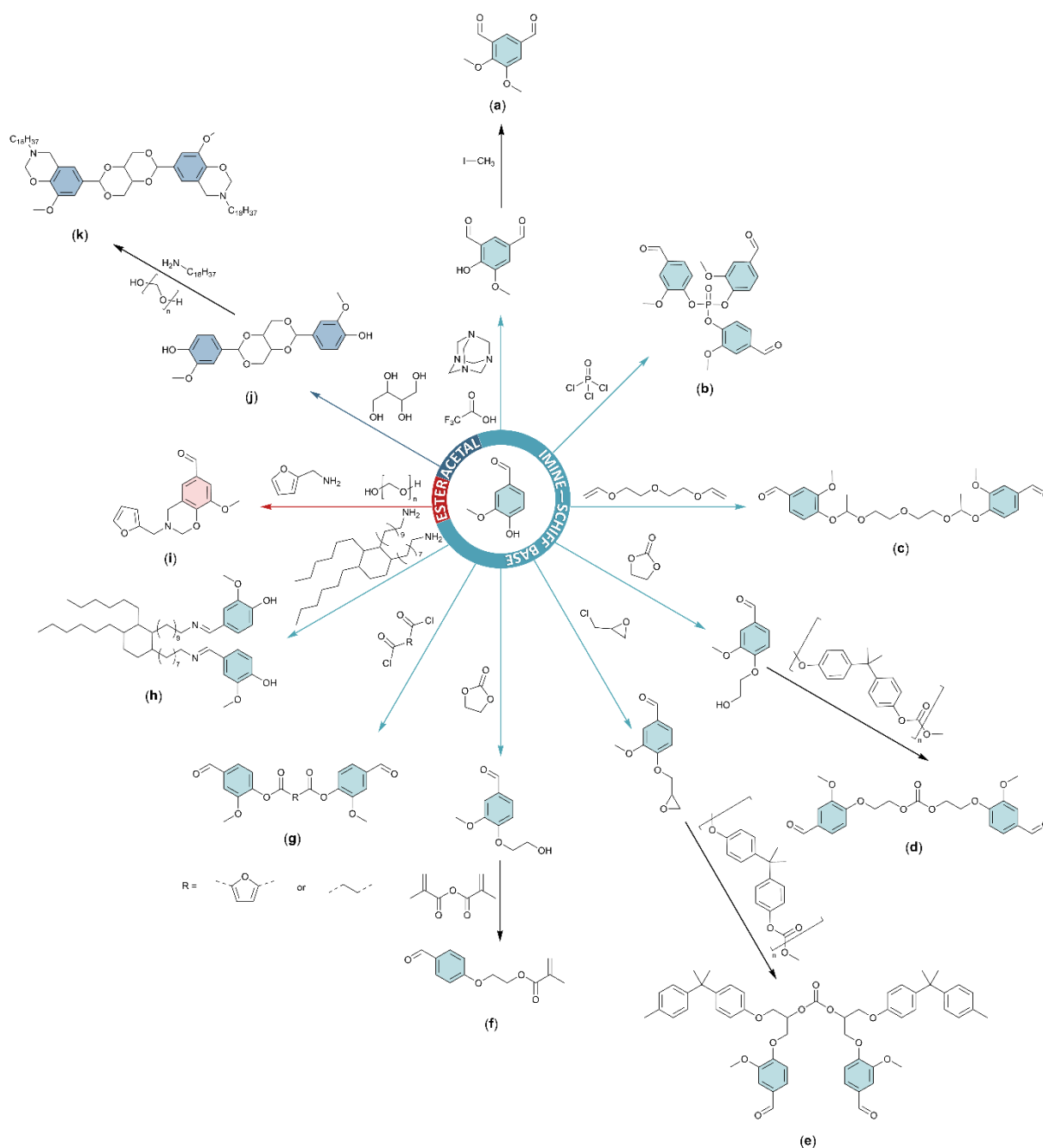


Figure 1-11. Vanillin chemical modifications into precursors for the synthesis of acetal, ester, and imine-based CANs.

Dynamic networks through transesterification reaction were prepared from a vanillin and furfurylamine benzoxazine monomer (Figure 1-11i) (Amornkitbamrung et al., 2022). Benzoxazine/epoxy copolymers were obtained after the reaction with epoxidized castor oil and glutaric anhydride. Photothermal effect of the copolymers was exploited to induce self-healing upon irradiation with near-infrared light. Poly(benzoxazine) dynamic through acetal metathesis were recently reported (J. Chen et al., 2023). Acetal dialdehyde monomers were prepared from the reaction of vanillin with erythritol, catalyzed with *p*TsOH (Figure 1-11j). Resulting diphenol structures were reacted with stearylamine and paraformaldehyde to obtain a benzoxazine monomer which was cured (Figure 1-11k).

The network was successfully degraded in acidic tetrahydrofuran (THF) aqueous solution owing to the cleavage of acetal bonds into aldehyde and hydroxyl moieties. Fully biobased spirocyclic diacetal-based networks were also synthesized from the reaction of vanillin (VA), ethyl vanillin (EV), or syringaldehyde (SA) with erythritol and soybean oil as crosslinker (Figure 1-11j) (W. Zhang et al., 2023). T_g between 41 and 59 °C were obtained by DSC for EV, VA and SA-based materials. The distinct mechanical properties between networks were attributed to the variation of chemical structure of phenol monomers. The two methoxy groups of syringaldehyde might limit the flexibility and mobility of polymer chains, resulting in increased structural rigidity (Young modulus and stress at break reaching 449 MPa and 15 MPa, respectively). Second generation (2G) materials were prepared through chemical recycling induced by acid degradation of the diacetals.

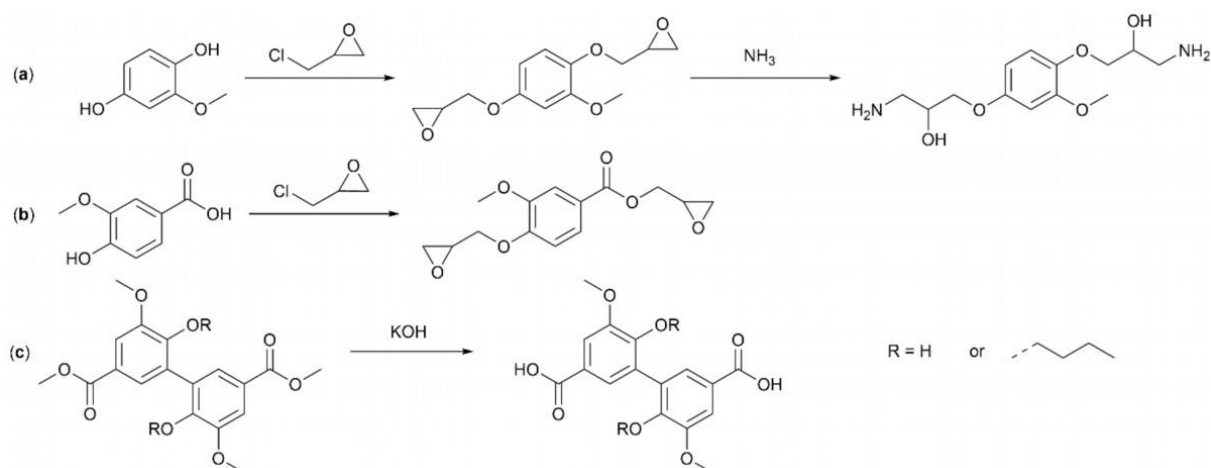


Figure 1-12. Vanillin derivatives as precursors for the synthesis of CANs.

Engelen *et al.* (Engelen et al., 2022) reported the first vanillin-derived vinylogous urethane vitrimers with renewable carbon content up to 86%, synthesized from the epoxidation and further amination by aqueous ammonia of 2-methoxyhydroquinone, a vanillin derivative, to form a bifunctional β-hydroxyamine (Figure 1-12a). Vitrimers were cured with terpene-based bis-acetoacetate. Vinylogous urethane epoxy networks were also prepared from vanillic acid (Yang et al., 2023). Firstly, linear VU prepolymers were prepared through the condensation of isosorbide-bis-acetoacetate with triethylenetetramine and diamines. Then, permanent crosslinks were obtained by ring opening of epoxy groups of epoxidized vanillic acid with the pendant amines of the prepolymer (Figure 1-12b).

Finally, the use of divanillic acid (DVA), a symmetrical dimer of vanillic acid, was reported to prepare ester containing vitrimers after the reaction of DVA or butoxylated DVA monomers with epoxidized soybean oil in the presence of zinc acetylacetonate hydrate (Figure 1-12c) (Yunfan Zhang et al., 2023).

4-hydroxybenzaldehyde

Analogously to vanillin, aromatic building blocks with aldehyde reactive groups are mainly valorized in imine-based CANs (Figure 1-13) (X. Lin et al., 2022; Trinh et al., 2023; Xu et al., 2021; Yuan et al., 2023; Zhu et al., 2023). Imine-based reactive mesogen i.e., the fundamental unit of a liquid crystal inducing structural order, and exchangeable liquid crystal elastomer were prepared (X. Lin et al., 2022). 4-hydroxybenzaldehyde (4-HBA) was etherified to graft aliphatic hydroxyls which were further reacted with acryloyl chloride (Figure 1-13a). Following the condensation of the aldehyde-based acrylate monomer with an aromatic diamine, a reactive mesogen was obtained and further crosslinked using “thiol-ene” click reaction. The presence of imine moieties within the mesogenic cores enabled fast and catalyst-free reprocessing of the liquid crystal elastomer through imine metathesis. Imine and esters functional groups in conjugation with aromatic structures enhance liquid crystal assembly based on π-π

interactions. In this regard, liquid-crystalline epoxy vitrimers bearing imine and esters dynamic linkages were also prepared from 4-HBA (Figure 1-13b) (Trinh et al., 2023). Mesogenic vitrimers present easy reprocessing via transimination and transesterification rearrangements, as well as efficient degradation in both acidic and basic media, through the hydrolysis of imine and esters, respectively. The combination of associative imine and dissociative disulfide bonds within 4-HBA-derived epoxy monomers was investigated (Figure 1-13c) (Xu et al., 2021). Dissociative bonds provided the highly crosslinked and rigid networks with fast exchange rate and reprocessability via both remolding and extrusion. Dissociation of aromatic disulfide bonds at elevated temperature improved the mobility of imine moieties, leading to acceleration of bonds rearrangements and enhanced reprocessing efficiency. Dually crosslinked CANs inspired by supramolecular interactions within natural materials were synthesized by combining covalent imine groups and hydrogen bonding in a styrene-butadiene rubber (SBR) vitrimer (Zhu et al., 2023). An epoxidized SBR was synthesized by reaction-controlled-phase-transfer catalysis and cured with an imine-containing crosslinker derived from 4-HBA to form the vitrimer elastomer (Figure 1-13d). Through the introduction of controlled contents of hydrogen bonds as physical crosslinks, mechanical and dynamic properties of the vitrimers were significantly improved, without compromising their reprocessability. 4-HBA was employed to generate polyimine vitrimers from solvent-free, melt processing of benzoxazine resins (Figure 1-13e). These materials exhibited excellent thermomechanical tunability (T_g from 34 to 160 °C and tensile strength up to 80 MPa), rapid stress relaxation, and moderate creep resistance at elevated temperatures (150 °C) and sustained force (1 MPa). Not only did these materials adhere to a greener approach (solvent-free crosslinking) but also demonstrated mild chemical depolymerizability (Hamernik et al., 2023).

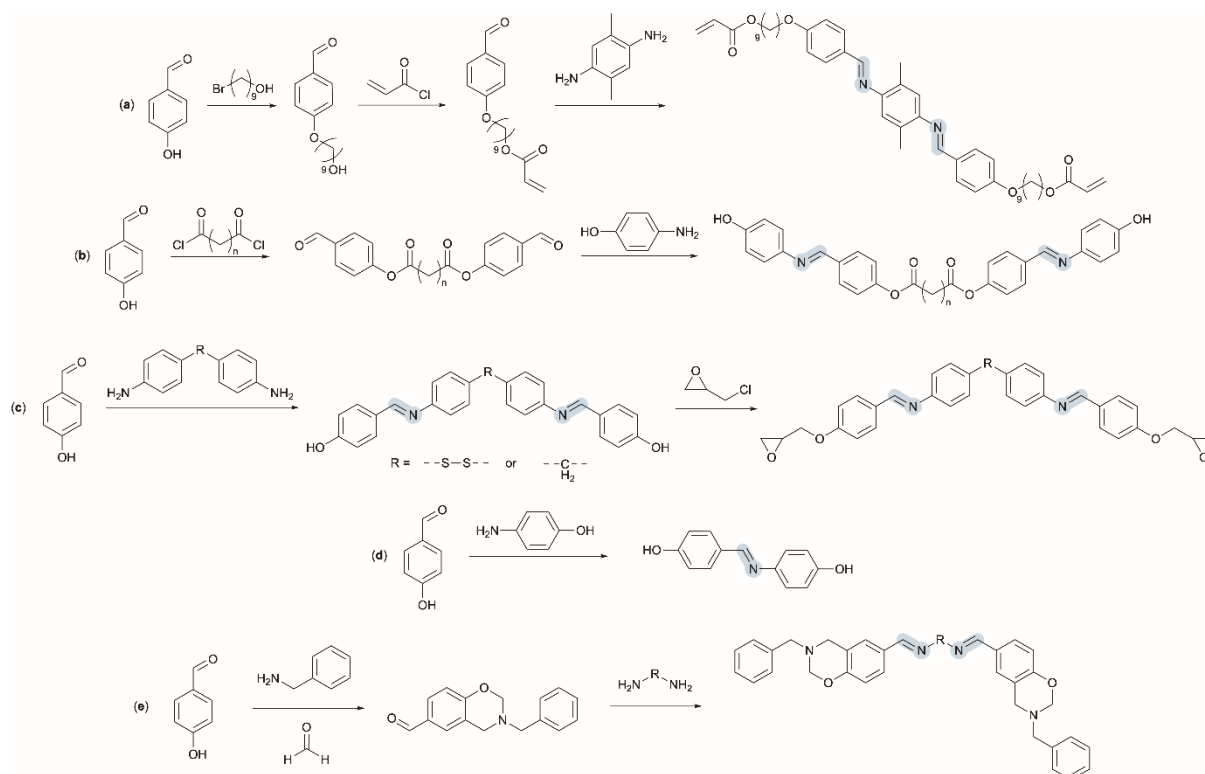


Figure 1-13. 4-hydroxybenzaldehyde as platform chemical for the synthesis of imine-containing monomers.

3,4-dihydroxybenzaldehyde

This building block is composed of a reactive aldehyde and two phenolic hydroxyls (Figure 1-14). The integration of 3,4-dihydroxybenzaldehyde (3,4-DHBA) within poly(epoxy imine) network containing siloxane flexible segments was recently disclosed (Ding et al., 2022). An epoxy monomer

was prepared via the glycidylation of 3,4-DHBA followed by the condensation of its reactive aldehyde group with a synthetic siloxane diamine (Figure 1-14a). The rigid aromatic imine moieties endow high mechanical properties while the high flexibility provided by the siloxane chains ensure fast rearrangement of imine bonds although a storage modulus plateau was observed after 600 s, indicating the remaining of permanent crosslinks. 3,4-DHBA-derived epoxy monomer was also reported in the preparation of an ester and diacetal containing epoxy resin (Figure 1-14b) (Yajie Zhang et al., 2023). Monomer was synthesized by acetalization of 3,4-DHBA with erythritol followed by glycidylation with bioderived epichlorohydrin and exhibited good reactivity with glutaric anhydride in the presence of zinc acetylacetonate, a transesterification catalyst. Degradation in acidic media was ensured by the cleavage of spirocyclic diacetal structures.

High-performance epoxy-vitrimer derived from 3,4-dihydroxybenzoic acid (3,4-DHBAc), also designated as protocatechuic acid, were developed as a sustainable alternative to bisphenol A (Tao et al., 2020). 3,4-DHBAc was modified into its allyl ether derivative followed by the glycidylation of the three allyl groups (Figure 1-14c). Epoxy monomer was cured with maleic anhydride, varying the epoxy/anhydride ratios, in presence of zinc acetylacetonate. Regardless of the epoxy/anhydride ratio, the vitrimers exhibited much better mechanical and thermal properties compared to bisphenol A-based epoxy resin while displaying efficient degradation in NaOH.

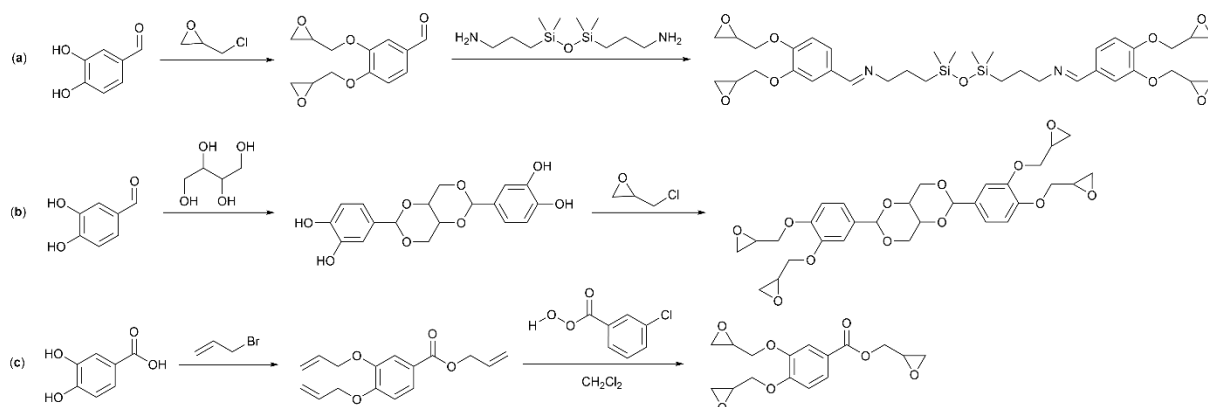


Figure 1-14. 3,4-dihydroxybenzaldehyde and 3,4-dihydroxybenzoic acid as precursors for the synthesis of epoxy building blocks.

Guaiacol

To design novel biobased epoxy network, a strategy for the conversion of guaiacol into aromatic amines through nitration and reduction of nitroarenes was developed (Figure 1-15a) (J. Li et al., 2022). This sustainable aromatic amine undergone a condensation reaction with vanillin to obtain an imine monomer, which was further modified by epichlorohydrin to obtain an epoxy precursor containing 96.4% biobased content. The cured resin with 4,4'-diaminodiphenyl methane exhibited high T_g (220°C), excellent mechanical properties (Young's modulus of 4489 MPa), and intrinsic flame retardancy compared to commercial petroleum-based bisphenol A epoxy resin. Another approach consists in the preparation of a triepoxy monomer from guaiacol and vanillin (Figure 1-15b), which was then cured by 4-methylcyclohexane-1,2-dicarboxylic anhydride (Liu et al., 2018). In this instance, zinc(II) acetylacetonate hydrate is used as curing and transesterification catalyst. The cured epoxy materials exhibit high T_g between 157 and 187 °C. The authors note the close relationship between the reparability and the magnitude of the rubbery modulus. The more rigid network (modulus at rubbery state of 73 MPa) is more difficult to heal compared to the material with a lower modulus (51 MPa), for which the deformation is favored under the same external stress. Closed-loop recycling and degradation of guaiacol-based epoxy resin reinforced with carbon fibers was successfully achieved by introducing disulfide bonds (Figure 1-15c) (Tang et al., 2023). A guaiacol-based bisphenol monomer was

CHAPITRE 1

synthesized and further functionalized by glycidylation, then 4-aminophenyl disulfide was used as curing agent. Two other materials were synthesized with curing agents which do not include dynamic bonds (4,4'-methylenedianiline and 4,4'-diaminodiphenylsulfone) for comparative purpose. The results indicated that S-S bonds enabled the epoxy resin to be reprocessed and restored owing to the rearrangement of the network topology. Co-poly(ether sulfone)s were reported from aromatic nucleophilic substitution polycondensation of guaiacol-based bisphenol monomer containing pendant furyl groups (Figure 1-15d) (Nagane et al., 2019). The latter, provide reactive sites for click Diels-Alder addition with maleimides and bismaleimides. Thermally-reversible crosslinking were achieved on both copoly(ether sulfone)-based films and gels.

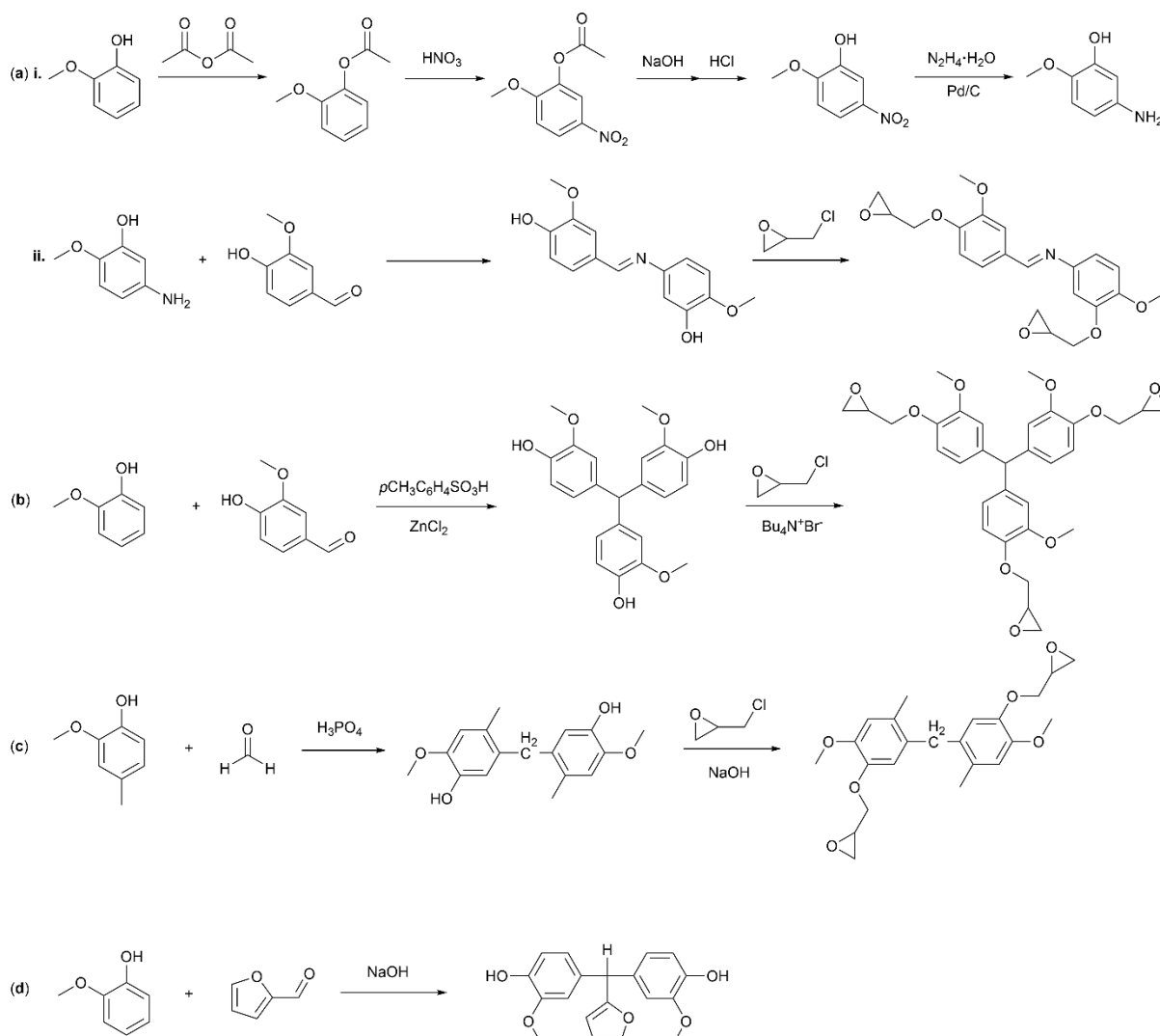


Figure 1-15. Guaiacol and 4-methyl guaiacol as precursors for the preparation of different CANs.

The recent review published by Tiz et al can be used to compare the chemical modifications reported for lignin-based CANs and thermoset polymers derived from the same lignin-derived precursors (Tiz et al., 2023).

CHAPITRE 1

Table 1-2. Main stress-relaxation, physical and chemical recycling parameters of CANs from lignin-derived precursors.

Biomass	Dynamic linkage	E_a (kJ mol ⁻¹)	τ	Physical recycling conditions ^a	Chemical recycling conditions	Ref.
Vanillin	Imine	57.0 – 83.0	0.85 – 1.90 min at 150 °C	180 °C, 3 MPa, 2 h	1 M HCl, RT, 24 h	(Roig et al., 2022a)
Vanillin	Imine	52.5 – 77.2	43 – 48 s at 190 °C	190 °C, 9.25 MPa, –	2 M HCl, 70 °C, 24 h	(Roig et al., 2022b)
Vanillin + Syringaldehyde	Imine	88.0 – 90.0	-15 – 20 s at 80 °C ^b	170 °C, 0.3 MPa, 30 min	excess bisaminomethyl cyclohexane, reflux, 6h	(Muhammad A. Rashid et al., 2023b)
Vanillin	Imine	21.9 – 35.9	6 – 44 s at 160 °C	180 °C, 20 MPa, 10 min	n/a	(F. Zhao et al., 2022)
Vanillin	Imine + acetal	36.7 – 55.0	14 – 730 s at 120 °C	120 °C, 75 kN, 1 h	1 M HCl, 65 °C, 2 h	(Türel and Tomović, 2023)
Vanillin	Imine	47.6 – 126.0	< 13 s at 130 °C	150 °C, 1 kN, 30 min	0.1 M HCl, RT, 16 h	(Klein et al., 2023)
Vanillin	Imine	54.0	115 s at 40 °C	120 °C, 5 MPa, 5 min + 10 MPa, 2 min	0.1 M HCl, – , 3 min	(Hong et al., 2022)
Vanillin	Imine + acetal	95.8	<5 s at 130 °C ^b	120 °C, 50 kN, 30 min	0.1 M HCl, 50 °C, 30 min	(Saito et al., 2023)
Vanillin	Imine + carbonate	78.0 – 115.0	1 – 18 s at 120 °C	120 °C, 10 MPa, 1 h	0.1 M HCl, RT, 2 h	(Saito et al., 2022)
Vanillin	Imine	n/a	n/a	240 °C, 10 MPa, 2 h	0.1M H ₂ SO ₄ , 50 °C, 6 h	(Reddy et al., 2023)
Vanillin	Imine	57.0 – 63.0	<3 s at 120 °C ^b	150 °C, 50 bar, 15 – 45 min	n/a	(Stouten et al., 2023)
Vanillin + 2,5-furandicarboxylic acid	Imine + ester	57.1 – 66.9	≤ 100 s at 50 °C ^b	120 °C, 10 MPa, 5 min	1 M HCl + EtOH (THF) or 1 M NaOH + EtOH (THF), RT, 72 h	(Jiang et al., 2023)
Vanillin	Imine	51.1 – 75.9	377 – 552 at 100 °C	80 °C, 10 MPa, 2 h	n/a	(H. Wang et al., 2023)
Vanillin + furfurylamine	Ester	n/a	n/a	n/a	n/a	(Amornkitbamrung et al., 2022)
Vanillin	Acetal	74.0	0.595 s at 60 °C	120 °C, 1 MPa, 10 min	1 M HCl/THF, 50 °C, 5 min	(J. Chen et al., 2023)
Vanillin + Ethyl vanillin + Syringaldehyde	Acetal	58.4 – 82.9	40 – 109 s at 170 °C	170 °C, 10 MPa, 60 min	0.1 – 1 M HCl, 70 °C, 150 min	(W. Zhang et al., 2023)
Vanillin	Vinylogous urethane	162.0	3 – 27 s at 160 °C	150 °C, 2 tons, 15 min	n/a	(Engelen et al., 2022)
Vanillic acid	Vinylogous urethane	n/a	n/a	180 °C, 15 MPa, 30 min	excess benzylamine in DMF, 60 °C, 12 h	(Yang et al., 2023)
Divanillic acid	Ester	111.8 – 118.6	5600 – 82000 s at 200 °C	230 °C, 5 MPa, 1h	n/a	(Yunfan Zhang et al., 2023)
4-HBA	Imine	54.0	n/a	120 °C, 0.1 MPa, 2 min	n/a	(X. Lin et al., 2022)
4-HBA	Imine + Ester	42.5	<1000 s at 130 °C	160 °C, 2 MPa, 1 h	0.125 M HCl in THF, 50 °C, 1 h and 0.5 M NaOH in ms, 60 °C, 5 h	(Trinh et al., 2023)
4-HBA	Imine + Disulfide	42.1 – 147.5	80 – 2275 s at 140 °C	160 °C, 10 MPa, 20 min	1 M HCl in ms at 50 °C, 8 h	(Xu et al., 2021)
4-HBA	Imine + Hydrogen	89.4 – 96.1	900 – 25000 at 140 °C	150 °C, – , 30 min	excess butylamine in toluene, 50 °C, 24 h	(Zhu et al., 2023)
4-HBA	Imine	70.0 – 177.0	<30 s at 180 °C	180 °C, 1.7 MPa, 15 min	1 M HCl/THF (1 : 1 v/v) at 25 °C	(Hamernik et al., 2023)
3,4-DHBA	Imine	66.1	<600 s at 150 °C	180 °C, 10 MPa, 1 h	n/a	(Ding et al., 2022)
3,4-DHBA	Ester	57.6 – 74.8	2605 – 3699 at 180 °C	n/a	0.1 and 1 M HCl, 25 – 80 °C, 15 – 45 min	(Yajie Zhang et al., 2023)
3,4-DHBAc	Ester	65.8	> 200 s at 240 °C	230 °C, 10 MPa, 2 h	1 M NaOH, RT, 24 h	(Tao et al., 2020)
Guaiacol + Vanillin	Imine	170.0	504 s at 225 °C	230 °C, 10 MPa, 2 h	0.1 M H ₂ SO ₄ (DMSO/H ₂ O) 90 °C, 24 h	(J. Li et al., 2022)
Guaiacol + Vanillin	Ester	n/a	>20 s at 220 °C ^b	n/a	n/a	(Liu et al., 2018)
Guaiacol	Disulfide	140.0	27.5 s at 200 °C	180 °C, 10 MPa, 15 min	DMF/2-mercaptoethanol (50/50), RT, 7 days	(Tang et al., 2023)
Guaiacol	Diels-Alder	n/a	n/a	60 °C, – , 12 h	120 °C, 10 min	(Nagane et al., 2019)

^a conditions of physical recycling are given as follow: temperature, time, applied pressure or force. ms = multiple solvents. ^b graphical values.

To outline the current trends in the field of dynamic networks prepared from lignin-derived precursors and derivatives such as vanillin, 4-hydroxybenzaldehyde, 3,4-dihydroxybenzaldehyde, or guaiacol, the main stress-relaxation, physical and chemical recycling parameters of aforementioned CANs are summarized in Table 1-2. This state of art highlights that research focused mainly on the

synthesis of imine containing networks, mostly in the context of developing epoxy resins, owing to the presence of aldehyde reactive groups on the building blocks. Moreover, imine bonds overall provide fast relaxation times and a wide range of activation energy from 22 to 126 kJ mol⁻¹, offering milder reprocessing conditions compared to ester groups, while enabling facile chemical recycling by hydrolysis. One drawback of the imine bond, which is one of the most commonly leveraged exchange platform within vanillin-based and generally biobased aromatic CANs, is the need for excess amine to induce transamination reactions, which also limits creep resistance. In addition to being sensitive to applied pressure and temperature, creep amplitude in polyimines materials was reported to be directly correlated with the Hammett equation representing the sensitivity of the reaction towards the substituent effect (Schoustra et al., 2021, p. 202). The extent of creep becomes tunable by selecting the appropriate Hammett parameter, thus choosing an aromatic monomer with the appropriate para and meta substituents. Supramolecular reinforcement through metal-ligand coordination was also employed to efficiently suppress creep in polyimine vitrimers (Wang et al., 2020). Finally, Du Prez and co-workers suggested creep suppression via the temporary shielding of free amines inside the network backbone which could be released as reactive chain ends via thermally cyclisation to an imide moiety. Although the strategy was employed on vinylogous urethane materials it could also be suitable for polyimine networks (Van Lijsebetten et al., 2022).

The challenge in processing high modulus CANs hampering physical recycling is addressed. Because of high structural rigidity the flow necessary for processability can be compromised. Conversely, low modulus CANs may present easier recycling opportunities but may show restricted practical applications due to limited mechanical properties.

4.2.2. Tannins and derived building blocks

Condensed tannins

Duval *et al.* (Duval et al., 2017) reported the first thermo-reversible network obtained from tannins (Table 1-3). Furfuryl glycidyl ether was grafted on condensed tannin from mimosa tree to prepare furan-bearing tannins. The latter were reacted with telechelic oligomers containing maleimide end groups to obtain dynamic networks. The dynamicity of the crosslinks was demonstrated by fast liquefaction upon heating at 120 °C. Later, thermo-reversible PU prepared from propyl gallate and polyester diol was disclosed (Soleimani and Sadeghi, 2022). Owing the phenol-carbamate dynamic linkages, the dissociation of phenolic urethane was observed at 110 °C followed by a reformation of the network at lower temperatures. The enrichment of the matrix with nano-silica increased the thermal resistance of the material.

Tannic acid

The first reversible network derived from tannic acid was developed by Feng *et al.* (Feng et al., 2020) in 2020. Researchers employed tannic acid as a multifunctional curing agent to a diglycidyl ether of bisphenol A (Figure 1-16). However, although the epoxy network could be reprocessed under long temperature exposure, very limited stress-relaxation was observed because of a restricted network mobility of the hierarchical molecular structure. They suggested to use a suitable catalyst to promote both curing and transesterification reactions and enhance dynamicity. Later, dynamic β -hydroxyl phosphate esters were prepared from epoxidized soybean oil, 2-hydroxyethyl methacrylate phosphate as flame retardant and tannic acid as charring agent (Yizhen Chen et al., 2023). Herein, flexibility brought by soybean oil aliphatic chains facilitated transesterification reactions, leading to faster stress-relaxation.

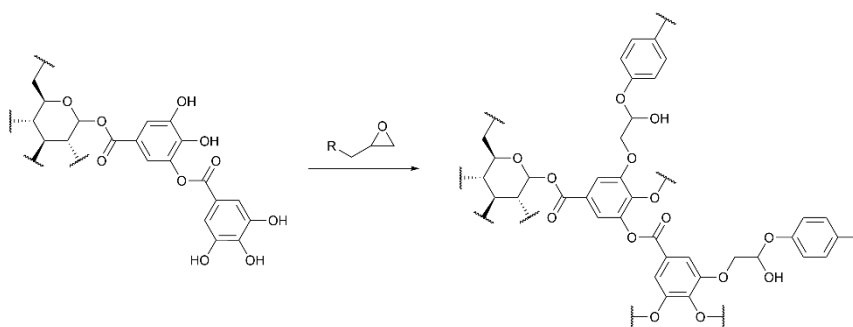


Figure 1-16. Tannic acid as curing agent for the preparation of dynamic epoxy networks. Refs. (Yizhen Chen et al., 2023; Feng et al., 2020).

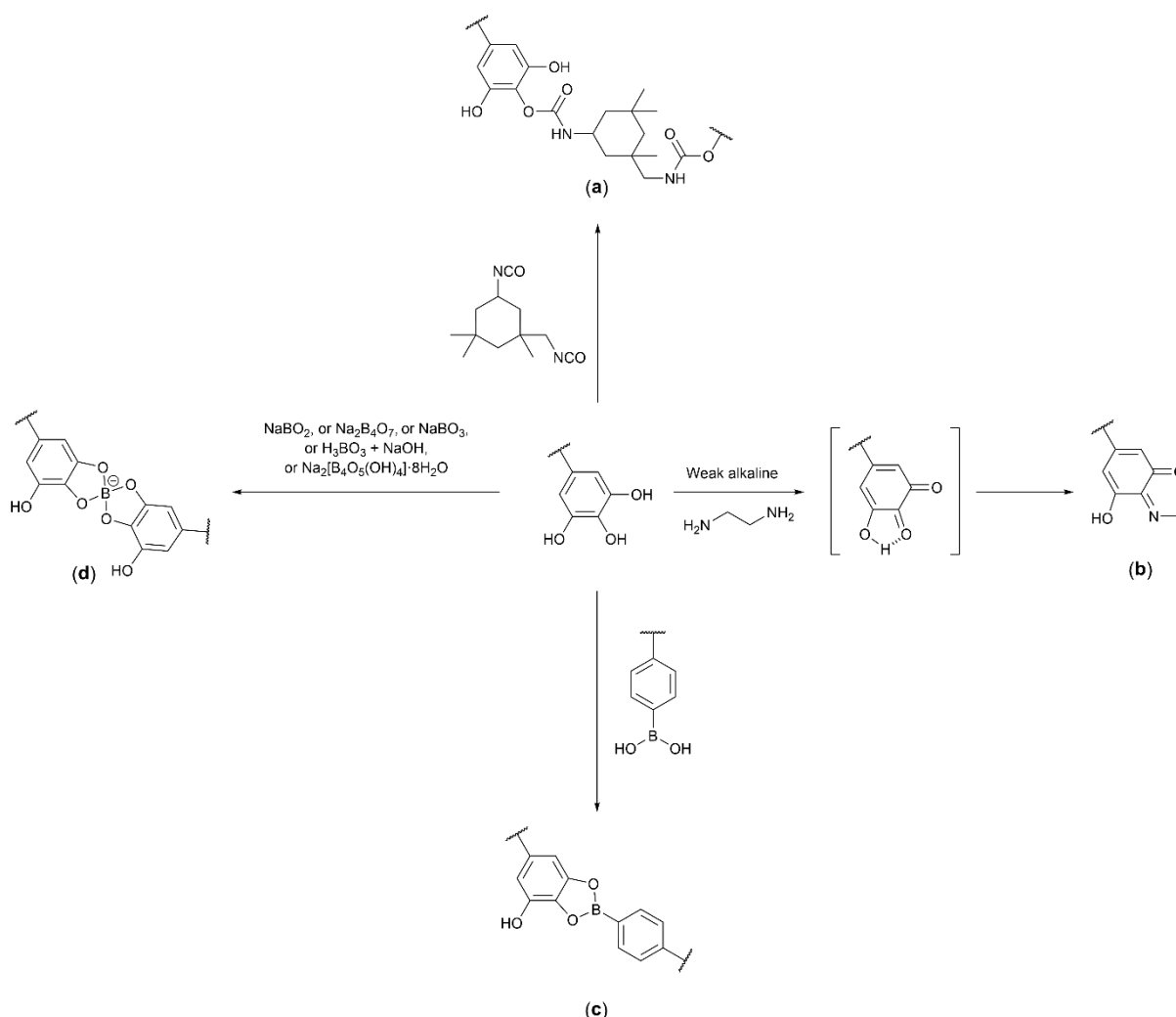


Figure 1-17. Tannic acid as precursor for the preparation of CANs.

A strategy to prepare dynamic phenol-carbamate networks PUs by introducing tannic acid (2.2 to 8.4 wt%) with isocyanate was disclosed (Figure 1-17a) (Y. Liu et al., 2021). A good balance between robust mechanical properties (up to 12.9 MPa of tensile strength and 844% of elongation) and efficient self-healing was achieved by adjusting the content of dynamic linkages. Furthermore, the influence of tannic acid on the structural organization of PUs was discussed, more particularly on the crystallinity

and the micro-phase separation. It was established that the crystallization and melting of crystalline domains, acting as switching segments, was responsible for the shape fixing ability. Leveraging from pH-responsive imine chemistry resulting from the one-pot imine condensation of oxidized tannic acid bearing aldehyde groups with ethylenediamine, blue emitting carbon dots with reversible room temperature polymerization were prepared (Figure 1-17b) (B.-B. Chen et al., 2022).

Owing to the diverse bonding abilities, particular topology, antiviral, and antibacterial properties, the preparation of tannic acid-based responsive hydrogels and smart antibacterial systems is widely studied (Kaczmarek, 2020; Montanari et al., 2016). Phenol compounds bearing three hydroxyl groups (pyrogallol and tannic acid) were demonstrated to reversibly form trigonal planar boronic esters, with a remaining free hydroxyl group (Figure 1-17c) (Zhao et al., 2021). The latter possess a donor and Lewis base character, promoting the dynamic B-O exchange by acting as a proximal base. In this context, boronate esters are attractive reversible linkages for the reaction with the catechols and pyrogallol groups of tannic acids. By incorporating boronate esters within a dynamic oxime hydrogel, the control of the gels properties was achieved (Collins et al., 2017). Mechanical strength was increased, while an orthogonal reversibility of the dual network to recover the initial gel was demonstrated. Several other dynamic interactions can be combined with boronate esters, such as hydrogen bonds and coordination bonds to develop ultra-stretchable, highly adhesive and self-healable hydrogels (Mo et al., 2021). For the purpose of developing multi stimuli-responsive soft materials, series of all-small-molecule dynamic covalent gels prepared by direct gelation of tannic acid with inorganic borates and organic boronates were also reported (Figure 1-17d) (Cheng et al., 2022, 2020). This strategy avoids the need for pre-synthesis of macromolecular building blocks, while enabling predictable degradation properties.

Catechol

Epoxy vitrimers were prepared from bisphenolic compounds obtained by the reaction of 4-methylcatechol with vanillyl alcohol (Figure 1-18a) (Zhao and Abu-Omar, 2019). The glycidylation of resulting structure composed of a phenol and a catechol moieties led to two products, a mono-epoxide or a triepoxide-derivative. Indeed, in contrast to phenol which mainly yield glycidyl ether, the glycidylation of catechol can yield glycidyl ether or benzodioxane. The reaction time and alkaline equivalents, factors influencing the ratio of both products were investigated, and successfully tuned via a two-step synthetic pathway, enabling the adjustment of thermomechanical properties of the final vitrimers.

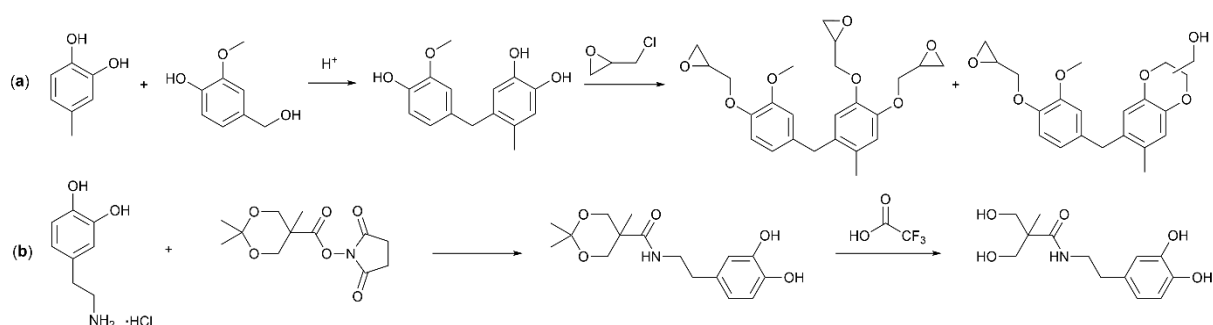


Figure 1-18. Catechol-derived structures as precursors for the preparation of CANs.

Due to their polyvalence, phenolic hydroxyl groups are performing systems to combine several dynamic chemistries. For instance, the combination of boronic esters and hydrogen bonds dynamic chemistries within catechol-based PU networks enabled the preparation of PU elastomeric vitrimers exhibiting high stretching and healing abilities (Figure 1-18b) (Y. Yang et al., 2020). A model study to understand the metathesis kinetics of boronic esters was performed with catechol molecules (Dong et al., 2023). PU elastomers were prepared from linear PU containing pendant catechol moieties which

were cured with 1,4-phenylenediboric acid. The influence of crosslinking density and content of free catechol groups on the mechanical properties and rheological behavior of the vitrimer was discussed. Residual catechol moieties increase the mechanical properties through hydrogen bonding and π - π stacking while the excess of free hydroxyl groups accelerate the network relaxation by catalyzing the rearrangements.

Epigallocatechin gallate

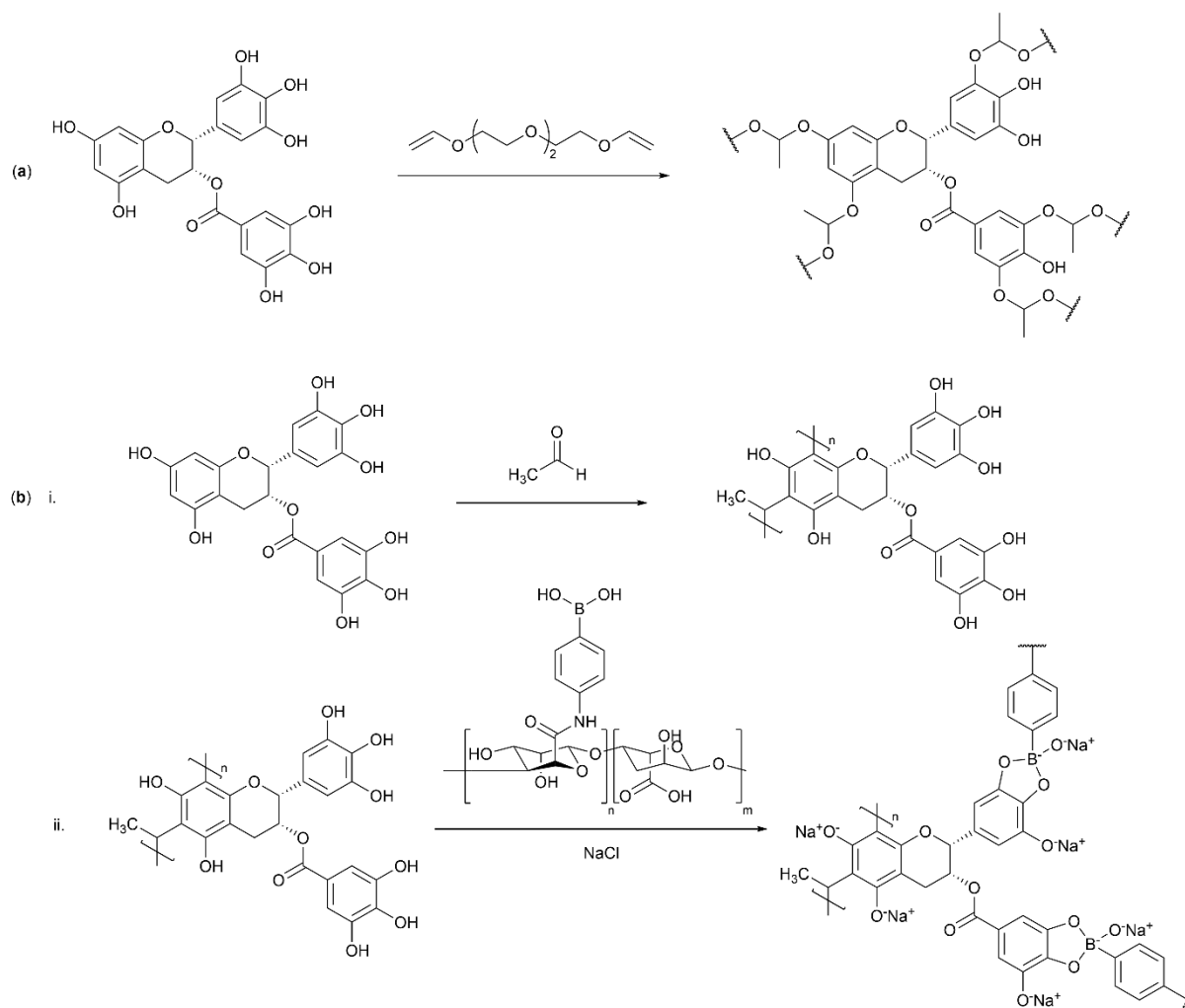


Figure 1-19. Epigallocatechin gallate as precursor for the preparation of CANs.

Acetal containing network were synthesized from epigallocatechin gallate and tri(ethylene glycol) divinyl ether via single step “click” catalyst-free reaction (Figure 1-19a) (Q. Li et al., 2021b). Creep resistance was observed until 80 °C on the more crosslinked material (molar ratio of double bond/phenolic hydroxyl of 0.9) while the less crosslinked material (R=0.7) already exhibited permanent deformation due to faster bond rearrangements occurring at this temperature. Reprocessing of the acetal CANs was examined through several methods such as compression remolding, welding and extrusion. Although defects and cracks were observed at the surface of the extrudates, neighboring phenolic hydroxyl groups revealed to greatly improve the rate exchange of acetal in CANs. This study constitutes a noticeable improvement from previously reported work on acetal CANs derived from phenolic resins which could not undergo physical recycling by extrusion, but which demonstrated degradability under mild acidic conditions and good creep resistance below their T_v (from 95 to 103 °C) (Q. Li et al., 2020). The authors suggested herein that the dimensional stability might be improved by the employment of asymmetric acetal bonds compared to regular acetal linkages. Plant-inspired self-healing hydrogel

composed of oligomerized epigallocatechin gallate and boronic acid functionalized alginate was also disclosed (Figure 1-19b) (Choi et al., 2021).

Gallic acid

Waterborne PU with dynamic phenol-carbamate crosslinks prepared from gallic acid was recently disclosed (Figure 1-20) (Y. Liu et al., 2022). Gallic acid and an isocyanate were polymerized into waterborne PU showing excellent emulsion stability. The phenol-carbamate network exhibits a good balance between robust thermal and mechanical properties (tensile strength 45.1 MPa and elongation at break 576.5%) and desirable self-healing ability (81%).

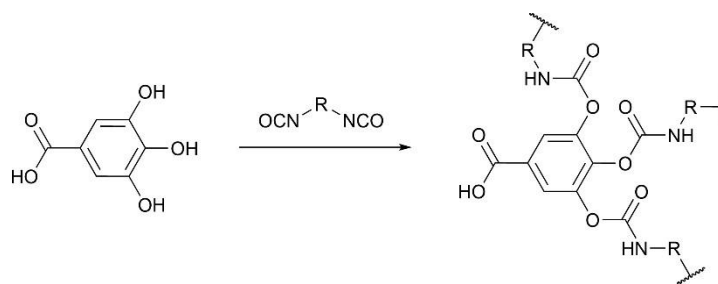


Figure 1-20. Gallic acid as precursor for the preparation of CANs.

Resorcinol

Tournillac and co-workers (Bakkali-Hassani et al., 2021) recently reported an enzymatic approach toward mild-temperature synthesis of dynamic poly(hydroxyester) networks (Figure 1-21a). In this work, the potential of lipase to promote epoxy-acid addition and transesterification up to 100 °C was demonstrated, enabling the synthesis of reversible resorcinol-based poly(hydroxyesters). The first consideration was thereupon investigated with the preparation and characterization of lipase-catalyzed epoxy vitrimers (Bakkali-Hassani et al., 2023). The vitrimer demonstrated stress-relaxation, albeit limited by the temperature window between the T_g of 7 °C and 100 °C at which the lipase denatures. Complete recovery of mechanical strength was observed after multiple physical recycling steps, highlighting the potential of this new approach.

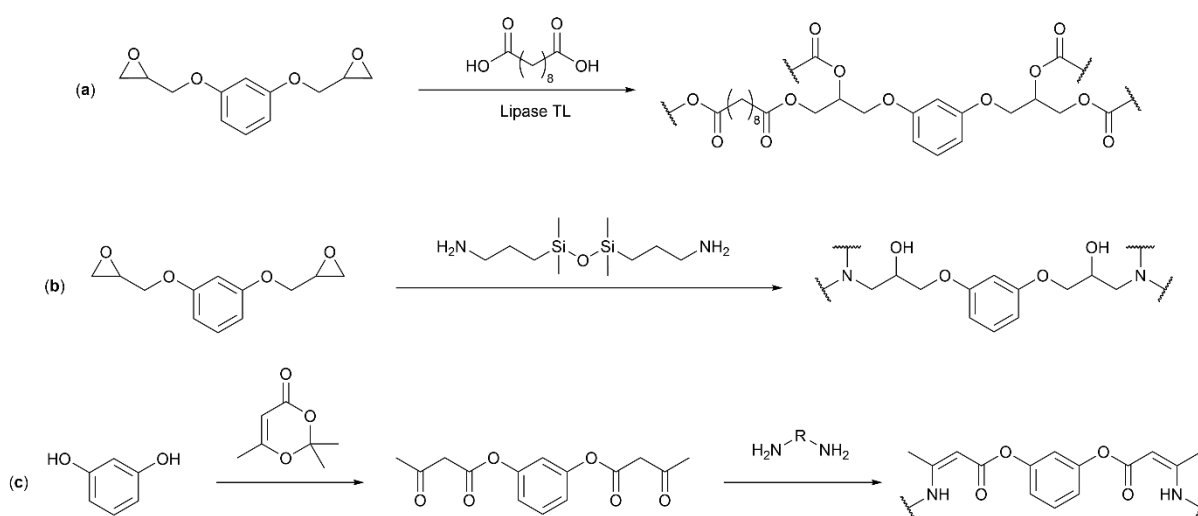


Figure 1-21. Resorcinol and resorcinol diglycidyl ether as CANs precursors.

Du Prez and co-workers (Debsharma et al., 2023) described the integration of a resorcinol-based epoxy resin into vitrimers demonstrating fast siloxane bond exchanges. Diglycidyl resorcinol ether was synthesized biobased epichlorohydrin alternative Epicerol®, commercialized by Solvay, and cured with a siloxane diamine hardener (Figure 1-21b). The material exhibited fast stress relaxation reaching 6 s at 220 °C and good property recovery over several recycling steps.

Resorcinol aromatic structure was also part of a study developing a feasible synthetic route for the acetoacetylation of aromatic alcohols (Figure 1-21c) (Haida et al., 2022). The novel aromatic acetoacetylated precursors were then employed for the preparation of blended vinylogous urethane and urea showing a wide range of properties, short relaxation times down to 0.7 s at 130 °C and activation energies between 45 and 150 kJ mol⁻¹.

Flavonoids

Although aromatic rich and highly-functional structures of flavonoid present high-value benefits, the integration of flavonoids into CANs is still underexploited. To this day, flavonoid-derivatives were exclusively employed in the synthesis of reversible epoxy networks (Fang Chen et al., 2021; Rashid et al., 2022). The preparation of a biobased epoxy hardener from quercetin and succinic anhydride via a mild one-step synthesis was disclosed (Rashid et al., 2022). The epoxy was successfully reprocessed through several cycles and degraded in an alkali medium while remaining stable in acidic and neutral media. An epoxy composite containing Diels-Alder bonds which was reinforced non-covalently with hexagonal boron nitride sheets functionalized with flavonoid dihydromyricetin was reported (Fang Chen et al., 2021). The material demonstrated crack-healing due to Diels-Alder reversible bonds, enabling the network to recover its structural integrity. Naringenin, a triphenolic building block, was readily derivatized into a biobased epoxide monomer and then crosslinked in a solvent-free manner with carboxylic acid-functionalized PEG to yield vitrimers operating under transesterification exchanges. The material displayed notable shape-memory behavior but also significantly faster relaxation times (430 to 24 s) at significantly lower temperatures (45 to 60 °C) compared to many other transesterification-based networks. Finally, these networks were readily chemically degraded in methanol-water mixtures at a relatively low temperature of 70 °C. However, this report does lack creep examination which would have been an asset to the study because of the low relaxation temperatures (Oh et al., 2019).

Phloroglucinol

The development of bi- and tri-functional epoxy monomers from vanillin and phloroglucinol were disclosed for the preparation of epoxy-amine vitrimers (Genua et al., 2020). Through the incorporation of aromatic disulfide-based diamine hardener, the build-to-specification vitrimers demonstrated comparable performances to commonly used fossil-based epoxy thermosets while showing advanced reprocessing features.

To outline the current trends in the field of dynamic networks prepared from tannin-derived precursors the main stress-relaxation, physical and chemical recyclability parameters of CANs are listed in Table 1-3. This overview highlights the compatibility of tannin derivatives compounds with a wide range of dynamic covalent chemistries owing to their reactive hydroxyl groups. Thus, urethane, ester, imine, boronic ester, acetal, siloxane, and Diels-Alder containing networks were reported. Herein, it is noticeable that a significant proportion of research focused on the preparation of boronic esters from catechol-bearing compounds such as tannic acid and epigallocatechin gallate, enabling one-step syntheses. Benefiting from the wide range of dynamic covalent chemistries, the best suited linkage can be chosen to enable the tuning of recycling conditions and meet specific requirements. For instance, urethane and boronic esters need tens of seconds at maximum 130 °C to fully relax, whereas esters and siloxane bonds generally need higher temperatures (>160 °C) or longer times.

CHAPITRE 1

Table 1-3. Main stress-relaxation, physical and chemical recycling parameters of tannin-derived CANs.

Biomass	Dynamic linkage	E_a (kJ mol ⁻¹)	τ	Physical recycling conditions ^a	Chemical recycling conditions	Ref.
Condensed tannins	Diels-Alder	n/a	n/a	n/a	DMSO, 120 °C, 1 h	(Duval et al., 2017)
Propyl gallate	Urethane	n/a	n/a	n/a	110 °C, –	(Soleimani and Sadeghi, 2022)
Tannic acid	Ester	n/a	Uncompleted at 175 °C	180 °C, 2 h, 14 MPa; or 210 °C, 4 h, 14 MPa	n/a	(Feng et al., 2020)
Tannic acid	Ester	118.9	750 s at 160 °C ^b	140 °C, 3 h, 10 MPa	n/a	(Yizhen Chen et al., 2023)
Tannic acid	Urethane	68.6	~300 s at 130 °C ^b	120 °C, 2 h, 5 kg	DMF, 120 °C, 2 h	(Y. Liu et al., 2021)
Tannic acid	Imine	n/a	n/a	n/a	1 M NaOH, RT	(B.-B. Chen et al., 2022)
Tannic acid	Boronic esters	67.2 – 74.1	~27.5 s at 120 °C ^b	25 °C, 50 kPa, 3h	THF, 25°C, 1 h	(Zhao et al., 2021)
Tannic acid	Boronic esters + Oxime	n/a	n/a	n/a	Excess of trifluoroacetic acid, RT, 2 h	(Collins et al., 2017, p. 201)
Tannic acid	Boronic esters	n/a	n/a	n/a	1 M HCl, 1 M NaOH, 10% (w/w) H ₂ O ₂ or 10% (w/w) 1,4-dithiothreitol, RT, 30 min	(Cheng et al., 2020)
Catechol + Vanillyl alcohol	Ester	24.3 – 59.5	456 s at 120 °C	100 °C, –, 30 s	n/a	(Zhao and Abu-Omar, 2019)
Catechol	Boronic ester + hydrogen bonds	28.0 – 33.0	13 – 436 s at 50 °C	60 – 80 °C, 2 – 3 MPa, 2 – 3 h	n/a	(Y. Yang et al., 2020)
Epigallocatechin gallate	Acetal	88.9 – 115.9	20 – 78 s at 180 °C	120 – 150 °C, 10 MPa, 20 min	0.1 M HCl acetone/H ₂ O, 25 – 50 °C, –	(Q. Li et al., 2021b)
Epigallocatechin gallate	Boronic ester	n/a	n/a	n/a	n/a	(Choi et al., 2021)
Gallic acid	Urethane	75.7	75 s at 130 °C	n/a	DMF, 120 °C, 1.5 h	(Y. Liu et al., 2022)
Resorcinol	Ester	n/a	4 – 18 h at 100 °C	100 °C, 3 tons, 24 h	n/a	(Bakkali-Hassani et al., 2023)
Resorcinol	Siloxane	86.9	6 s at 220 °C	220 °C, 1 ton, 2 min	n/a	(Debsharma et al., 2023)
Quercetin	Ester	n/a	n/a	n/a	1 M NaOH, RT, 6 h	(Rashid et al., 2022)
Dihydromyricetin	Diels-Alder	n/a	n/a	130 °C, 2 MPa, 30 min	N-methyl pyrrolidone, 130 °C, 24 h	(Fang Chen et al., 2021)
Naringenin	Ester	115.3	24 s at 60 °C	140 °C, 14 MPa, 5 h	Water/MeOH (1/9), 70 °C, 1 day	(Oh et al., 2019)
Phloroglucinol + vanillin	Disulfide	n/a	35 s at 200 °C	200 °C, 100 bar, 10 min	n/a	(Genua et al., 2020)

^a conditions of physical recycling are given as follow: temperature, time, applied pressure or force. ^b values obtained graphically.

4.2.3. Cashew nutshell liquid and its derivatives

CNSL

In the context of developing reconfigurable shape memory polymers, epoxy networks obtained from a phenolic epoxy resin cured with CNSL (Table 1-4) were reported. Resulting network (T_g between 41.6 and 55.4 °C) combined permanent ether linkage and exchangeable ester linkages, brought by anarcadic acid (AA) (Kasemsiri et al., 2018). Although relaxation was observed at 150 °C, the limited content of AA limited the relaxation of the materials, revealed by a remaining normalized storage modulus plateau of 0.75. The epoxy matrix exhibited shape memory behavior upon irradiation with near-infrared light. To increase the ester linkage content and promote relaxation, citric acid was added as co-curing agent to the initial phenolic epoxy resin/CNSL formulation (Lorwanishpaisarn et al., 2022, 2021). Faster stress relaxation was observed, with a relaxation time approximately of 200 s at 100 °C.

Torkelson's team took advantage of the aminolysis and decarboxylation of CNSL-based cyclic carbonate with thiol, releasing CO₂ as blowing agent to develop self-blowing PHU flexible foams containing up to 80 wt% biobased content (Purwanto et al., 2023). Owing to the dynamic hydroxyurethane dynamic linkages, the low T_g foams (-2 to 6 °C) were successfully reprocessed into bulk materials showing full property retention. The same group also uncovered the synthesis of non-isocyanate polythiourethanes (NIPTU) synthesized from a flexible biobased difunctional glycidyl ether

epoxy resin derived from CNSL (Cardolite NC-514, from Cardolite Corporation), and cyclic dithiocarbonate derived from p-xylene (Yixuan Chen et al., 2023). Resultant NIPTU networks presented dual dynamic linkages: thiourethane and disulfide dynamic linkages, the latter obtained by auto-oxidation of pendant thiols moieties. NIPTU were compared with structurally equivalent PHU networks and showed several benefits such as superior reactivity, mechanical properties, crosslinking density, and water resistance. Excellent reprocessability was assessed with complete recovery of the crosslinking density through several physical recycling cycles, along with potential self-healing.

Cardanol

This compound containing a phenolic alcohol on its aromatic ring and up to three unsaturations on the long alkyl chain provide CANs with interesting properties (Figure 1-22, Figure 1-23, and Table 1-4). Cardanol-based polybenzoxazine vitrimer containing disulfide dynamic bonds (Figure 1-22a) was reported (Trejo-Machin et al., 2020). Benzoxazine monomer was synthesized, purified and was further cured by ring-opening polymerization at temperature to obtain a vitrimer. The resulting network exhibited efficient chemical and physical recycling, enabled by a fast relaxation reaching 18 seconds at 120 °C. Subsequently, cardanol-derived polybenzoxazine containing boronic esters were also reported (Bo et al., 2022; X. Wang et al., 2022). High T_g networks (up to 224 °C) were prepared employing benzoxazine monomer obtained through one-pot Mannich reaction using cardanol, allylamine and paraformaldehyde, which was further cured at temperature and crosslinked with boronic esters crosslinkers via thiol-ene click reaction (Figure 1-22b) (X. Wang et al., 2022). On the other hand, boronic esters linkages were introduced by condensation of 1,4-phenylenebisboronic acid with a cardanol benzoxazine-based thiol (Figure 1-22c) (Bo et al., 2022). Boronic esters were also recently integrated within fluorescent epoxy polymer networks (Ke et al., 2021). Herein, a multi-arms epoxy monomer with hard core structures was synthesized from the reaction of cardanol with hexachlorocyclotriphosphazene, followed by epoxidation of the unsaturations using m-chloroperoxybenzoic acid (Figure 1-23a). Epoxy monomer was cured with four thiols monomers, one of which contained boronic esters.

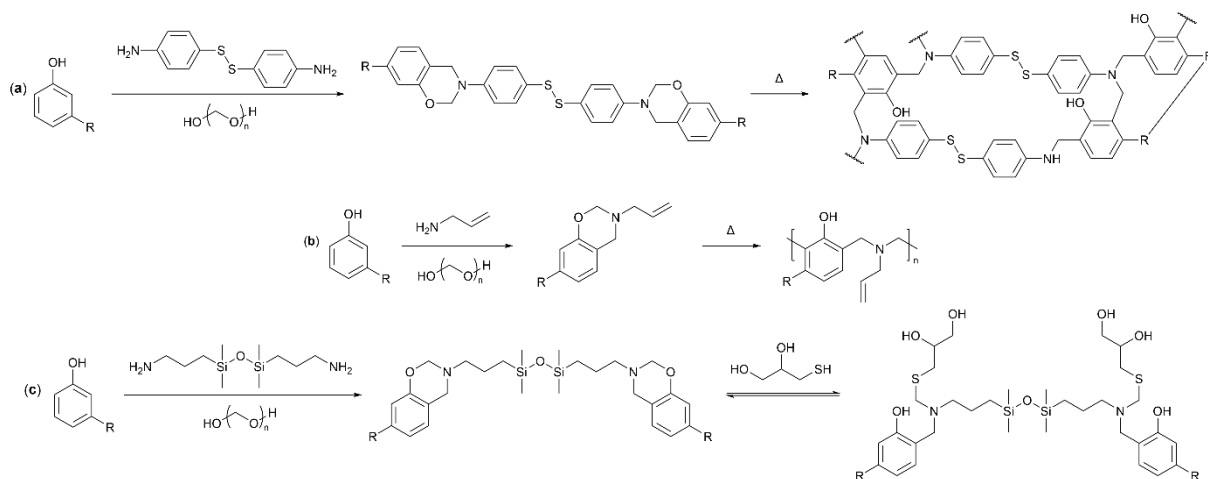


Figure 1-22. Chemical pathways for the synthesis of cardanol-derived benzoxazines.

Cardanol-based vinylogous urethane vitrimers were reported (Chen et al., 2020; Fengbiao Chen et al., 2021). Principally, the blend of urethane vitrimers with distinct mechanical properties was studied. Cardanol was subjected to sequential esterification, thiol-ene click reaction, and ester exchange to give an acetoacetate monomer (Figure 1-23b). Then, two specific vitrimers were synthesized by condensation of the acetoacetate-modified cardanol with two diamines (m-xylylenediamine and 4,4-diaminocyclohexylmethane). Cardanol-based shape memory vitrimers were subsequently used in the examination of the effect of latent plasticity on the shape recovery (Fengbiao Chen et al., 2021). It was

CHAPITRE 1

demonstrated that dissipation of stored energy was caused during longer shape-programming time due to bond rearrangements. The stress-relaxation of the strained regions showed to be detrimental to shape recovery of the material.

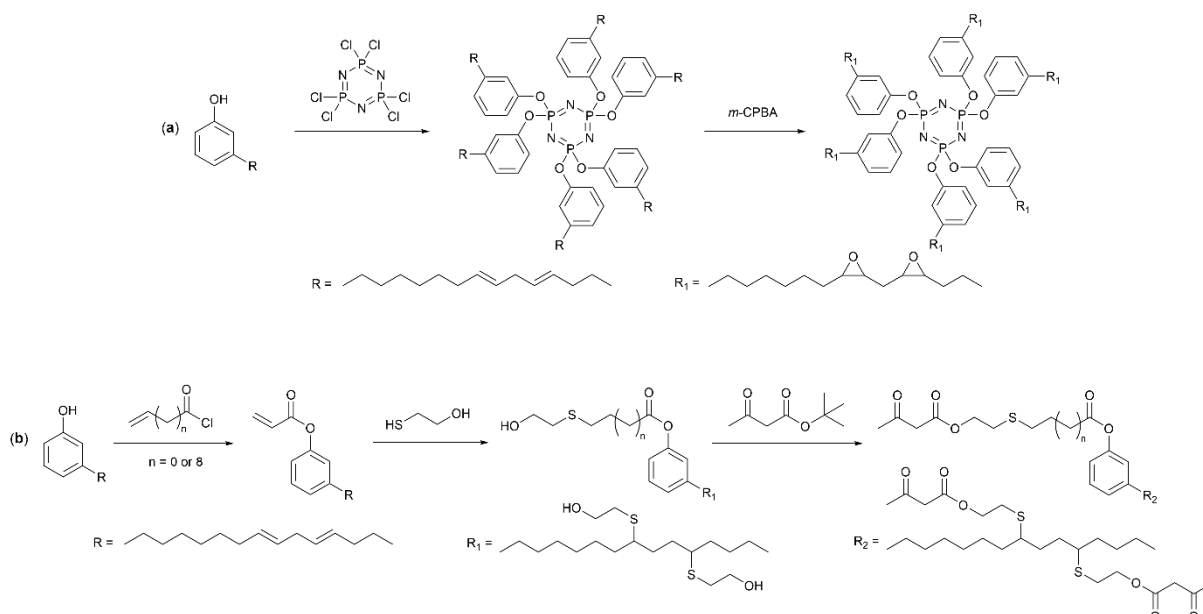


Figure 1-23. Cardanol as precursor for the preparation of CANs.

Table 1-4. Main stress-relaxation, physical and chemical recycling parameters of CNSL-derived CANs.

Biomass	Dynamic linkage	E_a (kJ mol ⁻¹)	τ	Physical recycling conditions ^a	Chemical recycling conditions	Ref.
CNSL	Ester	40.7 – 54.9	n/a	n/a	n/a	(Kasemsiri et al., 2018)
CNSL	Ester	51.4 – 55.7	~200 s at 100 °C	n/a	DMF, 100 °C, 2 h	(Lorwanishpaisarn et al., 2021)
CNSL	Ester	55.7 – 62.4	~200 s at 100 °C	n/a	n/a	(Lorwanishpaisarn et al., 2022)
CNSL	PHU	n/a	n/a	n/a	n/a	(Purwanto et al., 2023)
CNSL	Thiourethane + disulfide	33.0 – 66.0 ^c	n/a	140 °C, 7-ton ram, 1 h.	n/a	(Yixuan Chen et al., 2023)
Cardanol	Disulfide	64.5	18 s at 120 °C	120 °C, 5 bars, 1 min	n/a	(Trejo-Machin et al., 2020)
Cardanol	Boronic ester	n/a	n/a	160 °C, 16 MPa, 2 h	n/a	(X. Wang et al., 2022)
Cardanol	Boronic ester	50.2 – 63.5	40 – 60 s at 40 °C ^b	120 °C, 10 MPa, 5 min	THF, 35 °C, 96 h	(Bo et al., 2022)
Cardanol	Boronic ester	n/a	n/a	150 °C, 10 MPa, 15 min	n/a	(Ke et al., 2021)
Cardanol	Vinylogous urethane	n/a	n/a	130 °C, 10 MPa, 40 min	cyclohexylamine/benzylamine, 130 °C, 40 min	(Chen et al., 2020)
Cardanol	Vinylogous urethane	33.0	55 s at 130 °C	130 °C, 10 MPa, 30 min	n/a	(Fengbiao Chen et al., 2021)

^a conditions of physical recycling are given as follow: temperature, time, applied pressure or force. ^b graphical values. ^c activation energies obtained via creep experiments.

To outline the current trends in the field of dynamic networks prepared from CNSL-derived precursors, the main stress-relaxation, physical and chemical recycling parameters of aforementioned CANs are summarized in Table 1-4. The potential of CNSL and cardanol as building blocks for the preparation of CANs was herein highlighted, in particular owing to their combination potential with several dynamic bonds. Boronic esters, disulfides, and vinylogous urethane offered overall mild physical recycling conditions requiring acceptable temperatures and compression times. However, although physical recycling was studied, a lack of critical rheological characterizations required to properly demonstrate the dynamicity of networks can be observed in several studies.

4.2.4. Furan and derivatives

5-(hydroxymethyl)furfural and 2,5-furandicarboxaldehyde

Although the versatility of 5-(hydroxymethyl)furfural (HMF) was demonstrated in multiple research fields such as fine chemicals and polymers, the full potential of its rich chemistry has not been fully exploited in CANs till now (Table 1-5, Figure 1-24, and Figure 1-25) (Zhang and Dumont, 2017). For concision purpose, this section only discusses the utilization of furan derivatives as main building blocks in the preparation of CANs. Thus, the grafting of furan groups on end-chain to undergo Diels-Alder reactions for instance is not covered since different reviews have already discussed this topic (Briou et al., 2021; Gandini et al., 2016; Gevrek and Sanyal, 2021; Karlinskii and Ananikov, 2023; Liu and Chuo, 2013; van den Tempel et al., 2022). Avérous and co-workers (Dhers et al., 2019) reported the very first fully biobased polyimine vitrimer containing 100% renewable carbons, by combining a fructose-derived furan dialdehyde with biobased amines. This vitrimer was prepared from the oxidation of HMF into 2,5-furandicarboxaldehyde (FDC), followed by its condensation with a mixture of biobased di- and triamines derived from fatty acids (Figure 1-24a). Fast network rearrangement via transamination was observed through short relaxation times at low temperatures because of a relatively large excess of amines, enabling swift physical recycling but simultaneously leading to significant amount of creep deformation at low temperatures (0 to 40 °C) and under relatively low stress (2000 Pa). With the highlighted potential of furan-based polyimine towards environmentally-friendly vitrimers, it was latter demonstrated that by varying the di- and triamine ratios and the molar mass of the diamine, the network crosslinking densities would influence its dynamicity (Figure 1-24b) (Hajj et al., 2020, p. 20). Although similar chemical structures were obtained, a decreasing crosslinking density reduced the relaxation times and activation energies of the materials. In addition to a chemical control with for instance the introduction of an excess free reactive groups, physical control is also a key to tune the relaxations properties, facilitating the recycling of vitrimers. Moreover, the peculiar structure of furan within associative polyimine vitrimer was further exploited by introducing dissociative dynamic linkages (Figure 1-24c) (Lucherelli et al., 2023). CANs combining two rearrangement mechanisms, also referred as dual dynamic networks, have recently emerged with the pursuit of achieving more refined and engineered properties (Hammer et al., 2021; Jiang et al., 2019). The strategy disclosed enables the introduction of dual mechanisms without adding extra synthesis steps through Diels—Alder reactions of the furan ring with bismaleimides. The combination of the two mechanisms facilitates stress-relaxation, even at low temperature, while preserving the mechanical properties after several physical recycling steps. The combination of thiol-Michael addition and Diels-Alder reaction to prepare elastomers from HMF (Figure 1-25a) was reported (Zhang and Dumont, 2018). The network was synthesized via thiol-Michael addition of 2,5-furan diacrylate and 1,3-propanedithiol followed by the Diels-Alder reaction between furan rings and maleimides (Zhang et al., 2016). Although the study was preliminary, the resulting networks exhibit a potentially interesting dual dynamicity which would benefit further investigations. The dynamic crosslinked films were nonetheless recycled by dissolution in dimethylformamide at 130 °C and prepared again by solvent casting.

A fully biobased poly(acetal) network prepared in a single atom-efficient step (>90% atom economy) from FDC and sorbitol, a sugar alcohol obtained from reduction of glucose, was recently uncovered (Figure 1-24d) (Mao Png et al., 2023; Png et al., 2022). Material could be physically recycled at temperatures around its T_g of 120°C. Initial mechanical properties were recovered via water-mediated recycling and the monomers were retrieved by heating in green solvents such as water and ethanol.

Although the dynamicity was not studied, it is worth mentioning the recently reported preparation of an epoxy resin abundant in furan-derived compounds containing hydrazone bonds as potential CANs (Figure 1-25b) (Nabipour et al., 2023). The resin was synthesized from HMF and cured with a difurfurylamine curing agent in a two-pot synthesis. Imine-induced relaxation was not studied however the material was successfully degraded through acid hydrolysis, thus implying its potential as dynamic network. Recently, an alternative route to furfuryl derivation was suggested apart from typical

CHAPITRE 1

oxidation of HMF into FDC, which often requires heavy metal catalysis (Figure 1-25c). Authors subject HMF to straightforward self-etherification under *p*TsOH catalysis for the preparation of high biobased content polyimine networks (78 to 90 wt%). Good tunability was achieved by virtue of the multiamine functionality and excellent closed-loop chemical recyclability (Türel et al., 2024).

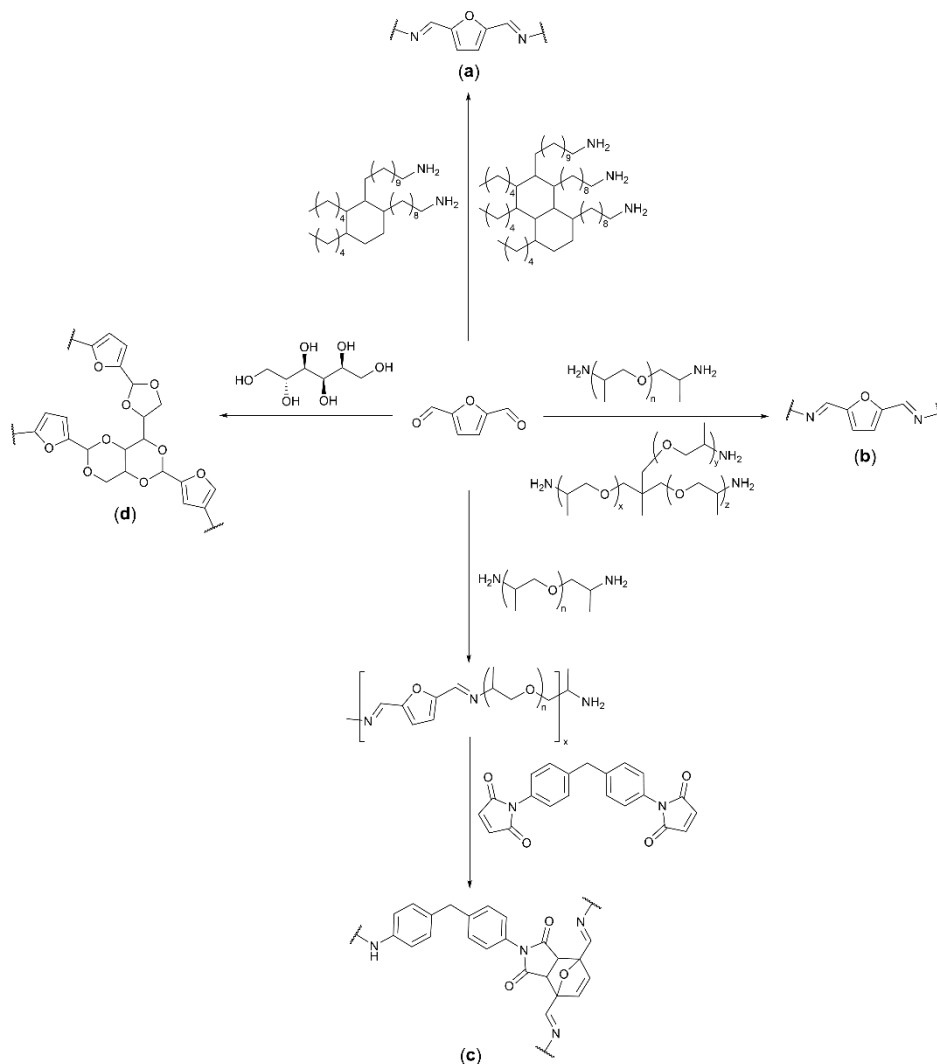


Figure 1-24. 2,5-furandicarboxaldehyde as a precursor for the preparation of CANs.

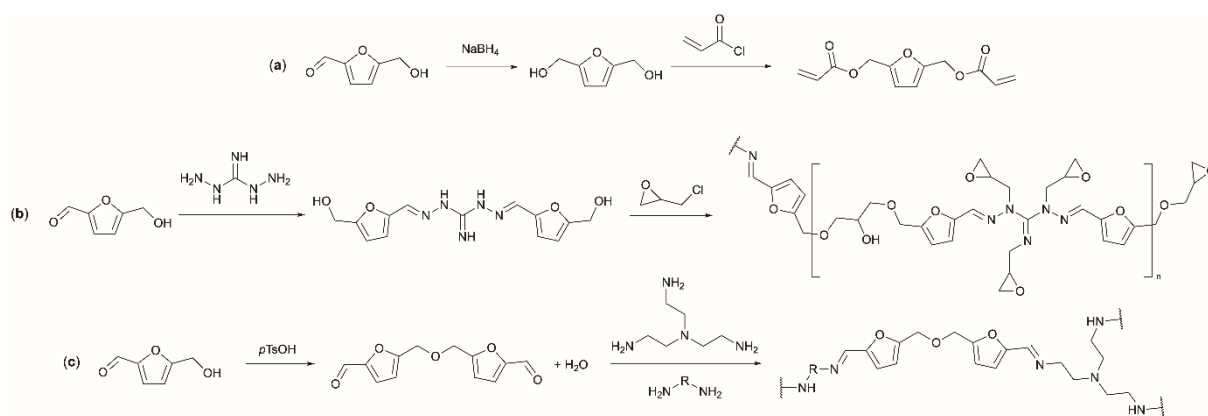


Figure 1-25. 5-(hydroxymethyl)furfural as precursor for the preparation of CANs.

Furfural

PU networks combining acetal and Diels-Alder dynamic linkages were synthesized from acetal diol derived from furfural and 1,6-hexanediol with trifunctional isocyanate (Q. Li et al., 2021a). The properties of the network could be tuned by Diels-Alder reaction between furan ring and bismaleimides. Density functional theory (DFT) calculations and model studies demonstrated that acetal linkages substituted by a furan ring or a benzene ring undergone a dissociative exchange rearrangement via a carbocation mechanism. PUs combined excellent recyclability and outstanding high-temperature creep resistance. Materials containing only acetal exhibited strain recovery after the creep experiments of 100% at 110 °C and 98% at 120 °C, while networks combining acetal and DA bonds could only return to its initial strain at 110 °C because of the retro-DA reaction occurring above this temperature.

2,5-bis(hydroxymethyl)furan (BHMF)

The potential of mechanochemical processes for the production of environmentally benign networks was highlighted through the preparation of PUs-based CANs under facile, solvent-free and ball milling condition (Kim et al., 2021). The networks were synthesized from BHMF, 1,6-hexanediol, *meso*-Erythritol, 1,6-hexamethylene diisocyanate and dibutyltin dilaurate. Authors reported surprisingly fast relaxation for the dissociation of alkyl-NCO/alkyl-OH (around 15 s at 190 °C). Usually, cleavage of such urethanes occurs at higher temperatures (250 °C) and over longer timescale of temperature exposition as discussed in section 3.2.4. Dissociative cleave of urethane bonds was suspected to occur instantaneously enabling facilitated reprocessing, self-healing and shape memory ability.

2,5-furandicarboxylic acid (FDCA)

Fully biobased star-shaped non-isocyanate poly(ester urethane) were prepared by step growth polymerization of FDCA with PHU adducts bearing hydroxyl groups (Quienne et al., 2020). PHU building blocks were obtained by aminolysis of glycerol carbonate with two aliphatic diamines of different chain length. Preliminary results indicated possible transcarbamoylation revealed by thermal changes within the networks upon repetitive heating cycles. This vitrimer-like behavior was then reported for the first time in poly(ester hydroxyurethane) networks, paving the way toward the development of a new range of dynamic materials. Recently, FDCA was used as curing agent for the preparation of diglycidyl ether bisphenol A (DGEBA) derived epoxy vitrimer, in the presence of triazabicyclodecene as catalyst (Manarin et al., 2023). Faster topology rearrangement was observed for a FDCA/DGEBA molar ratio of 0.6, reaching a relaxation time of 30 s at 180 °C, making this system quite attractive compared with analogous proposed epoxy vitrimers.

To conclude on the latest trends on furan-derived CANs, the main stress-relaxation, physical and chemical recycling parameters of studies in the field are listed in Table 1-5. This overview highlights the considerable versatility of furan-derived compounds. Owing to their wide range of reactive groups, they can be suitable with various dynamic covalent chemistries, such as imine, acetal, urethane or esters. Moreover, the combination of dynamic imine bonds with HMF for instance allows facile synthesis of materials following limited reaction steps and showing excellent stress relaxation in mild conditions (few seconds at 65 °C for instance), thus enabling rapid reprocessing. Finally, some furan groups used in the preparation of CANs can also be involved in Diels-Alder reactions, with the ability of combining different exchange mechanisms and/or post-polymerization modifications.

Table 1-5. Main stress-relaxation, physical and chemical recycling parameters of furan-derived CANs.

Biomass	Dynamic linkage	E_a (kJ mol ⁻¹)	τ	Physical recycling conditions ^a	Chemical recycling conditions	Ref.
HMF	Imine	64	40 s at 80 °C	120 °C, 20 tons, 10 min	1 M butylamine in THF, 24 h, 25 °C	(Dhers et al., 2019)
HMF	Imine	64 – 103	4 – 60 s at 65 °C	120 °C, –, 1 h	1 M HCl, RT, 24 h	(Hajji et al., 2020)
HMF	Imine + Diels-Alder	86 – 104	5 – 50 s at 65 °C ^b	80 °C, –, 40 min	n/a	(Lucherelli et al., 2023)
HMF	Thiol-Michael + Diels-Alder	n/a	n/a	n/a	DMF, 130 °C, 2 h	(Zhang and Dumont, 2018)
FDC	Acetal	110	8 s at 150 °C	140 °C, 5 bars, 30 min	H ₂ O, methanol, of ethanol, 80 °C, 16 h	(Png et al., 2022)
HMF	Imine	n/a	n/a	n/a	HCl in THF, RT, 24 h	(Nabipour et al., 2023)
HMF	Imine	n/a	n/a	n/a	1 M HCl, 50 °C, 24 h	(Tirel et al., 2024)
Furfural	Acetal + Diels-Alder	118 – 126	33 min at 200 °C ^b	190 °C, 10 MPa, 1 h	0.1 M HCl acetone/H ₂ O, 25 °C, 10 min	(Q. Li et al., 2021a)
BHMF	PU	109 – 196	15 – 50 s at 190 °C ^b	160 °C, 30 MPa, 4 h	n/a	(Kim et al., 2021)
FDCA	Ester	93 – 219	30 – 2499 s at 180 °C	160 °C, 100 bar, 30 min	n/a	(Manarin et al., 2023)

^a conditions of physical recycling are given as follow: temperature, time, applied pressure or force. ^b graphical values.

4.2.5. Other aromatic building blocks

Eugenol

Its unique structure including methoxy-substituted phenolic ring and allyl group makes eugenol an interesting compound in the preparation of dynamic epoxy resins. Diepoxy monomer was reported following the synthesis of a diene monomer by reaction of eugenol with 1,4-dibromobutane, which was further modified with meta-chloroperbenzoic acid (*m*-CPBA) (Figure 1-26a) (T. Liu et al., 2017). The ring opening reaction was performed with succinic anhydride in several ratios. Only material with 1:0.5 ratio was successfully physically recycled. However, the other systems could be chemically recycled in ethanol loaded with catalyst. Following similar chemical modification pathway, mixture of mono and diepoxy eugenol derivatives as model system were prepared to evaluate the effect of commercially available epoxy mixtures containing various epoxy fractions on the properties of the final vitrimers (Tannert et al., 2023). In this model system, monoepoxy monomers represented the effect of monofunctional impurities extending the polymer chain but not permitting crosslinking reactions. Overall, higher epoxy fractions and content were found to decrease the glass transition temperatures. However, exchange reactions remained unchanged with significant fraction of impurities, enabling unaffected reshaping and recycling, leading to proper vitrimers with still attractive properties. The synthesis of tri(epoxidized-eugenyl) phosphate epoxy monomer was considered via the treatment of eugenol with phosphorus oxychloride, followed by the epoxidation of allylic groups with *m*-CPBA (Figure 1-26b) (Miao et al., 2020; Ocando et al., 2020). The triepoxy monomer was cured with disulfide containing amine crosslinker (4-aminophenyl disulfide) to obtain high T_g materials (190 to 217 °C) with 70 to 100% renewable carbon content. Young modulus, strength at break and elongation at break reached 4145 MPa, 95.2 Mpa and 3.3%, respectively. Besides, the shape shifting ability of such network was observed by the spontaneous deformation from planar film to 3D “rocking chair”, as well as the flame retardancy property (Miao et al., 2020). Another strategy for the synthesis of eugenol epoxy precursor consists of the click thiol-ene reaction between eugenol allyl groups and previously prepared mercaptoesters by esterification of ethylene glycol, trimethylolpropane, and pentaerythritol with 3-mercaptopropionic acid (Figure 1-26c) (W. Li et al., 2022). The preparation of double functional epoxy was done through the hydrosilylation of eugenol with 1,1,3,3-tetramethyldisiloxane, followed by the glycidylation of the silicone monomer with epichlorohydrin (Figure 1-26d) (W. Li et al., 2021). 4-aminophenyl disulfide was used as curing agent to prepare the final epoxy resin. The different pathways all give materials with good self-healing ability and fast relaxation above 200 °C.

CHAPITRE 1

The combination of thiol-ene and thiol-oxidation reactions in a self-healing eugenol-derived material was disclosed (Cheng et al., 2016). This study reported the first self-healing eugenol-derived benzoxazine network by leveraging from reversible S-S bonds. In this context, eugenol was modified by 1,4-phenylenediamine and formaldehyde through a Mannich condensation (Figure 1-26e), followed by thiol-ene click polymerization with 1,6-hexanedithiol. The benzoxazine precursor was then crosslinked with trimethylolpropane tris(3-mercaptopropionate) under oxidative conditions to form disulfide bonds and was compared with a second polymer obtained from *O*-allylic eugenol previously prepared by reaction of eugenol with allyl bromide (Figure 1-26f), and cured with the former crosslinker by thiol-ene reaction. The reversibility imputed to the disulfide exchange was demonstrated through self-healing triggered by UV exposure. Subsequently, the synthesis of a benzoxazine precursor through Mannich condensation reaction between eugenol, 3-amino-1-propanol and paraformaldehyde (Figure 1-26g) was recently disclosed (Sriharshitha et al., 2022). Then, the polymer was simultaneously crosslinked via thermal ring opening polymerization of the benzoxazine monomer and thiol-ene reaction performed on the allyl reactive sites employing 3-mercaptopropyl trimethoxysilane and thiol-bearing bio-silica in various ratios, the latter forming S-S bonds with SH reactive end groups. Reshaping was observed at room temperature without the application of an external pressure, owing to the disulfide bonds and strong hydrogen interactions between S-H and phenolic O-H groups.

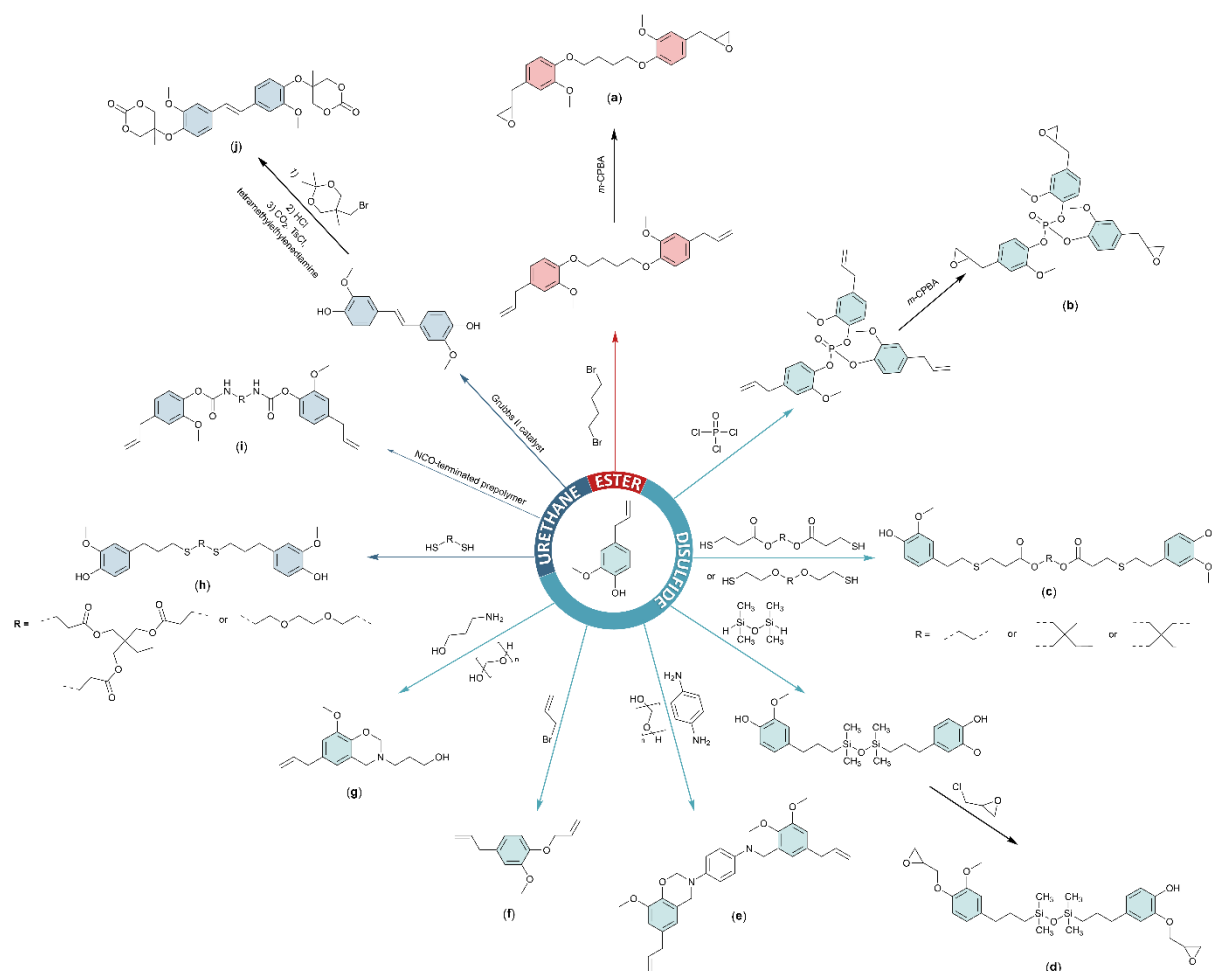


Figure 1-26. Different Eugenol chemical modifications into precursors for the synthesis of ester, disulfide, and urethane-based CANs.

Self-healable eugenol-derived PU networks were reported by leveraging from the reversible phenol-carbamate reaction (Figure 1-26h) (Liang et al., 2019; Y. Lin et al., 2022). In that respect, polyphenols were prepared from the addition reaction of eugenol with 3,6-dioxo-1,8-octanedithiol or

trimethylolpropane tris(3-mercaptopropionate) in the presence of 2-dimethoxy-2-phenyl-acetophenone (Y. Lin et al., 2022). Polyphenols were used to crosslink a commercial isocyanate prepolymer derived from polytetrahydrofuran to obtain the final network. Unsurprisingly, the healing ability at 120 °C of the bisphenol-derived PU was improved compared to the triphenol counterpart because of the chain diffusion in absence of crosslinks leading to thermoplastic behavior. Healing abilities of tensile strength of 73.5 and 24.1% were obtained respectively. Moreover, the difficulties to repair some samples was attributed to the partial dissociation of urethane bonds and passivation of resulting free isocyanates by water vapor present in air. Another proposed synthetic pathway consists of solvent and catalyst-free addition of eugenol in a poly(tetramethylene ether glycol)/4,4'-methylene bis(phenyl isocyanate) prepolymer (Figure 1-26i) (Liang et al., 2019). A crosslinked network was obtained through the radical copolymerization of the linear eugenol-derived PU with styrene. Here, mechanical properties were poorly recovered after healing of the copolymers at 160 °C for 24 h. However, increasing the eugenol-derived PU content enabled the improvement of the healing efficiency, by increasing the amount of reversible phenyl-carbamate bonds.

Finally, chemically recyclable non-isocyanate PU (NIPU) networks derived from eugenol were recently reported (Liu et al., 2023). Bis-eugenol molecule was obtained by cross-metathesis of isoeugenol and was further modified by protection-deprotection procedures and reacted with CO₂ to obtain cyclic carbonates (Figure 1-26 j). Eugenol-derived cyclic carbonate was cured with different content of polyether diamine and tris(2-aminoethyl)amine to obtain the final NIPU. In addition to successful reprocessing, the materials were degraded through alcoholysis into bis(1,3-diol) precursors of high purity (>99%) and yield (>99%) and can be reused to generate a novel generation of structurally similar NIPUs.

Hydroxycinnamic acids

Cinnamic acid and its derivatives, are known for decades to undergo reversible [2 + 2] cycloaddition under UV light at a specific wavelength (Kaur et al., 2014; Poplata et al., 2016). Crack healing polymers through [2 + 2] cycloaddition of cinnamoyl groups was already reported in 2004 (Chung et al., 2004), as well as light-induced shape memory polymers by Lendlein in 2005 (Lendlein et al., 2005). Latter, triple shape memory PU based on poly(ϵ -caprolactone) containing photo-crosslinkable cinnamoyl groups were disclosed (Wang et al., 2013). Rochette and Ashby prepared a library of poly(ester urethane)s from novel bifunctional monomers derived from cinnamoyl chloride (Rochette and Ashby, 2013). Ensuing materials showed to be crosslinkable under UV light at 302 nm, with temporary fixed macroscopic shapes, and de-crosslinkable at 254 nm, with the shape recovery.

For concision purpose, this section is only focused on biobased cinnamic derivatives in CANs. Moreover, only studies which examined the reversibility of [2 + 2] cycloaddition on polymeric materials are mentioned. Recently, researchers have renewed their interest on cinnamic acid as a building block for the development of biobased photo-reversible epoxy resins, or epoxy vitrimers (Cao et al., 2023; D. Jin et al., 2023). The first epoxy vitrimer containing N-heterocycle was recently synthesized from cinnamic acid and succinic anhydride-derived epoxy monomer obtained via a four-step procedure: i) Fridel-Crafts reaction, ii) cyclization, iii) dehydrogenation, and iv) glycidylation (Cao et al., 2023). The epoxy monomer was then cured with 4,4'-diaminodiphenyl methane. Resultant vitrimer, in addition to exhibiting stress-relaxation through transesterification bond exchange, was also successfully upcycled by dissolution in ethylene glycol.

Other hydroxycinnamic acids such as caffeic acid, ferulic acid and *p*-coumaric acid, have gained interest as renewable and aromatic structures. In this context, photo-crosslinkable polyesters were synthesized from caffeic acid (CA) through selective lipase-catalyzed polymerization (Bazin et al., 2022). A novel aromatic diol containing a pendant α,β -unsaturated ester was prepared from esterified and further oxyalkylated CA. Caffeic-derived monomer was polymerized with 1,6-hexanediol and diethyl adipate employing lipase B from *Candida Antarctica* as catalyst. Under 350 nm irradiation, a

three-dimensional network was created via the formation of cyclobutane units between carbon-carbon double bonds. A similar approach was reported where the same CA-derived aromatic diol (EC-diol) was integrated within a thermoplastic PU elastomer with unsaturated esters as pendant chains (Figure 1-27) (Duval and Avérous, 2023). In both cases, decrosslinking was achieved under irradiation of UV light at 254 nm. However, the decrosslinking was only partial because of the limited penetration depth of the UV radiation in the materials.

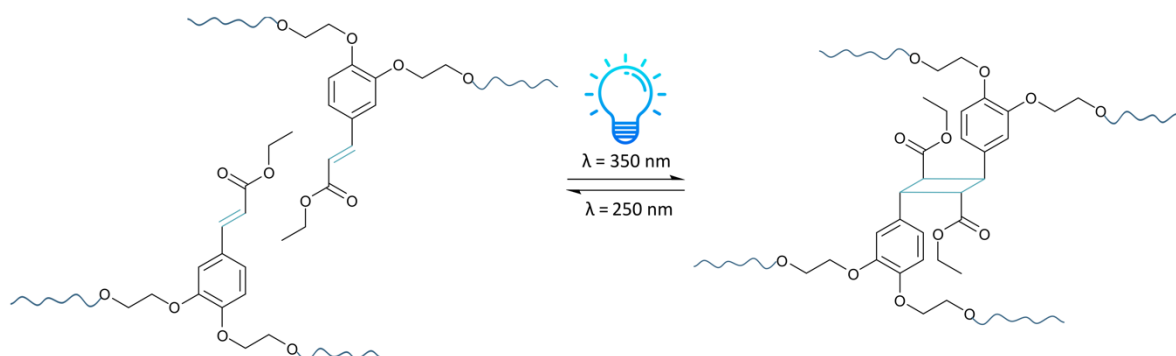


Figure 1-27. Reversible crosslinking by [2 + 2] photocycloaddition of TPU prepared from EC-diol.

To design further sustainable epoxy thermosets from cinnamic acid derivatives, closed-loop recyclable fully biobased networks prepared from ferulic acid (FA)-derived epoxy resin (FEP) and FA-based hyperbranched epoxy resin (FEHBP) obtained by glycidylation, and cured with citric acid (CA) were developed (Zhong et al., 2022). The integration of FEHBP significantly improved the mechanical properties of the vitrimers by increasing their free-volume and crosslinking density, reaching high tensile strength of 126.4 MPa and T_g of 94 °C while exhibiting fast relaxation (45 s at 140 °C). The materials demonstrated efficient reprocessing and healing ability through transesterification exchange reactions as well as closed-loop chemical recycling following basic treatment with NaOH. The recovered ferulic and citric acids were reused in the preparation of 2G vitrimers exhibiting excellent mechanical and thermal properties.

Urushiol

To date, only the preparation of sulfur-urushiol self-healable copolymer synthesized through inverse vulcanization, a catalyst and solvent-free process, was reported (Shen et al., 2022). By combining the catechol rich structure of urushiol and S-S metathesis, the dynamic network showed adhesion performance comparable to polydopamine derivatives while exhibiting heat and nucleophilic solvent-induced reparability. The influence of the sulfur content was discussed on the thermal, mechanical, and rheological properties. For instance, higher sulfur content increased the crosslinking density and improved the S-S metathesis kinetics, reflected by a faster stress-relaxation.

Phloretic acid and tyrosol

To this day, the only reports of phloretic acid utilization as CANs precursor were published in the context of polybenzoxazine vitrimers preparation (Adjaoud et al., 2023, 2022). In the two studies, this structure was reacted via Fischer esterification with isosorbide or lignin, followed by Mannich-like ring-closure reactions with amines to prepare biobased benzoxazine monomer with a high atom economy of 85% (Figure 1-28a and b). Isosorbide-based precursors could reach 100% biobased content. High T_g networks were obtained for the two systems, with values from 143 to 193 °C and from 136 to 197 °C, for isosorbide and lignin-based vitrimers, respectively. Good circularity was also achieved through fast relaxation enabling facile recycling.

Similarly, tyrosol-based benzoxazine monomer was synthesized via Mannich-like condensation with dodecylamine and paraformaldehyde (Figure 1-28c) (Wen et al., 2022). From the precursor, a catalyst-free crosslinked biobased polybenzoxazine-PU network was prepared leveraging from dynamic carbamate chemistry, showing successful reprocessability in mild conditions (130 °C, 10 min).

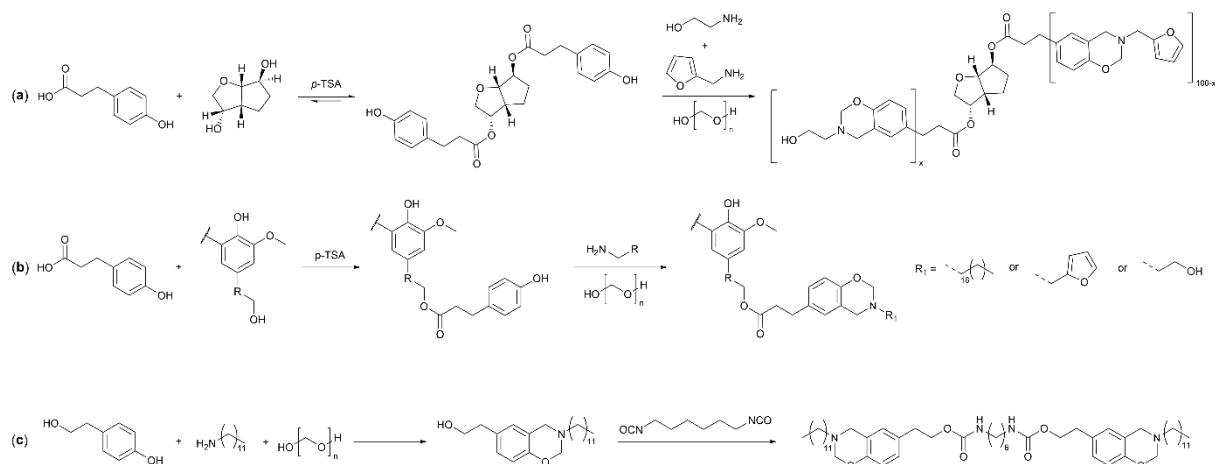


Figure 1-28. Synthetic pathways for the preparation of biobased benzoxazine precursors from phloretic acid and tyrosol.

Resveratrol

To overcome the concern raised about catalyst leaching and accelerating the aging of vitrimers upon reprocessing, resveratrol-based polyesters networks containing α,α -difluoro esters to promote transesterification reactions due to strong electron-withdrawing character of CF₂ moieties were developed (Cuminet et al., 2023). A trifunctional epoxy monomer and a trifunctional α,α -difluoro carboxylic acid were synthesized from resveratrol, by reactions with epichlorohydrin and ethyl bromodifluoroacetate, respectively. The vitrimer obtained upon the reaction of both precursors exhibited high biobased carbon content of 86%, of which between 50 and 56% are aromatic, resulting in a high T_g of 117 °C, making it one of the first high- T_g catalyst-free biobased vitrimer.

To conclude on the latest trends in literature, the main stress-relaxation, physical and chemical recycling parameters of eugenol, hydroxycinnamic acids, urushiol, phloretic acid, and tyrosol-derived CANs are listed in Table 1-6. This overview highlights the benefits of the valorization of the reactive sites present on the building blocks. For instance, hydroxyl and allylic moieties of eugenol makes it easily suitable for ester and disulfide chemistries, whereas cinnamoyl groups of hydroxycinnamic acids can easily undergo photodimerization. However, it is noteworthy to mention that limited recovery is often observed owing to restrained penetration depth of the UV radiation in the materials and leading to a restricted amount of crosslinking/decrosslinking cycles. Moreover, employing an aromatic compound enabling the combination of light-induced and thermally-induced dynamic bonds proved to be an efficient strategy to unite the conflicting properties of dimensional stability (creep resistance) and reversibility of the CANs.

Table 1-6. Main stress-relaxation, physical and chemical recycling parameters of eugenol, hydroxycinnamic acids, urushiol, phloretic acid, and tyrosol-derived CANs.

Biomass	Dynamic linkage	E _a (kJ mol ⁻¹)	τ	Physical recycling conditions ^a	Chemical recycling conditions	Ref.
Eugenol	Ester	n/a	128 s at 200 °C	200 °C, –, 1 h	Ethanol, 160 °C, 5 h	(T. Liu et al., 2017)
Eugenol	Ester	n/a	n/a	200 °C, –, 0.5 h	n/a	(Tannert et al., 2023)
Eugenol	Disulfide	146.0	37 s at 230 °C	230 °C, 20 bar, 3000 s	n/a	(Ocando et al., 2020)
Eugenol	Disulfide	90.7	27 s at 230 °C	n/a	n/a	(Miao et al., 2020)
Eugenol	Disulfide	70.5 – 110.6	107 – 301 s at 200 °C	60 °C, 20 MPa, 4 h + 180 °C, 20 MPa, 2 h	phosphotungstic acid + zinc (II) acetylacetonate + DMF in ethanol, 160 °C, 2 h	(W. Li et al., 2022)
Eugenol	Disulfide	50.5	28 s at 200 °C	200 °C, 20 MPa, 240 min	<i>m</i> -CPBA/DMF (1:1), 30 °C, 5 h, 60 Hz	(W. Li et al., 2021)
Eugenol	Disulfide	n/a	n/a	RT, –, 10 h	n/a	(Sriharshitha et al., 2022)
Eugenol	Urethane	110.0 – 115.0	21 – 40 min at 200 °C	210 °C, 8 – 12 MPa, 2 h	30 wt% NaOH, 90 °C, 4 h	(Liu et al., 2023)
Cinnamic acid	Ester	168.0	88 s at 250 °C	n/a	ethylene glycol, 230 °C, 4 h	(Cao et al., 2023)
CA	[2 + 2] CA	n/a	n/a	n/a	350 nm, 250 min/254 nm, 5 min	(Bazin et al., 2022)
CA	[2 + 2] CA	n/a	n/a	n/a	355 nm, 180 min/254 nm, 60 min	(Duval and Avérous, 2023)
FA	Ester	98.0 – 135.0	45 – 2745 s at 140 °C	140 °C, 5 MPa, 30 min	30 wt % NaOH, 80 °C, 30 min	(Zhong et al., 2022)
Urushiol	Disulfide	65.9 – 102.9	100 – 500 s at 80 °C ^b	n/a	n/a	(Shen et al., 2022)
Phloretic acid	Ester	126.0	300 s at 180 °C	175 °C, <10 Pa, 1 h	Acetic acid, 25 °C, 60 days	(Adjaoud et al., 2022)
Tyrosol	Urethane	92.0	~2 s at 130 °C ^b	130 °C, 10 MPa, 10 min	n/a	(Wen et al., 2022)
Resveratrol	Ester	107.0	156 s at 210 °C	170 °C, 8 MPa, 2 h	n/a	(Cuminet et al., 2023)

^a conditions of physical recycling are given as follow: temperature, time, applied pressure or force. ^b graphical values.

5. APPLICATIONS OF BIOBASED AND AROMATIC CANS

The combination of CANs reprocessing/recycling features with performances brought by biobased aromatic structures confer to these sustainable materials outstanding and unprecedented functionalities. This section discusses the strong contribution of aromatic and conjugated structures in the achievement of specific properties required for targeted applications, including biomedical devices, flame retardants, adhesives, or coatings.

5.1. Biomedical applications

Dynamic covalent bonds within biomedical devices is of utmost relevance to provide materials with excellent features including advanced mechanical properties, self-healing, controlled degradability and recyclability (Wendels and Avérous, 2021; Xu et al., 2019). These smart structures, adaptable to their environments, have already emerged for applications including for instance wound dressing (M. Chen et al., 2022; Konieczynska et al., 2016), tissue engineering (Kim et al., 2019), or drug delivery (Boyer and Hoogenboom, 2015; Solanki and Thakore, 2015).

5.1.1. Wound sealants

Adhesive hydrogel sealants containing dynamic crosslinks can offer infected wound healing and on-demand removability for post-wound closure (Liang et al., 2021). Dynamic imine bonds and catechol-Fe coordinate crosslinks were combined in a network containing protocatechualdehyde providing catechol and aldehyde groups, ferric iron, and quaternized chitosan as in-vivo skin sealing promoting the healing of infected wound. The pH-responsive hydrogel presented outstanding

autonomous healing and on-demand dissolution revealing good removal features. Good injectability, biocompatibility, antibacterial activity, adhesiveness, and hemostasis enabled high wound closure effectiveness.

5.1.2. Implants and tissue engineering

Conductive hydrogels containing dynamic boronic ester bonds formed between boronic acid-functionalized alginate and cis-diol moieties of an oligomerized epigallocatechin gallate were found to behave like electrical interconnectors when soaked in NaCl solution (Choi et al., 2021). The hydrogels were employed for “electrophysiological bridging” for the transfer of electromyographic signals in an ex vivo muscle defect model. When placed between the parallel rat hind limb muscle tissues, similar muscle-to-muscle amplitude and pattern was observed for muscle-hydrogel-muscle signal revealing satisfactory performance as a biocompatible and self-healable implantable electronics.

Scaffolds showing self-healing under ambient conditions and increased cell growth properties were reported from vanillin precursor (Yasar et al., 2023). Hydrogels were synthesized from UV-polymerized vanillin methacrylate monomer bearing aldehyde groups enabling imine linkages. Scaffolds were coated with collagen to increase the cell growth compared to the pristine hydrogel. Cell viability of the coated samples reached between 124 to 163% of increase compared to the control sample, showing high potential for tissue engineering applications.

5.1.3. Drug release

All-small-molecules hydrogels offer a promising strategy for the preparation of smart hydrogels presenting unique features including facile synthesis, bio-responsiveness and minimized material toxicity. In this context, formylboronic acids (FBA) bearing aldehyde and boronic acid reactive sites were used as bifunctional crosslinkers to integrate tannic acid (TA) and tobramycin (TOB) in the fabrication of an antibacterial and multi-stimuli responsive covalent hydrogel (Cheng et al., 2022). TA is an interesting precursor with antimicrobial action thanks to its strong complexation with iron (Chung et al., 1998). Controlled drug release profile was demonstrated through temperature-induced dissolution of the gel, linked to the diminution of intermolecular hydrogen bondings, via acid hydrolysis of imine and catechol-boronate network. This system is particularly suitable for the release of TOB in the acidic micro-environment created by bacterial colonization. Similarly, hyaluronan/tannic acid nanoparticles leveraged from the pH-induced reversibility of catechol/boronate bonds to act as a smart antibacterial system (Montanari et al., 2016). Herein, the boronate dynamic linkage enables the protection and controlled delivery of TA, leading to the reduction of the bacterial density.

5.2. Flame retardant applications

To minimize fire risk and meet fire safety requirements, it is necessary to retard ignition and lower the heat released during the combustion of polymer materials (Laoutid et al., 2009). In this context, biobased aromatic structures can be effective sources of carbon for flame retardant (FR) applications (M. Wang et al., 2023). The assets of biobased aromatic compounds for the design of FR polymer materials has been reported through several reviews (Wang et al., 2023; Costes et al., 2017; Yang et al., 2020; Sonnier et al., 2018; Hobbs, 2019), and has not gone unnoticed in the realm of CANs. To turn a combustible CAN into a self-extinguishing one, strategies either rely on the incorporation of phosphorus within networks acting as catalyst for char formation, or on the char-forming ability of aromatic building blocks and specific dynamic covalent bonds.

9,10-dihydro-9-oxa-10-phosphaphenanthrene-10-oxide (DOPO) was used as reactive FR agent in the preparation of an epoxy resin employing vanillin-derived imine compound as hardener alongside with biobased glycerol triglycidyl ether as epoxy monomer, increasing limiting oxygen index (LOI) values from 20 to 26% (Tian et al., 2023). Reprocessing of the vitrimers was enabled because of the fast

stress relaxation of imine bonds. Epoxy vitrimers prepared from the condensation of two vanillin-derived epoxy monomers in different ratios with diamino diphenylmethane were also reported to reach UL-94 V0 rating while only containing 0.66% of DOPO (W. Yang et al., 2022). Phosphorus can also be integrated within CANs matrixes through the synthesis of cyclophosphazene-based monomers from vanillin bearing imine bonds (Zamani et al., 2022; Peng et al., 2022; T. Liu et al., 2021). Owing to a rich P/N content and the benzene rings, vitrimers not only exhibited excellent resistance to flame but also to UV (Peng et al., 2022). Indeed, imines exhibit outstanding char-forming while allowing network degradability in acidic conditions. Reminiscent of the aforementioned studies, nucleophilic aromatic substitution of pentafluoropyridine in a straightforward, scalable manner was employed to develop vanillin-based polyimines containing high biomass content (>90 wt%). The aromatic scaffold is fully organic yet boasts thermal stability and charring which competes those of the inorganic-organic monomers discussed above. Furthermore, creep resistance could be dramatically increased as the aromaticity of the network increased, and mild chemical recyclability was achieved (A. Stewart et al., 2023).

Thus, fire resistant polyimine networks derived from syringaldehyde (Xie et al., 2021), or carbon fiber-reinforced epoxy vitrimer derived from HMF could undergo degradation through hydrolysis (Nabipour et al., 2023). Moreover, the structure of the diamine used as hardener for vanillin-based reprocessable polyimines containing hexasubstituted cyclotriphosphazene was found to influence the fire resistance of vitrimers (X. Yang et al., 2022). It was demonstrated that alkyl-containing diamines could delay ignition owing to the absence of oxygen in the segments in comparison to alkoxy-containing diamines.

The chemical structures and substituents of aromatic-rich building blocks can impart CANs with fire retardant properties as observed with the synthesis of a fully degradable imine-containing network prepared from *p*-coumaric acid-derived epoxy monomer and cured with a fluorinated imine compound derived from syringaldehyde (Z. Wang et al., 2023). Outstanding LOI value of 43.3% was attained likely owing to the supplementary methoxyl groups on syringaldehyde, compared to vanillin, positively impacting char formation. Tannic acid used in complement to a reactive phosphate FR in the preparation of an ester-based network containing epoxidized soybean oil, proved to effectively delay the pyrolysis of long aliphatic chains by forming dense carbon layers owing to its multiple aromatic rings (Yizhen Chen et al., 2023).

Sulfur-containing matrixes were reported to positively impact flame resistance by exerting the shielding and dilutions effects, while hindering energy and oxygen exchanges (Howell and Daniel, 2018; Zou et al., 2020). Disulfide reversible bonds were integrated in eugenol-derived networks to provide both reprocessing ability and fire resistance (Li et al., 2022; Miao et al., 2020). The surface combustion of sulfur-containing vitrimers can form smooth, highly crosslinked, and thermally stable char protective layers minimizing the contact area between oxygen/heat and the polymeric network, limiting combustion intensity (Li et al., 2022).

5.3. Coatings applications

Smart coatings are of utmost relevance to improve the protection of a substrate by effectively responding to environmental changes, heal coating defects, or release active species (Cui et al., 2020). In this context, smart anticorrosive epoxy coatings based on copolymer assemblies were prepared for controlled release of corrosion inhibitor (Cao et al., 2022). Owing to a difference of compatibility between the syringaldehyde methacrylate and dopamine methacrylate units of poly(syringaldehyde methacrylate)-co-poly(dopamine methacrylate) copolymer with the epoxy resin, the copolymer exhibited “semi-amphiphilic” behavior. Dopamine units were self-assembled with the epoxy resin, whereas guanine, a corrosion inhibitor, was covalently linked to syringaldehyde moieties through imine bond, enabling its release from the core upon corrosion in acidic medium. The strong influence of the assemblies on the anticorrosion properties has been shown.

Responsive fluorescence was reported to be an efficient self-detecting feature in anticorrosion coatings (Luo et al., 2022). A fluorescent polymer was prepared by coupling in-situ imine condensation with epoxy ring-opening polymerization by reaction of an hyperbranched polyamidoamine (HPAMAM) with a vanillin-derived epoxy monomer. Owing to the $n-\pi^*$ transition of the amide groups and tertiary amines, HPAMAM emits low-intensity blue fluorescence when excited between 446 and 365 nm UV light. The fluorescence intensity of the resulting materials, which was found to have a linear correlation with the crosslinking density, enabled real time monitoring of self-healing of the coating because the scraped and intact areas presented distinctive fluorescent boundary. Moreover, fluorescent molecules are widely used for metal ion detection. The result reveals high potential for applications in areas of self-detecting anticorrosive coatings, engineering damage assessment, fluorescent sensors, and anti-counterfeiting labels.

Compared to neat epoxy network, incorporation of carbon nanotubes in a CNSL-derived dynamic epoxy network is another strategy to reduce corrosion rates by forming uniform coating layers (Lorwanishpaisarn et al., 2022).

5.4. Adhesive applications

Compared to conventional adhesive systems, CANs offer several advantages. The presence of dynamic bonds makes a broken joint repairable, enables the disassembly and recycling of precious components in fields such as batteries and electronics, and dissipates energy via reversible bond cleavage, thus limiting crack propagation (Jarach et al., 2021; Shi et al., 2023). In this context, debonding-on-demand (DoD) adhesives based on photoreversible [2 + 2] cycloaddition was reported from tri-, tetra- and hexa-core monomers derived from vanillin and 3,4-dihydroxybenzaldehyde UV switchable adhesive (Roy et al., 2023). The adhesive strength was optimized to reach 1.74 MPa using a design of experiments. The adhesive was shown to provide adhesion after three cycles, although the adhesiveness decreases with each cycle.

Polymers bearing imine and ester dynamic bonds proved to be efficient adhesives by combining multiple groups enabling interaction between the polymer and the substrate. For instance, aldehyde groups, benzene rings and ester groups can form interactions such as metal chelating, hydrogen bonds, or electrostatic interactions with the substrate. Adhesion ability of 4-hydroxybenzaldehyde-derived highly crosslinked polymer network was examined on steel, aluminum, glass, PVC, and PTFE substrates (Ren et al., 2022). The main source of mechanical strength of the adhesive was attributed to the highly abundant non-covalent interactions present in the network. On the other hand, imine imparted to the adhesive good reusability with the absence of fatigue over 18 gluing-debonding-gluing on glass and steel substrates. Moreover, C=N bonds in conjugated systems containing aromatic groups were reported to confer vanillin epoxy-based recoverable adhesive with outstanding UV shielding performances (Zhao et al., 2023). Linear bottlebrush polymers derived from vanillin and ethyl cellulose containing imine bonds were also reported as efficient adhesives (Gong et al., 2020). Owing to controlled RAFT polymerization the structures were tuned to meet the required properties. Adhesion tests on wood revealed that higher crosslinking density increased adhesiveness to the detriment of reparability, pointing out the need for a good balance between those two fundamental properties. The same observation was made for lignin-based antifungal and conductive adhesives, where the authors proposed a balanced crosslinking density permitting the network to partially diffuse into the wood substrate (Gao et al., 2020). Damage and repair cycles were conducted 4 times, enabling the recovery of 42.8% of the original adhesion strength. The combination of imine bonds with boronic ester and B-N coordinate linkages revealed to be an efficient strategy for the development of organic-inorganic adhesives containing 3,4-dihydroxybenzaldehyde, soybean proteins, and mica (Zhou et al., 2023). Sacrificial B-N coordination was proved to increase the work of adhesion by facilitating energy transfer and dissipation, while borate and phenolic components provide strong flame retardancy and mildew resistance. Due to the dynamic B-O, imine and B-N coordination bonds, adhesives showed good recyclability under mild conditions, highlighting their potential for the fabrication of plywood. By providing hydrogen bonding,

tannic acid was reported to enhance interfacial interactions of hydrogels with substrates in combination with imine, B-O and coordination bonds, to attain robust interfacial adhesion (Mo et al., 2021). This point was also discussed in the case of catechol-derived network containing boronic esters (Y. Yang et al., 2020).

Disulfide dissociative bond rearrangement present convenient features for application as self-healable adhesives, as bonding/debonding cycles demand mild conditions (relatively low temperatures and short times). Significant adhesive strength up to 2.8 MPa was obtained on aluminum substrates for a cardanol-based polybenzoxazine vitrimer (Trejo-Machin et al., 2020). The material showed to be reusable 5 times without any sign of deterioration. However, authors notify that in the case of remaining cardanol double bonds in a disulfide-containing network, there is a possibility for sulfur radical to be irreversibly consumed via thiol-ene reactions, limiting the dynamicity of the network. Disulfide bonds were also incorporated in lignin-based polyurea adhesives (W. Liu et al., 2020). Strong adhesion strength was obtained after introduction of lignin and PEG-functionalized lignin by constructing more intensive hydrogen bonds.

Furfuryl alcohol (FFA) was demonstrated to be an interesting crosslinking agent in dynamic adhesives for the fabrication of wood-based panels (Aladejana et al., 2023). FFA was functionalized with 2,5-diamino-1,4-benzenedithiol hydrochloride (DBH) and reacted with soybean proteins containing disulfide bonds so that the free SH on the crosslinker could recombine with the S-S bonds. Adhesion strength on plywood specimen reached 1.9 MPa in dry conditions. Although the reversibility of adhesion was not examined by the authors, this approach could be an interesting alternative glue for the production of recyclable and mildew-resistant wood-based panels.

The first lignin-based vitrimers synthesized already showed potential as recoverable adhesives (Zhang et al., 2018). Lap-shear strength performed on aluminum sheets reached 6.5 MPa, comparable to commercial epoxy adhesives. The joint could easily be re-established owing to transesterification reactions. Similar results were obtained by investigating the potential of lignin-based acetal networks as recoverable adhesive on aluminum and nontreated birch wood sheets (Moreno et al., 2021). Adhesion strength of 6.0 MPa were obtained on aluminum sheets, with 93% of adhesion strength recovery (5.6 MPa) after rebonding. On birch wood substrates, lap shear strength of 2.6 MPa were obtained. Successful adhesion in harsh conditions was also observed after immersion in concentrated saline water. Recently, lignin-based vinylogous urethane also showed good adhesive properties on wood imparted by interactions between N-H and C=O moieties with COOH groups present in the substrate. Moreover, by penetrating the surface of the wood, the vitrimer could form nails inside the wood, improving adhesion by mechanical interlocking. The adhesive was detached from the substrate by solvent removal method after immersion in 2-MeTHF, and by thermal removal method after temperature activation of the dynamic covalent bonds (Liu et al., 2024).

5.5. Other applications

Thermoset matrix composites and nanocomposites are industrially demanded for high performances applications. However, available recycling techniques to recover the fillers/reinforcements often leads to thermal or mechanical degradation of the polymer matrix (Pickering, 2006). To increase the contribution of composites to the circular bioeconomy, it is critical to recover not only the fiber/filler but also the polymer matrix. The research for novel biobased and composites CANs has flourished in the last decade to overcome sustainability challenges (Andrew and Dhakal, 2022; Hubbard et al., 2022a; Schenk et al., 2022; Sharma et al., 2022). Indeed, the substitution of conventional thermoset resins by CANs matrixes is an approach to considerably increase the durability of composites, by providing materials with reparability, and enabling both the matrix and filler/reinforcement recovery through recycling. Among the available fibers, carbon fibers have broad application prospects because they provide lightweight materials with high specific strength and stiffness (Zheng et al., 2022). Several studies report the development of CANs containing carbon-fibers,

generally leading to the recovery of the fiber and the recycling of the polymer matrix. Numerous vanillin-derived epoxy composites based on imine bond exchange reactions were prepared and characterized (X. Liu et al., 2021; Y.-Y. Liu et al., 2021, 2020; Memon et al., 2020; Wang et al., 2019; Y. Wang et al., 2022a, 2022b). The presence of imine moieties in the network enabled facile dissolution of the polymer matrix in the presence of an excess of amine groups owing to transimination reactions (Y.-Y. Liu et al., 2021; Memon et al., 2020; Y. Wang et al., 2022a), or in acidic media as a result of imine hydrolysis (X. Liu et al., 2021; Y.-Y. Liu et al., 2020; Wang et al., 2019; Y. Wang et al., 2022b). The dissolution of the networks led to efficient recovery of the fibers with preserved morphology and mechanical properties, showing reusable potential for the preparation of new generation composites. Similarly, carbon fiber reinforcement of imine containing PU prepared from vanillin derivative, isosorbide, castor oil and 4,4'-dicyclohexylmethane diisocyanate was also discussed (Sun et al., 2022). Natural fibers, such as flax fibers, are interesting load-bearing component showing some safety advantages compared to glass fibers, such as low density and good sound-absorbing properties. In this context, flax-reinforced resorcinol-based vitrimer composite showing fast dynamic siloxane exchanges was prepared, enabling reshaping through thermoforming (Debsharma et al., 2023). To overcome the difficulty of mixing hydrophilic cellulose nanocrystals (CNCs) in a hydrophobic epoxy matrix, the incorporation of CNCs in the cured vitrimer epoxy during mechanochemical ball milling recycling was reported (Yue et al., 2021). Transesterification exchange reactions are promoted by the free hydroxyl groups present on CNCs, enabling reshaping through compression molding.

Some specific fibers or fillers can also provide additional stimuli-responsiveness to CANs composites. The incorporation of graphene and graphene oxide to vanillin-based polyimine CANs could allow to convert electromagnetic and electric energy into heat. In addition to conventional heating, self-healing can thus be induced by exposition to microwave or electrical fields (Jia et al., 2022). Similarly, carbon nanotubes (CNTs) can absorb near-infrared radiation and convert it to thermal energy, leading to heating of the entire material. This electro-thermal conversion was used to trigger cardanol-based benzoxazine network containing boronic esters (Bo et al., 2022), and to improve the shape memory behavior of CNSL epoxy composites showing self-welding properties (Kasemsiri et al., 2018). Carbon fiber-reinforced CNSL epoxy vitrimer were later used as an external self-welding repair patch (Lorwanishpaisarn et al., 2021). Fe₃O₄ nanoparticles were also demonstrated efficient for non-contact welding within vanillin-derived network dynamic through imine bond exchange (Kou et al., 2023). By driving and approaching the polymer using a magnet, and applying near infrared light, bond rearrangements were induced, welding the fracture within few minutes and highlighting the potential of this approach for the welding of large-size samples.

6. CONCLUSIONS AND OUTLOOKS

Current environmental challenges have demonstrated the need to develop materials with controlled end-of-life. Recycling of conventional polymers only reaches today around 10% of the global production. Novel approaches for the design of high-performance materials became a major concern in the last decades to consider both the cradle and the end-of-life of these materials. CANs and more particularly biobased CANs are a solution of choice in the development of more sustainable materials featuring circularity and performance. This review analyses the recent literature on the pathways for the valorization of biobased aromatic structures in dynamic crosslinked networks to obtain high-performance materials with controlled end-of-life. This overview puts particular emphasis on the benefits of combining biobased aromatic structures and dynamic covalent chemistries to meet specification requirements for targeted applications.

Aromatic structures have proven to be of utmost relevance for the design of materials with advanced properties such as high T_g and robust mechanical properties. The wide array of reactive functional groups makes them suitable for direct incorporation into networks through straightforward and atom-efficient syntheses, but also allows various chemical modifications. Benzene rings, in addition to reinforcing materials with interactions such as π -stacking, impart fire resistance due to their ability to form dense

protective char layers. Paired with a large choice of dynamic chemistries, controlled degradation of networks for specific applications can be achieved in various operating environments. Biomedical field is particularly leveraging from this feature for drug delivery systems or self-resorbing implants for instance. Coatings also relied on this specification to release protective compounds such as anticorrosion agents. Reversible chemistries in combination to inter and intramolecular interactions provided by phenolic structures confer materials with good adhesion properties.

Biobased and aromatic CANs owing to their flowing ability have proved to be increasingly suitable to conventional thermoplastic processing techniques such as extrusion, or thermoforming. In the coming years, the expansion of research on biobased CANs processing via 3D/4D printing technologies, such as liquid deposition modelling, is expected. This is offering new processing perspectives for the fabrication of construct with high reproducibility, cost-effectiveness, and reduced wastes. This aspect is utmost relevance for paving the way of facile industrialization and potential large-scale production of those smart materials in the coming years.

One shortcoming in the field of CANs stems from the difficulty of solid-state reaction monitoring resulting in the use of liquid-phase model systems, or DFT simulations, which characterized properties are transposed to the networks. Such extrapolation can give clues on the mechanistic pathway, although it is insufficient to precisely investigate the behavior of reactions in crosslinked systems in which the reactivity is reduced due to a lack of mobility. Rheological characterizations are essential for obtaining a better understanding of bond exchanges rate and behavior. However, a lack of critical rheological characterizations required to properly demonstrate the dynamicity of networks should be noted. The vitrimer designation is still widely used in the absence of thorough rheological demonstration.

The insufficient creep resistance of CANs constitutes a major drawback continually under scrutiny. Strategies are developed to improve their dimensional stability over time by incorporating considerable yet subcritical fraction of non-dynamic crosslinks, or by combining dynamic linkages with disparate triggers. For that matter, aromatic and oxygen-rich aromatic compounds may reinforce structure and organization within networks through physical interactions such as π - π stacking and hydrogen bonding, mitigating creep deformation. Dimensional stability might also be impaired by restricted long-term and/or temperature stability of excess reactive functions needed for network rearrangement, that may not be available over time to induce bond exchanges (e.g. free amines in vinyllogous urethane that are often reported to undergo oxidation at physical recycling temperature). Although covalently bonded dynamic linkages are supposedly stable, chemical stability of reversible bonds must also be considered as some are prone to hydrolysis (e.g. boronic esters), light or temperature-induced alteration for instance. Such phenomena can lead to variations in crosslinking density over time which constitutes key challenges associated with achieving consistent performance in CANs.

Another major challenge consists in the transposition of these fairly academic concepts into materials adapted to concrete applications. Several variables need to be addressed to make the manufacturing of aromatic CANs economically and environmentally viable. Aromatic compounds derived from renewable feedstocks are more expensive than petrol-derived chemicals, mainly due to their availability and to their extraction/transformation processes. Although renewable structures as lignins are accessible as by-product of the pulp and paper industry, other specific structures such as hydroxycinnamic acid derivatives are niche markets partly owing to low production yield from sustainable feedstock. The production share obtained from renewable resources of some widely studied structures such as vanillin are in fact negligible. This demonstrates a real demand and need for the upgrade and expand of new production lines of renewable fractions. The limitation of manufacturing costs of sustainable CANs can be improved by privileging syntheses with a minimal number of steps and, when possible, substantial atom-economy synthetic pathway are to be recommended to minimize wastes of valuable fractions. The restricted use of reagents and solvent, according to green chemistry principles, is also a key factor in maximizing the positive impact of CANs and facilitating their scale-up production. In this respect, the production of biobased and aromatic CANs is encouraged to exploit

the already existing infrastructures for the manufacturing of conventional polymer materials to promote its expansion at lower costs.

A necessary gap to be filled in this emerging field of study concerns CANs end-of-life. Firstly, trade-off between melt-processability and mechanical properties of high and low modulus CANs is necessary to combine facile flow-induced recyclability and robust mechanical properties for demanding applications like thermosets and engineering materials. Furthermore, recycling aspects are approached by the academics in a purely theoretical context and do not address the practical difficulties of recycling such as contamination, or mixed waste stream. One future trend in the field echoing large-scale industrialization might involve the establishment of facilities responsible for the collection and sorting of used CANs to consider their physical or chemical recycling.

Finally, no threshold percentage value for minimal renewable carbon content is universally agreed-upon to classify a material as bioplastic. A direct consequence is that some so-called biobased CANs contain in fact only marginal amounts of renewable carbon, limiting their positive environmental impact. A clear universal definition could encourage the production of high biobased content materials. It is noteworthy to mention that the amount of biomass included in specific materials and products should be specified anyway. In that matter, independent certifications and labels such as “OK biobased”, “DIN-Geprüft biobased, or “USDA certified biobased products” specify the amount of renewable carbon or the percentage of biobased of materials based on norms for the determination of biobased content like EN 16640 or EN 16785-1.

Although various challenges need to be addressed to support the global expansion of aromatic and biobased CANs, the field is a tremendously promising solution for the development of robust materials with positive environmental impact for a more sustainable future.

7. REFERENCES

- Adisakwattana, S., Moonsan, P., Yibchok-anun, S., 2008. Insulin-Releasing Properties of a Series of Cinnamic Acid Derivatives in Vitro and in Vivo. *J. Agric. Food Chem.* 56, 7838–7844. <https://doi.org/10.1021/jf801208t>
- Adjaoud, A., Puchot, L., Federico, C.E., Das, R., Verge, P., 2023. Lignin-based benzoxazines: A tunable key-precursor for the design of hydrophobic coatings, fire resistant materials and catalyst-free vitrimers. *Chem. Eng. J.* 453, 139895. <https://doi.org/10.1016/j.cej.2022.139895>
- Adjaoud, A., Puchot, L., Verge, P., 2022. High-Tg and Degradable Isosorbide-Based Polybenzoxazine Vitriimer. *ACS Sustain. Chem. Eng.* 10, 594–602. <https://doi.org/10.1021/acssuschemeng.1c07093>
- Ahmadi, M., Hanifpour, A., Ghiassinejad, S., van Ruymbeke, E., 2022. Polyolefins Vitrimers: Design Principles and Applications. *Chem. Mater.* 34, 10249–10271. <https://doi.org/10.1021/acs.chemmater.2c02853>
- Ahmed Khalil, A., ur Rahman, U., Rafiq Khan, M., Sahar, A., Mehmood, T., Khan, M., 2017. Essential oil eugenol: sources, extraction techniques and nutraceutical perspectives. *RSC Adv.* 7, 32669–32681. <https://doi.org/10.1039/C7RA04803C>
- Aladejana, J.T., Zeng, G., Zhang, F., Li, K., Li, X., Dong, Y., Li, J., 2023. Tough, waterproof, and mildew-resistant fully biobased soybean protein adhesives enhanced by furfuryl alcohol with dynamic covalent linkages. *Ind. Crops Prod.* 198, 116759. <https://doi.org/10.1016/j.indcrop.2023.116759>
- Allen, C.F.H., Fournier, J.O., Humphlett, W.J., 1964. THE THERMAL REVERSIBILITY OF THE MICHAEL REACTION: IV. THIOL ADDUCTS. *Can. J. Chem.* 42, 2616–2620. <https://doi.org/10.1139/v64-383>
- Amornkitbamrung, L., Leungpuangkaew, S., Panklang, T., Jubsilp, C., Ekgasit, S., Um, S.H., Rimdusit, S., 2022. Effects of glutaric anhydride functionalization on filler-free benzoxazine/epoxy copolymers with shape memory and self-healing properties under near-infrared light actuation. *J. Sci. Adv. Mater. Devices* 7, 100446.
- Anastas, P., Eghbali, N., 2010. Green Chemistry: Principles and Practice. *Chem. Soc. Rev.* 39, 301–312. <https://doi.org/10.1039/B918763B>
- Andrew, J.J., Dhakal, H.N., 2022. Sustainable biobased composites for advanced applications: recent trends and future opportunities – A critical review. *Compos. Part C Open Access* 7, 100220. <https://doi.org/10.1016/j.jcomc.2021.100220>

CHAPITRE 1

- Arbenz, A., Avérous, L., 2015. Chemical modification of tannins to elaborate aromatic biobased macromolecular architectures. *Green Chem.* 17, 2626–2646. <https://doi.org/10.1039/C5GC00282F>
- A. Stewart, K., J. Lessard, J., J. Cantor, A., F. Rynk, J., S. Bailey, L., S. Sumerlin, B., 2023. High-performance polyimine vitrimers from an aromatic bio-based scaffold. *RSC Appl. Polym.* 1, 10–18. <https://doi.org/10.1039/D3LP00019B>
- Bajwa, D.S., Pourhashem, G., Ullah, A.H., Bajwa, S.G., 2019. A concise review of current lignin production, applications, products and their environmental impact. *Ind. Crops Prod.* 139, 111526. <https://doi.org/10.1016/j.indcrop.2019.111526>
- Bakkali-Hassani, C., Edera, P., Langenbach, J., Poutrel, Q.-A., Norvez, S., Gresil, M., Tournilhac, F., 2023. Epoxy Vitriimer Materials by Lipase-Catalyzed Network Formation and Exchange Reactions. *ACS Macro Lett.* 12, 338–343. <https://doi.org/10.1021/acsmacrolett.2c00715>
- Bakkali-Hassani, C., Poutrel, Q.-A., Langenbach, J., Chappuis, S., Blaker, J.J., Gresil, M., Tournilhac, F., 2021. Lipase-Catalyzed Epoxy–Acid Addition and Transesterification: from Model Molecule Studies to Network Build-Up. *Biomacromolecules* 22, 4544–4551. <https://doi.org/10.1021/acs.biomac.1c00820>
- Banchereau, E., Lacombe, S., Ollivier, J., 1995. Solution reactivity of thiyl radicals with molecular oxygen: Unsensitized photooxidation of dimethyldisulfide. *Tetrahedron Lett.* 36, 8197–8200. [https://doi.org/10.1016/0040-4039\(95\)01698-H](https://doi.org/10.1016/0040-4039(95)01698-H)
- Bapat, A.P., Roy, D., Ray, J.G., Savin, D.A., Sumerlin, B.S., 2011. Dynamic-Covalent Macromolecular Stars with Boronic Ester Linkages. *J. Am. Chem. Soc.* 133, 19832–19838. <https://doi.org/10.1021/ja207005z>
- Bazin, A., Duval, A., Avérous, L., Pollet, E., 2022. Synthesis of Bio-Based Photo-Cross-Linkable Polyesters Based on Caffeic Acid through Selective Lipase-Catalyzed Polymerization. *Macromolecules* 55, 4256–4267. <https://doi.org/10.1021/acs.macromol.2c00499>
- Beller, H.R., Lee, T.S., Katz, L., 2015. Natural products as biofuels and bio-based chemicals: fatty acids and isoprenoids. *Nat. Prod. Rep.* 32, 1508–1526. <https://doi.org/10.1039/C5NP00068H>
- Belowich, M.E., Stoddart, J.F., 2012. Dynamic imine chemistry. *Chem. Soc. Rev.* 41, 2003–2024. <https://doi.org/10.1039/C2CS15305J>
- Berne, D., Coste, G., Morales-Cerrada, R., Boursier, M., Pinaud, J., Ladmiraal, V., Caillol, S., 2022a. Taking advantage of β -hydroxy amine enhanced reactivity and functionality for the synthesis of dual covalent adaptable networks. *Polym. Chem.* 13, 3806–3814. <https://doi.org/10.1039/D2PY00274D>
- Berne, D., Ladmiraal, V., Leclerc, E., Caillol, S., 2022b. Thia-Michael Reaction: The Route to Promising Covalent Adaptable Networks. *Polymers* 14, 4457. <https://doi.org/10.3390/polym14204457>
- Berne, D., Quienne, B., Caillol, S., Leclerc, E., Ladmiraal, V., 2022c. Biobased catalyst-free covalent adaptable networks based on CF 3 -activated synergistic aza-Michael exchange and transesterification. *J. Mater. Chem. A* 10, 25085–25097. <https://doi.org/10.1039/D2TA05067F>
- Biron, M., 2018. Thermoplastics and thermoplastic composites. William Andrew.
- Black, S.P., Sanders, J.K.M., Stefankiewicz, A.R., 2014. Disulfide exchange: exposing supramolecular reactivity through dynamic covalent chemistry. *Chem. Soc. Rev.* 43, 1861–1872. <https://doi.org/10.1039/C3CS60326A>
- Bo, C., Sha, Y., Song, F., Zhang, M., Hu, L., Jia, P., Zhou, Y., 2022. Renewable benzoxazine-based thermosets from cashew nut: Investigating the self-healing, shape memory, recyclability and antibacterial activity. *J. Clean. Prod.* 341, 130898. <https://doi.org/10.1016/j.jclepro.2022.130898>
- Boul, P.J., Reutenauer, P., Lehn, J.-M., 2005. Reversible Diels–Alder Reactions for the Generation of Dynamic Combinatorial Libraries. *Org. Lett.* 7, 15–18. <https://doi.org/10.1021/ol048065k>
- Bowman, C.N., Kloxin, C.J., 2012. Covalent Adaptable Networks: Reversible Bond Structures Incorporated in Polymer Networks. *Angew. Chem. Int. Ed.* 51, 4272–4274. <https://doi.org/10.1002/anie.201200708>
- Boyer, C., Hoogenboom, R., 2015. Multi-responsive polymers. *Eur. Polym. J.* 69, 438–440. <https://doi.org/10.1016/j.eurpolymj.2015.06.032>
- Brachvogel, R.-C., von Delius, M., 2016. The Dynamic Covalent Chemistry of Esters, Acetals and Orthoesters. *Eur. J. Org. Chem.* 2016, 3662–3670. <https://doi.org/10.1002/ejoc.201600388>
- Briou, B., Améduri, B., Boutevin, B., 2021. Trends in the Diels–Alder reaction in polymer chemistry. *Chem. Soc. Rev.* 50, 11055–11097. <https://doi.org/10.1039/D0CS01382J>
- Britt, P.F., Coates, G.W., Winey, K.I., Byers, J., Chen, E., Coughlin, B., Ellison, C., Garcia, J., Goldman, A., Guzman, J., Hartwig, J., Helms, B., Huber, G., Jenks, C., Martin, J., McCann, M., Miller, S., O’Neill, H., Sadow, A., Scott, S., Sita, L., Vlachos, D., Waymouth, R., 2019. Report of the Basic Energy Sciences Roundtable on Chemical Upcycling of Polymers. USDOE Office of Science (SC) (United States). <https://doi.org/10.2172/1616517>
- Brutman, J.P., Delgado, P.A., Hillmyer, M.A., 2014. Poly lactide Vitrimers. *ACS Macro Lett.* 3, 607–610. <https://doi.org/10.1021/mz500269w>

- Buono, P., Duval, A., Averous, L., Habibi, Y., 2018. Clicking Biobased Polyphenols: A Sustainable Platform for Aromatic Polymeric Materials. *ChemSusChem* 11, 2472–2491. <https://doi.org/10.1002/cssc.201800595>
- Buono, P., Duval, A., Averous, L., Habibi, Y., 2017. Thermally healable and remendable lignin-based materials through Diels – Alder click polymerization. *Polymer* 133, 78–88. <https://doi.org/10.1016/j.polymer.2017.11.022>
- Cacciapaglia, R., Di Stefano, S., Mandolini, L., 2005. Metathesis Reaction of Formaldehyde Acetals: An Easy Entry into the Dynamic Covalent Chemistry of Cyclophane Formation. *J. Am. Chem. Soc.* 127, 13666–13671. <https://doi.org/10.1021/ja054362o>
- Caffy, F., Nicolaÿ, R., 2019. Transformation of polyethylene into a vitrimer by nitroxide radical coupling of a bis-dioxaborolane. *Polym. Chem.* 10, 3107–3115. <https://doi.org/10.1039/C9PY00253G>
- Caillol, S., 2023. The future of cardanol as small giant for biobased aromatic polymers and additives. *Eur. Polym. J.* 193, 112096. <https://doi.org/10.1016/j.eurpolymj.2023.112096>
- Caillol, S., 2018. Cardanol: A promising building block for biobased polymers and additives. *Curr. Opin. Green Sustain. Chem., Bioresources and Biochemicals / Biofuels and Bioenergy* 14, 26–32. <https://doi.org/10.1016/j.cogsc.2018.05.002>
- Candolle, A. de, 1885. *Origin of Cultivated Plants*. D. Appleton.
- Cao, Q., Li, J., Liu, B., Zhao, Y., Zhao, J., Gu, H., Wei, Z., Li, F., Jian, X., Weng, Z., 2023. Toward versatile biobased epoxy vitrimers by introducing aromatic N-heterocycles with stiff and flexible segments. *Chem. Eng. J.* 469, 143702. <https://doi.org/10.1016/j.cej.2023.143702>
- Cao, Y., He, J., Wu, J., Wang, X., Lu, W., Lin, J., Xu, Y., Chen, G., Zeng, B., Dai, L., 2022. A Smart Anticorrosive Epoxy Coating Based on Environmental-Stimuli-Responsive Copolymer Assemblies for Controlled Release of Corrosion Inhibitors. *Macromol. Mater. Eng.* 307, 2100983. <https://doi.org/10.1002/mame.202100983>
- Capelot, M., Montarnal, D., Tournilhac, F., Leibler, L., 2012. Metal-Catalyzed Transesterification for Healing and Assembling of Thermosets. *J. Am. Chem. Soc.* 134, 7664–7667. <https://doi.org/10.1021/ja302894k>
- Cash, J.J., Kubo, T., Bapat, A.P., Sumerlin, B.S., 2015. Room-Temperature Self-Healing Polymers Based on Dynamic-Covalent Boronic Esters. *Macromolecules* 48, 2098–2106. <https://doi.org/10.1021/acs.macromol.5b00210>
- Celotti, E., Ferrarini, R., Zironi, R., Conte, L.S., 1996. Resveratrol content of some wines obtained from dried Valpolicella grapes: Recioto and Amarone. *J. Chromatogr. A, 19th International Symposium on Column Liquid Chromatography* 730, 47–52. [https://doi.org/10.1016/0021-9673\(95\)00962-0](https://doi.org/10.1016/0021-9673(95)00962-0)
- Chakma, P., Konkolewicz, D., 2019. Dynamic Covalent Bonds in Polymeric Materials. *Angew. Chem. Int. Ed.* 58, 9682–9695. <https://doi.org/10.1002/anie.201813525>
- Chandel, A.K., Garlapati, V.K., Jeevan Kumar, S.P., Hans, M., Singh, A.K., Kumar, S., 2020. The role of renewable chemicals and biofuels in building a bioeconomy. *Biofuels Bioprod. Biorefining* 14, 830–844. <https://doi.org/10.1002/bbb.2104>
- Chatterjee, M., Ishizaka, T., Chatterjee, A., Kawanami, H., 2017. Dehydrogenation of 5-hydroxymethylfurfural to diformylfuran in compressed carbon dioxide: an oxidant free approach. *Green Chem.* 19, 1315–1326. <https://doi.org/10.1039/C6GC02977A>
- Chen, B.-B., Chang, S., Jiang, L., Lv, J., Gao, Y.-T., Wang, Y., Qian, R.-C., Li, D.-W., Hafez, M.E., 2022. Reversible polymerization of carbon dots based on dynamic covalent imine bond. *J. Colloid Interface Sci.* 621, 464–469. <https://doi.org/10.1016/j.jcis.2022.04.089>
- Chen, Fengbiao, Cheng, Q., Gao, F., Zhong, J., Shen, L., Lin, C., Lin, Y., 2021. The effect of latent plasticity on the shape recovery of a shape memory vitrimer. *Eur. Polym. J.* 147, 110304. <https://doi.org/10.1016/j.eurpolymj.2021.110304>
- Chen, F., Gao, F., Zhong, J., Shen, L., Lin, Y., 2020. Fusion of biobased vinylogous urethane vitrimers with distinct mechanical properties. *Mater. Chem. Front.* 4, 2723–2730. <https://doi.org/10.1039/D0QM00302F>
- Chen, Fang, Xiao, H., Peng, Z.Q., Zhang, Z.P., Rong, M.Z., Zhang, M.Q., 2021. Thermally conductive glass fiber reinforced epoxy composites with intrinsic self-healing capability. *Adv. Compos. Hybrid Mater.* 4, 1048–1058. <https://doi.org/10.1007/s42114-021-00303-3>
- Chen, J., Lu, X., Xin, Z., 2023. A bio-based reprocessable and degradable polybenzoxazine with acetal structures. *React. Funct. Polym.* 191, 105653. <https://doi.org/10.1016/j.reactfunctpolym.2023.105653>
- Chen, M., Si, H., Zhang, H., Zhou, L., Wu, Y., Song, L., Kang, M., Zhao, X.-L., 2021. The Crucial Role in Controlling the Dynamic Properties of Polyester-Based Epoxy Vitrimers: The Density of Exchangeable Ester Bonds (v). *Macromolecules* 54, 10110–10117. <https://doi.org/10.1021/acs.macromol.1c01289>
- Chen, M., Wu, Y., Chen, B., Tucker, A.M., Jagota, A., Yang, S., 2022. Fast, strong, and reversible adhesives with dynamic covalent bonds for potential use in wound dressing. *Proc. Natl. Acad. Sci.* 119, e2203074119. <https://doi.org/10.1073/pnas.2203074119>

- Chen, X., Dam, M.A., Ono, K., Mal, A., Shen, H., Nutt, S.R., Sheran, K., Wudl, F., 2002. A Thermally Remendable Cross-Linked Polymeric Material. *Science* 295, 1698–1702. <https://doi.org/10.1126/science.1065879>
- Chen, X., Li, L., Jin, K., Torkelson, J.M., 2017. Reprocessable polyhydroxyurethane networks exhibiting full property recovery and concurrent associative and dissociative dynamic chemistry via transcarbamoylation and reversible cyclic carbonate aminolysis. *Polym. Chem.* 8, 6349–6355. <https://doi.org/10.1039/C7PY01160A>
- Chen, Yixuan, Chen, B., Torkelson, J.M., 2023. Biobased, Reprocessable Non-isocyanate Polythiourethane Networks with Thionourethane and Disulfide Cross-Links: Comparison with Polyhydroxyurethane Network Analogues. *Macromolecules* 56, 3687–3702. <https://doi.org/10.1021/acs.macromol.3c00220>
- Chen, Yizhen, Zeng, Y., Wu, Y., Chen, T., Qiu, R., Liu, W., 2023. Flame-Retardant and Recyclable Soybean Oil-Based Thermosets Enabled by the Dynamic Phosphate Ester and Tannic Acid. *ACS Appl. Mater. Interfaces* 15, 5963–5973. <https://doi.org/10.1021/acsami.2c21279>
- Cheng, C., Zhang, X., Chen, X., Li, J., Huang, Q., Hu, Z., Tu, Y., 2016. Self-healing polymers based on eugenol via combination of thiol-ene and thiol oxidation reactions. *J. Polym. Res.* 23, 110. <https://doi.org/10.1007/s10965-016-1001-x>
- Cheng, X., Li, L., Yang, L., Huang, Q., Li, Y., Cheng, Y., 2022. All-Small-Molecule Dynamic Covalent Hydrogels with Heat-Triggered Release Behavior for the Treatment of Bacterial Infections. *Adv. Funct. Mater.* 32, 2206201. <https://doi.org/10.1002/adfm.202206201>
- Cheng, X., Li, M., Wang, H., Cheng, Y., 2020. All-small-molecule dynamic covalent gels with antibacterial activity by boronate-tannic acid gelation. *Chin. Chem. Lett.* 31, 869–874. <https://doi.org/10.1016/j.ccllet.2019.07.013>
- Choi, Y., Park, K., Choi, H., Son, D., Shin, M., 2021. Self-Healing, Stretchable, Biocompatible, and Conductive Alginate Hydrogels through Dynamic Covalent Bonds for Implantable Electronics. *Polymers* 13, 1133. <https://doi.org/10.3390/polym13071133>
- Chung, C.-M., Roh, Y.-S., Cho, S.-Y., Kim, J.-G., 2004. Crack Healing in Polymeric Materials via Photochemical [2+2] Cycloaddition. *Chem. Mater.* 16, 3982–3984. <https://doi.org/10.1021/cm049394+>
- Chung, K.-T., Lu, Z., Chou, M.W., 1998. Mechanism of inhibition of tannic acid and related compounds on the growth of intestinal bacteria. *Food Chem. Toxicol.* 36, 1053–1060. [https://doi.org/10.1016/S0278-6915\(98\)00086-6](https://doi.org/10.1016/S0278-6915(98)00086-6)
- Ciaccia, M., Stefano, S.D., 2014. Mechanisms of imine exchange reactions in organic solvents. *Org. Biomol. Chem.* 13, 646–654. <https://doi.org/10.1039/C4OB02110J>
- Collins, J., Nadgorny, M., Xiao, Z., Connal, L.A., 2017. Doubly Dynamic Self-Healing Materials Based on Oxime Click Chemistry and Boronic Acids. *Macromol. Rapid Commun.* 38, 1600760. <https://doi.org/10.1002/marc.201600760>
- Cordes, E.H., Bull, H.G., 1974. Mechanism and catalysis for hydrolysis of acetals, ketals, and ortho esters. *Chem. Rev.* 74, 581–603. <https://doi.org/10.1021/cr60291a004>
- Costes, L., Laoutid, F., Brohez, S., Dubois, P., 2017. Bio-based flame retardants: When nature meets fire protection. *Mater. Sci. Eng. R Rep.* 117, 1–25. <https://doi.org/10.1016/j.mser.2017.04.001>
- Cromwell, O.R., Chung, J., Guan, Z., 2015. Malleable and Self-Healing Covalent Polymer Networks through Tunable Dynamic Boronic Ester Bonds. *J. Am. Chem. Soc.* 137, 6492–6495. <https://doi.org/10.1021/jacs.5b03551>
- Cui, G., Bi, Z., Wang, S., Liu, J., Xing, X., Li, Z., Wang, B., 2020. A comprehensive review on smart anti-corrosive coatings. *Prog. Org. Coat.* 148, 105821. <https://doi.org/10.1016/j.porgcoat.2020.105821>
- Cuminet, F., Berne, D., Lemouzy, S., Dantras, É., Joly-Duhamel, C., Caillol, S., Leclerc, É., Ladmiral, V., 2022. Catalyst-free transesterification vitrimers: activation via α -difluoroesters. *Polym. Chem.* 13, 2651–2658. <https://doi.org/10.1039/D2PY00124A>
- Cuminet, F., Caillol, S., Dantras, É., Leclerc, É., Ladmiral, V., 2021. Neighboring Group Participation and Internal Catalysis Effects on Exchangeable Covalent Bonds: Application to the Thriving Field of Vitrimer Chemistry. *Macromolecules* 54, 3927–3961. <https://doi.org/10.1021/acs.macromol.0c02706>
- Cuminet, F., Lemouzy, S., Dantras, É., Leclerc, É., Ladmiral, V., Caillol, S., 2023. From vineyards to reshapable materials: α -CF₂ activation in 100% resveratrol-based catalyst-free vitrimers. *Polym. Chem.* 14, 1387–1395. <https://doi.org/10.1039/D3PY00017F>
- Czarny-Krzywińska, K., Krawczyk, B., Szczukocki, D., 2023. Bisphenol A and its substitutes in the aquatic environment: Occurrence and toxicity assessment. *Chemosphere* 315, 137763. <https://doi.org/10.1016/j.chemosphere.2023.137763>
- D’Adamo, I., Gastaldi, M., Morone, P., Rosa, P., Sassanelli, C., Settembre-Blundo, D., Shen, Y., 2022. Bioeconomy of Sustainability: Drivers, Opportunities and Policy Implications. *Sustainability* 14, 200. <https://doi.org/10.3390/su14010200>

- Danthu, P., Simanjuntak, R., Fawbush, F., Leong Pock Tsy, J.M., Razafimamonjison, G., Abdillahi, M.M., Jahiel, M., Penot, E., 2020. The clove tree and its products (clove bud, clove oil, eugenol): prosperous today but what of tomorrow's restrictions? *Fruits* 75, 224–242. <https://doi.org/10.17660/th2020/75.5.5>
- de Hoyos-Martínez, P.L., Merle, J., Labidi, J., Charrier – El Bouhtoury, F., 2019. Tannins extraction: A key point for their valorization and cleaner production. *J. Clean. Prod.* 206, 1138–1155. <https://doi.org/10.1016/j.jclepro.2018.09.243>
- Debnath, S., Kaushal, S., Ojha, U., 2020. Catalyst-Free Partially Bio-Based Polyester Vitrimers. *ACS Appl. Polym. Mater.* 2, 1006–1013. <https://doi.org/10.1021/acsapm.0c00016>
- Debnath, S., Tiwary, S.K., Ojha, U., 2021. Dynamic Carboxylate Linkage Based Reprocessable and Self-Healable Segmented Polyurethane Vitrimers Displaying Creep Resistance Behavior and Triple Shape Memory Ability. *ACS Appl. Polym. Mater.* 3, 2166–2177. <https://doi.org/10.1021/acsapm.1c00199>
- Debsharma, T., Engelen, S., De Baere, I., Van Paeppegem, W., Du Prez, F., 2023. Resorcinol-Derived Vitrimers and Their Flax Fiber-Reinforced Composites Based on Fast Siloxane Exchange. *Macromol. Rapid Commun.* 44, 2300020. <https://doi.org/10.1002/marc.202300020>
- Decostanzi, M., Auvergne, R., Boutevin, B., Caillol, S., 2019. Biobased phenol and furan derivatives coupling for the synthesis of functional monomers. *Green Chem.* 21, 724–747. <https://doi.org/10.1039/C8GC03541E>
- del Río, J.C., Rencoret, J., Gutiérrez, A., Elder, T., Kim, H., Ralph, J., 2020. Lignin Monomers from beyond the Canonical Monolignol Biosynthetic Pathway: Another Brick in the Wall. *ACS Sustain. Chem. Eng.* 8, 4997–5012. <https://doi.org/10.1021/acssuschemeng.0c01109>
- Denissen, W., Drosbeke, M., Nicolaÿ, R., Leibler, L., Winne, J.M., Du Prez, F.E., 2017. Chemical control of the viscoelastic properties of vinylogous urethane vitrimers. *Nat. Commun.* 8, 14857. <https://doi.org/10.1038/ncomms14857>
- Denissen, W., M. Winne, J., Prez, F.E.D., 2016. Vitrimers: permanent organic networks with glass-like fluidity. *Chem. Sci.* 7, 30–38. <https://doi.org/10.1039/C5SC02223A>
- Denissen, W., Rivero, G., Nicolaÿ, R., Leibler, L., Winne, J.M., Du Prez, F.E., 2015. Vinylogous Urethane Vitrimers. *Adv. Funct. Mater.* 25, 2451–2457. <https://doi.org/10.1002/adfm.201404553>
- Dessbesell, L., Paleologou, M., Leitch, M., Pulkki, R., Xu, C. (Charles), 2020. Global lignin supply overview and kraft lignin potential as an alternative for petroleum-based polymers. *Renew. Sustain. Energy Rev.* 123, 109768. <https://doi.org/10.1016/j.rser.2020.109768>
- Dhers, S., Vantomme, G., Avérous, L., 2019. A fully bio-based polyimine vitrimer derived from fructose. *Green Chem.* 21, 1596–1601. <https://doi.org/10.1039/C9GC00540D>
- Ding, X.-M., Chen, L., Luo, X., He, F.-M., Xiao, Y.-F., Wang, Y.-Z., 2022. Biomass-derived dynamic covalent epoxy thermoset with robust mechanical properties and facile malleability. *Chin. Chem. Lett.* 33, 3245–3248. <https://doi.org/10.1016/j.ccl.2021.10.079>
- Dong, L., Wang, Y., Dong, Y., Zhang, Y., Pan, M., Liu, X., Gu, X., Antonietti, M., Chen, Z., 2023. Sustainable production of dopamine hydrochloride from softwood lignin. *Nat. Commun.* 14, 4996. <https://doi.org/10.1038/s41467-023-40702-2>
- Dorigato, A., 2021. Recycling of polymer blends. *Adv. Ind. Eng. Polym. Res., Recycling of Polymer Blends and Composites* 4, 53–69. <https://doi.org/10.1016/j.aiepr.2021.02.005>
- Du, L., Jin, X., Qian, G., Yang, W., Su, L., Ma, Y., Ren, S., Li, S., 2022. Lignin-based vitrimer for circulation in plastics, coatings, and adhesives with tough mechanical properties, catalyst-free and good chemical solvent resistance. *Ind. Crops Prod.* 187, 115439. <https://doi.org/10.1016/j.indcrop.2022.115439>
- Dusek, K., Matejka, L., 1984. Transesterification and Gelation of Polyhydroxy Esters Formed from Diepoxides and Dicarboxylic Acids, in: *Rubber-Modified Thermoset Resins, Advances in Chemistry*. American Chemical Society, pp. 15–26. <https://doi.org/10.1021/ba-1984-0208.ch002>
- Duval, A., Avérous, L., 2023. From thermoplastic polyurethane to covalent adaptable network via reversible photo-crosslinking of a biobased chain extender synthesized from caffeic acid. *Polym. Chem.* 14, 2685–2696. <https://doi.org/10.1039/D3PY00162H>
- Duval, A., Couture, G., Caillol, S., Avérous, L., 2017. Biobased and Aromatic Reversible Thermoset Networks from Condensed Tannins via the Diels–Alder Reaction. *ACS Sustain. Chem. Eng.* 5, 1199–1207. <https://doi.org/10.1021/acssuschemeng.6b02596>
- Duval, A., Lange, H., Lawoko, M., Crestini, C., 2015. Reversible crosslinking of lignin via the furan–maleimide Diels–Alder reaction. *Green Chem.* 17, 4991–5000. <https://doi.org/10.1039/C5GC01319D>
- Duval, A., Lawoko, M., 2014. A review on lignin-based polymeric, micro- and nano-structured materials. *React. Funct. Polym.* 85, 78–96. <https://doi.org/10.1016/j.reactfunctpolym.2014.09.017>
- Elling, B.R., Dichtel, W.R., 2020. Reprocessable Cross-Linked Polymer Networks: Are Associative Exchange Mechanisms Desirable? *ACS Cent. Sci.* 6, 1488–1496. <https://doi.org/10.1021/acscentsci.0c00567>

- Emblem, A., 2012. 13 - Plastics properties for packaging materials, in: Emblem, Anne, Emblem, H. (Eds.), *Packaging Technology*. Woodhead Publishing, pp. 287–309. <https://doi.org/10.1533/9780857095701.2.287>
- Emiliani, G., Fondi, M., Fani, R., Gribaldo, S., 2009. A horizontal gene transfer at the origin of phenylpropanoid metabolism: a key adaptation of plants to land. *Biol. Direct* 4, 7. <https://doi.org/10.1186/1745-6150-4-7>
- Engelen, S., Wróblewska, A.A., Bruycker, K.D., Aksakal, R., Admiral, V., Caillol, S., Du Prez, F.E., 2022. Sustainable design of vanillin-based vitrimers using vinylogous urethane chemistry. *Polym. Chem.* <https://doi.org/10.1039/D2PY00351A>
- Eraghi Kazzaz, A., Fatehi, P., 2020. Technical lignin and its potential modification routes: A mini-review. *Ind. Crops Prod.* 154, 112732. <https://doi.org/10.1016/j.indcrop.2020.112732>
- Fache, M., Boutevin, B., Caillol, S., 2016. Vanillin Production from Lignin and Its Use as a Renewable Chemical. *ACS Sustain. Chem. Eng.* 4, 35–46. <https://doi.org/10.1021/acssuschemeng.5b01344>
- Fache, M., Boutevin, B., Caillol, S., 2015. Vanillin, a key-intermediate of biobased polymers. *Eur. Polym. J.* 68, 488–502. <https://doi.org/10.1016/j.eurpolymj.2015.03.050>
- Fairbanks, B.D., Singh, S.P., Bowman, C.N., Anseth, K.S., 2011. Photodegradable, Photoadaptable Hydrogels via Radical-Mediated Disulfide Fragmentation Reaction. *Macromolecules* 44, 2444–2450. <https://doi.org/10.1021/ma200202w>
- Fan, X., Zhou, W., Chen, Y., Yan, L., Fang, Y., Liu, H., 2020. An Antifreezing/Antiheating Hydrogel Containing Catechol Derivative Urushiol for Strong Wet Adhesion to Various Substrates. *ACS Appl. Mater. Interfaces* 12, 32031–32040. <https://doi.org/10.1021/acscami.0c09917>
- Feng, X., Fan, J., Li, A., Li, G., 2020. Biobased Tannic Acid Cross-Linked Epoxy Thermosets with Hierarchical Molecular Structure and Tunable Properties: Damping, Shape Memory, and Recyclability. *ACS Sustain. Chem. Eng.* 8, 874–883. <https://doi.org/10.1021/acssuschemeng.9b05198>
- Ferry, J.D., 1980. *Viscoelastic Properties of Polymers*. John Wiley & Sons.
- Flourat, A.L., Combes, J., Bailly-Maitre-Grand, C., Magnien, K., Haudrechy, A., Renault, J.-H., Allais, F., 2021. Accessing p-Hydroxycinnamic Acids: Chemical Synthesis, Biomass Recovery, or Engineered Microbial Production? *ChemSusChem* 14, 118–129. <https://doi.org/10.1002/cssc.202002141>
- Ford, L., Theodoridou, K., Sheldrake, G.N., Walsh, P.J., 2019. A critical review of analytical methods used for the chemical characterisation and quantification of phlorotannin compounds in brown seaweeds. *Phytochem. Anal.* 30, 587–599. <https://doi.org/10.1002/pca.2851>
- Fortman, D.J., Brutman, J.P., Cramer, C.J., Hillmyer, M.A., Dichtel, W.R., 2015. Mechanically Activated, Catalyst-Free Polyhydroxyurethane Vitrimers. *J. Am. Chem. Soc.* 137, 14019–14022. <https://doi.org/10.1021/jacs.5b08084>
- Fortman, D.J., Brutman, J.P., De Hoe, G.X., Snyder, R.L., Dichtel, W.R., Hillmyer, M.A., 2018. Approaches to Sustainable and Continually Recyclable Cross-Linked Polymers. *ACS Sustain. Chem. Eng.* 6, 11145–11159. <https://doi.org/10.1021/acssuschemeng.8b02355>
- Frutos, P., Hervás, G., Giráldez, F.J., Mantecón, A.R., 2004. Review. Tannins and ruminant nutrition. *Span. J. Agric. Res.* 2, 191–202. <https://doi.org/10.5424/sjar/2004022-73>
- Galkin, K.I., Ananikov, V.P., 2019. When Will 5-Hydroxymethylfurfural, the “Sleeping Giant” of Sustainable Chemistry, Awaken? *ChemSusChem* 12, 2976–2982. <https://doi.org/10.1002/cssc.201900592>
- Gandini, A., 2013. The furan/maleimide Diels–Alder reaction: A versatile click–unclick tool in macromolecular synthesis. *Prog. Polym. Sci., Topical Issue on Polymer Chemistry* 38, 1–29. <https://doi.org/10.1016/j.progpolymsci.2012.04.002>
- Gandini, A., Belgacem, M.N., 1997. Furans in polymer chemistry. *Prog. Polym. Sci.* 22, 1203–1379. [https://doi.org/10.1016/S0079-6700\(97\)00004-X](https://doi.org/10.1016/S0079-6700(97)00004-X)
- Gandini, A., Lacerda, T.M., Carvalho, A.J.F., Trovatti, E., 2016. Progress of Polymers from Renewable Resources: Furans, Vegetable Oils, and Polysaccharides. *Chem. Rev.* 116, 1637–1669. <https://doi.org/10.1021/acs.chemrev.5b00264>
- Gao, S., Cheng, Z., Zhou, X., Liu, Y., Wang, J., Wang, C., Chu, F., Xu, F., Zhang, D., 2020. Fabrication of lignin based renewable dynamic networks and its applications as self-healing, antifungal and conductive adhesives. *Chem. Eng. J.* 394, 124896. <https://doi.org/10.1016/j.cej.2020.124896>
- García-Astrain, C., Gandini, A., Coelho, D., Mondragon, I., Retegi, A., Eceiza, A., Corcuera, M.A., Gabilondo, N., 2013. Green chemistry for the synthesis of methacrylate-based hydrogels crosslinked through Diels–Alder reaction. *Eur. Polym. J.* 49, 3998–4007. <https://doi.org/10.1016/j.eurpolymj.2013.09.004>
- Gedam, P.H., Sampathkumaran, P.S., 1986. Cashew nut shell liquid: Extraction, chemistry and applications. *Prog. Org. Coat.* 14, 115–157. [https://doi.org/10.1016/0033-0655\(86\)80009-7](https://doi.org/10.1016/0033-0655(86)80009-7)
- Genua, A., Montes, S., Azcune, I., Rekondo, A., Malburet, S., Daydé-Cazals, B., Graillet, A., 2020. Build-To-Specification Vanillin and Phloroglucinol Derived Biobased Epoxy-Amine Vitrimers. *Polymers* 12, 2645. <https://doi.org/10.3390/polym12112645>

- Gevrek, T.N., Sanyal, A., 2021. Furan-containing polymeric Materials: Harnessing the Diels-Alder chemistry for biomedical applications. *Eur. Polym. J.* 153, 110514. <https://doi.org/10.1016/j.eurpolymj.2021.110514>
- Gong, X., Cheng, Z., Gao, S., Zhang, D., Ma, Y., Wang, J., Wang, C., Chu, F., 2020. Ethyl cellulose based self-healing adhesives synthesized via RAFT and aromatic schiff-base chemistry. *Carbohydr. Polym.* 250, 116846. <https://doi.org/10.1016/j.carbpol.2020.116846>
- Guerre, M., Taplan, C., Nicolaÿ, R., Winne, J.M., Du Prez, F.E., 2018. Fluorinated Vitrimer Elastomers with a Dual Temperature Response. *J. Am. Chem. Soc.* 140, 13272–13284. <https://doi.org/10.1021/jacs.8b07094>
- Guo, X., Gao, F., Chen, F., Zhong, J., Shen, L., Lin, C., Lin, Y., 2021. Dynamic Enamine-one Bond Based Vitrimer via Amino-yne Click Reaction. *ACS Macro Lett.* 10, 1186–1190. <https://doi.org/10.1021/acsmacrolett.1c00550>
- Haida, P., Signorato, G., Abetz, V., 2022. Blended vinylogous urethane/urea vitrimers derived from aromatic alcohols. *Polym. Chem.* 13, 946–958. <https://doi.org/10.1039/D1PY01237A>
- Hajj, R., Duval, A., Dhers, S., Avérous, L., 2020. Network Design to Control Polyimine Vitrimer Properties: Physical Versus Chemical Approach. *Macromolecules* 53, 3796–3805. <https://doi.org/10.1021/acs.macromol.0c00453>
- Hamernik, L.J., Guzman, W., Wiggins, J.S., 2023. Solvent-free preparation of imine vitrimers: leveraging benzoxazine crosslinking for melt processability and tunable mechanical performance. *J. Mater. Chem. A* 11, 20568–20582. <https://doi.org/10.1039/D3TA04351G>
- Hammer, L., Van Zee, N.J., Nicolaÿ, R., 2021. Dually Crosslinked Polymer Networks Incorporating Dynamic Covalent Bonds. *Polymers* 13, 396. <https://doi.org/10.3390/polym13030396>
- Hao, C., Liu, T., Zhang, S., Brown, L., Li, R., Xin, J., Zhong, T., Jiang, L., Zhang, J., 2019. A High-Lignin-Content, Removable, and Glycol-Assisted Repairable Coating Based on Dynamic Covalent Bonds. *ChemSusChem* 12, 1049–1058. <https://doi.org/10.1002/cssc.201802615>
- Hatano, T., Shida, S., Han, L., Okuda, T., 1991. Tannins of Theaceous Plants. III. Camelliatannins A and B, Two New Complex Tannins from *Camellia japonica* L. *Chem. Pharm. Bull. (Tokyo)* 39, 876–880. <https://doi.org/10.1248/cpb.39.876>
- Hobbs, C.E., 2019. Recent Advances in Bio-Based Flame Retardant Additives for Synthetic Polymeric Materials. *Polymers* 11, 224. <https://doi.org/10.3390/polym11020224>
- Hocking, M.B., 1997. Vanillin: Synthetic Flavoring from Spent Sulfite Liquor. *J. Chem. Educ.* 74, 1055. <https://doi.org/10.1021/ed074p1055>
- Holloway, J.O., Taplan, C., Prez, F.E.D., 2022. Combining vinylogous urethane and β -amino ester chemistry for dynamic material design. *Polym. Chem.* 13, 2008–2018. <https://doi.org/10.1039/D2PY00026A>
- Hong, J., Hong, Y., Jeong, J., Oh, D., Goh, M., 2023. Robust Biobased Vitrimers and Its Application to Closed-Loop Recyclable Carbon Fiber-Reinforced Composites. *ACS Sustain. Chem. Eng.* 11, 14112–14123. <https://doi.org/10.1021/acssuschemeng.3c03468>
- Hong, K., Sun, Q., Zhang, X., Fan, L., Wu, T., Du, J., Zhu, Y., 2022. Fully Bio-Based High-Performance Thermosets with Closed-Loop Recyclability. *ACS Sustain. Chem. Eng.* 10, 1036–1046. <https://doi.org/10.1021/acssuschemeng.1c07523>
- Hopewell, J., Dvorak, R., Kosior, E., 2009. Plastics recycling: challenges and opportunities. *Philos. Trans. R. Soc. B Biol. Sci.* 364, 2115–2126. <https://doi.org/10.1098/rstb.2008.0311>
- Hoppe, C.E., Galante, M.J., Oyanguren, P.A., Williams, R.J.J., 2005. Epoxies Modified by Palmitic Acid: From Hot-Melt Adhesives to Plasticized Networks. *Macromol. Mater. Eng.* 290, 456–462. <https://doi.org/10.1002/mame.200400348>
- Howell, B.A., Daniel, Y.G., 2018. The impact of sulfur oxidation level on flame retardancy. *J. Fire Sci.* 36, 518–534. <https://doi.org/10.1177/0734904118806155>
- Huang, S., Kong, X., Xiong, Y., Zhang, X., Chen, H., Jiang, W., Niu, Y., Xu, W., Ren, C., 2020. An overview of dynamic covalent bonds in polymer material and their applications. *Eur. Polym. J.* 141, 110094. <https://doi.org/10.1016/j.eurpolymj.2020.110094>
- Hubbard, A.M., Ren, Y., Papaioannou, P., Sarvestani, A., Picu, C.R., Konkolewicz, D., Roy, A.K., Varshney, V., Nepal, D., 2022a. Vitrimer Composites: Understanding the Role of Filler in Vitrimer Applicability. *ACS Appl. Polym. Mater.* 4, 6374–6385. <https://doi.org/10.1021/acsapm.2c00770>
- Hubbard, A.M., Ren, Y., Picu, C.R., Sarvestani, A., Konkolewicz, D., Roy, A.K., Varshney, V., Nepal, D., 2022b. Creep Mechanics of Epoxy Vitrimer Materials. *ACS Appl. Polym. Mater.* 4, 4254–4263. <https://doi.org/10.1021/acsapm.2c00230>
- ISO 15270, 2008. ISO 15270:2008(en), Plastics — Guidelines for the recovery and recycling of plastics waste [WWW Document]. URL <https://www.iso.org/obp/ui/en/#iso:std:iso:15270:ed-2:v1:en> (accessed 1.10.24).

- Jarach, N., Zuckerman, R., Naveh, N., Dodiuk, H., Kenig, S., 2021. Bio- and Water-Based Reversible Covalent Bonds Containing Polymers (Vitrimers) and Their Relevance to Adhesives – A Critical Review, in: *Progress in Adhesion and Adhesives*. John Wiley & Sons, Ltd, pp. 587–619. <https://doi.org/10.1002/9781119846703.ch13>
- Jehanno, C., Alty, J.W., Roosen, M., De Meester, S., Dove, A.P., Chen, E.Y.-X., Leibfarth, F.A., Sardon, H., 2022. Critical advances and future opportunities in upcycling commodity polymers. *Nature* 603, 803–814. <https://doi.org/10.1038/s41586-021-04350-0>
- Jia, P., Shi, Y., Song, F., Bei, Y., Huang, C., Zhang, M., Hu, L., Zhou, Y., 2022. Bio-based and degradable vitrimer-graphene/graphene oxide composites with self-healing ability stimulated by heat, electricity and microwave as temperature and fire warning sensors. *Compos. Sci. Technol.* 227, 109573. <https://doi.org/10.1016/j.compscitech.2022.109573>
- Jiang, L., Tian, Y., Wang, X., Zhang, J., Cheng, J., Gao, F., 2023. A fully bio-based Schiff base vitrimer with self-healing ability at room temperature. *Polym. Chem.* 14, 862–871. <https://doi.org/10.1039/D2PY00900E>
- Jiang, Z., Bhaskaran, A., Aitken, H.M., Shackelford, I.C.G., Connal, L.A., 2019. Using Synergistic Multiple Dynamic Bonds to Construct Polymers with Engineered Properties. *Macromol. Rapid Commun.* 40, 1900038. <https://doi.org/10.1002/marc.201900038>
- Jin, D., Dai, J., Zhao, W., Liu, X., 2023. Biobased Epoxy Resin with Inherently Deep-UV Photodegradability for a Positive Photoresist and Anticounterfeiting. *ACS Appl. Polym. Mater.* 5, 3138–3147. <https://doi.org/10.1021/acsapm.3c00291>
- Jin, X., Li, X., Liu, X., Du, L., Su, L., Ma, Y., Ren, S., 2023. Simple lignin-based, light-driven shape memory polymers with excellent mechanical properties and wide range of glass transition temperatures. *Int. J. Biol. Macromol.* 228, 528–536. <https://doi.org/10.1016/j.ijbiomac.2022.12.098>
- J. Kloxin, C., N. Bowman, C., 2013. Covalent adaptable networks: smart, reconfigurable and responsive network systems. *Chem. Soc. Rev.* 42, 7161–7173. <https://doi.org/10.1039/C3CS60046G>
- John, G., Nagarajan, S., Vemula, P.K., Silverman, J.R., Pillai, C.K.S., 2019. Natural monomers: A mine for functional and sustainable materials – Occurrence, chemical modification and polymerization. *Prog. Polym. Sci.* 92, 158–209. <https://doi.org/10.1016/j.progpolymsci.2019.02.008>
- Johnson, R.M., Cortés-Guzmán, K.P., Perera, S.D., Parikh, A.R., Ganesh, V., Voit, W.E., Smaldone, R.A., 2023. Lignin-based covalent adaptable network resins for digital light projection 3D printing. *J. Polym. Sci. n/a*. <https://doi.org/10.1002/pol.20230026>
- Jourdain, A., Asbaï, R., Anaya, O., Chehimi, M.M., Drockenmuller, E., Montarnal, D., 2020. Rheological Properties of Covalent Adaptable Networks with 1,2,3-Triazolium Cross-Links: The Missing Link between Vitrimers and Dissociative Networks. *Macromolecules* 53, 1884–1900. <https://doi.org/10.1021/acs.macromol.9b02204>
- Kaczmarek, B., 2020. Tannic Acid with Antiviral and Antibacterial Activity as A Promising Component of Biomaterials—A Minireview. *Materials* 13, 3224. <https://doi.org/10.3390/ma13143224>
- Karlinskii, B.Y., Ananikov, V.P., 2023. Recent advances in the development of green furan ring-containing polymeric materials based on renewable plant biomass. *Chem. Soc. Rev.* 52, 836–862. <https://doi.org/10.1039/D2CS00773H>
- Kasemsiri, P., Lorwanishpaisarn, N., Pongsa, U., Ando, S., 2018. Reconfigurable Shape Memory and Self-Welding Properties of Epoxy Phenolic Novolac/Cashew Nut Shell Liquid Composites Reinforced with Carbon Nanotubes. *Polymers* 10, 482. <https://doi.org/10.3390/polym10050482>
- Kaur, G., Johnston, P., Saito, K., 2014. Photo-reversible dimerisation reactions and their applications in polymeric systems. *Polym. Chem.* 5, 2171–2186. <https://doi.org/10.1039/C3PY01234D>
- Ke, Y., Yang, X., Chen, Q., Xue, J., Song, Z., Zhang, Y., Madbouly, S.A., Luo, Y., Li, M., Wang, Q., Zhang, C., 2021. Recyclable and Fluorescent Epoxy Polymer Networks from Cardanol Via Solvent-Free Epoxy-Thiol Chemistry. *ACS Appl. Polym. Mater.* 3, 3082–3092. <https://doi.org/10.1021/acsapm.1c00284>
- Kim, H., Cha, I., Yoon, Y., Cha, B.J., Yang, J., Kim, Y.D., Song, C., 2021. Facile Mechanochemical Synthesis of Malleable Biomass-Derived Network Polyurethanes and Their Shape-Memory Applications. *ACS Sustain. Chem. Eng.* 9, 6952–6961. <https://doi.org/10.1021/acssuschemeng.1c00390>
- Kim, N.K., Cha, E.J., Jung, M., Kim, J., Jeong, G.-J., Kim, Y.S., Choi, W.J., Kim, B.-S., Kim, D.-G., Lee, J.-C., 2019. 3D hierarchical scaffolds enabled by a post-patternable, reconfigurable, and biocompatible 2D vitrimer film for tissue engineering applications. *J. Mater. Chem. B* 7, 3341–3345. <https://doi.org/10.1039/C9TB00221A>
- Kisszekelyi, P., Hardian, R., Vovusha, H., Chen, B., Zeng, X., Schwingenschlögl, U., Kupai, J., Szekeley, G., 2020. Selective Electrocatalytic Oxidation of Biomass-Derived 5-Hydroxymethylfurfural to 2,5-Diformylfuran: from Mechanistic Investigations to Catalyst Recovery. *ChemSusChem* 13, 3127–3136. <https://doi.org/10.1002/cssc.202000453>

- Klein, F.C., Vogt, M., Abetz, V., 2023. Reprocessable Vanillin-Based Schiff Base Vitrimers: Tuning Mechanical and Thermomechanical Properties by Network Design. *Macromol. Mater. Eng.* n/a, 2300187. <https://doi.org/10.1002/mame.202300187>
- Kloxin, C.J., Scott, T.F., Adzima, B.J., Bowman, C.N., 2010. Covalent Adaptable Networks (CANs): A Unique Paradigm in Cross-Linked Polymers. *Macromolecules* 43, 2643–2653. <https://doi.org/10.1021/ma902596s>
- Konieczynska, M.D., Villa-Camacho, J.C., Ghobril, C., Perez-Viloria, M., Tevis, K.M., Blessing, W.A., Nazarian, A., Rodriguez, E.K., Grinstaff, M.W., 2016. On-Demand Dissolution of a Dendritic Hydrogel-based Dressing for Second-Degree Burn Wounds through Thiol–Thioester Exchange Reaction. *Angew. Chem. Int. Ed.* 55, 9984–9987. <https://doi.org/10.1002/anie.201604827>
- Konuray, O., Fernández-Francos, X., Ramis, X., 2023. Structural Design of CANs with Fine-Tunable Relaxation Properties: A Theoretical Framework Based on Network Structure and Kinetics Modeling. *Macromolecules* 56, 4855–4873. <https://doi.org/10.1021/acs.macromol.3c00482>
- Korley, L.T.J., Epps, T.H., Helms, B.A., Ryan, A.J., 2021. Toward polymer upcycling—adding value and tackling circularity. *Science* 373, 66–69. <https://doi.org/10.1126/science.abg4503>
- Košir, T., Slavič, J., 2023. Manufacturing of single-process 3D-printed piezoelectric sensors with electromagnetic protection using thermoplastic material extrusion. *Addit. Manuf.* 73, 103699. <https://doi.org/10.1016/j.addma.2023.103699>
- Kou, Z., Hu, Y., Ma, Y., Yuan, L., Hu, L., Zhou, Y., Jia, P., 2023. Bio-based dynamically crosslinked networks/Fe₃O₄ nanoparticles composites with self-healing ability driven by multiple stimuli for non-contact welding. *Ind. Crops Prod.* 195, 116401. <https://doi.org/10.1016/j.indcrop.2023.116401>
- Krishnakumar, B., Pucci, A., Wadgaonkar, P.P., Kumar, I., Binder, W.H., Rana, S., 2022. Vitrimers based on bio-derived chemicals: Overview and future prospects. *Chem. Eng. J.* 433, 133261. <https://doi.org/10.1016/j.cej.2021.133261>
- Krishnakumar, B., Sanka, R.V.S.P., Binder, W.H., Parthasarthy, V., Rana, S., Karak, N., 2020. Vitrimers: Associative dynamic covalent adaptive networks in thermoset polymers. *Chem. Eng. J.* 385, 123820. <https://doi.org/10.1016/j.cej.2019.123820>
- K. Schoustra, S., Groeneveld, T., J. Smulders, M.M., 2021. The effect of polarity on the molecular exchange dynamics in imine-based covalent adaptable networks. *Polym. Chem.* 12, 1635–1642. <https://doi.org/10.1039/D0PY01555E>
- Kuhl, N., Bode, S., Hager, M.D., Schubert, U.S., 2015. Self-Healing Polymers Based on Reversible Covalent Bonds, in: Hager, M.D., van der Zwaag, S., Schubert, U.S. (Eds.), *Self-Healing Materials, Advances in Polymer Science*. Springer International Publishing, Cham, pp. 1–58. https://doi.org/10.1007/12_2015_336
- Kumar, A., Connal, L.A., 2023. Biobased Transesterification Vitrimers. *Macromol. Rapid Commun.* 44, 2200892. <https://doi.org/10.1002/marc.202200892>
- Lalanne, L., Nyahongo, G.S., Guebitz, G.M., Pellis, A., 2021. Biotechnological production and high potential of furan-based renewable monomers and polymers. *Biotechnol. Adv.* 48, 107707. <https://doi.org/10.1016/j.biotechadv.2021.107707>
- Laoutid, F., Bonnaud, L., Alexandre, M., Lopez-Cuesta, J.-M., Dubois, Ph., 2009. New prospects in flame retardant polymer materials: From fundamentals to nanocomposites. *Mater. Sci. Eng. R Rep.* 63, 100–125. <https://doi.org/10.1016/j.mser.2008.09.002>
- Laurichesse, S., Avérous, L., 2014. Chemical modification of lignins: Towards biobased polymers. *Prog. Polym. Sci.* 39, 1266–1290. <https://doi.org/10.1016/j.progpolymsci.2013.11.004>
- Leibler, L., Rubinstein, M., Colby, R.H., 1991. Dynamics of reversible networks. *Macromolecules* 24, 4701–4707. <https://doi.org/10.1021/ma00016a034>
- Lendlein, A., Jiang, H., Jünger, O., Langer, R., 2005. Light-induced shape-memory polymers. *Nature* 434, 879–882. <https://doi.org/10.1038/nature03496>
- Lessard, J.J., Garcia, L.F., Easterling, C.P., Sims, M.B., Bentz, K.C., Arencibia, S., Savin, D.A., Sumerlin, B.S., 2019. Catalyst-Free Vitrimers from Vinyl Polymers. *Macromolecules* 52, 2105–2111. <https://doi.org/10.1021/acs.macromol.8b02477>
- Li, H., Zhang, B., Wang, R., Yang, X., He, X., Ye, H., Cheng, J., Yuan, C., Zhang, Y.-F., Ge, Q., 2022. Solvent-Free Upcycling Vitrimers through Digital Light Processing-Based 3D Printing and Bond Exchange Reaction. *Adv. Funct. Mater.* 32, 2111030. <https://doi.org/10.1002/adfm.202111030>
- Li, J., Weng, Z., Cao, Q., Qi, Y., Lu, B., Zhang, S., Wang, J., Jian, X., 2022. Synthesis of an aromatic amine derived from biomass and its use as a feedstock for versatile epoxy thermoset. *Chem. Eng. J.* 433, 134512. <https://doi.org/10.1016/j.cej.2022.134512>

- Li, L., Chen, X., Jin, K., Torkelson, J.M., 2018. Vitrimers Designed Both To Strongly Suppress Creep and To Recover Original Cross-Link Density after Reprocessing: Quantitative Theory and Experiments. *Macromolecules* 51, 5537–5546. <https://doi.org/10.1021/acs.macromol.8b00922>
- Li, L., Chen, X., Torkelson, J.M., 2020. Covalent Adaptive Networks for Enhanced Adhesion: Exploiting Disulfide Dynamic Chemistry and Annealing during Application. *ACS Appl. Polym. Mater.* 2, 4658–4665. <https://doi.org/10.1021/acsapm.0c00720>
- Li, Q., Ma, S., Li, P., Wang, B., Feng, H., Lu, N., Wang, S., Liu, Y., Xu, X., Zhu, J., 2021a. Biosourced Acetal and Diels–Alder Adduct Concurrent Polyurethane Covalent Adaptable Network. *Macromolecules* 54, 1742–1753. <https://doi.org/10.1021/acs.macromol.0c02699>
- Li, Q., Ma, S., Li, P., Wang, B., Yu, Z., Feng, H., Liu, Y., Zhu, J., 2021b. Fast Reprocessing of Acetal Covalent Adaptable Networks with High Performance Enabled by Neighboring Group Participation. *Macromolecules* 54, 8423–8434. <https://doi.org/10.1021/acs.macromol.1c01046>
- Li, Q., Ma, S., Wang, S., Liu, Y., Taher, M.A., Wang, B., Huang, K., Xu, X., Han, Y., Zhu, J., 2020. Green and Facile Preparation of Readily Dual-Recyclable Thermosetting Polymers with Superior Stability Based on Asymmetric Acetal. *Macromolecules* 53, 1474–1485. <https://doi.org/10.1021/acs.macromol.9b02386>
- Li, Q., Ma, S., Wang, S., Yuan, W., Xu, X., Wang, B., Huang, K., Zhu, J., 2019. Facile catalyst-free synthesis, exchanging, and hydrolysis of an acetal motif for dynamic covalent networks. *J. Mater. Chem. A* 7, 18039–18049. <https://doi.org/10.1039/C9TA04073K>
- Li, S., Li, W., Khashab, N.M., 2012. Stimuli responsive nanomaterials for controlled release applications. *Nanotechnol. Rev.* 1, 493–513. <https://doi.org/10.1515/ntrev-2012-0033>
- Li, W., Xiao, L., Wang, Y., Chen, J., Nie, X., 2021. Self-healing silicon-containing eugenol-based epoxy resin based on disulfide bond exchange: Synthesis and structure-property relationships. *Polymer* 229, 123967. <https://doi.org/10.1016/j.polymer.2021.123967>
- Li, W., Xiao, L., Wang, Y., Huang, J., Liu, Z., Chen, J., Nie, X., 2022. Thermal-induced self-healing bio-based vitrimers: Shape memory, recyclability, degradation, and intrinsic flame retardancy. *Polym. Degrad. Stab.* 202, 110039. <https://doi.org/10.1016/j.polymdegradstab.2022.110039>
- Liang, J.-Y., Shin, S.-R., Lee, S.-H., Lee, D.-S., 2019. Characteristics of Self-Healable Copolymers of Styrene and Eugenol Terminated Polyurethane Prepolymer. *Polymers* 11, 1674. <https://doi.org/10.3390/polym11101674>
- Liang, Y., Li, Z., Huang, Y., Yu, R., Guo, B., 2021. Dual-Dynamic-Bond Cross-Linked Antibacterial Adhesive Hydrogel Sealants with On-Demand Removability for Post-Wound-Closure and Infected Wound Healing. *ACS Nano* 15, 7078–7093. <https://doi.org/10.1021/acsnano.1c00204>
- Liguori, A., Hakkarainen, M., 2022. Designed from Biobased Materials for Recycling: Imine-Based Covalent Adaptable Networks. *Macromol. Rapid Commun.* 43, 2100816. <https://doi.org/10.1002/marc.202100816>
- Lijsebetten, F.V., Bruycker, K.D., Ruymbeke, E.V., M. Winne, J., Prez, F.E.D., 2022. Characterising different molecular landscapes in dynamic covalent networks. *Chem. Sci.* 13, 12865–12875. <https://doi.org/10.1039/D2SC05528G>
- Lin, X., Gablier, A., Terentjev, E.M., 2022. Imine-Based Reactive Mesogen and Its Corresponding Exchangeable Liquid Crystal Elastomer. *Macromolecules* 55, 821–830. <https://doi.org/10.1021/acs.macromol.1c02432>
- Lin, Y., Yan, R., Zhang, Y., Yang, X., Ding, H., Xu, L., Li, S., Li, M., 2022. Synthesis of biobased polyphenols for preparing phenolic polyurethanes with self-healing properties. *Polym. Test.* 112, 107644. <https://doi.org/10.1016/j.polymertesting.2022.107644>
- Liu, H., Cheng, T., Xian, M., Cao, Y., Fang, F., Zou, H., 2014. Fatty acid from the renewable sources: A promising feedstock for the production of biofuels and biobased chemicals. *Biotechnol. Adv.* 32, 382–389. <https://doi.org/10.1016/j.biotechadv.2013.12.003>
- Liu, J., Miao, P., Leng, X., Che, J., Wei, Z., Li, Y., 2023. Chemically Recyclable Biobased Non-Isocyanate Polyurethane Networks from CO₂-Derived Six-membered Cyclic Carbonates. *Macromol. Rapid Commun.* 44, 2300263. <https://doi.org/10.1002/marc.202300263>
- Liu, J., Pich, A., Bernaerts, K.V., 2024. Preparation of lignin-based vinylogous urethane vitrimer materials and their potential use as on-demand removable adhesives. *Green Chem.* <https://doi.org/10.1039/D3GC02799F>
- Liu, T., Hao, C., Wang, L., Li, Y., Liu, W., Xin, J., Zhang, J., 2017. Eugenol-Derived Biobased Epoxy: Shape Memory, Repairing, and Recyclability. *Macromolecules* 50, 8588–8597. <https://doi.org/10.1021/acs.macromol.7b01889>
- Liu, T., Hao, C., Zhang, S., Yang, X., Wang, L., Han, J., Li, Y., Xin, J., Zhang, J., 2018. A Self-Healable High Glass Transition Temperature Bioepoxy Material Based on Vitrimer Chemistry. *Macromolecules* 51, 5577–5585. <https://doi.org/10.1021/acs.macromol.8b01010>

- Liu, T., Peng, J., Liu, J., Hao, X., Guo, C., Ou, R., Liu, Z., Wang, Q., 2021. Fully recyclable, flame-retardant and high-performance carbon fiber composites based on vanillin-terminated cyclophosphazene polyimine thermosets. *Compos. Part B Eng.* 224, 109188. <https://doi.org/10.1016/j.compositesb.2021.109188>
- Liu, W., Fang, C., Chen, F., Qiu, X., 2020. Strong, Reusable, and Self-Healing Lignin-Containing Polyurea Adhesives. *ChemSusChem* 13, 4691–4701. <https://doi.org/10.1002/cssc.202001602>
- Liu, W., Fang, C., Wang, S., Huang, J., Qiu, X., 2019. High-Performance Lignin-Containing Polyurethane Elastomers with Dynamic Covalent Polymer Networks. *Macromolecules* 52, 6474–6484. <https://doi.org/10.1021/acs.macromol.9b01413>
- Liu, W., Yang, S., Huang, L., Xu, J., Zhao, N., 2022. Dynamic covalent polymers enabled by reversible isocyanate chemistry. *Chem. Commun.* 58, 12399–12417. <https://doi.org/10.1039/D2CC04747K>
- Liu, W.-X., Zhang, C., Zhang, H., Zhao, N., Yu, Z.-X., Xu, J., 2017. Oxime-Based and Catalyst-Free Dynamic Covalent Polyurethanes. *J. Am. Chem. Soc.* 139, 8678–8684. <https://doi.org/10.1021/jacs.7b03967>
- Liu, X., Zhang, E., Feng, Z., Liu, J., Chen, B., Liang, L., 2021. Degradable bio-based epoxy vitrimers based on imine chemistry and their application in recyclable carbon fiber composites. *J. Mater. Sci.* 56, 15733–15751. <https://doi.org/10.1007/s10853-021-06291-5>
- Liu, Y., Zhang, Z., Fan, W., Yang, K., Li, Z., 2022. Preparation of renewable gallic acid-based self-healing waterborne polyurethane with dynamic phenol–carbamate network: toward superior mechanical properties and shape memory function. *J. Mater. Sci.* 57, 5679–5696. <https://doi.org/10.1007/s10853-022-07000-6>
- Liu, Y., Zhang, Z., Wang, J., Xie, T., Sun, L., Yang, K., Li, Z., 2021. Renewable tannic acid based self-healing polyurethane with dynamic phenol-carbamate network: Simultaneously showing robust mechanical properties, reprocessing ability and shape memory. *Polymer* 228, 123860. <https://doi.org/10.1016/j.polymer.2021.123860>
- Liu, Y.-L., Chuo, T.-W., 2013. Self-healing polymers based on thermally reversible Diels–Alder chemistry. *Polym. Chem.* 4, 2194–2205. <https://doi.org/10.1039/C2PY20957H>
- Liu, Y.-Y., He, J., Li, Y.-D., Zhao, X.-L., Zeng, J.-B., 2020. Biobased epoxy vitrimer from epoxidized soybean oil for reprocessable and recyclable carbon fiber reinforced composite. *Compos. Commun.* 22, 100445. <https://doi.org/10.1016/j.coco.2020.100445>
- Liu, Y.-Y., Liu, G.-L., Li, Y.-D., Weng, Y., Zeng, J.-B., 2021. Biobased High-Performance Epoxy Vitrimer with UV Shielding for Recyclable Carbon Fiber Reinforced Composites. *ACS Sustain. Chem. Eng.* 9, 4638–4647. <https://doi.org/10.1021/acssuschemeng.1c00231>
- Llevot, A., Grau, E., Carlotti, S., Grelier, S., Cramail, H., 2016. From Lignin-derived Aromatic Compounds to Novel Biobased Polymers. *Macromol. Rapid Commun.* 37, 9–28. <https://doi.org/10.1002/marc.201500474>
- Lochab, B., Shukla, S., Varma, I.K., 2014. Naturally occurring phenolic sources: monomers and polymers. *RSC Adv.* 4, 21712–21752. <https://doi.org/10.1039/C4RA00181H>
- Lorwanishpaisarn, N., Kasemsiri, P., Srikhao, N., Son, C., Kim, S., Theerakulpisut, S., Chindaprasirt, P., 2021. Carbon fiber/epoxy vitrimer composite patch cured with bio-based curing agents for one-step repair metallic sheet and its recyclability. *J. Appl. Polym. Sci.* 138, 51406. <https://doi.org/10.1002/app.51406>
- Lorwanishpaisarn, N., Srikhao, N., Jetsrisuparb, K., Knijnenburg, J.T.N., Theerakulpisut, S., Okhawilai, M., Kasemsiri, P., 2022. Self-healing Ability of Epoxy Vitrimer Nanocomposites Containing Bio-Based Curing Agents and Carbon Nanotubes for Corrosion Protection. *J. Polym. Environ.* 30, 472–482. <https://doi.org/10.1007/s10924-021-02213-3>
- Lucherelli, M.A., Duval, A., Averous, L., 2023. Combining Associative and Dissociative Dynamic Linkages in Covalent Adaptable Networks from Biobased 2,5-Furandicarboxaldehyde. *ACS Sustain. Chem. Eng.* 11, 2334–2344. <https://doi.org/10.1021/acssuschemeng.2c05956>
- Lucherelli, M.A., Duval, A., Avérous, L., 2022. Biobased vitrimers: Towards sustainable and adaptable performing polymer materials. *Prog. Polym. Sci.* 127, 101515. <https://doi.org/10.1016/j.progpolymsci.2022.101515>
- Lucintel, 2021. Management Consulting, Market Research Company, Market Research Firms [WWW Document], 2021. URL <https://www.lucintel.com/press/eugenol-market.aspx> (accessed 7.21.23).
- Ludmila, H., Michal, J., Andrea, Š., Aleš, H., 2015. LIGNIN, POTENTIAL PRODUCTS AND THEIR MARKET. *Wood Res.* 60, 973–986.
- Luo, W., Yu, H., Liu, Z., Ou, R., Guo, C., Tao liu, Zhang, J., 2022. Construction and application of hybrid covalent adaptive network with non-conjugated fluorescence, self-healing and Fe³⁺ ion sensing. *J. Mater. Res. Technol.* 19, 1699–1710. <https://doi.org/10.1016/j.jmrt.2022.05.157>
- Ma, X., Li, S., Wang, F., Wu, J., Chao, Y., Chen, X., Chen, P., Zhu, J., Yan, N., Chen, J., 2023a. Catalyst-Free Synthesis of Covalent Adaptable Network (CAN) Polyurethanes from Lignin with Editable Shape Memory Properties. *ChemSusChem* 16, e202202071. <https://doi.org/10.1002/cssc.202202071>

- Ma, X., Wang, X., Zhao, H., Xu, X., Cui, M., Stott, N.E., Chen, P., Zhu, J., Yan, N., Chen, J., 2023b. High-Performance, Light-Stimulation Healable, and Closed-Loop Recyclable Lignin-Based Covalent Adaptable Networks. *Small* 19, 2303215. <https://doi.org/10.1002/sml.202303215>
- Mahajan, J.S., O'Dea, R.M., Norris, J.B., Korley, L.T.J., Epps, T.H., 2020. Aromatics from Lignocellulosic Biomass: A Platform for High-Performance Thermosets. *ACS Sustain. Chem. Eng.* 8, 15072–15096. <https://doi.org/10.1021/acssuschemeng.0c04817>
- Manarin, E., Da Via, F., Rigatelli, B., Turri, S., Griffini, G., 2023. Bio-Based Vitrimers from 2,5-Furandicarboxylic Acid as Repairable, Reusable, and Recyclable Epoxy Systems. *ACS Appl. Polym. Mater.* 5, 828–838. <https://doi.org/10.1021/acsapm.2c01774>
- Mao Png, Z., Zheng, J., Kamarulzaman, S., Wang, S., Li, Z., S. Goh, S., 2023. Correction: Fully biomass-derived vitrimeric material with water-mediated recyclability and monomer recovery. *Green Chem.* 25, 789–790. <https://doi.org/10.1039/D2GC90119F>
- Martins, M.L., Zhao, X., Demchuk, Z., Luo, J., Carden, G.P., Toleutay, G., Sokolov, A.P., 2023. Viscoelasticity of Polymers with Dynamic Covalent Bonds: Concepts and Misconceptions. *Macromolecules* 56, 8688–8696. <https://doi.org/10.1021/acs.macromol.3c01545>
- Mather, B.D., Viswanathan, K., Miller, K.M., Long, T.E., 2006. Michael addition reactions in macromolecular design for emerging technologies. *Prog. Polym. Sci.* 31, 487–531. <https://doi.org/10.1016/j.progpolymsci.2006.03.001>
- McBride, M.K., Worrell, B.T., Brown, T., Cox, L.M., Sowan, N., Wang, C., Podgorski, M., Martinez, A.M., Bowman, C.N., 2019. Enabling Applications of Covalent Adaptable Networks. *Annu. Rev. Chem. Biomol. Eng.* 10, 175–198. <https://doi.org/10.1146/annurev-chembioeng-060718-030217>
- Memon, H., Wei, Y., Zhang, L., Jiang, Q., Liu, W., 2020. An imine-containing epoxy vitrimer with versatile recyclability and its application in fully recyclable carbon fiber reinforced composites. *Compos. Sci. Technol.* 199, 108314. <https://doi.org/10.1016/j.compscitech.2020.108314>
- Mgaya, J., Shombe, G.B., Masikane, S.C., Mlowe, S., Mubofu, E.B., Revaprasadu, N., 2019. Cashew nut shell: a potential bio-resource for the production of bio-sourced chemicals, materials and fuels. *Green Chem.* 21, 1186–1201. <https://doi.org/10.1039/C8GC02972E>
- Miao, J.-T., Ge, M., Wu, Y., Chou, T.Y., Wang, H., Zheng, L., Wu, L., 2020. Eugenol-derived reconfigurable high-performance epoxy resin for self-deployable smart 3D structures. *Eur. Polym. J.* 134, 109805. <https://doi.org/10.1016/j.eurpolymj.2020.109805>
- Mo, J., Dai, Y., Zhang, C., Zhou, Y., Li, W., Song, Y., Wu, C., Wang, Z., 2021. Design of ultra-stretchable, highly adhesive and self-healable hydrogels via tannic acid-enabled dynamic interactions. *Mater. Horiz.* 8, 3409–3416. <https://doi.org/10.1039/D1MH01324F>
- Molina-Gutiérrez, S., Ladmiral, V., Bongiovanni, R., Caillol, S., Lacroix-Desmazes, P., 2019. Emulsion Polymerization of Dihydroeugenol-, Eugenol-, and Isoeugenol-Derived Methacrylates. *Ind. Eng. Chem. Res.* 58, 21155–21164. <https://doi.org/10.1021/acs.iecr.9b02338>
- Montanari, E., Gennari, A., Pelliccia, M., Gourmel, C., Lallana, E., Matricardi, P., McBain, A.J., Tirelli, N., 2016. Hyaluronan/Tannic Acid Nanoparticles Via Catechol/Boronate Complexation as a Smart Antibacterial System. *Macromol. Biosci.* 16, 1815–1823. <https://doi.org/10.1002/mabi.201600311>
- Montarnal, D., Capelot, M., Tourmilhac, F., Leibler, L., 2011. Silica-Like Malleable Materials from Permanent Organic Networks. *Science* 334, 965–968. <https://doi.org/10.1126/science.1212648>
- Morales-Cerrada, R., Molina-Gutiérrez, S., Lacroix-Desmazes, P., Caillol, S., 2021. Eugenol, a Promising Building Block for Biobased Polymers with Cutting-Edge Properties. *Biomacromolecules* 22, 3625–3648. <https://doi.org/10.1021/acs.biomac.1c00837>
- More, A., Elder, T., Pajer, N., Argyropoulos, D.S., Jiang, Z., 2023. Novel and Integrated Process for the Valorization of Kraft Lignin to Produce Lignin-Containing Vitrimers. *ACS Omega* 8, 1097–1108. <https://doi.org/10.1021/acsomega.2c06445>
- Moreau, C., Belgacem, M.N., Gandini, A., 2004. Recent Catalytic Advances in the Chemistry of Substituted Furans from Carbohydrates and in the Ensuing Polymers. *Top. Catal.* 27, 11–30. <https://doi.org/10.1023/B:TOCA.0000013537.13540.0e>
- Moreno, A., Morsali, M., Sipponen, M.H., 2021. Catalyst-Free Synthesis of Lignin Vitrimers with Tunable Mechanical Properties: Circular Polymers and Recoverable Adhesives. *ACS Appl. Mater. Interfaces* 13, 57952–57961. <https://doi.org/10.1021/acsami.1c17412>
- Morinval, A., Averous, L., 2022. Systems Based on Biobased Thermoplastics: From Bioresources to Biodegradable Packaging Applications. *Polym. Rev.* 62, 653–721. <https://doi.org/10.1080/15583724.2021.2012802>
- Mouren, A., Avérous, L., 2023. Sustainable cycloaliphatic polyurethanes: from synthesis to applications. *Chem. Soc. Rev.* 52, 277–317. <https://doi.org/10.1039/D2CS00509C>

- Mubofu, E.B., Mgaya, J.E., 2018. Chemical Valorization of Cashew Nut Shell Waste. *Top. Curr. Chem.* 376, 8. <https://doi.org/10.1007/s41061-017-0177-9>
- Murphy, J.C., Watson, E.S., Harland, E.C., 1983. Toxicology evaluation of poison oak urushiol and its esterified derivative. *Toxicology* 26, 135–142. [https://doi.org/10.1016/0300-483X\(83\)90064-1](https://doi.org/10.1016/0300-483X(83)90064-1)
- Nabipour, H., Wang, X., Kandola, B., Song, L., Kan, Y., Chen, J., Hu, Y., 2023. A bio-based intrinsically flame-retardant epoxy vitrimer from furan derivatives and its application in recyclable carbon fiber composites. *Polym. Degrad. Stab.* 207, 110206. <https://doi.org/10.1016/j.polymdegradstab.2022.110206>
- Naderi Kalali, E., Lotfian, S., Entezar Shabestari, M., Khayat-zadeh, S., Zhao, C., Yazdani Nezhad, H., 2023. A critical review of the current progress of plastic waste recycling technology in structural materials. *Curr. Opin. Green Sustain. Chem.* 40, 100763. <https://doi.org/10.1016/j.cogsc.2023.100763>
- Nagane, S.S., Kuhire, S.S., Mane, S.R., Wadgaonkar, P.P., 2019. Partially bio-based aromatic poly(ether sulfone)s bearing pendant furyl groups: synthesis, characterization and thermo-reversible cross-linking with a bismaleimide. *Polym. Chem.* 10, 1089–1098. <https://doi.org/10.1039/C8PY01477A>
- Nagasaka, R., Chotimarkorn, C., Shafiqul, I.Md., Hori, M., Ozaki, H., Ushio, H., 2007. Anti-inflammatory effects of hydroxycinnamic acid derivatives. *Biochem. Biophys. Res. Commun.* 358, 615–619. <https://doi.org/10.1016/j.bbrc.2007.04.178>
- Nasar, A.S., Shrinivas, V., Shanmugam, T., Raghavan, A., 2004. Synthesis and deblocking of cardanol- and anacardate-blocked toluene diisocyanates. *J. Polym. Sci. Part Polym. Chem.* 42, 4047–4055. <https://doi.org/10.1002/pola.20211>
- Nie, J., Xie, J., Liu, H., 2013. Activated carbon-supported ruthenium as an efficient catalyst for selective aerobic oxidation of 5-hydroxymethylfurfural to 2,5-diformylfuran. *Chin. J. Catal.* 34, 871–875. [https://doi.org/10.1016/S1872-2067\(12\)60551-8](https://doi.org/10.1016/S1872-2067(12)60551-8)
- Nishimura, Y., Chung, J., Muradyan, H., Guan, Z., 2017. Silyl Ether as a Robust and Thermally Stable Dynamic Covalent Motif for Malleable Polymer Design. *J. Am. Chem. Soc.* 139, 14881–14884. <https://doi.org/10.1021/jacs.7b08826>
- Nishiyabu, R., Kubo, Y., James, T.D., Fossey, J.S., 2011. Boronic acid building blocks: tools for self assembly. *Chem. Commun.* 47, 1124–1150. <https://doi.org/10.1039/C0CC02921A>
- Ocando, C., Ecochard, Y., Decostanzi, M., Caillol, S., Avérous, L., 2020. Dynamic network based on eugenol-derived epoxy as promising sustainable thermoset materials. *Eur. Polym. J.* 135, 109860. <https://doi.org/10.1016/j.eurpolymj.2020.109860>
- Offenbach, J.A., Tobolsky, A.V., 1956. Chemical relaxation of stress in polyurethane elastomers. *J. Colloid Sci.* 11, 39–47. [https://doi.org/10.1016/0095-8522\(56\)90017-4](https://doi.org/10.1016/0095-8522(56)90017-4)
- Oh, Y., Lee, K.M., Jung, D., Chae, J.A., Kim, H.J., Chang, M., Park, J.-J., Kim, H., 2019. Sustainable, Naringenin-Based Thermosets Show Reversible Macroscopic Shape Changes and Enable Modular Recycling. *ACS Macro Lett.* 8, 239–244. <https://doi.org/10.1021/acsmacrolett.9b00008>
- Organization for Economic Co-operation and Development, 2022. Global plastics outlook: economic drivers, environmental impacts and policy options. OECD publishing.
- Osthoff, R.C., Bueche, A.M., Grubb, W.T., 1954. Chemical Stress-Relaxation of Polydimethylsiloxane Elastomers ¹. *J. Am. Chem. Soc.* 76, 4659–4663. <https://doi.org/10.1021/ja01647a052>
- Pagliaro, M., Albanese, L., Scurria, A., Zabini, F., Meneguzzo, F., Ciriminna, R., 2021. Tannin: a new insight into a key product for the bioeconomy in forest regions. *Biofuels Bioprod. Biorefining* 15, 973–979. <https://doi.org/10.1002/bbb.2217>
- Pan, X., Sengupta, P., Webster, D.C., 2011. High Biobased Content Epoxy–Anhydride Thermosets from Epoxidized Sucrose Esters of Fatty Acids. *Biomacromolecules* 12, 2416–2428. <https://doi.org/10.1021/bm200549c>
- Pemba, A.G., Miller, S.A., 2019. Acetal Metathesis: Mechanistic Insight. *Synlett* 30, 1971–1976. <https://doi.org/10.1055/s-0037-1611833>
- Peng, J., Xie, S., Liu, T., Wang, D., Ou, R., Guo, C., Wang, Q., Liu, Z., 2022. High-performance epoxy vitrimer with superior self-healing, shape-memory, flame retardancy, and antibacterial properties based on multifunctional curing agent. *Compos. Part B Eng.* 242, 110109. <https://doi.org/10.1016/j.compositesb.2022.110109>
- Perego, A., Lazarenko, D., Cloitre, M., Khabaz, F., 2022. Microscopic Dynamics and Viscoelasticity of Vitrimers. *Macromolecules* 55, 7605–7613. <https://doi.org/10.1021/acs.macromol.2c00588>
- Phani Kumar, P., Paramashivappa, R., Vithayathil, P.J., Subba Rao, P.V., Srinivasa Rao, A., 2002. Process for Isolation of Cardanol from Technical Cashew (*Anacardium occidentale* L.) Nut Shell Liquid. *J. Agric. Food Chem.* 50, 4705–4708. <https://doi.org/10.1021/jf020224w>
- Picinelli, A., Dapena, E., Mangas, J.J., 1995. Polyphenolic Pattern in Apple Tree Leaves in Relation to Scab Resistance. A Preliminary Study. *J. Agric. Food Chem.* 43, 2273–2278. <https://doi.org/10.1021/jf00056a057>

- Pickering, S.J., 2006. Recycling technologies for thermoset composite materials—current status. *Compos. Part Appl. Sci. Manuf., The 2nd International Conference: Advanced Polymer Composites for Structural Applications in Construction* 37, 1206–1215. <https://doi.org/10.1016/j.compositesa.2005.05.030>
- Pinto, O., Romero, R., Carrier, M., Appelt, J., Segura, C., 2018. Fast pyrolysis of tannins from pine bark as a renewable source of catechols. *J. Anal. Appl. Pyrolysis* 136, 69–76. <https://doi.org/10.1016/j.jaap.2018.10.022>
- Pizzi, A., 2019. Tannins: Prospectives and Actual Industrial Applications. *Biomolecules* 9, 344. <https://doi.org/10.3390/biom9080344>
- Pizzi, A., Daling, G.M.E., 1980. Laminating wood adhesives by generation of resorcinol from tannin extracts. *J. Appl. Polym. Sci.* 25, 1039–1048. <https://doi.org/10.1002/app.1980.070250606>
- Png, Z.M., Zheng, J., Kamarulzaman, S., Wang, S., Li, Z., Goh, S.S., 2022. Fully biomass-derived vitrimeric material with water-mediated recyclability and monomer recovery. *Green Chem.* 24, 5978–5986. <https://doi.org/10.1039/D2GC01556K>
- Poplata, S., Tröster, A., Zou, Y.-Q., Bach, T., 2016. Recent Advances in the Synthesis of Cyclobutanes by Olefin [2 + 2] Photocycloaddition Reactions. *Chem. Rev.* 116, 9748–9815. <https://doi.org/10.1021/acs.chemrev.5b00723>
- Popp, J., Kovács, S., Oláh, J., Divéki, Z., Balázs, E., 2021. Bioeconomy: Biomass and biomass-based energy supply and demand. *New Biotechnol.* 60, 76–84. <https://doi.org/10.1016/j.nbt.2020.10.004>
- Porath, L., Huang, J., Ramlawi, N., Derkaloustian, M., Ewoldt, R.H., Evans, C.M., 2022. Relaxation of Vitrimers with Kinetically Distinct Mixed Dynamic Bonds. *Macromolecules* 55, 4450–4458. <https://doi.org/10.1021/acs.macromol.1c02613>
- Porath, L.E., Evans, C.M., 2021. Importance of Broad Temperature Windows and Multiple Rheological Approaches for Probing Viscoelasticity and Entropic Elasticity in Vitrimers. *Macromolecules* 54, 4782–4791. <https://doi.org/10.1021/acs.macromol.0c02800>
- Post, W., Susa, A., Blaauw, R., Molenveld, K., Knoop, R.J.I., 2020. A Review on the Potential and Limitations of Recyclable Thermosets for Structural Applications. *Polym. Rev.* 60, 359–388. <https://doi.org/10.1080/15583724.2019.1673406>
- Purwanto, N.S., Chen, Y., Torkelson, J.M., 2023. Reprocessable, Bio-Based, Self-Blowing Non-Isocyanate Polyurethane Network Foams from Cashew Nutshell Liquid. *ACS Appl. Polym. Mater.* 5, 6651–6661. <https://doi.org/10.1021/acsapm.3c01196>
- Qiu, J., Ma, S., Wang, S., Tang, Z., Li, Q., Tian, A., Xu, X., Wang, B., Lu, N., Zhu, J., 2021. Upcycling of Polyethylene Terephthalate to Continuously Reprocessable Vitrimers through Reactive Extrusion. *Macromolecules* 54, 703–712. <https://doi.org/10.1021/acs.macromol.0c02359>
- Quienne, B., Kasmi, N., Dieden, R., Caillol, S., Habibi, Y., 2020. Isocyanate-Free Fully Biobased Star Polyester-Urethanes: Synthesis and Thermal Properties. *Biomacromolecules* 21, 1943–1951. <https://doi.org/10.1021/acs.biomac.0c00156>
- Ragaert, K., Ragot, C., Van Geem, K.M., Kersten, S., Shiran, Y., De Meester, S., 2023. Clarifying European terminology in plastics recycling. *Curr. Opin. Green Sustain. Chem.* 44, 100871. <https://doi.org/10.1016/j.cogsc.2023.100871>
- Ralph, J., Lundquist, K., Brunow, G., Lu, F., Kim, H., Schatz, P.F., Marita, J.M., Hatfield, R.D., Ralph, S.A., Christensen, J.H., Boerjan, W., 2004. Lignins: Natural polymers from oxidative coupling of 4-hydroxyphenyl-propanoids. *Phytochem. Rev.* 3, 29–60. <https://doi.org/10.1023/B:PHYT.0000047809.65444.a4>
- Raquez, J.-M., Deléglise, M., Lacrampe, M.-F., Krawczak, P., 2010. Thermosetting (bio)materials derived from renewable resources: A critical review. *Prog. Polym. Sci., Topical Issue on Biomaterials* 35, 487–509. <https://doi.org/10.1016/j.progpolymsci.2010.01.001>
- Rashid, Muhammad Abdur, Dayan, Md.A.R., Jiang, Q., Wei, Y., Liu, W., 2023a. Optimizing mechanical and thermomechanical properties of the self-healable and recyclable biobased epoxy thermosets. *J. Polym. Res.* 30, 70. <https://doi.org/10.1007/s10965-023-03456-5>
- Rashid, Muhammad Abdur, Hasan, M.N., Dayan, M.A.R., Ibna Jamal, M.S., Patoary, M.K., 2023b. A Critical Review of Sustainable Vanillin-modified Vitrimers: Synthesis, Challenge and Prospects. *Reactions* 4, 66–91. <https://doi.org/10.3390/reactions4010003>
- Rashid, Muhammad A., Zhu, S., Jiang, Q., Wei, Y., Liu, W., 2023a. Developing Easy Processable, Recyclable, and Self-Healable Biobased Epoxy Resin through Dynamic Covalent Imine Bonds. *ACS Appl. Polym. Mater.* 5, 279–289. <https://doi.org/10.1021/acsapm.2c01501>
- Rashid, M.A., Zhu, S., Jiang, Q., Zhang, L., Wei, Y., Liu, W., 2022. A Quercetin-Derived Polybasic Acid Hardener for Reprocessable and Degradable Epoxy Resins Based on Transesterification. *ACS Appl. Polym. Mater.* 4, 5708–5716. <https://doi.org/10.1021/acsapm.2c00674>

- Rashid, Muhammad A., Zhu, S., Zhang, L., Jin, K., Liu, W., 2023b. High-performance and fully recyclable epoxy resins cured by imine-containing hardeners derived from vanillin and syringaldehyde. *Eur. Polym. J.* 187, 111878. <https://doi.org/10.1016/j.eurpolymj.2023.111878>
- Reddy, K.S.K., Chen, Y.-C., Jeng, R.-J., Abu-Omar, M.M., Lin, C.-H., 2023. Upcycling Waste Polycarbonate to Poly(carbonate imine) Vitrimers with High Thermal Properties and Unprecedented Hydrolytic Stability. *ACS Sustain. Chem. Eng.* 11, 8580–8591. <https://doi.org/10.1021/acssuschemeng.3c01454>
- Rekondo, A., Martin, R., Luzuriaga, A.R. de, Cabañero, G., Grande, H.J., Odriozola, I., 2014. Catalyst-free room-temperature self-healing elastomers based on aromatic disulfide metathesis. *Mater. Horiz.* 1, 237–240. <https://doi.org/10.1039/C3MH00061C>
- Ren, J., Yang, H., Wu, Y., Liu, S., Ni, K., Ran, X., Zhou, X., Gao, W., Du, G., Yang, L., 2022. Dynamic reversible adhesives based on crosslinking network via Schiff base and Michael addition. *RSC Adv.* 12, 15241–15250. <https://doi.org/10.1039/D2RA02299K>
- Renders, T., Bosch, S.V. den, Koelewijn, S.-F., Schutyser, W., Sels, B.F., 2017. Lignin-first biomass fractionation: the advent of active stabilisation strategies. *Energy Environ. Sci.* 10, 1551–1557. <https://doi.org/10.1039/C7EE01298E>
- Ricarte, R.G., Tournilhac, F., Cloître, M., Leibler, L., 2020. Linear Viscoelasticity and Flow of Self-Assembled Vitrimers: The Case of a Polyethylene/Dioxaborolane System. *Macromolecules* 53, 1852–1866. <https://doi.org/10.1021/acs.macromol.9b02415>
- Rinaldi, R., Jastrzebski, R., Clough, M.T., Ralph, J., Kennema, M., Bruijninx, P.C.A., Weckhuysen, B.M., 2016. Paving the Way for Lignin Valorisation: Recent Advances in Bioengineering, Biorefining and Catalysis. *Angew. Chem. Int. Ed.* 55, 8164–8215. <https://doi.org/10.1002/anie.201510351>
- Rocha, L.D., Monteiro, M.C., Teodoro, A.J., 2012. Anticancer Properties of Hydroxycinnamic Acids -A Review. *Cancer Clin. Oncol.* 1, 109–121. <https://doi.org/10.5539/cc.v1n2p109>
- Rochette, J.M., Ashby, V.S., 2013. Photoresponsive Polyesters for Tailorable Shape Memory Biomaterials. *Macromolecules* 46, 2134–2140. <https://doi.org/10.1021/ma302354a>
- Rodrigues Pinto, P.C., Borges da Silva, E.A., Rodrigues, A.E., 2012. Lignin as Source of Fine Chemicals: Vanillin and Syringaldehyde, in: Baskar, C., Baskar, S., Dhillon, R.S. (Eds.), *Biomass Conversion: The Interface of Biotechnology, Chemistry and Materials Science*. Springer, Berlin, Heidelberg, pp. 381–420. https://doi.org/10.1007/978-3-642-28418-2_12
- Roig, A., Hidalgo, P., Ramis, X., De la Flor, S., Serra, À., 2022a. Vitrimeric Epoxy-Amine Polyimine Networks Based on a Renewable Vanillin Derivative. *ACS Appl. Polym. Mater.* 4, 9341–9350. <https://doi.org/10.1021/acsapm.2c01604>
- Roig, A., Petrauskaitė, A., Ramis, X., Flor, S.D. la, Serra, À., 2022b. Synthesis and characterization of new bio-based poly(acylhydrazone) vanillin vitrimers. *Polym. Chem.* 13, 1510–1519. <https://doi.org/10.1039/D1PY01694F>
- Romero, C., Brenes, M., 2012. Analysis of Total Contents of Hydroxytyrosol and Tyrosol in Olive Oils. *J. Agric. Food Chem.* 60, 9017–9022. <https://doi.org/10.1021/jf3026666>
- Rosato, D.V., Rosato, M.G., 2012. *Injection molding handbook*. Springer Science & Business Media.
- Röttger, M., Domenech, T., van der Weegen, R., Breuillac, A., Nicolaÿ, R., Leibler, L., 2017. High-performance vitrimers from commodity thermoplastics through dioxaborolane metathesis. *Science* 356, 62–65. <https://doi.org/10.1126/science.aah5281>
- Roy, P.S., Mention, M.M., Patti, A.F., Garnier, G., Allais, F., Saito, K., 2023. Photo-responsive lignin fragment-based polymers as switchable adhesives. *Polym. Chem.* 14, 913–924. <https://doi.org/10.1039/D2PY01474B>
- Rubinstein, M., Semenov, A.N., 1998. Thermoreversible Gelation in Solutions of Associating Polymers. 2. Linear Dynamics. *Macromolecules* 31, 1386–1397. <https://doi.org/10.1021/ma970617+>
- Ruiz, E., Romero-García, J.M., Romero, I., Manzanares, P., Negro, M.J., Castro, E., 2017. Olive-derived biomass as a source of energy and chemicals. *Biofuels Bioprod. Biorefining* 11, 1077–1094. <https://doi.org/10.1002/bbb.1812>
- Saito, K., Eisenreich, F., Türel, T., Tomović, Ž., 2022. Closed-Loop Recycling of Poly(Imine-Carbonate) Derived from Plastic Waste and Bio-based Resources. *Angew. Chem. Int. Ed.* 61, e202211806. <https://doi.org/10.1002/anie.202211806>
- Saito, K., Türel, T., Eisenreich, F., Tomović, Ž., 2023. Closed-Loop Recyclable Poly(imine-acetal)s with Dual-Cleavable Bonds for Primary Building Block Recovery. *ChemSusChem* 16, e202301017. <https://doi.org/10.1002/cssc.202301017>
- Sardon, H., Mecerreyes, D., Basterretxea, A., Avérous, L., Jehanno, C., 2021. From Lab to Market: Current Strategies for the Production of Biobased Polyols. *ACS Sustain. Chem. Eng.* 9, 10664–10677. <https://doi.org/10.1021/acssuschemeng.1c02361>

- Sarika, P.R., Nancarrow, P., Khansaheb, A., Ibrahim, T., 2020. Bio-Based Alternatives to Phenol and Formaldehyde for the Production of Resins. *Polymers* 12, 2237. <https://doi.org/10.3390/polym12102237>
- Sastri, V.R., Tesoro, G.C., 1990. Reversible crosslinking in epoxy resins. II. New approaches. *J. Appl. Polym. Sci.* 39, 1439–1457. <https://doi.org/10.1002/app.1990.070390703>
- Schenk, V., Labastie, K., Destarac, M., Olivier, P., Guerre, M., 2022. Vitrimers: current status and future challenges. *Mater. Adv.* 3, 8012–8029. <https://doi.org/10.1039/D2MA00654E>
- Schmolke, W., Perner, N., Seiffert, S., 2015. Dynamically Cross-Linked Polydimethylsiloxane Networks with Ambient-Temperature Self-Healing. *Macromolecules* 48, 8781–8788. <https://doi.org/10.1021/acs.macromol.5b01666>
- Schoustra, S.K., Dijkman, J.A., Zuilhof, H., Smulders, M.M.J., 2021. Molecular control over vitrimer-like mechanics – tuneable dynamic motifs based on the Hammett equation in polyimine materials. *Chem. Sci.* 12, 293–302. <https://doi.org/10.1039/D0SC05458E>
- Schutyser, W., Renders, T., Bosch, S.V. den, Koelewijn, S.-F., Beckham, G.T., Sels, B.F., 2018. Chemicals from lignin: an interplay of lignocellulose fractionation, depolymerisation, and upgrading. *Chem. Soc. Rev.* 47, 852–908. <https://doi.org/10.1039/C7CS00566K>
- Scott, T.F., Schneider, A.D., Cook, W.D., Bowman, C.N., 2005. Photoinduced Plasticity in Cross-Linked Polymers. *Science* 308, 1615–1617. <https://doi.org/10.1126/science.1110505>
- Semenov, A.N., Rubinstein, M., 1998. Thermoreversible Gelation in Solutions of Associative Polymers. 1. Statics. *Macromolecules* 31, 1373–1385. <https://doi.org/10.1021/ma970616h>
- Sharma, H., Rana, S., Singh, P., Hayashi, M., Binder, W.H., Rossegger, E., Kumar, A., Schögl, S., 2022. Self-healable fiber-reinforced vitrimer composites: overview and future prospects. *RSC Adv.* 12, 32569–32582. <https://doi.org/10.1039/D2RA05103F>
- Shen, H., Qiao, H., Zhang, H., 2022. Sulfur-urushiol copolymer: A material synthesized through inverse vulcanization from renewable resources and its latent application as self-repairable and antimicrobial adhesive. *Chem. Eng. J.* 450, 137905. <https://doi.org/10.1016/j.cej.2022.137905>
- Shi, B., Greaney, M.F., 2005. Reversible Michael addition of thiols as a new tool for dynamic combinatorial chemistry. *Chem. Commun.* 7, 886–888. <https://doi.org/10.1039/B414300K>
- Shi, J., Zheng, T., Guo, B., Xu, J., 2019. Solvent-free thermo-reversible and self-healable crosslinked polyurethane with dynamic covalent networks based on phenol-carbamate bonds. *Polymer* 181, 121788. <https://doi.org/10.1016/j.polymer.2019.121788>
- Shi, Q., Jin, C., Chen, Z., An, L., Wang, T., 2023. On the Welding of Vitrimers: Chemistry, Mechanics and Applications. *Adv. Funct. Mater.* 33, 2300288. <https://doi.org/10.1002/adfm.202300288>
- Shrestha, S., Zhang, W., Smid, S.D., 2021. Phlorotannins: A review on biosynthesis, chemistry and bioactivity. *Food Biosci.* 39, 100832. <https://doi.org/10.1016/j.fbio.2020.100832>
- Simon, J., Barla, F., Kelemen-Haller, A., Farkas, F., Kraxner, M., 1988. Thermal stability of polyurethanes. *Chromatographia* 25, 99–106. <https://doi.org/10.1007/BF02259024>
- Solanki, A., Thakore, S., 2015. Cellulose crosslinked pH-responsive polyurethanes for drug delivery: α -hydroxy acids as drug release modifiers. *Int. J. Biol. Macromol.* 80, 683–691. <https://doi.org/10.1016/j.ijbiomac.2015.07.003>
- Soleimani, A., Sadeghi, G.M.M., 2022. Synthesis, Characterization and Thermal Properties of Intrinsic Self-Healing Polyurethane Nanocomposites. *ChemistrySelect* 7, e202103978. <https://doi.org/10.1002/slct.202103978>
- Song, P., Du, L., Pang, J., Jiang, G., Shen, J., Ma, Y., Ren, S., Li, S., 2023. Preparation and properties of lignin-based vitrimer system containing dynamic covalent bonds for reusable and recyclable epoxy asphalt. *Ind. Crops Prod.* 197, 116498. <https://doi.org/10.1016/j.indcrop.2023.116498>
- Sonnier, R., Taguet, A., Ferry, L., Lopez-Cuesta, J.-M., 2018. Towards Bio-based Flame Retardant Polymers, *SpringerBriefs in Molecular Science*. Springer International Publishing, Cham. <https://doi.org/10.1007/978-3-319-67083-6>
- Sougrati, L., Duval, A., Averous, L., 2023. From Lignins to Renewable Aromatic Vitrimers based on Vinylogous Urethane. *ChemSusChem* 16, e202300792. <https://doi.org/10.1002/cssc.202300792>
- Souto, F., Calado, V., 2022. Mystifications and misconceptions of lignin: revisiting understandings. *Green Chem.* 24, 8172–8192. <https://doi.org/10.1039/D2GC01914K>
- Spiesschaert, Y., Danneels, J., Van Herck, N., Guerre, M., Acke, G., Winne, J., Du Prez, F., 2021. Polyaddition Synthesis Using Alkyne Esters for the Design of Vinylogous Urethane Vitrimers. *Macromolecules* 54, 7931–7942. <https://doi.org/10.1021/acs.macromol.1c01049>
- Sridhar, L.M., Oster, M.O., E. Herr, D E., Gregg, J.B.D., Wilson, J.A., Slark, A.T., 2020. Re-usable thermally reversible crosslinked adhesives from robust polyester and poly(ester urethane) Diels–Alder networks. *Green Chem.* 22, 8669–8679. <https://doi.org/10.1039/D0GC02938F>

- Sriharshitha, S., Krishnadevi, K., Prasanna, D., 2022. Vitrimers trigger covalent bonded bio-silica fused composite materials for recycling, reshaping, and self-healing applications. *RSC Adv.* 12, 26934–26944. <https://doi.org/10.1039/D2RA03794G>
- Stadler, R., 1988. Association phenomena in macromolecular systems - influence of macromolecular constraints on the complex formation. *Macromolecules* 21, 121–126. <https://doi.org/10.1021/ma00179a025>
- Statista, 2021. Cashew nut: global production. URL <https://www.statista.com/statistics/967702/global-cashew-nut-production/> (accessed 7.13.23).
- Stouten, J., de Roy, M.K.N., Bernaerts, K.V., 2023. Synthesis and characterization of water-borne vanillin derived copolymers containing dynamic imine cross-links. *Mater. Today Sustain.* 22, 100396. <https://doi.org/10.1016/j.mtsust.2023.100396>
- Stricker, L., Taplan, C., Du Prez, F.E., 2022. Biobased, Creep-Resistant Covalent Adaptable Networks Based on β -Amino Ester Chemistry. *ACS Sustain. Chem. Eng.* 10, 14045–14052. <https://doi.org/10.1021/acssuschemeng.2c04822>
- Sultania, M., Rai, J.S.P., Srivastava, D., 2011. Process modeling, optimization and analysis of esterification reaction of cashew nut shell liquid (CNSL)-derived epoxy resin using response surface methodology. *J. Hazard. Mater.* 185, 1198–1204. <https://doi.org/10.1016/j.jhazmat.2010.10.031>
- Sun, Y., Tian, X., Xie, H., Shi, B., Zhong, J., Liu, X., Yang, Y., 2022. Reprocessable and degradable bio-based polyurethane by molecular design engineering with extraordinary mechanical properties for recycling carbon fiber. *Polymer* 258, 125313. <https://doi.org/10.1016/j.polymer.2022.125313>
- Sun, Z., Fridrich, B., de Santi, A., Elangovan, S., Barta, K., 2018. Bright Side of Lignin Depolymerization: Toward New Platform Chemicals. *Chem. Rev.* 118, 614–678. <https://doi.org/10.1021/acs.chemrev.7b00588>
- Symes, W.F., Dawson, C.R., 1954. Poison Ivy “Urushiol.” *J. Am. Chem. Soc.* 76, 2959–2963. <https://doi.org/10.1021/ja01640a030>
- Symes, W.F., Dawson, C.R., 1953. Separation and Structural Determination of the Olefinic Components of Poison Ivy Urushiol, Cardanol and Cardol. *Nature* 171, 841–842. <https://doi.org/10.1038/171841b0>
- Takahashi, Y., Tobolsky, A.V., 1971. Chemorheological Study on Natural Rubber Vulcanizates. *Polym. J.* 2, 457–467. <https://doi.org/10.1295/polymj.2.457>
- Tang, R., Xue, B., Tan, J., Guan, Y., Wen, J., Li, X., Zhao, W., 2022. Regulating Lignin-Based Epoxy Vitrimer Performance by Fine-Tuning the Lignin Structure. *ACS Appl. Polym. Mater.* 4, 1117–1125. <https://doi.org/10.1021/acsapm.1c01541>
- Tang, S., Lin, H., Dong, K., Zhang, J., Zhao, C., 2023. Closed-loop recycling and degradation of guaiacol-based epoxy resin and its carbon fiber reinforced composites with S-S exchangeable bonds. *Polym. Degrad. Stab.* 210, 110298. <https://doi.org/10.1016/j.polymdegradstab.2023.110298>
- Tannert, R., Taubert, A., Weber, J., 2023. Biobased Epoxy Eugenol Vitrimers: Influence of Impurities of Technical Grade Monomers on the Network Characteristics. *Macromol. Mater. Eng.* n/a, 2300236. <https://doi.org/10.1002/mame.202300236>
- Tao, Y., Fang, L., Dai, M., Wang, C., Sun, J., Fang, Q., 2020. Sustainable alternative to bisphenol A epoxy resin: high-performance recyclable epoxy vitrimers derived from protocatechuic acid. *Polym. Chem.* 11, 4500–4506. <https://doi.org/10.1039/D0PY00545B>
- Tao, Y., Liang, X., Zhang, J., Lei, I.M., Liu, J., 2023. Polyurethane vitrimers: Chemistry, properties and applications. *J. Polym. Sci.* 61, 2233–2253. <https://doi.org/10.1002/pol.20220625>
- Taofiq, O., González-Paramás, A.M., Barreiro, M.F., Ferreira, I.C.F.R., 2017. Hydroxycinnamic Acids and Their Derivatives: Cosmeceutical Significance, Challenges and Future Perspectives, a Review. *Molecules* 22, 281. <https://doi.org/10.3390/molecules22020281>
- Taplan, C., Guerre, M., Du Prez, F.E., 2021. Covalent Adaptable Networks Using β -Amino Esters as Thermally Reversible Building Blocks. *J. Am. Chem. Soc.* 143, 9140–9150. <https://doi.org/10.1021/jacs.1c03316>
- Taplan, C., Guerre, M., Winne, J.M., Du Prez, F.E., 2020. Fast processing of highly crosslinked, low-viscosity vitrimers. *Mater. Horiz.* 7, 104–110. <https://doi.org/10.1039/C9MH01062A>
- Tellers, J., Pinalli, R., Soliman, M., Vachon, J., Dalcanale, E., 2019. Reprocessable vinylogous urethane cross-linked polyethylene via reactive extrusion. *Polym. Chem.* 10, 5534–5542. <https://doi.org/10.1039/C9PY01194C>
- Tesoro, G.C., Sastri, V., 1990. Reversible crosslinking in epoxy resins. I. Feasibility studies. *J. Appl. Polym. Sci.* 39, 1425–1437. <https://doi.org/10.1002/app.1990.070390702>
- Thomas, S., Yang, W., 2009. *Advances in polymer processing: from macro-to nano-scales.* Elsevier.
- Thys, M., Brancart, J., Van Assche, G., Van den Brande, N., Vendamme, R., 2023a. LignoSwitch: A Robust Yet Reversible Bioaromatic Superglue for Enhanced Materials Circularity and Ecodesign. *ACS Sustain. Chem. Eng.* 11, 17941–17950. <https://doi.org/10.1021/acssuschemeng.3c04477>

- Thys, M., Brancart, J., Van Assche, G., Vendamme, R., Van den Brande, N., 2021. Reversible Lignin-Containing Networks Using Diels–Alder Chemistry. *Macromolecules* 54, 9750–9760. <https://doi.org/10.1021/acs.macromol.1c01693>
- Thys, M., Kaya, G.E., Soetemans, L., Van Assche, G., Bourbigot, S., Baytekin, B., Vendamme, R., Van den Brande, N., 2023b. Bioaromatic-Associated Multifunctionality in Lignin-Containing Reversible Elastomers. *ACS Appl. Polym. Mater.* 5, 5846–5856. <https://doi.org/10.1021/acsapm.3c00491>
- Tian, P.-X., Li, Y.-D., Weng, Y., Hu, Z., Zeng, J.-B., 2023. Reprocessable, chemically recyclable, and flame-retardant biobased epoxy vitrimers. *Eur. Polym. J.* 193, 112078. <https://doi.org/10.1016/j.eurpolymj.2023.112078>
- Tiz, D.B., Vicente, F.A., Kroflič, A., Likozar, B., 2023. Lignin-Based Covalent Adaptable Network Polymers—When Bio-Based Thermosets Meet Recyclable by Design. *ACS Sustain. Chem. Eng.* 11, 13836–13867. <https://doi.org/10.1021/acssuschemeng.3c03248>
- Tobolsky, A.V., MacKnight, W.J., Takahashi, M., 1964. Relaxation of Disulfide and Tetrasulfide Polymers. *J. Phys. Chem.* 68, 787–790. <https://doi.org/10.1021/j100786a013>
- Tong, X., Ma, Y., Li, Y., 2010. Biomass into chemicals: Conversion of sugars to furan derivatives by catalytic processes. *Appl. Catal. Gen.* 385, 1–13. <https://doi.org/10.1016/j.apcata.2010.06.049>
- Trejo-Machin, A., Puchot, L., Verge, P., 2020. A cardanol-based polybenzoxazine vitrimer: recycling, reshaping and reversible adhesion. *Polym. Chem.* 11, 7026–7034. <https://doi.org/10.1039/D0PY01239D>
- Tremblay-Parrado, K.-K., Avérous, L., 2020a. Renewable Responsive Systems Based on Original Click and Polyurethane Cross-Linked Architectures with Advanced Properties. *ChemSusChem* 13, 238–251. <https://doi.org/10.1002/cssc.201901991>
- Tremblay-Parrado, K.-K., Avérous, L., 2020b. Synthesis and behavior of responsive biobased polyurethane networks cross-linked by click chemistry: Effect of the cross-linkers and backbone structures. *Eur. Polym. J.* 135, 109840. <https://doi.org/10.1016/j.eurpolymj.2020.109840>
- Tremblay-Parrado, K.-K., Bordin, C., Nicholls, S., Heinrich, B., Donnio, B., Avérous, L., 2020. Renewable and Responsive Cross-Linked Systems Based on Polyurethane Backbones from Clickable Biobased Bismaleimide Architecture. *Macromolecules* 53, 5869–5880. <https://doi.org/10.1021/acs.macromol.0c01115>
- Tretbar, C.A., Neal, J.A., Guan, Z., 2019. Direct Silyl Ether Metathesis for Vitrimers with Exceptional Thermal Stability. *J. Am. Chem. Soc.* 141, 16595–16599. <https://doi.org/10.1021/jacs.9b08876>
- Tribot, A., Amer, G., Abdou Alio, M., De Baynast, H., Delattre, C., Pons, A., Mathias, J.-D., Callois, J.-M., Vial, C., Michaud, P., Dussap, C.-G., 2019. Wood-lignin: Supply, extraction processes and use as bio-based material. *Eur. Polym. J.* 112, 228–240. <https://doi.org/10.1016/j.eurpolymj.2019.01.007>
- Trinh, T.E., Ku, K., Yeo, H., 2023. Reprocessable and Chemically Recyclable Hard Vitrimers Based on Liquid-Crystalline Epoxides. *Adv. Mater.* 35, 2209912. <https://doi.org/10.1002/adma.202209912>
- Türel, T., Saito, K., Glišić, I., Middelhoek, T., Tomović, Ž., 2024. Closing the loop: polyimine thermosets from furfural derived bioresources. *RSC Appl. Polym.* 2, 395–402. <https://doi.org/10.1039/D3LP00268C>
- Türel, T., Tomović, Ž., 2023. Chemically Recyclable and Upcyclable Epoxy Resins Derived from Vanillin. *ACS Sustain. Chem. Eng.* 11, 8308–8316. <https://doi.org/10.1021/acssuschemeng.3c00761>
- van den Tempel, P., Picchioni, F., Bose, R.K., 2022. Designing End-of-Life Recyclable Polymers via Diels–Alder Chemistry: A Review on the Kinetics of Reversible Reactions. *Macromol. Rapid Commun.* 43, 2200023. <https://doi.org/10.1002/marc.202200023>
- van Es, D.S., 2013. Rigid Biobased Building Blocks. *J. Renew. Mater.* 1, 61–72. <https://doi.org/10.7569/JRM.2012.634108>
- Van Lijsebetten, F., De Bruycker, K., Spiesschaert, Y., Winne, J.M., Du Prez, F.E., 2022. Suppressing Creep and Promoting Fast Reprocessing of Vitrimers with Reversibly Trapped Amines. *Angew. Chem. Int. Ed.* 61, e202113872. <https://doi.org/10.1002/anie.202113872>
- Van Lijsebetten, F., Holloway, J.O., Winne, J.M., Prez, F.E.D., 2020. Internal catalysis for dynamic covalent chemistry applications and polymer science. *Chem. Soc. Rev.* 49, 8425–8438. <https://doi.org/10.1039/D0CS00452A>
- van Putten, R.-J., van der Waal, J.C., de Jong, E., Rasrendra, C.B., Heeres, H.J., de Vries, J.G., 2013. Hydroxymethylfurfural, A Versatile Platform Chemical Made from Renewable Resources. *Chem. Rev.* 113, 1499–1597. <https://doi.org/10.1021/cr300182k>
- Van Zee, N.J., Nicolaj, R., 2020. Vitrimers: Permanently crosslinked polymers with dynamic network topology. *Prog. Polym. Sci.* 104, 101233. <https://doi.org/10.1016/j.progpolymsci.2020.101233>
- Vanholme, R., Demedts, B., Morreel, K., Ralph, J., Boerjan, W., 2010. Lignin Biosynthesis and Structure. *Plant Physiol.* 153, 895–905. <https://doi.org/10.1104/pp.110.155119>

- Vantomme, G., Lehn, J.-M., 2014. Reversible Adaptation to Photoinduced Shape Switching by Oligomer–Macrocyclic Interconversion with Component Selection in a Three-State Constitutional Dynamic System. *Chem. – Eur. J.* 20, 16188–16193. <https://doi.org/10.1002/chem.201404561>
- Vidil, T., Llevot, A., 2022. Fully Biobased Vitrimers: Future Direction toward Sustainable Cross-Linked Polymers. *Macromol. Chem. Phys.* 223, 2100494. <https://doi.org/10.1002/macp.202100494>
- Wahyudiono, Sasaki, M., Goto, M., 2008. Recovery of phenolic compounds through the decomposition of lignin in near and supercritical water. *Chem. Eng. Process. Process Intensif.* 47, 1609–1619. <https://doi.org/10.1016/j.cep.2007.09.001>
- Wang, H., Fu, Y., Liu, Y., Li, J., Sun, X., Liu, T., 2023. Synthesis of facilely healable and recyclable imine vitrimers using biobased branched diamine and vanillin. *Eur. Polym. J.* 196, 112309. <https://doi.org/10.1016/j.eurpolymj.2023.112309>
- Wang, L., Yang, X., Chen, H., Gong, T., Li, W., Yang, G., Zhou, S., 2013. Design of Triple-Shape Memory Polyurethane with Photo-cross-linking of Cinnamoyl Groups. *ACS Appl. Mater. Interfaces* 5, 10520–10528. <https://doi.org/10.1021/am402091m>
- Wang, M., Yin, G.-Z., Yang, Y., Fu, W., Díaz Palencia, J.L., Zhao, J., Wang, N., Jiang, Y., Wang, D.-Y., 2023. Bio-based flame retardants to polymers: A review. *Adv. Ind. Eng. Polym. Res., Advances in Flame Retardant Materials and Technologies* 6, 132–155. <https://doi.org/10.1016/j.aiepr.2022.07.003>
- Wang, S., Ma, S., Li, Q., Xu, X., Wang, B., Huang, K., Liu, Y., Zhu, J., 2020. Facile Preparation of Polyimine Vitrimers with Enhanced Creep Resistance and Thermal and Mechanical Properties via Metal Coordination. *Macromolecules* 53, 2919–2931. <https://doi.org/10.1021/acs.macromol.0c00036>
- Wang, S., Ma, S., Li, Q., Xu, X., Wang, B., Yuan, W., Zhou, S., You, S., Zhu, J., 2019. Facile in situ preparation of high-performance epoxy vitrimer from renewable resources and its application in nondestructive recyclable carbon fiber composite. *Green Chem.* 21, 1484–1497. <https://doi.org/10.1039/C8GC03477J>
- Wang, X., Zhang, S., He, Y., Guo, W., Lu, Z., 2022. Reprocessable Polybenzoxazine Thermosets with High T_gs and Mechanical Strength Retentions Using Boronic Ester Bonds as Crosslinkages. *Polymers* 14, 2234. <https://doi.org/10.3390/polym14112234>
- Wang, Y., Jin, B., Ye, D., Liu, Z., 2022a. Fully recyclable carbon fiber reinforced vanillin-based epoxy vitrimers. *Eur. Polym. J.* 162, 110927. <https://doi.org/10.1016/j.eurpolymj.2021.110927>
- Wang, Y., Xu, A., Zhang, L., Chen, Z., Qin, R., Liu, Y., Jiang, X., Ye, D., Liu, Z., 2022b. Recyclable Carbon Fiber Reinforced Vanillin-Based Polyimine Vitrimers: Degradation and Mechanical Properties Study. *Macromol. Mater. Eng.* 307, 2100893. <https://doi.org/10.1002/mame.202100893>
- Wang, Z., Zhang, X., Cai, J., Xie, J., 2023. Plant-derived p-hydroxyphenylacrylic acid-derived epoxy resins exhibit excellent flame retardancy, hydrophobicity, degradability, and low dielectric loss after curing with bio-based fluorinated Schiff bases. *Polym. Degrad. Stab.* 209, 110270. <https://doi.org/10.1016/j.polymdegradstab.2023.110270>
- Wen, Z., Bonnaud, L., Dubois, P., Raquez, J.-M., 2022. Catalyst-free reprocessable crosslinked biobased polybenzoxazine-polyurethane based on dynamic carbamate chemistry. *J. Appl. Polym. Sci.* 139, 52120. <https://doi.org/10.1002/app.52120>
- Wendels, S., Avérous, L., 2021. Biobased polyurethanes for biomedical applications. *Bioact. Mater.* 6, 1083–1106. <https://doi.org/10.1016/j.bioactmat.2020.10.002>
- Winne, J.M., Leibler, L., Prez, F.E.D., 2019. Dynamic covalent chemistry in polymer networks: a mechanistic perspective. *Polym. Chem.* 10, 6091–6108. <https://doi.org/10.1039/C9PY01260E>
- Xie, W., Huang, S., Liu, S., Zhao, J., 2021. Imine-functionalized biomass-derived dynamic covalent thermosets enabled by heat-induced self-crosslinking and reversible structures. *Chem. Eng. J.* 404, 126598. <https://doi.org/10.1016/j.cej.2020.126598>
- Xu, J., Liu, Y., Hsu, S., 2019. Hydrogels Based on Schiff Base Linkages for Biomedical Applications. *Molecules* 24, 3005. <https://doi.org/10.3390/molecules24163005>
- Xu, N., Gong, J., Huang, Z., 2016. Review on the production methods and fundamental combustion characteristics of furan derivatives. *Renew. Sustain. Energy Rev.* 54, 1189–1211. <https://doi.org/10.1016/j.rser.2015.10.118>
- Xu, X., Ma, S., Feng, H., Qiu, J., Wang, S., Yu, Z., Zhu, J., 2021. Dissociate transfer exchange of tandem dynamic bonds endows covalent adaptable networks with fast reprocessability and high performance. *Polym. Chem.* 12, 5217–5228. <https://doi.org/10.1039/D1PY01045J>
- Xue, B., Tang, R., Xue, D., Guan, Y., Sun, Y., Zhao, W., Tan, J., Li, X., 2021. Sustainable alternative for bisphenol A epoxy resin high-performance and recyclable lignin-based epoxy vitrimers. *Ind. Crops Prod.* 168, 113583. <https://doi.org/10.1016/j.indcrop.2021.113583>
- Yan, P., Zhao, W., Fu, X., Liu, Z., Kong, W., Zhou, C., Lei, J., 2017. Multifunctional polyurethane-vitrimers completely based on transcarbamoylation of carbamates: thermally-induced dual-shape memory effect and self-welding. *RSC Adv.* 7, 26858–26866. <https://doi.org/10.1039/C7RA01711A>

- Yang, H., Yu, B., Xu, X., Bourbigot, S., Wang, H., Song, P., 2020. Lignin-derived bio-based flame retardants toward high-performance sustainable polymeric materials. *Green Chem.* 22, 2129–2161. <https://doi.org/10.1039/D0GC00449A>
- Yang, R., Li, W., Mo, R., Zhang, X., 2023. Recyclable and Degradable Vinylous Urethane Epoxy Thermosets with Tunable Mechanical Properties from Isosorbide and Vanillic Acid. *ACS Appl. Polym. Mater.* 5, 2553–2561. <https://doi.org/10.1021/acsapm.2c02186>
- Yang, W., Ding, H., Zhou, W., Liu, T., Xu, P., Puglia, D., Kenny, J.M., Ma, P., 2022. Design of inherent fire retarding and degradable bio-based epoxy vitrimer with excellent self-healing and mechanical reprocessability. *Compos. Sci. Technol.* 109776. <https://doi.org/10.1016/j.compscitech.2022.109776>
- Yang, X., Ke, Y., Chen, Q., Shen, L., Xue, J., Quirino, R.L., Yan, Z., Luo, Y., Zhang, C., 2022. Efficient transformation of renewable vanillin into reprocessable, acid-degradable and flame retardant polyimide vitrimers. *J. Clean. Prod.* 333, 130043. <https://doi.org/10.1016/j.jclepro.2021.130043>
- Yang, Y., Du, F.-S., Li, Z.-C., 2020. Highly Stretchable, Self-Healable, and Adhesive Polyurethane Elastomers Based on Boronic Ester Bonds. *ACS Appl. Polym. Mater.* 2, 5630–5640. <https://doi.org/10.1021/acsapm.0c00941>
- Yasar, M., Oktay, B., Dal Yontem, F., Haciosmanoglu Aldogan, E., Kayaman Apohan, N., 2023. Development of self-healing vanillin/PEI hydrogels for tissue engineering. *Eur. Polym. J.* 188, 111933. <https://doi.org/10.1016/j.eurpolymj.2023.111933>
- Yazaki, Y., 2015. Utilization of Flavonoid Compounds from Bark and Wood: A Review. *Nat. Prod. Commun.* 10, 513–520. <https://doi.org/10.1177/1934578X1501000333>
- Ye, C., Voet, V.S.D., Folkersma, R., Loos, K., 2021. Robust Superamphiphilic Membrane with a Closed-Loop Life Cycle. *Adv. Mater.* 33, 2008460. <https://doi.org/10.1002/adma.202008460>
- Yu, S., Wu, S., Zhang, C., Tang, Z., Luo, Y., Guo, B., Zhang, L., 2020. Catalyst-Free Metathesis of Cyclic Acetals and Spirocyclic Acetal Covalent Adaptable Networks. *ACS Macro Lett.* 9, 1143–1148. <https://doi.org/10.1021/acsmacrolett.0c00527>
- Yuan, Y., Chen, H., Jia, L., Lu, X., Yan, S., Zhao, J., Liu, S., 2023. Aromatic polyimine covalent adaptable networks with superior water and heat resistances. *Eur. Polym. J.* 187, 111912. <https://doi.org/10.1016/j.eurpolymj.2023.111912>
- Yue, L., Ke, K., Amirhosravi, M., Gray, T.G., Manas-Zloczower, I., 2021. Catalyst-Free Mechanochemical Recycling of Biobased Epoxy with Cellulose Nanocrystals. *ACS Appl. Bio Mater.* 4, 4176–4183. <https://doi.org/10.1021/acsabm.0c01670>
- Zamani, P., Zabihi, O., Ahmadi, M., Mahmoodi, R., Kannangara, T., Joseph, P., Naebe, M., 2022. Biobased Carbon Fiber Composites with Enhanced Flame Retardancy: A Cradle-to-Cradle Approach. *ACS Sustain. Chem. Eng.* 10, 1059–1069. <https://doi.org/10.1021/acssuschemeng.1c07859>
- Zeng, C., Seino, H., Ren, J., Hatanaka, K., Yoshie, N., 2013. Self-healing bio-based furan polymers cross-linked with various bis-maleimides. *Polymer* 54, 5351–5357. <https://doi.org/10.1016/j.polymer.2013.07.059>
- Zhang, C., Xue, J., Yang, X., Ke, Y., Ou, R., Wang, Y., Madbouly, S.A., Wang, Q., 2022. From plant phenols to novel bio-based polymers. *Prog. Polym. Sci.* 125, 101473. <https://doi.org/10.1016/j.progpolymsci.2021.101473>
- Zhang, D., Dumont, M.-J., 2018. Reprocessable 5-hydroxymethylfurfural derivative-based thermoset elastomers synthesized through the thiol-Michael and Diels–Alder reactions. *J. Mater. Sci.* 53, 11116–11129. <https://doi.org/10.1007/s10853-018-2375-4>
- Zhang, D., Dumont, M.-J., 2017. Advances in polymer precursors and bio-based polymers synthesized from 5-hydroxymethylfurfural. *J. Polym. Sci. Part Polym. Chem.* 55, 1478–1492. <https://doi.org/10.1002/pola.28527>
- Zhang, D., Dumont, M.-J., Cherestes, A., 2016. An efficient strategy for the synthesis of 5-hydroxymethylfurfural derivative based poly(β -thioether ester) via thiol-Michael addition polymerization. *RSC Adv.* 6, 83466–83470. <https://doi.org/10.1039/C6RA17532E>
- Zhang, H., Cui, J., Hu, G., Zhang, B., 2022. Recycling strategies for vitrimers. *Int. J. Smart Nano Mater.* 13, 367–390. <https://doi.org/10.1080/19475411.2022.2087785>
- Zhang, L., Rowan, S.J., 2017. Effect of Sterics and Degree of Cross-Linking on the Mechanical Properties of Dynamic Poly(alkylurea–urethane) Networks. *Macromolecules* 50, 5051–5060. <https://doi.org/10.1021/acs.macromol.7b01016>
- Zhang, S., Liu, T., Hao, C., Wang, L., Han, J., Liu, H., Zhang, J., 2018. Preparation of a lignin-based vitrimer material and its potential use for recoverable adhesives. *Green Chem.* 20, 2995–3000. <https://doi.org/10.1039/C8GC01299G>
- Zhang, W., Gao, F., Chen, X., Shen, L., Chen, Y., Lin, Y., 2023. Recyclable, Degradable, and Fully Bio-Based Covalent Adaptable Polymer Networks Enabled by a Dynamic Diacetal Motif. *ACS Sustain. Chem. Eng.* 11, 3065–3073. <https://doi.org/10.1021/acssuschemeng.2c06870>

- Zhang, X., Wang, S., Jiang, Z., Li, Y., Jing, X., 2020. Boronic Ester Based Vitrimers with Enhanced Stability via Internal Boron–Nitrogen Coordination. *J. Am. Chem. Soc.* 142, 21852–21860. <https://doi.org/10.1021/jacs.0c10244>
- Zhang, Y., Yuan, L., Liang, G., Gu, A., 2023. Bio-based Tetrafunctional Epoxy Monomer Containing a Dicyclo Diacetal Structure and Its Medium-Temperature-Cured Epoxy Vitrimer System with Excellent Mechanical and Multifunctional Properties. *ACS Sustain. Chem. Eng.* 11, 9264–9280. <https://doi.org/10.1021/acssuschemeng.3c02568>
- Zhang, Y., Yukiko, E., Tadahisa, I., 2023. Bio-based vitrimers from divanillic acid and epoxidized soybean oil. *RSC Sustain.* 1, 543–553. <https://doi.org/10.1039/D2SU00140C>
- Zhao, F., Lian, W.-Q., Li, Y.-D., Weng, Y., Zeng, J.-B., 2022. Synthesis of epoxidized soybean oil-derived covalent adaptable networks through melt Schiff base condensation. *Ind. Crops Prod.* 187, 115499. <https://doi.org/10.1016/j.indcrop.2022.115499>
- Zhao, S., Abu-Omar, M.M., 2019. Catechol-Mediated Glycidylation toward Epoxy Vitrimers/Polymers with Tunable Properties. *Macromolecules* 52, 3646–3654. <https://doi.org/10.1021/acs.macromol.9b00334>
- Zhao, X.-L., Li, Y.-D., Weng, Y., Zeng, J.-B., 2023. Biobased epoxy covalent adaptable networks for high-performance recoverable adhesives. *Ind. Crops Prod.* 192, 116016. <https://doi.org/10.1016/j.indcrop.2022.116016>
- Zhao, X.-L., Tian, P.-X., Li, Y.-D., Zeng, J.-B., 2022. Biobased covalent adaptable networks: towards better sustainability of thermosets. *Green Chem.* 24, 4363–4387. <https://doi.org/10.1039/D2GC01325H>
- Zhao, Z.-H., Wang, D.-P., Zuo, J.-L., Li, C.-H., 2021. A Tough and Self-Healing Polymer Enabled by Promoting Bond Exchange in Boronic Esters with Neighboring Hydroxyl Groups. *ACS Mater. Lett.* 3, 1328–1338. <https://doi.org/10.1021/acsmaterialslett.1c00314>
- Zheng, H., Zhang, W., Li, B., Zhu, J., Wang, C., Song, G., Wu, G., Yang, X., Huang, Y., Ma, L., 2022. Recent advances of interphases in carbon fiber-reinforced polymer composites: A review. *Compos. Part B Eng.* 233, 109639. <https://doi.org/10.1016/j.compositesb.2022.109639>
- Zheng, P., McCarthy, T.J., 2012. A Surprise from 1954: Siloxane Equilibration Is a Simple, Robust, and Obvious Polymer Self-Healing Mechanism. *J. Am. Chem. Soc.* 134, 2024–2027. <https://doi.org/10.1021/ja2113257>
- Zheng, Y., Liu, T., He, H., Lv, Z., Xu, J., Ding, D., Dai, L., Huang, Z., Si, C., 2023. Lignin-based epoxy composite vitrimers with light-controlled remoldability. *Adv. Compos. Hybrid Mater.* 6, 53. <https://doi.org/10.1007/s42114-023-00633-4>
- Zhong, L., Hao, Y., Zhang, J., Wei, F., Li, T., Miao, M., Zhang, D., 2022. Closed-Loop Recyclable Fully Bio-Based Epoxy Vitrimers from Ferulic Acid-Derived Hyperbranched Epoxy Resin. *Macromolecules* 55, 595–607. <https://doi.org/10.1021/acs.macromol.1c02247>
- Zhou, Y., Goossens, J.G.P., Sijbesma, R.P., Heuts, J.P.A., 2017. Poly(butylene terephthalate)/Glycerol-based Vitrimers via Solid-State Polymerization. *Macromolecules* 50, 6742–6751. <https://doi.org/10.1021/acs.macromol.7b01142>
- Zhou, Y., Zeng, G., Zhang, F., Li, K., Li, X., Luo, J., Li, Jiongjiong, Li, Jianzhang, 2023. Design of tough, strong and recyclable plant protein-based adhesive via dynamic covalent crosslinking chemistry. *Chem. Eng. J.* 460, 141774. <https://doi.org/10.1016/j.cej.2023.141774>
- Zhu, L., Xu, L., Jie, S., Li, B.-G., 2023. Preparation of Styrene–Butadiene Rubber Vitrimers with High Strength and Toughness through Imine and Hydrogen Bonds. *Ind. Eng. Chem. Res.* 62, 2299–2308. <https://doi.org/10.1021/acs.iecr.2c03133>
- Zia, K.M., Noreen, A., Zuber, M., Tabasum, S., Mujahid, M., 2016. Recent developments and future prospects on bio-based polyesters derived from renewable resources: A review. *Int. J. Biol. Macromol.* 82, 1028–1040. <https://doi.org/10.1016/j.ijbiomac.2015.10.040>
- Zou, J., Duan, H., Chen, Y., Ji, S., Cao, J., Ma, H., 2020. A P/N/S-containing high-efficiency flame retardant endowing epoxy resin with excellent flame retardance, mechanical properties and heat resistance. *Compos. Part B Eng.* 199, 108228. <https://doi.org/10.1016/j.compositesb.2020.108228>
- Zou, W., Dong, J., Luo, Y., Zhao, Q., Xie, T., 2017. Dynamic Covalent Polymer Networks: from Old Chemistry to Modern Day Innovations. *Adv. Mater.* 29, 1606100. <https://doi.org/10.1002/adma.201606100>

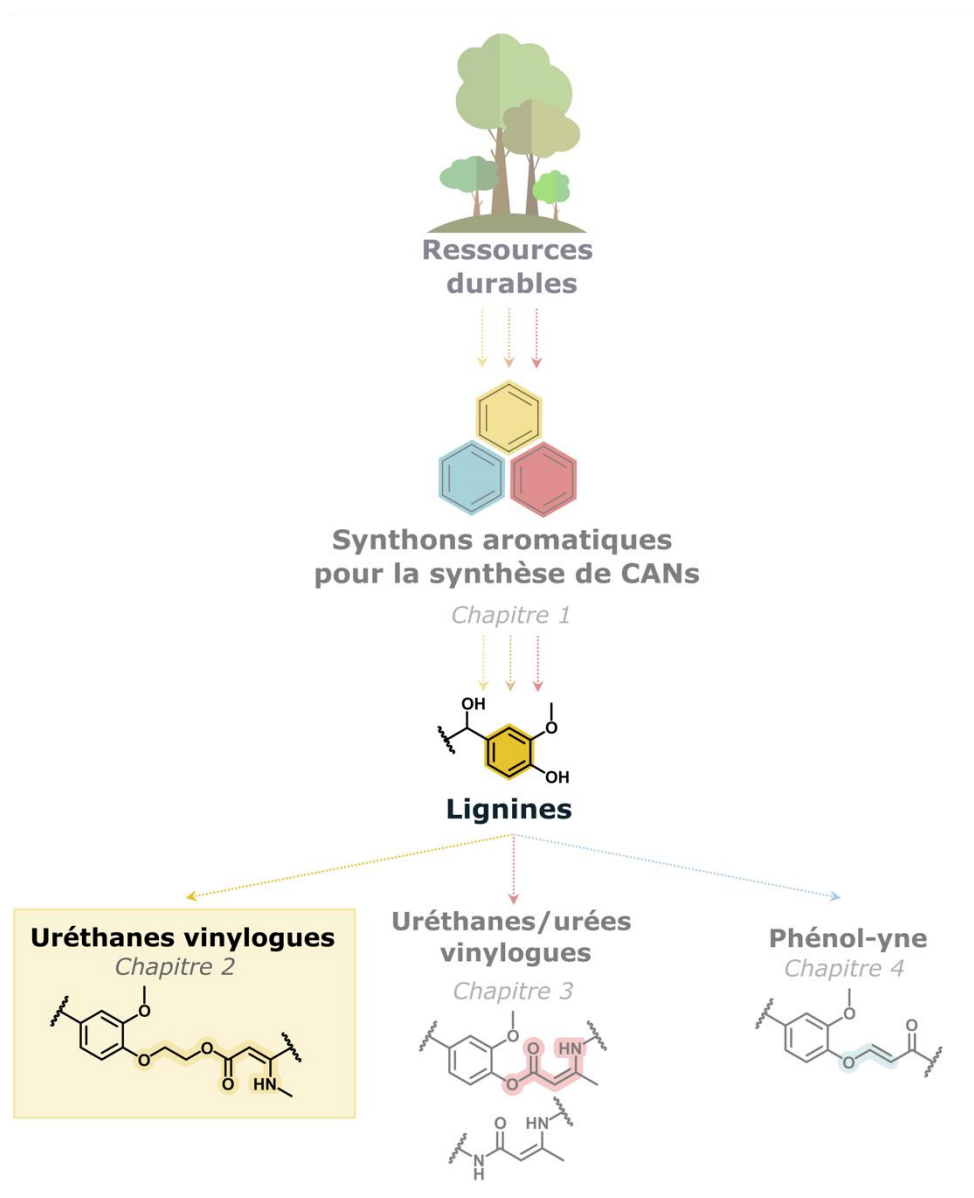
CONCLUSION DU CHAPITRE 1

Cette revue de littérature a montré la richesse des chimies et des voies de synthèse de CANs à partir de synthons aromatiques biosourcés. Cet état de l'art a mis en évidence la grande variété des composés aromatiques disponibles issus de ressources renouvelables tels que la biomasse lignocellulosique ou les dérivés de polysaccharides. Les lignines, les tannins, le liquide de coques de noix de cajou et leurs dérivés ont montré, grâce à leurs multiples sites fonctionnels, pouvoir être facilement intégrés dans des réseaux dynamiques par des voies de synthèse simples, économes en atomes et innovantes. Ce chapitre bibliographique a mis en exergue l'intérêt de ces molécules plateformes pour la synthèse, entre autres, de polyesters, polyimines, ou polyuréthanes plus durables. De plus, l'utilisation de molécules aromatiques dans la synthèse de polymères a montré renforcer les propriétés mécaniques des matériaux et être à l'origine de fonctionnalités dites avancées. Les polymères aromatiques présentent une excellente résistance au feu et de bonnes propriétés d'adhésion. La fin de vie de ces polymères aromatiques peut être contrôlée par recyclage physique, mais aussi par recyclage chimique dans divers environnements. De nombreux domaines d'applications tirent parti des caractéristiques exceptionnelles des CANs aromatiques pour obtenir des propriétés spécifiques requises pour des applications ciblées. Ces matériaux ont montré leur pertinence pour le développement de systèmes d'administration de médicaments, d'implants résorbables, ou de revêtements relarguant des agents anticorrosion. Enfin, les CANs ont révélé être de plus en plus adaptés aux techniques de transformation utilisées pour les thermoplastiques conventionnels, telles que l'extrusion ou le thermoformage, et être compatibles avec les technologies d'impression 3D/4D, offrant de nouvelles perspectives de mise en forme.

Des nombreux défis restent à relever dans ce domaine en pleine expansion, notamment en raison d'un contrôle difficile des réactions à l'état solide ou le manque de caractérisation rhéologiques critiques altérant la compréhension des mécanismes en jeu. De plus, la stabilité dimensionnelle induite par la présence de liaisons dynamiques peut être une limitation de ces matériaux. Ce domaine constitue néanmoins une solution ambitieuse pour le développement de matériaux durables et performants, dans contexte de bioéconomie circulaire.

Ce chapitre bibliographique sera à la base des orientations de recherche des études développées dans la suite de ce mémoire de doctorat.

CHAPITRE 2. DES LIGNINES AUX VITRIMÈRES AROMATIQUES RENOUVELABLES À BASE D'URETHANE VINYLOGUES



INTRODUCTION DU CHAPITRE 2

Dans un contexte de bioéconomie circulaire, ce premier chapitre expérimental a pour objectif de mettre en évidence l'intérêt de la lignine pour la synthèse de vitrimère uréthane vinylogues recyclable. Il fait l'objet d'un article scientifique intitulé « From Lignins to renewable Aromatic Vitrimers Based on Vinylogous Urethane », publié dans *ChemSusChem* en 2023.

Le chapitre bibliographique présenté précédemment a clairement mis en évidence le fort potentiel de la lignine comme synthon aromatique pour la synthèse d'architectures macromoléculaires dynamiques aux propriétés innovantes et à la fin de vie contrôlée dans divers environnements. En raison de sa fonctionnalité élevée en groupements hydroxyles aliphatiques et phénoliques, la lignine est compatible avec une grande variété de liaisons dynamiques potentielles. Parmi elles, les uréthanes vinylogues, obtenus par condensation de groupements acétoacétates et amines, se démarquent par leur fort potentiel de réarrangement induit par des réactions de transamination en présence d'un excès d'amines. Les échanges de liaisons présentent l'avantage d'avoir lieu à des températures relativement basses et sans catalyseur, rendant cette chimie compatible avec de nombreux principes de chimie verte.

Dans ce chapitre, une voie de synthèse a été développée pour la modification chimique d'une lignine organosolv en polyacétoacétates liquides réactifs. Ces macromonomères acétoacétates, contenant différentes teneurs en lignines et des chaînes de polyéthylène glycol de masses molaires variables, ont été utilisés pour synthétiser une gamme de matériaux par condensation avec de l'hexaméthylènediamine. La structure chimique et les propriétés des réseaux tridimensionnels ont été largement caractérisés. L'influence de la teneur en lignine et de la longueur de la chaîne de polyéthylène glycol sur les caractéristiques structurales ainsi que sur propriétés mécaniques et rhéologiques a été étudiée. Enfin, dans une approche du berceau-au-berceau (cradle-to-cradle), le potentiel de recyclage des matériaux a été évalué au cours de plusieurs cycles de recyclage physique. De même, la capacité de dépolymérisation des réseaux par recyclage chimique et leur cicatrisation à température ont été étudiées.

FROM LIGNINS TO RENEWABLE AROMATIC VITIRMERS BASED ON VINYLOGOUS URETHANE

Lisa Sougrati ^a, Antoine Duval ^{a, b, *}, Luc Avérous ^{a, *}

^a BioTeam/ICPEES-ECPM, UMR CNRS 7515, Université de Strasbourg, 25 rue Becquerel, 67087 Strasbourg, Cedex 2, France

^b Soprema, 15 rue de Saint Nazaire, 67100, Strasbourg, France

*Corresponding authors.



1. ABSTRACT

During the two last decades, Covalent Adaptable Networks (CANs) have proven to be an important new class of polymer materials combining the main advantages of thermoplastics and thermosets. For instance, materials can undergo reprocessing cycles by incorporating dynamic covalent bonds within a crosslinked network. Due to their versatility, renewable resources can be easily integrated into these innovative systems to develop sustainable materials, which can be related to the context of the recent development of a circular bioeconomy. Lignins, the main renewable sources of aromatic structures, is a major candidate in the design of novel and biobased stimuli-responsive materials such as vitrimers due to their high functionality and specific chemical architectures. In the aim of developing recyclable lignin-based vinylogous urethane (VU) networks, an innovative strategy was elaborated in which lignin was first modified into liquid polyols, and then into polyacetoacetates. Resulting macromonomers were integrated into aromatic VU networks and fully characterized through thermal, mechanical, and rheological experiments. Viscoelastic behaviors of the different aromatic vitrimers exhibited fast stress relaxations (e.g., 39 s at 130 °C) allowing easy and fast mechanical reprocessing. A thermomechanical recycling study was successfully performed. Then, the developed strategy enabled the fabrication of healing biobased aromatic vitrimers with tunable structural design and properties.

2. INTRODUCTION

Polymers are commonly categorized into thermoplastics or thermosets (Pascault and Williams, 2018; Peters, 2017). In regard to environmental issues, thermosets' inability to undergo thermomechanical recycling because of their covalent crosslinks highly limits their sustainability at the end-of-life (Post et al., 2020). To overcome this issue while still achieving efficient performances, covalent adaptable networks (CANs) have recently shown to be an attractive strategy, since they combine the main advantages of thermosets (mechanical performance and thermal resistance) and thermoplastics (recyclability and reprocessability) (Denissen et al., 2016; J. Kloxin and N. Bowman, 2013; Kloxin et al., 2010; Scheutz et al., 2019). For instance, incorporating dynamic covalent bonds into polymer network can endow macroscopic flow at high temperature without compromising the properties at usage temperature.

CANs are classified into two main categories depending on their bond exchange mechanisms (McBride et al., 2019). Dissociative CANs depend on dynamic bonds that can be reverted into their initial chemical structure. The covalent bond is first broken before being reformed, resulting in an intermediate state with a reduced crosslinking density (Winne et al., 2019). On the other hand, associative CANs rely on the formation of an intermediate before fragmentation of the initial connection, maintaining the crosslinking density of the network throughout the bond exchange process. Thermally induced associatively exchanging materials have been named vitrimers, in reference to vitreous silica, because their viscosity decreases gradually with temperature, following an Arrhenius law (Capelot et al., 2012). However, the frontier between associative and dissociative CANs is sometimes difficult to draw, and the Arrhenius behavior should not be taken as sole criterion, since numerous examples of dissociative CANs behave as "vitriemer-like" upon heating (Elling and Dichtel, 2020; Liu et al., 2017; Zhang and Rowan, 2017).

To develop sustainable materials, biobased building blocks have been exploited in the design of innovative and dynamic macromolecular architectures (Lucherelli et al., 2022). Aliphatic building blocks such as triglycerides and fatty acid derivatives (Altuna et al., 2013; Mauro et al., 2020; Patel et al., 2016; Tremblay-Parrado et al., 2021), polysaccharides (Chen et al., 2020; Liu et al., 2016; Zhao et al., 2019), biobased diacids and polyesters, (Altuna et al., 2019; Demongeot et al., 2017) or natural rubber have shown great interest in the production of renewable CANs (Imbernon et al., 2016; Pire et al., 2010). Biobased aromatic precursors such as furan derivatives (Hajj et al., 2020; Tremblay-Parrado et al., 2020; Tremblay-Parrado and Avérous, 2020), and some phenolic building blocks have been also employed in the preparation of sustainable dynamic materials (Ocando et al., 2020; Tao et al., 2020). Considering

both the beginning, with biogenic resources, and the end of life, with the various recycling options, these adaptable and stimuable materials can be fully integrated in a circular bioeconomy.

Considered as polyphenols, lignins are the most abundant sources of renewable aromatic structures on Earth, with a great variability of structures according to the botanical resource and the fractionation process. Different types of lignins can be obtained with varying architectures for a same lignocellulosic feedstock. Alkaline processes enable the production of Kraft (KL) and soda lignins (SL), treated with sodium hydroxide in the presence or absence of sodium hydrosulfide (NaSH), respectively. Besides, organosolv lignins (OSL) are obtained from solvent pulping, in sulfur-free processes. Depending on the treatment conditions, structures relatively rich in β -ether bonds, the most abundant in native lignin, may be produced (Constant *et al.*, 2016). OSL are great candidates for industrial and environmental applications due to the absence of sulfur in its structure, especially in catalyzed systems. Its high purity as well as good solubility in organic solvents make it suitable for controlled synthetic processes (Lora and Glasser, 2002). For instance, methylation with trimethyl phosphate and oxyalkylation using ethylene carbonate (EC) were successfully achieved on OSL in our group (Duval *et al.*, 2021; Duval and Avérous, 2020).

Advanced properties of lignin-based materials are enhanced by its aromaticity, which improve thermal stability, mechanical strength and chemical resistance (Kimura *et al.*, 2006). Only few work attempted to valorize lignins in aromatic vitrimers. First, Zhang *et al.* reported the modification of KL by ozonation to introduce carboxylic acid groups that were reacted with aliphatic diepoxy monomers to obtain polyester networks dynamic through transesterification (Zhang *et al.*, 2018). Recently, other lignin-based transesterification vitrimers were prepared to develop self-healing materials using a zinc catalyst (Hao *et al.*, 2019; More *et al.*, 2023; Xue *et al.*, 2021), catalyst-free coatings and adhesives (Du *et al.*, 2022), and light-controlled networks (Zheng *et al.*, 2023). Dynamic lignin-based adhesives were also prepared using acetal exchange reactions (Moreno *et al.*, 2021), or disulfide metathesis within a polyurea matrix (Liu *et al.*, 2020). Hydrophobic and fire resistant lignin-based benzoxazine coatings were also prepared through Mannich-like condensation reaction (Adjaoud *et al.*, 2023), as well as shape memory lignin-based polyurethanes (PUs), dynamic through transcarbamylation reactions (Ma *et al.*, 2023).

The integration of vinylogous urethane (VU) dynamic bonds into associative networks was first reported by Denissen *et al.* (Denissen *et al.*, 2015). It has been significantly used in the design of different advanced materials. This covalent bond was suggested as an alternative to transesterification exchange reaction. VU can be synthesized from the condensation of acetoacetate and amine moieties. The dynamicity is brought by transamination reactions with an excess of amine groups. Due to tunable parameters, VU-based vitrimers can easily achieve fast reprocessing, through rapid network rearrangements at reasonable temperatures and without catalyst. Subsequently, it was established that viscoelastic properties could be further controlled via acid-mediated catalysis, enabling remarkably fast stress relaxation (Denissen *et al.*, 2017; Haida and Abetz, 2020; Taplan *et al.*, 2020). Recently, Van Lijsebetten *et al.* showed attractive strategies limiting creep through dicarboxamide dissociation, to protect amine moieties and restrict network defects (Van Lijsebetten *et al.*, 2022a, 2022b). VU network based on vanillin, a building block which can be potentially obtained from lignins, was recently reported (Engelen *et al.*, 2022).

To the best of our knowledge, we here report the first work incorporating lignin into the design of VU vitrimers. Following several green chemistry principles, OSL was valorized in the synthesis of novel biobased VU networks using solvent-free reactions and non-toxic compounds. OSL was modified by oxyalkylation into an aliphatic polyol using ethylene carbonate (EC) in mixture with polyethylene glycols (PEG) of different average molar masses (Duval *et al.*, 2022; Duval and Avérous, 2017a). Resulting polyols were further modified into reactive polyacetoacetates that enabled the preparation of VU containing networks by condensation with hexamethylenediamine (HMDA), as illustrated in Figure 2-1. Chemical and physico-chemical characterizations were performed on both polyols and the

corresponding polyacetoacetates. Chemical, thermal, dynamic mechanical analysis, rheological behavior (stress relaxation) and uniaxial tensile tests of the series of vitrimers were carried out. Lastly, the recyclability and healing ability of the different vitrimers was studied.

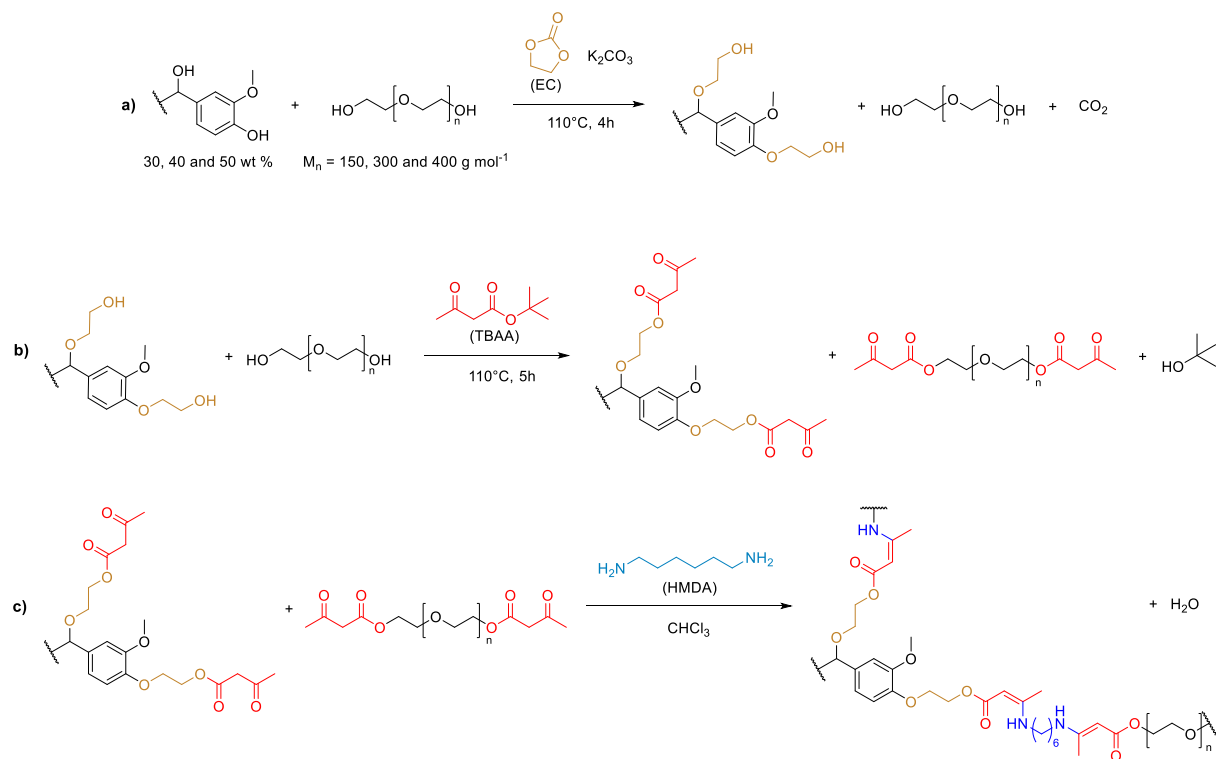


Figure 2-1. Synthetic pathways for the preparation of a) polyols, b) polyacetoacetate, and c) VU networks from OSL.

3. EXPERIMENTAL SECTION

3.1. Materials

Organosolv lignin (OSL) was isolated at pilot scale from industrial size beech wood using the aqueous acetone Fabiola™ process. It was precipitated from the pulping liquor using the LigniSep technology of a continuous falling film precipitator. Detailed characterization of this lignin has been previously detailed (as P-BEC-3) (Smit et al., 2022). OSL is a low number-average molar mass lignin (M_n below 1400 g mol^{-1}) with an aliphatic hydroxyl content of 1.74 mmol g^{-1} and phenolic hydroxyl content of 2.89 mmol g^{-1} . The lignin was dried overnight at $50 \text{ }^\circ\text{C}$ before utilization.

Triethylene glycol (TEG), PEGs with number-average molar masses of 300 and 400 g mol^{-1} , EC (99%), *tert*-butyl acetoacetate (TBAA, 97%) and ethyl acetoacetate were purchased from Acros Organics. Potassium carbonate anhydrous (K_2CO_3 , $\geq 99\%$), chloroform (CHCl_3 , $\geq 99\%$), 3,4,5-trichloropyridine (TCP, 98%) and magnesium sulfate were obtained from Thermo Fisher Scientific. Hexamethylene diamine (HMDA) was obtained from BASF. *n*-Octylamine was purchased from TCI Chemicals. Hydrochloric acid (37% in water), chromium (III) acetyl acetonate ($\text{Cr}(\text{acac})_3$, 97%), cholesterol ($> 99\%$), deuterated chloroform (CDCl_3) and 2-chloro-4,4,5,5-tetramethyl-1,3,2-dioxaphospholane (Cl-TMDP, 95%) and *N,N*-Dimethylformamide anhydrous (DMF, 99.8%) were purchased from Sigma-Aldrich. Acetone was obtained from CARLO ERBA Reagents. All chemicals were used without additional purification.

3.2. Synthesis of lignin-based liquid polyols

A series of lignin-based liquid polyols were synthesized with lignin content from 30 to 50 wt % and different PEG chain length, following a protocol developed previously (Duval et al., 2022). 50 g of a lignin and PEG mixture, ethylene carbonate (1.1 molar equivalent with respect to the total OH groups of lignin) and K_2CO_3 (0.1 molar equivalent to EC) were introduced in a three-necked round bottom flask equipped with a mechanical stirred. The reaction was stirred under argon flow and heated in an oil bath at 110 °C for 4 h.

3.3. Synthesis of lignin-based polyacetoacetate

In a round bottom flask equipped with a distillation apparatus and a magnetic stirrer, 25 g of lignin-based polyol and TBAA (2.5 molar equivalent with respect to total aliphatic OH groups of the polyol) were added. The reaction mixture was stirred vigorously and heated in an oil bath at 110 °C for 3 h enabling the distillation of *tert*-butanol (*t*-BuOH). Then, TBAA excess was evaporated *in vacuo*, gradually. Following the removal of reagent's excess, the reaction was stopped after 4 to 5 h. The remaining quantity of K_2CO_3 in polyacetoacetates was calculated and neutralized with an excess of HCl (2 equivalents). The polyacetoacetates were dissolved in 200 mL of acetone and HCl (2M) was added. The mixture was stirred 5 minutes, dried with anhydrous magnesium sulfate, and filtered. The remaining salt was removed by centrifugation, and the product was concentrated under reduced pressure and dried overnight at 50 °C in a vacuum oven.

3.4. Synthesis of VU networks

In a 50 mL round bottom flask was added 15 g of polyacetoacetate diluted in 10 mL of $CHCl_3$ at room temperature. HMDA (1.1 equivalent with respect to the total acetoacetate) was introduced and the resulting solution was stirred vigorously for 30 seconds until homogenization. The mixture was poured into a Teflon mold (10 cm x 10 cm) and let at room temperature for solvent evaporation overnight. The material was further cured at 90 °C for 24 h and post cured at 150 °C for 30 minutes. The resulting material was cut into pieces and hot pressed at 140 °C for 20 minutes in a mold (10 cm x 10 cm x 1 mm).

3.5. Materials designation

The designations are established as follow: product type (OL, AC or VU) – lignin content (30,40 or 50 in wt %) – PEG chain length (150, 300 or 400 g mol⁻¹), with OL standing for OSL-based polyol, AC for the corresponding polyacetoacetate and VU for the final material. For instance, OL-30-300 corresponds to the polyol synthesized with a lignin content of 30 wt % in a mixture with PEG₃₀₀.

3.6. Reprocessing study of VU networks

To analyze the reprocessing ability of the VU networks, they were first dipped into liquid nitrogen and grinded using a rotating blade coffee grinder (Bosch, TSM6A013B). The thin powder was reprocessed by compression molding using a LabTech Scientific hot press at 140 °C in a 10 cm x 10 cm x 1 mm mold. The materials were placed in the center of the tile and left to undergo a 4 min preheating to soften the material. Then, several venting steps were performed before a final pressing of 15 minutes under a constant applied force of 16 MPa. Reprocessed materials were cut into dumbbell-shaped samples to undergo uniaxial tensile tests and further FT-IR and DMA measurements.

3.7. Characterization techniques

¹H and ³¹P-NMR spectra were acquired with a Bruker 400 MHz spectrometer. ¹H-NMR calibration was performed based on CDCl₃ (δH = 7.26 ppm) chemical shift, with 16 scans. Quantitative ¹H-NMR (15 s relaxation delay) was performed using TCP as internal standard. Around 20 mg of sample were dissolved in 500 μL of solvent and 100 μL of a standard solution of TCP (0.5 M) was added. ³¹P-NMR was obtained after reaction of a phosphorylating reagent following standard protocols (Archipov et al., 1991; Granata and Argyropoulos, 1995). 128 scans were recorded with 15 s relaxation delay. Hydroxyl (OH) content (in mmol g⁻¹) were calculated using Equation 1, where C_s (M) is the concentration of cholesterol standard, V_s (μL) is the volume of cholesterol standard, A is the area of the OH groups peak obtained on the ³¹P NMR spectrum, and m (mg) is the sample's weight:

$$OH\ content = \frac{C_s \times V_s \times A}{m} \quad (1)$$

Fourier transform infrared (FT-IR) spectra were obtained with a Nicolet 380 spectrometer (Thermo Electron Corporation) equipped with an attenuated total reflectance (ATR) diamond module. Each analysis was acquired with 32 scans in the range 4000-500 cm⁻¹.

Size-exclusion Chromatography (SEC) enabled the determination of the number-average molar mass (M_n) and dispersity (Đ) using an Acquity APC apparatus from Waters, with THF as eluent (0.6 mL min⁻¹) at 40 °C. The detection was performed by an Acquity refractive index detector. Three columns (Acquity APC XT 450 Å 2.5 μm 4.6 × 150 mm, 200 and 45) were connected. The calibration was based on polystyrene (PS) standards.

Thermogravimetric analysis (TGA) was performed on a TA Instrument Hi-Res TGA Q5000. Samples of approximately 2-3 mg were heated in a platinum crucible from room temperature to 700 °C at a rate of 20 °C min⁻¹ under an air atmosphere (25 mL min⁻¹ flow rate).

Differential scanning calorimetry (DSC) measurements were recorded on a TA instruments Discovery DSC-25 apparatus under 50 mL min⁻¹ dry nitrogen flow. 2-3 mg samples were placed in aluminum pans, with an empty pan as reference. To erase thermal history, the samples were first equilibrated at 150 °C for 3 minutes. They were then cooled down at -80 °C with a ramp of 5 °C min⁻¹ rate and equilibrated for 3 min. Finally, the samples were heated up to 150 °C with a 10 °C min⁻¹ ramp. T_g was measured as the change of slope during the last heating ramp.

Oxidation induction time (OIT) were performed on a TA instruments Discovery DSC-25 device. Around 2-3 mg of sample were precisely weighed and placed in open alumina pans, using an empty pan as reference. Samples were heated under nitrogen to 140°C at a 10°C min⁻¹ rate. Then the gas was switched to air at a mass flow of 50 mL min⁻¹ for 120 minutes. The experiment would abort if the normalized heat flow would exceed 0.8 W g⁻¹.

Shear viscosity of polyols and polyacetoacetates was measured at 25 °C with a TA Instrument Discovery Hybrid Rheometer HR-3 equipped with 25 mm parallel plates. A 500 nm gap and frequency range from 10⁻⁵ to 10⁻² s⁻¹ were applied.

Dynamic mechanical analyses (DMA) were recorded on a TA Instrument Discovery Hybrid Rheometer HR-3 equipped with rectangular torsion geometry. Samples were heated at 3 °C min from -60 to 150 °C, with a 0.01 % strain and 1 Hz frequency. The theory of rubber elasticity for small deformations on the rubbery plateau enabled the calculation of the crosslinking density (*ν*) from Equation 2, where *G'* (Pa) is the storage modulus, and R the molar gas constant (8.314 J mol⁻¹ K⁻¹). T_α (K), the temperature of the α transition is determined at the maximum of tan δ curve (Chenal et al., 2007; Palmese and McCullough, 1992).

CHAPITRE 2

$$v \text{ (mol m}^{-3}\text{)} = \frac{G'_{T_{\alpha+60}}}{3R(T_{\alpha+60})} \quad (2)$$

Molar mass between crosslinks (M_c) was calculated with Equation 3, where ρ is the density of the materials (g m^{-3}) which was calculated by measuring the volume and the mass of materials discs of 0.8 cm diameter and approximately 1 mm thickness. Detailed values are available in Table S2-4 in appendices (SI).

$$M_c \text{ (g mol}^{-1}\text{)} = \frac{\rho}{v} \quad (3)$$

Stress relaxation experiment were performed on a TA Instrument Discovery Hybrid Rheometer HR-3 equipped with ETC-steel 25 mm parallel plates geometry. Disks of 25 mm diameter and 1 mm thickness were prepared. The series of stress relaxation at different temperatures were carried out successively on the same sample after equilibration at temperature for 10 minutes, with a fixed gap of approximately 1 mm and 1 % strain. Resulting curves were fitted with Equation 4, using Kohlrausch-William-Watts stretched exponential decay where $G(t)/G_0$ is the normalized stress at relaxation time t , τ^* is a characteristic relaxation time, and β ($0 \leq \beta \leq 1$) the exponent indicating the distribution of relaxation times (Dhinojwala et al., 1994; Williams and Watts, 1970).

$$\frac{G(t)}{G_0} = \frac{G_{perm}}{G_0} + \left(1 - \frac{G_{perm}}{G_0}\right) \exp \left\{ -\left(t/\tau^*\right)^\beta \right\} \quad (4)$$

For stress exponential decay, average relaxation time $\langle \tau \rangle$ is given by Equation 5.

$$\langle \tau \rangle = \frac{\tau^* \Gamma\left(\frac{1}{\beta}\right)}{\beta} \quad (5)$$

Activation energies (E_a) were calculated by plotting $\ln \langle \tau \rangle = f(1000/T)$, with $\langle \tau \rangle$ given by Equation 6.

$$\langle \tau \rangle = A \exp\left(\frac{-E_a}{RT}\right) \quad (6)$$

Uniaxial tensile tests were carried out on an Instron 5567H dynamometer equipped with a 10 kN load cell. Experiments were performed on a set of 5 dumbbell-shaped samples with dimension of approximately $45 \times 5 \times 1 \text{ mm}^3$ in a room set at $23 \text{ }^\circ\text{C}$ with a constant crosshead speed of 20 mm min^{-1} until sample failure. Young's modulus (E), stress at break (σ) and elongation at break (ϵ) were recorded. Exhibited tensile curves were selected to be representative of the average values.

Swelling ratio (SR) of each material was determined by immersion of three separate samples of around 100 mg in both acetone and water for 48 h. SR were calculated using Equation 7, where m_1 is the mass of material after swelling in either acetone or water and m_i is the initial mass of dried material.

$$SR \text{ (\%)} = \frac{m_1 - m_i}{m_i} \times 100 \quad (7)$$

After swelling, the samples were dried for 24 h in an oven at $50 \text{ }^\circ\text{C}$ under vacuum. Gel fraction (GF) was calculated according to Equation 8, where m_f is the final mass of dried material and m_i the initial mass of material.

$$GF \text{ (\%)} = \frac{m_f}{m_i} \times 100 \quad (8)$$

To study the macroscopic healing ability of the materials, a razor blade was used to scratch the surface of a specimen. The sample was healed in an oven at $140 \text{ }^\circ\text{C}$ for 0, 2 and 6 h and the healing

process was recorded using an Olympus BX41 optical microscope equipped with a MPlan N 10_x/0.25 objective.

4. RESULTS AND DISCUSSION

4.1. Polyacetoacetates from OSL

The synthesis of lignin-based VU networks first requires grafting acetoacetate groups onto lignin. Previous studies show that TBAA is an efficient reagent in the modification of aliphatic alcohols into acetoacetate without catalyst, releasing *t*-BuOH as side product (Witzeman and Nottingham, 1991). However, this pathway is not adequate to achieve high conversion rate on lignins, because of the diversity of reactive groups present, with carboxylic acids, aliphatic and phenolic OHs groups. Indeed, Krall et al. showed that acetoacetylation of phenolic OH present on Indulin Kraft Lignin using TBAA led to poor conversion (Krall et al., 2018), because of their low nucleophilicity induced by electron delocalization. To overcome the potential sluggishness of this reaction and OSL heterogeneous structure, OSL was first modified by EC to graft aliphatic OH moieties on each of its reactive sites, as illustrated in Figure 2-1a (Duval et al., 2022; Duval and Avérous, 2017b). Reaction of EC with aliphatic OH can also lead to the formation of carbonate linkages, but was not represented here (Duval and Avérous, 2017b). The reaction was performed on a mixture of OSL and PEG, to integrate soft segments in the final architecture, reduce the global viscosity, and avoid the use of solvents, in agreement with green chemistry principles. This strategy has already been successfully developed by our group to prepare lignin-based polyols suitable for the preparation of polyurethane foams (Duval et al., 2022).

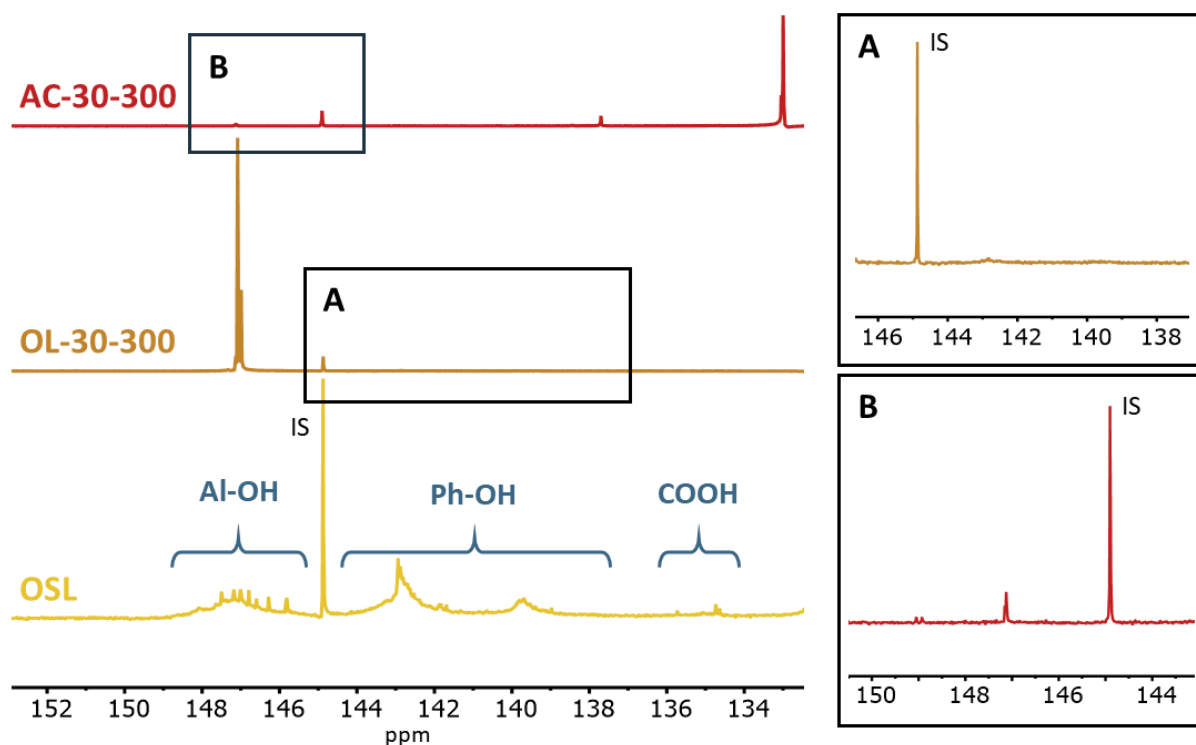


Figure 2-2. Stacked ³¹P NMR of OSL, OL-30-300 and AC-30-300 with details of (A) phenolic hydroxyls conversion after the OL-30-300 synthesis, and (B) aliphatic hydroxyls conversion after AC-30-300 synthesis; IS = Internal standard.

A series of polyol varying lignin content (30, 40 and 50 wt %) and PEG chain length (150, 300 and 400 g mol⁻¹) was synthesized. The polyols were analyzed by ³¹P NMR, as illustrated in Figure 2-2.

CHAPITRE 2

This technique relies on the reaction of a phosphorylating agent, Cl-TMDP, with the different OH groups of lignin (Archipov et al., 1991; Granata and Argyropoulos, 1995). Aliphatic OH (Al-OH) are visible from 145.4 to 150.0 ppm, phenolic hydroxyls (Ph-OH) from 137.6 to 144.0 ppm, and carboxylic acids (COOH) 133.6 to 136.0 (Pu et al., 2011). Spectra of polyols are available from Figure S2-10 to Figure S2-14 in SI. The disappearance of peaks corresponding to phenolic OH between 144.3 and 138.8 ppm and the appearance of peaks corresponding to aliphatic OH from 147.2 to 146.8 ppm show an almost complete grafting of EC moieties onto OSL reactive groups. Conversions of phenolic OH between 87 and 100 % were obtained. Values are given in Table 2-1 for each polyol. According to the reaction conditions and the stoichiometry of 1.1 equivalents of EC, PEG moieties should be only slightly modified by EC (Duval et al., 2022). FT-IR spectra available in Figure S2-15 in SI exhibit an increasing intensity of the vibration OH band around 3394 cm^{-1} . OH content of the different polyols, from Equation 2, and the viscosities at $25\text{ }^{\circ}\text{C}$ are given in Table 2-1. OH content is increasing with (i) decreasing PEG chain length, and (ii) increasing lignin content due to its high content in OH groups. The viscosity of the polyols increases significantly with the lignin content, from 10 to 9520 Pa s with 30 and 50 wt %, respectively. Besides, the viscosity drops when the PEG molar mass is reduced, from 267 to 30 Pa s, from PEG₄₀₀ to TEG, respectively, as previously observed (Duval et al., 2022).

Table 2-1. Main physico-chemical properties of the polyols.

Polyol (Designations)	Lignin content [wt %]	PEG [g mol ⁻¹]	Ph-OH conversion [%]	OH content [mmol g ⁻¹]	Viscosity [Pa s]
OL-30-300	30	300	90	5.05	10 ± 1
OL-40-300	40	300	96	6.55	170 ± 2
OL-50-300	50	300	100	6.12	9520 ± 1000
OL-40-400	40	400	95	5.40	267 ± 5
OL-40-150	40	150	87	8.16	30 ± 3

Synthesized polyols were further modified using TBAA as depicted in Figure 2-1b in order to obtain polyacetoacetates (Krall et al., 2018). As evidenced in the literature, bases slow down bond exchange reactions in VU-based networks (Denissen et al., 2017), thus K₂CO₃ used as a catalyst in the polyol synthesis had to be removed. ³¹P NMR, displayed in Figure 2-2 and from Figure S2-16 to Figure S2-20 in SI, exhibit the vanishing of peaks corresponding to aliphatic OHs between 147.1 and 147.0 ppm, indicating their full conversion. The appearance of a peak around 133.0 ppm is caused by the reaction between the grafted acetoacetate groups and Cl-TMDP. It is also observed on the ³¹P NMR of TBAA, as depicted in Figure S2-22 in SI, confirming that acetoacetate moieties react with the phosphorus agent, although not quantitatively. The reaction should be related to the presence of enol moieties in the product resulting from acetoacetate tautomerization, as illustrated in Figure S2-21 in SI. An unknown peak at 138.6 ppm is also observed on the ³¹P NMR spectrum of the reagent but could not be assigned.

¹H NMR further confirmed the successful grafting with the appearance of peaks at 3.47 ppm and 2.25 ppm corresponding to methyl and methylene of acetoacetate moieties, as displayed in Figure S2-23 to Figure S2-27 in SI. In FT-IR spectra, new bands appear at 1738 and 1712 cm⁻¹, corresponding to the esters and ketones, respectively, as illustrated in Figure 2-3. Additional physico-chemical analysis of the series of polyacetoacetate are available in Table S2-5 in SI. The amount in acetoacetate of each macromolecular architecture was comprised between 3.27 and 3.43 mmol g⁻¹. Viscosity of the polyacetoacetates is much lower than the corresponding polyols, making it convenient for various synthetic processes. M_n are comprised between 560 and 760 g mol⁻¹. They strongly increase with the PEG chain length but are almost unaffected by the variation of the lignin content. The SEC curves are displayed in Figure S2-28.

4.2. VU networks

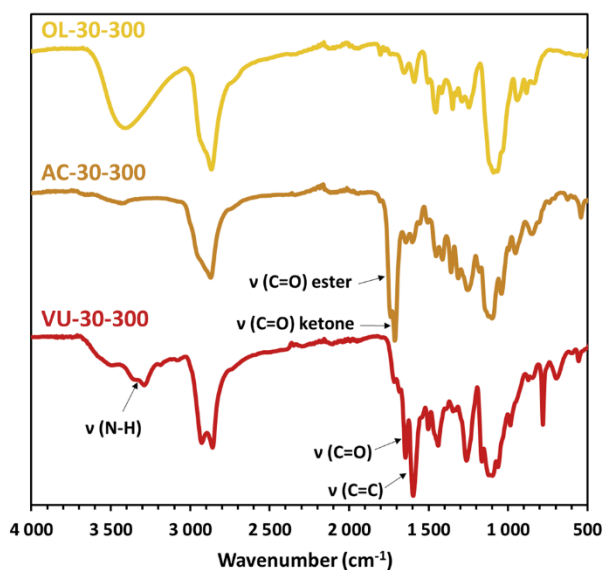


Figure 2-3. FT-IR spectra with some examples of lignin-based polyol, polyacetoacetate and VU network, from top to bottom.

VU networks were prepared by condensation of the different polyacetoacetates with HMDA, a diamine which can be potentially biobased. The synthetic pathway is illustrated in Figure 2-1c. HMDA can be synthesized from adipodinitrile and hexanediol derived from biobased adipic acid originating from carbohydrates (Froidevaux et al., 2016; Pelckmans et al., 2017). FT-IR spectra, displayed in Figure 2-3 exhibit the appearance of characteristic bands of C=O and C=C vibrations in VU at 1646 and 1598 cm^{-1} , respectively (Liu et al., 2018). Almost complete consumption of acetoacetate moieties is observed with only small remaining acetoacetate bands at 1738 and 1712 cm^{-1} , corresponding to the esters and ketones, respectively. Remaining acetoacetate might result from incomplete conversion after gelation due to OSL's high functionality. Stacked FT-IR spectra of the materials series are available in Figure S2-29 in SI.

To assess reprocessing conditions, thermal properties of VU networks were determined by TGA. Resulting values are summarized in Table 2-2. Curves are displayed in Figure S2-30 in SI. For all materials, thermal degradation corresponding to a 5 % mass loss occurs between 244 and 270 $^{\circ}\text{C}$ under air. $T_{d5\%}$ increases with lignin content, whereas the value is slightly higher with a longer PEG chain. Similar values are reported for other lignin-based vitrimers (Moreno et al., 2021). DSC measurements were performed to determine the glass transition temperatures (T_g). The resulting curves are available in Figure S2-31 in SI. As reported in Table 2-2, T_g strongly increases from -28 to 18 $^{\circ}\text{C}$, with the lignin content from 30 to 50 wt %, respectively. T_g values are unaffected by the PEG chain length, probably because the different PEG have relatively similar T_g values (from -60 to -47 $^{\circ}\text{C}$ for TEG and PEG₄₀₀ respectively, as shown in Figure S2-32 to Figure S2-34).

Rheological properties were assessed by DMA. Results are given in Table 2-2 and the corresponding curves are available in Figure S2-35. Alpha relaxation temperatures (T_{α}) increase from 2 to 65 $^{\circ}\text{C}$, with lignin content from 30 to 50 wt %, respectively, whereas T_{α} values' variation can be considered as minors with PEG chain length, which is in accordance with the trend observed by DSC. Crosslinking density of the tridimensional networks (ν) and the average molar mass between two crosslink nodes (M_c) were calculated and summarized in Table 2-2. As expected, ν increases from 208 to 269 with lignin content (from 30 to 50 wt %) because of OSL high functionality forming a higher number of crosslinking nodes, and thus reducing M_c from 2400 to 1800 g mol^{-1} . An analogous tendency

CHAPITRE 2

is shown with increasing the length of the PEG chains. From TEG to PEG₄₀₀, ν increases from 151 to 294 mol m⁻³. The polyols were synthesized from the same lignin / PEG ratio in mass, but with PEGs of different molar masses. The molar ratio between lignin and PEG is thus increasing with the PEG chain length. Since crosslinking nodes in the network are brought by the lignin high functionality, increasing its molar content increases crosslinking density and decreases M_c value.

Table 2-2. Thermal and physico-chemical properties of the VU networks.

VU (Designations)	$T_{d5\%}$ [°C]	T_g [°C]	T_α [°C]	ν [mol m ⁻³]	M_c [g mol ⁻¹]	R^a	E [MPa]	σ [MPa]	ϵ [%]
VU-30-300	244	-28	2	208	2400	3.4	0.2 ± 0.1	0.2 ± 0.1	98 ± 10
VU-40-300	263	-10	23	231	2100	2.9	10.9 ± 1.3	3.3 ± 0.7	67 ± 20
VU-50-300	270	18	65	269	1800	2.6	420 ± 30	17.2 ± 0.7	22 ± 3
VU-40-400	267	-11	27	294	1700	2.3	4.3 ± 0.6	1.6 ± 0.3	65 ± 8
VU-40-150	245	-13	17	151	3200	5.7	0.5 ± 0.1	0.7 ± 0.1	141 ± 10

^aR correspond to the M_c / M_n ratio (measured by SEC), of the respective polyacetoacetates.

Furthermore, M_c values of the materials are often greater than M_n of their corresponding precursors possibly owing to topological defects in the networks (Liu et al., 2022). The ratio R between M_c and M_n can be defined as a theoretical fraction of defects, resulting from unreacted functionalized dangling chains. The higher R is, the greater is the quantity of defects in the network. Values are reported in Table 2-2. Furthermore, R decreases with lignin content and with longer PEG chain length. This suggest that the presence of shorter precursors during the materials synthesis favors the probability of creating defects in the networks. However, it should be kept in mind that this value of defect is only indicative of a trend. Indeed, the molar mass values obtained from SEC present a well-known bias since the calibration is based on linear PS standards.

Flow behavior of vinylogous urethane networks was assessed by stress relaxation experiment. Heat-induced transamination exchange reactions were analyzed from 100 to 140 °C, as displayed in Figure 2-4. Stress relaxation experimental curves were successfully fitted with Kohlrausch-William-Watts stretched exponential decay using equation 4, given that our networks dissipates stress through plural relaxation modes (Li et al., 2018). This model enables the determination of the characteristic relaxation time τ^* and the exponent that reflects the homogeneity of the network via the distribution of relaxation times β ($0 < \beta \leq 1$), a decreasing β value indicating a broader distribution. The fit parameters are summarized in Table 2-3. Full stress relaxation was observed, indicating that no permanent crosslinks were formed during networks syntheses. Thus, the G_{perm}/G_0 in equation 4 is equal to 0. Vitrimers exhibited relaxation time from 488 to 39 s at 130 °C, depending on the macromolecular architecture. No clear trend can be seen with the lignin content or PEG chain length evolutions. However, the results suggest that an optimal network structure was reached for VU-40-300 and VU-40-400. Relaxations times are faster by a combination of sufficient crosslinking density favoring the probability of dynamic bond exchange and an acceptable mobility of the involved chains (Liu et al., 2022). As expected, β values, comprised between 0.50 and 0.69, indicated relatively broad relaxation times distributions due to dynamic bonds connected to lignin or to PEG moiety. Moreover, OSL structural heterogeneity may also impact β values. Activation energies E_a required for macroscopic flow via transamination reaction were calculated according to Arrhenius plot of $\langle \tau \rangle$ (equation 6). For each vitrimer, stress relaxation and Arrhenius plots are available from Figure S2-36 to Figure S2-43, in SI. This Arrhenius behavior upon heating confirms the vitrimer character of the synthesized materials. Resulting E_a values were ranged between 51 and 114 kJ mol⁻¹, which is in good agreement with previously reported values for VU networks (Chen et al., 2021; Denissen et al., 2015; Wei et al., 2021). Materials having higher lignin content exhibited increased E_a , which can be correlated with the evolution

CHAPITRE 2

of the T_g and the crosslinking density between the different macromolecular architectures (Breuillac et al., 2019; Hajj et al., 2020). However, no significant trend was observed concerning the variation of E_a as a function of PEG chain length. The variation of E_a cannot be fully correlated to the structural parameters of the networks. Plots of E_a as a function of lignin content, PEG molar mass, and crosslinking density are available in Figure S2-44.

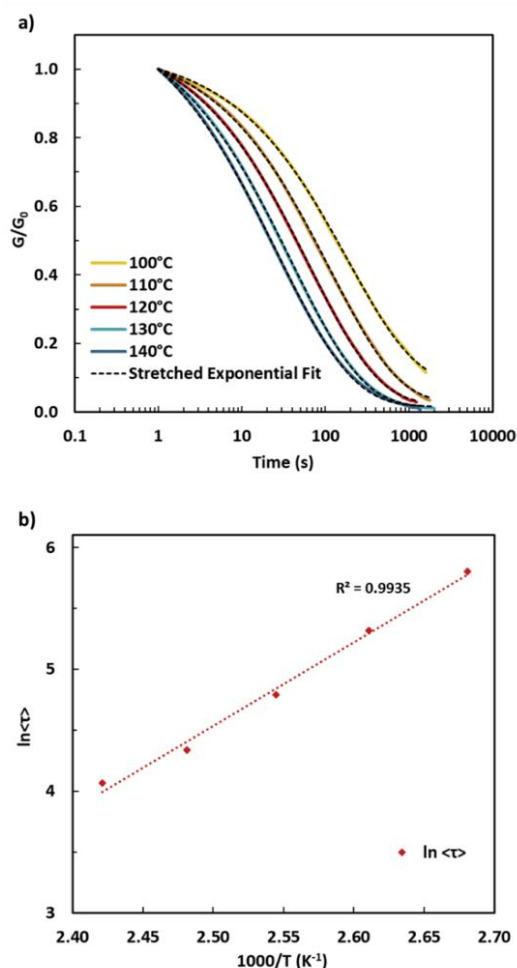


Figure 2-4. Flow behavior of VU-40-300 with a) stress relaxation curves from 100 to 140°C, and b) Arrhenius plot.

Table 2-3. Main stress relaxation parameters.

VU (Designations)	$\tau^*_{130^\circ\text{C}}$ [s]	β	E_a [kJ mol ⁻¹]	T_v [°C]
VU-30-300	243	0.62 ± 0.02	51	-15
VU-40-300	40	0.52 ± 0.03	57	-17
VU-50-300	97	0.57 ± 0.05	72	12
VU-40-400	39	0.50 ± 0.04	81	16
VU-40-150	488	0.69 ± 0.06	114	51

Theoretical topology freezing temperature (T_v) can be defined as temperature above which a macroscopic flow can be achieved via dynamic exchange (elastic solid to viscoelastic liquid). T_v were calculated by extrapolation from the Arrhenius plot for a conventional viscosity of 10^{12} Pa s (Brutman

et al., 2014; Lessard et al., 2019), and the details are reported in SI (Table S2-6). Resulting values, summarized in Table 2-3, show two viscoelastic behaviors. VU-40-300 and VU-50-300 exhibit slightly lower T_v than T_g , indicating that bond exchange reactions are first limited by the network's rigidity. Whereas the macromolecular architectures displaying higher T_v than T_g demonstrate a flow mainly controlled by the bond exchange kinetics (Denissen et al., 2016). Overall, bond exchange reactions might theoretically already take place at room temperature.

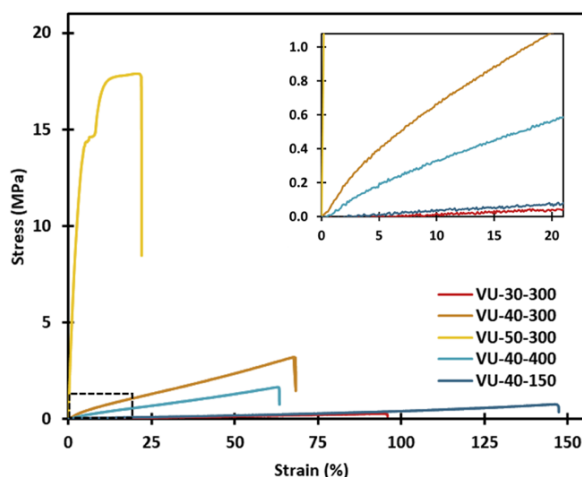


Figure 2-5. Uniaxial tensile tests of vitrimer series.

Mechanical properties of lignin-based vitrimers were evaluated at 23 °C by uniaxial tensile tests. They are reported in Table 2-2 and Figure 2-5. As expected, the results indicated that increasing lignin content led to increased tensile strength (from 0.2 to 17.2 MPa) and decreased elongation at break (from 98 to 22 %), correlated to an increased crosslinking density and aromaticity (Zhang et al., 2018). Young's modulus was also greatly improved, from 0.2 to 420 MPa for systems based on 30 to 50 wt % lignin, respectively. Whereas lignin adds rigidity to the backbone, increasing PEG content promote higher mobility within the network which results in lower stress at break and higher elongation at break, especially when using TEG. In this latter case, elastomer-like behavior can be obtained. Thus, the system used to develop the networks can be tuned to achieve the desired properties, particularly by adjusting the lignin content.

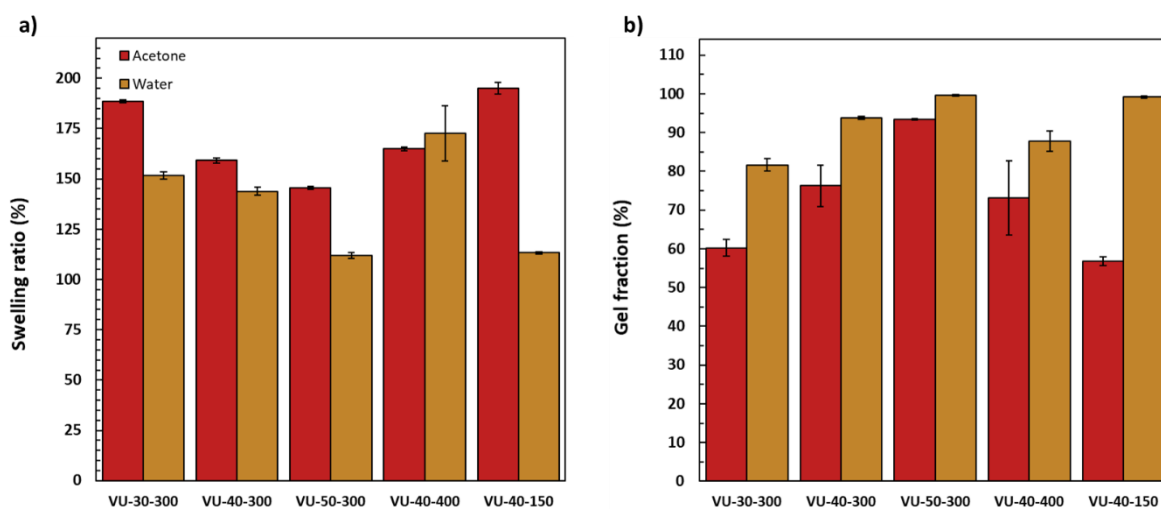


Figure 2-6. a) Swelling ratios and b) gel fractions of the vitrimer series.

CHAPITRE 2

Network's structures were further studied via swelling ratio (SR) and gel fraction (GF) experiments in both acetone and water, as illustrated in Figure 2-6. Acetone was chosen as organic solvent in this study because it can easily solubilize the polyacetoacetates. Detailed data are reported in Table S2-7. A preliminary kinetic study was first performed to determine the adequate time of immersion of the vitrimers in both solvents. Resulting curves on Figure S2-45, show that 48h is necessary to reach an equilibrium. After 48 h hours of immersion, excess of solvent was carefully wiped from VU samples before weighing. Higher SR were reached in acetone (from 146 to 195 %) because of a better affinity of polyacetoacetates compared to water (112 to 173 %). Values decreased with higher crosslinking density due to smaller available interspace and free volumes inside the networks, with the shorter distance between crosslinked points, for both selected solvents. Higher GF were obtained in water (82 to 100 %) compared to acetone (57 to 93 %). This is linked to the respective solubility of the precursors. Overall, the lowest GF were obtained for networks with the greatest theoretical fraction of defects, such as VU-30-300 and VU-40-150, as previously mentioned. Such relatively low GF values are not unprecedented for lignin-based vitrimers (Xue et al., 2021). Furthermore, Nicolaÿ and co-workers discussed the solubility of dynamic networks compared to their static counterparts containing permanent linkages (Breuillac et al., 2019; Nicolaÿ et al., 2010). Vitrimers can partially or even completely dissolve during swelling tests, because of the rearrangement into soluble structure, depending on several parameters such as the crosslinking density, the exchangeable bonds content, the dynamics of the rearrangements, the time of observation or the quality of the solvent (Breuillac et al., 2019; Hajj et al., 2020). The partial dissolution of the systems herein prepared might be favored by their low T_g and T_v , enabling mobility and theoretical bond exchanges reactions in these conditions.

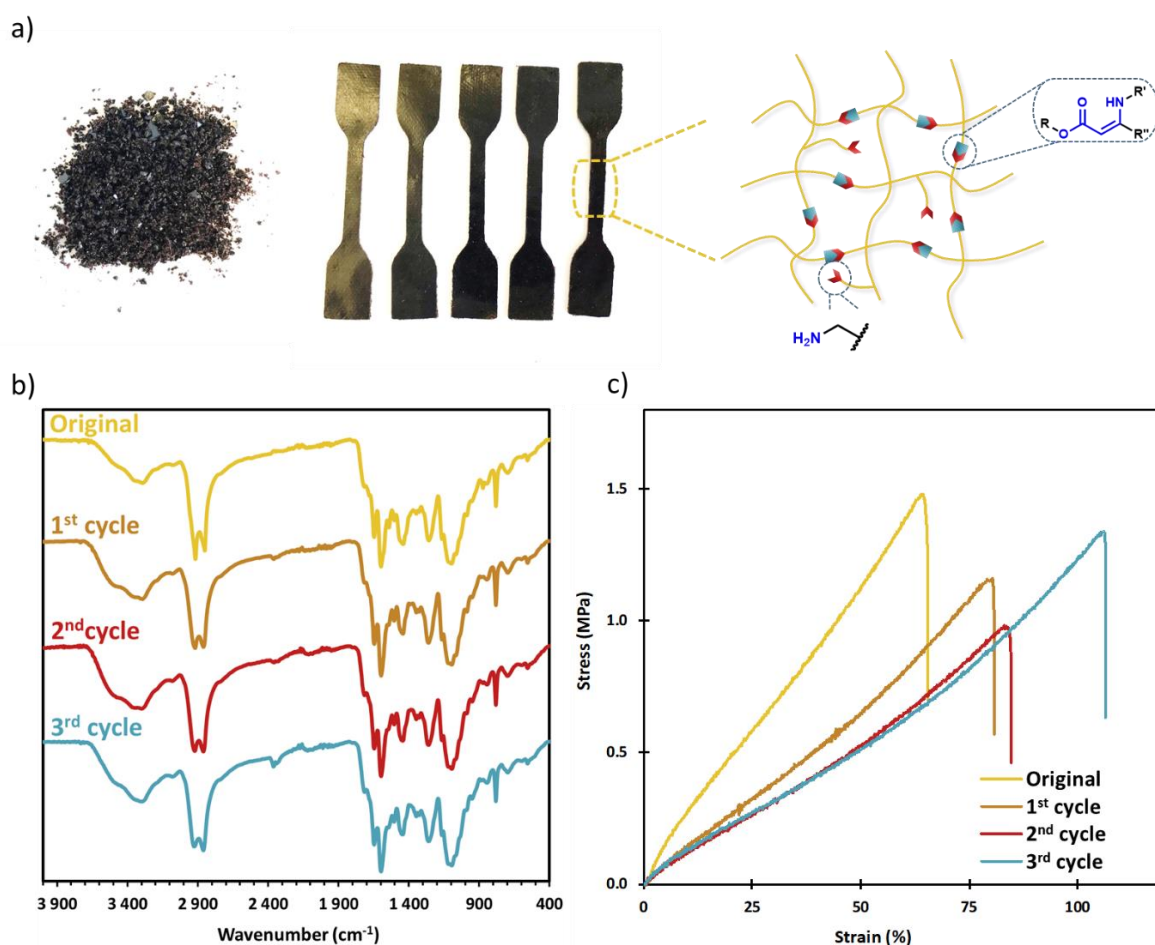


Figure 2-7. Reprocessing study. a) Thermomechanical reprocessing of VU-40-400, b) FT-IR analysis, and c) uniaxial tensile tests after each reprocessing cycle.

CHAPITRE 2

The reprocessing of VU vitrimers was studied during three cycles, with grinding and remolding steps (Figure 2-7). Chemical structure, mechanical and rheological properties were carried out after each cycle to evaluate the evolution of properties induced by mechanical reprocessing. FT-IR analyses, depicted in Figure 2-7b, exhibited unchanged spectra for recycled materials compared to their corresponding first generations, inducing no significant modification of the chemical structure of the network. Uniaxial tensile tests indicated relatively small mechanical losses, and especially after the first recycling step where 71 % of the initial stress at break is recovered as illustrated in Figure 2-7c. Elongation at break was increased after each recycling steps, to achieve a final value of 109 %, compared to 65 % for the original material. A stabilization of the Young's modulus was achieved after the 2nd recycling cycle. Lastly, DMA measurements, available in Figure S2-46 and Table S2-8 in SI, evidenced a noticeable decreasing crosslinking density throughout the first recycling cycle, followed by a stabilization for the other two cycles. This evolution is in accordance with the data of uniaxial tensile tests.

A hypothesis often mentioned in the literature for VU vitrimers' loss of properties throughout recycling steps is the oxidation of pendant amine after long duration exposure to air at high temperatures (Fortman et al., 2018; Spiesschaert et al., 2021, 2020). In order to control this phenomenon, OIT were performed on the different generation of materials to further understand the property loss induced by the reprocessing cycles. The experiments were conducted under conditions mimicking hot press cycles with an isothermal far superior to 20 minutes at 140 °C. From the resulting curves displayed in SI from Figure S2-47 to Figure S2-50, no oxidation peak was observed during the isotherm for unrecycled and recycled materials. Then, the previously given hypothesis found in the literature is not validated in this case. The degradation of the network is most likely resulting from mechanical recycling and the corresponding thermal and mechanical treatments, especially from the grinding step that might alter the integrity of the vitrimers structures. Not only dynamic bonds but all bonds forming the network, especially lignin's bulky structure could potentially be affected (Gamardella et al., 2020).

To demonstrate healing ability of the prepared materials, a scratching test was performed on VU-40-400. The sample was scratched and healed at 140 °C in an oven. Pictures captured using an optical microscope at 0, 2 and 6 h of healing are available in Figure S2-51 in SI. After 2 h, the scratch size was already significantly reduced due to thermally activated bond exchange reactions occurring at the scratched surfaces and thus restructuring the network. The crack almost completely faded after 6 h at 140 °C, revealing good reparability potential which is an interesting feature to increase lifecycle and sustainability of the materials. Such materials could reveal a good candidate as flexible membrane for instance.



Figure 2-8. Study of transamination reactions: a) VU in DMF, b) VU in DMF after heating at 100°C, c) VU in DMF after heating with an excess of n-octylamine, and d) VU in DMF after heating, with an excess of ethyl acetoacetate.

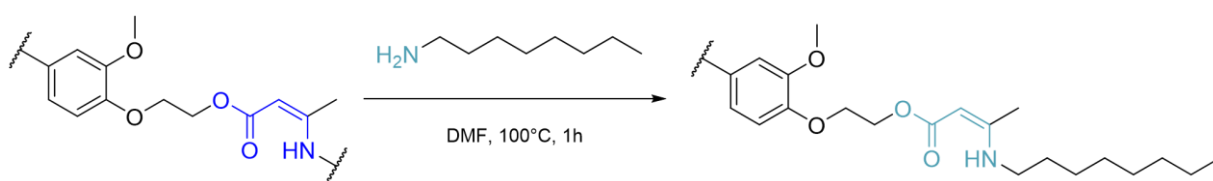


Figure 2-9. Transamination reaction between VU networks and n-octylamine in DMF.

In presence of an excess of n-octylamine at 100 °C, VU networks were completely dissolved, as illustrated in Figure 2-8c (Denissen et al., 2015; Guerre et al., 2018). This result reveals potential for chemical recycling, although this point was not studied in this work. In the presence of an excess of ethyl acetoacetate at 100 °C (Figure 2-8d), the network showed significant swelling and the liquid phase got a slightly orange coloration due to the soluble fraction, but deconstruction of the network did not occur. It confirms that the fast bond exchange reaction requires free amine groups, as depicted in Figure 2-9.

5. CONCLUSION

The valorization of lignin towards adaptable and performing aromatic materials was successfully demonstrated through the synthesis of novel and sustainable lignin-based VU networks. To the best of our knowledge, this is the first work reporting the integration of lignin into the design of dynamic VU networks. Starting from OSL, a series of five liquid polyols was successfully synthesized by chemical modification from a mixture of lignin and PEG. These systems were thereafter used for the synthesis of polyacetoacetates. Different macromolecular architectures were then elaborated from polyacetoacetates condensation with HMDA and were also fully characterized. The influence of the lignin content and PEG chain length was particularly analyzed. The systems exhibited different network structures through the various macromolecular architectures, with T_g from -28 to 18 °C and crosslinking densities from 151 to 294 mol m⁻³.

The vitrimer behavior of these systems has been clearly evidenced with stress relaxation as short as 39 s at 130 °C, and activation energies from 51 to 114 kJ mol⁻¹, enabling fast reprocessing and healing ability. After two recycling cycles, no major property loss was observed. Mechanical and rheological properties achieved stabilized values, whereupon crosslinking density and Young's modulus remained constant after the first recycling cycle. Oxidation tests indicated that networks were probably more damaged by the grinding step of the mechanical recycling (thermo-mechanical treatment) than by the oxidation of amines moieties upon heating, unlike hypotheses that can be found in the literature.

Finally, organosolv lignins proved to be a promising and relevant precursor in the development of novel sustainable, recyclable and healable aromatic materials. These performing and adaptable materials could be developed for industrial and long-term applications (e.g., building and automotive) with a controlled end-of life by thermomechanical reprocessing.

In accordance with societal expectations for a more sustainable future, the structure-property relationship of lignin-based VU vitrimers could be further evaluated with other types of lignins, from other resources and fractionation process, to prepare novel biobased materials which can be fully integrated in the circular bioeconomy.

6. REFERENCES

Adjaoud, A., Puchot, L., Federico, C.E., Das, R., Verge, P., 2023. Lignin-based benzoxazines: A tunable key-precursor for the design of hydrophobic coatings, fire resistant materials and catalyst-free vitrimers. *Chem. Eng. J.* 453, 139895. <https://doi.org/10.1016/j.cej.2022.139895>

- Altuna, F.I., Hoppe, C.E., Williams, R.J.J., 2019. Epoxy vitrimers with a covalently bonded tertiary amine as catalyst of the transesterification reaction. *Eur. Polym. J.* 113, 297–304. <https://doi.org/10.1016/j.eurpolymj.2019.01.045>
- Altuna, F.I., Pettarin, V., Williams, R.J.J., 2013. Self-healable polymer networks based on the cross-linking of epoxidised soybean oil by an aqueous citric acid solution. *Green Chem.* 15, 3360–3366. <https://doi.org/10.1039/C3GC41384E>
- Archipov, Y., Argyropoulos, D.S., Bolker, H.I., Heitner, C., 1991. 31P NMR Spectroscopy in Wood Chemistry. I. Model Compounds. *J. Wood Chem. Technol.* 11, 137–157. <https://doi.org/10.1080/02773819108050267>
- Breuillac, A., Kassalias, A., Nicolaÿ, R., 2019. Polybutadiene Vitrimers Based on Dioxaborolane Chemistry and Dual Networks with Static and Dynamic Cross-links. *Macromolecules* 52, 7102–7113. <https://doi.org/10.1021/acs.macromol.9b01288>
- Brutman, J.P., Delgado, P.A., Hillmyer, M.A., 2014. Polylactide Vitrimers. *ACS Macro Lett.* 3, 607–610. <https://doi.org/10.1021/mz500269w>
- Capelot, M., Montarnal, D., Tournilhac, F., Leibler, L., 2012. Metal-Catalyzed Transesterification for Healing and Assembling of Thermosets. *J. Am. Chem. Soc.* 134, 7664–7667. <https://doi.org/10.1021/ja302894k>
- Chen, F., Cheng, Q., Gao, F., Zhong, J., Shen, L., Lin, C., Lin, Y., 2021. The effect of latent plasticity on the shape recovery of a shape memory vitrimer. *Eur. Polym. J.* 147, 110304. <https://doi.org/10.1016/j.eurpolymj.2021.110304>
- Chen, Z., Wang, J., Qi, H.J., Wang, T., Naguib, H.E., 2020. Green and Sustainable Layered Chitin–Vitrimer Composite with Enhanced Modulus, Reprocessability, and Smart Actuator Function. *ACS Sustain. Chem. Eng.* 8, 15168–15178. <https://doi.org/10.1021/acssuschemeng.0c04235>
- Chenal, J.-M., Chazeau, L., Guy, L., Bomal, Y., Gauthier, C., 2007. Molecular weight between physical entanglements in natural rubber: A critical parameter during strain-induced crystallization. *Polymer* 48, 1042–1046. <https://doi.org/10.1016/j.polymer.2006.12.031>
- Constant, S., Wienk, H.L.J., Frissen, A.E., Peinder, P. de, Boelens, R., Es, D.S. van, Grisel, R.J.H., Weckhuysen, B.M., Huijgen, W.J.J., Gosselink, R.J.A., Bruijninx, P.C.A., 2016. New insights into the structure and composition of technical lignins: a comparative characterisation study. *Green Chem.* 18, 2651–2665. <https://doi.org/10.1039/C5GC03043A>
- Demongeot, A., Groote, R., Goossens, H., Hoeks, T., Tournilhac, F., Leibler, L., 2017. Cross-Linking of Poly(butylene terephthalate) by Reactive Extrusion Using Zn(II) Epoxy-Vitrimer Chemistry. *Macromolecules* 50, 6117–6127. <https://doi.org/10.1021/acs.macromol.7b01141>
- Denissen, W., Droesbeke, M., Nicolaÿ, R., Leibler, L., Winne, J.M., Du Prez, F.E., 2017. Chemical control of the viscoelastic properties of vinylogous urethane vitrimers. *Nat. Commun.* 8, 14857. <https://doi.org/10.1038/ncomms14857>
- Denissen, W., M. Winne, J., Prez, F.E.D., 2016. Vitrimers: permanent organic networks with glass-like fluidity. *Chem. Sci.* 7, 30–38. <https://doi.org/10.1039/C5SC02223A>
- Denissen, W., Rivero, G., Nicolaÿ, R., Leibler, L., Winne, J.M., Du Prez, F.E., 2015. Vinylogous Urethane Vitrimers. *Adv. Funct. Mater.* 25, 2451–2457. <https://doi.org/10.1002/adfm.201404553>
- Dhinojwala, A., Hooker, J.C., Torkelson, J.M., 1994. Retardation of rotational reorientation dynamics in polymers near the glass transition: a novel study over eleven decades in time using second-order non-linear optics. *J. Non-Cryst. Solids, Relaxations in Complex Systems* 172–174, 286–296. [https://doi.org/10.1016/0022-3093\(94\)90447-2](https://doi.org/10.1016/0022-3093(94)90447-2)
- Du, L., Jin, X., Qian, G., Yang, W., Su, L., Ma, Y., Ren, S., Li, S., 2022. Lignin-based vitrimer for circulation in plastics, coatings, and adhesives with tough mechanical properties, catalyst-free and good chemical solvent resistance. *Ind. Crops Prod.* 187, 115439. <https://doi.org/10.1016/j.indcrop.2022.115439>
- Duval, A., Avérous, L., 2020. Mild and controlled lignin methylation with trimethyl phosphate: towards a precise control of lignin functionality. *Green Chem.* 22, 1671–1680. <https://doi.org/10.1039/C9GC03890F>

- Duval, A., Avérous, L., 2017a. Solvent- and Halogen-Free Modification of Biobased Polyphenols to Introduce Vinyl Groups: Versatile Aromatic Building Blocks for Polymer Synthesis. *ChemSusChem* 10, 1813–1822. <https://doi.org/10.1002/cssc.201700066>
- Duval, A., Avérous, L., 2017b. Cyclic Carbonates as Safe and Versatile Etherifying Reagents for the Functionalization of Lignins and Tannins. *ACS Sustain. Chem. Eng.* 5, 7334–7343. <https://doi.org/10.1021/acssuschemeng.7b01502>
- Duval, A., Layrac, G., van Zomeren, A., Smit, A.T., Pollet, E., Avérous, L., 2021. Isolation of Low Dispersity Fractions of Acetone Organosolv Lignins to Understand their Reactivity: Towards Aromatic Building Blocks for Polymers Synthesis. *ChemSusChem* 14, 387–397. <https://doi.org/10.1002/cssc.202001976>
- Duval, A., Vidal, D., Sarbu, A., René, W., Avérous, L., 2022. Scalable single-step synthesis of lignin-based liquid polyols with ethylene carbonate for polyurethane foams. *Mater. Today Chem.* 24, 100793. <https://doi.org/10.1016/j.mtchem.2022.100793>
- Elling, B.R., Dichtel, W.R., 2020. Reprocessable Cross-Linked Polymer Networks: Are Associative Exchange Mechanisms Desirable? *ACS Cent. Sci.* 6, 1488–1496. <https://doi.org/10.1021/acscentsci.0c00567>
- Engelen, S., Wróblewska, A.A., Bruycker, K.D., Aksakal, R., Ladmiral, V., Caillol, S., Du Prez, F.E., 2022. Sustainable design of vanillin-based vitrimers using vinylogous urethane chemistry. *Polym. Chem.* <https://doi.org/10.1039/D2PY00351A>
- Fortman, D.J., Brutman, J.P., De Hoe, G.X., Snyder, R.L., Dichtel, W.R., Hillmyer, M.A., 2018. Approaches to Sustainable and Continually Recyclable Cross-Linked Polymers. *ACS Sustain. Chem. Eng.* 6, 11145–11159. <https://doi.org/10.1021/acssuschemeng.8b02355>
- Froidevaux, V., Negrell, C., Caillol, S., Pascault, J.-P., Boutevin, B., 2016. Biobased Amines: From Synthesis to Polymers; Present and Future. *Chem. Rev.* 116, 14181–14224. <https://doi.org/10.1021/acs.chemrev.6b00486>
- Gamardella, F., De la Flor, S., Ramis, X., Serra, A., 2020. Recyclable poly(thiourethane) vitrimers with high T_g. Influence of the isocyanate structure. *React. Funct. Polym.* 151, 104574. <https://doi.org/10.1016/j.reactfunctpolym.2020.104574>
- Granata, A., Argyropoulos, D.S., 1995. 2-Chloro-4,4,5,5-tetramethyl-1,3,2-dioxaphospholane, a Reagent for the Accurate Determination of the Uncondensed and Condensed Phenolic Moieties in Lignins. *J. Agric. Food Chem.* 43, 1538–1544. <https://doi.org/10.1021/jf00054a023>
- Guerre, M., Taplan, C., Nicolaÿ, R., Winne, J.M., Du Prez, F.E., 2018. Fluorinated Vitriimer Elastomers with a Dual Temperature Response. *J. Am. Chem. Soc.* 140, 13272–13284. <https://doi.org/10.1021/jacs.8b07094>
- Haida, P., Abetz, V., 2020. Acid-Mediated Autocatalysis in Vinylogous Urethane Vitrimers. *Macromol. Rapid Commun.* 41, 2000273. <https://doi.org/10.1002/marc.202000273>
- Hajj, R., Duval, A., Dhers, S., Avérous, L., 2020. Network Design to Control Polyimine Vitriimer Properties: Physical Versus Chemical Approach. *Macromolecules* 53, 3796–3805. <https://doi.org/10.1021/acs.macromol.0c00453>
- Hao, C., Liu, T., Zhang, S., Brown, L., Li, R., Xin, J., Zhong, T., Jiang, L., Zhang, J., 2019. A High-Lignin-Content, Removable, and Glycol-Assisted Repairable Coating Based on Dynamic Covalent Bonds. *ChemSusChem* 12, 1049–1058. <https://doi.org/10.1002/cssc.201802615>
- Imbernon, L., Norvez, S., Leibler, L., 2016. Stress Relaxation and Self-Adhesion of Rubbers with Exchangeable Links. *Macromolecules* 49, 2172–2178. <https://doi.org/10.1021/acs.macromol.5b02751>
- J. Kloxin, C., N. Bowman, C., 2013. Covalent adaptable networks: smart, reconfigurable and responsive network systems. *Chem. Soc. Rev.* 42, 7161–7173. <https://doi.org/10.1039/C3CS60046G>
- Kimura, K., Kohama, S., Yamazaki, S., 2006. Morphology Control of Aromatic Polymers in Concert with Polymerization. *Polym. J.* 38, 1005–1022. <https://doi.org/10.1295/polymj.PJ2006083>
- Kloxin, C.J., Scott, T.F., Adzima, B.J., Bowman, C.N., 2010. Covalent Adaptable Networks (CANs): A Unique Paradigm in Cross-Linked Polymers. *Macromolecules* 43, 2643–2653. <https://doi.org/10.1021/ma902596s>

- Krall, E.M., Serum, E.M., Sibi, M.P., Webster, D.C., 2018. Catalyst-free lignin valorization by acetoacetylation. Structural elucidation by comparison with model compounds. *Green Chem.* 20, 2959–2966. <https://doi.org/10.1039/C8GC01071D>
- Lessard, J.J., Garcia, L.F., Easterling, C.P., Sims, M.B., Bentz, K.C., Arencibia, S., Savin, D.A., Sumerlin, B.S., 2019. Catalyst-Free Vitrimers from Vinyl Polymers. *Macromolecules* 52, 2105–2111. <https://doi.org/10.1021/acs.macromol.8b02477>
- Li, L., Chen, X., Jin, K., Torkelson, J.M., 2018. Vitrimers Designed Both To Strongly Suppress Creep and To Recover Original Cross-Link Density after Reprocessing: Quantitative Theory and Experiments. *Macromolecules* 51, 5537–5546. <https://doi.org/10.1021/acs.macromol.8b00922>
- Liu, H., Sui, X., Xu, H., Zhang, L., Zhong, Y., Mao, Z., 2016. Self-Healing Polysaccharide Hydrogel Based on Dynamic Covalent Enamine Bonds. *Macromol. Mater. Eng.* 301, 725–732. <https://doi.org/10.1002/mame.201600042>
- Liu, J., Li, J.-J., Luo, Z.-H., Zhou, Y.-N., 2022. Mapping crosslinking reaction–structure–property relationship in polyether-based vinylogous urethane vitrimers. *AIChE J.* 68, e17587. <https://doi.org/10.1002/aic.17587>
- Liu, W., Fang, C., Chen, F., Qiu, X., 2020. Strong, Reusable, and Self-Healing Lignin-Containing Polyurea Adhesives. *ChemSusChem* 13, 4691–4701. <https://doi.org/10.1002/cssc.202001602>
- Liu, W.-X., Zhang, C., Zhang, H., Zhao, N., Yu, Z.-X., Xu, J., 2017. Oxime-Based and Catalyst-Free Dynamic Covalent Polyurethanes. *J. Am. Chem. Soc.* 139, 8678–8684. <https://doi.org/10.1021/jacs.7b03967>
- Liu, Z., Zhang, C., Shi, Z., Yin, J., Tian, M., 2018. Tailoring vinylogous urethane chemistry for the cross-linked polybutadiene: Wide freedom design, multiple recycling methods, good shape memory behavior. *Polymer* 148, 202–210. <https://doi.org/10.1016/j.polymer.2018.06.042>
- Lora, J.H., Glasser, W.G., 2002. Recent industrial applications of lignin: a sustainable alternative to nonrenewable materials. *J. Polym. Environ.* 10, 39–48.
- Lucherelli, M.A., Duval, A., Avérous, L., 2022. Biobased vitrimers: Towards sustainable and adaptable performing polymer materials. *Prog. Polym. Sci.* 127, 101515. <https://doi.org/10.1016/j.progpolymsci.2022.101515>
- Ma, X., Li, S., Wang, F., Wu, J., Chao, Y., Chen, X., Chen, P., Zhu, J., Yan, N., Chen, J., 2023. Catalyst-Free Synthesis of Covalent Adaptable Network (CAN) Polyurethanes from Lignin with Editable Shape Memory Properties. *ChemSusChem* 16, e202202071. <https://doi.org/10.1002/cssc.202202071>
- Mauro, C.D., Genua, A., Mija, A., 2020. Building thermally and chemically reversible covalent bonds in vegetable oil based epoxy thermosets. Influence of epoxy–hardener ratio in promoting recyclability. *Mater. Adv.* 1, 1788–1798. <https://doi.org/10.1039/D0MA00370K>
- McBride, M.K., Worrell, B.T., Brown, T., Cox, L.M., Sowan, N., Wang, C., Podgorski, M., Martinez, A.M., Bowman, C.N., 2019. Enabling Applications of Covalent Adaptable Networks. *Annu. Rev. Chem. Biomol. Eng.* 10, 175–198. <https://doi.org/10.1146/annurev-chembioeng-060718-030217>
- More, A., Elder, T., Pajer, N., Argyropoulos, D.S., Jiang, Z., 2023. Novel and Integrated Process for the Valorization of Kraft Lignin to Produce Lignin-Containing Vitrimers. *ACS Omega* 8, 1097–1108. <https://doi.org/10.1021/acsomega.2c06445>
- Moreno, A., Morsali, M., Sipponen, M.H., 2021. Catalyst-Free Synthesis of Lignin Vitrimers with Tunable Mechanical Properties: Circular Polymers and Recoverable Adhesives. *ACS Appl. Mater. Interfaces* 13, 57952–57961. <https://doi.org/10.1021/acsami.1c17412>
- Nicolaÿ, R., Kamada, J., Van Wassen, A., Matyjaszewski, K., 2010. Responsive Gels Based on a Dynamic Covalent Trithiocarbonate Cross-Linker. *Macromolecules* 43, 4355–4361. <https://doi.org/10.1021/ma100378r>
- Ocando, C., Ecochard, Y., Decostanzi, M., Caillol, S., Avérous, L., 2020. Dynamic network based on eugenol-derived epoxy as promising sustainable thermoset materials. *Eur. Polym. J.* 135, 109860. <https://doi.org/10.1016/j.eurpolymj.2020.109860>
- Palmese, G.R., McCullough, R.L., 1992. Effect of epoxy–amine stoichiometry on cured resin material properties. *J. Appl. Polym. Sci.* 46, 1863–1873. <https://doi.org/10.1002/app.1992.070461018>

- Pascault, J.-P., Williams, R.J.J., 2018. Chapter 1 - Overview of thermosets: Present and future, in: Guo, Q. (Ed.), *Thermosets (Second Edition)*. Elsevier, pp. 3–34. <https://doi.org/10.1016/B978-0-08-101021-1.00001-0>
- Patel, V.R., Dumancas, G.G., Viswanath, L.C.K., Maples, R., Subong, B.J.J., 2016. Castor Oil: Properties, Uses, and Optimization of Processing Parameters in Commercial Production. *Lipid Insights* 9, LPI.S40233. <https://doi.org/10.4137/LPI.S40233>
- Pelckmans, M., Renders, T., Vyver, S.V. de, Sels, B.F., 2017. Bio-based amines through sustainable heterogeneous catalysis. *Green Chem.* 19, 5303–5331. <https://doi.org/10.1039/C7GC02299A>
- Peters, E.N., 2017. 1 - Engineering Thermoplastics—Materials, Properties, Trends, in: Kutz, M. (Ed.), *Applied Plastics Engineering Handbook (Second Edition)*, *Plastics Design Library*. William Andrew Publishing, pp. 3–26. <https://doi.org/10.1016/B978-0-323-39040-8.00001-8>
- Pire, M., Norvez, S., Iliopoulos, I., Le Rossignol, B., Leibler, L., 2010. Epoxidized natural rubber/dicarboxylic acid self-vulcanized blends. *Polymer* 51, 5903–5909. <https://doi.org/10.1016/j.polymer.2010.10.023>
- Post, W., Susa, A., Blaauw, R., Molenveld, K., Knoop, R.J.I., 2020. A Review on the Potential and Limitations of Recyclable Thermosets for Structural Applications. *Polym. Rev.* 60, 359–388. <https://doi.org/10.1080/15583724.2019.1673406>
- Pu, Y., Cao, S., Ragauskas, A.J., 2011. Application of quantitative ³¹P NMR in biomass lignin and biofuel precursors characterization. *Energy Environ. Sci.* 4, 3154–3166. <https://doi.org/10.1039/C1EE01201K>
- Scheutz, G.M., Lessard, J.J., Sims, M.B., Sumerlin, B.S., 2019. Adaptable Crosslinks in Polymeric Materials: Resolving the Intersection of Thermoplastics and Thermosets. *J. Am. Chem. Soc.* 141, 16181–16196. <https://doi.org/10.1021/jacs.9b07922>
- Smit, A.T., Verges, M., Schulze, P., van Zomeren, A., Lorenz, H., 2022. Laboratory- to Pilot-Scale Fractionation of Lignocellulosic Biomass Using an Acetone Organosolv Process. *ACS Sustain. Chem. Eng.* 10, 10503–10513. <https://doi.org/10.1021/acssuschemeng.2c01425>
- Spiesschaert, Y., Danneels, J., Van Herck, N., Guerre, M., Acke, G., Winne, J., Du Prez, F., 2021. Polyaddition Synthesis Using Alkyne Esters for the Design of Vinylogous Urethane Vitrimers. *Macromolecules* 54, 7931–7942. <https://doi.org/10.1021/acs.macromol.1c01049>
- Spiesschaert, Y., Guerre, M., De Baere, I., Van Paepegem, W., Winne, J.M., Du Prez, F.E., 2020. Dynamic Curing Agents for Amine-Hardened Epoxy Vitrimers with Short (Re)processing Times. *Macromolecules* 53, 2485–2495. <https://doi.org/10.1021/acs.macromol.9b02526>
- Tao, Y., Fang, L., Dai, M., Wang, C., Sun, J., Fang, Q., 2020. Sustainable alternative to bisphenol A epoxy resin: high-performance recyclable epoxy vitrimers derived from protocatechuic acid. *Polym. Chem.* 11, 4500–4506. <https://doi.org/10.1039/D0PY00545B>
- Taplan, C., Guerre, M., Winne, J.M., Du Prez, F.E., 2020. Fast processing of highly crosslinked, low-viscosity vitrimers. *Mater. Horiz.* 7, 104–110. <https://doi.org/10.1039/C9MH01062A>
- Tremblay-Parrado, K.-K., Avérous, L., 2020. Renewable Responsive Systems Based on Original Click and Polyurethane Cross-Linked Architectures with Advanced Properties. *ChemSusChem* 13, 238–251. <https://doi.org/10.1002/cssc.201901991>
- Tremblay-Parrado, K.-K., Bordin, C., Nicholls, S., Heinrich, B., Donnio, B., Avérous, L., 2020. Renewable and Responsive Cross-Linked Systems Based on Polyurethane Backbones from Clickable Biobased Bismaleimide Architecture. *Macromolecules* 53, 5869–5880. <https://doi.org/10.1021/acs.macromol.0c01115>
- Tremblay-Parrado, K.-K., García-Astrain, C., Avérous, L., 2021. Click chemistry for the synthesis of biobased polymers and networks derived from vegetable oils. *Green Chem.* 23, 4296–4327. <https://doi.org/10.1039/D1GC00445J>
- Van Lijsebetten, F., De Bruycker, K., Spiesschaert, Y., Winne, J.M., Du Prez, F.E., 2022a. Suppressing Creep and Promoting Fast Reprocessing of Vitrimers with Reversibly Trapped Amines. *Angew. Chem. Int. Ed.* 61, e202113872. <https://doi.org/10.1002/anie.202113872>
- Van Lijsebetten, F., De Bruycker, K., Winne, J.M., Du Prez, F.E., 2022b. Masked Primary Amines for a Controlled Plastic Flow of Vitrimers. *ACS Macro Lett.* 11, 919–924. <https://doi.org/10.1021/acsmacrolett.2c00255>

- Wei, X., Ge, J., Gao, F., Chen, F., Zhang, W., Zhong, J., Lin, C., Shen, L., 2021. Bio-based self-healing coating material derived from renewable castor oil and multifunctional alamine. *Eur. Polym. J.* 160, 110804. <https://doi.org/10.1016/j.eurpolymj.2021.110804>
- Williams, G., Watts, D.C., 1970. Non-symmetrical dielectric relaxation behaviour arising from a simple empirical decay function. *Trans. Faraday Soc.* 66, 80–85. <https://doi.org/10.1039/TF9706600080>
- Winne, J.M., Leibler, L., Prez, F.E.D., 2019. Dynamic covalent chemistry in polymer networks: a mechanistic perspective. *Polym. Chem.* 10, 6091–6108. <https://doi.org/10.1039/C9PY01260E>
- Witzeman, J.S., Nottingham, W.D., 1991. Transacetoacetylation with tert-butyl acetoacetate: synthetic applications. *J. Org. Chem.* 56, 1713–1718. <https://doi.org/10.1021/jo00005a013>
- Xue, B., Tang, R., Xue, D., Guan, Y., Sun, Y., Zhao, W., Tan, J., Li, X., 2021. Sustainable alternative for bisphenol A epoxy resin high-performance and recyclable lignin-based epoxy vitrimers. *Ind. Crops Prod.* 168, 113583. <https://doi.org/10.1016/j.indcrop.2021.113583>
- Zhang, L., Rowan, S.J., 2017. Effect of Sterics and Degree of Cross-Linking on the Mechanical Properties of Dynamic Poly(alkylurea-urethane) Networks. *Macromolecules* 50, 5051–5060. <https://doi.org/10.1021/acs.macromol.7b01016>
- Zhang, S., Liu, T., Hao, C., Wang, L., Han, J., Liu, H., Zhang, J., 2018. Preparation of a lignin-based vitrimer material and its potential use for recoverable adhesives. *Green Chem.* 20, 2995–3000. <https://doi.org/10.1039/C8GC01299G>
- Zhao, W., Feng, Z., Liang, Z., Lv, Y., Xiang, F., Xiong, C., Duan, C., Dai, L., Ni, Y., 2019. Vitrimer-Cellulose Paper Composites: A New Class of Strong, Smart, Green, and Sustainable Materials. *ACS Appl. Mater. Interfaces* 11, 36090–36099. <https://doi.org/10.1021/acsami.9b11991>
- Zheng, Y., Liu, T., He, H., Lv, Z., Xu, J., Ding, D., Dai, L., Huang, Z., Si, C., 2023. Lignin-based epoxy composite vitrimers with light-controlled remoldability. *Adv. Compos. Hybrid Mater.* 6, 53. <https://doi.org/10.1007/s42114-023-00633-4>

7. APPENDICES (SI)

Table S2-4. Detailed values used for density calculations of each material.

Material (Designations)	Diameter (cm)	Thickness (cm)	V (cm ³)	m (g)	ρ (g cm ⁻³)
VU-30-300	0.8	0.106	0.2135	0.1045	0.4894
VU-40-300	0.8	0.113	0.2272	0.1075	0.4732
VU-50-300	0.8	0.120	0.2409	0.1149	0.4770
VU-40-400	0.8	0.112	0.2252	0.1095	0.4863
VU-40-150	0.8	0.107	0.2143	0.1026	0.4787

CHAPITRE 2

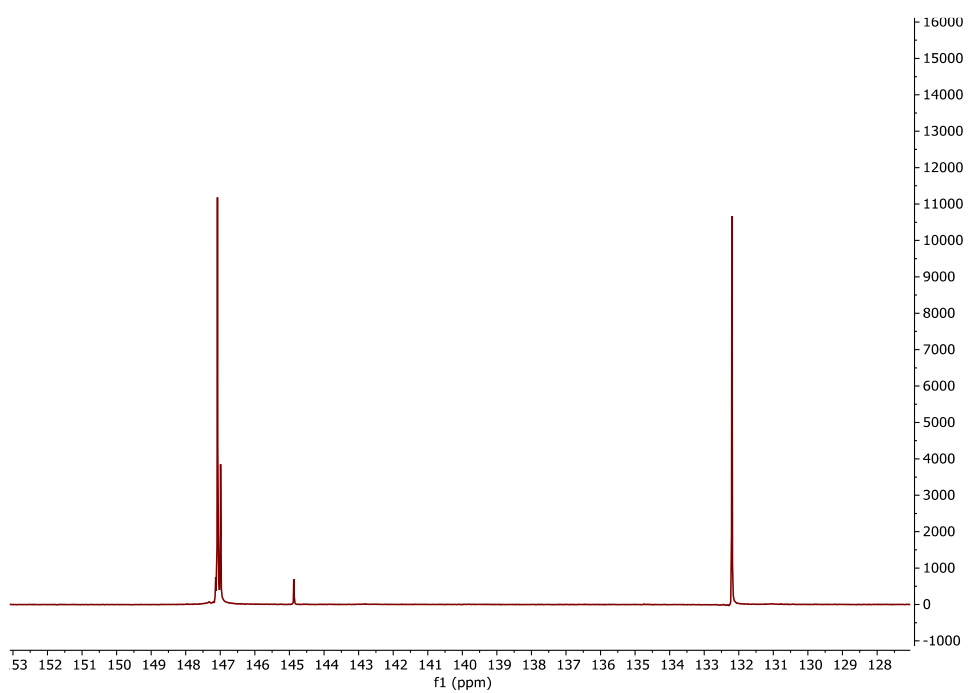


Figure S2-10. ^{31}P NMR of OL-30-300.

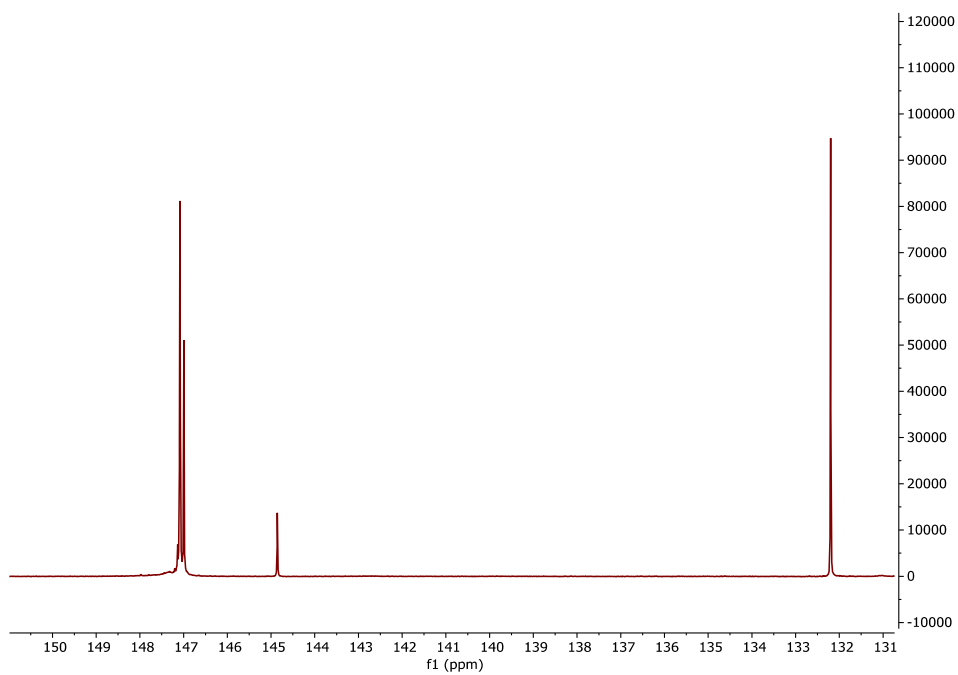


Figure S2-11. ^{31}P NMR of OL-40-300.:

CHAPITRE 2

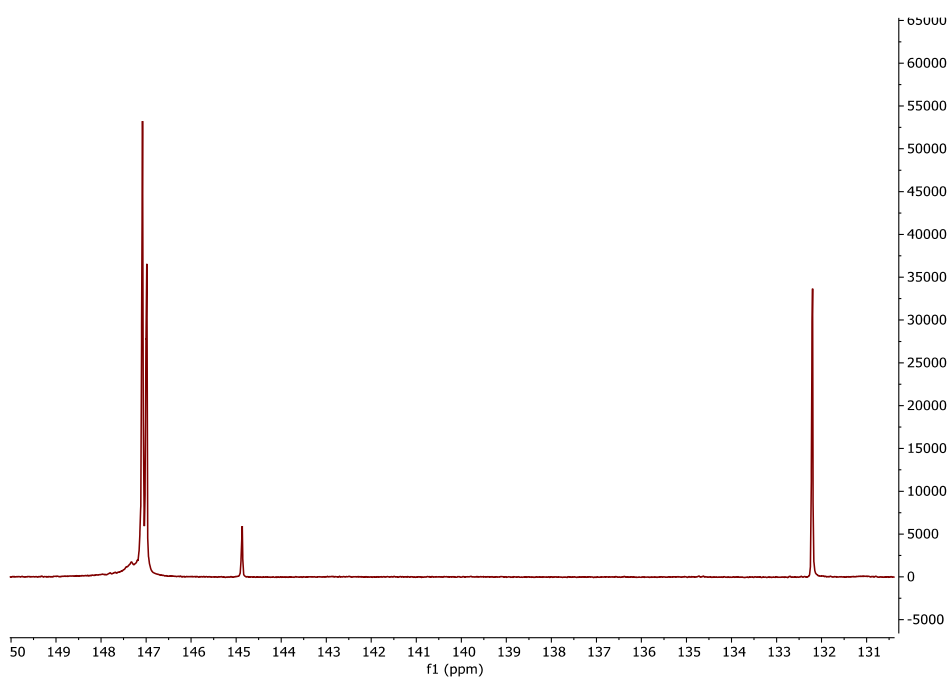


Figure S2-12. ^{31}P NMR of OL-50-300.

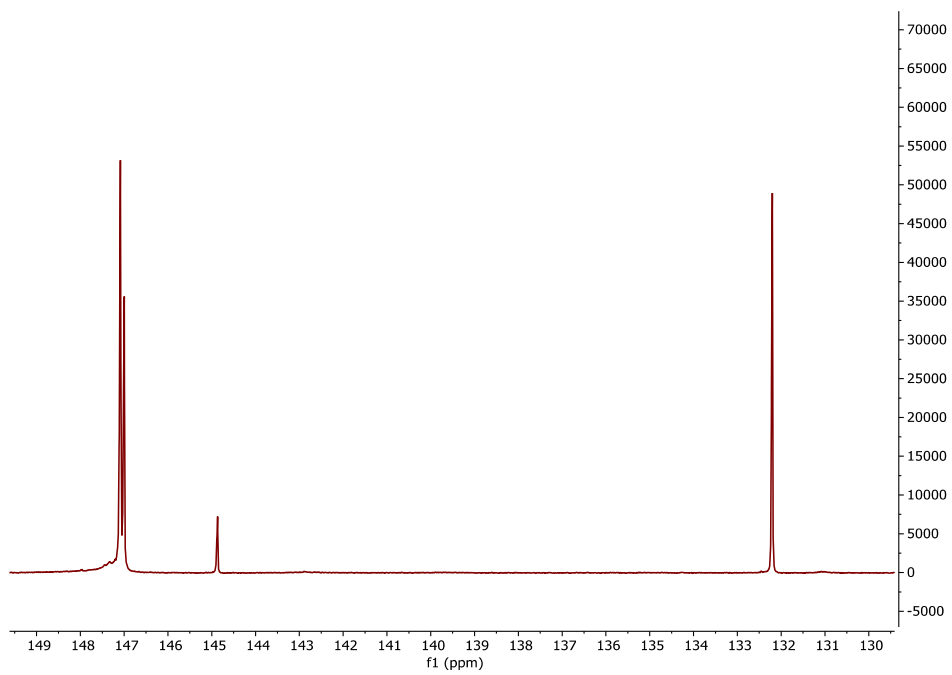


Figure S2-13. ^{31}P NMR of OL-40-400.

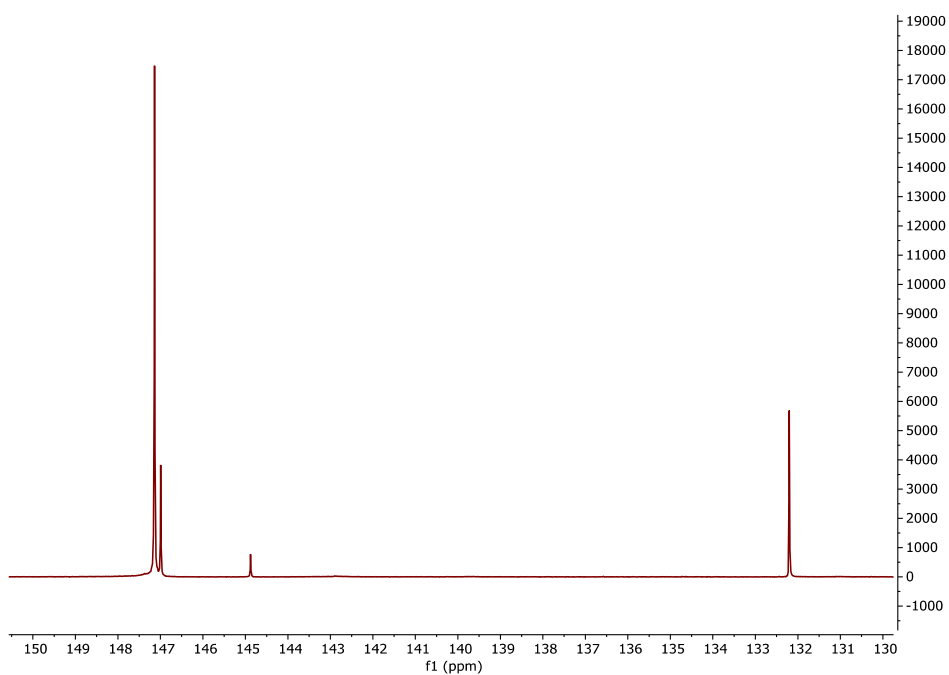


Figure S2-14. ^{31}P NMR of OL-40-150.

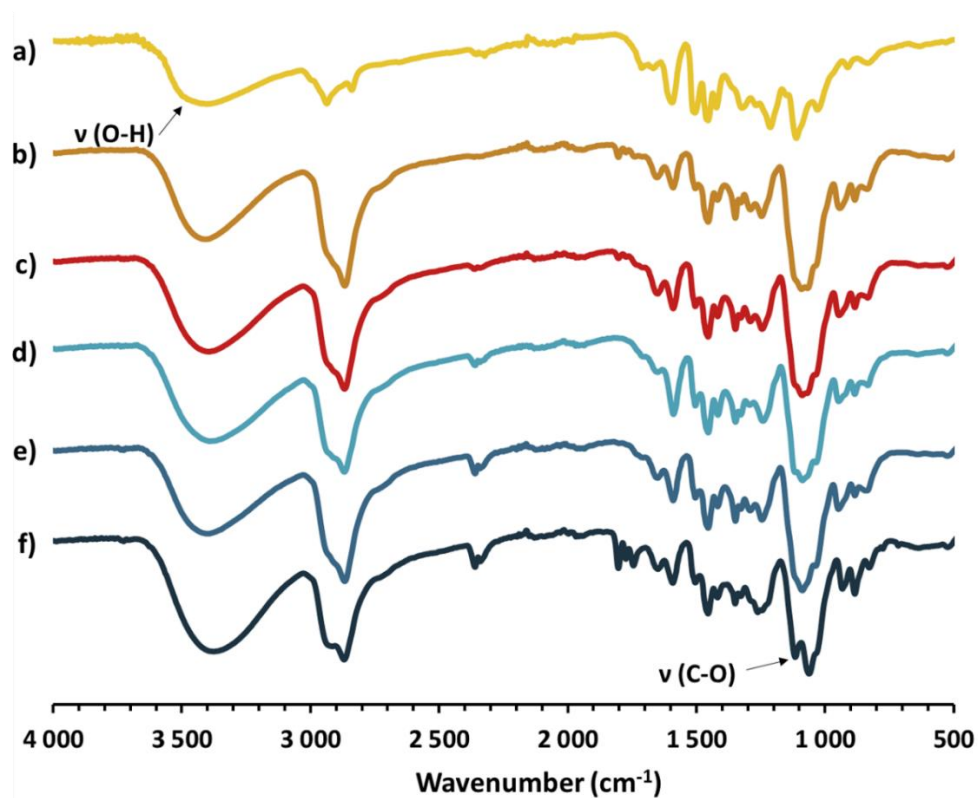


Figure S2-15. Stacked FT-IR spectra of the different polyols, with a) OSL, b) OL-30-300, c) OL-40-300, d) OL-50-300, e) OL-40-400, and f) OL-40-150

CHAPITRE 2

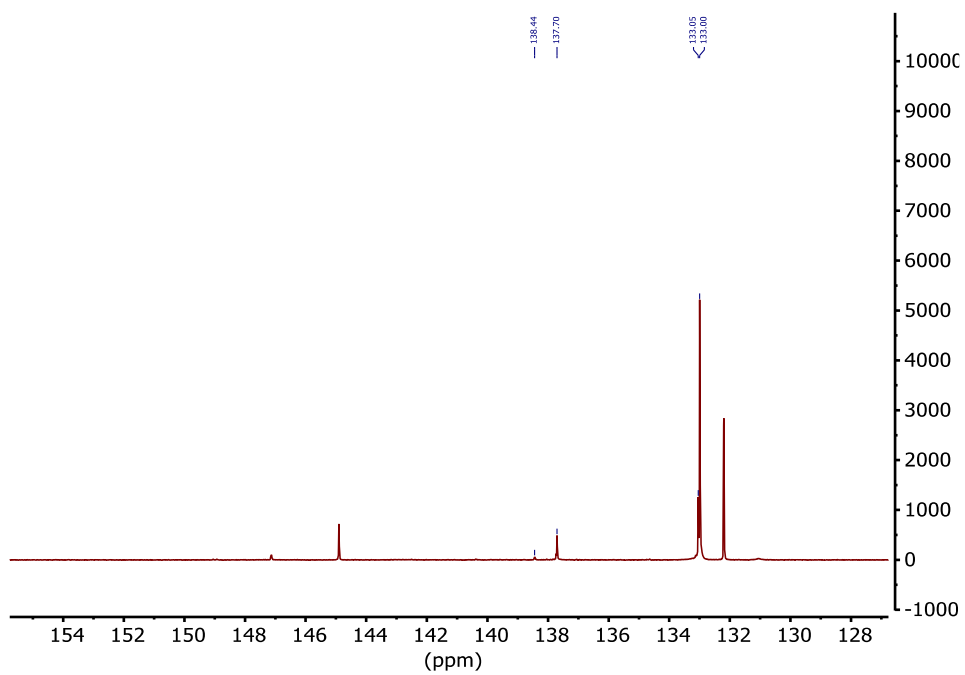


Figure S2-16. ^{31}P NMR of AC-30-300.

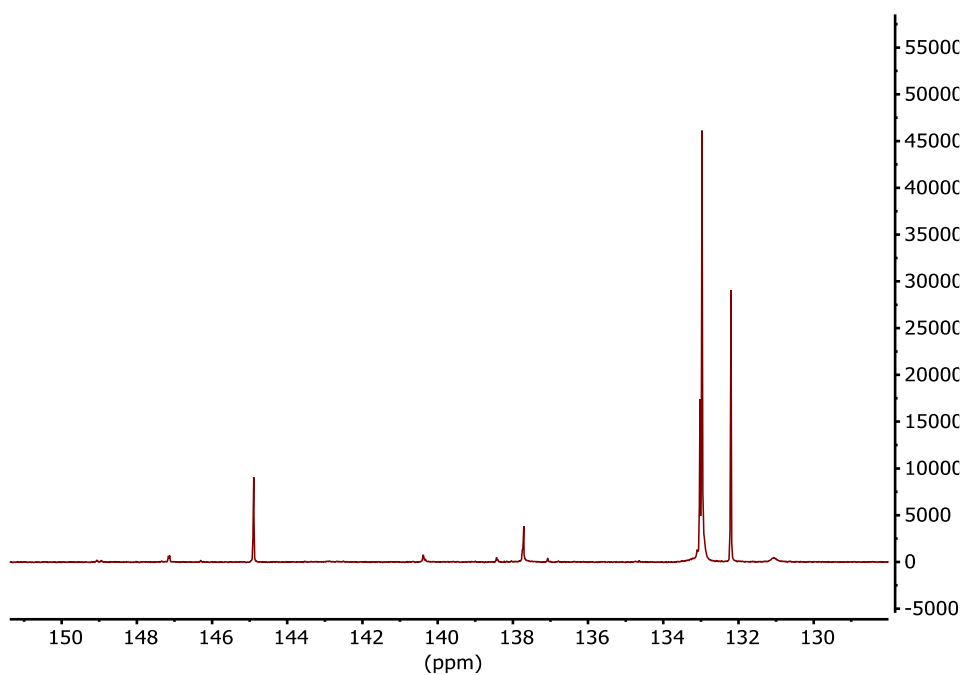


Figure S2-17. ^{31}P NMR of AC-40-300.

CHAPITRE 2

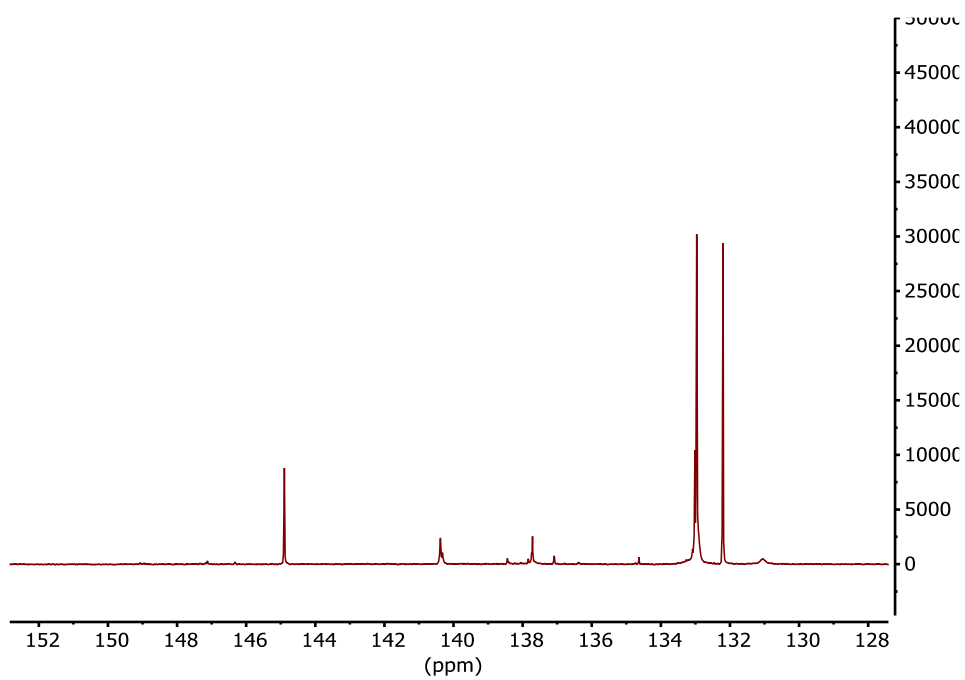


Figure S2-18. ^{31}P NMR of AC-50-300.

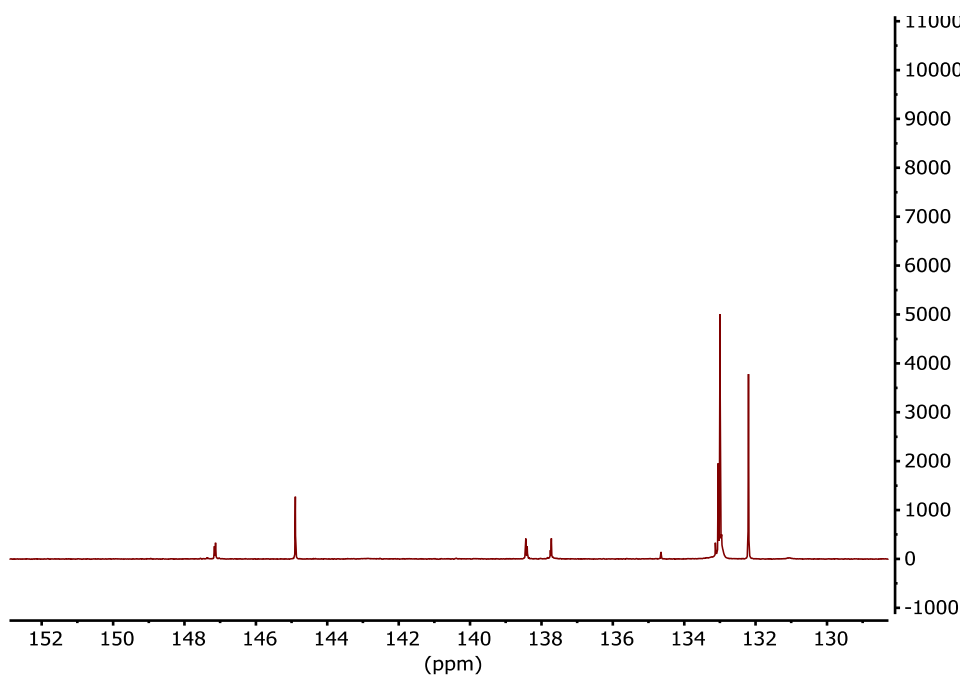


Figure S2-19. ^{31}P NMR of AC-40-400.

CHAPITRE 2

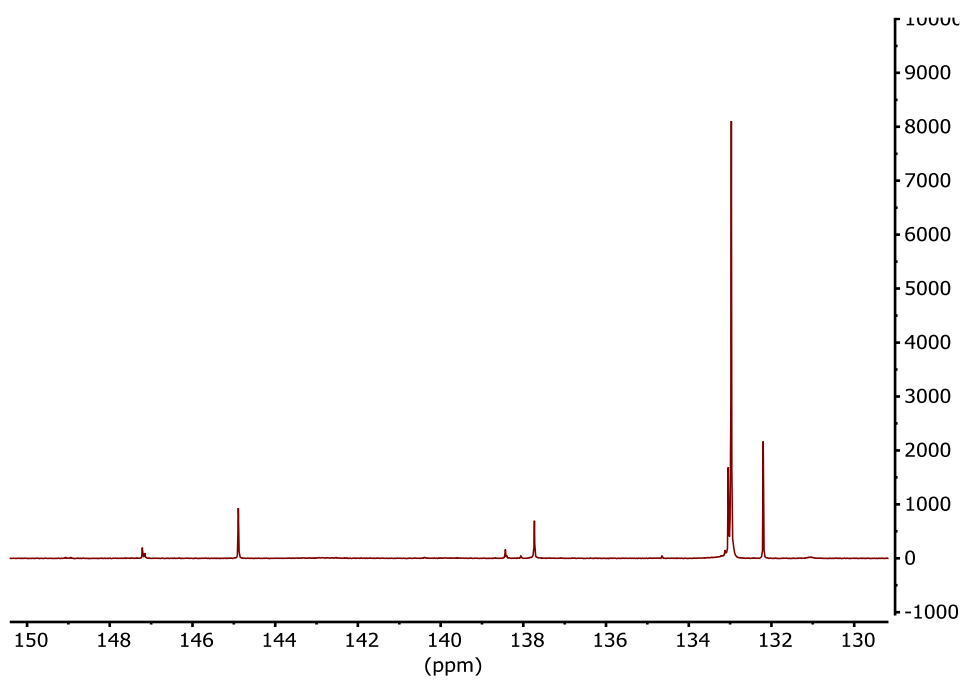


Figure S2-20. ^{31}P NMR of AC-40-150.

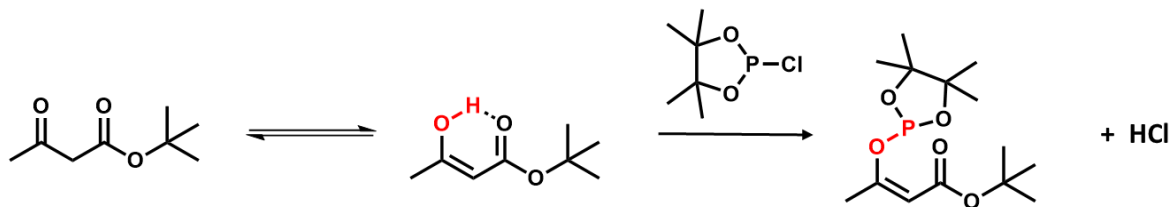


Figure S2-21. Potential reaction of TBAA with Cl-TMDP.

CHAPITRE 2

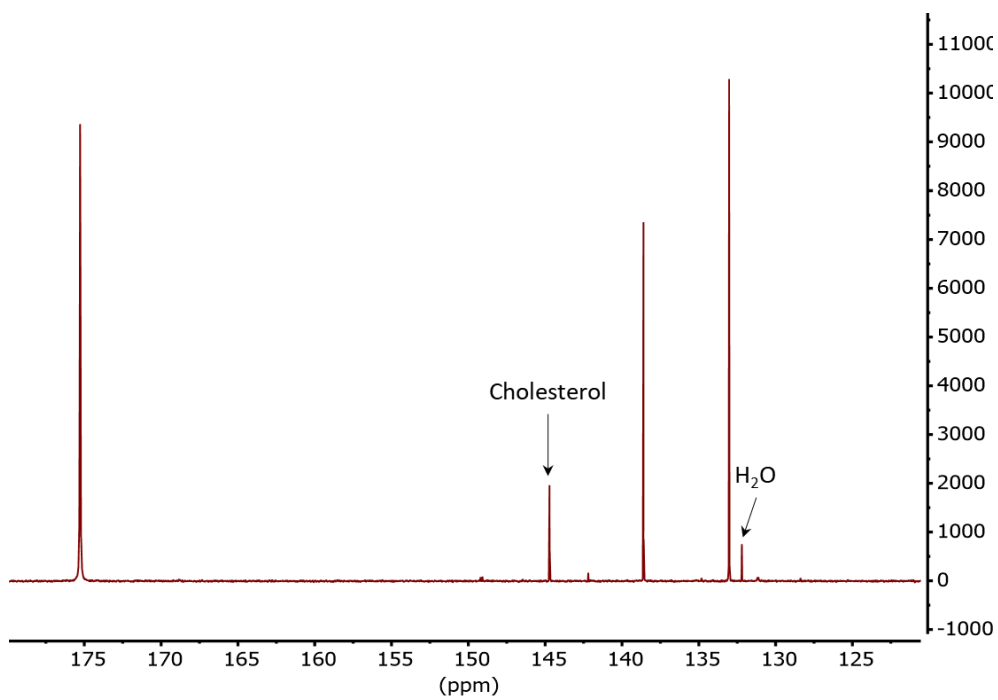


Figure S2-22. ^{31}P NMR of TBAA.

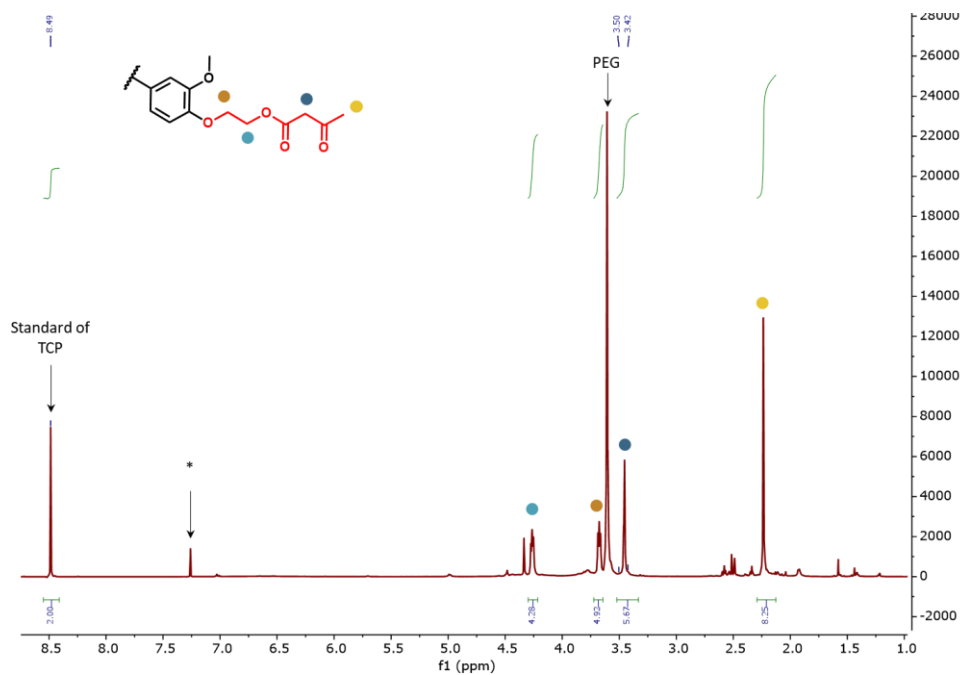


Figure S2-23. ^1H NMR of AC-30-300 in CDCl_3 .

CHAPITRE 2

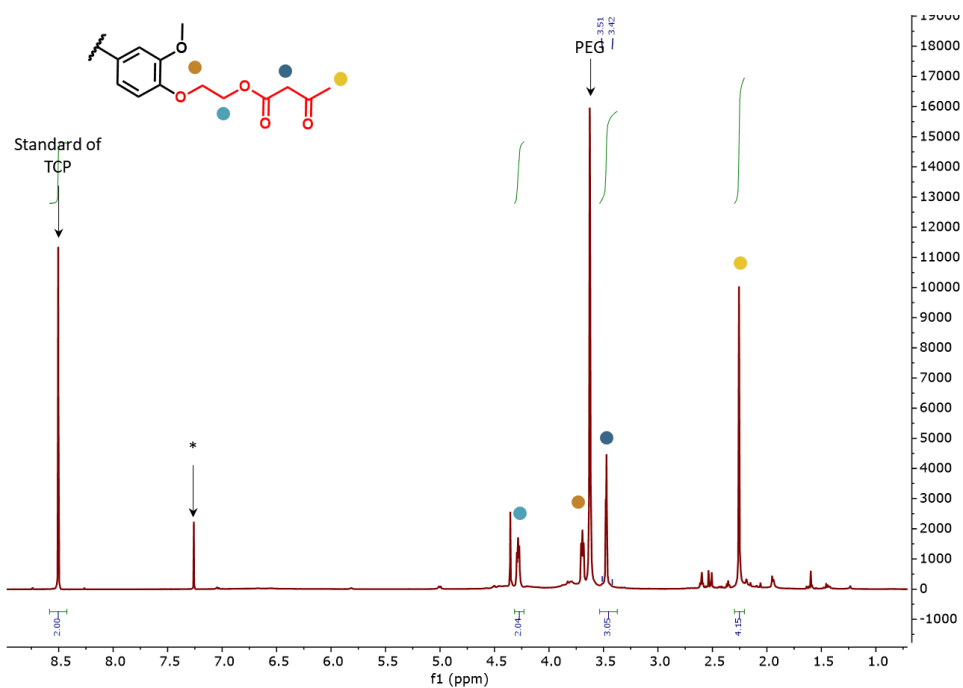


Figure S2-24. ^1H NMR of AC-40-300 in CDCl_3 .

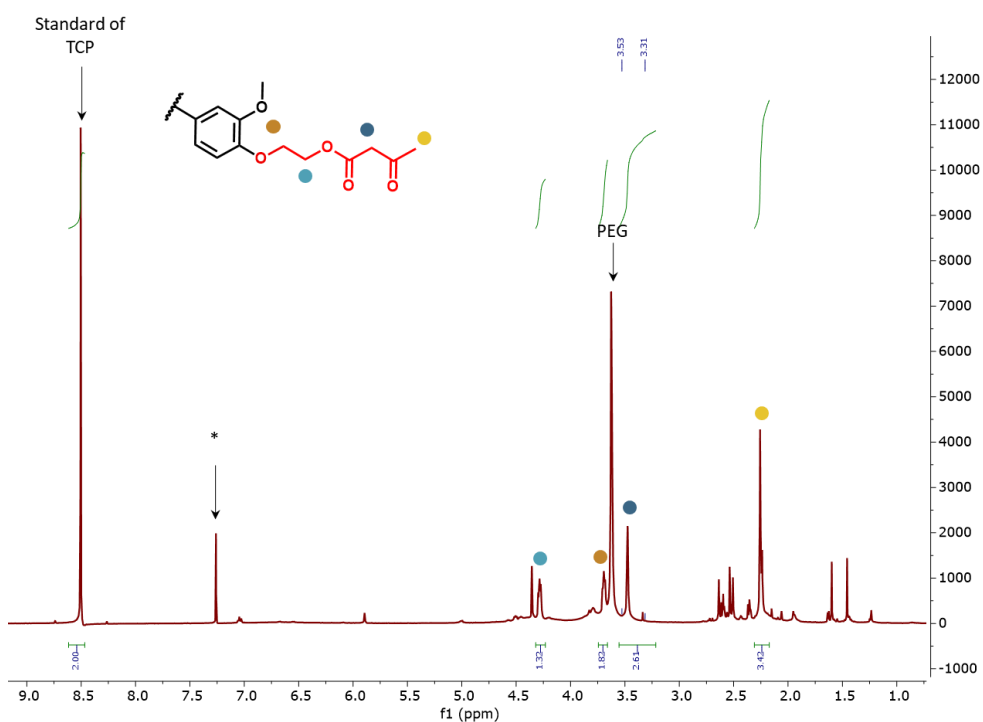


Figure S2-25. ^1H NMR of AC-50-300 in CDCl_3 .

CHAPITRE 2

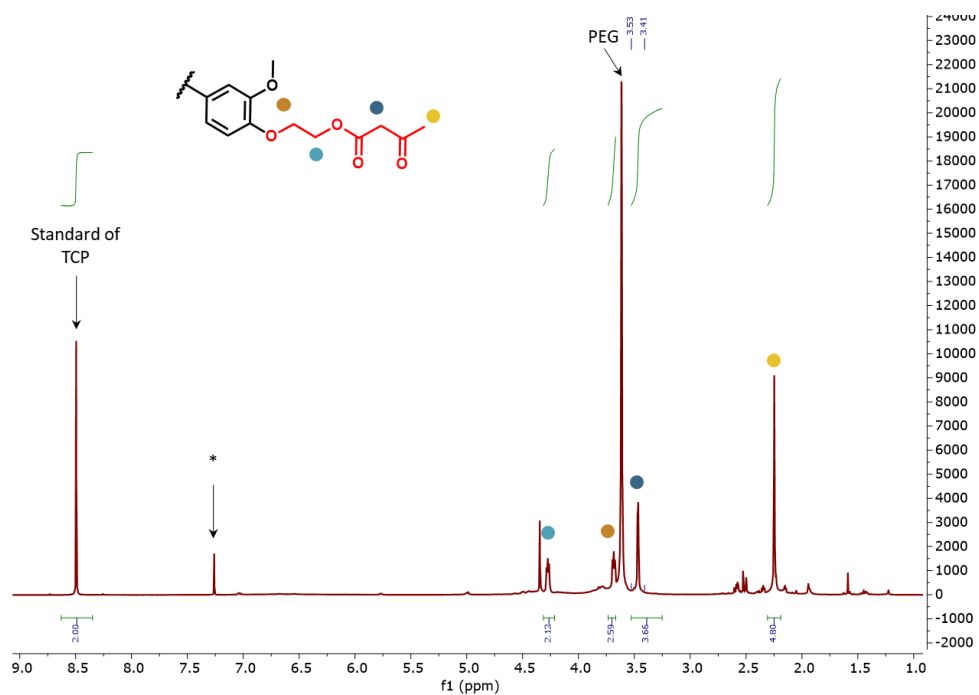


Figure S2-26. ^1H NMR of AC-40-400 in CDCl_3 .

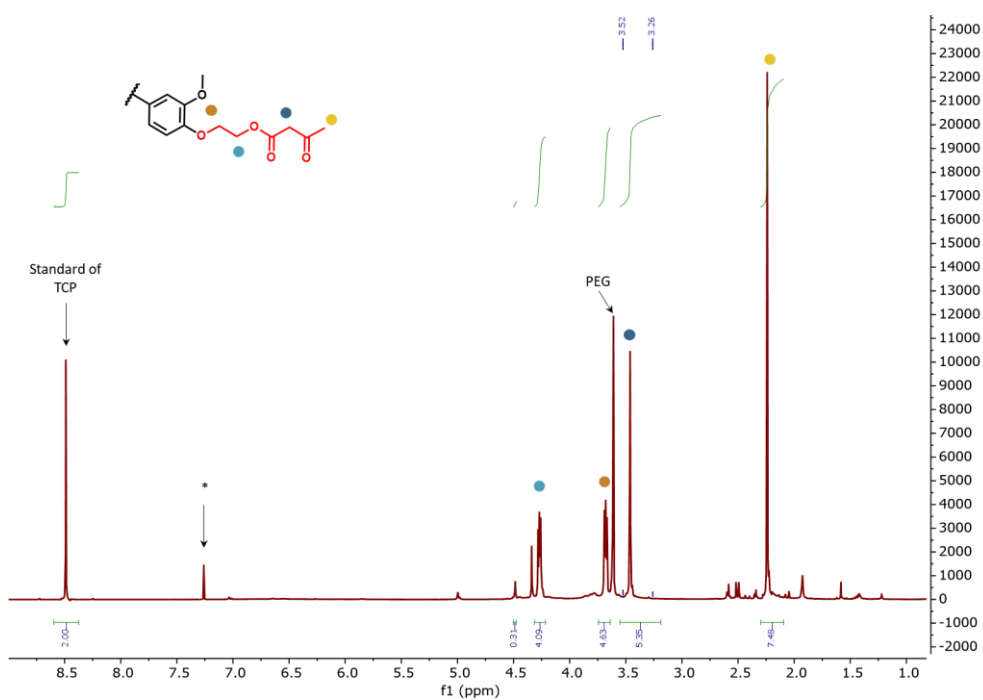


Figure S2-27. ^1H NMR of AC-40-150 in CDCl_3 .

CHAPITRE 2

Table S2-5. Main physico-chemical properties of polyacetoacetates.

Polyacetoacetate (Designations)	Lignin content (%)	n _{acetoacetate} (mmol g ⁻¹)	M _n (g mol ⁻¹)	Dispersity	Viscosity (Pa s)
AC-30-300	17	3.27	710	2.4	1.59 ± 0.08
AC-40-300	21	3.29	710	2.6	11.7 ± 0.2
AC-50-300	24	3.38	700	2.4	153 ± 5
AC-40-400	22	3.37	760	2.4	13 ± 2
AC-40-150	19	3.43	560	2.9	1.53 ± 0.01

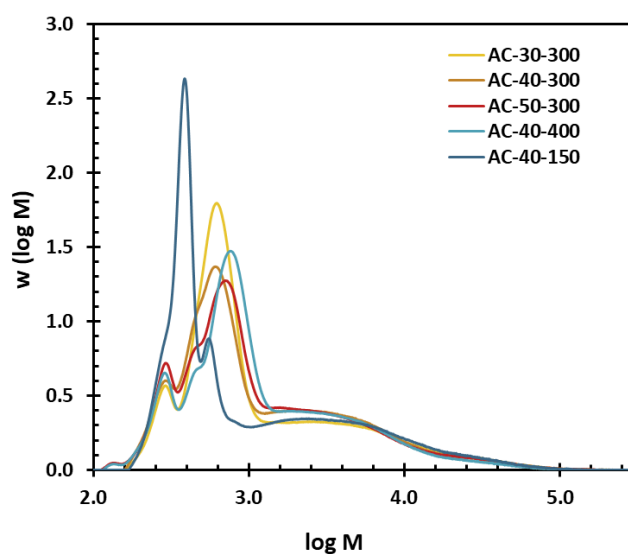


Figure S2-28. SEC curves of polyacetoacetates (RID detection, THF as eluent, calibration with PS standards).

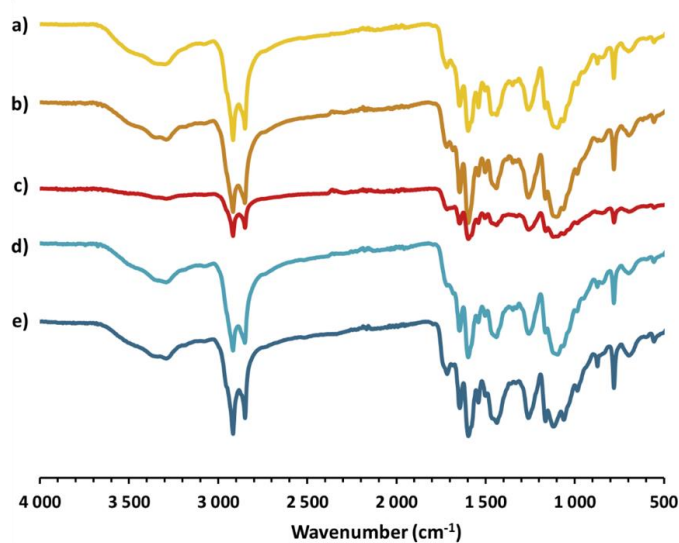


Figure S2-29. Stacked FT-IR spectra of a) VU-30-300, b) VU-40-300, c) VU-50-300, d) VU-40-400, and e) VU-40-150.

CHAPITRE 2

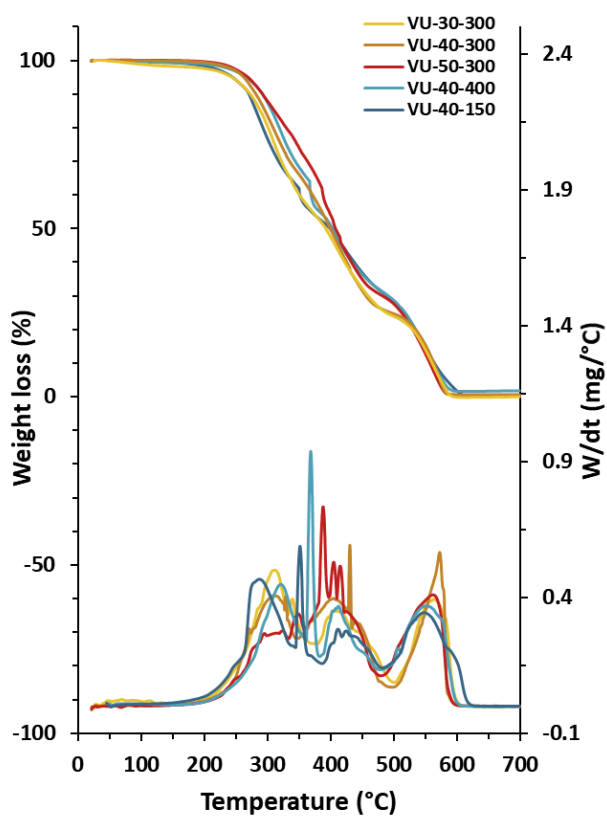


Figure S2-30. TGA curves of the different final materials.

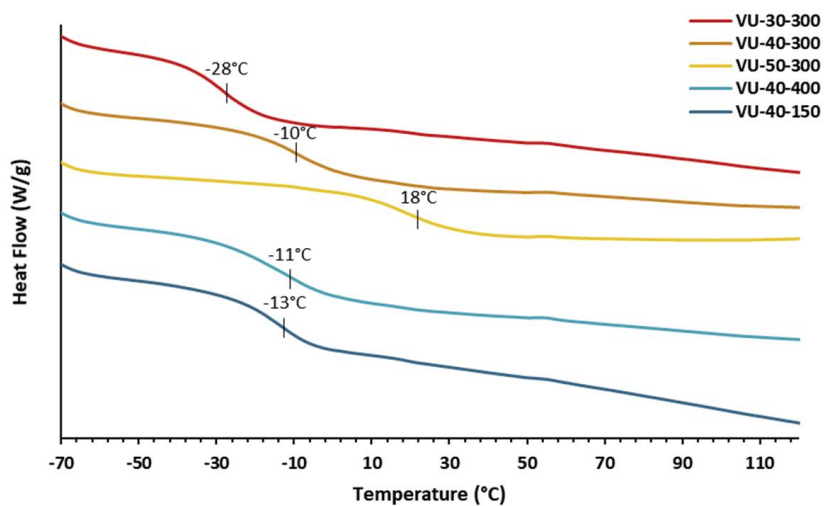


Figure S2-31. DSC curves of the series of materials.

CHAPITRE 2

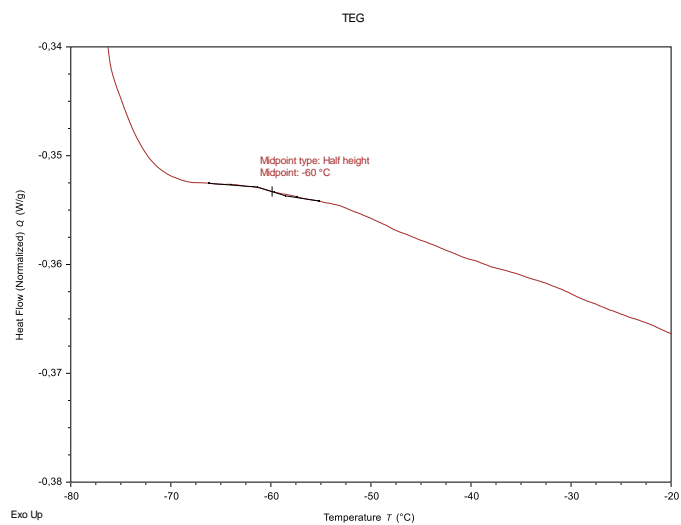


Figure S2-32. DSC curve of TEG.

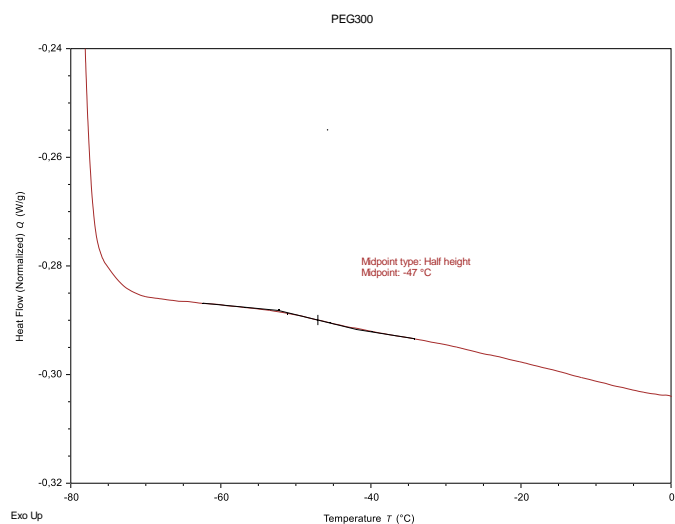


Figure S2-33. DSC curve of PEG₃₀₀.

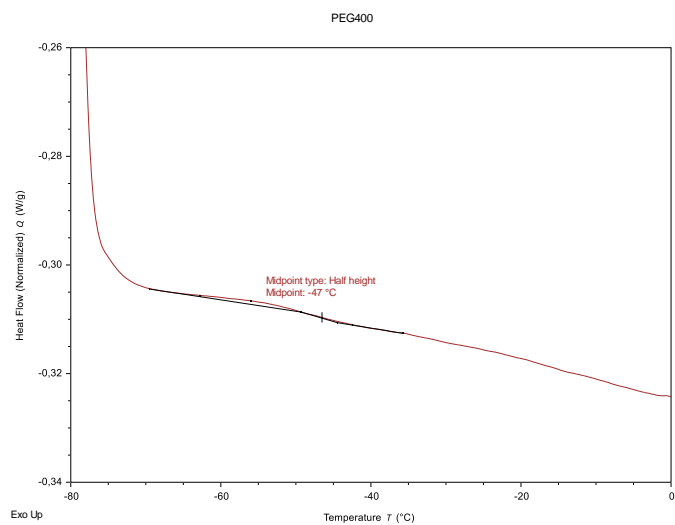


Figure S2-34. DSC curve of PEG₄₀₀.

CHAPITRE 2

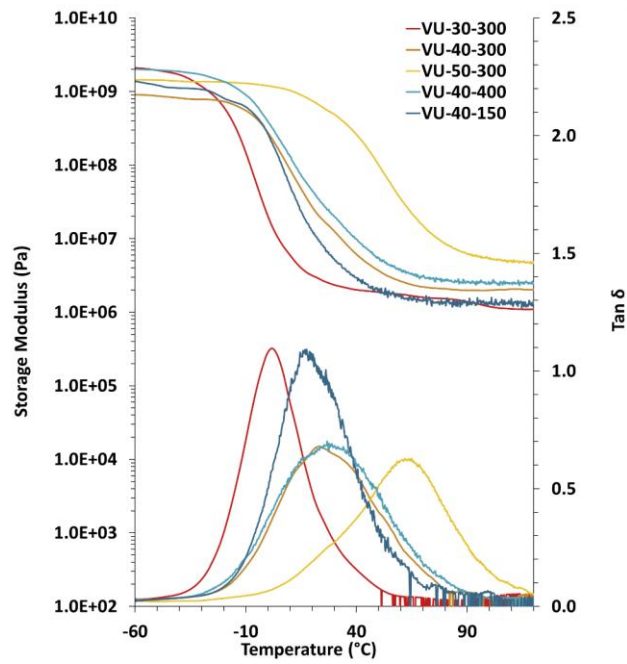


Figure S2-35. DMA curves of the different final VU.

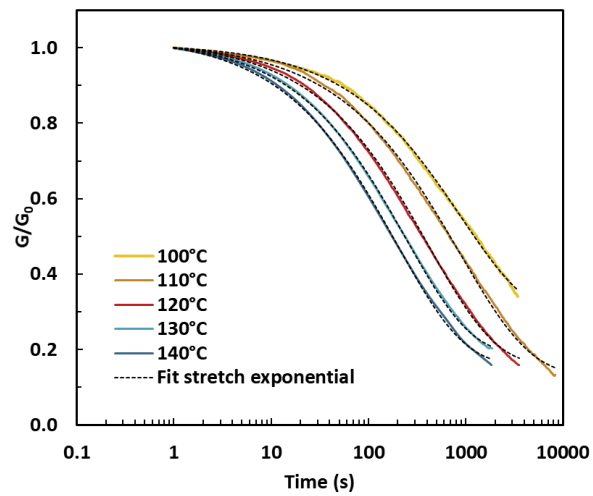


Figure S2-36. Stress relaxation curves of VU-30-300.

CHAPITRE 2

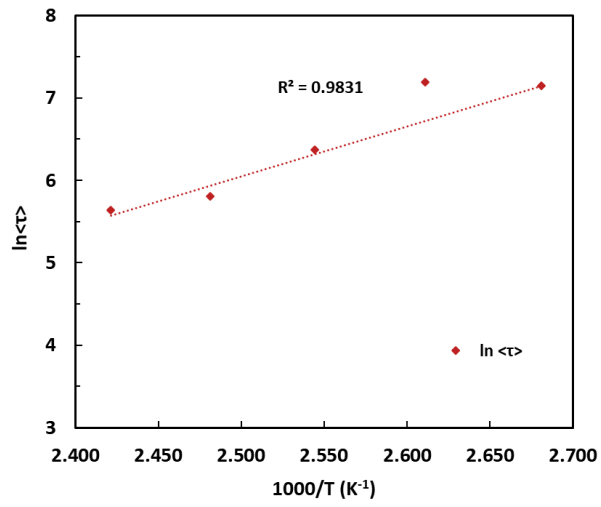


Figure S2-37. Arrhenius relationship of VU-30-300.

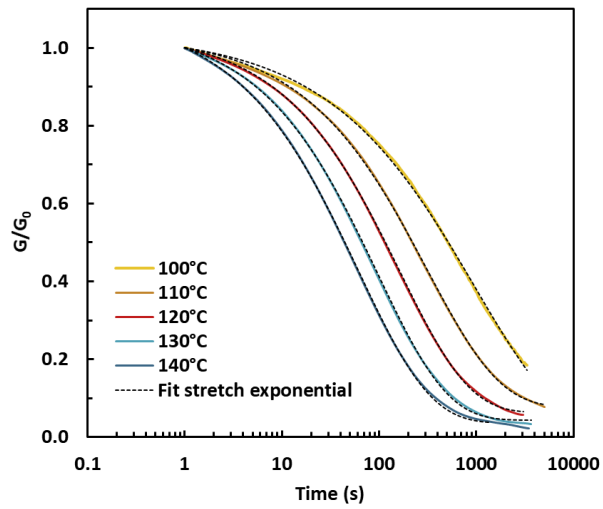


Figure S2-38. Stress relaxation curves of VU-50-300.

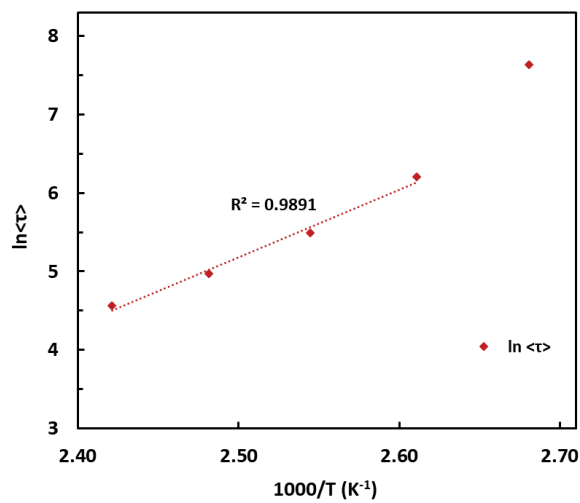


Figure S2-39. Arrhenius relationship of VU-50-300.

CHAPITRE 2

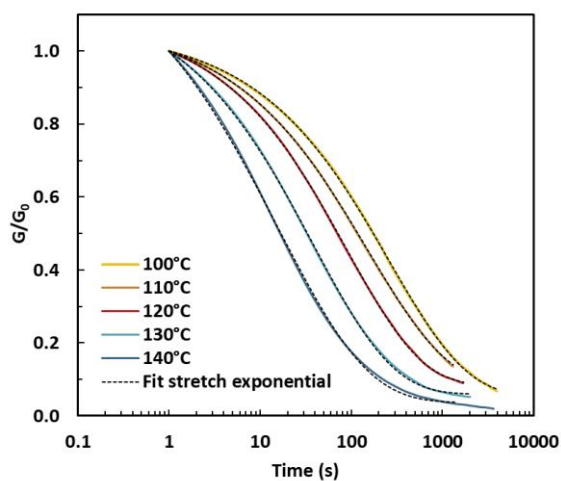


Figure S2-40. Stress relaxation curves of VU-40-400.

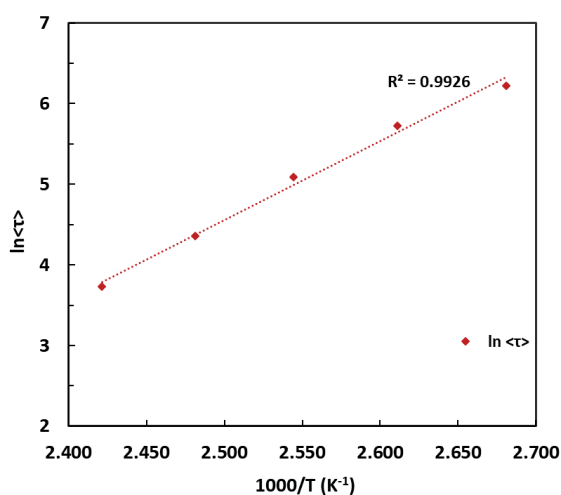


Figure S2-41. Arrhenius relationship of VU-40-400.

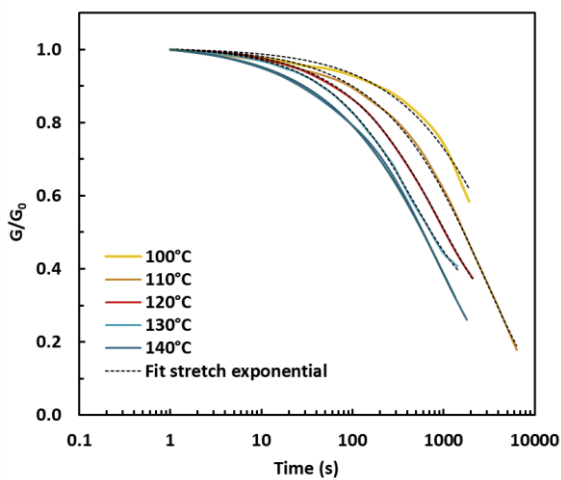


Figure S2-42. Stress-relaxation curves of VU-40-150.

CHAPITRE 2

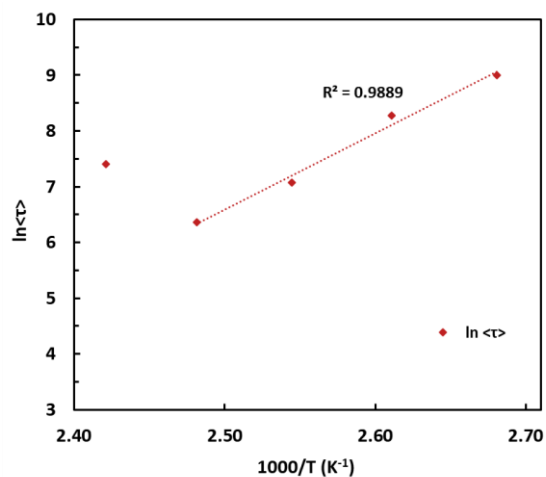


Figure S2-43. Arrhenius relationship of VU-40-150.

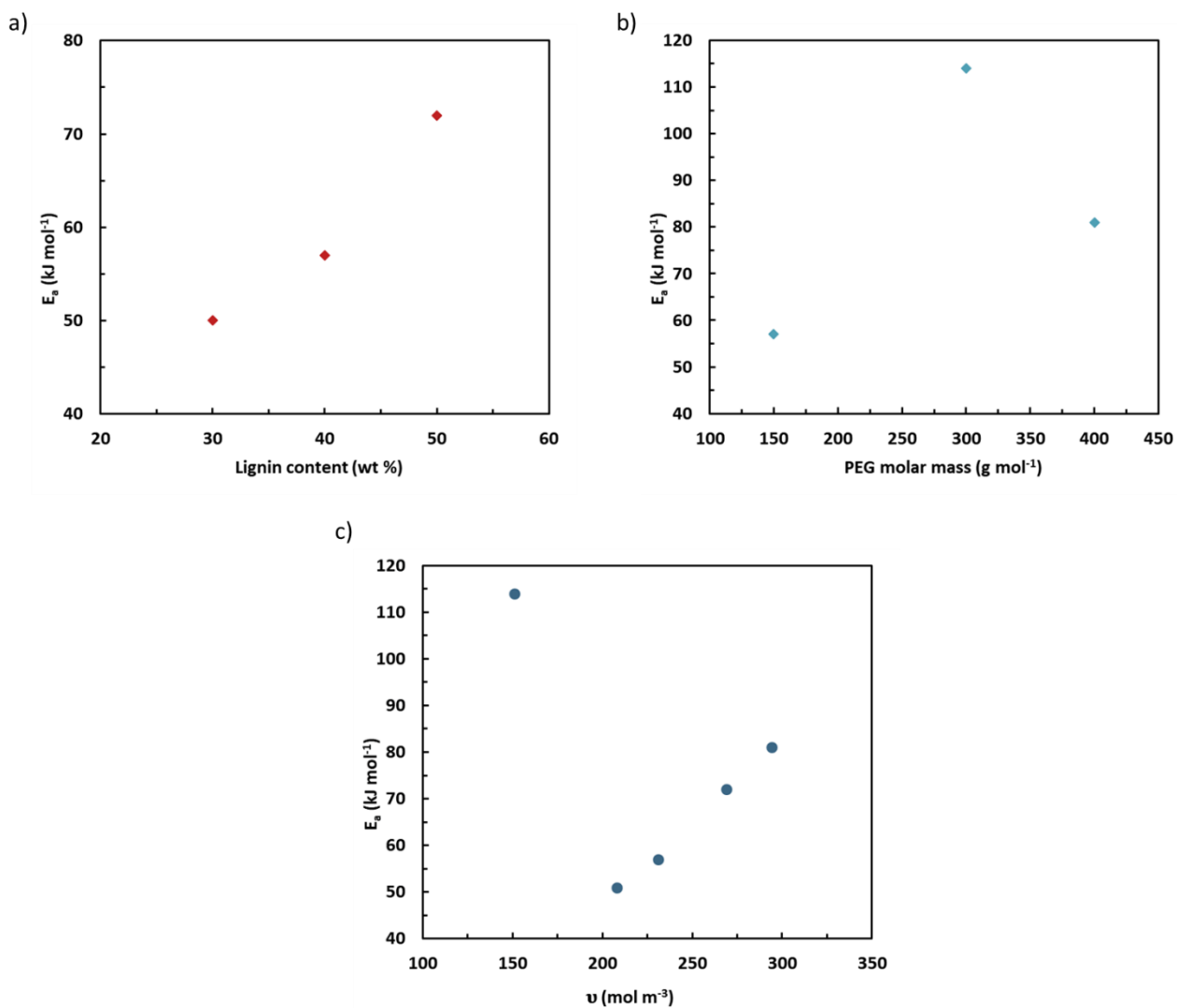


Figure S2-44. Plot of E_a as a function of a) lignin content, b) PEG molar mass, and c) crosslinking density.

Theoretical topology freezing temperatures (T_v) determination

Maxwell equation was used to first calculate the relaxation time τ^* in s:

$$\eta = \frac{1}{3} G' \times \tau^*$$

Where η is the viscosity in Pa s, G' the storage modulus obtained by DMA in Pa. τ^* was calculated for a conventional viscosity of 10^{12} Pa s.

Arrhenius equations were used to calculate T_v for each vitrimer by extrapolation.

$$\ln \tau^* = \ln \tau_0 \times \frac{E_a}{RT}$$

And thus the corresponding T_v is determined by the following Equation:

$$\frac{1000}{T} = \frac{\ln \tau^* - B}{A}$$

With A et B, the parameters obtained from Arrhenius relationship of experimental data.

Table S2-6. Parameters used for T_v calculation of each vitrimers.

VU (Designations)	G' (Pa)	τ^* (s)	A	B	T_v (°C)
VU-30-300	1.73E+06	1.73E+06	6.074	-9.140	-15
VU-40-300	2.05E+06	1.46E+06	6.866	-12.632	-17
VU-50-300	2.67E+06	1.12E+06	8.638	-16.414	12
VU-40-400	2.64E+06	1.14E+06	9.778	-19.887	16
VU-40-150	1.32E+06	2.27E+06	13.698	-27.653	51

Table S2-7. Swelling ratio and gel fraction data.

VU (Designations)	GF _{acetone} (%)	SR _{acetone} (%)	GF _{Water} (%)	SR _{Water} (%)
VU-30-300	60	188	82	152
VU-40-300	76	159	94	144
VU-50-300	93	146	100	112
VU-40-400	73	165	88	173
VU-40-150	57	195	99	113

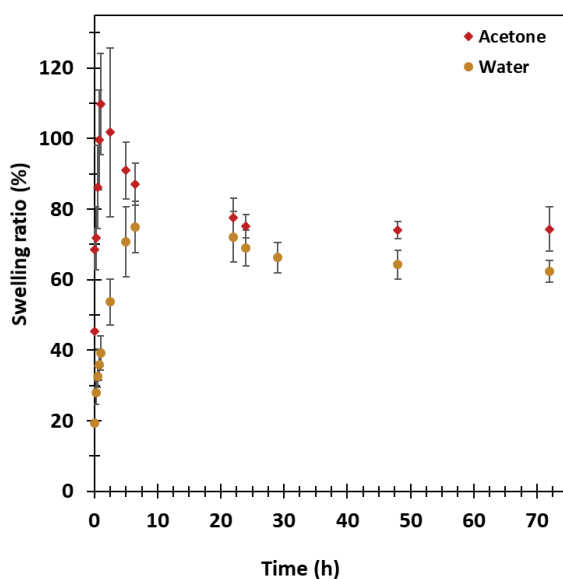


Figure S2-45. Swelling kinetics study of VU-40-400 in acetone and water.

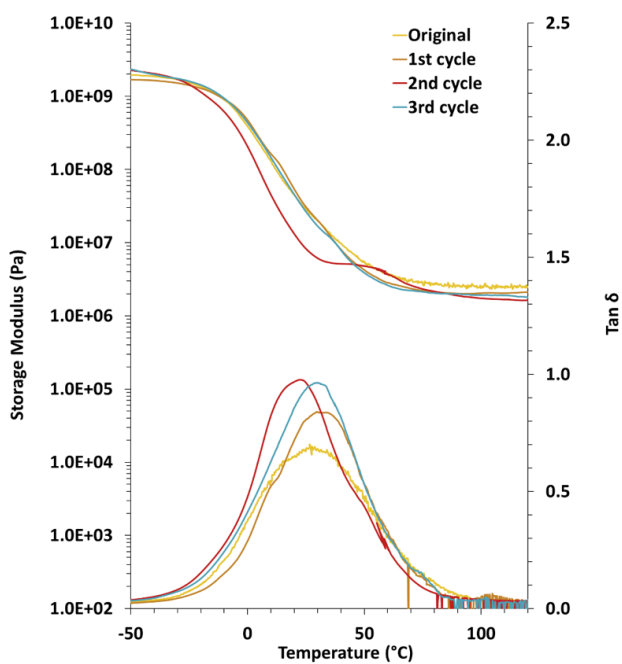


Figure S2-46. DMA curves of unrecycled and recycled VU-40-400.

Table S2-8. DMA measurements on original and recycled VU-40-400.

VU	T_{α} [°C]	ν [mol m ³]	M_c [g mol ⁻¹]
Original	27	294	1660
1 st cycle	29	224	2170
2 nd cycle	23	234	2080
3 rd cycle	29	220	2210

CHAPITRE 2

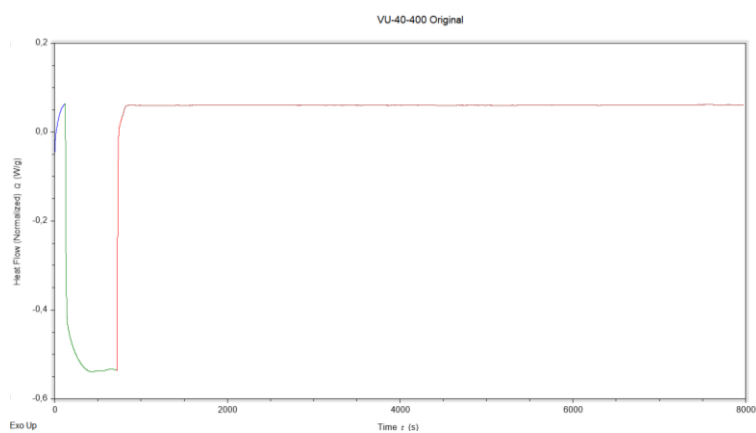


Figure S2-47. OIT curve of original VU-40-400.

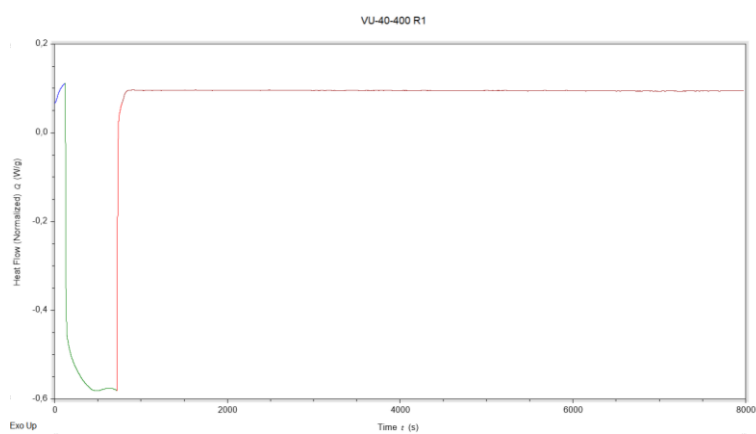


Figure S2-48. OIT curve of VU-40-400 after 1st recycling.

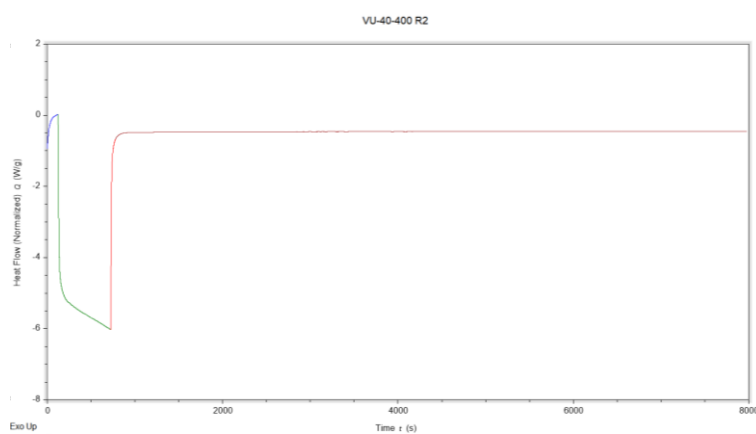


Figure S2-49. OIT curve of VU-40-400 after 2nd recycling.

CHAPITRE 2

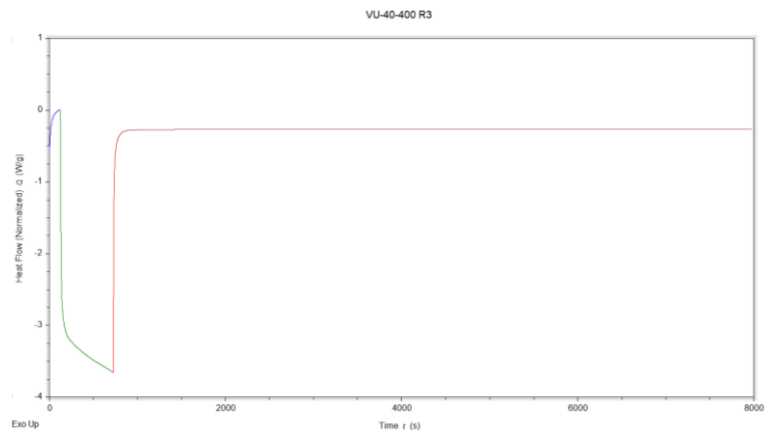


Figure S2-50. OIT curve of VU-40-400 after 3rd recycling.

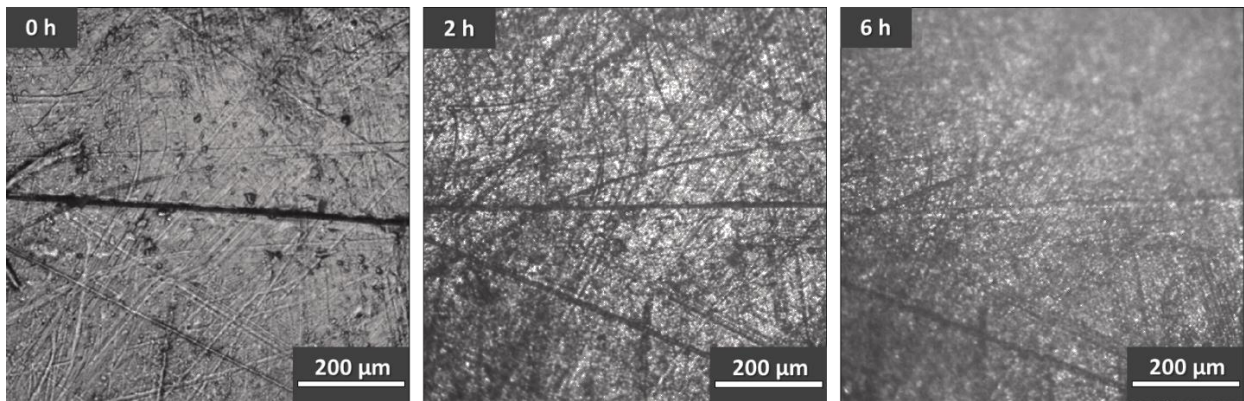


Figure S2-51. Images of self-healed samples after 0, 2 and 6 h at 140 °C.

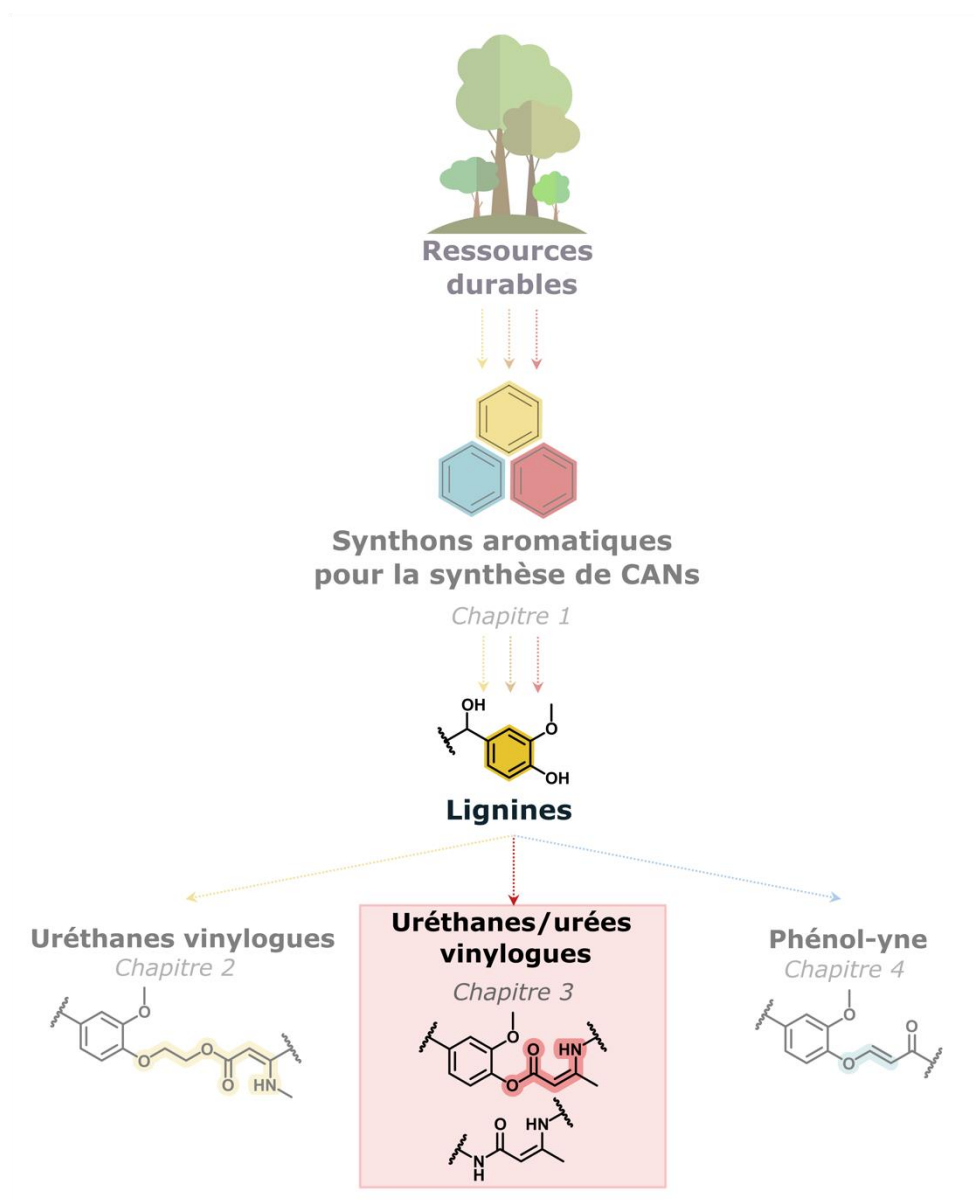
CONCLUSION DU CHAPITRE 2

Ce premier chapitre expérimental a mis en évidence le grand intérêt de la lignine (ici organosolv) comme synthon aromatique renouvelable pour la synthèse de polymères uréthane vinylogues durables dont les propriétés peuvent être modulées en fonction de la teneur en lignine et de la longueur de chaîne de polyéthylène glycol.

La première partie de ce chapitre a présenté une nouvelle voie de synthèse pour la préparation de polyacétoacétates liquides réactifs et hautement fonctionnalisés à partir de lignine. Cette voie chimique en deux étapes et sans solvant ni composés toxiques, en accord avec de nombreux principes de chimie verte, a montré être aisément réalisable sur des mélanges de plusieurs dizaines de grammes, offrant des possibilités de montée en échelle. Ces macromonomères acétoacétates ont ensuite pu être utilisés pour la préparation d'une gamme de matériaux contenant jusqu'à 20% massiques de lignine. De larges gammes de propriétés mécaniques et rhéologiques ont été obtenues. Une augmentation de la teneur en lignine permet d'augmenter la stabilité thermique et la rigidité des matériaux, dont le comportement mécanique est semblable à des thermodurcissables traditionnels. En revanche, une augmentation de la longueur de la chaîne de polyéthylène glycol permet d'obtenir des matériaux présentant des caractéristiques d'élastomères.

Le comportement de vitrimère de ces systèmes a été clairement étudié et analysé. Une relaxation de contrainte minimale de quelques dizaines de secondes à 130 °C, permettant un recyclage physique rapide par moulage par compression tout en conservant de bonnes propriétés mécaniques après des cycles de remise en forme, a clairement été établie. Alternativement, la possibilité de recyclage chimique des vitrimères par dépolymérisation avec une monoamine courte a été démontrée, offrant de nouvelles opportunités de (re)valorisation en fin de vie. Enfin, les réarrangements de liaisons au sein des matériaux rendent leur cicatrization (auto-réparation) en température possible, renforçant ainsi la pertinence de ces matériaux dynamiques biosourcés pour des applications industrielle à long terme.

CHAPITRE 3. VITRIMERES URETHANE VINYLOGUES DURABLES A PARTIR DE LIGNINE : ANALYSE DES RELATIONS « CONCEPTION-STRUCTURE-PROPRIETES »



INTRODUCTION DU CHAPITRE 3

Le chapitre expérimental précédent a montré l'excellent choix de la lignine pour synthétiser de nouveaux polymères uréthanes vinylogues dynamiques, aromatiques, renouvelables et durable (dans le sens long terme et de développement durable), avec un fort potentiel de recyclabilité. En revanche, la multiplicité des fonctions portées par la lignine nécessite plusieurs étapes de modifications chimiques pour obtenir un macromonomère acétoacétate fortement fonctionnalisé. Dans une approche de chimie verte, et pour faciliter un éventuel futur changement d'échelle et d'expansion industrielle des CANs aromatiques et biosourcés, la diminution du nombre d'étapes de synthèse est un point clé.

Dans ce second chapitre expérimental, il est donc question de développer une nouvelle stratégie de design par synthèse, pour modifier les hydroxyles aliphatiques et phénoliques de la lignine en une seule étape, pour le développement de nouveaux polymères uréthanes vinylogues aromatiques renouvelables. Une optimisation des conditions de synthèse est d'abord proposée pour obtenir une haute conversion des fonctions réactives de la lignine organosolv. La condensation des groupements acétoacétates aromatiques de la lignine modifiée par des amines a été étudiée, dans le but de favoriser la formation de liaisons uréthane vinylogues au détriment des urée vinylogues. Fort de cela, des matériaux contenant jusqu'à 50% massique de lignine ont pu être synthétisés à partir de la lignine acétoacétylée et de différentes diamines dérivées de polypropylène glycol et d'un copolymère à blocs polypropylène-b-polyéthylène glycol. L'influence de la structure et de la masse molaire des diamines utilisées sur les morphologies et propriétés des CANs a été analysée. Les propriétés rhéologiques ont été étudiées de manière à évaluer la capacité des liaisons dynamiques à se réarranger au sein des réseaux tridimensionnels. Enfin, la possibilité de (re)valorisation des matériaux en fin de vie a été examinée via leur recyclage physique sur plusieurs cycles consécutifs. Une nouvelle approche de recyclage chimique par dépolymérisation en milieu acide a fait l'objet d'une preuve de concept comme une alternative non-toxique aux dépolymérisations classiques à base d'amines courtes et toxiques.

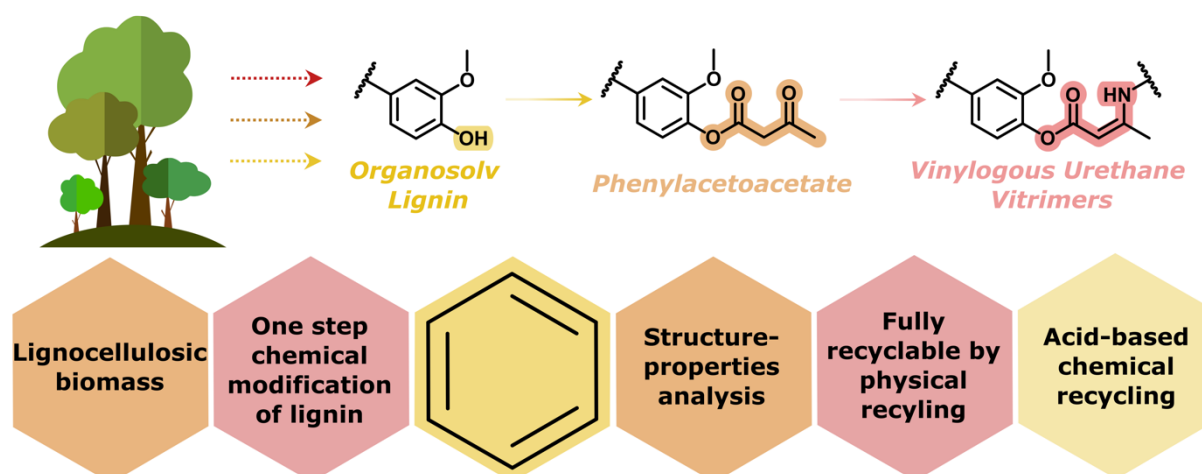
SUSTAINABLE LIGNIN-BASED VINYLOGOUS URETHANE VITRIMERS: “STRUCTURAL DESIGN-PROPERTIES” RELASHIONSHIP ANALYSIS

Lisa Sougrati ^a, Antoine Duval ^{a, b, *}, Luc Avérous ^{a, *}

^a BioTeam/ICPEES-ECPM, UMR CNRS 7515, Université de Strasbourg, 25 rue Becquerel, 67087 Strasbourg, Cedex 2, France

^b Soprema, 15 rue de Saint Nazaire, 67100, Strasbourg, France

*Corresponding authors.



1. ABSTRACT

Lignins are the most abundant source of renewable aromatics on Earth. They are macromonomers (polyphenols) with high functionality to develop performing aromatic materials. However, a major drawback of ensuing polymers is their lack of efficient recyclability. In the global context of environmental crisis, the need for the development of sustainable polymers with controlled end-of-life is urgent. In this respect and to tackle this challenge, the design of lignin-based vitrimers is an elegant strategy to overcome the recycling limits of thermosets without compromising properties. In this work we report the synthesis and evaluation of lignin-based vinylogous urethane vitrimers. A novel one-step route for the chemical modification of organosolv lignin into an acetoacetate macromonomer is proposed, enabling full conversion of aliphatic and phenolic moieties. The reaction of phenylacetoacetate groups with amines generating the dual formation of vinylogous urethane and vinylogous urea moieties was examined in a model study. Subsequently, a series of materials was prepared by condensation of the acetoacetylated lignin with polyetheramines of different lengths and chemical structures. The materials were chemically, morphologically, rheologically and mechanically characterized. Structure-property relationships were established. The structure of the diamine was found to strongly influence the morphological and mechanical properties of the vitrimers. Relaxation times from 156 and 1319 s at 200 °C and E_a from 32.9 to 80.0 kJ mol⁻¹ were obtained, allowing swift networks rearrangements. The physical recycling potential was demonstrated through three cycles of thermo-mechanical recycling and chemical recycling was also investigated.

2. INTRODUCTION

Lignocellulosic biomass represents the largest source of renewable aromatic structures. Among the diverse compounds derived from this feedstock, lignin has emerged as an attractive source of phenols for the synthesis of sustainable aromatic polymers (Laurichesse and Avérous, 2014). This polyphenol has an amorphous and complex structure which highly depends on its botanical origin and extraction process (Tribot et al., 2019). The main extraction technics are sulfite, producing lignosulfonates, Kraft, soda and organosolv. This polyfunctional oligomer offers numerous possibilities for chemical modifications owing to its high aliphatic and phenolic hydroxyl content, as well as small amount of carboxylic acids. Due to its high functionality, lignin is widely used for the design of a large range of thermosets, including polyesters, polyurethanes, epoxy and phenolic resins (Upton and Kasko, 2016; Lawoko and Samec, 2023). Its aromaticity provides materials with attractive properties such as thermal resistance and stiffness, due to the phenol groups and π - π interactions between aromatic rings. One shortcoming of these high-performance materials, inherent to lignin high functionality, is the limited recyclability of crosslinked networks. Due to their inability to melt they are unsuitable for thermoplastics recycling techniques.

To overcome thermosets recycling limitations without compromising on properties, covalent adaptable networks (CANs) were introduced as a novel category of polymer combining the advantages of thermosets and thermoplastics (Bowman and Kloxin, 2012; Kloxin et al., 2010). By incorporating dynamic covalent bonds within the tridimensional network, the material can undergo macroscopic flow in response to stimuli (e.g. temperature, pH, light). CANs are generally categorized by their bond exchange mechanism. Dissociative CANs rely on the initial bond dissociation prior to the formation of a new one, leading to a viscosity decrease and in some cases to depolymerization. Associative CANs are based on the formation of a new bond prior to the breaking of the initial linkage, maintaining a constant crosslinking density within the network. This category on CANs is also known as vitrimers (Montarnal et al., 2011; Capelot et al., 2012). Due to the wide range of dynamic bonds available, polyolefins, polyesters, polyurethanes, and polyimines with cutting-edge properties including recyclability, self-healing, or shape memory are developed (Breuillac et al., 2019; Delavarde et al., 2024; McBride et al., 2019; Zhao et al., 2022a).

In the frame of a circular bioeconomy approach, CANs recyclability at end of life can be combined with the use of biobased building blocks. Numerous studies have highlighted the potential of biobased aliphatic, cycloaliphatic, and aromatic compounds (Lucherelli et al., 2022; Zhao et al., 2022b). In this respect, aromatic structures such as vanillin and lignin have demonstrated their attractiveness for the synthesis of sustainable materials using a cradle-to-cradle approach (Tiz et al., 2023). The potential of lignin-based vitrimers has not ceased to attract attention in recent years. Following the pioneering work of Zhang *et al.* on the design of polyester vitrimers (Zhang et al., 2018), many chemical strategies were considered for the development of repairable coatings, recoverable adhesives or fire resistant materials based on transesterification (Adjaoud et al., 2023; Du et al., 2022; Hao et al., 2019). Subsequently, dynamic polyurethane (X. Ma et al., 2023a, 2023b), polyacetal (Moreno et al., 2021; Yang et al., 2023), disulfide (Liu et al., 2020), and polyimine networks were developed from lignin (Gao et al., 2020). Diels-Alder dissociative CANs were also reported from Kraft and soda lignins (Duval et al., 2015; Buono et al., 2017; Thys et al., 2021, 2023a, 2023b).

More particularly and recently, lignin-based vinylogous urethane (VU) vitrimers were reported with distinct synthetic strategies (Sougrati et al., 2023; Liu et al., 2024). VUs are obtained by the condensation of acetoacetate and amine. Unlike many reversible bonds, VUs do not require the use of hazardous compounds nor catalyst to generate fast macroscopic flow at moderate temperatures (above 100 °C) (Denissen et al., 2015, 2017). These features make VU-based materials compatible with most green chemistry principles and energy-efficient to produce and recycle, which are key parameters in the design of sustainable materials. Our group recently developed a two-step pathway to prepare reactive lignin-based liquid polyacetoacetates (Sougrati et al., 2023). Mixtures of lignin/polyethylene glycol (PEG) were oxyalkylated into low viscosity aliphatic polyols using ethylene carbonate and further acetoacetylated with *tert*-butyl acetoacetate (TBAA). Another approach reported was based on the direct modification of kraft lignin hydroxyls with TBAA leading to the full conversion of aliphatic groups but partially grafted phenols (Liu et al., 2024).

In this work, we report the preparation of high lignin content (from 20 to 50 wt%) VU vitrimers. A one-step catalyst-free and easily scalable strategy was developed to achieve the full conversion of both aliphatic and phenolic hydroxyls of an organosolv lignin (OSL) into acetoacetate groups by employing 2,2,6-trimethyl-4H-1,3-dioxin-4-one (TMDO) (Figure 3-1a). The reaction of phenylacetoacetate groups with amines enabling the dual formation of vinylogous urethane and vinylogous urea (VU_N) moieties was examined in a model study by reacting acetoacetylated lignin with benzylamine, in the aim of shifting the reaction towards the formation of the VU product over the VU_N product. A series of vitrimers was synthesized from the condensation of the modified lignin with polyetheramines with chain length between 400 and 2000 g mol⁻¹ (Figure 3-1b). The materials chemical structures and morphologies were examined, and their rheological and mechanical behaviors were characterized. The physical recycling potential was demonstrated through several cycles of thermo-mechanical recycling and subsequent characterizations. Finally, chemical recycling was also investigated via acid-catalyzed hydrolysis as an alternative recycling route.

3. EXPERIMENTAL SECTION

3.1. Materials

OSL was isolated at pilot scale from industrial size beech wood using the aqueous acetone Fabiola™ process (TNO, Petten, Netherland). It was precipitated from the pulping liquor using the LigniSep technology of a continuous falling film precipitator. Detailed characterization of this lignin has been formerly described as P-BEC-3 (Smit et al., 2022). OSL is a low number-average molar mass lignin (M_n below 1400 g mol⁻¹) with an aliphatic hydroxyl content of 1.74 mmol g⁻¹ and phenolic hydroxyl content of 2.89 mmol g⁻¹. OSL was dried overnight at 50 °C before utilization. ¹H NMR is available in Figure S7-1 in Appendices (SI). Poly(propylene glycol) bis(2-aminopropyl ether) with weight-average molar masses 400 and 2000 g mol⁻¹ (J₄₀₀ and J₂₀₀₀) were kindly supplied by Hunstman.

2,2,6-Trimethyl-4H-1,3-dioxin-4-one, benzylamine (BA, 99%), chloroform (CHCl₃, ≥ 99%), 3,4,5-trichloropyridine (TCP, 98%), ethyl acetate (99%), and magnesium sulfate were obtained from Thermo Fisher Scientific. Acetic acid glacial (AA) was purchased from VWR Chemicals. *p*-Toluenesulfonic acid monohydrate (*p*TsOH, 99%), tert-butyl acetoacetate (TBAA, 97%), sodium bicarbonate (NaHCO₃, 99.7%), and dimethyl sulfoxide anhydrous (DMSO, ≥ 99.7%) were obtained from Acros Organics. O,O'-Bis(2-aminopropyl) polypropylene glycol-block-polyethylene glycol-block-polypropylene glycol with weight-average molar masses 600 and 900 g mol⁻¹ (J₆₀₀ and J₉₀₀), 4-Methyl-2,6-dimethoxyphenol (MDMP, ≥ 97%), chromium (III) acetyl acetonate (Cr(acac)₃, 97%), cholesterol (> 99%), deuterated chloroform (CDCl₃) and 2-chloro-4,4,5,5-tetramethyl-1,3,2-dioxaphospholane (Cl-TMDP, 95%) and *N,N*-Dimethylformamide anhydrous (DMF, 99.8%) were purchased from Sigma-Aldrich. Acetone was obtained from CARLO ERBA Reagents. Deuterated dimethyl sulfoxide (DMSO-d₆, 99.8%) was purchased from Eurisotop.

3.2. Synthesis of acetoacetylated lignin (OL-AC)

In a round-bottom flask equipped a magnetic stirrer and a distillation apparatus, 40 g of OSL were dissolved in 75 mL of DMF. Then, TMDO (3 equivalents with respect to the total of OH groups of OSL) was introduced. The reaction was stirred vigorously and heated at 120 °C, enabling the distillation of the acetone formed. Following acetone distillation, the reaction was stopped after 10 h (for the modification of 5 g of lignin, only 4 h of reaction are needed). The resulting mixture was precipitated in a saturated aqueous solution of NaHCO₃ to remove the reagent excess, solvent and dehydroacetic acid by-product. The product was filtered and washed abundantly with distilled water. OL-AC was dried overnight at 50 °C in a vacuum oven. ¹H NMR of OL-AC is available in Figure S7-2 in SI.

3.3. Model reaction of OL-AC with benzylamine

In a round bottom flask equipped with a cooler, 0.2 g of OL-AC (2.94 mmol g⁻¹ of acetoacetate groups) were dissolved into 2 mL of solvent, then BA (1 molar equivalent with respect to acetoacetate groups), and catalyst (AA or *p*TsOH, 1 molar equivalent to BA) were added. The reaction mixture was stirred vigorously 24 h under reflux when CHCl₃ was used, or at 100 °C with DMSO. The product was precipitated in distilled water and filtered. The resulting powder was dried overnight at 50 °C in a vacuum oven. ¹H NMR of Ph-VU-L is available in Figure S7-3 in SI.

3.4. Model compound synthesis

3.4.1. Synthesis of 2,6-dimethoxy-4-methylphenyl (Z)-3-(benzylamino)but-2-enoate (Ph-VU)

In a 25 mL round bottom flask equipped with a distillation apparatus were added 2 g of MDMP (10.98 mmol) and TMDO (12.63 mmol, 1.15 equivalent). The mixture was agitated and heated at 130 °C to remove acetone by distillation. After 4 h of reaction, the product (MDMP-AC) was obtained. Then, in a 10 mL round bottom flask, 0.2 g of MDMP-AC (0.75 mmol), benzylamine (0.825 mmol, 1.1 equivalent), and AA (0.75 mmol, 1 equivalent) were dissolved in 2 mL CHCl₃. After 24 h of reaction at 60 °C, the product (Ph-VU) was diluted in ethyl acetate, washed with water to remove AA, dried with anhydrous magnesium sulfate, filtered, and concentrated under reduced pressure and dried overnight at 50 °C in a vacuum oven. ¹H NMR is available in Figure S7-4 in SI.

3.4.2. Synthesis of tert-butyl (Z)-3-(benzylamino)but-2-enoate (Al-VU)

In a 10 mL round bottom flask, 0.2 g of TBAA (1.26 mmol) and benzylamine (1.39 mmol, 1.1 equivalent) were dissolved in 2 mL of CHCl₃. The mixture was stirred vigorously at 60 °C and the

desired product (Al-VU) was obtained after 24 h. The solvent was removed under reduced pressure. Al-VU was dried overnight in a vacuum oven at 50 °C. ¹H NMR is available in Figure S7-5 in SI.

3.4.3. Synthesis of *N*-benzyl-3-(benzylamino)but-2-enamide (Ph-VU_N)

In a 10 mL round bottom flask equipped with a distillation apparatus, 1 g of benzylamine (9.33 mmol) and 696 μL of TMDO (4.66 mmol, 0.5 equivalents) were added. The mixture was vigorously agitated with a magnetic stirrer at 120 °C and the formed acetone was distilled. The neat product was obtained after 30 minutes of reaction. ¹H NMR is available in Figure S7-6 in SI.

3.5. Synthesis of lignin-based VU networks

In a 50 mL round bottom flask was added 15 g of OL-AC diluted in 10 mL of CHCl₃ at room temperature. Diamine (1.3 molar equivalents of amine functions with respect to acetoacetate groups of OL-AC) was introduced. The reactive mixture was stirred vigorously for 30 seconds to obtain a homogeneous solution. The mixture was poured into a Teflon mold (10 cm x 10 cm) and let under the fume hood overnight for solvent evaporation. The material was cured in an oven 100 °C for 24 h. The resulting network was cut into pieces and hot pressed for 25 minutes at 160 °C under a constant applied force of 16 MPa in a mold (10 cm × 10 cm × 1 mm).

The materials designations were established as follow: Ph-VU-X, where X (X = 400, 600, 900, or 2000) stands for the chain length of the diamine used for the network synthesis. For example, Ph-VU-400 is a material synthesized from OL-AC and J₄₀₀.

3.6. Physical and chemical recycling studies of VU networks

Three physical recycling cycles were performed. For each cycle, the resulting material was grinded into a fine and homogenous powder using a 200 W Livoo DOD192 grinder. The powder was hot pressed 25 minutes (Scientific hydraulic press from LabTech, Thailand) at 160 °C under a constant applied force of 16 MPa in a mold (10 cm × 10 cm × 1 mm) to shape a new material generation to be tested.

Chemical recycling was performed by immersion of a 1.85 g VU-based sample in acetic acid (0.033 g mL⁻¹ concentration). The mixture was heated 48 h at 110 °C under vigorous agitation. Then, acetic acid was distilled using a distillation apparatus at 110 °C under 440 mbar until the obtention of slightly viscous mixture. The product was poured into a Teflon mold and the rest of acetic acid was evaporated in a vacuum oven at 60 °C for 48 h. The material was finally hot pressed (Scientific hydraulic press from LabTech, Thailand) at 80 °C for 10 min before evaluation.

3.7. Characterization techniques

¹H and ³¹P NMR spectra were recorded on a Bruker 400 MHz spectrometer (United States of America). ¹H NMR calibration was assessed based on CDCl₃ (δH = 7.26 ppm) chemical shift, with 16 scans. Quantitative ¹H NMR (15 s relaxation delay) was obtained using TCP as internal standard. Approximately 20 mg of sample were dissolved in 500 μL of solvent and 100 μL of a standard solution of TCP (0.5 M) was added. ³¹P NMR was performed following the reaction with a phosphorylating reagent (Cl-TMDP) according to standard protocols, and 128 scans were acquired with 15 s relaxation delays (Archipov et al., 1991; Granata and Argyropoulos, 1995; Meng et al., 2019). Equation 1 gives the hydroxyl (OH) content (in mmol g⁻¹), with C_s (M) is the concentration of cholesterol standard, V_s (μL) is the volume of cholesterol standard, A is the area of the OH groups peak obtained on the ³¹P NMR spectrum, and m (mg) is the weight of the sample:

$$OH\ content = \frac{c_S \times V_S \times A}{m} \quad (1)$$

^1H - ^{15}N HMBC NMR spectra at natural abundance were recorded on a Bruker 500 MHz spectrometer with 64 scans and 2 s relaxation delays. All analysis consisted of approximately 100 mg of sample in 600 μL of CDCl_3 .

Fourier transform infrared (FT-IR) spectra were acquired with a Nicolet 380 spectrometer from Thermo Electron Corporation (United States of America), equipped with an attenuated total reflectance (ATR) diamond module. 32 scans were recorded for each analysis in the range 4000-500 cm^{-1} .

Size-exclusion Chromatography (SEC) was performed on a Acquity APC apparatus from Waters (United States of America) for the determination of the number-average molar mass (M_n), weight-average molar mass (M_w) and dispersity (Đ). THF was employed as eluent (0.6 mL min^{-1}) at 40 $^\circ\text{C}$. Three columns (Acquity APC XT 450 \AA 2.5 μm 4.6 \times 150 mm, 200 and 45) were connected and the detection was assessed with a UV detector. Polystyrene (PS) standards were used for the calibration.

Thermogravimetric analysis (TGA) was recorded on a TA Instrument Hi-RES TGA Q5000 (United States of America). Samples of around 2 to 3 mg were heated in a platinum crucible from room temperature to 700 $^\circ\text{C}$ at a rate of 20 $^\circ\text{C min}^{-1}$ under an air atmosphere (25 mL min^{-1} flow rate).

Differential scanning calorimetry (DSC) was performed on a TA instruments Discovery DSC-25 (United States of America) apparatus under 50 mL min^{-1} dry nitrogen flow. Around 2 to 3 mg of sample were weighted in aluminum pans, using an empty pan as reference. Samples were first equilibrated at 150 $^\circ\text{C}$ for 3 minutes to erase their thermal history. They were then cooled down at -80 $^\circ\text{C}$ at a 5 $^\circ\text{C min}^{-1}$ rate and equilibrated for 3 minutes. Finally, samples were heated at 150 $^\circ\text{C}$ at a 10 $^\circ\text{C min}^{-1}$ rate. The glass transition temperature (T_g) was measured on the last heating ramp as the change of slope.

Wide Angle X-ray Scattering (WAXS) measurements were conducted on a Bruker D-8 Advance diffractometer (United States of America) with $\text{Cu K}\alpha$ radiation ($\lambda = 1.5406 \text{\AA}$) at room temperature in the 2θ range of 3 to 60 $^\circ$, with a scan step of 0.03 $^\circ$ and a step time of 0.5 s. Samples of 1 mm thickness were analyzed. The scattering vectors (q) and the real-space distances (D) were calculated using Equations 2 and 3, where 2θ (rad) is the scattering angle and λ is the X-rays wavelength (\AA).

$$q \text{ (\AA}^{-1}\text{)} = \left(\frac{4\pi}{\lambda}\right) \sin \theta \quad (2)$$

$$D \text{ (\AA)} = \frac{2\pi}{q} \quad (3)$$

The peaks deconvolutions were assessed by fitting 4 Gaussian functions, using Scipy library openly developed on GitHub, on Python 3.0. The areas under each Gaussian were integrated and the resulting values were used to calculate the proportions of the different interactions.

Dynamic mechanical analyses (DMA) were assessed on a TA Instrument Discovery Hybrid Rheometer HR-3 (United States of America) equipped with a rectangular torsion geometry. Rectangular samples of around 2 $\text{cm} \times 1 \text{ cm} \times 1 \text{ mm}$ were heated at 3 $^\circ\text{C min}^{-1}$ from -60 to 150 $^\circ\text{C}$, with a 0.01 % strain at 1 Hz frequency. Crosslinking densities (ν) were calculated according to the theory of rubber elasticity for small deformations on the rubbery plateau using Equation 4, where G' (Pa) is the storage modulus, and R the molar gas constant (8.314 $\text{J mol}^{-1} \text{K}^{-1}$). T_α (K), the α transition temperature, is determined at the maximum of $\tan \delta$ curve (Chenal et al., 2007; Palmese and McCullough, 1992).

$$\nu \text{ (mol m}^{-3}\text{)} = \frac{G'_{T_\alpha+60}}{3R(T_\alpha+60)} \quad (4)$$

Stress relaxation experiment were carried out on a TA Instrument Discovery Hybrid Rheometer HR-3 (United States of America) equipped with ETC-steel 25 mm parallel plates geometry. Samples were cut into discs of 25 mm diameter and 1 mm thickness. The series of experiment at different temperatures were performed successively on the same sample after equilibration at temperature for 10 min, with a fixed gap around 1 mm and 1% strain. The curves were fitted with Kohlrausch-William-Watts stretched exponential decay using Equation 5, where $G(t)/G_0$ is the normalized stress at relaxation time t , τ^* is a characteristic relaxation time, and β ($0 \leq \beta \leq 1$) the exponent indicating the distribution of relaxation times (Dhinojwala et al., 1994; Williams and Watts, 1970). Average relaxation time $\langle \tau \rangle$ is given by Equation 6. Activation energies (E_a) were determined by plotting $\ln \langle \tau \rangle = f(1000/T)$, with $\langle \tau \rangle$ given by Equation 7.

$$\frac{G(t)}{G_0} = \frac{G_{perm}}{G_0} + \left(1 - \frac{G_{perm}}{G_0}\right) \exp \left\{ -\left(t/\tau^*\right)^\beta \right\} \quad (5)$$

$$\langle \tau \rangle = \frac{\tau^* \Gamma\left(\frac{1}{\beta}\right)}{\beta} \quad (6)$$

$$\langle \tau \rangle = A \exp\left(\frac{-E_a}{RT}\right) \quad (7)$$

Uniaxial tensile tests were assessed on an Instron 5567H dynamometer (United States of America) equipped with a 10 kN load cell. Tests were carried out in a room set at 23 °C on a set of 5 dumbbell-shaped samples of dimension $45 \times 5 \times 1 \text{ mm}^3$ with a constant crosshead speed of 20 mm min⁻¹. Young's modulus (E), stress at break (σ), and elongation at break were obtained. Representative curves of the average values were selected.

Swelling ratio (SR) of the series of materials was studied by immersion of previously dried samples of around 100 mg in both acetone and water for 48 h. The test was performed in triplicate. SR were calculated with Equation 8, where m_i is the mass of material after swelling in either acetone or water and m_f is the final mass of dried material.

$$SR (\%) = \frac{m_i - m_f}{m_f} \times 100 \quad (8)$$

Following swelling, the samples were dried in a vacuum oven for 24 h at 50 °C. Gel fraction (GF) was determined using Equation 9, where m_f is the final mass of dried material and m_i the initial mass of material.

$$GF (\%) = \frac{m_f}{m_i} \times 100 \quad (9)$$

4. RESULTS AND DISCUSSION

4.1. Analysis of lignin acetoacetylation

The preparation of VU containing networks requires the condensation of acetoacetate and amine-bearing building blocks. In this context, *tert*-butyl acetoacetate (TBAA) is commonly used for the modification of aliphatic alcohols into acetoacetates without catalyst (Denissen et al., 2017; Engelen et al., 2022; Witzeman and Nottingham, 1991). However, this reagent was reported to poorly modify phenolic OH, leading to partially modified lignins with phenolic OH conversion between 15 and 55% (Krall et al., 2018; Liu et al., 2024). To overcome this limitation and achieve a full conversion of all reactive groups of lignin, we previously reported a two-step strategy based on several green chemistry principles consisting on the modifications of phenolic OH into reactive aliphatic OH employing ethylene carbonate, followed by acetoacetylation of hydroxyl moieties with TBAA (Sougrati et al., 2023).

CHAPITRE 3

However, with the intention of minimizing synthesis steps, a one-step and catalyst-free pathway can be envisaged by employing TMDO as reactant for the grafting of reactive acetoacetates moieties onto all OSL hydroxyl moieties, both aliphatic and phenolic, as illustrated in Figure 3-1a. Upon heating, TMDO generates a reactive acetylketene and acetone via retro-Diels-Alder reaction (Figure S3-24a in SI) (Clemens and Witzeman, 1989). Acetoacetylation reactions between the formed acetylketene and nucleophile groups on OSL proceed efficiently, while acetone is removed via distillation to push the equilibrium (Figure S3-24b in SI). To increase the positive impact of this reaction, the distilled acetone can be recovered and reused in syntheses, for instance.

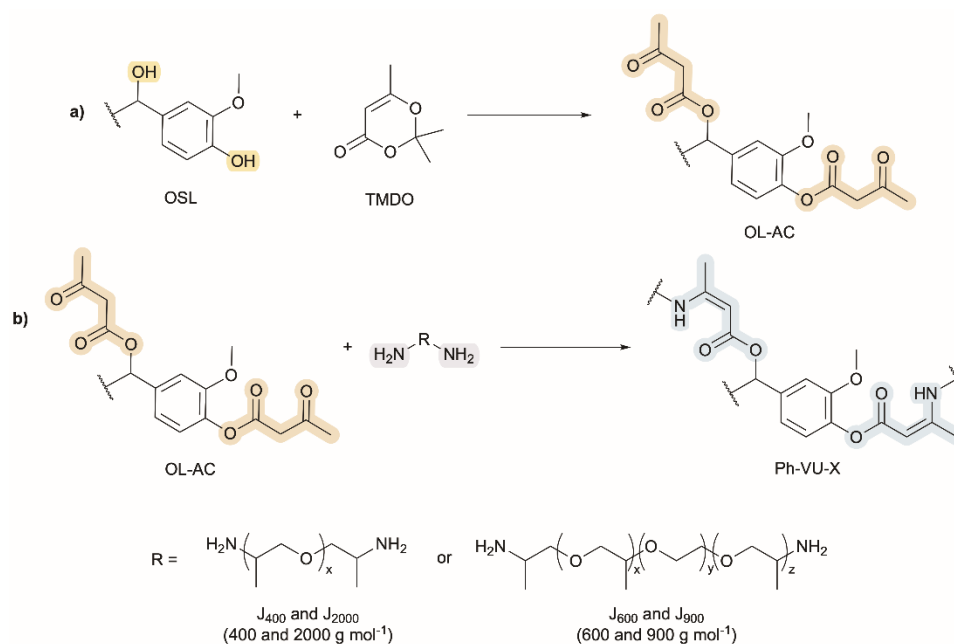


Figure 3-1. Synthetic pathway for the preparation of a) acetoacetylated lignin, and b) VU networks from OSL.

Table 3-1. Acetoacetylation conditions optimization from OSL.

Entry	TMDO equiv.	Solvent	T (°C)	Time (h)	Al-OH conversion (%)	Ph-OH conversion (%)
1	1.05	Cyrene	110	2.5	54	6
2	3	Cyrene	110	2.5	91	51
3	1.05	DMF	110	2.5	85	2
4	3	DMF	110	2.5	95	89
5	1.05	DMF	130	2.5	94	22
6	3	DMF	130	2.5	91	60
7	3	DMF	120	2.5	94	90
8	3	DMSO	120	2.5	100	23
9	1.5	DMF	120	2.5	100	48
10	2	DMF	120	2.5	100	47

The acetoacetylation reaction was optimized on 0.2 g of OSL and the different tested conditions are available in Table 3-1. The molar equivalent of TMDO, the solvent, and the temperature were varied. Better conversion of aliphatic and phenolic hydroxyls, respectively of 94 and 90%, was obtained with 3 equivalents of TMDO in DMF at 120 °C. Overall, increasing TMDO equivalent from 1.05 to 3.00 increased considerably the conversion of lignin hydroxyls, particularly the phenols. The latter, which could not exceed 22% of conversion, reached up to 90% of conversion with more reactant equivalents. Cyrene, a biobased non-toxic and eco-friendly solvent, was tested as green solvent but showed limited conversion of the phenols of 51% in the same conditions (Duval and Avérous, 2022; Citarella et al., 2022). DMSO, which can be biobased, was also surveyed but also showed poor conversion of phenolic hydroxyl of 23% (Marcos Celada et al., 2024). DMF was then chosen as solvent for the synthesis but only the minimal quantity needed for the lignin solubilization was used (less than 2 mL of solvent per gram of lignin). Finally, the optimal temperature was found to be 120 °C.

The complete conversion of all nucleophilic phenols of OSL was almost but not fully achieved. This can be explained by the formation of dehydroacetic acid. This by-product is reported to result from the dimerization of the reactive acetylketene, even at low temperatures (Hyatt et al., 1984; Clemens and Witzeman, 1989). It is also formed by the self-condensation of phenylacetoacetates, generating phenols alongside dehydroacetic acid under the reaction conditions (Clemens and Hyatt, 1985). This explains why full conversion of phenols is challenging, even with TMDO excess.

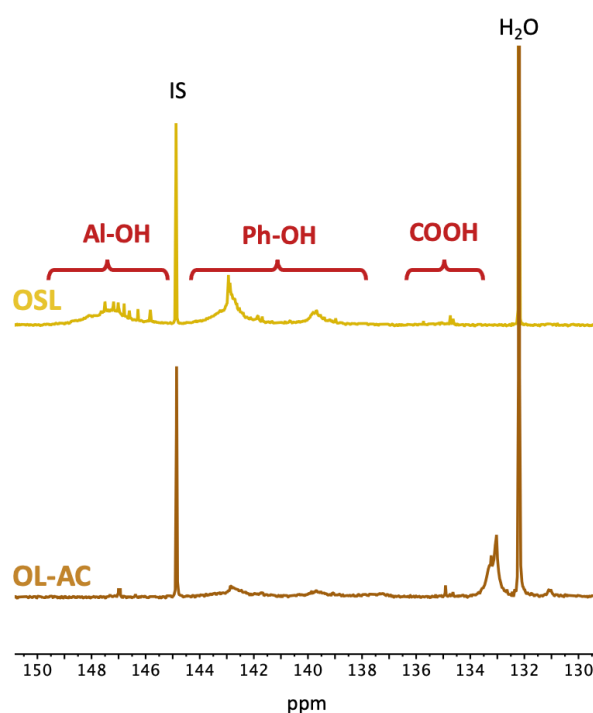


Figure 3-2. Stacked ^{31}P NMR of OSL and OL-AC. IS= Internal standard.

The product of OSL acetoacetylation (OL-AC) was analyzed by ^{31}P NMR, as illustrated in Figure 3-2. This method enables the quantification of aliphatic alcohols (Al-OH) from 145.4 to 150.0 ppm, phenolic hydroxyls (Ph-OH) from 137.6 to 144.0 ppm, and carboxylic acids (COOH) from 133.3 to 136.0 ppm (Pu et al., 2011). The spectra show the disappearance of the signals between 145.4 and 149.0 ppm, and between 138.2 and 144.5 ppm, indicating the consumption of Al-OH and Ph-OH. The appearance of a signal around 133.0 ppm is observed, resulting from the reaction of acetoacetate groups with the phosphorylating agent (Cl-TMDP) as discussed in a previous work (Sougrati et al., 2023). The conversion of Al-OH and Ph-OH of the 40 g batch of lignin reached 100% and 71%. It is noteworthy to mention that under the same experimental conditions, 98 and 94% of Al-OH and Ph-OH of 5 g batches

of lignin were reproducibly converted in only 4 hours, respectively. It is assumed that differences in conversions linked to changes in the scales of reaction might be due to a small temperature inhomogeneities in the large flask, and the need for longer reaction times favoring secondary reactions which consume the reactive acetylketene by forming dehydroacetic acid.

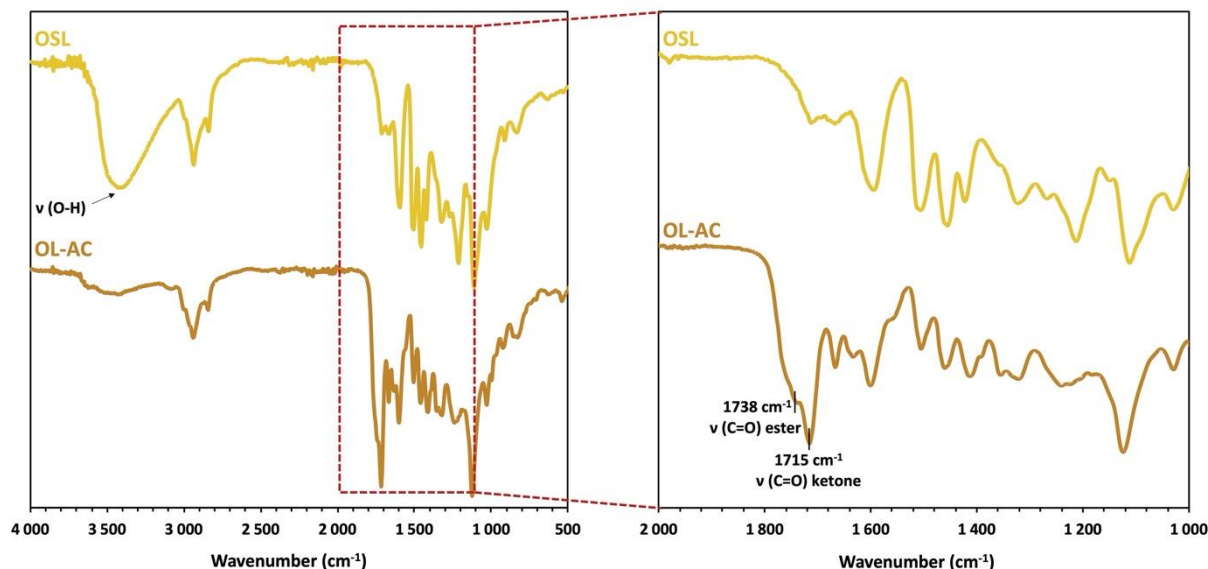


Figure 3-3. FT-IR spectra of OSL and OL-AC from top to bottom. Right spectra are magnifications of the left spectra, between 2000 and 1000 cm^{-1} .

The grafting of acetoacetate groups onto OSL was successfully confirmed by FT-IR analysis, as illustrated in Figure 3-3. Characteristic peaks of acetoacetate appeared at 1738 and 1715 cm^{-1} , corresponding to esters and ketones, respectively, while the band corresponding to the OH vibration at 3403 cm^{-1} of alcohol groups almost completely disappeared. ^1H NMR of OSL and OL-AC are displayed in Figure S3-18 and Figure S3-19 in SI. Broad signals around 3.47 ppm and 2.25 ppm were attributed to methyl and methylene of acetoacetate moieties, respectively. SEC analysis of OSL and OL-AC are given in Figure S3-25 and Table S3-8 in SI. M_n of 1340 and 1180 g mol^{-1} and \bar{D} of 2.48 and 2.44 were respectively obtained for OSL and OL-AC.

4.2. Analysis of the reaction of aromatic acetoacetate with amines

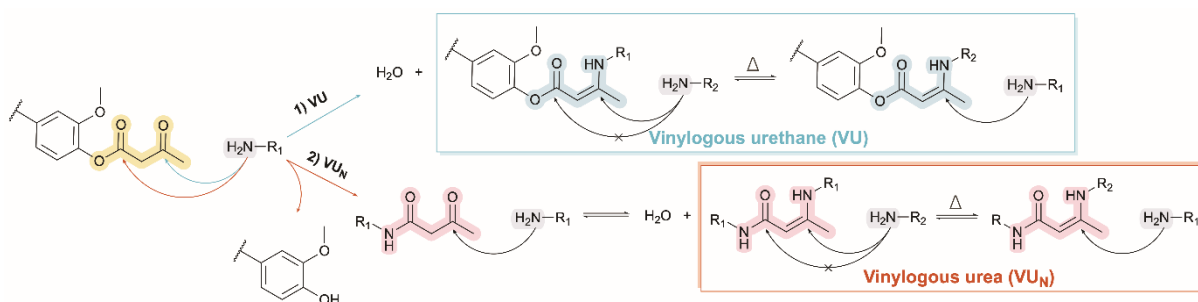


Figure 3-4. Two potential mechanistic pathways for the reaction of aromatic acetoacetates with an excess amine groups forming 1) vinylogous urethanes, and 2) vinylogous ureas. Adapted from Ref (Haida et al., 2022).

Although the reaction of aliphatic acetoacetate with amines have been extensively studied for vinylogous urethanes synthesis, the use of aromatic acetoacetates remains partially unexplored. Haida

et al. discussed the reaction between phenylacetoacetate and amines, revealing a dual mechanism as illustrated in Figure 3-4 (Haida et al., 2022). Vinylogous urethane are formed through the nucleophilic attack of the amine on the keto group, whereas vinylogous urea are obtained via the nucleophilic attack on the ester moiety of the acetoacetate. Although both covalent bonds enable dynamicity in networks, the second pathway implies the degrafting of phenol units. In the case of a lignin-based dynamic network, the formation of vinylogous ureas would lead to the rupture of the crosslinking bonds, with degrafting of the phenol groups of lignin. Thus, it is crucial to understand and quantify the formation of VU_N occurring during the synthesis of lignin-based CANs.

To investigate the simultaneous formation of vinylogous urethane and urea, OL-AC was reacted with a monoamine (benzylamine) in different solvents and catalytic conditions. From previous reported results (Haida et al., 2022), DMSO and CHCl₃ were chosen as solvents, while AA and *p*TsOH were selected as catalysts. The subsequent products were characterized by ³¹P NMR to quantify the amount of degrafted phenol during the condensation of acetoacetate and amine groups. The content of degrafted phenol for each reaction conditions are reported in Table 3-2 and the ³¹P spectra are available from Figure S3-26 to Figure S3-29 in SI. Full conversion of acetoacetate moieties was reached for each reaction as indicted by the disappearance of acetoacetate peaks around 133.0 ppm on ³¹P NMRs. The results show limited influence of the catalyst on the content of degrafted phenol in DMSO. The use of AA marginally decreases the amount of degrafted phenol because of the protonation of acetoacetate keto groups resulting in an increased nucleophilicity which shifts the reaction toward the VU product. Nonetheless, CHCl₃ significantly decreases by a 2-fold factor this content. This indicates that the solvent dipole moment reflecting the polarity is a key parameter to tune the product formation. It is suggested that solvents with high dipole moments as DMSO (3.96 D, with D as a nonstandard unit Debye) seem to shift the reaction towards the VU_N formation, while solvents with low dipole moments as CHCl₃ (1.03 D) seem to favor the VU formation (Clark et al., 2008, p. 20; Davidson et al., 2006). From DMSO high dipole moment originate large array of positive and negative sites which allow various intermolecular interactions between its positive regions and π electrons of aromatic compounds (Clark et al., 2008). This makes it an effective solvent for OL-AC, but it might also generate interactions with phenylacetoacetate moieties that promote VU_N formation. However, it was reported that when the dipole moment becomes too low, as for benzene, the VU_N product is favored yet again (Haida et al., 2022).

Table 3-2. Conditions and corresponding parameters obtained from the formation of vinylogous urethanes and ureas.

Designation	Solvent	Catalyst	Catalyst equiv.	Degrifted Ph-OH (%)	M _n (g mol ⁻¹)	M _w (g mol ⁻¹)	Đ
Ph-VU-01	DMSO	-	-	51	1030	2270	2.2
Ph-VU-02	DMSO	AA	1	49	1020	2250	2.2
Ph-VU-03	DMSO	<i>p</i> TsOH	1	55	920	1860	2.0
Ph-VU-L	CHCl ₃	AA	1	25	1130	3010	2.6

The products were characterized by SEC and the main values (M_n, M_w and Đ) are listed in Table 3-2. The resulting curves in Figure 3-5 show one main signal with two shoulders at approximately log M of 2.56 and 2.79 that are respectively attributed to THF impurities and urea by-product. When BA reacts on OL-AC at the ester position, the acetoacetate moiety initially grafted on lignin is removed, leading to the release of a small vinylogous urea molecule (Figure 3-1). The released VU_N molecules give rise to the signal at log M = 2.79, whereas the degrafting the acetoacetate from the lignin leads to a decrease of the M_n of the modified lignin. Ph-VU-L, which exhibit the higher M_n of 1130 g mol⁻¹, contains less urea compound (Ph-VU_N) and degrafted lignin. In contrast Ph-VU-03 is composed of greater amount of VU_N reducing its M_n to 920 g mol⁻¹, as suggested by a greater degrafted Ph-OH content. This observation is also reflected by the evolution of M_w values. It is suggested that the formation of a small amount of urea increases the heterogeneity of molar mass in the product by

CHAPITRE 3

increasing \bar{M}_w values. This heterogeneity is smoothed out when more ureas are generated because fewer large molar mass structures are formed, limiting the discrepancy with small molar masses.

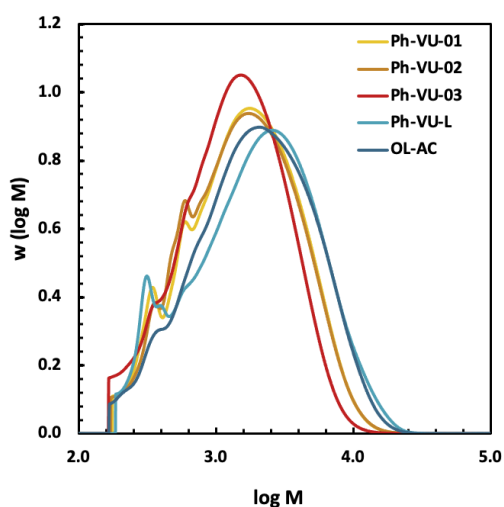


Figure 3-5. SEC curves in THF of OL-AC and the products of the formation of vinyllogous urethanes and ureas.

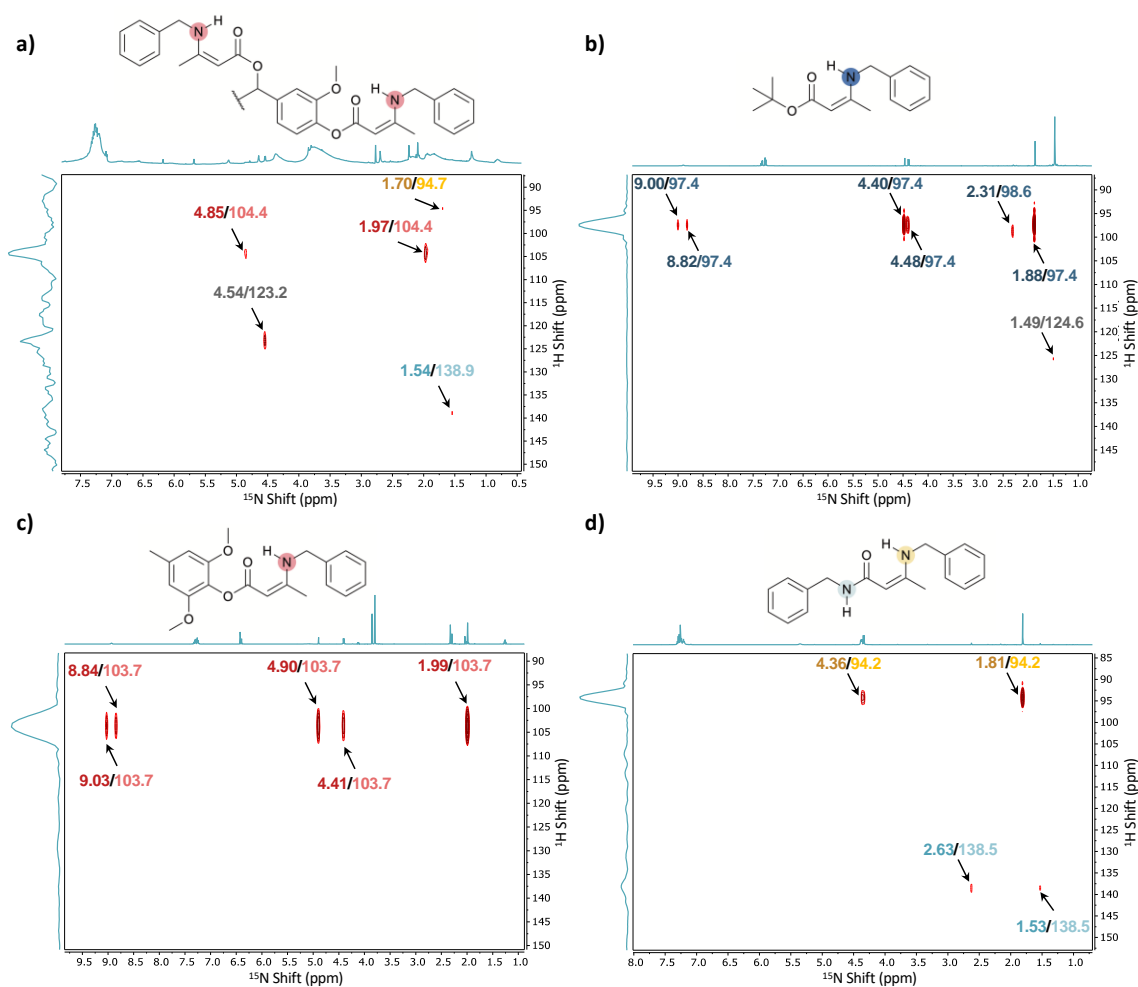


Figure 3-6. ^1H - ^{15}N HMBC spectra of a) Ph-VU-L, b) Al-VU, c) Ph-VU, and d) Ph-VU_N.

The degrafting of phenol might indicate the formation of VU_N , however additional NMR investigations are required. Due to OSL structural heterogeneity, the formation of characteristic signals of VU/VU_N are not visible on 1H NMR spectra, as they are usually observed. Thus, 1H - ^{15}N HMBC was performed to confirm the dual formation of VU and VU_N . Ph- VU -L spectra is displayed in Figure 3-6a. Four different nitrogen atoms correlated with 1H signals are observed. The signals at 94.7, 104.4, and 138.9 ppm were attributed to VU_N -enaminone, VU -enaminone, and urea nitrogen atoms, while the signal at 123.2 ppm was unidentified. To support and confirm this attribution, three model molecules were synthesized to represent aliphatic VU (Figure 3-6b), aromatic VU (Figure 3-6c), and VU_N (Figure 3-6d). 1H - ^{15}N HMBC of each molecule was acquired to determine the exact chemical shift of the different nitrogen. A detailed attribution of the 1H NMR spectra are available from Figure S3-20 to Figure S3-23 in SI. The intensities of the signals observed on Ph- VU -L also indicates, although not quantitatively, nitrogen atoms grafted on OL-AC are mainly VU as previously observed with the ^{31}P NMR analyses. Finally, the signal observed at 123.2 and 124.6 ppm on Ph- VU -L and Al-Ph spectra could not be attributed and may result from impurities.

4.3. Analysis of the obtained aromatic VU networks

4.3.1. Results from FT-IR characterizations

A series of VU networks were prepared by reacting OL-AC with different chain length diamines. Two PPG diamines of molar mass 400 and 2000 $g\ mol^{-1}$ (J_{400} and J_{2000}), and two PPG-*b*-PEG-*b*-PPG diamines of molar mass 600 and 900 $g\ mol^{-1}$ (J_{600} and J_{900}) were selected. The quantity of amine used in the networks synthesis was adjusted to enable the presence of free amines in the materials to induce rearrangements, considering that some amines groups would form VU_N . Thus 1.3 equivalents of amine were used per equivalent of acetoacetate for the networks syntheses, in presence of AA and $CHCl_3$.

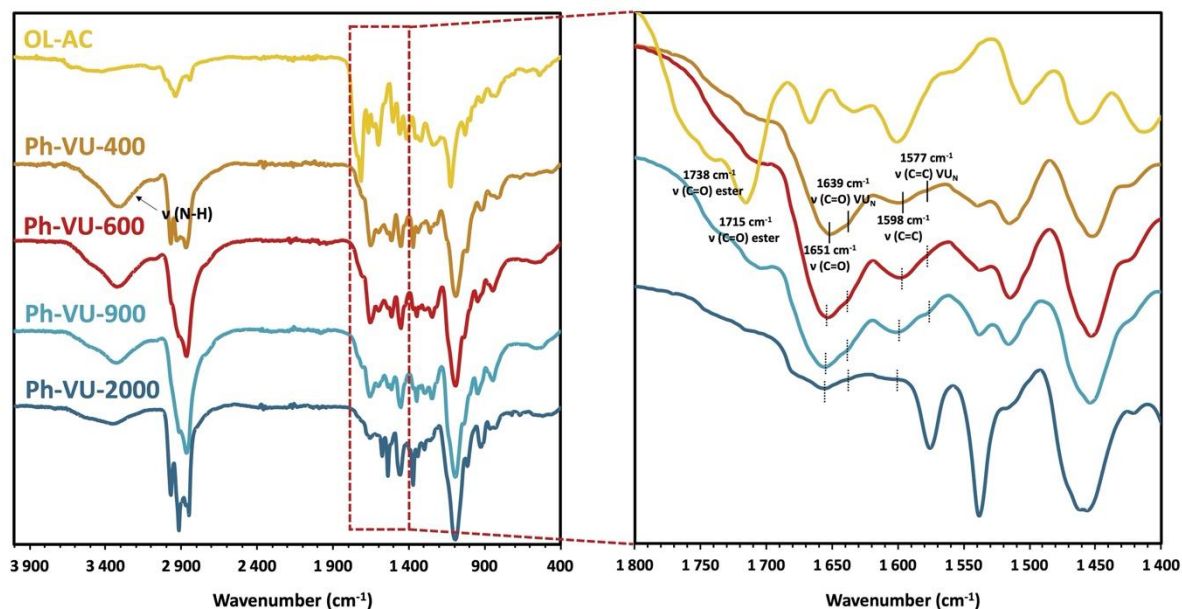


Figure 3-7. Stacked FT-IR spectra of OL-AC and Ph- VU -400, Ph- VU -600, Ph- VU -900, and Ph- VU -2000, from top to bottom. Right spectra are magnifications of the left spectra, between 1800 and 1400 cm^{-1} .

FT-IR analyses were performed on these materials. The spectra of OL-AC and materials are displayed in Figure 3-7. The disappearance of ester $C=O$ and ketone $C=O$ vibration bands of the

acetoacetate moieties is observed. New specific C=O and C=C vibration bands of vinylogous urethane are observed at 1651 and 1598 cm^{-1} indicating the successful condensation of acetoacetates and amine groups, respectively. Shoulders of lower intensity can be observed on these two signals which are attributed to vinylogous urea C=O stretch of the amide and C=C stretch of the enamine around 1639 and 1577 cm^{-1} , respectively (Engelen et al., 2024). Curiously, the peak at C=C stretch at 1577 cm^{-1} is more intense on Ph-VU-2000, but the corresponding C=O stretch at 1639 cm^{-1} exhibit a lower intensity, similar to other materials. This suggest that the peak attributed to VU_N is overlapping another signal which might be attributed to secondary amide in plane N–H bending (Asemani and Rabbani, 2020).

4.3.2. Results from the thermal characterizations by TGA and DSC

To assess their global behavior and suitable reprocessing conditions, thermal properties of VU networks were studied by TGA. Results are summarized in Table 3-3. The curves are displayed in Figure S3-30 in SI. TGA demonstrated high thermal resistances, with 5% mass loss ($T_{d5\%}$) under air attained at temperatures between 280 to 326 °C. Interestingly, a slight increase in $T_{d5\%}$ can be observed for networks synthesized with longer diamine chain length (J₉₀₀ and J₂₀₀₀). Those values are slightly higher than previously reported values for lignin-based vinylogous urethane networks containing poly(ethylene glycol) (PEG) chains, probably owing to their higher lignin content (Sougrati et al., 2023). DSC was performed to determine the main thermal transitions temperatures such as the glass transition temperatures (T_g) of the series of networks. Values are listed in Table 3-3 while the curves of the precursors and materials are available from Figure S3-31 to Figure S3-33 in SI. T_g increases almost exponentially from -57 to 18 °C with a higher lignin content and a smaller diamine chain length as displayed in Figure S3-34 in SI.

Table 3-3. Thermal and rheological properties of the aromatic VU networks.

VU (Designations)	Lignin content (wt%)	$T_{d5\%}$ (°C)	T_g (°C)	T_α (°C)	ν (mol m^{-3})
Ph-VU-400	50	290	18	59	140
Ph-VU-600	46	266	-10	28	205
Ph-VU-900	36	302	-39	-17	210
Ph-VU-2000	20	326	-57	-46	162

4.3.3. Results from the morphological characterizations using X-ray scattering

The morphological organization of OSL, OL-AC and the final networks was studied by WAXS as illustrated by the main results given in Figure 3-8. The building blocks and the corresponding polymers show patterns with broad backgrounds scattering signals typical to amorphous systems containing some regions with a certain degree of ordering. The order is attributed to physical interactions occurring between the chemical compounds. The scattering vectors (q_x) also called momentum transfer in reciprocal-space and their corresponding real-space distances also called Bragg spacings (D_x) were determined using Equations 2 and 3. The proportion of each type of interaction are estimated by deconvolution of the diffraction signal using Gaussian functions. D_x , q_x and the physical interaction proportions are summarized in Table 3-4. According to literature, interplanar distance around 4.2 – 4.6, 3.4 – 3.5, and 2.1 – 2.6 Å may be respectively attributed to hydrogen bonding (XH \cdots XH), π - π stacking, and carbonyl-hydrogen bonding (C=O \cdots HX), with X = O or N atoms, respectively (Babra et al., 2019; Merino et al., 2016; Xing et al., 2018). In the materials scattering pattern, the signal D_1 might be characteristic of VU and VU_N stacking (Feula et al., 2016). The attribution of D_1 signals in OSL and

OL-AC is still unclear and need some additional developments. The assembly by hydrogen bonding did not vary significantly between OSL and OL-AC (25 to 22% of D_2 and 14 to 10% of D_4). The content of π - π stacking (D_3) slightly increased by 7% overall suggesting that despite the grafting of acetoacetate moieties a similar organization is observed between the unmodified and modified lignin macromolecules.

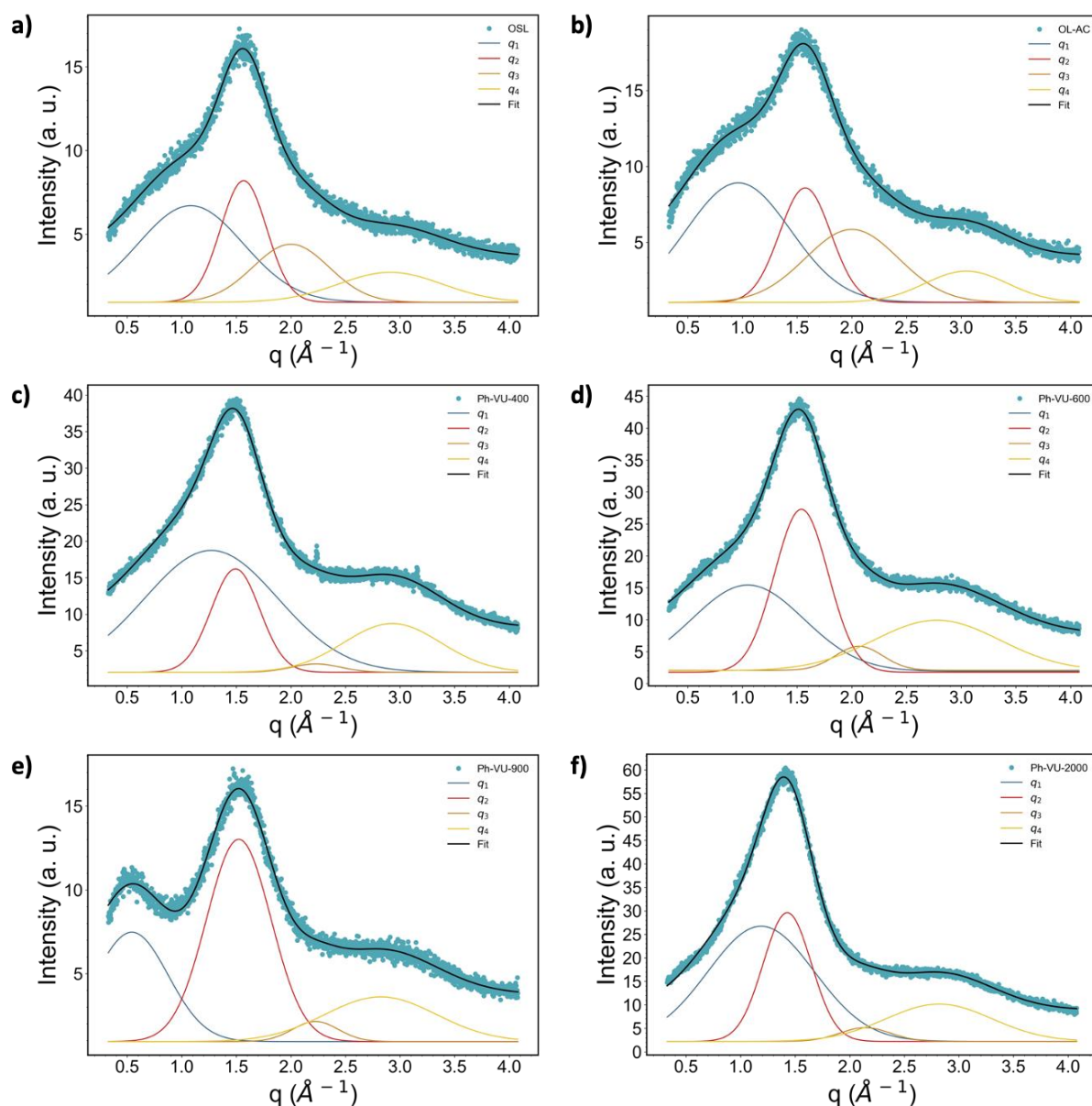


Figure 3-8. WAXS curves and corresponding deconvolutions of a) OSL, b) OL-AC, c) Ph-VU-400, d) Ph-VU-600, e) Ph-VU-900, and f) Ph-VU-2000.

The polymer networks show distinctive physical interactions in proportion. To different extent, hydrogen bonding is favored yet π - π stacking is restricted compared to the precursors. The stacking limitation might be explained by the dilution of lignin moieties in a constrained crosslinked network. The increase of hydrogen bonding may result from the addition of the oxygen-rich PPG and PPG/PEG-based diamines. It should be noted that Ph-VU-900 display a higher value for D_1 compared to the other materials. It is hypothesized that this signal might corresponds to a microphase-separated morphology arising from hard hydrogen bonded and rigid lignin moieties with the soft diamine backbone. The

different physical interaction proportions of the materials were plotted as a function of lignin content, as displayed in Figure S3-35 in SI. With increasing lignin contents hydrogen bonding decreases probably resulting from the lower amounts of oxygen-rich diamines. Lignin content does not seem to drastically influence the π - π stacking and carbonyl-OH bonding with limited values between 2 and 6% and 17 and 26%, respectively. Interestingly, the diamine backbone seems to impact the networks morphologies as diamines with PPG backbone (J₄₀₀ and J₂₀₀₀), corresponding to materials with 50 and 20 wt% lignin, present less hydrogen bonding, and consequently a higher content of VU/VU_N stacking. One hypothesis is that the methyl groups along the entire diamines backbones increase steric hinderance around oxygen atoms making them less inclined to physical bonding. In contrast, diamines containing PPG/PEG blocks (J₆₀₀ and J₉₀₀), employed in the networks containing 46 and 36 wt% lignin, promote hydrogen bonding over VU/VU_N stacking. Finally, the only network exhibiting a T_g close to ambient temperature (around 20 °C) at which the WAXS experiment were carried (Ph-VU-400) display narrow peaks at $q \approx 2.2 \text{ \AA}^{-1}$ and $q \approx 3.2 \text{ \AA}^{-1}$ indicating a better network organization associated to restricted segmental chain mobility.

Table 3-4. WAXS parameters and interaction proportions for OSL, OL-AC, and the series of materials.

Designation	OSL	OL-AC	Ph-VU-400	Ph-VU-600	Ph-VU-900	Ph-VU-2000
q₁ (Å⁻¹)	1.08	0.96	1.27	1.05	0.54	1.19
q₂ (Å⁻¹)	1.57	1.57	1.49	1.54	1.52	1.43
q₃ (Å⁻¹)	2.00	2.00	2.23	2.07	2.22	2.14
q₄ (Å⁻¹)	2.91	3.05	2.93	2.78	2.82	2.82
D₁ (Å)	5.81	6.53	4.95	5.99	11.58	5.29
D₂ (Å)	4.01	3.99	4.21	4.08	4.13	4.40
D₃ (Å)	3.14	3.14	2.82	3.04	2.82	2.94
D₄ (Å)	2.16	2.06	2.15	2.26	2.23	2.23
q₁ proportion (%)	42	43	60	35	24	52
XH...XH proportion (%)	25	22	20	33	53	27
π-π stacking proportion (%)	19	26	2	6	4	3
C=O...HX proportion (%)	14	10	19	26	20	17

4.3.4. Results from the rheological characterizations by DMA and stress relaxation

Rheological properties were investigated by DMA. Main curves are displayed in Figure S3-36 in SI, and the main rheological parameters are summarized in Table 3-3. Temperatures of alpha relaxation (T_α) from -46 to 59 °C were obtained with an increasing lignin content from 20 to 50 %. T_α can be associated to the T_g of the materials, in some conditions (Backfolk et al., 2007; Lei et al., 2014). Then T_α evolutions obtained by DMA follows the T_g one obtained by DSC. Crosslinking densities (ν) calculated with Equation 4 unexpectedly are not correlated to the lignin content. This observation is surprising because lignin high functionality provides crosslinking within the materials, yet ν increases between Ph-VU-400, Ph-VU-600 and Ph-VU-900 respectively containing 50, 46 and 36 wt% of lignin. The storage modulus in the rubbery plateau used for ν calculation is reported to be a function of both entanglements and crosslinks (Reinitz et al., 2015). Equation 4 may determine the density of physically effective crosslinks, which involve entanglements, physical and chemical crosslinks. Hydrogen bonding observed by WAXS may be perceived as crosslinks in addition to the covalent VU linkages, even at

high temperatures (above 150 °C) (Engelen et al., 2024; Sung and Schneider, 1977). The physical interaction proportions were plotted as a function of crosslinking densities as illustrated in Figure 3-9. As hypothesized, higher hydrogen bonding proportions leads to higher crosslinking densities which may explain why Ph-VU-900 exhibits higher ν than Ph-VU-600 and Ph-VU-400. Conversely, VU/VU_N clustering is more important for lower ν . The clustering may be favored with the use of diamines of lower molar mass which possibly restrict segmental chain mobility facilitating the aggregation of VU/VU_N units. No clear evolution of ν is observed depending on π - π stacking and C=O \cdots HX contents.

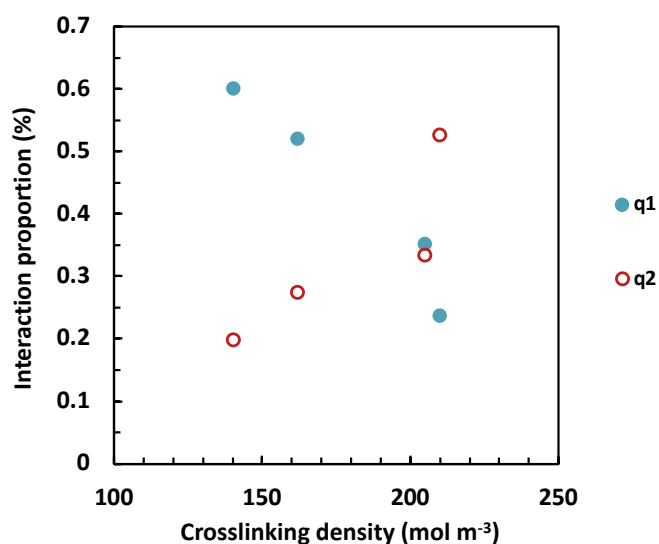


Figure 3-9. Physical interaction proportions as a function of crosslinking density.

To investigate the dynamicity of the series of lignin-based networks and to evaluate their vitrimer behavior, stress relaxation experiments were performed. The resulting curves were fitted using the KWW stretched exponential decay as illustrated in Figure 3-10a. This model enables the determination of τ^* and β exponent ($0 < \beta < 1$) characteristic of the distribution of relaxation times for networks dissipating energy through various relaxation modes. Detailed relaxation parameters are reported in Table 3-5. Stress relaxation curves of all materials are available from Figure S3-37 to Figure S3-39 in SI. At 200 °C, relaxation times were obtained in the range of 156 and 1319 s, originating from transamination reactions between VU moieties and free amines. Faster relaxation is observed when lignin content is increased, and then when a shorter diamine is used. This may result from a higher concentration in dynamic VU bonds and shorter free volumes within the network facilitating the free amine and VU bonds exchanges (Chen et al., 2021). The diamine backbones do not seem to influence the relaxation since a logical evolution of the relaxation times is observed following the diamine molar mass. The presence of the methyl group in β -position from the amines used for the networks formation might be responsible for the slower relaxation times compared to previously reported works that employed unsubstituted amines like hexamethylene diamine or 1,10-diaminodecane/fatty acid-derived diamine mixture (Sougrati et al., 2023; Liu et al., 2024). Polyetheramines with β -methylation are reported to be less reactive than classic aliphatic and cycloaliphatic amines (Mora et al., 2020). The reactivity issue is combined with the sterically hindered environment of amine groups, making the interactions and exchanges between VU moieties and free amines less favored. A computational study performed by Spiesschaert et al. revealed the steric and electronic influences of primary amines employed in VU formation and subsequent transamination reactions (Spiesschaert et al., 2021). It was concluded that an increase in steric hinderance of the primary amine leads to higher kinetic barrier and restricted thermodynamic driving force for the VU formation, which also results in limited transamination potential.

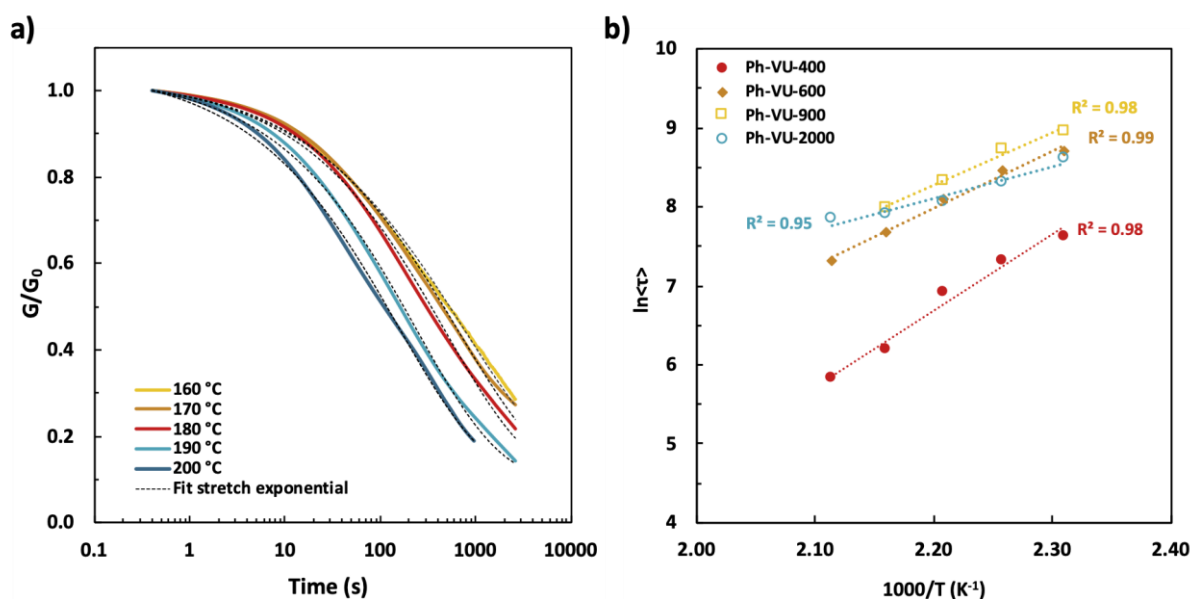


Figure 3-10. a) Stress relaxation curves of Ph-VU-400 with temperature variations between 160 and 200 °C, and b) Arrhenius plots of the different vitrimers.

Overall, no major variation of the parameter β is shown, with values fluctuating between 0.44 and 0.51 for the different networks. These results suggest an heterogeneous distribution of relaxation time, resulting from the different chemical environment of VU bonds (grafted to aliphatic or aromatic acetoacetates). Moreover, the presence of VU_N bonds, reported to have a different exchange kinetics than VU, may also contribute to increase the distribution of relaxation times. As Denissen et al. demonstrated, the rate of bond exchange of enamionone highly depends on the group bonded to the carbonyl function (Denissen et al., 2018). Better electro donating groups tend to generate faster bond rearrangements.

Table 3-5. Main stress-relaxation parameters.

VU (Designations)	$\tau^{*200\text{ °C}}$ (s)	β	E_a (kJ mol ⁻¹)	T_v (°C)
Ph-VU-400	156	0.47 ± 0.02	80.0	58
Ph-VU-600	454	0.44 ± 0.02	60.5	53
Ph-VU-900	890	0.46 ± 0.03	47.3	33
Ph-VU-2000	1319	0.51 ± 0.01	32.9	-6

Activation energies (E_a) between 32.9 and 80.0 kJ mol⁻¹ were obtained (Table 3-5). Vitrimers containing higher lignin content show greater E_a , which can be correlated with the evolution of the T_g . This phenomenon was already observed in our previous work (Sougrati et al., 2023). Vitrimers with higher E_a values undergo rapid viscosity decrease upon heating and exhibit high energy barrier of bond exchange, thus they combine fast relaxation and good dimensional stability. Contrarily, vitrimers with lower E_a are subjected to less pronounced viscosity changes and lower bond exchange energy barriers, resulting in altered dimensional stability at service conditions (Chen et al., 2021). While Ph-VU-400 and Ph-VU-600 E_a values are in accordance with typical values for VU networks, Ph-VU-900 and Ph-VU-2000 exhibit quite low activation energies.

Theoretical freezing temperatures (T_v) above which macroscopic flow can be induced via bond exchange (elastic solid to viscoelastic liquid) were determined by extrapolation from Arrhenius plot for

a conventional viscosity of 10^{12} Pa s (Table 3-5) (Brutman et al., 2014; Lessard et al., 2019; Sougrati et al., 2023). Parameters used for calculations are detailed in Table S3-9 in SI. Each vitrimer show a $T_v > T_g$ revealing a viscoelastic flow mainly controlled by the bond exchange kinetics (Denissen et al., 2016). At an ambient temperature around 25 °C (T_{amb}), Ph-VU-400 ($T_g \approx T_{amb} < T_v$) exhibit a network chemical fixity and restricted segmental motion because the rubber state may not be fully overstepped. Ph-VU-600 and Ph-VU-900 ($T_g < T_{amb} < T_v$) are under the rubbery state and behave like elastomers with a fixed network chemical structure since bond rearrangements are supposedly very slow and practically negligible. Finally, Ph-VU-2000 ($T_g < T_v < T_{amb}$) can already undergo bond rearrangement which are enhanced by a good chain mobility. Creep resistance at the usage temperature of these vitrimers, especially Ph-VU-2000, may be a concern for specific applications which are not compatible with elastomer behaviors.

4.3.5. Results from the mechanical characterizations by uniaxial tensile tests

Mechanical properties of the series of vitrimer were characterized by uniaxial tensile tests. The curves are displayed in Figure S3-40. Young's modulus (E), maximum stress at break (σ) and maximum elongation at break (ϵ) are summarized in Table 3-6. Most vitrimers present an elastomer-like behavior with long elastic zones and low modulus (Bueno-Ferrer et al., 2012). Two distinctive mechanical behaviors are observed. In the case of Ph-VU-400, the testing temperature (23 °C) is very close to the T_g (18 °C), thus the polymer is in a glassy to rubbery state transition. The other networks are in a rubbery state ($T_g \ll 23$ °C). Ph-VU-400 exhibits the higher Young's modulus and stress at break of 71.44 MPa and 3.77 MPa, respectively, with an elongation of 27%. Due to their lower T_g (-10 to -57 °C) Ph-VU-600, Ph-VU-900 and Ph-VU-2000 show decreased mechanical properties. E and σ increase with the lignin content from 0.23 to 2.40 MPa and from 0.22 to 1.02 MPa, as illustrated in Figure 3-11.

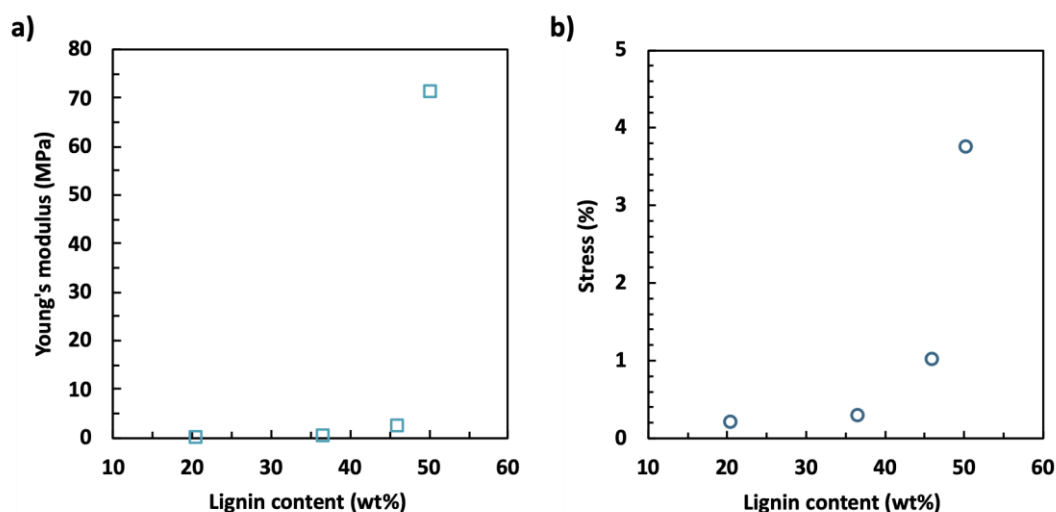


Figure 3-11. Variation of the Young's modulus and stress at break with lignin content.

Table 3-6. Mechanical properties of the series of vitrimers.

VU (Designations)	E (MPa)	σ (MPa)	ϵ (%)
Ph-VU-400	71.44 ± 5.50	3.77 ± 0.50	27 ± 3
Ph-VU-600	2.40 ± 0.10	1.02 ± 0.05	115 ± 4
Ph-VU-900	0.51 ± 0.20	0.31 ± 0.02	56 ± 5
Ph-VU-2000	0.23 ± 0.02	0.22 ± 0.02	91 ± 9

4.3.6. Results from the structural characterizations

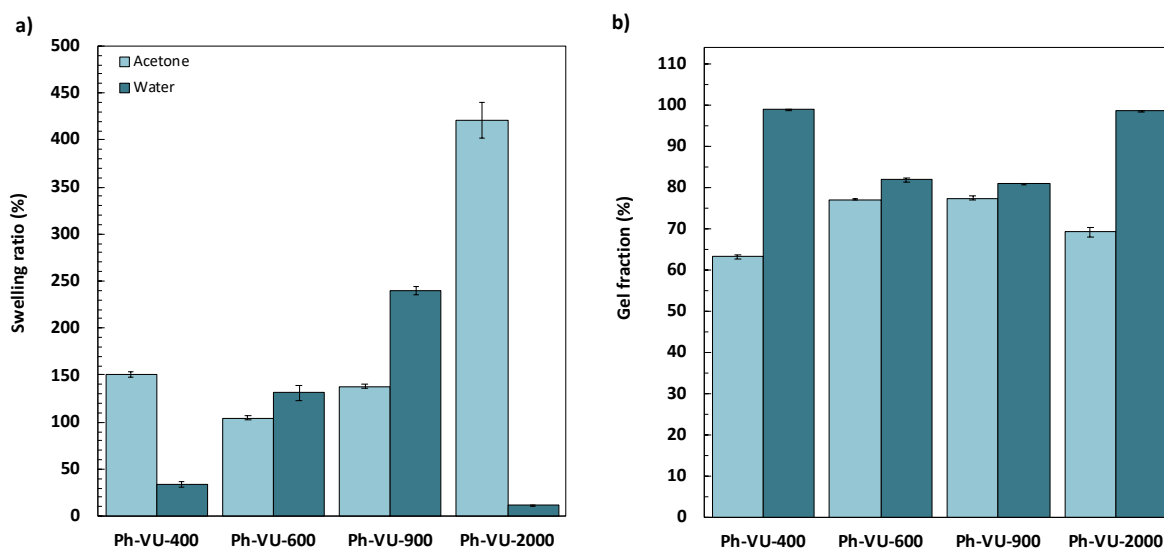


Figure 3-12. a) Swelling ratio and b) gel fraction of VU networks in acetone and water.

The integrity of the networks was investigated through swelling and gel fraction experiments both in acetone and water after 48 h of immersion, as illustrated in Figure 3-12. Detailed values are summarized in Table S3-10 in SI. Overall, the SR increases with lower lignin content. This evolution is correlated with the use of longer diamine chain length, allowing larger amounts of solvents into the network's cavities and free volume. This trend is observed for all materials in acetone. However, in water the materials prepared with J_{2000} exhibits surprisingly low swelling of 11.9% compared to the others (from 34.1 to 239.3%), although it would have been expected to show the larger SR. Interestingly, the backbone of the diamine seems to influence the affinity of the materials with specific solvents. Networks containing PPG-based diamines (Ph-VU-400 and 2000) exhibit greater swelling in acetone than in water. Instead, materials prepared with PPG/PEG-based diamines (Ph-VU-600 and 900) swell more in water, indicating a better affinity induced by PEG segments. These observations lead to hypothesize that the lower water SR of Ph-VU-2000 is due to the methyl groups of the PPG-based diamine and the lower lignin content in the material which bring an higher hydrophilic character, thus limiting its affinity with water compared to Ph-VU-400. GF between 80.9 and 99.1% were obtained in water, which are better than formerly reported GF for lignin-based VU networks (Sougrati et al., 2023). In acetone, slightly lower GF (from 63.2 and 77.5%) were reached, most likely arising from the good solubility of the acetoacetylated lignin and diamines precursors in this solvent. The results also confirm the impact of the diamine structure. In acetone, higher gel fractions are obtained for Ph-VU-600 and Ph-VU-900 synthesized with the PPG-based diamines. On the other hand, Ph-VU-400 and Ph-VU-2000 prepared with PPG/PEG-based diamines display higher GF in water compared to acetone.

4.3.7. Results from the physical and chemical recycling study

The physical recycling potential of the vitrimers series was assessed through three cycles of thermo-mechanical reprocessing. The materials were grinded and hot pressed at 160 °C for 25 minutes under a constant applied force of 16 MPa. The chemical structure of the recycled networks was analyzed by FT-IR. Upon three reprocessing cycles, materials retained their chemical integrity as displayed in Figure 3-13. Mechanical properties were assessed through uniaxial tensile tests on each generation of materials as showed in Figure S3-41 and Table 3-7. Young's modulus and stress at break slightly increased after the first reprocessing step. Yet both parameters slightly decreased after the second cycle and were not further affected after the third cycle, attaining E and σ plateau values of 3.23 MPa and 1.48 MPa, respectively. The elongation at break was very slightly expanded by the consecutive recycling

loops, from 115 to 129%. Finally, rheological properties were investigated on the recycled materials. The resulting parameters are summarized in Table 3-7 and the DMA curves are available in Figure S3-42 in SI. No variation of the T_g was observed. The crosslinking density also remained quite constant throughout the successive cycles, indicating a preserved network structural integrity.

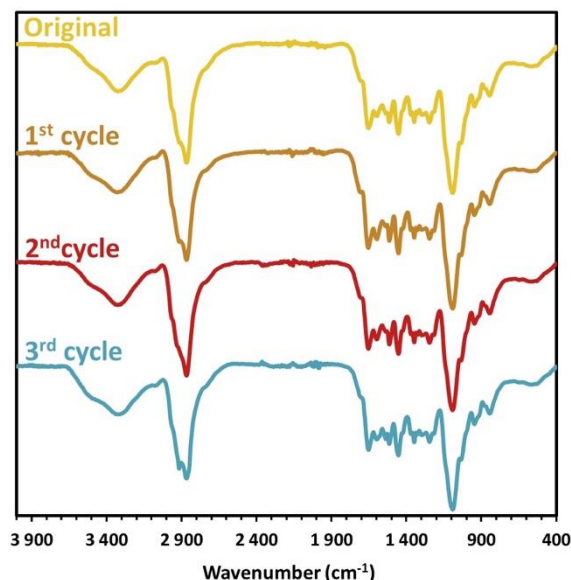


Figure 3-13. FT-IR of Ph-VU-600 upon three physical recycling cycles.

Table 3-7. Mechanical and rheological properties of pristine, physically, and chemically recycled Ph-VU-600.

VU (Designations)	E (MPa)	σ (MPa)	ϵ (%)	T_g (°C)	ν (mol m ⁻³)
Original	2.40 ± 0.10	1.03 ± 0.05	115 ± 4	28	205
1 st cycle	4.08 ± 0.90	1.68 ± 0.06	128 ± 7	32	191
2 nd cycle	3.56 ± 0.90	1.42 ± 0.20	124 ± 13	30	210
3 rd cycle	3.23 ± 0.40	1.48 ± 0.09	129 ± 4	26	253
Ph-VU-600-CR	n/a	n/a	n/a	30	115

In a global cradle-to-cradle approach, chemical recycling by depolymerization offers alternative end-of-life opportunities. Chemical recycling of VU networks is often reported in literature through transamination reactions upon heating, disintegrating the vitrimers. Such pathway generally includes the use of toxic monoamines that are chemical hazards and difficult to remove to reprocess the new-generation material. Recently, closed-loop recycling of PEG-based VU networks was reported via degradation in water, offering a novel and green depolymerization alternative (Y. Ma et al., 2023). This method was tried at 100 °C on Ph-VU-600 which was chosen because of its PEG-containing diamine and high swelling potential in water. However, the vitrimer has not undergone depolymerization in water after 48 h. Alternatively, the material was immersed into 1M HCl aqueous solution, 1M AA aqueous solution, and AA/H₂O (9:1) solution (Figure 3-14). The mixtures were heated at 90 °C for 24 h. Aqueous solutions containing catalytic amounts of acids could not depolymerized the material probably due to a poor ability to solubilize the network and its precursors. Conversely, concentrated aqueous solution of AA enabled an improved depolymerization, although not completed in 24 h at 90 °C. AA is suggested to have a better solubilization ability of the network and its precursors.

CHAPITRE 3

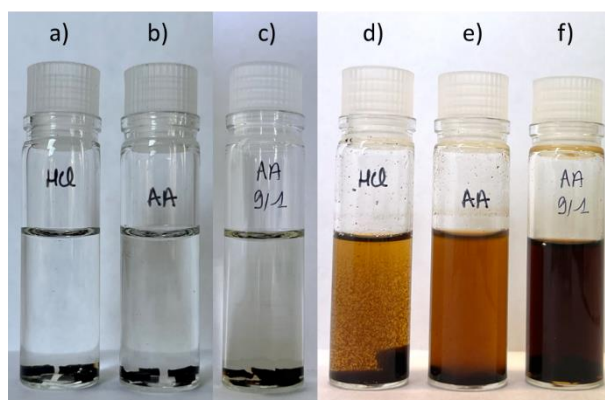


Figure 3-14. Depolymerization assays of Ph-VU-600 in a) 1M HCl, b) 1M AA, and c) aqueous solution of AA (9:1) before heating, and d) 1M HCl, e) 1M AA, and f) aqueous solution of AA (9:1) after heating at 90 °C for 24 h.

The material was immersed in acetic acid containing traces of water at 110 °C for 48 h. As illustrated in Figure 3-15, acid-catalyzed disintegration of the vitrimer was successfully obtained (Haida et al., 2023). A representation of the hypothesized mechanism is illustrated in Figure 3-16 (Huang and Jiang, 2018). It is suggested that enaminone intramolecular hydrogen bond between C=O and N-H, which stabilize the network can be destroyed by adding an excess of acid. The enaminone is further isomerized to form an imine bond which is less stable in acid media. Imine usually can dissociate into aldehyde and amine moieties (Hajj et al., 2020; Zhou et al., 2020), however because of the enaminone methyl substituent acetoacetate and amine are herein expected.

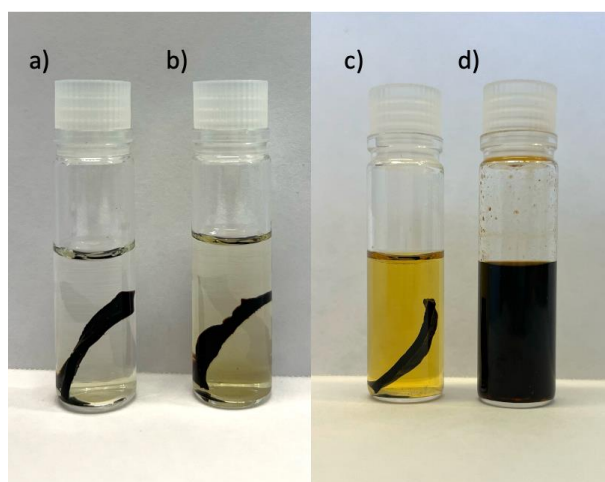


Figure 3-15. Study of acid-catalyzed depolymerization of VU networks: a) VU in H₂O, b) VU in acetic acid, c) VU in H₂O after heating at 100 °C for 48h, and d) VU in acetic acid after heating at 110 °C for 48h.

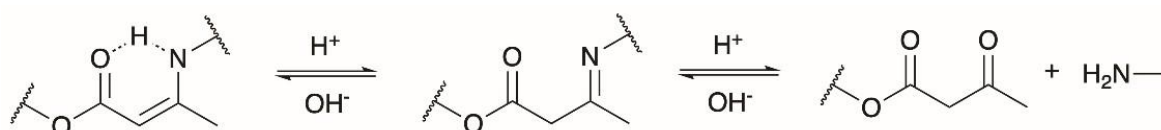


Figure 3-16. Hypothesized acid hydrolysis of VU.

The 2nd generation vitrimer (Ph-VU-600-CR) was recovered by evaporation of AA enabling the reformation of the network. The material was analyzed by FT-IR and DMA (Table 3-7). FT-IR spectra of pristine and chemically recycled Ph-VU-600 are displayed in Figure 3-17 and DMA curves are available in Figure S3-43 in SI. FT-IR spectra overall indicates the obtention of a similar chemical structure compared to the pristine material with the display of VU characteristic bands at 1651 and 1598 cm^{-1} . However, two C=O vibrations are visible at 1735 and 1708 cm^{-1} which can be attributed to acetoacetate ester and ketone groups. This might indicate the partial condensation of acetoacetates and amines leading to incomplete network reformation.

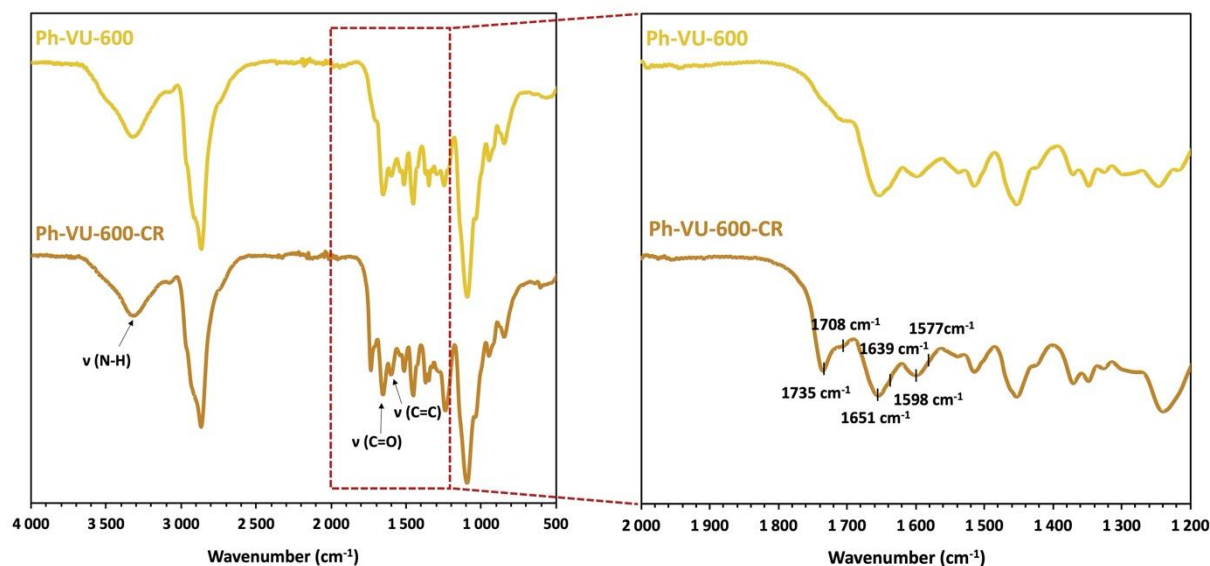


Figure 3-17. Stacked FT-IR spectra of pristine Ph-VU-600 and chemically recycled Ph-VU-600, from top to bottom. Right spectra are magnifications of the left spectra, between 2000 and 1200 cm^{-1} .

DMA results show a decrease of storage modulus from 1.85 to 1.04 MPa which leads to a drop of the crosslinking density from 205 to 115 mol m^{-3} . The network is suggested to have lost part of its integrity from the chemical recycling, as discussed above. This is suspected to result from the low temperature curing step. Lower curing temperatures (60 and 80 $^{\circ}\text{C}$) compared to the temperature used for thermo-mechanical recycling (160 $^{\circ}\text{C}$) were chosen to fully distinct the potential of chemical recycling from the physical recycling which is based on temperature-induced transamination rearrangements. A slightly higher intermediate temperature should enable the network to reform more successfully and regain its integrity.

Another approach could be investigated in the context of chemical recycling. Acetoacetylated lignin could be precipitated in water and recovered by filtration. The PPG and PPG/PEG based diamines could be recovered from the water using acidic ion exchange membranes according to reported protocols (Y. Ma et al., 2023). This alternative method could enable the recovery of both modified lignin and diamine macromonomers, allowing the synthesis of new chemically identical materials and offering upcycling opportunities.

5. CONCLUSION

Organosolv lignin was successfully used to obtain novel aromatic, sustainable and recyclable vitrimer materials. An easily scalable one-step synthetic pathway was developed to fully graft both aliphatic and phenolic hydroxyl with acetoacetate groups. The condensation of the highly functionalized lignin was studied through model reactions with benzylamine to understand the parameters influencing the conversion of phenylacetoacetates into vinylogous urethanes or vinylogous ureas. With the objective

of limiting the degrafting of phenol moieties leading to the dissociation of lignin from the network, low dipole solvent such as CHCl_3 was found to be a key parameter to shift the reaction towards the formation of VU bonds, compared to higher dipole solvents favoring VU_N formation. The use of acid catalyst was found to marginally favor VU products. Based on these observations, a series of vitrimer with high lignin content (20 to 50 wt%) was prepared through the condensation of acetoacetylated lignin with PPG and PPG/PEG-based β -methylated polyetheramines with chain length between 400 and 2000 g mol^{-1} . The structure of the diamine backbone (PPG or PPG/PEG) was found to strongly influence the morphological properties of the vitrimers. The presence of a methyl group on the backbone was observed to hampers hydrogen bonding and to increase materials water resistance leading to lower swelling and higher gel fractions compared to the methyl-free counterpart. Moreover, mechanical properties could be tuned by varying the diamine chain length.

Vitrimers could undergo network rearrangements through transamination bond exchanges. Relaxation times from 156 and 1319 s were obtained at 200 °C and E_a from 32.9 to 80.0 kJ mol^{-1} . The slower bond exchanges compared to previously reported lignin-based VU was attributed to highest steric hindrance of β -methylated polyetheramines compared to non-methylated amines, restricting the transamination potential. Physical recycling was nonetheless efficiently performed on Ph-VU-600 over three cycles. FT-IR, uniaxial tensile tests and DMA indicated no chemical and structural deterioration of the network over the reprocessing steps. Chemical recycling was examined through acid-catalyzed depolymerization of the VU/ VU_N moieties. Although the 2nd generation material displayed partially altered chemical structure, the results showed proofs-of-concept for a non-toxic alternative to VU standard depolymerization employing monoamines which are safety hazards. This approach has the advantage of theoretically allowing the recovery of acetoacetylated lignin by precipitation and filtration for the preparation of a structurally identical material but also offers further upcycling possibilities for the development of sustainable aromatic materials.

This work offers several perspectives. To improve the environmental impact of the condensation reaction of acetoacetylated lignin with amines, greener low boiling point solvents may be tested as alternative to CHCl_3 , which is the only CMR compound used for the vitrimers synthesis. Moreover, the study of the influence of acid catalysis could be further extended to other acid compounds in the aim of simultaneously favoring VU formation and improving stress relaxation by catalyzing transamination reactions. Finally, the structure-properties relationship of lignin-based VU networks could be further evaluated with various lignin structures obtained from other resources and fractionation processes, to develop novel materials fully integrated in the circular bioeconomy.

6. REFERENCES

- Adjaoud, A., Puchot, L., Federico, C.E., Das, R., Verge, P., 2023. Lignin-based benzoxazines: A tunable key-precursor for the design of hydrophobic coatings, fire resistant materials and catalyst-free vitrimers. *Chem. Eng. J.* 453, 139895. <https://doi.org/10.1016/j.cej.2022.139895>
- Archipov, Y., Argyropoulos, D.S., Bolker, H.I., Heitner, C., 1991. 31P NMR Spectroscopy in Wood Chemistry. I. Model Compounds. *J. Wood Chem. Technol.* 11, 137–157. <https://doi.org/10.1080/02773819108050267>
- Asemani, M., Rabbani, A.R., 2020. Detailed FTIR spectroscopy characterization of crude oil extracted asphaltene: Curve resolve of overlapping bands. *J. Pet. Sci. Eng.* 185, 106618. <https://doi.org/10.1016/j.petrol.2019.106618>
- Babra, T.S., Wood, M., Godleman, J.S., Salimi, S., Warriner, C., Bazin, N., Siviour, C.R., Hamley, I.W., Hayes, W., Greenland, B.W., 2019. Fluoride-responsive debond on demand adhesives: Manipulating polymer crystallinity and hydrogen bonding to optimise adhesion strength at low bonding temperatures. *Eur. Polym. J.* 119, 260–271. <https://doi.org/10.1016/j.eurpolymj.2019.07.038>

- Backfolk, K., Holmes, R., Ihalainen, P., Sirviö, P., Triantafillopoulos, N., Peltonen, J., 2007. Determination of the glass transition temperature of latex films: Comparison of various methods. *Polym. Test.* 26, 1031–1040. <https://doi.org/10.1016/j.polymeresting.2007.07.007>
- Bowman, C.N., Kloxin, C.J., 2012. Covalent Adaptable Networks: Reversible Bond Structures Incorporated in Polymer Networks. *Angew. Chem. Int. Ed.* 51, 4272–4274. <https://doi.org/10.1002/anie.201200708>
- Breuillac, A., Kassalias, A., Nicolaÿ, R., 2019. Polybutadiene Vitrimers Based on Dioxaborolane Chemistry and Dual Networks with Static and Dynamic Cross-links. *Macromolecules* 52, 7102–7113. <https://doi.org/10.1021/acs.macromol.9b01288>
- Brutman, J.P., Delgado, P.A., Hillmyer, M.A., 2014. Polylactide Vitrimers. *ACS Macro Lett.* 3, 607–610. <https://doi.org/10.1021/mz500269w>
- Bueno-Ferrer, C., Hablot, E., Perrin-Sarazin, F., Garrigós, M.C., Jiménez, A., Averous, L., 2012. Structure and Morphology of New Bio-Based Thermoplastic Polyurethanes Obtained From Dimeric Fatty Acids. *Macromol. Mater. Eng.* 297, 777–784. <https://doi.org/10.1002/mame.201100278>
- Buono, P., Duval, A., Averous, L., Habibi, Y., 2017. Thermally healable and remendable lignin-based materials through Diels – Alder click polymerization. *Polymer* 133, 78–88. <https://doi.org/10.1016/j.polymer.2017.11.022>
- Capelot, M., Unterlass, M.M., Tournilhac, F., Leibler, L., 2012. Catalytic Control of the Vitrimer Glass Transition. *ACS Macro Lett.* 1, 789–792. <https://doi.org/10.1021/mz300239f>
- Chen, M., Si, H., Zhang, H., Zhou, L., Wu, Y., Song, L., Kang, M., Zhao, X.-L., 2021. The Crucial Role in Controlling the Dynamic Properties of Polyester-Based Epoxy Vitrimers: The Density of Exchangeable Ester Bonds (ν). *Macromolecules* 54, 10110–10117. <https://doi.org/10.1021/acs.macromol.1c01289>
- Chenal, J.-M., Chazeau, L., Guy, L., Bomal, Y., Gauthier, C., 2007. Molecular weight between physical entanglements in natural rubber: A critical parameter during strain-induced crystallization. *Polymer* 48, 1042–1046. <https://doi.org/10.1016/j.polymer.2006.12.031>
- Citarella, A., Amenta, A., Passarella, D., Micale, N., 2022. Cyrene: A Green Solvent for the Synthesis of Bioactive Molecules and Functional Biomaterials. *Int. J. Mol. Sci.* 23, 15960. <https://doi.org/10.3390/ijms232415960>
- Clark, T., Murray, J.S., Lane, P., Politzer, P., 2008. Why are dimethyl sulfoxide and dimethyl sulfone such good solvents? *J. Mol. Model.* 14, 689–697. <https://doi.org/10.1007/s00894-008-0279-y>
- Clemens, R.J., Hyatt, J.A., 1985. Acetoacetylation with 2,2,6-trimethyl-4H-1,3-dioxin-4-one: a convenient alternative to diketene. *J. Org. Chem.* 50, 2431–2435. <https://doi.org/10.1021/jo00214a006>
- Clemens, R.J., Witzeman, J.S., 1989. Kinetic and spectroscopic studies on the thermal decomposition of 2,2,6-trimethyl-4H-1,3-dioxin-4-one. Generation of acetylketene. *J. Am. Chem. Soc.* 111, 2186–2193. <https://doi.org/10.1021/ja00188a037>
- Davidson, E.R., Eichinger, B.E., Robinson, B.H., 2006. Hyperpolarizability: Calibration of theoretical methods for chloroform, water, acetonitrile, and *p*-nitroaniline. *Opt. Mater.* 29, 360–364. <https://doi.org/10.1016/j.optmat.2006.03.031>
- Delavarde, A., Savin, G., Derkenne, P., Boursier, M., Morales-Cerrada, R., Nottelet, B., Pinaud, J., Caillol, S., 2024. Sustainable polyurethanes: toward new cutting-edge opportunities. *Prog. Polym. Sci.* 151, 101805. <https://doi.org/10.1016/j.progpolymsci.2024.101805>
- Denissen, W., De Baere, I., Van Paepegem, W., Leibler, L., Winne, J., Du Prez, F.E., 2018. Vinylogous Urea Vitrimers and Their Application in Fiber Reinforced Composites. *Macromolecules* 51, 2054–2064. <https://doi.org/10.1021/acs.macromol.7b02407>
- Denissen, W., Droesbeke, M., Nicolaÿ, R., Leibler, L., Winne, J.M., Du Prez, F.E., 2017. Chemical control of the viscoelastic properties of vinylogous urethane vitrimers. *Nat. Commun.* 8, 14857. <https://doi.org/10.1038/ncomms14857>
- Denissen, W., M. Winne, J., Prez, F.E.D., 2016. Vitrimers: permanent organic networks with glass-like fluidity. *Chem. Sci.* 7, 30–38. <https://doi.org/10.1039/C5SC02223A>

- Denissen, W., Rivero, G., Nicolaj, R., Leibler, L., Winne, J.M., Du Prez, F.E., 2015. Vinylogous Urethane Vitrimers. *Adv. Funct. Mater.* 25, 2451–2457. <https://doi.org/10.1002/adfm.201404553>
- Dhinojwala, A., Hooker, J.C., Torkelson, J.M., 1994. Retardation of rotational reorientation dynamics in polymers near the glass transition: a novel study over eleven decades in time using second-order non-linear optics. *J. Non-Cryst. Solids, Relaxations in Complex Systems* 172–174, 286–296. [https://doi.org/10.1016/0022-3093\(94\)90447-2](https://doi.org/10.1016/0022-3093(94)90447-2)
- Du, L., Jin, X., Qian, G., Yang, W., Su, L., Ma, Y., Ren, S., Li, S., 2022. Lignin-based vitrimer for circulation in plastics, coatings, and adhesives with tough mechanical properties, catalyst-free and good chemical solvent resistance. *Ind. Crops Prod.* 187, 115439. <https://doi.org/10.1016/j.indcrop.2022.115439>
- Duval, A., Avérous, L., 2022. Dihydrolevoglucosenone (CyreneTM) as a versatile biobased solvent for lignin fractionation, processing, and chemistry. *Green Chem.* 24, 338–349. <https://doi.org/10.1039/D1GC03395F>
- Duval, A., Lange, H., Lawoko, M., Crestini, C., 2015. Reversible crosslinking of lignin via the furan–maleimide Diels–Alder reaction. *Green Chem.* 17, 4991–5000. <https://doi.org/10.1039/C5GC01319D>
- Engelen, S., Dolinski, N.D., Chen, C., Ghimire, E., Lindberg, C.A., Crolais, A.E., Nitta, N., Winne, J.M., Rowan, S.J., Du Prez, F.E., 2024. Vinylogous Urea–Urethane Vitrimers: Accelerating and Inhibiting Network Dynamics through Hydrogen Bonding. *Angew. Chem.* 136, e202318412. <https://doi.org/10.1002/ange.202318412>
- Engelen, S., Wróblewska, A.A., Bruycker, K.D., Aksakal, R., Ladmiral, V., Caillol, S., Du Prez, F.E., 2022. Sustainable design of vanillin-based vitrimers using vinylogous urethane chemistry. *Polym. Chem.* <https://doi.org/10.1039/D2PY00351A>
- Feula, A., Tang, X., Giannakopoulos, I., M. Chippindale, A., W. Hamley, I., Greco, F., Buckley, C.P., R. Siviour, C., Hayes, W., 2016. An adhesive elastomeric supramolecular polyurethane healable at body temperature. *Chem. Sci.* 7, 4291–4300. <https://doi.org/10.1039/C5SC04864H>
- Gao, S., Cheng, Z., Zhou, X., Liu, Y., Wang, J., Wang, C., Chu, F., Xu, F., Zhang, D., 2020. Fabrication of lignin based renewable dynamic networks and its applications as self-healing, antifungal and conductive adhesives. *Chem. Eng. J.* 394, 124896. <https://doi.org/10.1016/j.cej.2020.124896>
- Granata, A., Argyropoulos, D.S., 1995. 2-Chloro-4,4,5,5-tetramethyl-1,3,2-dioxaphospholane, a Reagent for the Accurate Determination of the Uncondensed and Condensed Phenolic Moieties in Lignins. *J. Agric. Food Chem.* 43, 1538–1544. <https://doi.org/10.1021/jf00054a023>
- Haida, P., Chirachanchai, S., Abetz, V., 2023. Starch-Reinforced Vinylogous Urethane Vitrimer Composites: An Approach to Biobased, Reprocessable, and Biodegradable Materials. *ACS Sustain. Chem. Eng.* 11, 8350–8361. <https://doi.org/10.1021/acssuschemeng.3c01340>
- Haida, P., Signorato, G., Abetz, V., 2022. Blended vinylogous urethane/urea vitrimers derived from aromatic alcohols. *Polym. Chem.* 13, 946–958. <https://doi.org/10.1039/D1PY01237A>
- Hajj, R., Duval, A., Dhers, S., Avérous, L., 2020. Network Design to Control Polyimine Vitrimer Properties: Physical Versus Chemical Approach. *Macromolecules* 53, 3796–3805. <https://doi.org/10.1021/acs.macromol.0c00453>
- Hao, C., Liu, T., Zhang, S., Brown, L., Li, R., Xin, J., Zhong, T., Jiang, L., Zhang, J., 2019. A High-Lignin-Content, Removable, and Glycol-Assisted Repairable Coating Based on Dynamic Covalent Bonds. *ChemSusChem* 12, 1049–1058. <https://doi.org/10.1002/cssc.201802615>
- Huang, J., Jiang, X., 2018. Injectable and Degradable pH-Responsive Hydrogels via Spontaneous Amino–Yne Click Reaction. *ACS Appl. Mater. Interfaces* 10, 361–370. <https://doi.org/10.1021/acsmi.7b18141>
- Hyatt, J.A., Feldman, P.L., Clemens, R.J., 1984. Ketenes. 20. Thermal decomposition of 2,2,6-trimethyl-4H-1,3-dioxin-4-one and 1-ethoxybutyn-3-one. *Acetylketene. J. Org. Chem.* 49, 5105–5108. <https://doi.org/10.1021/jo00200a018>
- Kloxin, C.J., Scott, T.F., Adzima, B.J., Bowman, C.N., 2010. Covalent Adaptable Networks (CANs): A Unique Paradigm in Cross-Linked Polymers. *Macromolecules* 43, 2643–2653. <https://doi.org/10.1021/ma902596s>

- Krall, E.M., Serum, E.M., Sibi, M.P., Webster, D.C., 2018. Catalyst-free lignin valorization by acetoacetylation. Structural elucidation by comparison with model compounds. *Green Chem.* 20, 2959–2966. <https://doi.org/10.1039/C8GC01071D>
- Laurichesse, S., Avérous, L., 2014. Chemical modification of lignins: Towards biobased polymers. *Prog. Polym. Sci.* 39, 1266–1290. <https://doi.org/10.1016/j.progpolymsci.2013.11.004>
- Lawoko, M., Samec, J.S.M., 2023. Kraft lignin valorization: Biofuels and thermoset materials in focus. *Curr. Opin. Green Sustain. Chem.* 40, 100738. <https://doi.org/10.1016/j.cogsc.2022.100738>
- Lei, Z., Xing, W., Wu, J., Huang, G., Wang, X., Zhao, L., 2014. The proper glass transition temperature of amorphous polymers on dynamic mechanical spectra. *J. Therm. Anal. Calorim.* 116, 447–453. <https://doi.org/10.1007/s10973-013-3526-0>
- Lessard, J.J., Garcia, L.F., Easterling, C.P., Sims, M.B., Bentz, K.C., Arencibia, S., Savin, D.A., Sumerlin, B.S., 2019. Catalyst-Free Vitrimers from Vinyl Polymers. *Macromolecules* 52, 2105–2111. <https://doi.org/10.1021/acs.macromol.8b02477>
- Liu, J., Pich, A., Bernaerts, K.V., 2024. Preparation of lignin-based vinylogous urethane vitrimer materials and their potential use as on-demand removable adhesives. *Green Chem.* <https://doi.org/10.1039/D3GC02799F>
- Liu, W., Fang, C., Chen, F., Qiu, X., 2020. Strong, Reusable, and Self-Healing Lignin-Containing Polyurea Adhesives. *ChemSusChem* 13, 4691–4701. <https://doi.org/10.1002/cssc.202001602>
- Lucherelli, M.A., Duval, A., Avérous, L., 2022. Biobased vitrimers: Towards sustainable and adaptable performing polymer materials. *Prog. Polym. Sci.* 127, 101515. <https://doi.org/10.1016/j.progpolymsci.2022.101515>
- Ma, X., Li, S., Wang, F., Wu, J., Chao, Y., Chen, X., Chen, P., Zhu, J., Yan, N., Chen, J., 2023a. Catalyst-Free Synthesis of Covalent Adaptable Network (CAN) Polyurethanes from Lignin with Editable Shape Memory Properties. *ChemSusChem* 16, e202202071. <https://doi.org/10.1002/cssc.202202071>
- Ma, X., Wang, X., Zhao, H., Xu, X., Cui, M., Stott, N.E., Chen, P., Zhu, J., Yan, N., Chen, J., 2023b. High-Performance, Light-Stimulation Healable, and Closed-Loop Recyclable Lignin-Based Covalent Adaptable Networks. *Small* 19, 2303215. <https://doi.org/10.1002/sml.202303215>
- Ma, Y., Jiang, X., Shi, Z., Berrocal, J.A., Weder, C., 2023. Closed-Loop Recycling of Vinylogous Urethane Vitrimers. *Angew. Chem. Int. Ed.* 62, e202306188. <https://doi.org/10.1002/anie.202306188>
- Marcos Celada, L., Martín, J., Dvinskikh, S.V., Olsén, P., 2024. Fully Bio-Based Ionic Liquids for Green Chemical Modification of Cellulose in the Activated-State. *ChemSusChem* 17, e202301233. <https://doi.org/10.1002/cssc.202301233>
- McBride, M.K., Worrell, B.T., Brown, T., Cox, L.M., Sowan, N., Wang, C., Podgorski, M., Martinez, A.M., Bowman, C.N., 2019. Enabling Applications of Covalent Adaptable Networks. *Annu. Rev. Chem. Biomol. Eng.* 10, 175–198. <https://doi.org/10.1146/annurev-chembioeng-060718-030217>
- Meng, X., Crestini, C., Ben, H., Hao, N., Pu, Y., Ragauskas, A.J., Argyropoulos, D.S., 2019. Determination of hydroxyl groups in biorefinery resources via quantitative ³¹P NMR spectroscopy. *Nat. Protoc.* 14, 2627–2647. <https://doi.org/10.1038/s41596-019-0191-1>
- Merino, D.H., Feula, A., Melia, K., Slark, A.T., Giannakopoulos, I., Siviour, C.R., Buckley, C.P., Greenland, B.W., Liu, D., Gan, Y., Harris, P.J., Chippindale, A.M., Hamley, I.W., Hayes, W., 2016. A systematic study of the effect of the hard end-group composition on the microphase separation, thermal and mechanical properties of supramolecular polyurethanes. *Polymer, Self-Assembly* 107, 368–378. <https://doi.org/10.1016/j.polymer.2016.07.029>
- Montarnal, D., Capelot, M., Tournilhac, F., Leibler, L., 2011. Silica-Like Malleable Materials from Permanent Organic Networks. *Science* 334, 965–968. <https://doi.org/10.1126/science.1212648>
- Mora, A.-S., Tayouo, R., Boutevin, B., David, G., Caillol, S., 2020. A perspective approach on the amine reactivity and the hydrogen bonds effect on epoxy-amine systems. *Eur. Polym. J.* 123, 109460. <https://doi.org/10.1016/j.eurpolymj.2019.109460>

- Moreno, A., Morsali, M., Sipponen, M.H., 2021. Catalyst-Free Synthesis of Lignin Vitrimers with Tunable Mechanical Properties: Circular Polymers and Recoverable Adhesives. *ACS Appl. Mater. Interfaces* 13, 57952–57961. <https://doi.org/10.1021/acsami.1c17412>
- Palmese, G.R., McCullough, R.L., 1992. Effect of epoxy–amine stoichiometry on cured resin material properties. *J. Appl. Polym. Sci.* 46, 1863–1873. <https://doi.org/10.1002/app.1992.070461018>
- Pu, Y., Cao, S., Ragauskas, A.J., 2011. Application of quantitative ³¹P NMR in biomass lignin and biofuel precursors characterization. *Energy Environ. Sci.* 4, 3154–3166. <https://doi.org/10.1039/C1EE01201K>
- Reinitz, S.D., Carlson, E.M., Levine, R.A.C., Franklin, K.J., Van Citters, D.W., 2015. Dynamical mechanical analysis as an assay of cross-link density of orthopaedic ultra high molecular weight polyethylene. *Polym. Test.* 45, 174–178. <https://doi.org/10.1016/j.polymertesting.2015.06.008>
- Smit, A.T., Verges, M., Schulze, P., van Zomeren, A., Lorenz, H., 2022. Laboratory- to Pilot-Scale Fractionation of Lignocellulosic Biomass Using an Acetone Organosolv Process. *ACS Sustain. Chem. Eng.* 10, 10503–10513. <https://doi.org/10.1021/acssuschemeng.2c01425>
- Sougrati, L., Duval, A., Avérous, L., 2023. From Lignins to Renewable Aromatic Vitrimers based on Vinylogous Urethane. *ChemSusChem* 16, e202300792. <https://doi.org/10.1002/cssc.202300792>
- Spießschaert, Y., Danneels, J., Van Herck, N., Guerre, M., Acke, G., Winne, J., Du Prez, F., 2021. Polyaddition Synthesis Using Alkyne Esters for the Design of Vinylogous Urethane Vitrimers. *Macromolecules* 54, 7931–7942. <https://doi.org/10.1021/acs.macromol.1c01049>
- Sung, C.S.P., Schneider, N.S., 1977. Temperature Dependence of Hydrogen Bonding in Toluene Diisocyanate Based Polyurethanes. *Macromolecules* 10, 452–458. <https://doi.org/10.1021/ma60056a041>
- Thys, M., Brancart, J., Van Assche, G., Van den Brande, N., Vendamme, R., 2023a. LignoSwitch: A Robust Yet Reversible Bioaromatic Superglue for Enhanced Materials Circularity and Ecodesign. *ACS Sustain. Chem. Eng.* 11, 17941–17950. <https://doi.org/10.1021/acssuschemeng.3c04477>
- Thys, M., Brancart, J., Van Assche, G., Vendamme, R., Van den Brande, N., 2021. Reversible Lignin-Containing Networks Using Diels–Alder Chemistry. *Macromolecules* 54, 9750–9760. <https://doi.org/10.1021/acs.macromol.1c01693>
- Thys, M., Kaya, G.E., Soetemans, L., Van Assche, G., Bourbigot, S., Baytekin, B., Vendamme, R., Van den Brande, N., 2023b. Bioaromatic-Associated Multifunctionality in Lignin-Containing Reversible Elastomers. *ACS Appl. Polym. Mater.* 5, 5846–5856. <https://doi.org/10.1021/acsapm.3c00491>
- Tiz, D.B., Vicente, F.A., Kroflič, A., Likozar, B., 2023. Lignin-Based Covalent Adaptable Network Polymers—When Bio-Based Thermosets Meet Recyclable by Design. *ACS Sustain. Chem. Eng.* 11, 13836–13867. <https://doi.org/10.1021/acssuschemeng.3c03248>
- Tribot, A., Amer, G., Abdou Alio, M., De Baynast, H., Delattre, C., Pons, A., Mathias, J.-D., Callois, J.-M., Vial, C., Michaud, P., Dussap, C.-G., 2019. Wood-lignin: Supply, extraction processes and use as bio-based material. *Eur. Polym. J.* 112, 228–240. <https://doi.org/10.1016/j.eurpolymj.2019.01.007>
- Upton, B.M., Kasko, A.M., 2016. Strategies for the Conversion of Lignin to High-Value Polymeric Materials: Review and Perspective. *Chem. Rev.* 116, 2275–2306. <https://doi.org/10.1021/acs.chemrev.5b00345>
- Williams, G., Watts, D.C., 1970. Non-symmetrical dielectric relaxation behaviour arising from a simple empirical decay function. *Trans. Faraday Soc.* 66, 80–85. <https://doi.org/10.1039/TF9706600080>
- Witzeman, J.S., Nottingham, W.D., 1991. Transacetoacetylation with tert-butyl acetoacetate: synthetic applications. *J. Org. Chem.* 56, 1713–1718. <https://doi.org/10.1021/jo00005a013>
- Xing, P., Chen, H., Xiang, H., Zhao, Y., 2018. Selective Coassembly of Aromatic Amino Acids to Fabricate Hydrogels with Light Irradiation-Induced Emission for Fluorescent Imprint. *Adv. Mater.* 30, 1705633. <https://doi.org/10.1002/adma.201705633>

- Yang, Y., Zhou, H., Chen, X., Liu, T., Zheng, Y., Dai, L., Si, C., 2023. Green and ultrastrong polyphenol lignin-based vitrimer adhesive with photothermal conversion property, wide temperature adaptability, and solvent resistance. *Chem. Eng. J.* 477, 147216. <https://doi.org/10.1016/j.cej.2023.147216>
- Zhang, S., Liu, T., Hao, C., Wang, L., Han, J., Liu, H., Zhang, J., 2018. Preparation of a lignin-based vitrimer material and its potential use for recoverable adhesives. *Green Chem.* 20, 2995–3000. <https://doi.org/10.1039/C8GC01299G>
- Zhao, X.-L., Li, Y.-D., Zeng, J.-B., 2022a. Progress in the design and synthesis of biobased epoxy covalent adaptable networks. *Polym. Chem.* 13, 6573–6588. <https://doi.org/10.1039/D2PY01167K>
- Zhao, X.-L., Tian, P.-X., Li, Y.-D., Zeng, J.-B., 2022b. Biobased covalent adaptable networks: towards better sustainability of thermosets. *Green Chem.* 24, 4363–4387. <https://doi.org/10.1039/D2GC01325H>
- Zhou, Z., Su, X., Liu, J., Liu, R., 2020. Synthesis of Vanillin-Based Polyimine Vitrimers with Excellent Reprocessability, Fast Chemical Degradability, and Adhesion. *ACS Appl. Polym. Mater.* 2, 5716–5725. <https://doi.org/10.1021/acsapm.0c01008>

7. APPENDICES (SI)

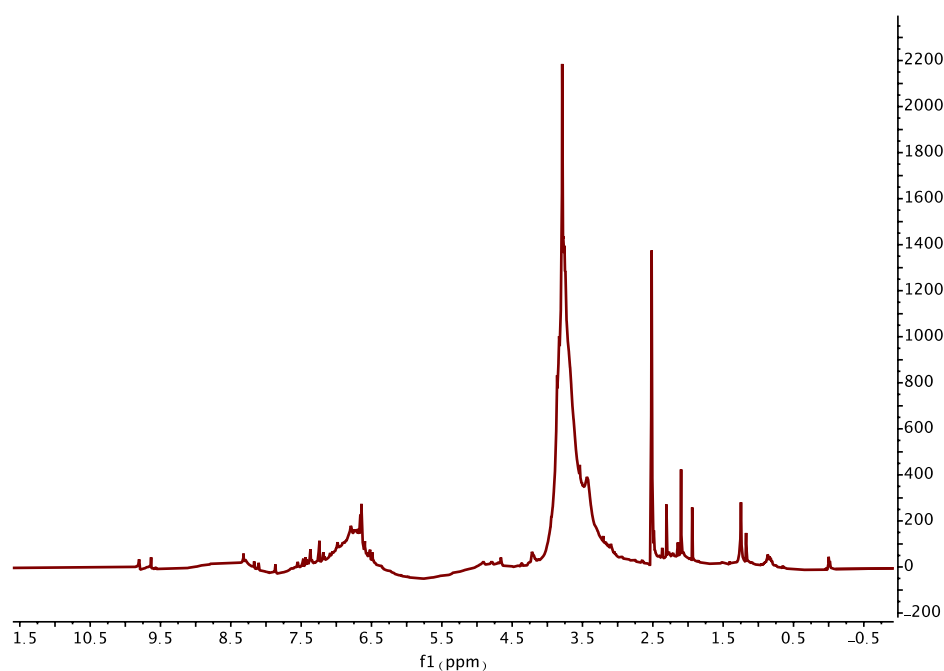


Figure S3-18. ¹H NMR of OSL in DMSO-*d*₆.

CHAPITRE 3

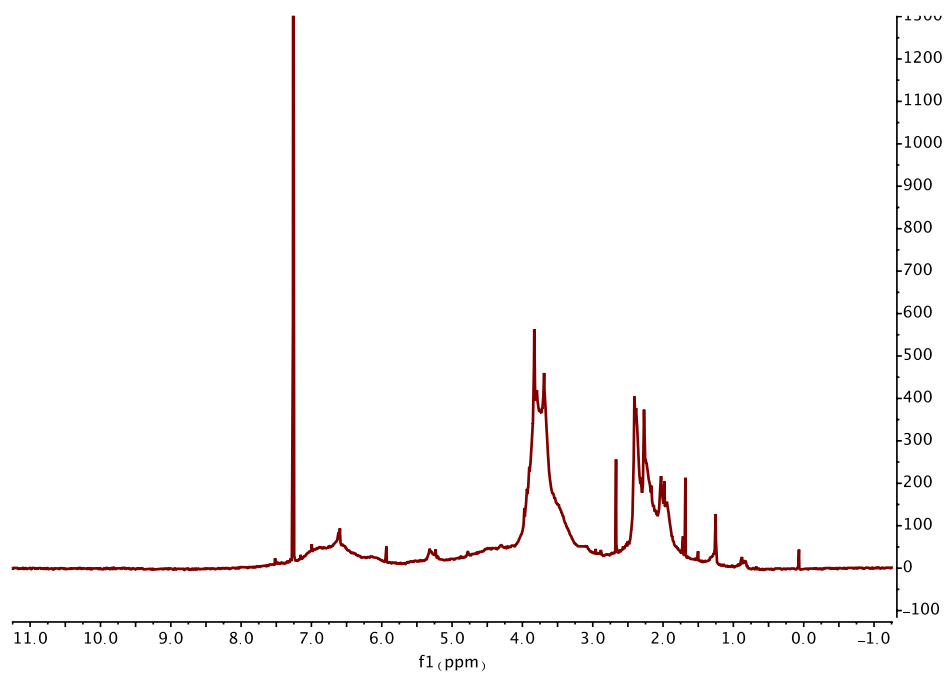


Figure S3-19. ¹H NMR of OL-AC in CDCl₃.

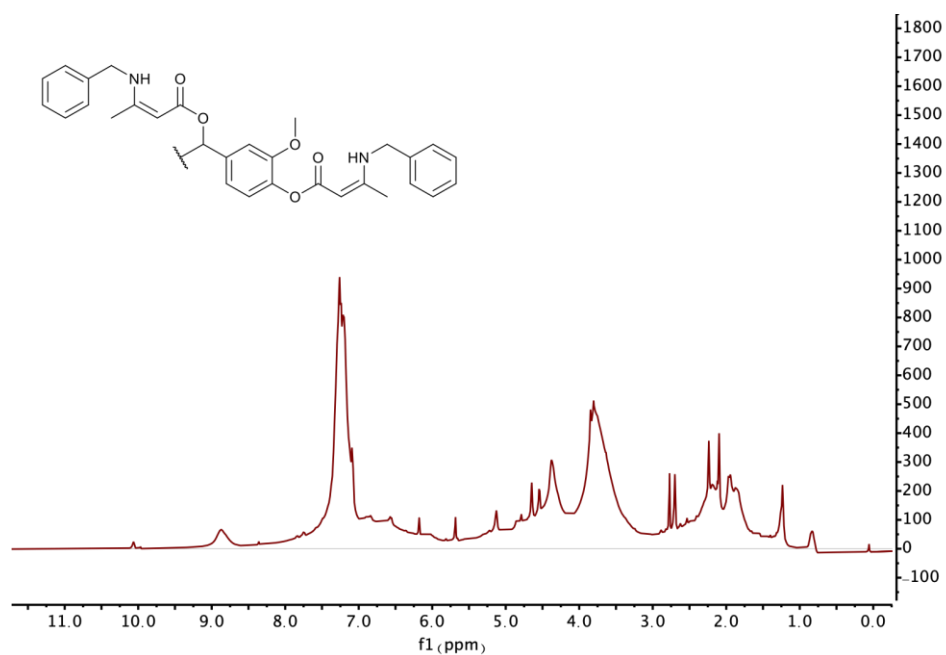


Figure S3-20. ¹H NMR Ph-VU-L in CDCl₃.

CHAPITRE 3

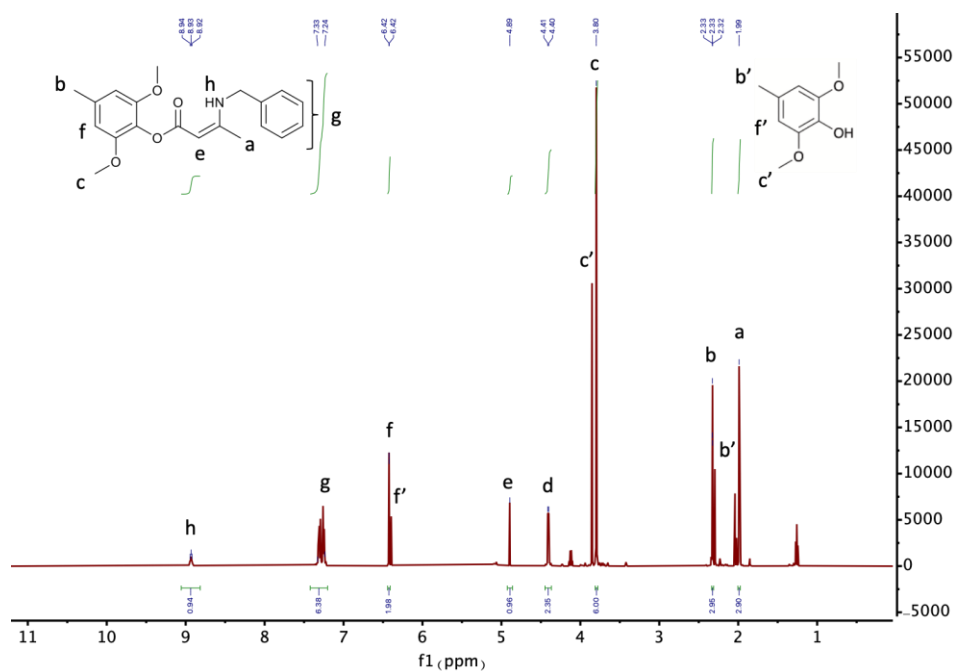


Figure S3-21. ^1H NMR Ph-VU in CDCl_3 .

^1H NMR (500 MHz, CDCl_3) δ 8.93 (t, $J = 6.2$ Hz, 1H), 7.24 (s, 6H), 6.42 (d, $J = 0.9$ Hz, 2H), 4.89 (s, 1H), 4.41 (d, $J = 6.3$ Hz, 2H), 3.80 (s, 6H), 2.34 – 2.31 (m, 3H), 1.99 (s, 3H).

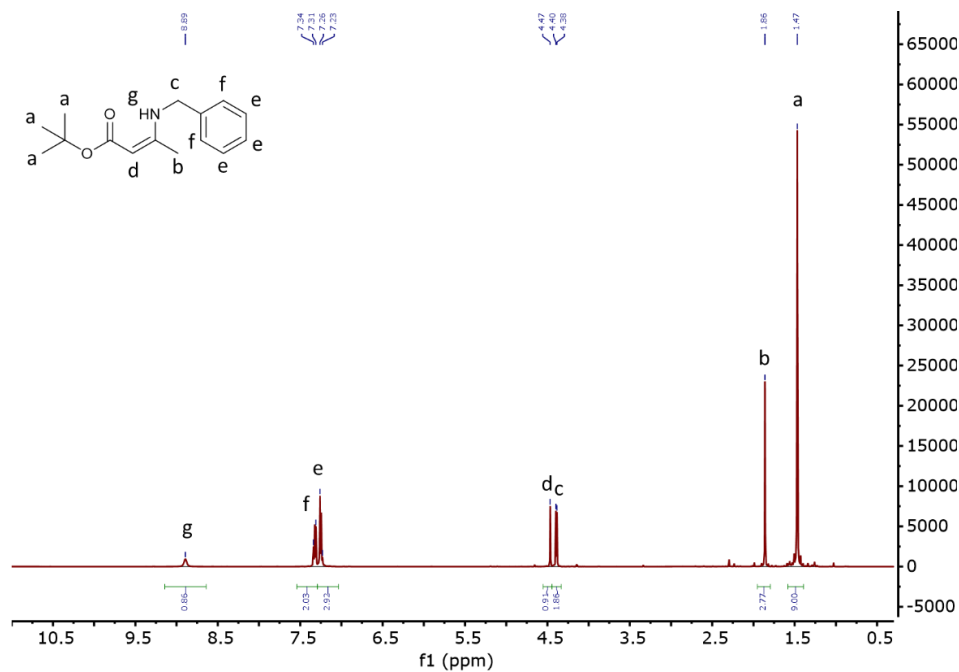


Figure S3-22. ^1H NMR of Al-VU in CDCl_3 .

^1H NMR (500 MHz, CDCl_3) δ 8.89 (s, 1H), 7.32 (d, $J = 15.0$ Hz, 2H), 7.24 (d, $J = 15.3$ Hz, 3H), 4.47 (s, 1H), 4.39 (d, $J = 6.5$ Hz, 2H), 1.86 (s, 3H), 1.47 (s, 9H).

CHAPITRE 3

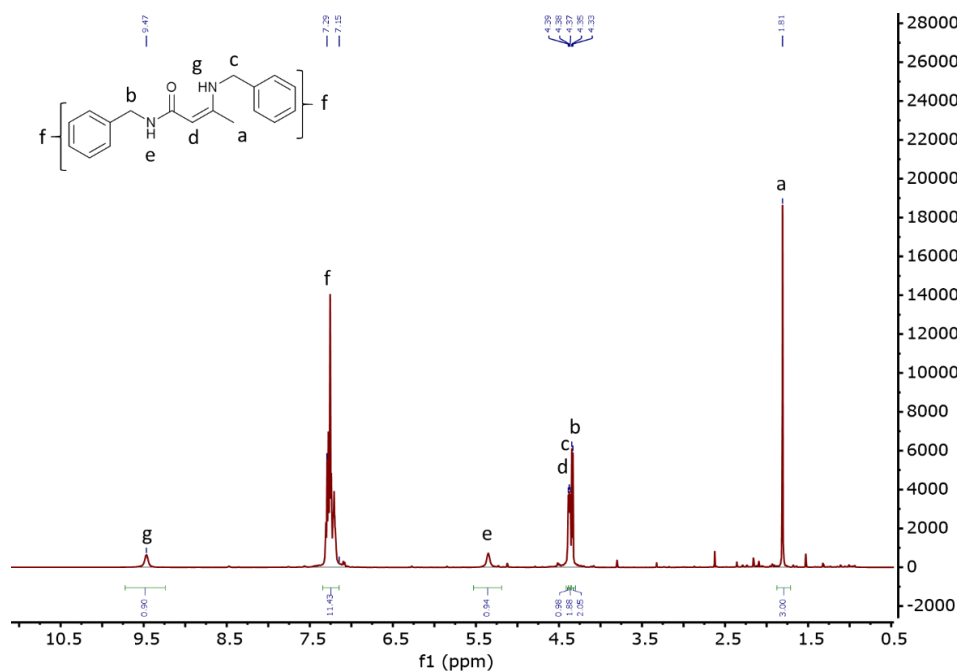


Figure S3-23. ¹H NMR of Ph-VU_N in CDCl₃.

¹H NMR (500 MHz, CDCl₃) δ 9.47 (s, 1H), 7.29 (s, 10H), 5.35 (s, 1H), 4.39 (s, 1H), 4.37 (d, J = 5.7 Hz, 2H), 4.34 (d, J = 6.5 Hz, 2H), 1.81 (s, 3H).

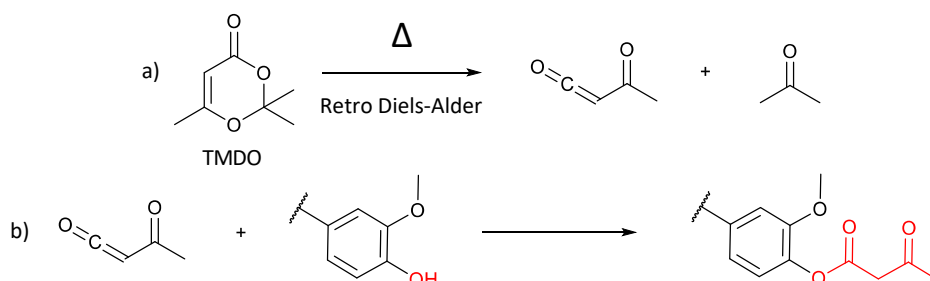


Figure S3-24. a) Production of a reactive acetylketene and acetone from TMDO via retro-Diels-Alder reaction, and b) acetoacetylation reactions between the formed acetylketene and nucleophile hydroxyls.

CHAPITRE 3

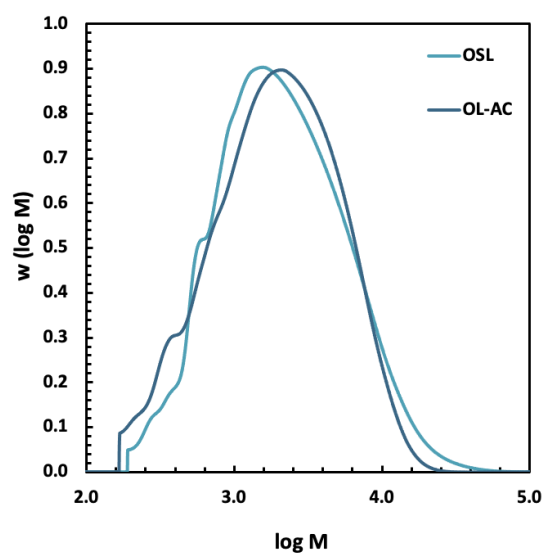


Figure S3-25. SEC curves of OSL and OL-AC in THF.

Table S3-8. SEC results of OSL and OL-AC.

Designation	M_n (g mol^{-1})	M_w (g mol^{-1})	\bar{D}
OSL	1340	3310	2.48
OL-AC	1180	2890	2.44

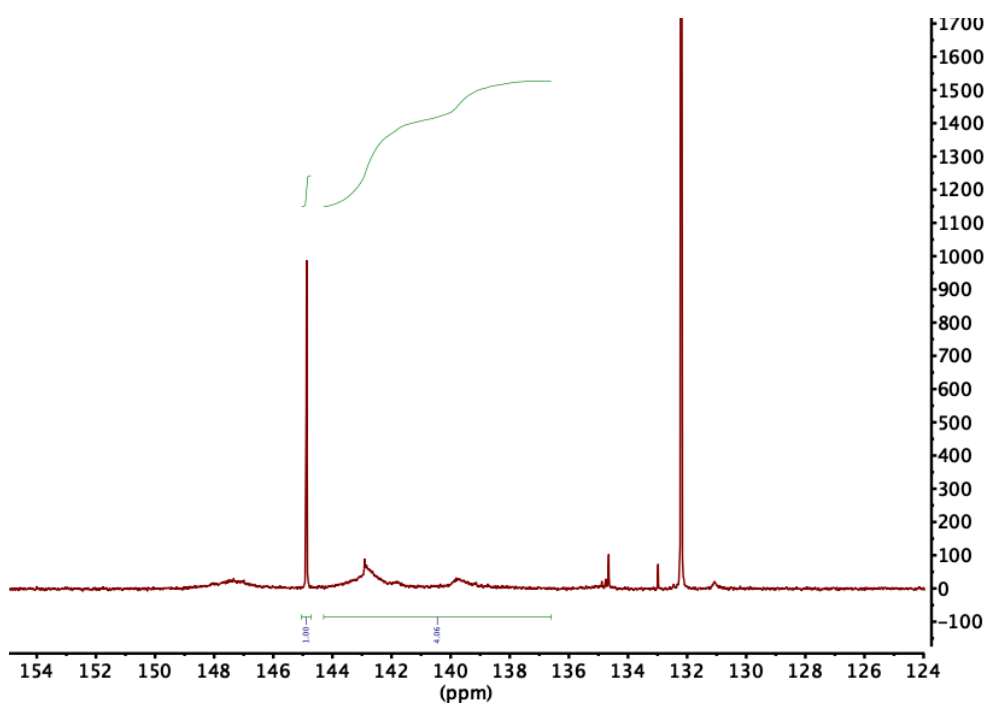


Figure S3-26. ^{31}P NMR of Ph-VU-01.

CHAPITRE 3

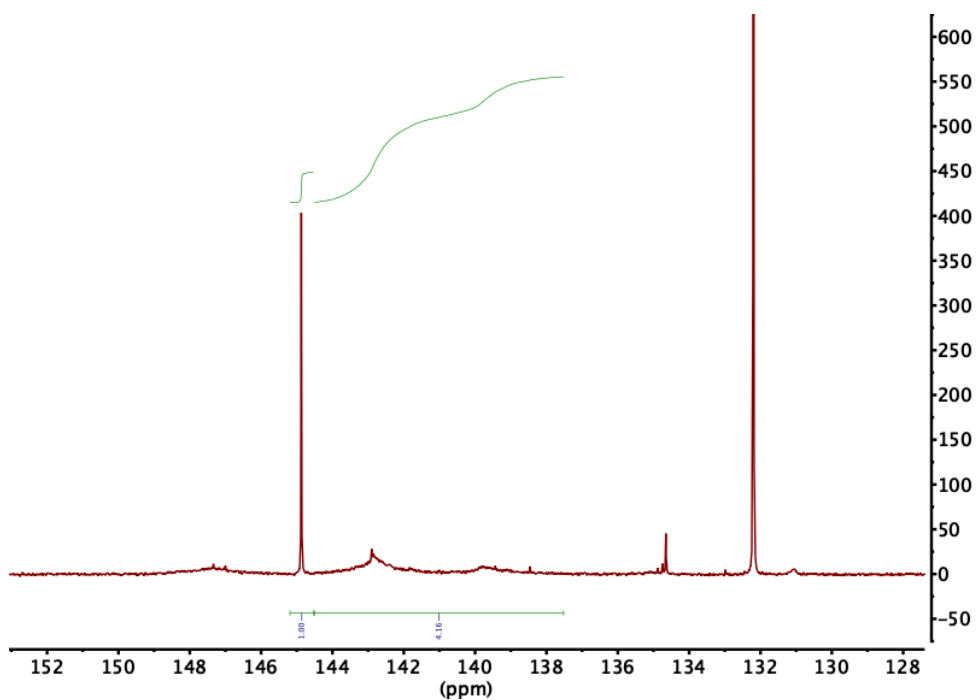


Figure S3-27. ^{31}P NMR of Ph-VU-02.

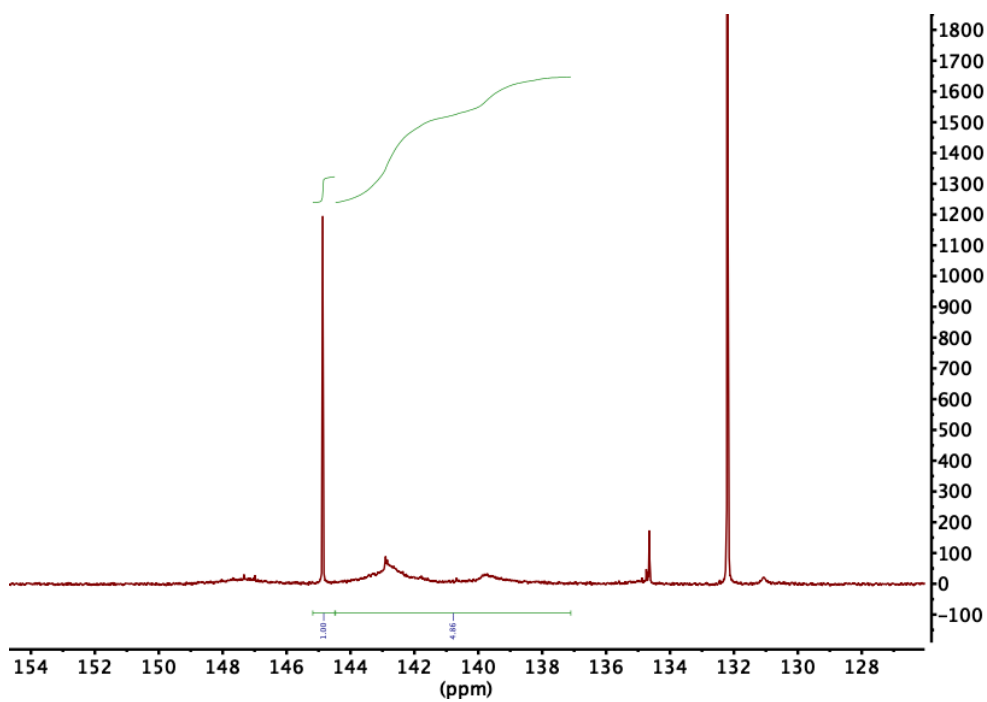


Figure S3-28. ^{31}P NMR of Ph-VU-03.

CHAPITRE 3

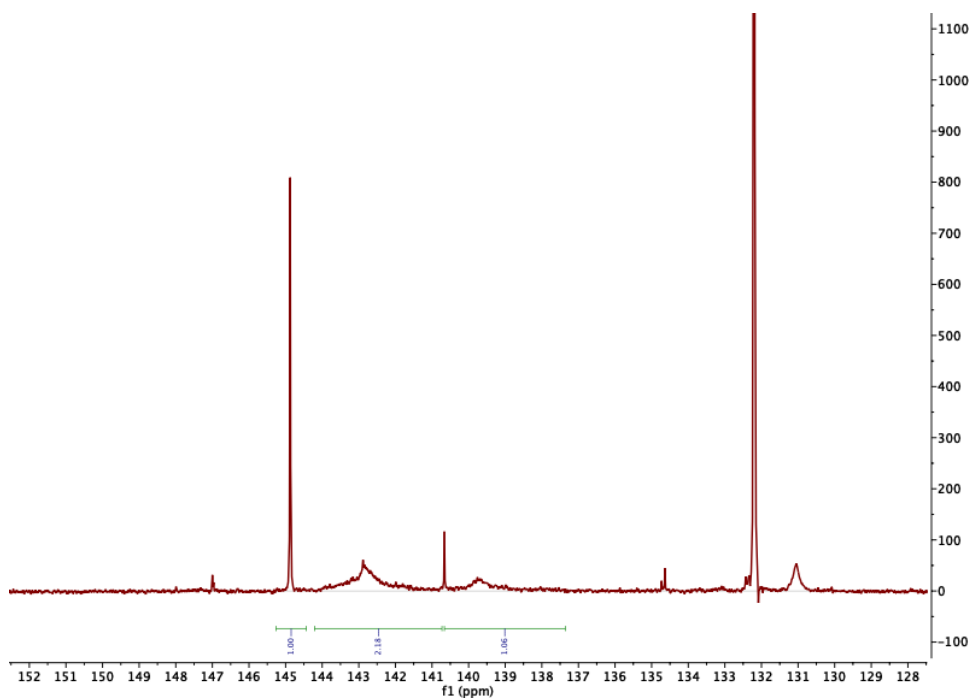


Figure S3-29. ^{31}P NMR of Ph-VU-L.

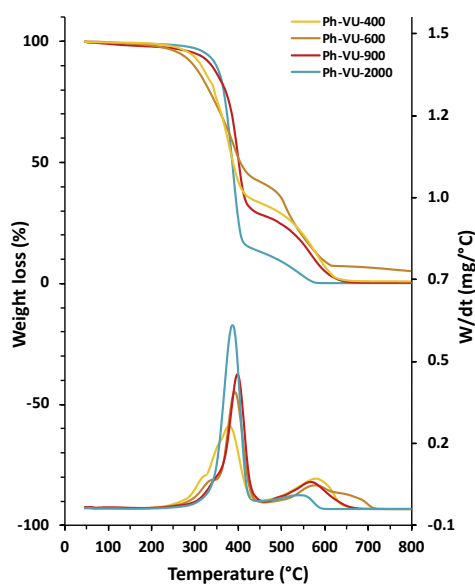


Figure S3-30. TGA curves of lignin-based VU networks.

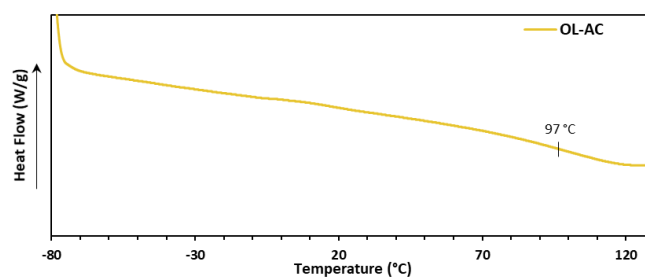


Figure S3-31. DSC curve of OL-AC.

CHAPITRE 3

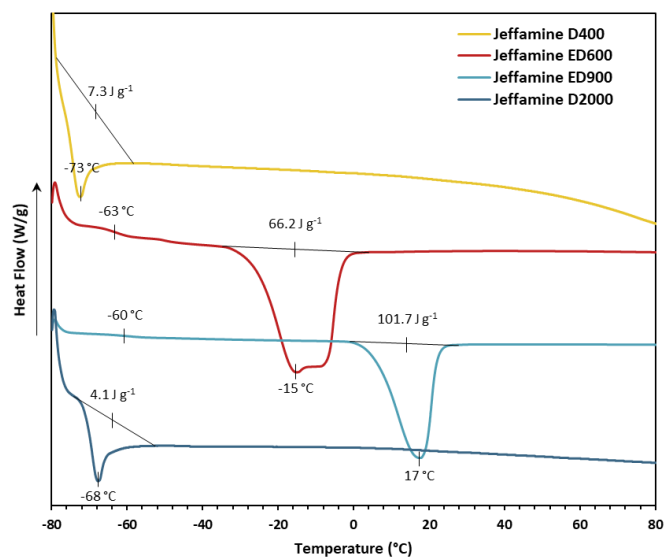


Figure S3-32. DSC curves of the diamines.

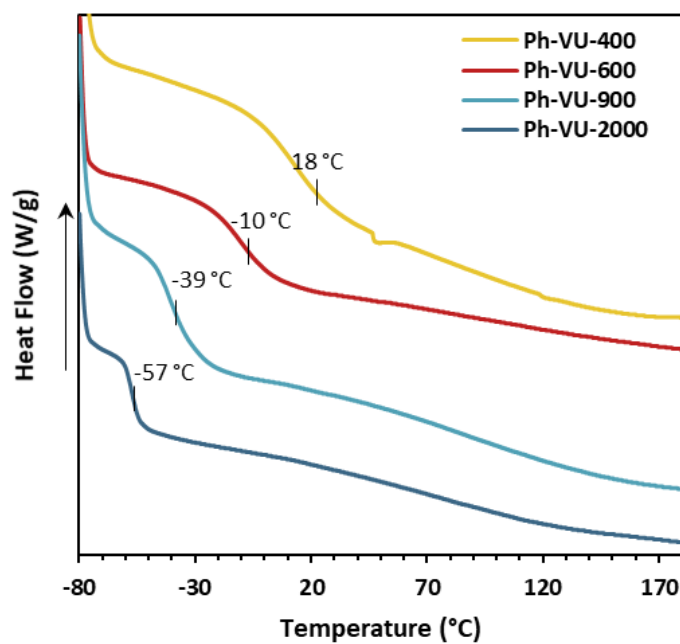


Figure S3-33. DSC curves of different Ph-VU materials.

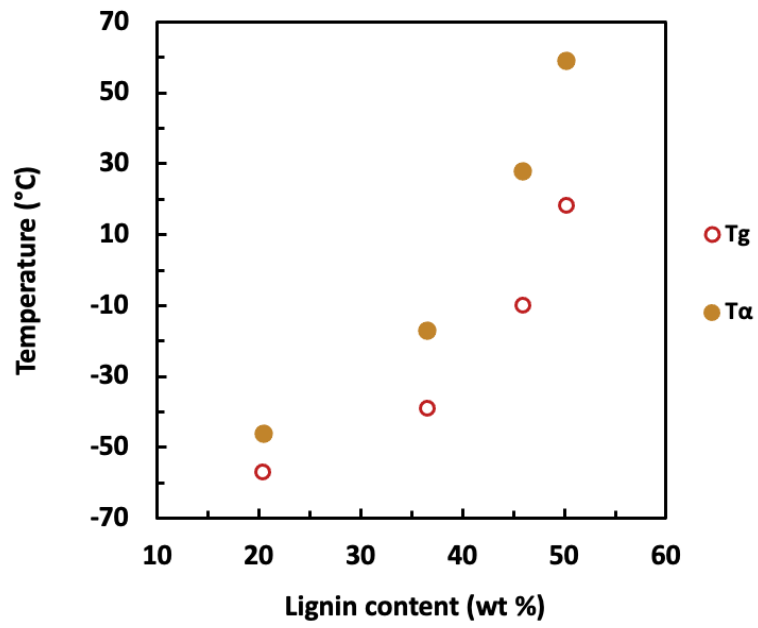


Figure S3-34. Evolutions of T_g and T_α with lignin content.

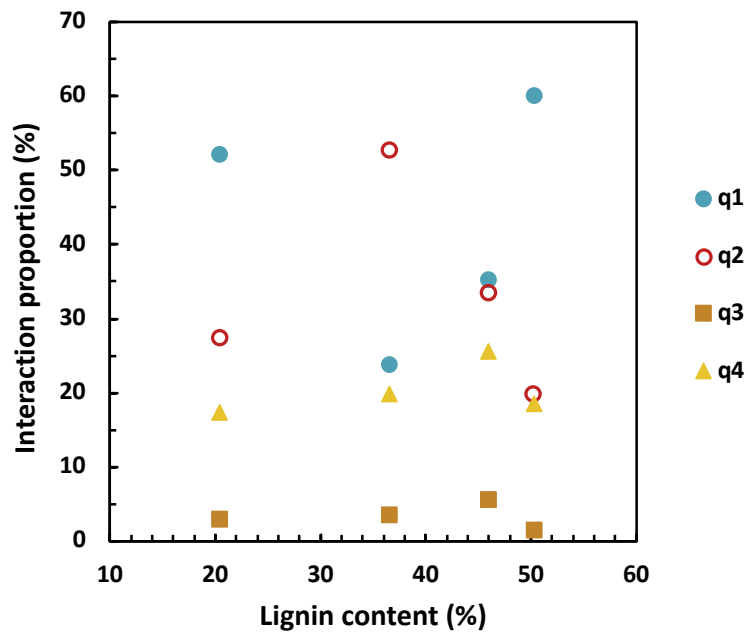


Figure S3-35. Evolutions of physical interaction proportions as a function of lignin content.

CHAPITRE 3

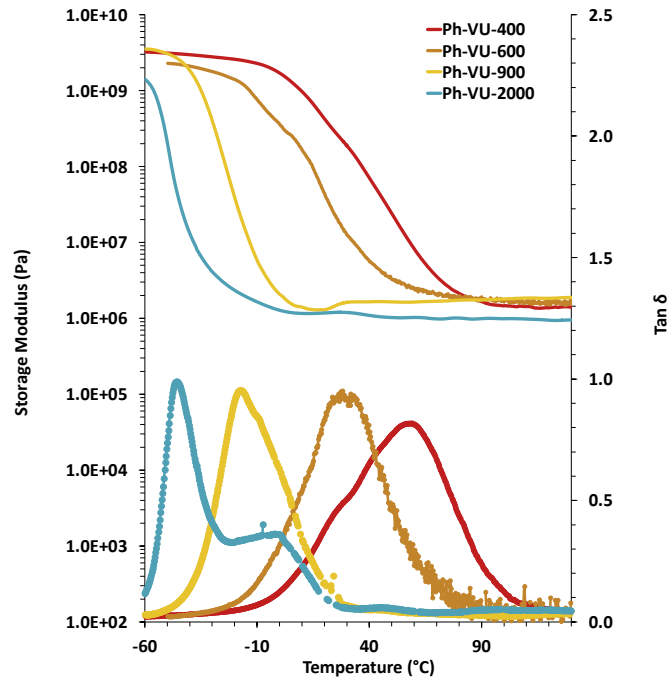


Figure S3-36. DMA curves of the Ph-VU materials.

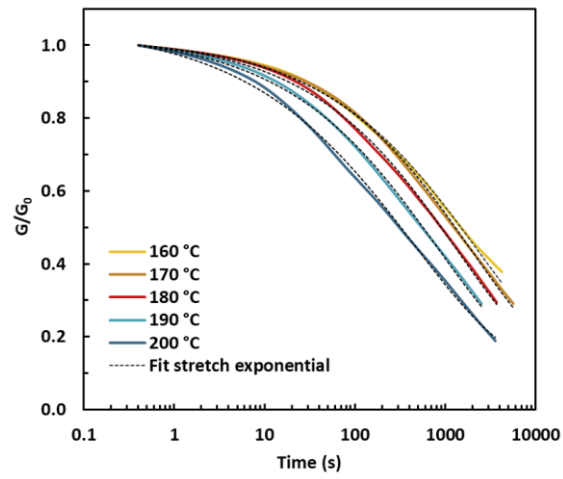


Figure S3-37. Stress relaxation curves of Ph-VU-600 at different temperatures.

CHAPITRE 3

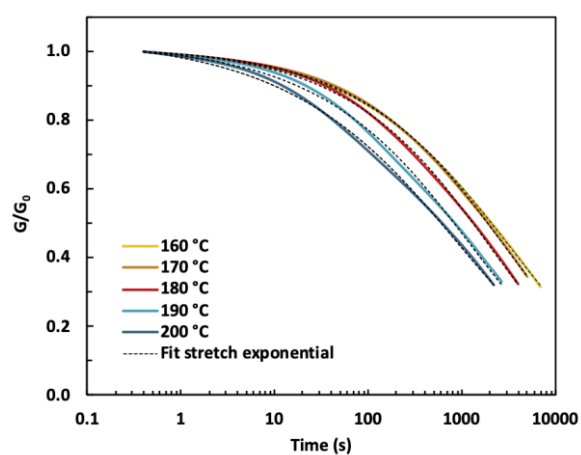


Figure S3-38. Stress relaxation curves of Ph-VU-900 at different temperatures.

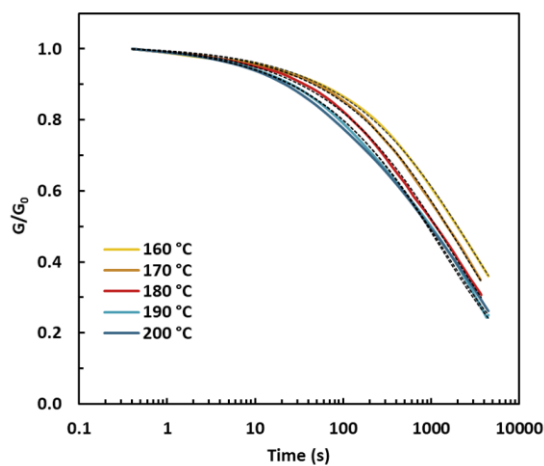


Figure S3-39. Stress relaxation of Ph-VU-2000 at different temperatures.

Table S3-9. Parameters used for T_v calculation of each vitrimer.

VU (Designations)	G' (Pa)	τ^* (s)	A	B	T_v (°C)
Ph-VU-400	1.37E+06	2.19E+06	9.619	-14.475	58
Ph-VU-600	1.85E+06	1.62E+06	7.273	-8.015	53
Ph-VU-900	1.65E+06	1.81E+06	5.690	-4.187	33
Ph-VU-2000	1.16E+06	2.59E+06	3.952	-0.059	-6

CHAPITRE 3

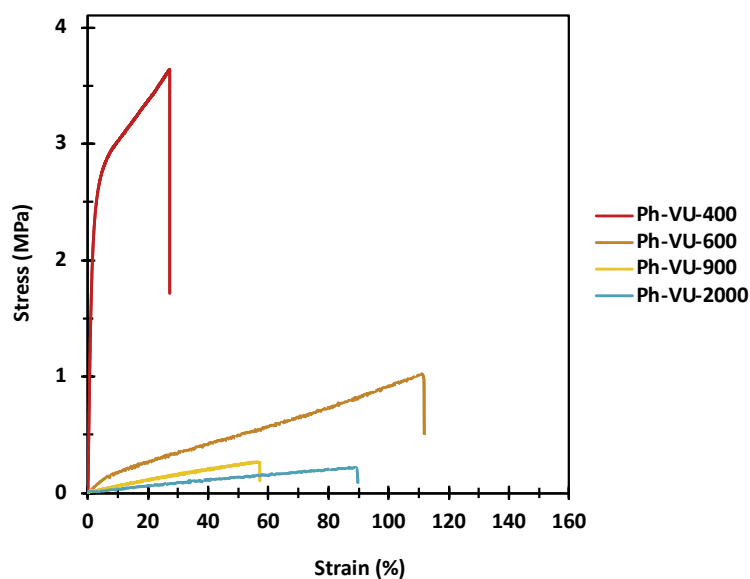


Figure S3-40. Stress-strain curves of the vitrimer series.

Table S3-10. Swelling ratios (SR) and gels fractions (GF) in acetone and water of the vitrimer series.

VU (Designations)	SR _{acetone}	SR _{water}	GF _{acetone}	GF _{water}
Ph-VU-400	150.9 ± 3.1	34.4 ± 2.9	63.2 ± 0.5	99.1 ± 0.1
Ph-VU-600	104.1 ± 2.3	130.9 ± 8.7	77.1 ± 0.2	81.9 ± 0.4
Ph-VU-900	138.0 ± 2.1	239.3 ± 4.5	77.5 ± 0.6	80.9 ± 0.2
Ph-VU-2000	421.1 ± 19.4	11.9 ± 0.1	69.2 ± 1.2	98.5 ± 0.2

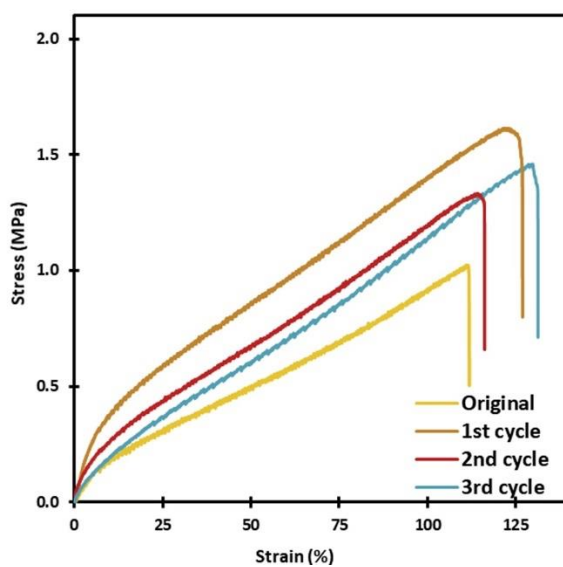


Figure S3-41. Uniaxial stress-strain curves of Ph-VU-600 upon three physical recycling cycles.

CHAPITRE 3

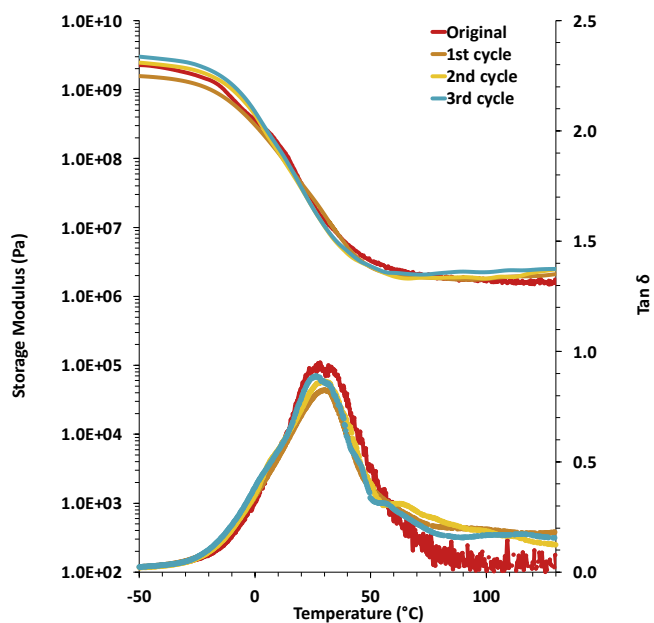


Figure S3-42. DMA curves of pristine and physically recycled Ph-VU-600 after different cycles.

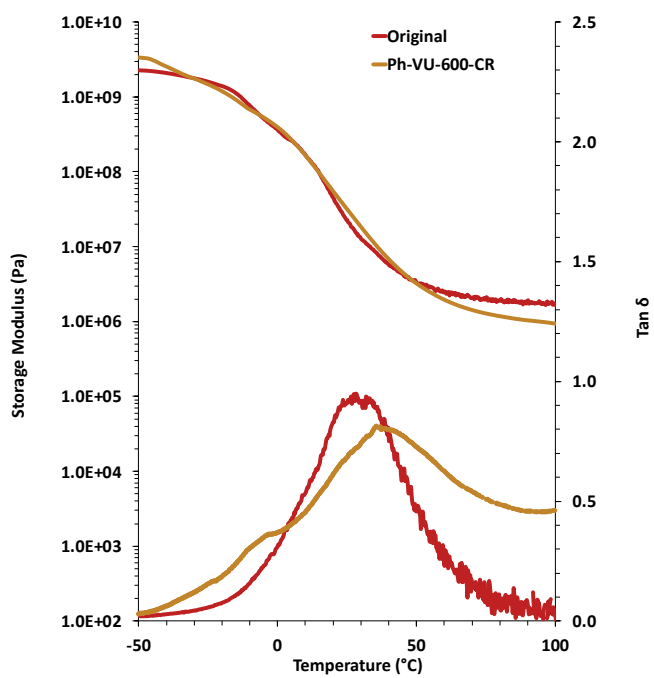


Figure S3-43. DMA of chemically recycled Ph-VU-600.

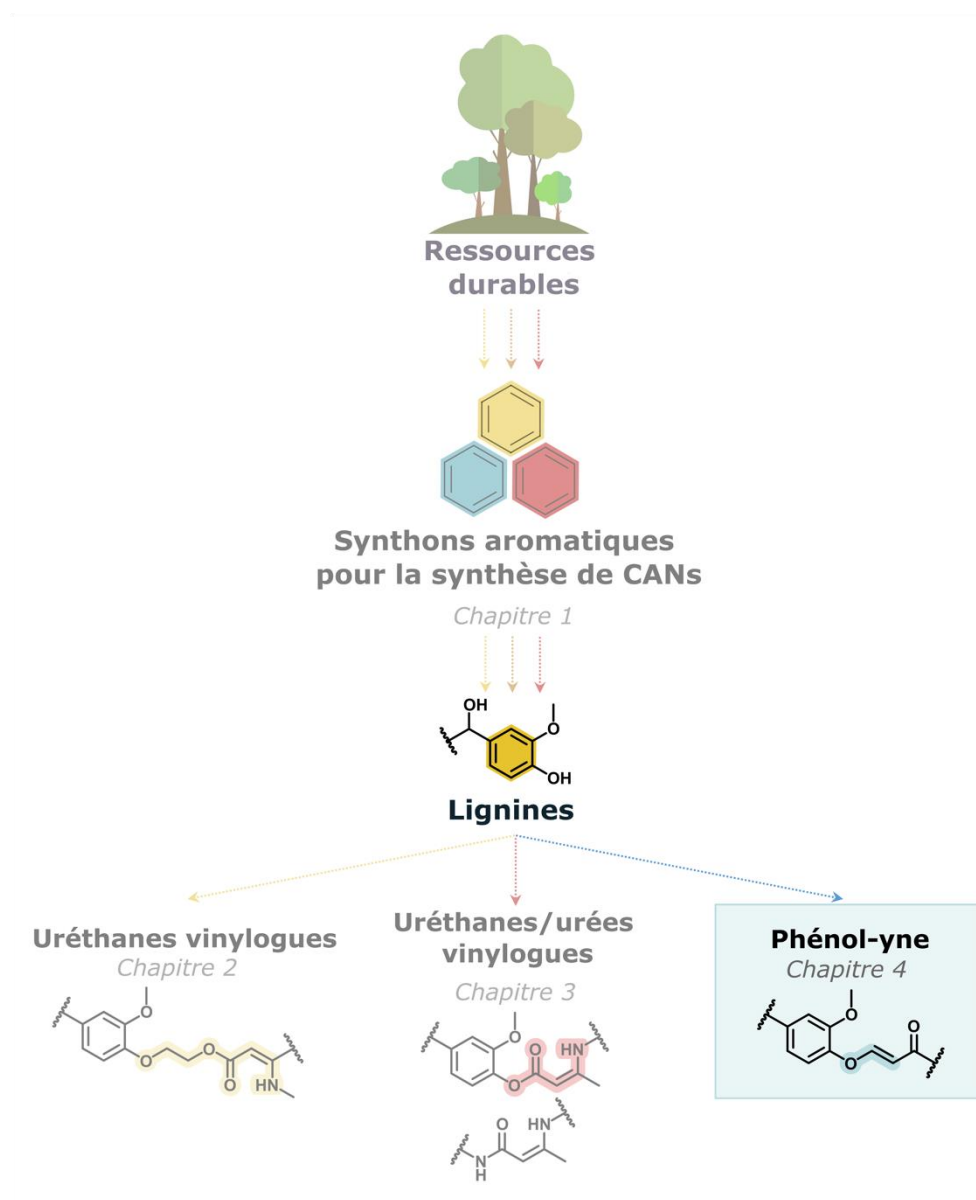
CONCLUSION DU CHAPITRE 3

Ce second chapitre expérimental propose une nouvelle voie de synthèse de polymères uréthanes vinylogues aromatiques, renouvelables, durables et recyclables à partir de lignine comportant un nombre d'étapes de modifications limité.

La modification chimique en une seule étape de synthèse d'une lignine organosolv en macromonomère acétoacétate a dans un premier temps été développée, permettant d'obtenir un synthon renouvelable hautement fonctionnalisé grâce à une bonne conversion des groupements hydroxyles aliphatiques et aromatiques de la lignine. L'utilisation du chloroforme, solvant à faible dipôle, lors de la condensation de cette lignine modifiée avec la benzylamine, a montré favoriser la formation de liaisons uréthanes vinylogues et ainsi limiter le dé-greffage de groupements phénoliques conduisant à la dissociation de la lignine du réseau. L'utilisation de l'acide acétique, également catalyseur des réactions de transaminations, a révélé favoriser que marginalement la génération d'uréthanes vinylogues par rapports aux urées vinylogues. Sur la base de ces observations, une gamme de matériaux contenant une forte teneur en lignine a pu être synthétisée par condensation de la lignine acétoacétylée avec des polyétheramines. La présence d'un groupement méthyl sur le squelette de la diamine a montré entraver la capacité des matériaux à former des liaisons hydrogènes, augmentant ainsi leur résistance à l'eau. Des gonflements plus faibles et des fractions de gel plus élevées ont ainsi pu être obtenus dans l'eau, par rapport aux matériaux comportant un bloc de polyéthylène glycol.

Les polymères obtenus présentent un comportement de vitrimère. L'utilisation des polyétheramines β -méthylées permettent de ralentir les échanges de liaisons par transaminations par rapports aux résultats précédemment obtenus sur les vitrimères uréthanes vinylogues dans le chapitre 2. Un des matériaux a cependant pu être recyclé par recyclage physique sur plusieurs cycles consécutifs en préservant sa structure chimique ainsi que ses propriétés mécaniques et rhéologiques. Enfin, dans un contexte de recyclage chimique, une nouvelle stratégie de valorisation des matériaux uréthanes vinylogues en fin de vie par dépolymérisation en milieu acide a fait l'objet d'une preuve de concept, permettant d'obtenir un réseau polymère de seconde génération. Cette approche rend donc normalement possible la récupération de la lignine acétoacétylée, ouvrant la voie à de nouvelles opportunités de revalorisation dans une approche circulaire "cradle to cradle".

CHAPITRE 4. CHIMIE PHENOL-YNE POUR LA CONCEPTION DE VITRIMERES A BASE DE LIGNINE : VERS DES MATERIAUX DURABLES ET RECYCLABLES



INTRODUCTION DU CHAPITRE 4

Ce dernier chapitre expérimental est aussi un chapitre d'ouverture sur l'utilisation de lignines pour la synthèse de nouvelles architectures aromatiques renouvelables dynamiques en exploitant la chimie émergente phénol-yne. Cette chimie covalente dynamique présente l'avantage d'être une addition-click entre un phénol et un alcyne activé. Cette réaction permet d'atteindre une économie totale en atomes. De plus, aucune modification chimique au préalable des lignines n'est nécessaire pour les rendre plus réactives, contrairement aux travaux précédents présentés dans les chapitres 2 et 3 de ce mémoire de thèse. Ainsi, la chimie phénol-yne semble parfaitement compatible avec les principes de chimie verte, pour le développement de nouveaux CANs aromatiques et biosourcés.

Une première étude porte sur l'évaluation et l'étude, à l'aide de molécules modèles mimant des parties de l'architecture de lignines, de l'impact de la substitution de phénols par des groupements méthoxy en position ortho sur la capacité des phénols à subir des réactions d'échanges. Les cinétiques d'addition des hydroxyles aliphatiques et phénoliques sur des alcynes activés a ensuite été étudiée sur des molécules modèles représentatives de la structure hétérogène des lignines. En accord avec les principes de chimie verte, différentes sources de lignine soufrée et non-soufrées (kraft et organosolv) ont été sélectionnées pour la synthèse de matériaux. De manière à évaluer l'influence de la masse molaire de la lignine, une lignine organosolv partiellement dépolymérisée a également été retenue pour cette étude. Les polymères ont été synthétisés par réaction des lignines avec un agent de réticulation dialcynes dérivé de polyéthylène glycol. Les propriétés thermiques, mécaniques et rhéologique des matériaux ont été largement analysées. La circularité en fin de vie des matériaux a été particulièrement étudiée par (i) recyclage physique, sur plusieurs cycles consécutifs, et (ii) recyclage chimique par hydrolyse acide des liaisons éthers d'énol et esters. Ceci a fait l'objet d'une étude finale, permettant de récupérer une lignine de seconde génération, dans une approche circulaire du type "cradle-to-cradle" (berceau-au-berceau).

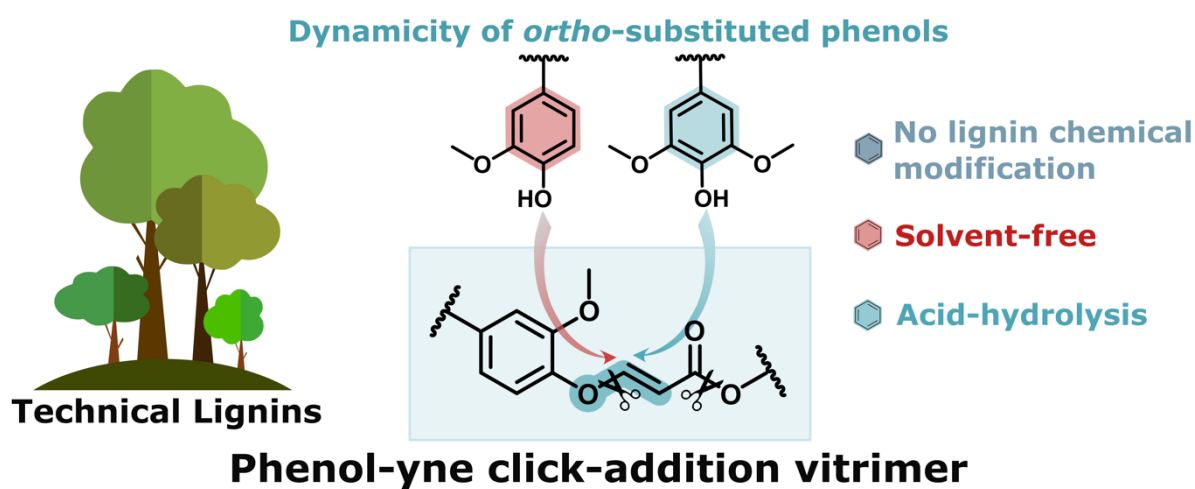
PHENOL-YNE CHEMISTRY FOR THE DESIGN OF LIGNIN-BASED VITRIMERS: TOWARDS SUSTAINABLE AND RECYCLABLE MATERIALS

Lisa Sougrati ^a, Antoine Duval ^{a, b, *}, Luc Avérous ^{a, *}

^a BioTeam/ICPEES-ECPM, UMR CNRS 7515, Université de Strasbourg, 25 rue Becquerel, 67087 Strasbourg, Cedex 2, France

^b Soprema, 15 rue de Saint Nazaire, 67100, Strasbourg, France

*Corresponding authors.



1. ABSTRACT

Lignins are the main source of renewable aromatic compounds on Earth. These polyphenols of high functionality are biobased building blocks of great interest for the development of performing aromatic polymer materials. However, one shortcoming of subsequent thermosets is their lack of efficient recyclability, increasing their environmental impact in a context where the need for performing materials with controlled end-of-life is paramount. In that frame, the conceptualization of lignin-based vitrimers is an attractive solution to tackle this global challenge. In this work, we report the synthesis, evaluation and recycling of lignin-based phenol-yne vitrimers, in a context of circular bioeconomy. The potential of *ortho*-substituted phenols by one or two methoxy groups (G and S units) to undergo vinyl ether bond exchanges was examined with model compounds. Then, the addition kinetics of aliphatic hydroxyls and di-substituted phenols was investigated on model molecules representatives of lignin heterogeneous reactive groups. Subsequently, a series of materials from different lignin sources were prepared via a one-step click-addition, in solvent-free conditions, and achieving full atom-economy, in accordance with green chemistry principles. These high lignin-content (from 39 to 49%) vitrimers were duly characterized. Thermal, morphological, rheological, and mechanical properties were fully assessed. The vitrimers could undergo rearrangement through vinyl ether bond exchanges. Relaxation times from 44 to 290 s were obtained at 200 °C. The determined activation energy are from 77.7 to 91.3 kJ mol⁻¹. The networks structures and properties were analyzed through successive physical recycling steps. Their chemical recycling potential via acid-catalyzed hydrolysis was also surveyed. The results clearly showed a proof-of-concept for the closed-loop recycling of lignin-based phenol-yne vitrimers, offering further upcycling opportunities for the development of sustainable aromatic materials for a greener future, towards a cradle-to-cradle approach.

2. INTRODUCTION

Lignocellulosic biomass is the main source of aromatic renewable compounds on Earth. Lignin is a major fraction of this feedstock, mainly associated with cellulose and hemicellulose, representing up to 40% of its dry weight. It has emerged as a large and attractive source of phenols for the design of sustainable and performant aromatic polymers. Lignin is an amorphous polyphenol with a complex structure, which arises from the polymerization of three main aromatic precursors called monolignols: coniferyl alcohol, sinapyl alcohol, and p-coumaryl alcohol, often referred to as G, S and H units, respectively. Lignin architecture mainly varies according to the feedstock botanical origin and the extraction process. According to the extraction method different lignins can be obtained, with or without sulfur (Figure 4-1).

The subsequent polyphenols are highly functionalized by aliphatic and phenolic (mainly G and S) hydroxyls (OHs), enabling facile utilization as building blocks for the preparation of high-performance thermosets. Nonetheless, the highly crosslinked structures of ensuing polymer networks present limited recycling opportunities due to their inability to melt, which is a major challenge in a global context of profound environmental concerns.

Tackling end-of-life issues for thermosets, covalent adaptable networks (CANs) are an ingenious novel class of polymers benefiting from thermosets and thermoplastic most sophisticated features by enabling recycling (as a thermoplastic) without compromising the mechanical properties (as a thermoset) (Kloxin et al., 2010; Bowman and Kloxin, 2012; J. Kloxin and N. Bowman, 2013). By incorporating within 3D networks stimuli responsive bonds sensible to temperature, light or pH variations for instance, these networks can undergo bond rearrangements inducing a macroscopic flow. CANs are generally divided in two main categories according to their bond exchange mechanisms. Dissociative CANs are subjected to the dissociation of the initial bond prior to the formation of a new one, resulting in a decreased viscosity and in some instance to depolymerization. Conversely, associative CANs, also classified as vitrimers, rely on the formation of a new bond onto the initial one prior to the bond cleavage, maintaining a constant crosslinking density (Montarnal et al., 2011; Capelot et al., 2012;

Winne et al., 2019). Because of the wide range of dynamic covalent chemistries, the development of recyclable alternatives to conventional polymers has been spread to different polymers types such as polyolefins, polyesters, polyimines, and polyurethanes (Ahmadi et al., 2022; Breuillac et al., 2019; Dhers et al., 2019; McBride et al., 2019; Zheng et al., 2021).

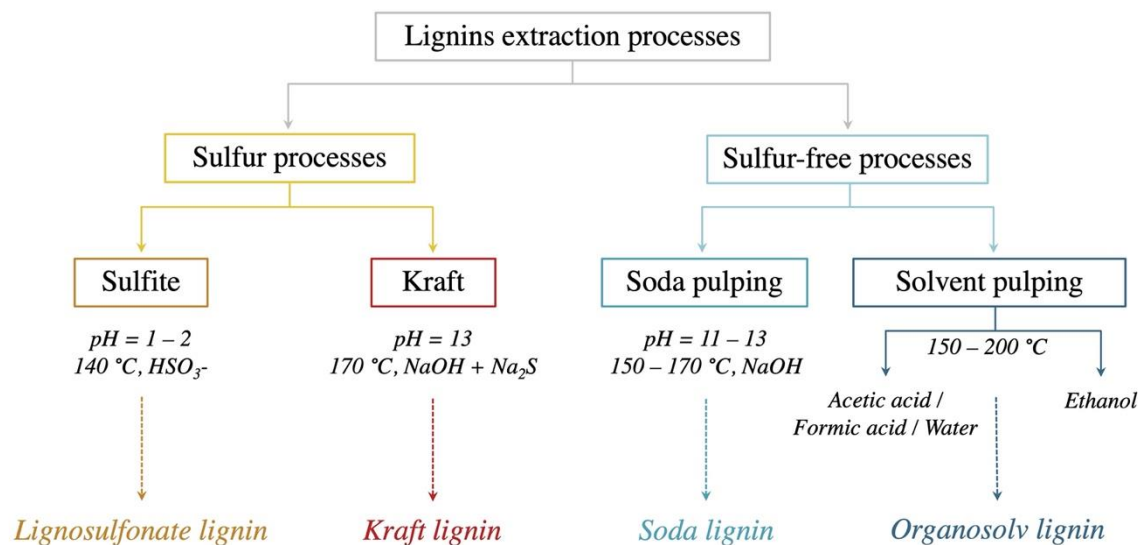


Figure 4-1. Extraction processes to separate lignin from lignocellulosic biomass for the production of technical lignins. Adapted from (Laurichesse and Avérous, 2014).

To reduce the environmental impact with sustainable materials and embrace a circular bioeconomy strategy, the design of vitrimers derived from biomass is an elegant answer to tackle both the valorization of biomass and the recyclability at the end-of-life (Lucherelli et al., 2022; Vidil and Llevot, 2022; Zhao et al., 2022). Aromatic structures present strong advantages such as high mechanical properties and fire resistance. Then, recently, they have also gained particular interest in the field of CANs (Tiz et al., 2023). Lignin has emerged as an attractive structure because of its compatibility with a great array of potential covalent dynamic chemistries. The valorization of lignin within CANs was successfully reported using various dynamic chemistries in polyester, polyurethane, vinylogous urethane, disulfide, and Diels-Alder networks (Buono et al., 2017; Duval et al., 2015, 2024, 2024; Gao et al., 2020; Liu et al., 2020; Ma et al., 2023; Moreno et al., 2021; Sougrati et al., 2023a; Thys et al., 2021). The design of these materials necessitates the chemical modification of lignin to enhance its reactivity, to homogenize its reactive end groups, or to graft new functions. This usually requires multi-step syntheses, consuming significant amounts of reagents and solvents and generating substantial wastes. In an approach aiming to reduce the environmental impact of polymer materials, the limitation of the number of chemical modifications is paramount to follow green chemistry principles and to facilitate eventual industrialization.

Green chemistry principles represent a powerful framework in the design of materials with a positive effect on the environmental. Those principles are mainly established on the use of renewable feedstock, less hazardous chemicals and solvents, atom-economy, for the design of safer and/or degradable products (Anastas and Eghbali, 2010). In that respect, it is crucial to thoroughly privilege pathways with a minimal number of steps and substantial atom-economy syntheses to minimize wastes of valuable fractions. In this context, the emerging and still under-exploited phenol-yne dynamic chemistry is an elegant and rich approach for the valorization of lignin into high performance, recyclable and sustainable materials. This strategy relies on the click-addition of phenols with activated alkynes under basic catalysis, which can undergo bond exchanges through addition/elimination pathways, inducing dynamicity (Fu et al., 2024; Santos et al., 2022; Shi et al., 2017; Zhang et al., 2022). Phenol-yne has the

potential to enable the rapid preparation of lignin-based materials in a single atom-efficient step, without the prior chemical modification of lignin.

The aim of this study is to report for the first time, as far as we know, the synthesis of phenol-yne (PY) vitrimers with high lignin content, till about 50 wt%. In a first step, the impact of phenols *ortho*-substitution by methoxy groups (G and S units) on the bond exchange process was carefully analyzed using different model molecules. The click-addition of aliphatic and phenolic OHs with activated alkynes was then investigated on model compounds representatives of lignin heterogeneous structure. A polyethylene glycol (PEG)-derived activated dialkyne crosslinker was synthesized by esterification with propiolic acid, in bulk. Following green chemistry principles, a series of vitrimers was prepared using different lignin sources based on sulfur and sulfur-free process such as kraft (KL) and organosolv (OSL) lignins. Besides, to analyze the effect of the lignin molar mass, partially depolymerized organosolv lignin (DOSL) was also used. They were reacted via a one-step click-addition with the PEG crosslinker in solvent-free conditions, leading to total atom-economy (Figure 4-2). Their structures, thermal, rheological, and mechanical properties were duly characterized. The end-of-life of these materials was investigated via physical recycling, after several cycles. Alternatively, chemical recycling potential was studied through acid-catalyzed hydrolysis of vinyl ether and ester bonds, paving the way to closed-loop recycling approach enabling to recover both pristine lignin and PEG, towards a cradle-to-cradle approach.

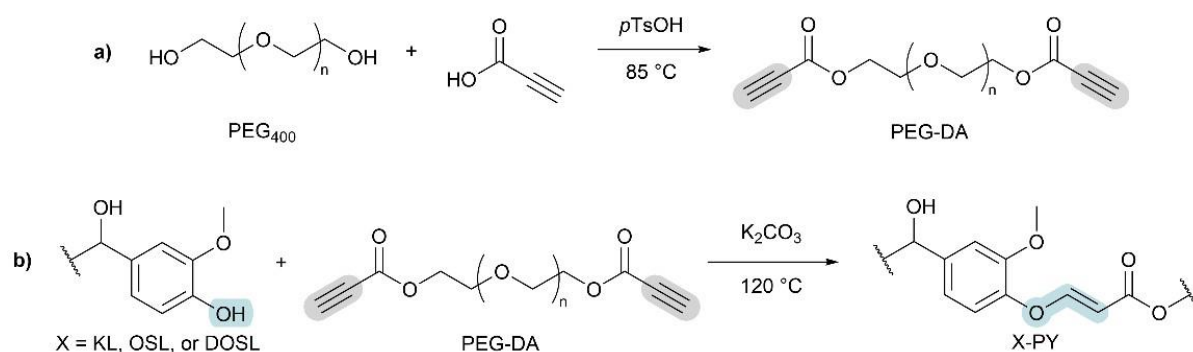


Figure 4-2. Synthetic pathway for the preparation of a) PEG dialkyne crosslinker (PEG-DA), and b) phenol-yne (PY) networks from KL, OSL, and DOSL.

3. EXPERIMENTAL SECTION

3.1. Materials

BioPivaTM100 softwood KL in powder was supplied by UPM Biochemicals (Helsinki, Finland). KL is a medium weight-average molar mass lignin (M_w around 5000 g mol⁻¹). OSL was isolated at pilot scale from industrial size beech wood using the aqueous acetone FabiolaTM process (TNO, Petten, Netherland). Detailed characterization of this lignin has been formerly described (as P-BEC-3) (Smit et al., 2022). OSL is a low number-average molar mass lignin (M_n below 1400 g mol⁻¹). Partially depolymerized lignin (DOSL) was obtained by catalytic depolymerization of OSL (TNO, Petten, Netherland). The steps of this reductive depolymerization and details of DOSL characterizations have been previously described (Smit et al., 2023). The aliphatic and phenolic OH contents of KL, OSL, and DOSL were measured by ³¹P NMR which rely on the reaction of lignin different OH groups with a phosphorylating agent (Cl-TMDP). Al-OH were integrated from 145.4 to 150.0 ppm and Ph-OH from 137.6 to 144.0 ppm (Pu et al., 2011). ³¹P NMR are available in Figure S4-27, in appendices (SI). OHs contents and physicochemical characterizations of KL, OSL, and DOSL are reported in Table 4-1. Size-exclusion chromatography curves are displayed in Figure S4-28 in SI. Lignins were dried overnight at 50 °C prior to utilization.

Table 4-1. Main chemical and physicochemical parameters of KL, OSL, and DOSL.

Lignin	Al-OH content (mmol g ⁻¹)	Ph-OH content (mmol g ⁻¹)	S and condensed units (mmol g ⁻¹)	G units (mmol g ⁻¹)	H units (mmol g ⁻¹)	M _n (g mol ⁻¹)	M _w (g mol ⁻¹)	Đ
KL	2.48	4.33	1.95	2.17	0.24	1580	5270	3.3
OSL	1.74	2.89	2.19	0.60	0.08	1340	3310	2.5
DOSL	2.17	3.27	2.39	0.78	0.09	1280	2310	1.8

Potassium carbonate anhydrous (K₂CO₃, ≥ 99%), benzyl alcohol (99%), 3,4,5-trichloropyridine (TCP, 98%), ethyl acetate (99%), and magnesium sulfate were obtained from Thermo Fisher Scientific. Polyethylene glycol with number-average molar mass of 400 g mol⁻¹ (PEG₄₀₀), *p*-Toluenesulfonic acid monohydrate (*p*TsOH, 99%), sodium bicarbonate (NaHCO₃, 99.7%), and dimethyl sulfoxide anhydrous (DMSO, ≥ 99.7%) were obtained from Acros Organics. Ethyl propiolate (EP, 99%), propiolic acid (95%), 2-methoxyphenol, 2,6-dimethoxyphenol (99%), 4-methyl-2,6-dimethoxyphenol (S, ≥ 97%), 2-methoxy-4-methylphenol (G, ≥ 98%), 1-butanol, chromium (III) acetyl acetonate (Cr(acac)₃, 97%), cholesterol (> 99%), deuterated chloroform (CDCl₃), hydrochloric acid (37% in water), 2-chloro-4,4,5,5-tetramethyl-1,3,2-dioxaphospholane (Cl-TMDP, 95%) and *N,N*-dimethylformamide anhydrous (DMF, 99.8%), dichloromethane (CH₂Cl₂, ≥ 99.8 %), were purchased from Sigma-Aldrich. Acetone was obtained from CARLO ERBA Reagents. Deuterated dimethyl sulfoxide (DMSO-d₆, 99.8%) was purchased from Eurisotop.

3.2. Synthesis of aromatic model compounds

In order to mimic some particular aromatics (G and S) from lignins architectures, ethyl-3-(2-methoxy-4-methylphenoxy)acrylate (G-VE) and ethyl-3-(2,6-dimethoxy-4-methylphenoxy)acrylate (S-VE) have been synthesized as aromatic models (Figure S4-29). For the synthesis of G-VE, 3 g of 2-methoxy-4-methylphenol (G) (21.71 mmol g⁻¹), 2.201 mL of ethyl propiolate (1 equivalent, 21.71 mmol g⁻¹) and 0.15 g of K₂CO₃ (0.05 equivalent, 1.09 mmol g⁻¹) were added to a 25 mL round bottom flask. The reactive mixture was stirred vigorously under argon flow and heated at 80 °C for 3 h. After cooling, the mixture was diluted in 25 mL of ethyl acetate and washed consecutively by 25 mL of 0.01M NaOH, brine and water. The product was dried with anhydrous magnesium sulfate, filtered, and concentrated under reduced pressure. The viscous liquid G-VE was dried overnight at 50 °C in a vacuum oven and yielded 96%.

¹H NMR (400 MHz, CDCl₃) δ 7.70 (d, *J* = 12.2 Hz, 1H), 6.92 (d, *J* = 7.9 Hz, 1H), 6.78 (s, 2H), 5.38 (d, *J* = 12.3 Hz, 1H), 4.28 – 4.08 (m, 2H), 3.84 (s, 3H), 2.34 (s, 3H), 1.26 (t, *J* = 7.2 Hz, 3H).

The same protocol was reproduced using 4-methoxy-2,6-dimethoxyphenol (S) for the production of S-VE precursor, yielding 89%.

¹H NMR (400 MHz, CDCl₃) δ 7.65 (d, *J* = 12.2 Hz, 1H), 6.55 (d, *J* = 7.0 Hz, 1H), 5.26 (d, *J* = 12.2 Hz, 1H), 4.98 (d, *J* = 7.0 Hz, 1H), 4.21 (q, *J* = 7.2 Hz, 3H), 4.15 (q, *J* = 7.2 Hz, 2H), 1.27 (d, *J* = 16.5 Hz, 4H).

¹H NMR of both compounds are available in Figure S4-30 and Figure S4-31 in SI.

3.3. Vinyl ether model exchange reactions

In a 10 mL round bottom flask were added 0.2 g of S-VE (0.85 mmol), 93 μL of 2-methoxyphenol (1 equivalent, 0.85 mmol) and 0.0059 g of K₂CO₃ (0.05 equivalent, 0.042 mmol). The mixture was heated at 120 °C for 24 h. The exchange reaction between GG' units was monitored by ¹H NMR. The protocol was adapted to study exchange kinetics for GS', SG', and SS' units. 2-Methoxyphenol (G') is used as G exchangeable unit, 2,6-dimethoxyphenol (S') as S exchangeable unit,

and benzyl alcohol as aliphatic OH unit. All the reaction conditions are summarized in Table S4-9 in SI. Reactions are designated as follow: XY, with X = G-VE or S-VE model compounds, and Y = G' or S'.

3.4. Click-addition kinetics study on aliphatic and phenolic models

To study the reactivity of phenolic model, 0.5 g of 4-methoxy-2,6-dimethoxyphenol (2.97 mmol), 0.301 mL of ethyl propiolate (1 equivalent, 2.97 mmol), and 0.0205 g of K₂CO₃ (0.05 equivalent, 0.15 mmol) were added to a 25 mL round bottom flask. The mixture was heated at 60, 80, or 120 °C for 6 h and the reaction kinetics was monitored by ¹H NMR. The same procedure was adopted with 1-butanol as a model for aliphatic OHs.

3.5. Lignin modification with ethyl propiolate

In a 25 mL round bottom flask equipped with a condenser 1 g of lignin was dissolved in 4 mL DMF or DMSO. Ethyl propiolate (1 equivalent with respect to phenol groups of lignin) and K₂CO₃ (0.05 equivalent with respect to phenol groups) were then added. The reactive mixture was stirred vigorously under an argon flow and heated at 80 or 120 °C. The reaction was stopped after consumption of the alkyne groups evaluated by ¹H NMR. The product was precipitated in acidified water (pH = 2), filtered, and washed with water. The powder was dried overnight at 50 °C in a vacuum oven. Detailed reaction conditions including quantities and time are available in Table S4-10 in SI. 2D HSQC spectra are available in Figure S4-32 in SI. ³¹P NMR are displayed from Figure S4-33 to Figure S4-36 in SI.

3.6. Synthesis of PEG dialkyne crosslinker (PEG-DA)

In a 250 mL round bottom flask equipped with a distillation apparatus connected to trap saturated with a NaHCO₃ aqueous solution were added 50 g of polyethylene glycol 400 g mol⁻¹ (0.273 mol), 33.65 mL of propiolic acid (2 equivalent, 0.547 mol), and 2.60 g of *p*-toluenesulfonic acid monohydrate (0.05 equivalent, 0.014 mol). The bulk mixture was heated at 85 °C under 550 mbar and vigorous stirring for 24 h. The mixture was diluted in 200 mL of dichloromethane and the product was washed consecutively with 200 mL of saturated NaHCO₃, brine, and water. The product was dried with anhydrous magnesium sulfate, filtered, and concentrated under reduced pressure. PEG-DA was dried 48 h at 60 °C in a vacuum oven. ¹H NMR is available in Figure S4-37 in SI. 82% conversion and yield of 58% were obtained.

3.7. Synthesis of lignin-based phenol-yne materials

In a mortar were added 5.50 g of KL (4.33 mmol g⁻¹ of phenol groups), 8.569 g of PED-DA (0.8 equivalent with respect to phenol groups), and 0.658 g of K₂CO₃ (0.2 equivalent with respect to phenol groups). The mixture was mixed using a pestle until complete homogenization. The resulting paste was poured into a Teflon mold and cured in an oven at 120 °C for 2.5 h. The material was compression molded 30 minutes at 160 °C under a constant applied force of 16 MPa to obtain a homogeneous film (10 cm × 10 cm × 1 mm). The same procedure was applied to OSL and DOSL. The experimental conditions are reported in Table S4-11 in SI. The materials designations were established as follow: X-PY, where X = KL, OSL, or DOSL.

3.8. Physical and chemical recycling studies of phenol-yne materials

Physical recycling was performed as follow: the material was grinded into a fine and homogenous powder using a 200 W Livoo DOD192 grinder. The powder was compression molded into a new generation material for 30 minutes at 160 °C under a constant applied force of 16 MPa, to obtain films (10 cm × 10 cm × 1 mm).

Chemical recycling was performed by acid-catalyzed hydrolysis. 1.2 g of KL-PY sample previously ground was immersed in 18 mL HCl 5M and 85 mL DMSO. The reaction was equipped with a cooler and heated at 70 °C for 72 h. The solid fraction was removed by centrifugation and washed with water for quantification which was determined to be of 0.5 wt% of the initial sample. The soluble fraction was precipitated in 400 mL of acidified water (pH around 2) and filtered. To ensure optimum purification, the product was resolubilized in a minimum of DMSO (3 mL) and reprecipitated in 100 mL of acidified water. The resulting powder was filtered and dried overnight at 50 °C in a vacuum oven.

3.9. Characterization techniques

¹H and ³¹P NMR spectra were acquired on a Bruker 400 MHz spectrometer (United States of America). ¹H NMR calibration was performed based on CDCl₃ (δH = 7.26 ppm) chemical shift over 16 scans. Quantitative ¹H NMR (15 s relaxation delay) was obtained using TCP as internal standard. Approximately 20 mg of sample were dissolved in 500 μL of solvent and 100 μL of a standard solution of TCP (0.5 M) was added. ³¹P NMR was prepared according to standard protocols employing the reaction with a phosphorylating reagent (Cl-TMDP) (Archipov et al., 1991; Granata and Argyropoulos, 1995; Meng et al., 2019). The spectra were acquired with 128 scans and 15 s relaxation delays. Equation 1 was used for the calculation of OH content (in mmol g⁻¹), where C_s (M) is the concentration of cholesterol standard, V_s (μL) is the volume of cholesterol standard, A is the area of the OH groups peak obtained on the ³¹P NMR spectrum, and m (mg) is the sample weight:

$$OH\ content = \frac{C_s \times V_s \times A}{m} \quad (1)$$

2D HSQC NMR spectra were recorded on a Bruker 500 MHz spectrometer at 25 °C. About 100 mg of sample were dissolved in DMSO-*d*₆, and 32 scans were recorded (1024 × 256 increments, 1.5 s relaxation delay, 0.13 s acquisition time).

Fourier transform infrared (FT-IR) spectra were assessed using a Nicolet 380 spectrometer from Thermo Electron Corporation (United States of America), equipped with an attenuated total reflectance (ATR) diamond module. Each analysis required 32 scans in the range 4000-500 cm⁻¹.

Diffuse reflectance FT-IR (DRIFT) spectra were collected on a Bruker VERTEX 70 spectrometer (United States of America) equipped with a MCT (HgCdTe) detector with a 4 cm⁻¹ spectral resolution in the range of 4000-500 cm⁻¹. The viscous samples were mixed with KBr to obtain powders before introduction in a Praying Mantis™ low temperature reaction chamber from Harrick Scientific. The samples were heated under a 10 mL min⁻¹ He flow rate with a ramp of 10 °C/min from room temperature to 80 or 120 °C, followed by an isotherm.

Size-exclusion Chromatography (SEC) was carried out on a Acquity APC apparatus from Waters (United States of America) for the determination of the number-average molar mass (M_n), weight-average molar mass (M_w) and dispersity (Đ). THF was employed as eluent (0.6 mL min⁻¹) at 40 °C. Three columns (Acquity APC XT 450 Å 2.5 μm 4.6 × 150 mm, 200 and 45) were connected and the detection was performed with a UV or a refractive index detector. The apparatus was calibrated using polystyrene (PS) standards. To increase lignins dispersions and solubilities in THF, samples were acetylated prior to analysis according to a formerly reported procedure (Duval and Avérous, 2017).

Thermogravimetric analysis (TGA) was recorded on a Mettler Toledo TGA 2 apparatus (Switzerland). Samples of around 3 to 5 mg were heated in a crucible from room temperature to 800 °C at a rate of 20 °C min⁻¹ under an air atmosphere (25 mL min⁻¹ flow rate).

Differential scanning calorimetry (DSC) was carried out on a TA instruments Discovery DSC-25 apparatus (United States of America) under dry nitrogen flow of 50 mL min⁻¹. Around 2 to 3 mg of sample were weighted in aluminum pans, using an empty pan as reference. Samples were first

CHAPITRE 4

equilibrated at 160 °C for 3 minutes to erase their thermal history. They were then cooled down at -80 °C at a 5 °C min⁻¹ rate and equilibrated for 3 minutes. Finally, samples were heated at 160 °C at a 10 °C min⁻¹ rate. The glass transition temperature (T_g) was measured on the last heating ramp as the change of slope.

Wide Angle X-ray Scattering (WAXS) analysis were performed on a Bruker D-8 Advance diffractometer (United States of America) using Cu K α radiation ($\lambda = 1.5406 \text{ \AA}$) at room temperature in the 2θ range of 3 to 60 °. Scan step of 0.03 ° and a step time of 0.5 s were used. Samples of 1 mm thickness were analyzed. Equation 2 and Equation 3 were employed for the calculation of the scattering vectors (q) and the real-space distances (D), where 2θ (rad) is the scattering angle and λ is the X-rays wavelength (\AA).

$$q (\text{\AA}^{-1}) = \left(\frac{4\pi}{\lambda}\right) \sin \theta \quad (2)$$

$$D(\text{\AA}) = \frac{2\pi}{q} \quad (3)$$

The peaks deconvolutions were fitted with 4 Gaussian functions, using Scipy library openly developed on GitHub, on Python 3.0. The proportion of the different interactions were calculated with the integrated areas under each Gaussian curves.

Dynamic mechanical analyses (DMA) were recorded on a TA Instrument Discovery Hybrid Rheometer HR-3 (United States of America) equipped with a rectangular torsion geometry. Rectangular samples of around 2 cm \times 1 cm \times 1 mm were heated at 3 °C min⁻¹ from -60 to 180 °C, with a 0.01 % strain at 1 Hz frequency. Equation 4 was used for the calculation of crosslinking densities (ν) in accordance with the theory of rubber elasticity for small deformations on the rubbery plateau, where G' (Pa) is the storage modulus, and R the molar gas constant (8.314 J mol⁻¹ K⁻¹). T_α (K), the temperature of the α transition is determined at the maximum of $\tan \delta$ curve (Chenal et al., 2007; Palmese and McCullough, 1992).

$$\nu (\text{mol m}^{-3}) = \frac{G'_{T_{150}}}{3R(T_{150})} \quad (4)$$

Stress relaxations were measured on a TA Instrument Discovery Hybrid Rheometer HR-3 (United States of America) equipped with ETC-steel 25 mm parallel plates geometry. Samples discs of 25 mm diameter and 1 mm thickness were analyzed. The series of experiment at different temperatures were carried out successively on the same sample after 10 min equilibration at temperature, with a fixed gap around 1 mm and 1% strain. The curves were fitted with Kohlrausch-William-Watts (KWW) stretched exponential decay using Equation 5, where $G(t)/G_0$ is the normalized stress at relaxation time t , τ^* is a characteristic relaxation time, and β ($0 \leq \beta \leq 1$) the exponent indicating the distribution of relaxation times (Williams and Watts, 1970; Dhinojwala et al., 1994; Martins et al., 2023). Average relaxation time $\langle \tau \rangle$ is calculated by Equation 6. Activation energies (E_a) were determined by plotting $\ln \langle \tau \rangle = f(1000/T)$, with $\langle \tau \rangle$ given by Equation 7.

$$\frac{G(t)}{G_0} = \frac{G_{perm}}{G_0} + \left(1 - \frac{G_{perm}}{G_0}\right) \exp \left\{ -\left(t/\tau^*\right)^\beta \right\} \quad (5)$$

$$\langle \tau \rangle = \frac{\tau^* \Gamma\left(\frac{1}{\beta}\right)}{\beta} \quad (6)$$

$$\langle \tau \rangle = A \exp\left(\frac{-E_a}{RT}\right) \quad (7)$$

Uniaxial tensile tests were carried out on an Instron 5567H dynamometer (USA) equipped with a 10 kN load cell. Tests were performed on a set of 5 dumbbell-shaped samples of dimension $45 \times 5 \times 1 \text{ mm}^3$ with a constant crosshead speed of 20 mm min^{-1} in a room set at $23 \text{ }^\circ\text{C}$. Young's modulus (E), stress at break (σ), and elongation at break (ε) were measured. Averages and standard deviations were determined. Representative curves were selected to be displayed.

Swelling ratio (SR) and gel fraction (GF) of the series of materials was investigated by immersion of previously dried samples of around 100 mg in both acetone and water for 48 h. The mass of material after swelling (m_i) was then measured. The materials were finally dried in a vacuum oven for 24 h at $50 \text{ }^\circ\text{C}$, and their final mass (m_f) was recorded. The test was conducted in triplicate. SR and GF were calculated according to Equations 8 and 9.

$$SR (\%) = \frac{m_i - m_f}{m_f} \times 100 \quad (8)$$

$$GF (\%) = \frac{m_f}{m_i} \times 100 \quad (9)$$

The apparent water contact angles (WCA) of final materials were measured by sessile test using a TRACKER™ goniometer from Teclis Scientific (France). 3 droplets of distilled water with volumes of $8 \text{ } \mu\text{L}$ were dropped on previously dried materials. WCA obtained by calculation are given as mean values with standard deviations.

4. RESULTS AND DISCUSSION

4.1. Analysis of the vinyl ether rearrangements: model study on mono- and di-substituted phenols

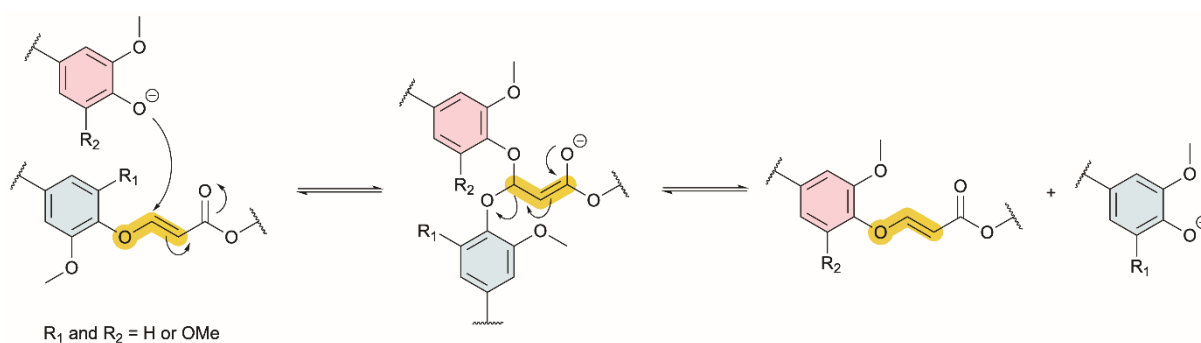


Figure 4-3. Mechanistic pathway for the exchange of phenyl vinyl ether dynamic bonds.

Emerging phenol-yne chemistry was reported to undergo exchange reactions on small organic molecules (Santos et al., 2022), and in polymer network using bisphenol A (Zhang et al., 2022). The mechanistic pathway for bond exchange was suggested to occur through: i) the deprotonation of phenol species under basic catalysis and subsequent nucleophilic addition of the phenol anion to the enol-one bond, forming a negatively charged enolate intermediate, and ii) the elimination of the substituted phenol, generating a new vinyl ether (Figure 4-3) (Zhang et al., 2022). Since these studies reports the facile rearrangements at low temperatures of vinyl ether bonds only on unsubstituted phenols in *ortho*-positions, it is necessary to evaluate whether vinyl ether rearrangements are also possible on mono- or di-*ortho*-substituted phenols for the development of lignin-based materials. This is a key point in the preparation of vinylene-ether CANs from lignin, in which phenols are substituted by one or two methoxy groups (G and S units).

CHAPITRE 4

In the present study, aiming to valorize lignin containing both aliphatic (Al-OH) and phenolic OHs (Ph-OH), K_2CO_3 was selected as an healthcare and environmentally friendly catalyst. Because of its pKa of 10, K_2CO_3 enables the deprotonation of phenols forming dynamic bonds while restricting the deprotonation of aliphatic OHs forming non-dynamic bonds.

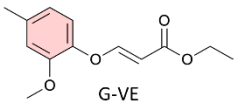
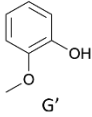
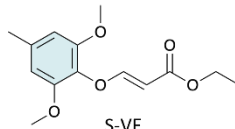
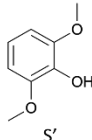
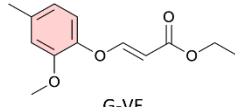
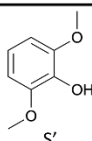
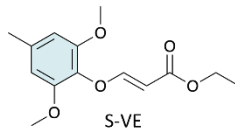
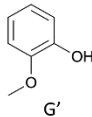
Exchange reaction	Vinyl ether	Exchangeable phenol	Equilibrium constant
GG'	 G-VE	 G'	K = 0.29
SS'	 S-VE	 S'	K = 0.18
GS'	 G-VE	 S'	K = 0.27
SG'	 S-VE	 G'	K = 0.37

Figure 4-4. Exchange reactions GG', SS', GS', and SG' conditions and equilibrium constants. For clarity purpose only *E*-isomers were represented.

Two model compounds were then synthesized to mimic lignin G and S units (G-VE and S-VE, respectively). 1H NMR of both compounds are available in Figure S4-30 and Figure S4-31 in SI. The reaction proceeds in an anti-Markovnikov fashion as confirmed by the absence of the Markovnikov product, revealing a good regioselectivity (Figure S4-38 in SI) (Shi et al., 2017; Jiang et al., 2023; Yao et al., 2014). G-VE and S-VE show the formation of *E* and *Z*-isomers readily assigned due to their distinct coupling constants. G-VE resonances at 5.36 and 7.68 were assigned to *E*-isomer vinylene protons ($J_{HH} = 12.2$ Hz) while doublets at 5.04 and 6.96 were attributed to *Z*-isomer ($J_{HH} = 7$ Hz) (Chiang et al., 1978; Song et al., 2022). S-VE resonances at 5.25 and 7.64 ppm were assigned to *E*-isomer while doublets at 4.97 and 6.54 ppm were attributed to *Z*-isomer. The proportion of *E/Z*-isomers in G-VE and S-VE were found to be 88/12 and 42/58, respectively. Whereas Santos *et al.* observed only *E*-isomer vinyl ether with unsubstituted phenols, the results herein suggest that the substituents in *ortho*-position tend to increase the proportion of the *Z*-isomer (Santos et al., 2022).

The dynamicity of the hydroxyl-yne reaction between the various units were studied (GG', GS', SG', and SS') by reacting the models with G' and S' (Figure 4-4). The reactions were monitored by 1H NMR over 24 h. The spectra sequences obtained and corresponding plotted kinetics are available from Figure S4-39 to Figure S4-47 in SI. G-VE and S-VE demonstrated to undergo exchange reactions when mixed with equimolar amount of G' and S' compounds (Figure 4-5).

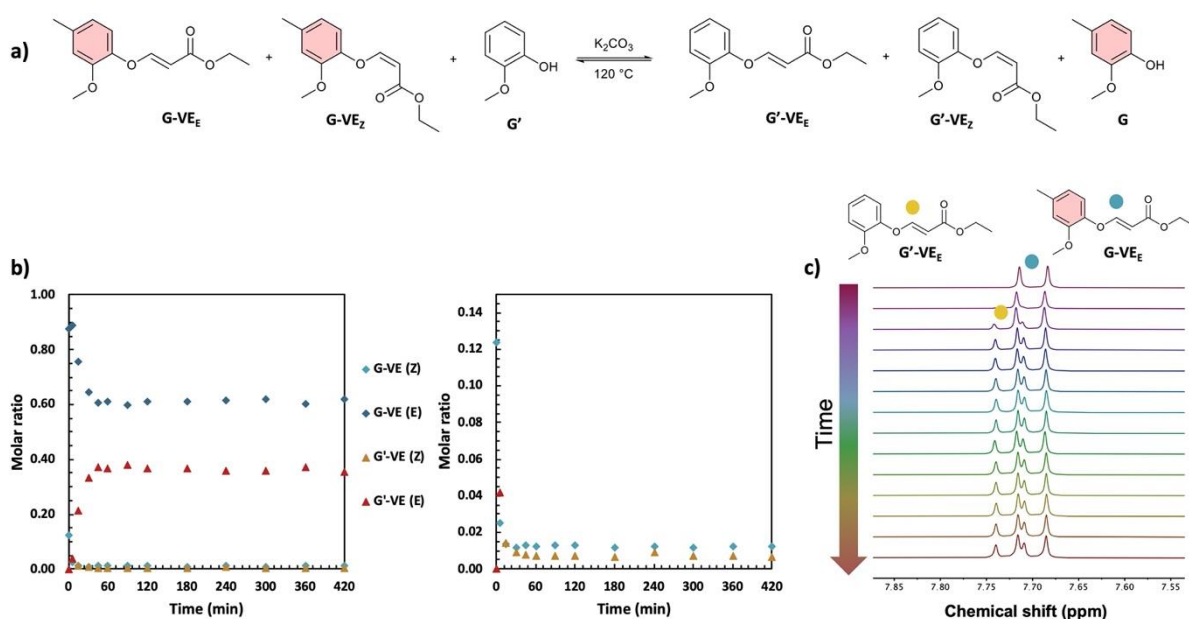


Figure 4-5. a) Illustration of the dynamic exchange of substituted phenols, b) kinetics of the exchange reaction with K₂CO₃ at 120 °C with a zoom on molar ratios from 0 to 0.15, and c) stacked ¹H NMR sequence of the exchange reaction at different times.

Equilibration constants (*K*) were determined (Figure 4-4), as detailed from Table S4-12 to Table S4-16 in SI. For all reactions, *K* < 1 is obtained. This is associated with reactions favorizing the formation of G-VE and S-VE structures over G'-VE and S'-VE compounds. Two influencing parameters were observed: i) the ability of mono- or di-substituted compounds to react on existing vinyl ether bonds, and ii) the ability of mono- or di-substituted bonds to undergo addition/elimination reactions. The higher *K* values of 0.37 and 0.29 obtained for SG' and GG' reactions suggest that G' undergo smoother addition onto G-VE and S-VE model compounds than S'. Interestingly, the addition of G' on S-VE is favored compared to G-VE, despite the larger steric hinderance induced by the two OMe substituents. This is suspected to result from the larger proportion of *Z*-isomer (58%) in S-VE making the addition site more accessible compared to an *E*-isomer, which is the main configuration of G-VE. S-VE *Z*-configuration appears to be more prone to the addition of a new phenol, as indicated by SG' and SS' kinetics (Figure S4-41 and Figure S4-45 in SI). In the case of SS' for instance, S-VE_Z is predominantly consumed in a first kinetic step, generating S'-VE_E compound and free S. Then, in a second step both S-VE_Z and newly generated S'-VE_Z are consumed to preferably reform S-VE_E and produce S'-VE_E structures. Eventually, all the *Z*-isomers will be consumed into the more stable *E*-compounds, leading to the reaction equilibrium. The same kinetic profile is observed with SG' reaction.

The influence of the methyl *para*-substituent (*p*-Me) on G-VE and S-VE inducing a slightly electron donating effect was investigated. Santos *et al.* demonstrated that electron-rich phenols tend to remain attached as ether while electron deficient phenols tend to be released and remain free in solution (Santos *et al.*, 2022). A reference reaction between G-VE and S (GSB) was carried out to determine the specific influence of the *p*-Me (Figure S4-46 and Figure S4-47 in SI). Although, the equilibrium was faster reached in around 2 h, compared to approximately 7 h for G-VE reaction with S', similar mixture composition was obtained at 24 h (83% of G-VE and 17% of S-VE (*E/Z*)). It is thus suspected that the *p*-Me and *p*-H substituents do not influence significantly the exchange potential between G and S units.

In literature, alkyl OHs are reported to form non-dynamic bonds after click reaction onto activated alkyne groups (Santos *et al.*, 2022). This point was confirmed by the synthesis of a benzyl alcohol precursor (Benz-VE) (Figure S4-48 in SI). Benz-VE was reacted with G, leading to no bond exchange (Figure S4-49 in SI). Inverse reaction of benzyl alcohol onto G-VE was investigated and

revealed the addition of aliphatic OH onto phenyl vinyl ethers and releasing of G compound (Figure S4-50 in SI). It is thus suggested that non-dynamic bonds can be generated from dynamic vinyl ether linkages. This might cause limitations in dynamicity potential when transposed to lignin, because of the presence of free aliphatic OHs moieties.

4.2. Kinetic study on aliphatic and phenolic alcohols: from models to lignins

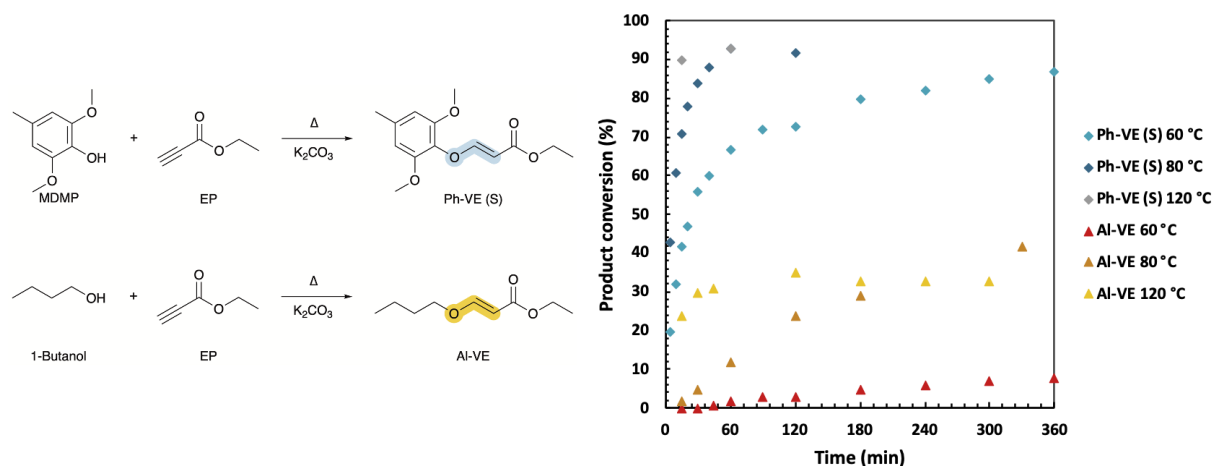


Figure 4-6. Kinetic monitoring of the conversion of vinyl ether aliphatic (Al-VE) and aromatic (Ph-VE) adducts.

The influence of aliphatic and aromatic OHs reactivity and the reaction temperature were investigated on model compounds. Butanol and S were selected as model molecules for Al-OH and S unit Ph-OH, respectively. They were reacted with ethyl propiolate. The conversion was followed by integration of the distinct doublet peaks corresponding to vinylenes protons (Figure 4-6). Ph-OH model shows the formation of *E* and *Z*-isomers, as formerly discussed and displayed in Figure S4-51 in SI. Resonances at 5.24 and 7.63 ppm were assigned to *E*-isomer vinylenes protons while doublets at 4.98 and 6.55 ppm were attributed to *Z*-isomer. The ratio *E/Z* was found to be 41/59, 37/63, and 52/48 at 120, 80, and 60 °C, respectively. *E/Z* stereochemistry is reported to be dependent on the temperature, catalyst and solvent conditions, enabling the tuning of the target isomeric configuration (Worch et al., 2021).

Similarly, Al-OH model shows the formation of *E/Z*-isomers. According to their coupling constants, resonance at 4.82 and 7.56 ppm were attributed to *E*-isomer vinylenes protons and signals at 4.81 and 6.49 ppm to *Z*-isomer protons. Additionally, the spectra evidence some transesterification occurring between butanol and esters, forming ethanol. The different potential products and their corresponding vinylenes protons signals are given in Figure S4-52, in SI. Transesterification reactions occur in the different tested conditions.

Overall, Ph-OH exhibit enhanced reactivity towards activated alkynes compared to Al-OH. At 120 °C, the conversion plateau at around 90 % is obtained in 15 minutes for Ph-OH, whereas the product conversion does not exceed 33%, after 5 h of reaction for Al-OH. This discrepancy in reactivity is observed for all the temperatures studied. This should be attributed to the relatively low pKa of K₂CO₃ which limits the deprotonation of aliphatic alcohols, while successfully deprotonating the phenols. Furthermore, the temperature is found to strongly influence the reaction kinetic by accelerating the formation of vinyl ether adducts. For Ph-OH, the adduct conversion reaches 87% in 6 h at 60 °C, and 90% in just 15 minutes at 120 °C. The same trend is observed for Al-OH, although significantly lower conversion rates are obtained. The reaction of Al-OH forming non-dynamic vinyl ether bonds is limited,

as opposed to Ph-OH generating dynamic phenyl vinyl ether covalent bonds. The results obtained in this kinetic study are then very positive.

From the above observations based on model molecules, three lignins (KL, OSL and DOSL) with different G/S units ratios and molar masses were then selected for the synthesis of a final series of materials. KL extracted from softwood is rich in G units. On the opposite, OSL and DOSL extracted from hardwood present a high S content and condensed units, and vary with their molar masses (Table 4-1).

To comprehend and to try to predict the structure of lignin-based phenol-yne networks, the reactivity of their different OHs must be assessed. As formerly evidenced in the study on model compounds, phenyl and aliphatic vinyl ether are mainly based on dynamic and non-dynamic covalent bonds, respectively (Figure S4-53 in SI). The reactivity of aliphatic and phenolic OHs of lignin towards click-addition with ethyl propiolate was investigated. Different lignin source (KL or OSL) were investigated. The influence of the reaction temperature (80 or 120 °C) was also analyzed to comprehend by extrapolation the impact of the curing temperature on the reactivity of Al-OH and Ph-OH. The structure of modified lignin with ethyl propiolate was analyzed by 2D HSQC NMR, and displayed in Figure S4-32 in SI. The formation of vinyl ether moieties was confirmed with the apparition of a "A signal" associated with vinylene protons, while "B signal" was attributed to the newly grafted ester groups. The modified lignins were analyzed by ³¹P NMR to quantify the amount of phenol and aliphatic OHs which have reacted with the monoalkyne. The spectra are available from Figure S4-33 to Figure S4-36 in SI. The dynamic and non-dynamic bonds contents could thus be calculated by dividing the amount of converted Ph-OH or Al-OH by the total amount of converted OH (Table S4-10 in SI).

The proportions of dynamic/non-dynamic bonds are reported in Table 4-2. Overall, between 73 and 78% of dynamic bonds were obtained in the different experiments. The source of lignin (KL or OSL) did not influence significantly this proportion, with values varying from 73 to 75%. As previously discussed in section 4.1, reaction temperature is a major concern because it may enhance the unwanted reactivity of Al-OH. Reactions were performed on KL at 80 and 120 °C. By increasing the temperature to 120 °C, the reaction time was significantly decreased (Table S4-10 in SI) while the proportion of dynamic bonds remained constant (73%). Finally, the click-addition was also tested in DMSO, which can be biobased (Marcos Celada et al., 2024), and showed a similar reactivity of Ph-OH and Al-OH groups than in DMF.

Table 4-2. Determination of dynamic and non-dynamic bonds contents, from the click-addition of a monoalkyne with different lignins and in different conditions.

Lignin	Temperature (°C)	Solvent	Dynamic bonds (%)	Non-dynamic bonds (%)
OSL	80	DMF	75	25
KL	80	DMF	73	27
KL	120	DMF	73	27
OSL	80	DMSO	78	22

4.3. Analysis of the lignin-derived CANs based on phenol-yne

4.3.1. Analysis of the synthesis of PEG-DA crosslinker

Esterification of PEG and derivatives with propiolic acid have been formerly reported in literature to graft alkyne moieties onto OHs of PEG (Katritzky et al., 2006; Truong and Dove, 2013;

Huang and Jiang, 2018; Maity et al., 2024). However, the reported syntheses used toxic and non-green solvents such as toluene or benzene. To reduce the environmental impact, we have developed a solvent-free synthesis of a PEG dialkyne (PEG-DA). The reaction is then based on the low viscosity of both reactants at 85 °C (Figure 4-2a).

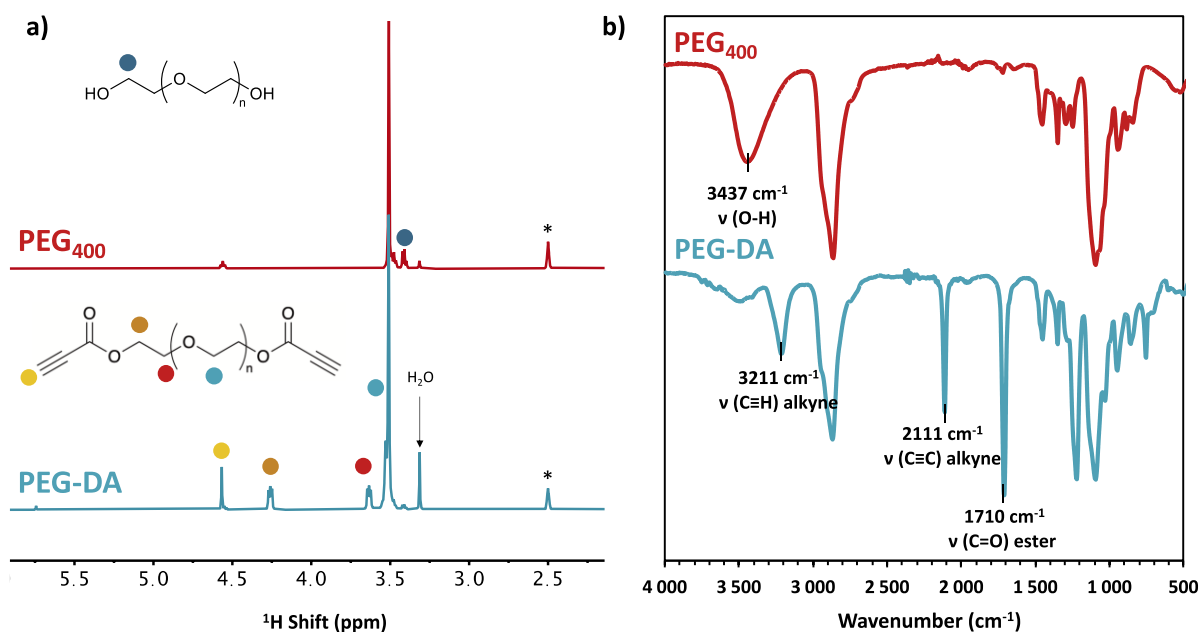


Figure 4-7. a) Stacked ¹H RMN in DMSO-*d*₆ and b) FT-IR spectra of PEG₄₀₀ and PEG-DA.

The product of PEG₄₀₀ Fischer esterification with propiolic acid was analyzed by ¹H NMR, as illustrated in Figure 4-7a. The conversion of PEG OH end groups was observed with the disappearance of the peaks at 3.41 ppm corresponding to the methylene next to OH end groups of PEG₄₀₀. New signals at 3.63 and 4.26 ppm were respectively attributed to methylene protons in α and β positions from the ester, confirming the grafting of ester moieties onto the PEG end chains (Huang and Jiang, 2018). Finally, the characteristic singlet of ethynyl protons appeared at 4.57 ppm confirming the grafting of alkyne moieties onto PEG₄₀₀. The amount of grafted alkyne measured by quantitative ¹H NMR using TCP as standard and was found to reach 2.22 mmol g⁻¹ (Table 4-3).

The successful modification of PEG₄₀₀ into PEG dialkyne (PEG-DA) was also confirmed by FT-IR, as displayed in Figure 4-7b. The effective grafting of alkyne moieties is shown by the emerging C≡C–H and C≡C bands at respectively 3211 and 2111 cm⁻¹, which are characteristic of alkyne functions (Cui et al., 2024). A new C=O band associated with ester resulting from the esterification is observed at 1710 cm⁻¹. Finally, the strong decrease of the absorption vibration of OH groups at 3337 cm⁻¹ is also indicative of the consumption of OH from PEG.

PEG₄₀₀ and PEG-DA were analyzed by SEC. The curves are displayed in Figure 4-8 and the physicochemical values (*M*_n, *M*_w and Đ) are reported in Table 4-3. *M*_n increased from 458 to 754 g mol⁻¹ after esterification. *M*_w and Đ slightly decreased from 2130 to 1950 g mol⁻¹ and from 4.6 to 2.6, respectively. It is suspected that the variation of *M*_w and Đ are resulting from interaction of PEG₄₀₀ OHs with the column using ethylene bridge hybrid technology, whereas PEG-DA is less subjected to such interactions with the column.

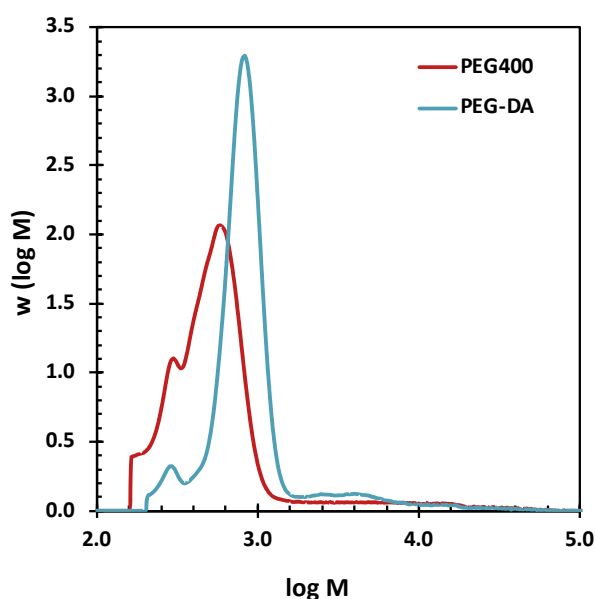


Figure 4-8. SEC curves of PEG₄₀₀ and PEG-DA in THF.

Table 4-3. Physicochemical values of PEG₄₀₀ and PEG-DA.

Designation	OH content (mmol g ⁻¹)	DA content (mmol g ⁻¹)	M _n (g mol ⁻¹)	M _w (g mol ⁻¹)	Đ
PEG ₄₀₀	5.47	-	458	2130	4.6
PEG-DA	-	2.22	754	1950	2.6

4.3.2. Analysis of the synthesis and the structural characterization of lignin-based phenol-yne materials

The influence of the temperature on the reaction kinetic was also studied in bulk. The kinetic of OSL and PEG-DA reaction was monitored by DRIFT spectroscopy at 80 and 120 °C. The evolution of the normalized absorbance of alkyne signal at 2111 cm⁻¹ was plotted as a function of time in Figure 4-9. 3D view of the of the reaction kinetics is available in Figure S4-54, in SI. At 120 °C, the absorbance of the characteristic alkyne band at 2111 cm⁻¹ decreased to less than 0.15 in 4 h, indicating a conversion around 85%. On the other hand, the experiment performed at 80 °C exhibited an absorbance of 0.66 revealing a lower conversion of 34%, after 4 h of reaction. This is suspected to originate from a restricted segmental mobility of lignin moieties at 80 °C, preventing reactive groups from interacting and forming covalent vinyl ether bonds. It is noteworthy to mention that because the samples are dispersed in KBr and the temperature is induced by IR light only at the surface of the materials, the reaction time is herein overestimated compared to an equivalent reaction in an oven. The curing temperature was set at 120 °C for the rest of the study.

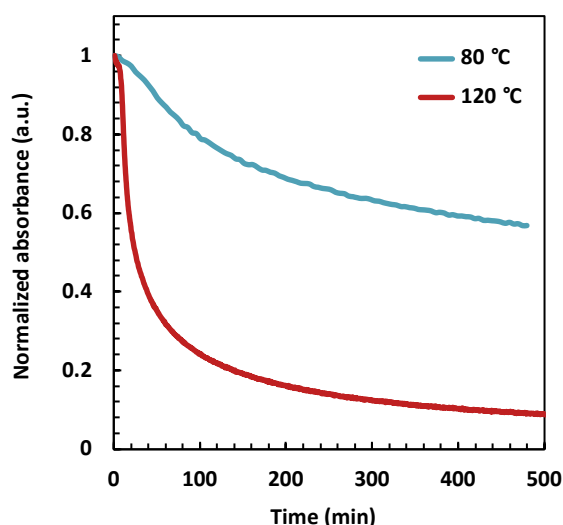


Figure 4-9. Evolution of the normalized absorbance of alkyne signal at 2111 cm^{-1} as a function of time, at 80 and 120°C .

Materials were synthesized by click-addition of KL phenols with PEG-DA under basic catalysis (Figure 4-2b). Two parameters were varied in the synthesis of KL-based networks, such as i) the amount of excess Ph-OH available to induce addition/elimination rearrangements, and ii) the molar equivalents of catalyst (K_2CO_3).

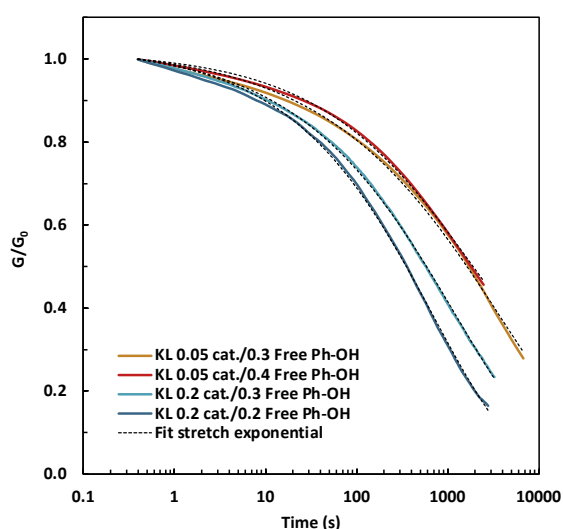


Figure 4-10. Stress relaxation curves obtained at 190°C on materials synthesized with different experimental conditions: varying the amount of free Ph-OH (from 0.2 to 0.4 equivalents), and the catalyst equivalents (from 0.05 to 0.2).

Since dynamic materials with recycling potential are designed, stress relaxation tests were performed at 190°C to determine the impact of materials architecture on the dynamicity. The resulting curves were fitted with KWW model to determine their relaxation time τ^* , as illustrated in Figure 4-10. The main relaxation parameters are available in Table S4-17, in SI. The free phenol content within the network was found to have a marginal influence on the stress relaxation. For instance, no difference is observed between 0.3 and 0.4 equivalents. Moreover, at 0.4 equivalents the material was extremely brittle due to higher lignin content. On the other hand, the amount of catalyst showed to strongly influence the network rearrangement. By increasing K_2CO_3 content from 0.05 to 0.2 equivalents, the

relaxation time decreased significantly from 3783 to 1238 s. In these catalytic conditions, the material with 0.2 equivalents of free Ph-OH was found to relax faster than the one containing 0.3 equivalents of free Ph-OH. It is assumed to arise from its slightly lower lignin content, facilitating segmental mobility and favoring addition/elimination rearrangements. Finally, optimal rheological behavior was obtained for the network containing 0.2 equivalents of free Ph-OH and 0.2 equivalents of K_2CO_3 (τ^* of 703 s). These conditions were then selected for the preparation of the final materials.

The chemical architectures of KL-PY, OSL-PY, and DOSL-PY materials were characterized by FT-IR, as displayed in Figure 4-11. The disappearance of peaks at 3211 and 2111 cm^{-1} characteristic of alkyne $C\equiv C-H$ and $C\equiv C$ stretching vibrations and the diminution of the absorption peak at 3390 cm^{-1} associated to OH stretching indicated full conversion of PEG-DA alkyne groups and partial conversion of lignin OHs. The appearance of a new absorption band at 1640 cm^{-1} attributed to $C=C$ stretching vibration confirmed the formation of vinyl ether moieties (Cui et al., 2024; Si et al., 2020).

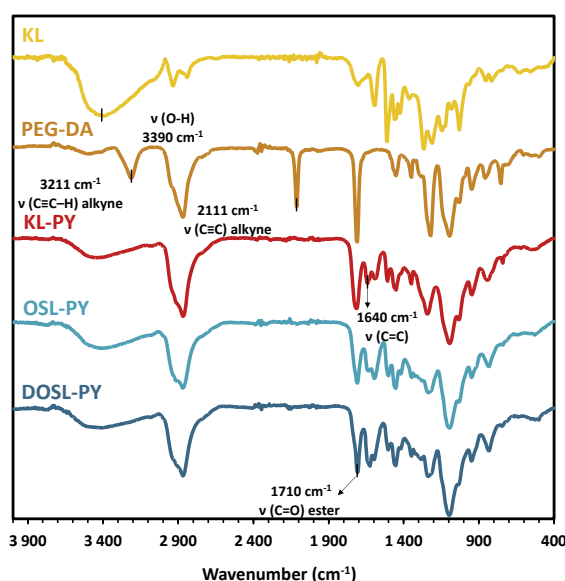


Figure 4-11. Stacked FT-IR spectra of KL, PEG-DA, and the series of materials.

The structural networks of the materials was assessed by swelling and gel fraction experiments, after immersion of materials in both acetone and water for 48 h. Resulting values are displayed in Figure 4-12 and are reported in Table S4-18 in SI. Swelling ratios of 30.6, 29.5, and 57.8% were obtained in acetone for KL-PY, OSL-PY, and DOSL-PY, respectively. Interestingly, KL-PY and OSL-PY prepared from non-depolymerized lignins exhibit similar low swelling ability in acetone at around 30%, while DOSL-PY derived from depolymerized organosolv lignin shows a higher (2-fold) value approaching 60%. This is first suggesting that kraft lignin and organosolv lignin, despite their distinct extraction processes, have a similar affinity with acetone when integrated into networks. On the other hand, catalytic treatments used to obtain DOSL from OSL enhance the affinity of the resulting structure with acetone, inducing greater swelling ability of the corresponding PY material. Swelling ratio of 64.8, 57.6, and 61.4% were obtained in water for KL-PY, OSL-PY, and DOSL-PY, respectively. Overall, smaller variations are observed between each material in water compared to in acetone. The evolution of the swelling ratio could be correlated with the Al-OH content, which are available in the network (Figure S4-55 in SI), since increased swellings are observed for the higher Al-OH contents through hydrogen bonding with water. Gel fractions (GF) were subsequently measured in both solvents. In acetone, excellent GF values of 98.0, 100.0, and 90.6% were obtained for KL-PY, OSL-PY, and DOSL-PY. As formerly discussed with SR, KL and OSL exhibit comparable behaviors in acetone resulting is similar GF, while DOSL structure induces a small reduction in GF. In water, GF slightly decreased at around 90.1 to 92.2% but stay rather high. This is believed to result from a difference of affinity of the materials

CHAPITRE 4

with water and acetone due to the polar/apolar balance and then the polymer-solvent interactions, between the solvents. Moreover, the results are in good accordance with reported GF in water for ester containing vitrimers (Gao et al., 2020; Song et al., 2023). Globally, very high gel fractions were obtained, indicating a good solvent resistance in both acetone and water. The developed lignin-based PY vitrimers herein showed better solvent resistance compared to previously reported lignin-based materials also containing PEG chains (Sougrati et al., 2023a). The results confirm that the materials were indeed highly crosslinked, and then soluble fractions remain marginal.

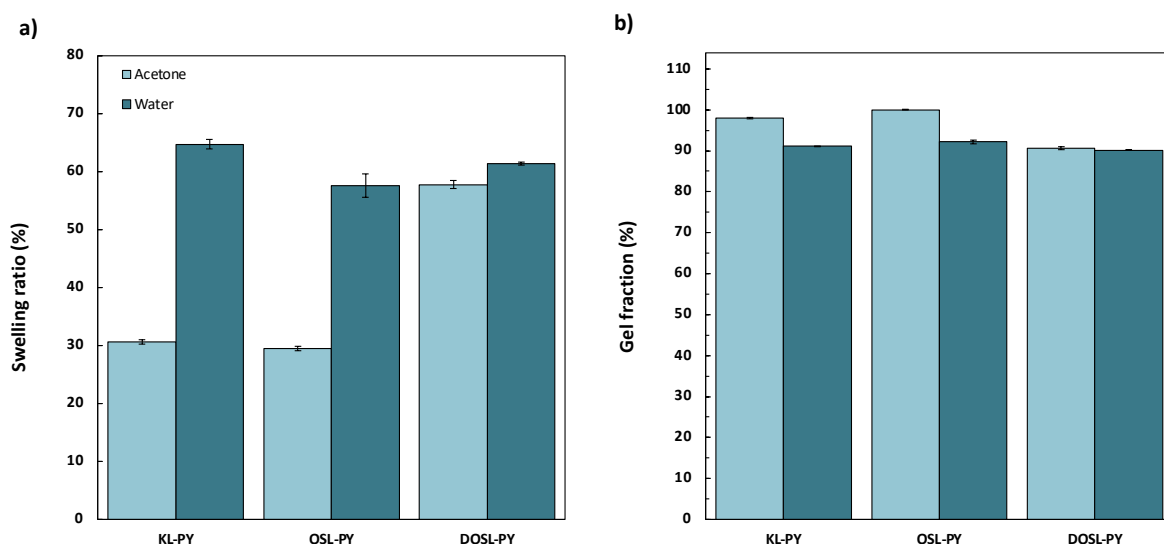


Figure 4-12. a) Swelling ratio, and b) gel fraction of the lignin-based CANs.

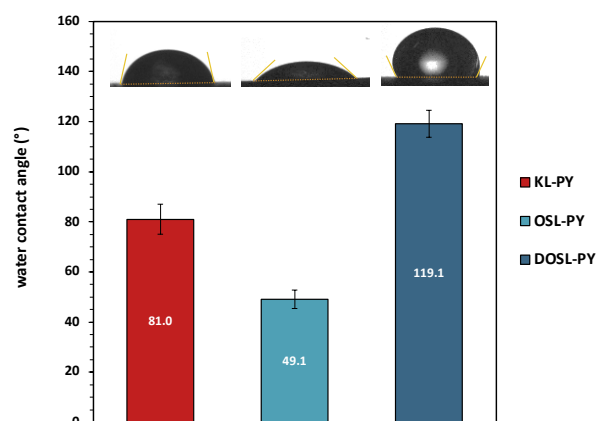


Figure 4-13. WCA of the series of material.

To determine the wettability with water of the materials surfaces and to approach the surface tension, water contact angle (WCA) assessments were carried out, as displayed in Figure 4-13. The values with their standard deviations are summarized in Table S4-18 in SI. WCA between 49.1 and 119.1 ° were measured, indicating very distinctive surface behaviors between materials. KL-PY and OSL-PY display WCA below 90 ° associated to hydrophilic surfaces (Sougrati et al., 2023b). Particularly, OSL-PY surface is considered very hydrophilic with a WCA of 49.1 °. Conversely, DOSL-PY surface is considered as hydrophobic, with a WCA above 90 °, reaching 119.1 °. This parameter is of utmost relevance to predict the materials surface behaviors in utilization conditions for specific applications. It is noteworthy to mention that apparent contact angle was also carried out in acetone but

could not be evaluated because of the immediate solvent absorption in the materials. Interestingly, the results could be correlated with gel fraction tests performed in water. The higher GF is observed for OSL-PY, the more hydrophilic material, whereas the lower GF is obtained for DOSL-PY, the more hydrophobic network (Figure S4-56 in SI).

The crystallinity and organization of the series of materials were analyzed by WAXS, as displayed in Figure 4-14. The materials exhibit pattern with broad background scattering signals which are specific to amorphous polymers comprising regions with a certain degree of ordering. The organization is associated with inter and intramolecular physical interactions occurring between the polymer segments. Scattering vectors q (also known as momentum transfer in reciprocal-space) and the associated real-space distances D (also known as Bragg spacings) were determined using Equations 2 and 3 (Table 4-4). The proportions of physical interactions were identified through the scattering signal deconvolution using four Gaussian functions.

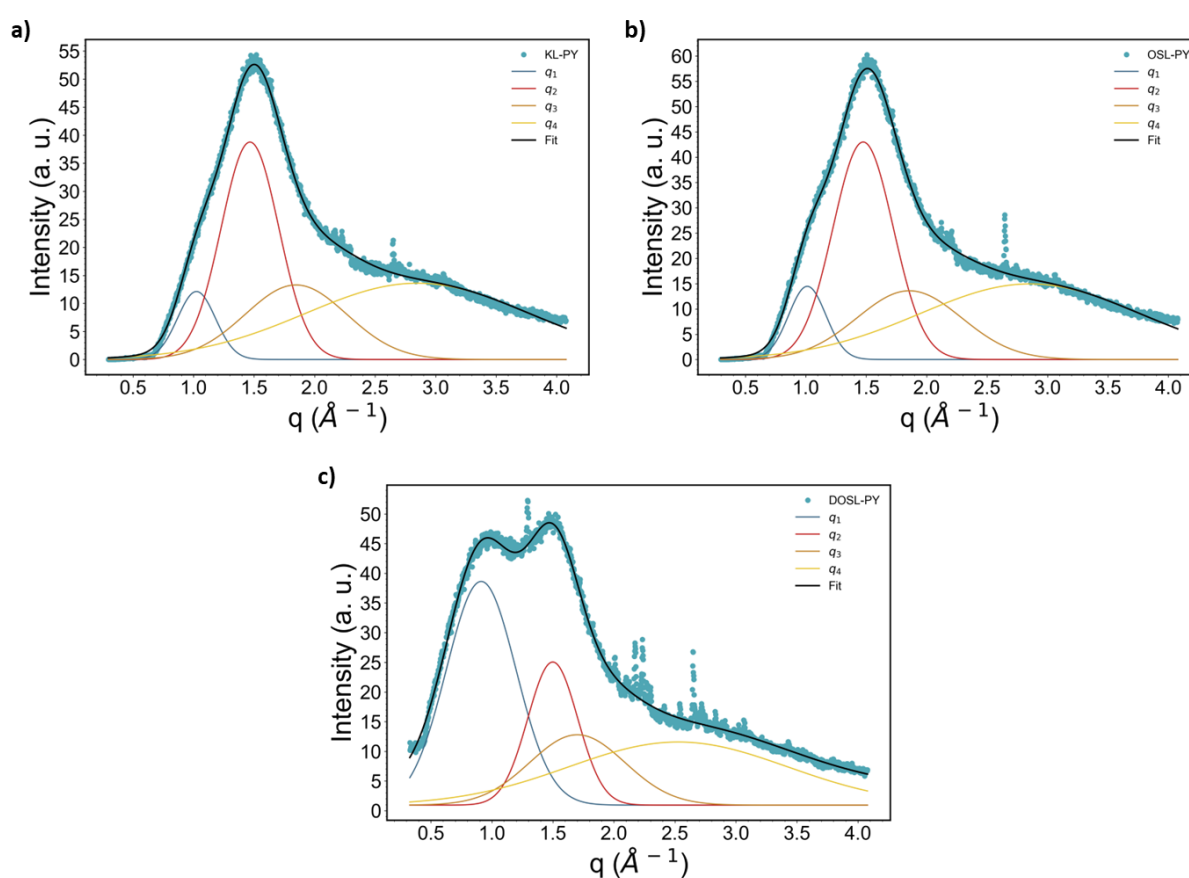


Figure 4-14. WAXS curves and deconvolutions of a) KL-PY, b) OSL-PY, and c) DOSL-PY.

Interplanar distance around 4.2 – 4.6 Å, 3.4 – 3.5 Å, and 2.1 – 2.6 Å could be respectively assigned to hydrogen bonding (OH \cdots OH), π - π stacking, and carbonyl-hydrogen bonding (C=O \cdots HO) (Babra et al., 2019; Merino et al., 2016). Materials microstructure organization was not found to significantly vary with the lignin (KL or OSL) source. This suggests that both lignins, despite their distinctive OH contents and inter-unit linkages, when integrated in polymer networks, have similar abilities towards the generation of hydrogen bonding (7%), π - π stacking (around 20%), and carbonyl-hydrogen bonding (40%). The use of depolymerized lignin is the source of diverging interactions proportions. A slight decrease π - π stacking (16%) and substantial reduction of hydrogen bonding (17%), and carbonyl-hydrogen bonding (31%) is observed in favor to the q_1 interaction, which might be attributed to a sort of microphase separation between the lignin rich regions and homogeneous phase in

CHAPITRE 4

which lignin is dispersed in the flexible PEG chains. Finally, the materials display narrow peaks in the regions from $q \approx 2.0$ to 3.0 \AA^{-1} . Those peaks indicate a higher organization of some domains. DOSL-PY shows the better network organization characterized by greater amounts of narrow peaks.

Table 4-4. WAXS parameters and interaction proportions for KL, OSL, DOSL, and the series of materials.

PY (Designation)	KL-PY	OSL-PY	DOSL-PY
$q_1 (\text{\AA}^{-1})$	1.02	1.01	0.91
$q_2 (\text{\AA}^{-1})$	1.47	1.47	1.50
$q_3 (\text{\AA}^{-1})$	1.85	1.86	1.70
$q_4 (\text{\AA}^{-1})$	2.85	2.85	2.53
$D_1 (\text{\AA})$	6.14	6.21	6.89
$D_2 (\text{\AA})$	4.29	4.26	4.19
$D_3 (\text{\AA})$	3.40	3.38	3.70
$D_4 (\text{\AA})$	2.21	2.20	2.49
q_1 proportion (%)	7	7	36
OH...OH proportion (%)	33	34	17
π - π stacking proportion (%)	20	19	16
C=O...HO proportion (%)	40	40	31

4.3.3. Analysis of the thermal, rheological, and mechanical behaviors of the materials

Thermal properties of the material were investigated by TGA to assess suitable reprocessing conditions. The results are summarized in Table 4-5 and the curves are available in Figure S4-57 in SI. The materials demonstrated 5% mass loss between 263 and 274 °C ($T_{d5\%}$), indicating a good thermal resistance. Those values are similar to previously reported lignin-based networks containing PEG-derived crosslinker (Sougrati et al., 2023a). Temperatures of maximal mass loss rate (T_{deg}) from 384 to 400 °C are observed for the different materials. Besides, these values enabled the choice of temperature range so that no major degradation occurs during the DSC scans. Glass transition temperatures (T_g) of the series of materials were determined by DSC. The values are reported in Table 4-5 while the curves of lignins and corresponding materials are displayed in Figure S4-58 and Figure S4-59 in SI. KL-PY, OSL-PY, and DOSL-PY exhibited T_g of 2, 19, and -2 °C. A second T_g of lower intensity seems to be visible on DOSL-PY spectra around 105 °C. This is probably resulting from partial phase separation between the aggregated lignin structures and more homogeneous phase in which lignin is dispersed in the flexible PEG chain. Since the T_g value is -2 °C, it is unlikely that the inhomogeneities are originating from PEG rich phases which would lead to lower T_g values. This would be in good agreement with the WAXS results indicating potential microphase separations in DOSL-PY. The phase separation of DOSL-PY is however surprising because the use of depolymerized lignin of lower M_n should theoretically improve the phase compatibility (Glasser, 2019). Lignin phase separation and clustering in resins is also intrinsic to its chemical structure and functionality. It is thus suspected that the distinctive compatibility of DOSL with PEG-DA is inherent to its chemical structure and inter-unit linkages resulting from the catalytic depolymerization treatment.

Table 4-5. Thermal and rheological properties of the PY-based networks.

PY-based Networks	Lignin content (wt%)	$T_{d5\%}$ (°C)	T_{deg} (°C)	T_g (°C)	T_α (°C)	ν (mol m ⁻³)
KL-PY	39	274	400	2	46	3321
OSL-PY	49	266	388	19	76	1207
DOSL-PY	46	263	384	-4	10	1563

Rheological properties of the series of networks were investigated by DMA. The main rheological parameters are reported in Table 4-5 and the curves are available in Figure S4-60 in SI. Only OSL-PY exhibits a well-marked α -transition at 19 °C. KL-PY exhibited a broader signal originating at around -30 °C and terminating around 140 °C, with a maximum at 2 °C. DOSL-PY demonstrated a main peak at -10 °C and a less intense second signal around 125 °C. The broad signal of KL-PY and the two maxima of DOSL-PY are suspected to be associated with phase separation. This partial phase separation is suggested to occur at the sub-micro scale, owing to partially aggregated KL and DOSL structures and homogeneous phase in which lignin is dispersed in the flexible PEG chains (Thys et al., 2021; Wang et al., 2016). This is in good agreements with the DSC and WAXS observations on DOSL-PY, which respectively indicated for the presence of two T_g and possible interactions originating from microphase separation.

Crosslinking densities (ν) were determined on the rubbery plateau (at 150 °C) according to Equation 4. ν between 1207 and 3321 mol m⁻³ were obtained. Unlike previously reported, the ν is not correlated to the lignin content (Sougrati et al., 2023a). However, it is well correlated to the lignin content in Ph-OH groups, which varies significantly between lignin samples. The evolution of ν was plotted as a function of Ph-OH content, as displayed in Figure 4-15, and show a very high linearity with $R^2 = 0.99$, in the studied range. Lignin high functionality is the only source of crosslinks generation in the designed materials. Thus, higher lignin Ph-OH content induces the formation of greater crosslinks contents within the networks.

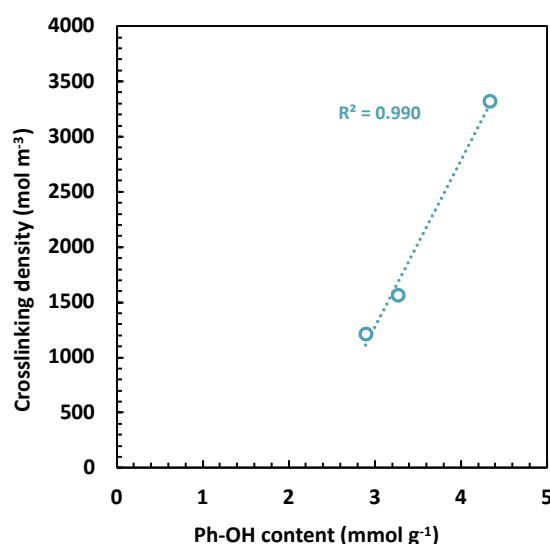


Figure 4-15. Evolution of the crosslinking density as a function of Ph-OH content.

The dynamicity of the lignin-based networks was investigated through stress relaxation experiments. Experimental curves were fitted using the KWW stretched exponential decay, as displayed in Figure 4-16. This model allowed the determination of τ^* and β exponent ($0 < \beta < 1$) which characterize

the distribution of relaxation times for materials dissipating energy through various relaxation modes. The main relaxation parameters are reported in Table 4-6. Relaxation times ranging from 44 to 384 s were obtained at 200 °C. The dynamicity is suspected to originate from vinyl ether addition/elimination bond exchange, although transesterification reactions involving lignin free aliphatic OHs might occur in the presence of the K_2CO_3 catalyst (Ochoa-Gómez et al., 2009). Transesterification in the networks is suspected to be marginal because of the weak reactivity of lignin primary and secondary aliphatic OH, especially in bulk. However, transesterification might nonetheless occur by K_2CO_3 activation, as discussed in section 4.1. Moreover, full stress relaxation is observed. Thus, G_{perm}/G_0 in equation 5 is equal to 0. It confirms that networks are mainly composed of dynamic phenyl vinyl ether bonds, and that potential non-dynamic bonds are marginal.

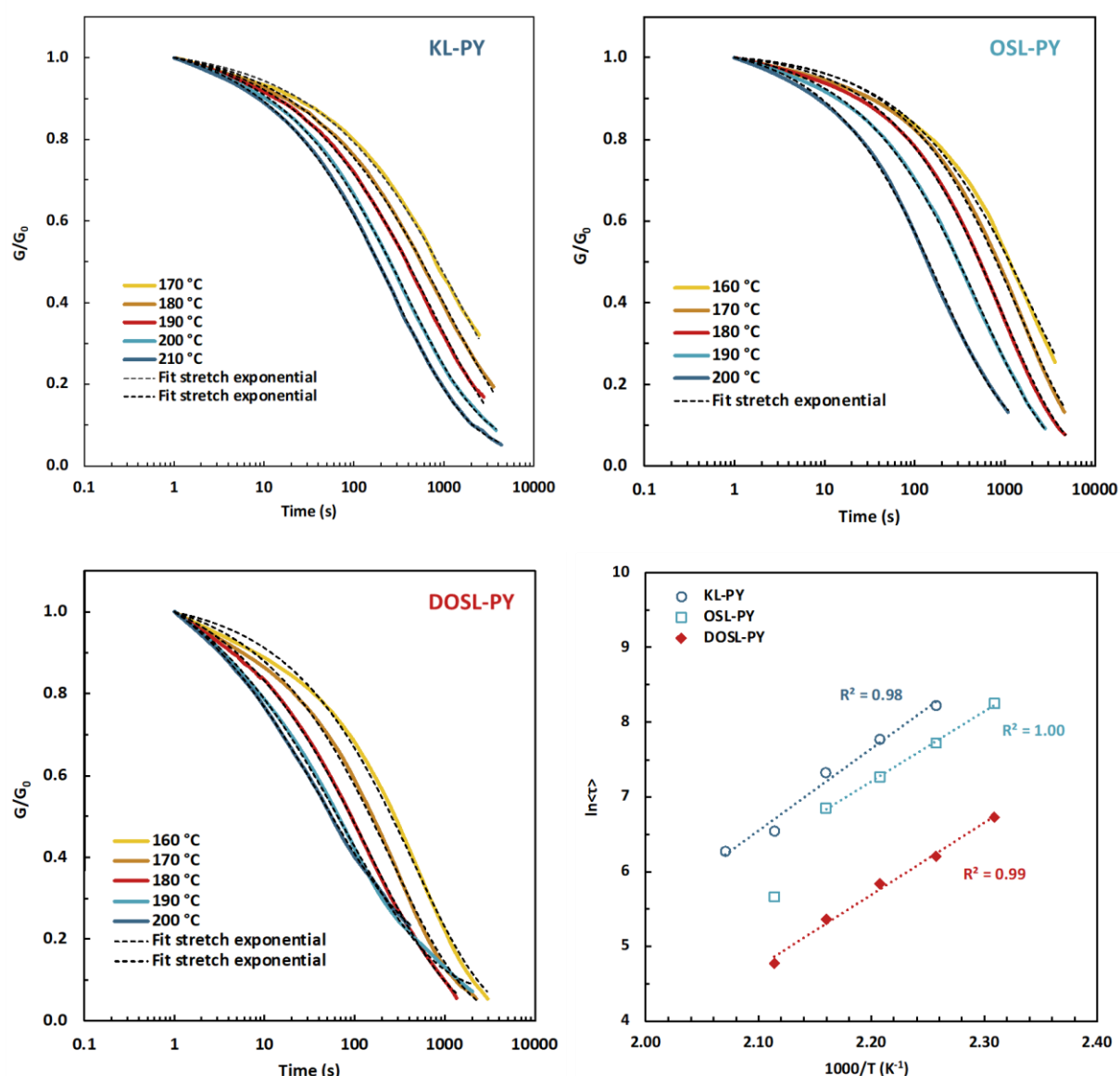


Figure 4-16. Stress relaxation curves of KL-PY, OSL-PY and DOSL-PY, and Arrhenius plots of the networks.

The relaxation times were also found to decrease with the molar mass of lignin, as illustrated in Figure 4-17. The fastest relaxation was observed for DOSL exhibiting the lower molar mass. It is

CHAPITRE 4

suggested that bond rearrangements are highly dependent on the network segmental mobility, which is improved by employing less bulky lignins with lower M_n .

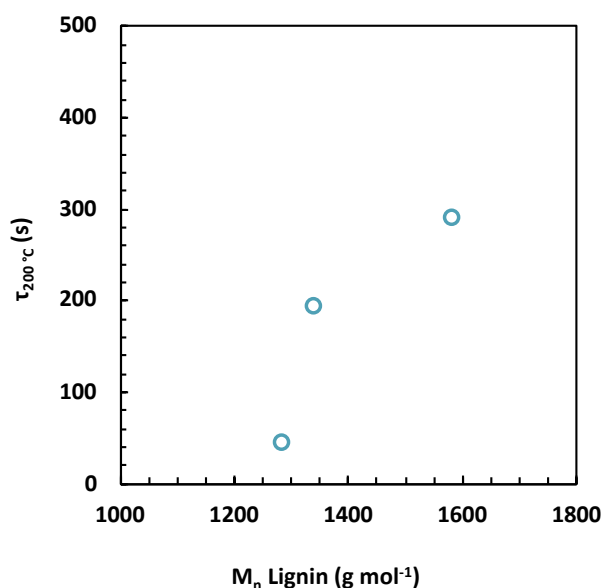


Figure 4-17. Evolution of the relaxation time at 200 °C with lignin molar mass.

β parameter was found to vary between 0.48 and 0.57. These values are characteristic to heterogenous distribution of relaxation times originating from the different chemical environments of the phenyl vinyl ether groups. The different *ortho*-substituents of phenols (H, G and S units) which showed distinctive bond exchange kinetics are suspected to be the source of this discrepancy in relaxation times.

Table 4-6. Main stress relaxation parameters.

PY (Designations)	$\tau_{200\text{ °C}}^*$ (s)	β	E_a (kJ mol ⁻¹)	T_v (°C)
KL-PY	290	0.50 ± 0.03	91.3	121
OSL-PY	193	0.57 ± 0.03	77.7	90
DOSL-PY	44	0.48 ± 0.05	80.4	76

Activation energies (E_a) values of 91.3, 77.7, and 80.4 kJ mol⁻¹ were obtained for KL-PY, OSL-PY, and DOSL-PY, respectively (Table 4-6). E_a was found to show a linear correlation with the crosslinking density as displayed in Figure 4-18a (Chen et al., 2021). This is in good agreement with previously reported results on lignin-based vitrimers (Sougrati et al., 2023a). This correlation is resulting from the Ph-OH content of lignin (Figure 4-18b). As formerly discussed, the use of lignin with higher Ph-OH content produces materials containing higher amounts of crosslinks which are reversible bonds. Finally, E_a values are in good agreement with the only reported E_a for phenol-yne vitrimers of 73.7 and 89.8 (Zhang et al., 2022). Overall, the stress relaxation experiments implied that KL-PY showing the greater E_a value exhibits a rapid decrease in viscosity but slower relaxation upon heating while OSL-PY and DOSL-PY demonstrating lower E_a are subjected to less pronounced viscosity changes but faster relaxation.

Theoretical topology freezing temperatures (T_v) associated with temperatures above which bond exchange induce a macroscopic flow (elastic solid to viscoelastic liquid) were calculated by extrapolation from Arrhenius plot for a viscosity conventionally set at 10^{12} Pa s (Table 4-6) (Brutman et

CHAPITRE 4

al., 2014; Lessard et al., 2019; Sougrati et al., 2023a). Parameters employed for the calculations are reported in Table S4-19 in SI. T_v of KL-PY, OSL-PY, and DOSL-PY were determined to be 121, 90, and 76 °C, respectively. Each vitrimer exhibits a $T_v > T_g$ which is characteristic to a viscoelastic flow mainly controlled by the bond exchange kinetics (Denissen et al., 2016). At an ambient temperature of 25 °C, KL-PY and DOSL-PY ($T_g < T_v < T_{amb}$) behave like elastomers under the rubbery state with fixed chemical structures because of their high T_v . OSL-PY ($T_g \approx T_{amb} < T_v$) has limited segmental movements because (i) the rubbery plateau has not been completely overtaken and (ii) the rigidity and structure of the chemical network induce such a behavior. Although creep was not measured for the series of vitrimers, OSL-PY is expected to demonstrate the better creep resistance at usage temperature amongst the synthesized materials.

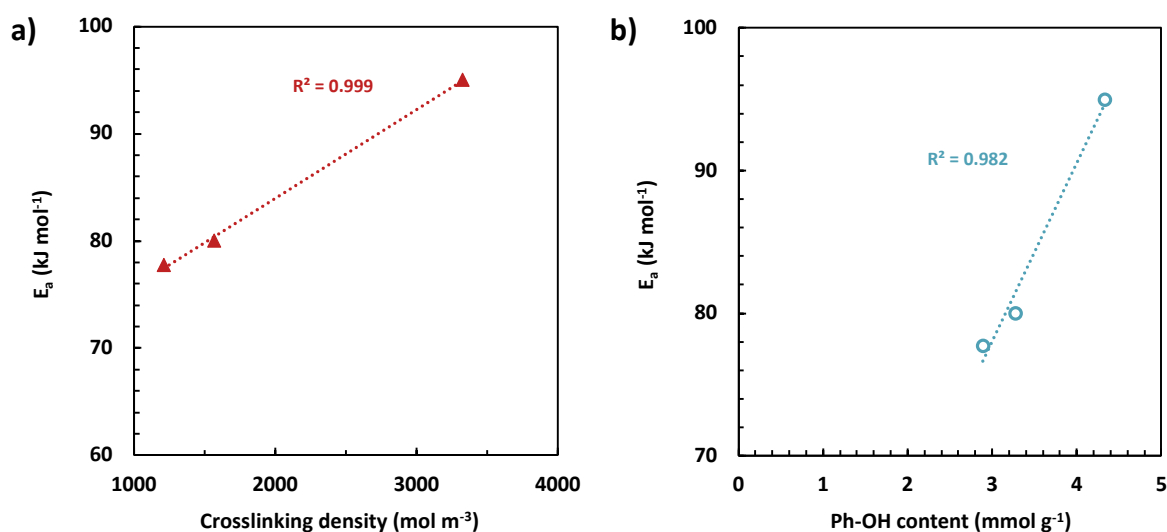


Figure 4-18. Evolution of E_a of the vitrimers with a) the crosslinking density, and b) the Ph-OH content.

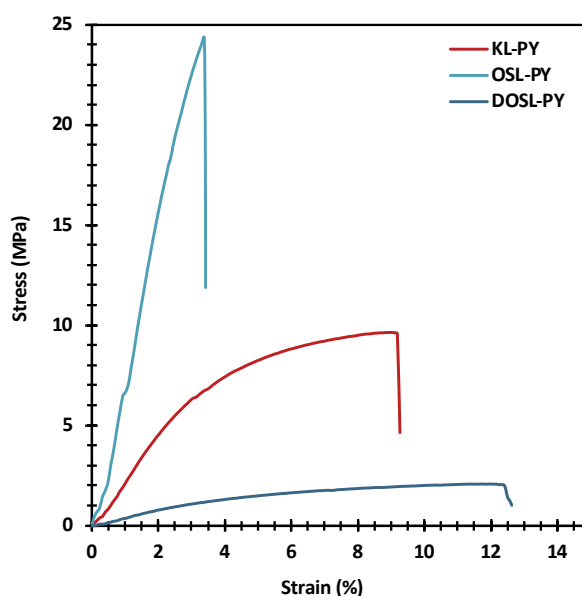


Figure 4-19. Stress-strain curves of the series of CANs.

Static mechanical properties were assessed by uniaxial tensile tests. The resulting stress-strain curves displayed in Figure 4-19 show that the materials globally have a typical thermoset behavior, with

rather steep slope in the initial linear region associated to high modulus, and limited elongation before break. The corresponding values of Young's modulus (E), maximal stress at break (σ), and maximal elongation at break (ϵ) are reported in Table 4-7. Two distinct mechanical behaviors are observed, since T_g of OSL-PY is close to the testing temperature (T_g of 19 °C). This material exhibits the greatest Young's modulus and maximal stress of 899 MPa and 24.6 MPa, respectively, while achieving an elongation of 4.0%. KL-PY and DOSL-PY, whose T_g are far below testing temperature, are in their rubbery state. They show respectively E values of 263 and 42 MPa, σ of 9.6 and 2.0 MPa, and ϵ of 10.0 and 13.1 %. E and σ values show a similar evolution than the dynamic storage modulus measured at 23 °C ($G'_{23\text{ °C}}$) reported in Table 4-7, with OSL-PY > KL-PY > DOSL-PY.

Table 4-7. Mechanical properties of the series of CANs.

PY (Designations)	E (MPa)	σ (MPa)	ϵ (%)	$G'_{23\text{ °C}}$ (MPa)
KL-PY	263 ± 21	9.6 ± 0.3	10.0 ± 1.0	586
OSL-PY	899 ± 41	24.6 ± 2.8	4.0 ± 1.2	915
DOSL-PY	42 ± 3	2.0 ± 0.2	13.1 ± 2.6	211

4.3.4. Analysis of the physical recycling

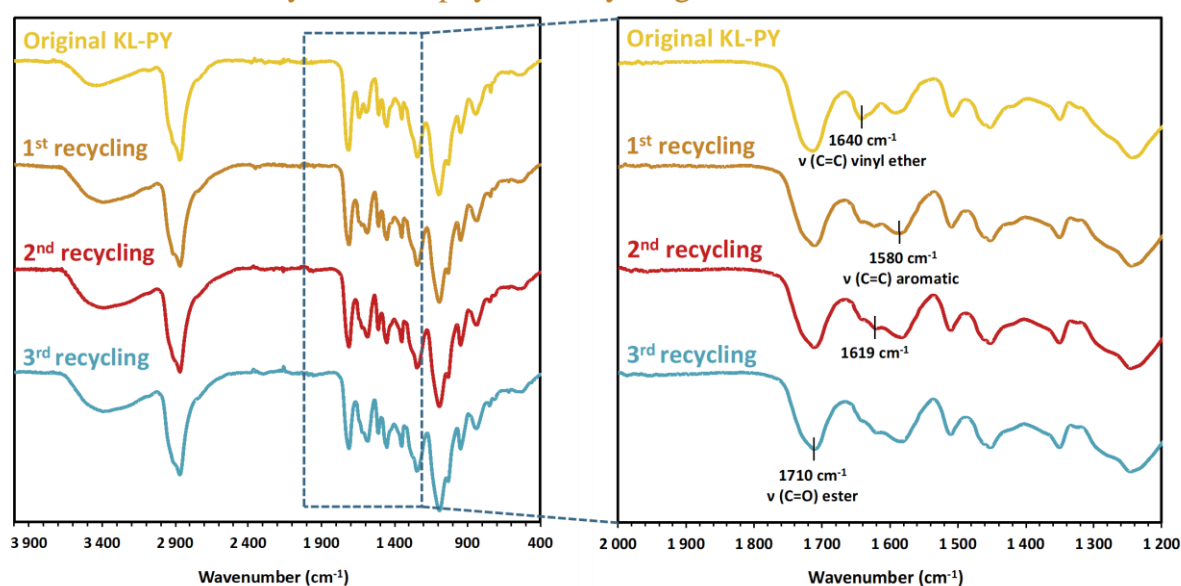


Figure 4-20. FT-IR spectra of pristine and recycled KL-PY.

The control of polymer networks end-of-life is of utmost relevance in the design of sustainable materials with reduced environmental impact. In this context, physical recycling potential of the lignin-based phenol-yne vitrimers was investigated. As a proof of concept, KL-PY was chosen for this study, as it is the network with intermediate mechanical properties. KL-PY was grinded and thermo-mechanically remolded at 160 °C over three cycles. The evolution of the chemical structure was also analyzed by FT-IR, as illustrated in Figure 4-20. The FT-IR spectra display a change in chemical structure after the first recycling with the slight intensity decrease of the ester band at 1710 cm^{-1} and the increase of the OH vibration band at 3390 cm^{-1} . The shape of the ester peak is subtly modified with the appearance of a small shoulder at 1720 cm^{-1} . Moreover, the region between 1640 and 1580 cm^{-1} evidences some alteration with the appearance of a new band around 1619 cm^{-1} . This new band is suspected to arise from the generation of alkyl vinyl ether by reaction of lignin free Al-OH onto existing

phenyl vinyl ethers, as observed on model compounds. This hypothesis is supported by FT-IR spectra of model molecules, displayed in Figure S4-61 in SI, which indicate that vinyl ether C=C bands wavenumber is slightly shifted depending on its chemical environment and stereoisomer configuration (Meunier et al., 2002). While the broadness of the peaks might result from the different isomeric configurations, the peaks maximum tends to reach 1620 cm^{-1} for alkyl vinyl ether (Benz-VE and Al-VE products) whereas phenyl vinyl ethers (S-VE and G-VE) maximum is slightly shifted towards 1640 cm^{-1} . To have a better understanding of the phenomenon occurring, thermally induced degradation under an air atmosphere was studied by applying an isotherm at $160\text{ }^{\circ}\text{C}$ on KL-PY for 4 h. The resulting curve is available in Figure S4-62 in SI. After 30 min at $160\text{ }^{\circ}\text{C}$, corresponding to the time and temperature of each compression molding cycle, only 1.3% of mass loss is observed (98.7% of remaining sample). The mass marginally decreases to 97.4% after 4 h. This suggests that KL-PY is relatively stable at temperature, or if there is any alteration in the network, only very low amounts of volatile compounds are generated. A sample of KL-PY was heated in an oven for 30 minutes at $160\text{ }^{\circ}\text{C}$ and analyzed by FT-IR as a reference (Figure S4-63 in SI). The spectra display a slight intensity decrease of the ester band and increase of the OH vibration, yet the C=C region shows no variation. It is thus suspected that the networks alteration may be partially induced by thermal treatment (linked to the esters bonds) but might also arises from the high mechanical constraints involved in the remolding process, favoring side reactions. This hypothesis is supported by stress relaxation experiments which indicated that heating the samples under low strain did not result in the formation of non-dynamic alkyl vinyl ether crosslinks. The side reaction generating alkyl vinyl ether might severely hamper the dynamic properties of the material over consecutive physical recycling cycles.

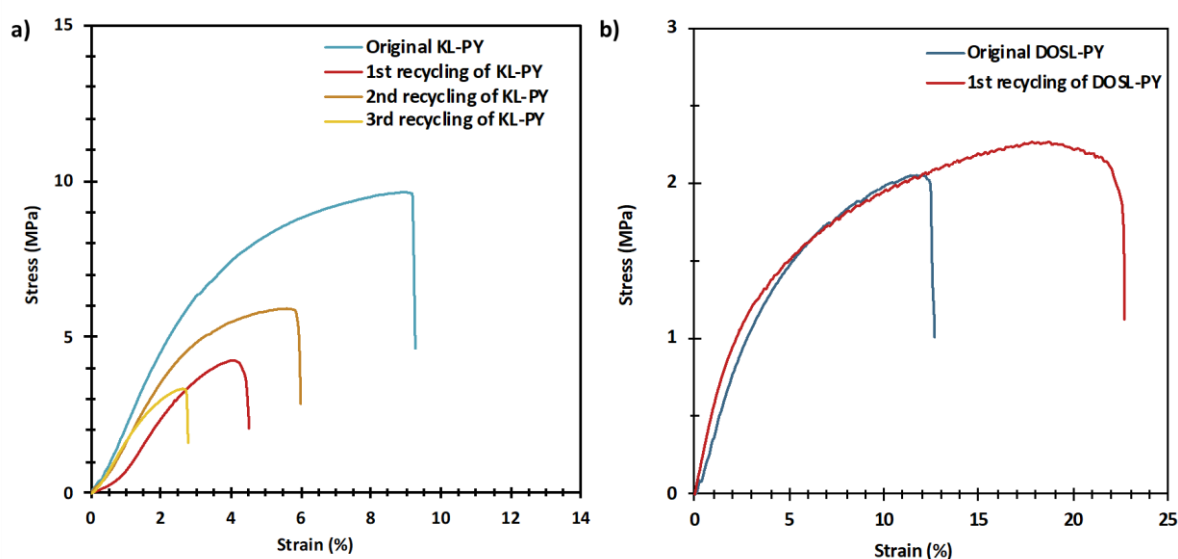


Figure 4-21. Stress-strain curves of a) pristine and recycled KL-PY, and b) pristine and recycled DOSL-PY.

The evolution of mechanical properties after various physical recycling were followed by uniaxial tensile tests. The resulting stress-strain curves are available in Figure 4-21a and the corresponding values are reported in Table 4-8. A considerable loss of mechanical performance can be observed over successive cycles, resulting in a substantial reduction in Young's modulus, maximum stress at break, and elongation at break from 263 MPa, 9.6 MPa, and 10.0% to 198 MPa, 3.2 MPa, and 2.9% for the pristine and three times recycled materials, respectively. DMA (Figure S4-64 in SI) shows a decrease in storage modulus leading to the collapse of crosslinking density from 3321 to 350 mol m^{-3} after the last recycling. Those results are indicative of a significant loss of network integrity during the remolding cycles. A suggested explanation for this crosslinking density loss is the successive cleavage of non-dynamic alkyl vinyl ether bonds during the grinding step that are no longer able of creating new

crosslinks. The materials might lose its dynamic properties during the successive physical recycling cycles. In addition to some chemical degradation of the structure observed by FT-IR, it is suspected that the physical recycling temperature of 160 °C for 30 minutes is too low and too short to induce sufficient bond exchange in KL-PY. These remolding conditions (temperature and time) were chosen to limit the thermal degradation during the physical recycling steps. However, according to the KL-PY stress relaxation experiments, a relaxation time of 1677 s (28 minutes) is observed at 170 °C, suggesting, that more than 30 minutes at 160 °C may be needed to achieve complete network rearrangement. It is noteworthy to mention that this extrapolation is only indicative.

To support this suggestion, DOSL-PY, which is the vitrimer displaying the fastest relaxation at temperature, was physically recycled once. As previously discussed for KL-PY, FT-IR of pristine and recycled DOSL-PY (Figure S4-65 in SI) exhibit diminished ester and alkene bonds but stronger OH band, indicating chemical alteration of the network. However, stress-strain results (Figure 4-21b and Table 4-8) show improved mechanical properties for the recycled material compared to pristine DOSL-PY. Young's modulus and stress at break have slightly increased from 42 to 52 MPa and from 2.0 to 2.4 MPa. Interestingly, elongation at break has almost doubled from 13.1 to 23.4% before and after recycling, respectively. Finally, crosslinking densities obtained by DMA (Figure S4-66 in SI) once again indicates a loss of network integrity with ν values that collapse from 1563 to 455 mol m⁻³ after remolding.

Table 4-8. Mechanical and rheological properties of pristine and physically recycled KL-PY and DOSL-PY.

Designations	E (MPa)	σ (MPa)	ϵ (%)	T_a (°C)	ν (mol m ⁻³)
Original KL-PY	263 ± 21	9.6 ± 0.3	10.0 ± 1.0	46	3321
KL-PY 1 st cycle	159 ± 6.8	4.2 ± 0.2	4.6 ± 0.4	53	1430
KL-PY 2 nd cycle	207.9 ± 4.1	5.9 ± 0.1	5.9 ± 0.1	49	790
KL-PY 3 rd cycle	198 ± 20.4	3.2 ± 0.7	2.9 ± 0.1	52	350
Original DOSL-PY	42 ± 3	2.0 ± 0.2	13.1 ± 2.6	10	1563
DOSL-PY 1 st cycle	52 ± 6	2.4 ± 0.1	23.4 ± 5.3	23	455

4.3.5. Analysis of the chemical recycling

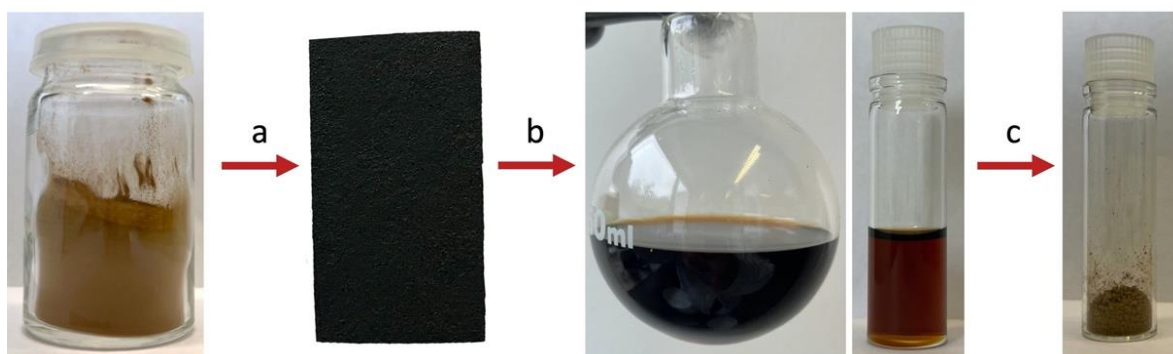


Figure 4-22. Full life cycle of PY material from a) the synthesis to b) the depolymerization, and c) the recovery of lignin.

In the aim of designing socially and economically sustainable material, closed-loop chemical recycling is an attractive “waste-to-high value” strategy in the field of CANs, in a global cradle-to-cradle potential approach. It consists of degrading networks and downstream materials into oligomers and monomers having the same structure as the starting building blocks (Liu et al., 2022) (Figure 4-22).

Closed-loop chemical recycling was then investigated. Hydroxyl-yne chemistry, including phenol-yne, is reported to be responsive to acid hydrolysis by cleavage of vinyl ether moieties (Shi et al., 2017). Moreover, ester bonds are also known to break under acidic condition in presence of excess of water (Rowe et al., 2016). Theoretically, acid-catalyzed hydrolytic degradation of the PY materials could lead to the recovery of both pristine lignin and PEG₄₀₀ by the cleavage of vinyl ethers and esters moieties as illustrated in Figure 4-23.

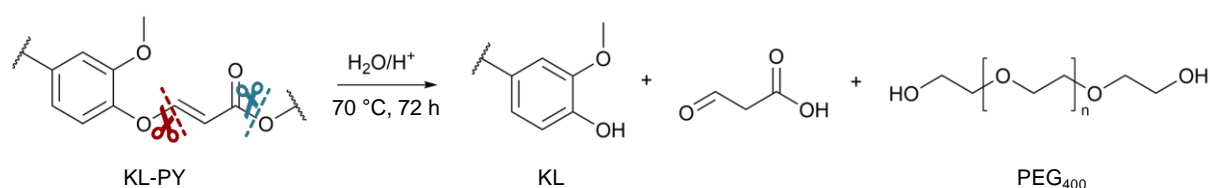


Figure 4-23. Acid-catalyzed hydrolysis of KL-PY vinyl ether and ester groups.

Various degradation conditions were investigated. Tested conditions are reported in Table S4-20 in SI and then displayed in Figure S4-67 in SI. It was found that aqueous 2M HCl and solutions of acetone/aqueous 2M HCl (7:3) could not degrade the network probably due to poor solubilization ability of the products of the depolymerization. The addition of two drops of concentrated HCl (37%) within the solution of acetone/aqueous 2M HCl (7:3) helped to disperse the material into small but insoluble particles in the mixture. DMSO/aqueous 1M HCl (8:2) was found to completely solubilize the materials over 48 h at 70 °C. The depolymerization was scale up on 1.2 g of KL-PY (0.012 g L⁻¹) was performed using the latter conditions over 72 h.

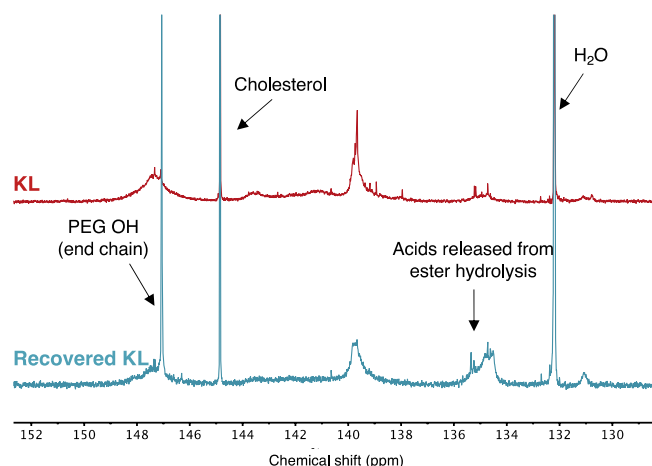


Figure 4-24. Stacked ³¹P NMR of pristine and chemically recovered KL.

Lignin was then precipitated from the DMSO/HCl solution. The recovered brown powder was analyzed by ³¹P NMR, as displayed in Figure 4-24. The content of degrafted phenols resulting from the cleavage of vinyl ether bonds was determined by integrating the Ph-OH area on the recovered KL spectrum (between 137.6 and 144.0 ppm). A resulting Ph-OH content of 1.62 mmol g⁻¹ was obtained (Table S4-21 in SI). Only 21% of Ph-OH were degrafted during this acid-catalyzed depolymerization. The ³¹P NMR spectrum also indicates the presence of OH end chains at 147.1 ppm corresponding to the chemical shift of PEG₄₀₀ (Figure S4-68 in SI), as well as an increase in signal intensity in the carboxylic

acid region from 133.6 to 136.0 (Pu et al., 2011). This suggests that the depolymerization conditions employed allow partial ester hydrolysis, but it is not sufficient to fully break all vinyl ether bonds. Finally, because PEG₄₀₀ is highly soluble in water which was used for the purification of the recovered powder, it is suspected that most PEG moieties are still grafted on one end onto vinyl ether linkages.

FT-IR analysis was performed on the recovered product, which spectra shows the presence of vinyl ether C=C band at 1640 cm⁻¹ and ester band at 1710 cm⁻¹ (Figure S4-69 in SI). The simultaneous increase in OH band at 3390 cm⁻¹, and decrease of C-H stretching (2863 cm⁻¹) and C–O–C ether stretching (1086 cm⁻¹) indicates that considerable PEG₄₀₀ amounts were removed during degradation, but some moieties are still linked by ester bonds to lignin (Shameli et al., 2012).

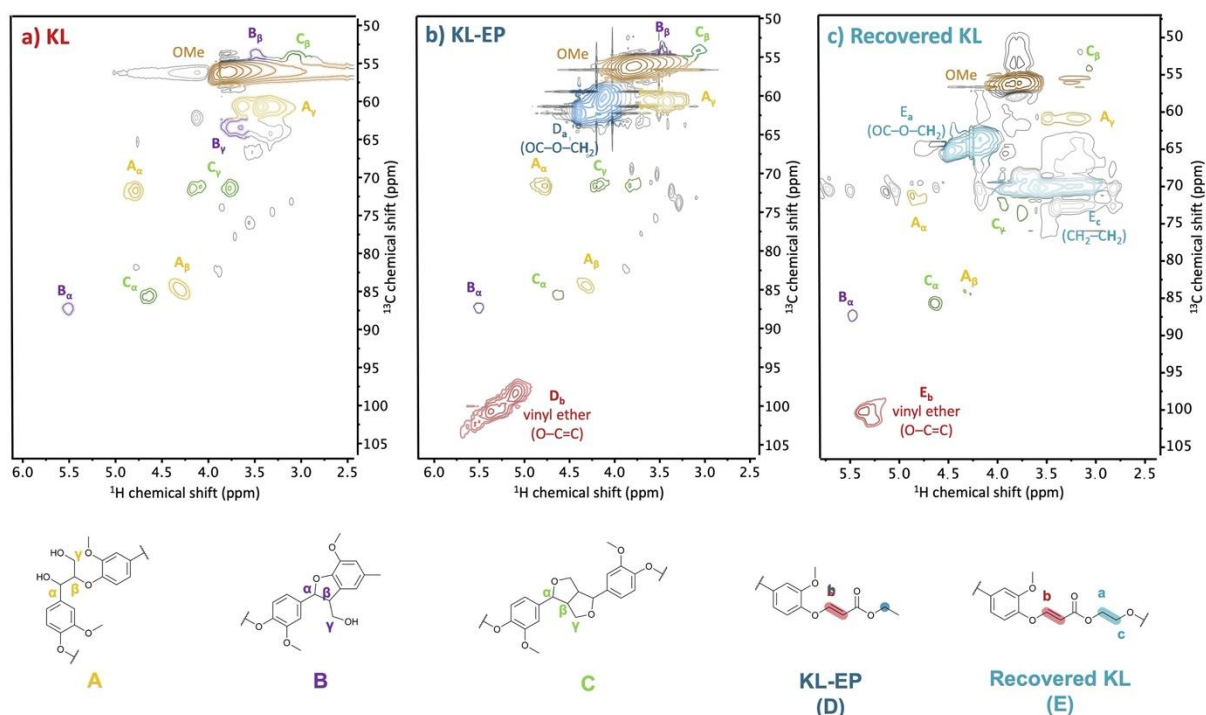


Figure 4-25. 2D HSQC of a) KL, b) KL-EP, and c) recovered KL.

To further analyze the depolymerized structure obtained, the product was analyzed by 2D HSQC NMR. The spectra of pristine KL, KL modified with ethyl propiolate (Table S2 in SI), and the recovered KL are displayed in Figure 4-25. 2D HSQC indicates that the main inter-linkages and end chains of KL remain unchanged before and after click-addition. Characteristic signals associated with B, and C structures are also observed on recovered KL. A related signals are less intense suggesting that some β-O-4 linkages might have been cleaved during the material preparation (processing) or during the depolymerization. These results overall indicate that hydrolysis conditions are not completely altering KL structure. However, the presence of PEG moieties in the recovered compound is evidenced with characteristic signals of methylene protons in α and β positions from the ester. Vinylene protons are also visible, confirming incomplete depolymerization, in agreement with ³¹P NMR and FT-IR results.

Finally, the depolymerized product was acetylated, and the soluble fractions were analyzed by SEC. Resulting curves are displayed in Figure 4-26 and detailed values are reported in Table S4-21 in SI. The soluble fraction of recovered KL showed a M_n of 1520 g mol⁻¹ indicating that the most depolymerized structures approach M_n of pristine KL. The presence of insoluble fractions after acetylation suggests the presence of structures with M_n > 1520 g mol⁻¹. Đ value reached 2.7 for the recovered KL while pristine KL Đ value was of 3.3.

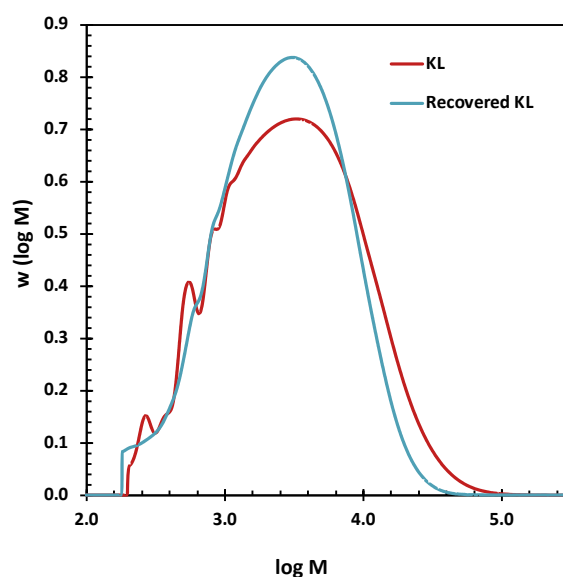


Figure 4-26. SEC curves of pristine and recovered KL.

At this level and for further development, the hydrolysis potential of materials prepared with OSL and DOSL should be assessed to compare the lignin structure influence on acid-catalyzed degradation. Hydrophilicity might be a determinant parameter in the degradation rates of the vitrimers (Liu et al., 2022; Zhou et al., 2023).

5. CONCLUSION

The under-exploited phenol-yne click-addition clearly demonstrated to be a very promising dynamic covalent chemistry for the development of highly aromatic and sustainable vitrimers, from lignin. The dynamicity of substituted phenyl vinyl ether was investigated on model compounds representatives of lignin heterogeneous reactive groups. *Ortho*-substitution of G and S units was found to strongly influence the bond exchange potential of vinyl ethers originating from different steric hinderance and *Z/E* isomerization. While G units are more easily submitted to addition on vinyl ether bonds owing to reduced steric hinderance, S units favoring *Z*-vinyl ethers undergo easier rearrangements due to their improved accessibility. The gradual replacement of *Z*-bonds into more stable *E*-linkages was found to eventually hamper bond exchanges. Kinetics studies on model compounds and on KL and OSL lignin showed the undeniably superior reactivity of phenols with activated alkynes compared to aliphatic OH, indicating the favored formation of dynamic phenyl vinyl ether bonds over non-dynamic alkyl vinyl ethers.

The valorization of different technical lignins from sulfur and free-sulfur processes, with or without molar mass fractionation, was successfully achieved by click phenol-yne addition to develop series of sustainable aromatic vitrimers. A PEG dialkyne crosslinker was prepared in a solvent-free way achieving full conversion in 24 h. The crosslinker was used in the synthesis of a series of vitrimers using different lignin sources via a one-step solvent-free click-polymerization achieving full atom-economy, in accordance with green chemistry principles. The high lignin-content vitrimers (till 49%) could undergo rearrangement through vinyl ether bond exchanges. Relaxation times from 44 to 290 s were obtained at 200 °C. E_a from 77.7 to 91.3 kJ mol⁻¹ were acquired. Network rearrangements were found to be favored with lower M_n lignin, facilitating segmental mobility needed for bond exchanges. Physical recycling was found to be hampered by the gradual formation over successive cycles of non-dynamic alkyl vinyl ether bonds resulting from the reaction of free aliphatic OHs onto dynamic phenyl vinylene moieties. Nonetheless, DOSL exhibited greater physical recycling ability compared to KL due to its lower relaxation times enabling the recovery of its initial mechanical properties. Finally, chemical

recycling was investigated through acid-catalyzed hydrolysis. Ester and vinyl ethers demonstrated to be cleavable and enabled the recovery of lignin-derived product. Although the tested conditions showed only partial hydrolysis of vinyl ether moieties with a recovery of 21% of the phenols, the results showed proofs-of-concepts for recovery of both pristine lignin and PEG. The closed-loop recycling of lignin-based phenol-yne vitrimer could also offer further upcycling opportunities for the development of sustainable aromatic materials.

This work paves the way to many new perspectives in the exploration of lignin-based phenol-yne materials. Dynamicity could be further investigated in the absence of ester bonds to enable the scrutiny of vinyl ether exchanges. A keto ether activated alkyne crosslinker could be herein employed instead of the ester activated PEG-DA. Lignin aliphatic OHs were identified as source of recyclability limitation by generating non-dynamic alkyl vinyl ether linkages and potential transesterification reactions altering the network chemical structure. It would be interesting to use protective groups to make them inert within the materials. Grafting of methyl or ethyl ethers could be good candidates if the group is wanted to remain permanently onto OHs groups because they cannot be removed except under drastic conditions. Conversely, benzyl and silyl ethers are suitable protecting groups for on-demand removability. Finally, an evaluation of the photoisomerization potential of lignin-based phenol-yne vitrimers could be utmost relevance to achieve on-demand dynamicity and thus recyclability of the materials. By shifting the configurations to *E*-isomer with the suitable wavelength the material may show hindered dynamicity and thus improved creep resistance, while shifting to the *Z*-configuration could accelerate rearrangements upon temperature rising during physical recycling.

6. REFERENCES

- Ahmadi, M., Hanifpour, A., Ghiassinejad, S., van Ruymbeke, E., 2022. Polyolefins Vitrimers: Design Principles and Applications. *Chem. Mater.* 34, 10249–10271. <https://doi.org/10.1021/acs.chemmater.2c02853>
- Anastas, P., Eghbali, N., 2010. Green Chemistry: Principles and Practice. *Chem. Soc. Rev.* 39, 301–312. <https://doi.org/10.1039/B918763B>
- Archipov, Y., Argyropoulos, D.S., Bolker, H.I., Heitner, C., 1991. 31P NMR Spectroscopy in Wood Chemistry. I. Model Compounds. *J. Wood Chem. Technol.* 11, 137–157. <https://doi.org/10.1080/02773819108050267>
- Babra, T.S., Wood, M., Godleman, J.S., Salimi, S., Warriner, C., Bazin, N., Siviour, C.R., Hamley, I.W., Hayes, W., Greenland, B.W., 2019. Fluoride-responsive debond on demand adhesives: Manipulating polymer crystallinity and hydrogen bonding to optimise adhesion strength at low bonding temperatures. *Eur. Polym. J.* 119, 260–271. <https://doi.org/10.1016/j.eurpolymj.2019.07.038>
- Bowman, C.N., Kloxin, C.J., 2012. Covalent Adaptable Networks: Reversible Bond Structures Incorporated in Polymer Networks. *Angew. Chem. Int. Ed.* 51, 4272–4274. <https://doi.org/10.1002/anie.201200708>
- Breuillac, A., Kassalias, A., Nicolaÿ, R., 2019. Polybutadiene Vitrimers Based on Dioxaborolane Chemistry and Dual Networks with Static and Dynamic Cross-links. *Macromolecules* 52, 7102–7113. <https://doi.org/10.1021/acs.macromol.9b01288>
- Brutman, J.P., Delgado, P.A., Hillmyer, M.A., 2014. Polylactide Vitrimers. *ACS Macro Lett.* 3, 607–610. <https://doi.org/10.1021/mz500269w>
- Buono, P., Duval, A., Averous, L., Habibi, Y., 2017. Thermally healable and remendable lignin-based materials through Diels – Alder click polymerization. *Polymer* 133, 78–88. <https://doi.org/10.1016/j.polymer.2017.11.022>
- Capelot, M., Unterlass, M.M., Tournilhac, F., Leibler, L., 2012. Catalytic Control of the Vitrimer Glass Transition. *ACS Macro Lett.* 1, 789–792. <https://doi.org/10.1021/mz300239f>

- Chen, M., Si, H., Zhang, H., Zhou, L., Wu, Y., Song, L., Kang, M., Zhao, X.-L., 2021. The Crucial Role in Controlling the Dynamic Properties of Polyester-Based Epoxy Vitrimers: The Density of Exchangeable Ester Bonds (v). *Macromolecules* 54, 10110–10117. <https://doi.org/10.1021/acs.macromol.1c01289>
- Chenal, J.-M., Chazeau, L., Guy, L., Bomal, Y., Gauthier, C., 2007. Molecular weight between physical entanglements in natural rubber: A critical parameter during strain-induced crystallization. *Polymer* 48, 1042–1046. <https://doi.org/10.1016/j.polymer.2006.12.031>
- Chiang, Y., Kresge, A.J., Young, C.I., 1978. Vinyl ether hydrolysis. XII. Use of *cis* – *trans* isomerism to probe the reaction mechanism. *Can. J. Chem.* 56, 461–464. <https://doi.org/10.1139/v78-074>
- Cui, C.-Y., Chen, W., Wang, H.-R., Ren, W.-M., Lu, X.-B., Zhou, H., 2024. Degradable sugar-derived poly(vinyl ether ester)s by hydroxyl-yne click polymerization. *Eur. Polym. J.* 211, 112997. <https://doi.org/10.1016/j.eurpolymj.2024.112997>
- Denissen, W., M. Winne, J., Prez, F.E.D., 2016. Vitrimers: permanent organic networks with glass-like fluidity. *Chem. Sci.* 7, 30–38. <https://doi.org/10.1039/C5SC02223A>
- Dhers, S., Vantomme, G., Avérous, L., 2019. A fully bio-based polyimine vitrimer derived from fructose. *Green Chem.* 21, 1596–1601. <https://doi.org/10.1039/C9GC00540D>
- Dhinojwala, A., Hooker, J.C., Torkelson, J.M., 1994. Retardation of rotational reorientation dynamics in polymers near the glass transition: a novel study over eleven decades in time using second-order non-linear optics. *J. Non-Cryst. Solids, Relaxations in Complex Systems* 172–174, 286–296. [https://doi.org/10.1016/0022-3093\(94\)90447-2](https://doi.org/10.1016/0022-3093(94)90447-2)
- Duval, A., Avérous, L., 2017. Cyclic Carbonates as Safe and Versatile Etherifying Reagents for the Functionalization of Lignins and Tannins. *ACS Sustain. Chem. Eng.* 5, 7334–7343. <https://doi.org/10.1021/acssuschemeng.7b01502>
- Duval, A., Benali, W., Avérous, L., 2024. Turning lignin into a recyclable bioresource: transesterification vitrimers from lignins modified with ethylene carbonate. *Green Chem.* <https://doi.org/10.1039/D4GC00567H>
- Duval, A., Lange, H., Lawoko, M., Crestini, C., 2015. Reversible crosslinking of lignin via the furan–maleimide Diels–Alder reaction. *Green Chem.* 17, 4991–5000. <https://doi.org/10.1039/C5GC01319D>
- Fu, X., Qin, A., Tang, B.Z., 2024. Dynamic covalent polymers generated from X-yne click polymerization. *J. Polym. Sci.* 62. <https://doi.org/10.1002/pol.20230383>
- Gao, S., Cheng, Z., Zhou, X., Liu, Y., Wang, J., Wang, C., Chu, F., Xu, F., Zhang, D., 2020. Fabrication of lignin based renewable dynamic networks and its applications as self-healing, antifungal and conductive adhesives. *Chem. Eng. J.* 394, 124896. <https://doi.org/10.1016/j.cej.2020.124896>
- Glasser, W.G., 2019. About Making Lignin Great Again—Some Lessons From the Past. *Front. Chem.* 7. <https://doi.org/10.3389/fchem.2019.00565>
- Granata, A., Argyropoulos, D.S., 1995. 2-Chloro-4,4,5,5-tetramethyl-1,3,2-dioxaphospholane, a Reagent for the Accurate Determination of the Uncondensed and Condensed Phenolic Moieties in Lignins. *J. Agric. Food Chem.* 43, 1538–1544. <https://doi.org/10.1021/jf00054a023>
- Huang, J., Jiang, X., 2018. Injectable and Degradable pH-Responsive Hydrogels via Spontaneous Amino–Yne Click Reaction. *ACS Appl. Mater. Interfaces* 10, 361–370. <https://doi.org/10.1021/acsmi.7b18141>
- Jiang, Qimin, Zhang, H., Jiang, Qilin, Zhang, S., Guan, S., Huang, W., Xue, X., Yang, H., Jiang, L., Jiang, B., Komarneni, S., 2023. Hydroxyl–yne click polymerization: a facile strategy toward poly(vinyl amino ether ester)s with color-tunable luminescence. *Polym. Chem.* 14, 1232–1240. <https://doi.org/10.1039/D2PY01581A>
- J. Kloxin, C., N. Bowman, C., 2013. Covalent adaptable networks: smart, reconfigurable and responsive network systems. *Chem. Soc. Rev.* 42, 7161–7173. <https://doi.org/10.1039/C3CS60046G>
- Katritzky, A.R., Singh, S.K., Meher, N.K., Doskocz, J., Suzuki, K., Jiang, R., Sommen, G.L., Ciaramitaro, D.A., Steel, P.J., 2006. Triazole-oligomers by 1,3-dipolar cycloaddition. *Arkivoc* 2006, 43–62. <https://doi.org/10.3998/ark.5550190.0007.505>

- Kloxin, C.J., Scott, T.F., Adzima, B.J., Bowman, C.N., 2010. Covalent Adaptable Networks (CANs): A Unique Paradigm in Cross-Linked Polymers. *Macromolecules* 43, 2643–2653. <https://doi.org/10.1021/ma902596s>
- Laurichesse, S., Avérous, L., 2014. Chemical modification of lignins: Towards biobased polymers. *Prog. Polym. Sci.* 39, 1266–1290. <https://doi.org/10.1016/j.progpolymsci.2013.11.004>
- Lessard, J.J., Garcia, L.F., Easterling, C.P., Sims, M.B., Bentz, K.C., Arencibia, S., Savin, D.A., Sumerlin, B.S., 2019. Catalyst-Free Vitrimers from Vinyl Polymers. *Macromolecules* 52, 2105–2111. <https://doi.org/10.1021/acs.macromol.8b02477>
- Liu, W., Fang, C., Chen, F., Qiu, X., 2020. Strong, Reusable, and Self-Healing Lignin-Containing Polyurea Adhesives. *ChemSusChem* 13, 4691–4701. <https://doi.org/10.1002/cssc.202001602>
- Liu, Y., Yu, Z., Wang, B., Li, P., Zhu, J., Ma, S., 2022. Closed-loop chemical recycling of thermosetting polymers and their applications: a review. *Green Chem.* 24, 5691–5708. <https://doi.org/10.1039/D2GC00368F>
- Lucherelli, M.A., Duval, A., Avérous, L., 2022. Biobased vitrimers: Towards sustainable and adaptable performing polymer materials. *Prog. Polym. Sci.* 127, 101515. <https://doi.org/10.1016/j.progpolymsci.2022.101515>
- Ma, X., Li, S., Wang, F., Wu, J., Chao, Y., Chen, X., Chen, P., Zhu, J., Yan, N., Chen, J., 2023. Catalyst-Free Synthesis of Covalent Adaptable Network (CAN) Polyurethanes from Lignin with Editable Shape Memory Properties. *ChemSusChem* 16, e202202071. <https://doi.org/10.1002/cssc.202202071>
- Maity, A., Chen, J., Wilson-Faubert, N., Laventure, A., Nazemi, A., 2024. Harnessing Activated Alkyne-Hydroxyl “Click” Chemistry for Degradable and Self-Healing Poly(urea vinyl ether ester)s. *Macromolecules* 57, 305–316. <https://doi.org/10.1021/acs.macromol.3c01574>
- Marcos Celada, L., Martín, J., Dvinskikh, S.V., Olsén, P., 2024. Fully Bio-Based Ionic Liquids for Green Chemical Modification of Cellulose in the Activated-State. *ChemSusChem* 17, e202301233. <https://doi.org/10.1002/cssc.202301233>
- Martins, M.L., Zhao, X., Demchuk, Z., Luo, J., Carden, G.P., Toletay, G., Sokolov, A.P., 2023. Viscoelasticity of Polymers with Dynamic Covalent Bonds: Concepts and Misconceptions. *Macromolecules* 56, 8688–8696. <https://doi.org/10.1021/acs.macromol.3c01545>
- McBride, M.K., Worrell, B.T., Brown, T., Cox, L.M., Sowan, N., Wang, C., Podgorski, M., Martinez, A.M., Bowman, C.N., 2019. Enabling Applications of Covalent Adaptable Networks. *Annu. Rev. Chem. Biomol. Eng.* 10, 175–198. <https://doi.org/10.1146/annurev-chembioeng-060718-030217>
- Meng, X., Crestini, C., Ben, H., Hao, N., Pu, Y., Ragauskas, A.J., Argyropoulos, D.S., 2019. Determination of hydroxyl groups in biorefinery resources via quantitative 31P NMR spectroscopy. *Nat. Protoc.* 14, 2627–2647. <https://doi.org/10.1038/s41596-019-0191-1>
- Merino, D.H., Feula, A., Melia, K., Slark, A.T., Giannakopoulos, I., Siviour, C.R., Buckley, C.P., Greenland, B.W., Liu, D., Gan, Y., Harris, P.J., Chippindale, A.M., Hamley, I.W., Hayes, W., 2016. A systematic study of the effect of the hard end-group composition on the microphase separation, thermal and mechanical properties of supramolecular polyurethanes. *Polymer, Self-Assembly* 107, 368–378. <https://doi.org/10.1016/j.polymer.2016.07.029>
- Meunier, F.C., Domokos, L., Seshan, K., Lercher, J.A., 2002. *In Situ* IR Study of the Nature and Mobility of Sorbed Species on H-FER during But-1-ene Isomerization. *J. Catal.* 211, 366–378. <https://doi.org/10.1006/jcat.2002.3703>
- Montarnal, D., Capelot, M., Tournilhac, F., Leibler, L., 2011. Silica-Like Malleable Materials from Permanent Organic Networks. *Science* 334, 965–968. <https://doi.org/10.1126/science.1212648>
- Moreno, A., Morsali, M., Sipponen, M.H., 2021. Catalyst-Free Synthesis of Lignin Vitrimers with Tunable Mechanical Properties: Circular Polymers and Recoverable Adhesives. *ACS Appl. Mater. Interfaces* 13, 57952–57961. <https://doi.org/10.1021/acsami.1c17412>
- Ochoa-Gómez, J.R., Gómez-Jiménez-Aberasturi, O., Maestro-Madurga, B., Pesquera-Rodríguez, A., Ramírez-López, C., Lorenzo-Ibarreta, L., Torrecilla-Soria, J., Villarán-Velasco, M.C., 2009. Synthesis of glycerol carbonate from glycerol and dimethyl carbonate by transesterification:

- Catalyst screening and reaction optimization. *Appl. Catal. Gen.* 366, 315–324. <https://doi.org/10.1016/j.apcata.2009.07.020>
- Palmese, G.R., McCullough, R.L., 1992. Effect of epoxy–amine stoichiometry on cured resin material properties. *J. Appl. Polym. Sci.* 46, 1863–1873. <https://doi.org/10.1002/app.1992.070461018>
- Pu, Y., Cao, S., Ragauskas, A.J., 2011. Application of quantitative ³¹P NMR in biomass lignin and biofuel precursors characterization. *Energy Environ. Sci.* 4, 3154–3166. <https://doi.org/10.1039/C1EE01201K>
- Rowe, M.D., Eyiler, E., Walters, K.B., 2016. Hydrolytic degradation of bio-based polyesters: Effect of pH and time. *Polym. Test.* 52, 192–199. <https://doi.org/10.1016/j.polymertesting.2016.04.015>
- Santos, T., Pérez-Pérez, Y., Rivero, D.S., Diana-Rivero, R., García-Tellado, F., Tejedor, D., Carrillo, R., 2022. Dynamic Hydroxyl–Yne Reaction with Phenols. *Org. Lett.* 24, 8401–8405. <https://doi.org/10.1021/acs.orglett.2c03518>
- Shameli, K., Bin Ahmad, M., Jazayeri, S.D., Sedaghat, S., Shabanzadeh, P., Jahangirian, H., Mahdavi, M., Abdollahi, Y., 2012. Synthesis and Characterization of Polyethylene Glycol Mediated Silver Nanoparticles by the Green Method. *Int. J. Mol. Sci.* 13, 6639–6650. <https://doi.org/10.3390/ijms13066639>
- Shi, Y., Bai, T., Bai, W., Wang, Z., Chen, M., Yao, B., Sun, J.Z., Qin, A., Ling, J., Tang, B.Z., 2017. Phenol-yne Click Polymerization: An Efficient Technique to Facilely Access Regio- and Stereoregular Poly(vinylene ether ketone)s. *Chem. – Eur. J.* 23, 10725–10731. <https://doi.org/10.1002/chem.201702966>
- Si, H., Wang, K., Song, B., Qin, A., Tang, B.Z., 2020. Organobase-catalysed hydroxyl–yne click polymerization. *Polym. Chem.* 11, 2568–2575. <https://doi.org/10.1039/D0PY00095G>
- Smit, A.T., Dezaire, T., Riddell, L.A., Bruijninx, P.C.A., 2023. Reductive Partial Depolymerization of Acetone Organosolv Lignin to Tailor Lignin Molar Mass, Dispersity, and Reactivity for Polymer Applications. *ACS Sustain. Chem. Eng.* 11, 6070–6080. <https://doi.org/10.1021/acssuschemeng.3c00617>
- Smit, A.T., Verges, M., Schulze, P., van Zomeren, A., Lorenz, H., 2022. Laboratory- to Pilot-Scale Fractionation of Lignocellulosic Biomass Using an Acetone Organosolv Process. *ACS Sustain. Chem. Eng.* 10, 10503–10513. <https://doi.org/10.1021/acssuschemeng.2c01425>
- Song, B., Lu, D., Qin, A., Tang, B.Z., 2022. Combining Hydroxyl–Yne and Thiol–Ene Click Reactions to Facilely Access Sequence-Defined Macromolecules for High-Density Data Storage. *J. Am. Chem. Soc.* 144, 1672–1680. <https://doi.org/10.1021/jacs.1c10612>
- Song, P., Du, L., Pang, J., Jiang, G., Shen, J., Ma, Y., Ren, S., Li, S., 2023. Preparation and properties of lignin-based vitrimer system containing dynamic covalent bonds for reusable and recyclable epoxy asphalt. *Ind. Crops Prod.* 197, 116498. <https://doi.org/10.1016/j.indcrop.2023.116498>
- Sougrati, L., Duval, A., Avérous, L., 2023a. From Lignins to Renewable Aromatic Vitrimers based on Vinylogous Urethane. *ChemSusChem* 16, e202300792. <https://doi.org/10.1002/cssc.202300792>
- Sougrati, L., Wendels, S., Dinescu, S., Balahura, L.-R., Sleiman, L., Avérous, L., 2023b. Renewable adhesives based on oleo-chemistry: From green synthesis to biomedical applications. *Sustain. Mater. Technol.* 37, e00656. <https://doi.org/10.1016/j.susmat.2023.e00656>
- Thys, M., Brancart, J., Van Assche, G., Vendamme, R., Van den Brande, N., 2021. Reversible Lignin-Containing Networks Using Diels–Alder Chemistry. *Macromolecules* 54, 9750–9760. <https://doi.org/10.1021/acs.macromol.1c01693>
- Tiz, D.B., Vicente, F.A., Kroflič, A., Likozar, B., 2023. Lignin-Based Covalent Adaptable Network Polymers—When Bio-Based Thermosets Meet Recyclable by Design. *ACS Sustain. Chem. Eng.* 11, 13836–13867. <https://doi.org/10.1021/acssuschemeng.3c03248>
- Truong, V.X., Dove, A.P., 2013. Organocatalytic, Regioselective Nucleophilic “Click” Addition of Thiols to Propiolic Acid Esters for Polymer–Polymer Coupling. *Angew. Chem.* 125, 4226–4230. <https://doi.org/10.1002/ange.201209239>
- Vidil, T., Llevot, A., 2022. Fully Biobased Vitrimers: Future Direction toward Sustainable Cross-Linked Polymers. *Macromol. Chem. Phys.* 223, 2100494. <https://doi.org/10.1002/macp.202100494>

- Wang, C., Kelley, S.S., Venditti, R.A., 2016. Lignin-Based Thermoplastic Materials. *ChemSusChem* 9, 770–783. <https://doi.org/10.1002/cssc.201501531>
- Williams, G., Watts, D.C., 1970. Non-symmetrical dielectric relaxation behaviour arising from a simple empirical decay function. *Trans. Faraday Soc.* 66, 80–85. <https://doi.org/10.1039/TF9706600080>
- Winne, J.M., Leibler, L., Prez, F.E.D., 2019. Dynamic covalent chemistry in polymer networks: a mechanistic perspective. *Polym. Chem.* 10, 6091–6108. <https://doi.org/10.1039/C9PY01260E>
- Worch, J.C., Stubbs, C.J., Price, M.J., Dove, A.P., 2021. Click Nucleophilic Conjugate Additions to Activated Alkynes: Exploring Thiol-yne, Amino-yne, and Hydroxyl-yne Reactions from (Bio)Organic to Polymer Chemistry. *Chem. Rev.* 121, 6744–6776. <https://doi.org/10.1021/acs.chemrev.0c01076>
- Yao, B., Mei, J., Li, J., Wang, J., Wu, H., Sun, J.Z., Qin, A., Tang, B.Z., 2014. Catalyst-Free Thiol–Yne Click Polymerization: A Powerful and Facile Tool for Preparation of Functional Poly(vinylene sulfide)s. *Macromolecules* 47, 1325–1333. <https://doi.org/10.1021/ma402559a>
- Zhang, W., Gao, F., Shen, L., Chen, Y., Lin, Y., 2022. Unexploited Design and Application of Dynamic Covalent Networks: Phenol-yne Click Reaction and Porous Film Generation. *ACS Mater. Lett.* 4, 2090–2096. <https://doi.org/10.1021/acsmaterialslett.2c00633>
- Zhao, X.-L., Tian, P.-X., Li, Y.-D., Zeng, J.-B., 2022. Biobased covalent adaptable networks: towards better sustainability of thermosets. *Green Chem.* 24, 4363–4387. <https://doi.org/10.1039/D2GC01325H>
- Zheng, J., Png, Z.M., Ng, S.H., Tham, G.X., Ye, E., Goh, S.S., Loh, X.J., Li, Z., 2021. Vitrimers: Current research trends and their emerging applications. *Mater. Today* 51, 586–625. <https://doi.org/d>
- Zhou, S., Huang, K., Xu, X., Wang, B., Zhang, W., Su, Y., Hu, K., Zhang, C., Zhu, J., Weng, G., Ma, S., 2023. Rigid-and-Flexible, Degradable, Fully Biobased Thermosets from Lignin and Soybean Oil: Synthesis and Properties. *ACS Sustain. Chem. Eng.* 11, 3466–3473. <https://doi.org/10.1021/acssuschemeng.2c06990>

7. APPENDICES (SI)

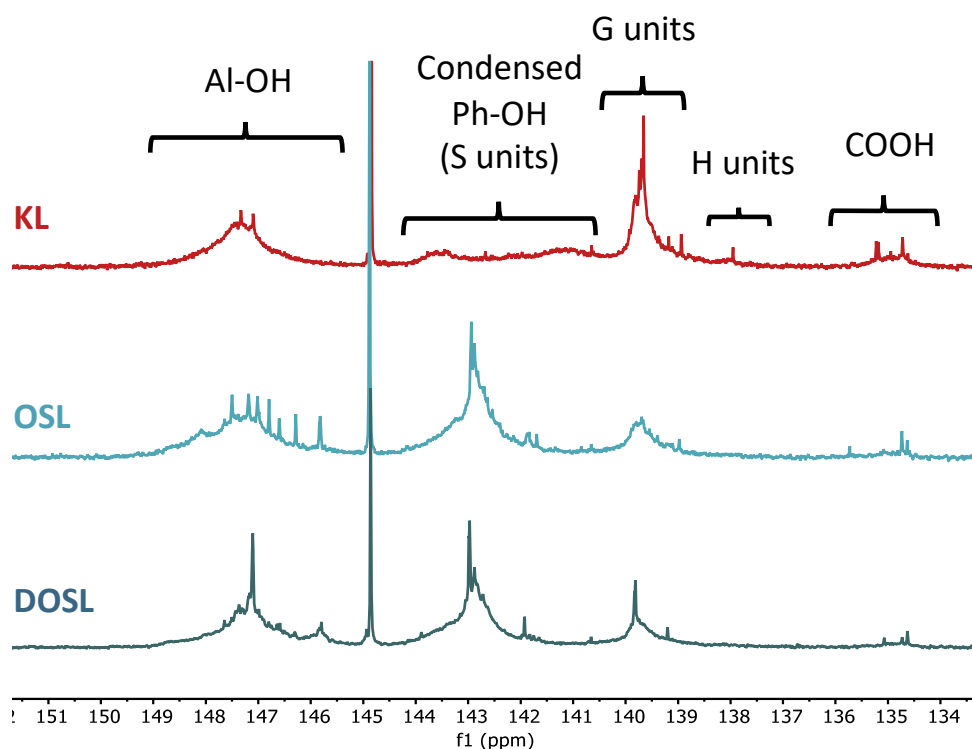


Figure S4-27. ^{31}P NMR spectra of KL, OSL, and DOSL.

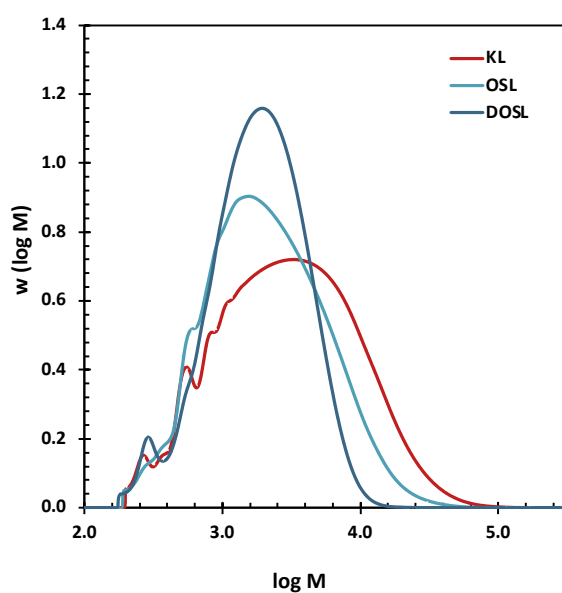


Figure S4-28. SEC curves of KL, OSL, and DOSL in THF.

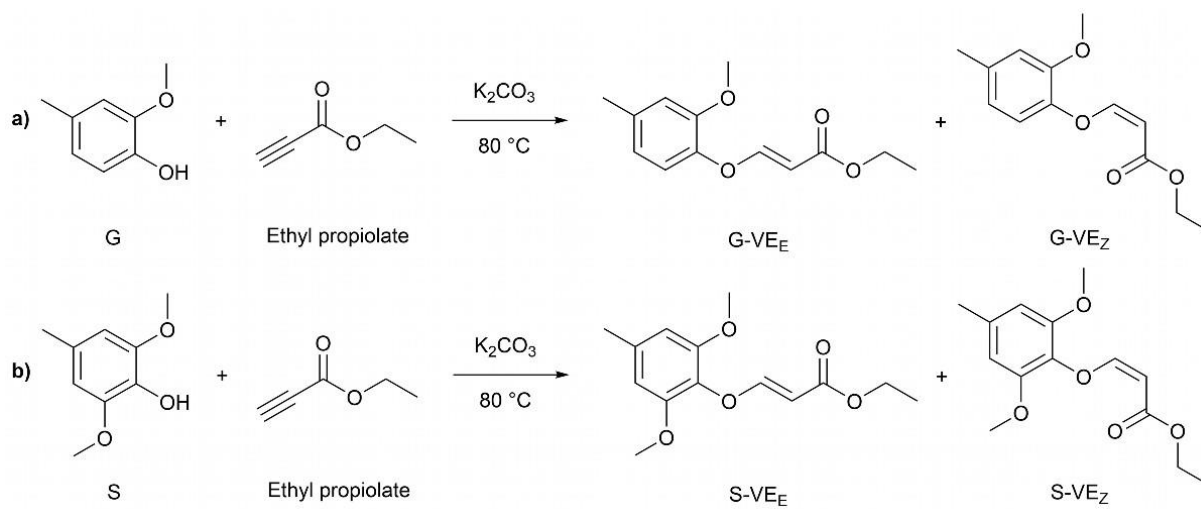


Figure S4-29. Synthesis of G-VE and S-VE model compounds by click-addition.

CHAPITRE 4

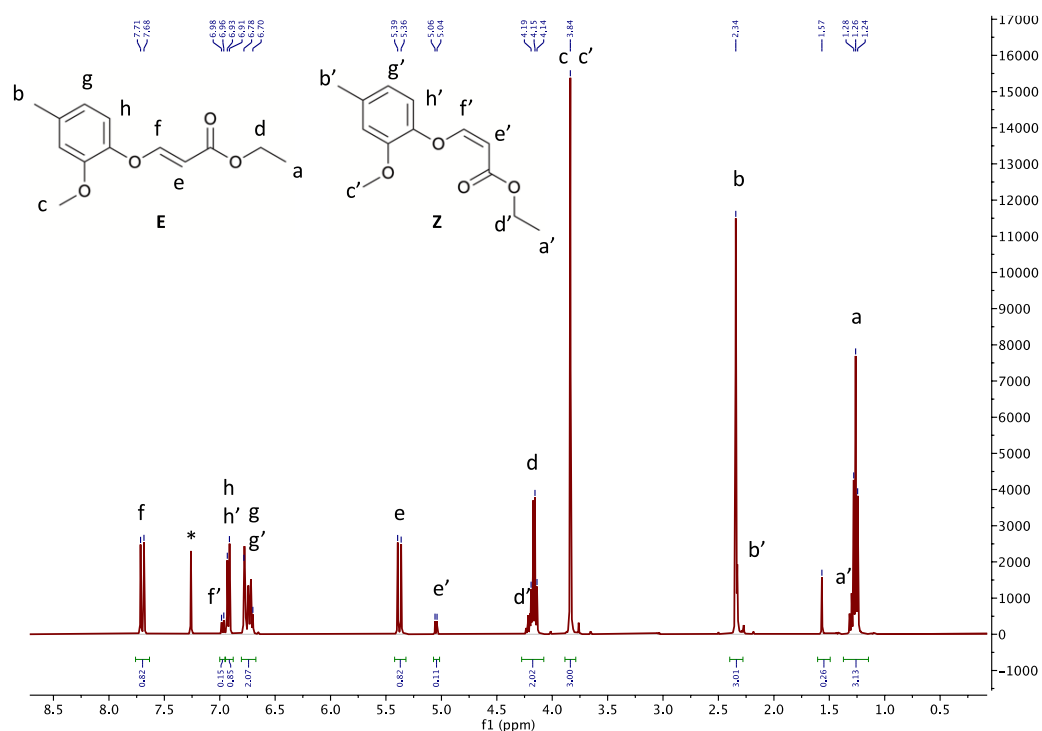


Figure S4-30. ^1H NMR of G-VE in CDCl_3 .

^1H NMR (400 MHz, CDCl_3) δ 7.70 (d, $J = 12.2$ Hz, 1H), 6.92 (d, $J = 7.9$ Hz, 1H), 6.78 (s, 2H), 5.38 (d, $J = 12.3$ Hz, 1H), 4.28 – 4.08 (m, 2H), 3.84 (s, 3H), 2.34 (s, 3H), 1.26 (t, $J = 7.2$ Hz, 3H).

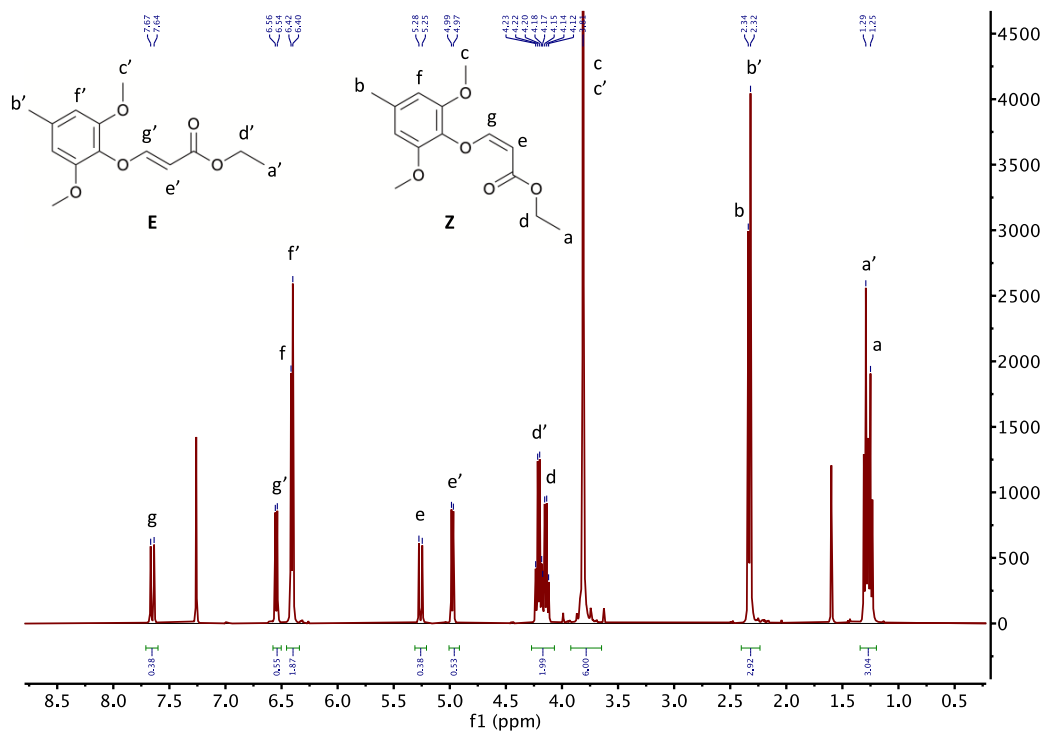


Figure S4-31. ^1H NMR of S-VE in CDCl_3 .

^1H NMR (400 MHz, CDCl_3) δ 7.65 (d, $J = 12.2$ Hz, 1H), 6.55 (d, $J = 7.0$ Hz, 1H), 5.26 (d, $J = 12.2$ Hz, 1H), 4.98 (d, $J = 7.0$ Hz, 1H), 4.21 (q, $J = 7.2$ Hz, 3H), 4.15 (q, $J = 7.2$ Hz, 2H), 1.27 (d, $J = 16.5$ Hz, 4H).

CHAPITRE 4

Table S4-9. Vinyl ether model exchange reactions conditions.

Exchange units	Model	Exchangeable unit	m_{model} (g)	Quantity exch. unit	$m_{\text{K}_2\text{CO}_3}$ (g)
GG'	G-VE	G'	0.2	93 μL	0.0059
GS'	G-VE	S'	0.2	0.1304 g	0.0059
SG'	S-VE	G'	0.2	83 μL	0.0052
SS'	S-VE	S'	0.2	0.1158 g	0.0052
G/Al	G-VE	Benzyl alcohol	0.2	88 μL	0.0059
Al/G	Benz	G	1	613 μL	0.0335

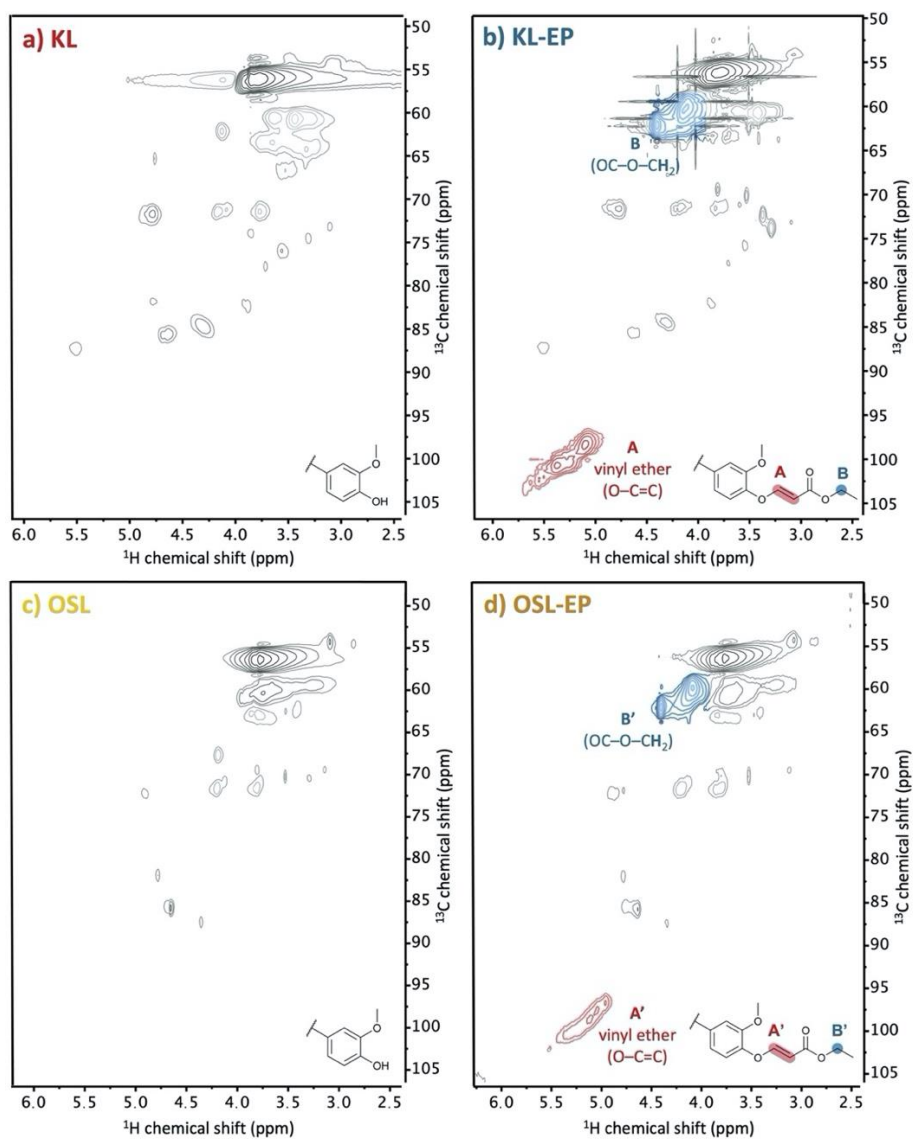


Figure S4-32. 2D HSQC spectra of a) KL, b) KL-EP, c) OSL, and d) OSL-EP in DMSO- d_6 .

CHAPITRE 4

Table S4-10. Reactional conditions of lignin modification with ethyl propiolate (EP) and conversion of Ph-OH and Al-OH.

Entry	Lignin	T (°C)	Solvent	Time (h)	m _{Lignin} (g)	V _{EP} (μL)	m _{K₂CO₃} (g)	Ph-OH converted (mmol g ⁻¹)	Al-OH converted (mmol g ⁻¹)	Conversion Ph-OH (%)	Conversion Al-OH (%)
OSL-80	OSL	80	DMF	23	1	293	0.02	1.26	0.43	43.7	24.8
KL-80	KL	80	DMF	23	0.5	219	0.015	2.93	1.10	67.8	44.0
KL-120	KL	120	DMF	4	0.5	219	0.015	3.01	1.11	69.6	44.2
OSL-DMSO	OSL	80	DMSO	23	1	293	0.02	1.40	0.40	48.6	23.2

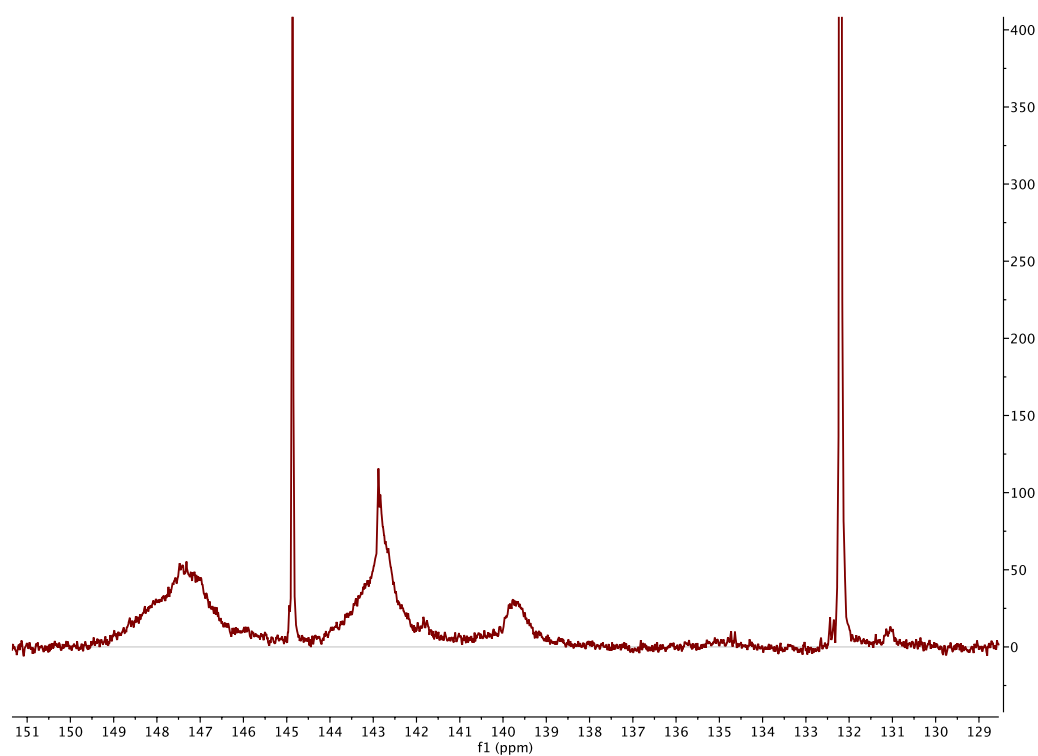


Figure S4-33. ³¹P NMR spectra of OSL-80 in DMSO-d₆.

CHAPITRE 4

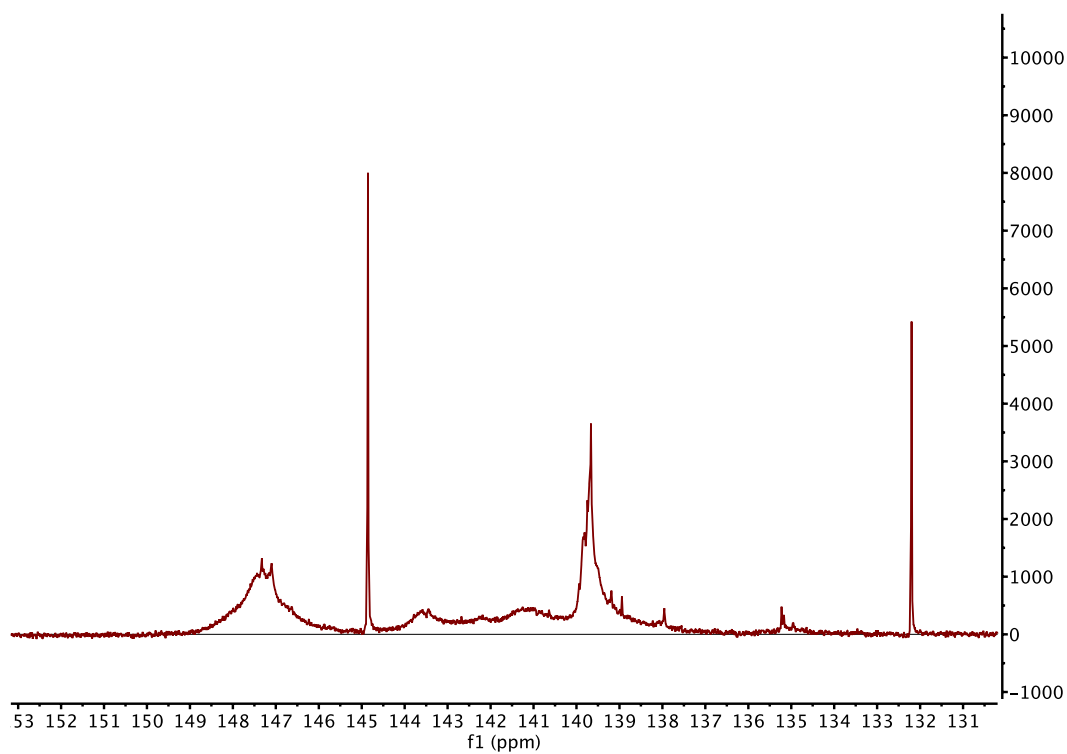


Figure S4-34. ^{31}P NMR spectra of KL-80 in $\text{DMSO-}d_6$.

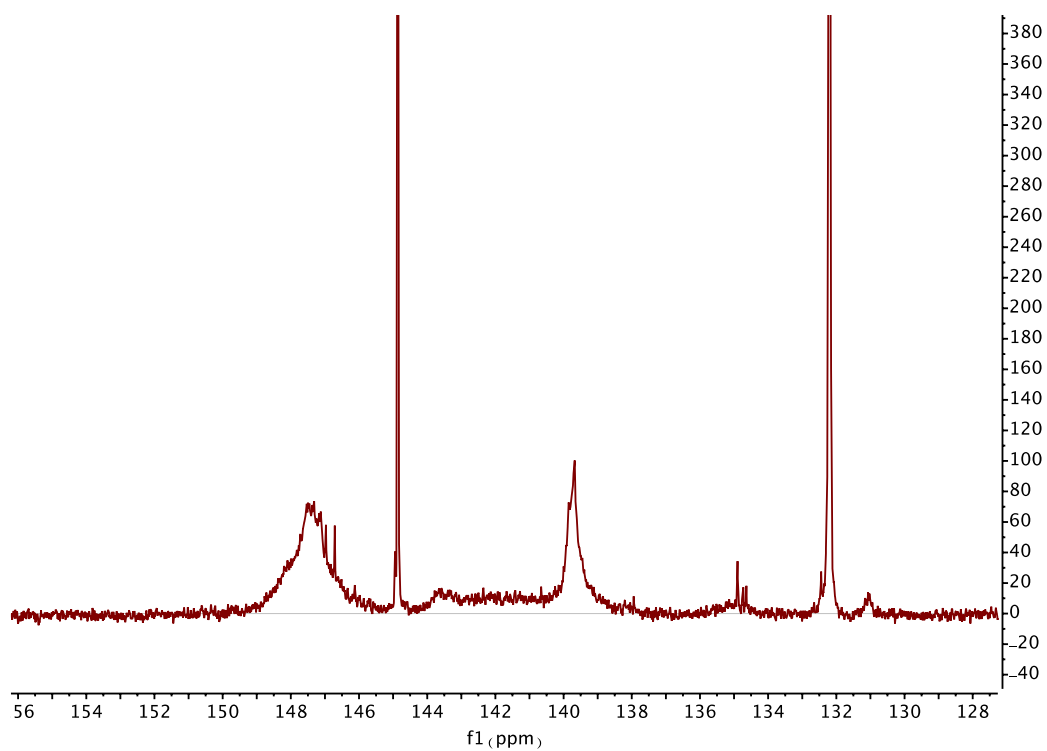


Figure S4-35. ^{31}P NMR spectra of KL-120 in $\text{DMSO-}d_6$.

CHAPITRE 4

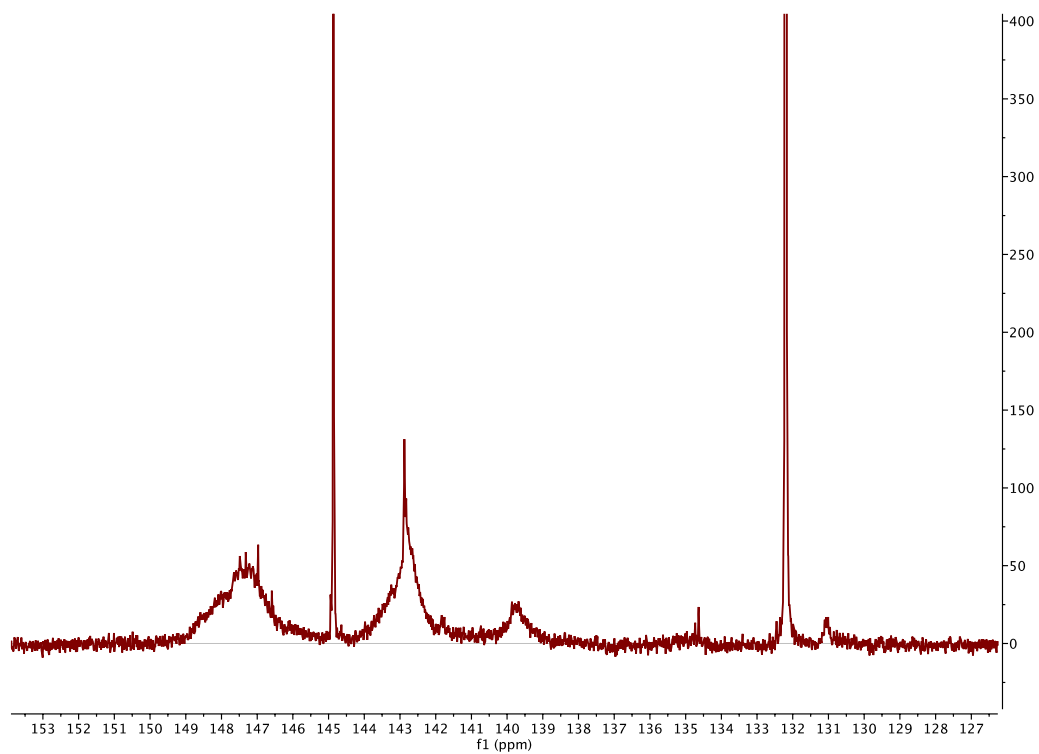


Figure S4-36. ^{31}P NMR spectra of OSL-DMSO in $\text{DMSO-}d_6$.

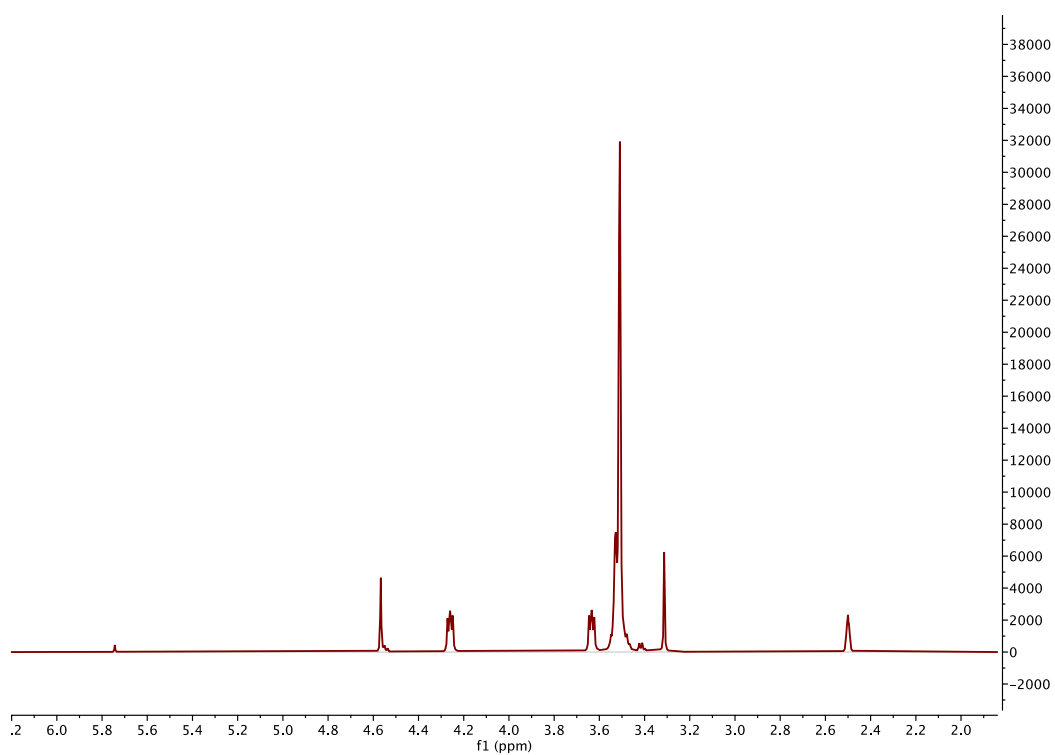


Figure S4-37. ^1H NMR spectra of PEG-DA in $\text{DMSO-}d_6$.

CHAPITRE 4

Table S4-11. Synthesis condition of lignin-based materials.

Material Designation	Lignin	Ph-OH content (mmol g ⁻¹)	m _{lignin} (g)	m _{MPEG-DA} (g)	m _{K₂CO₃} (g)
KL-PY	Kraft	4.33	5.500	8.569	0.658
OSL-PY	Organosolv	2.89	8.000	8.318	0.639
DOSL-PY	Depolymerized organosolv	3.27	8.000	9.417	0.723

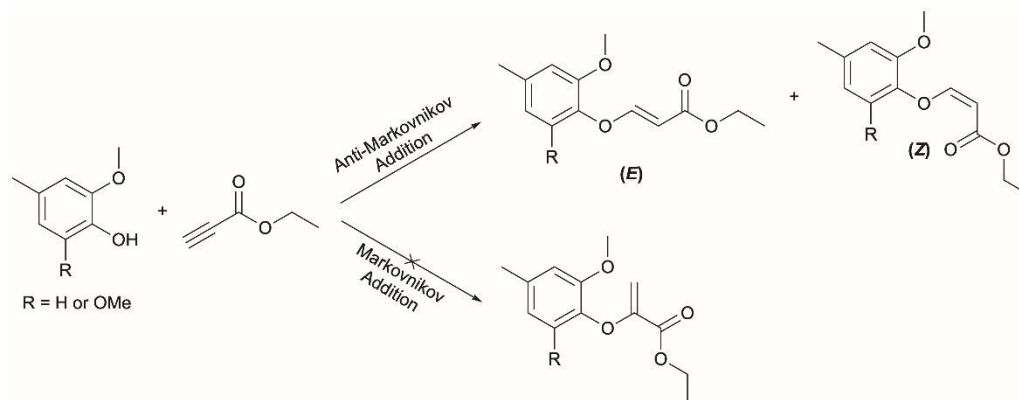


Figure S4-38. Markovnikov and anti-Markovnikov addition of ethyl propiolate and phenols.

System G/G'

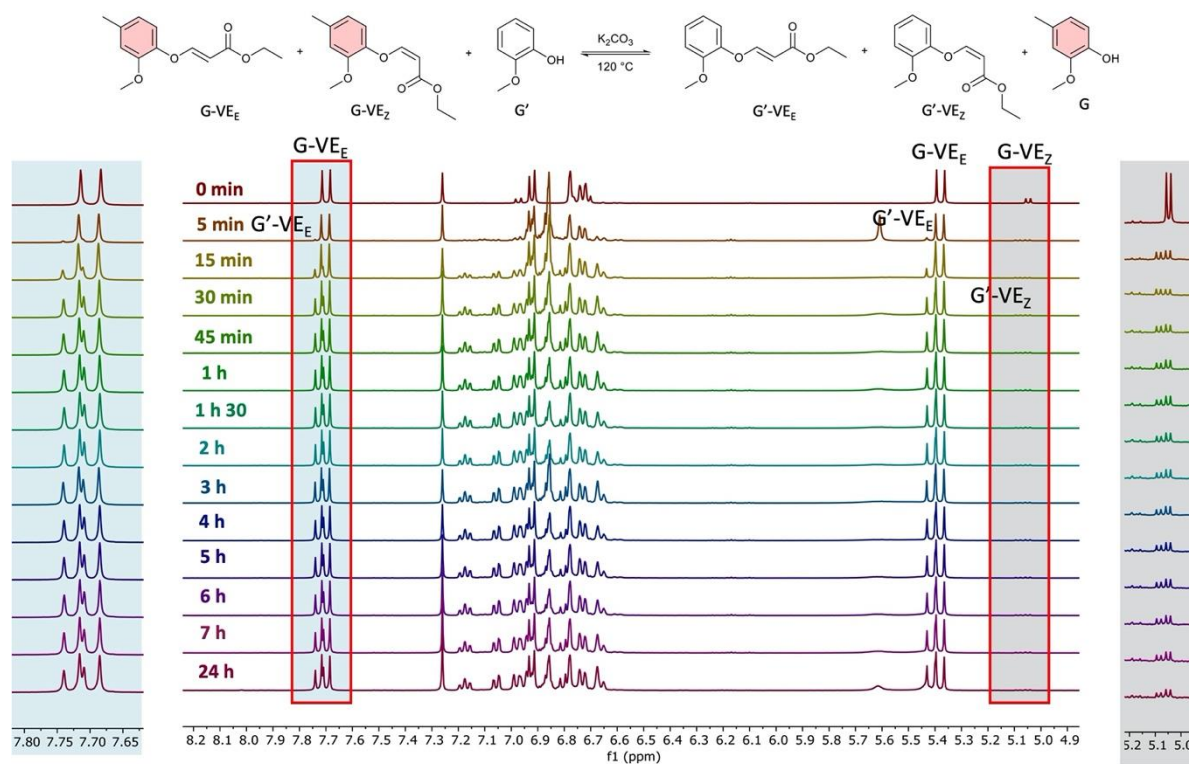


Figure S4-39. ¹H NMR sequence of GG' exchange reaction between G-VE and G in CDCl₃.

CHAPITRE 4

$$K_{GG'} = \frac{[G' - VE][G]}{[G - VE][G']} = 0.29$$

Table S4-12. Parameters used for $K_{GG'}$ calculation.

Compound	ppm	Area	Relative area	Molar fraction
G-VE ^a	5.04-5.06 (<i>Z</i>) 7.68-7.71 (<i>E</i>)	34409	34409	0.34
G'	3.89	95568	31855	0.31
G'-VE ^a	5.08-5.09 (<i>Z</i>) 7.71-7.74 (<i>E</i>)	18077	18077	0.18
G	3.87	52621	17540	0.17

^aSum of *E* and *Z*-isomers.

System SS'

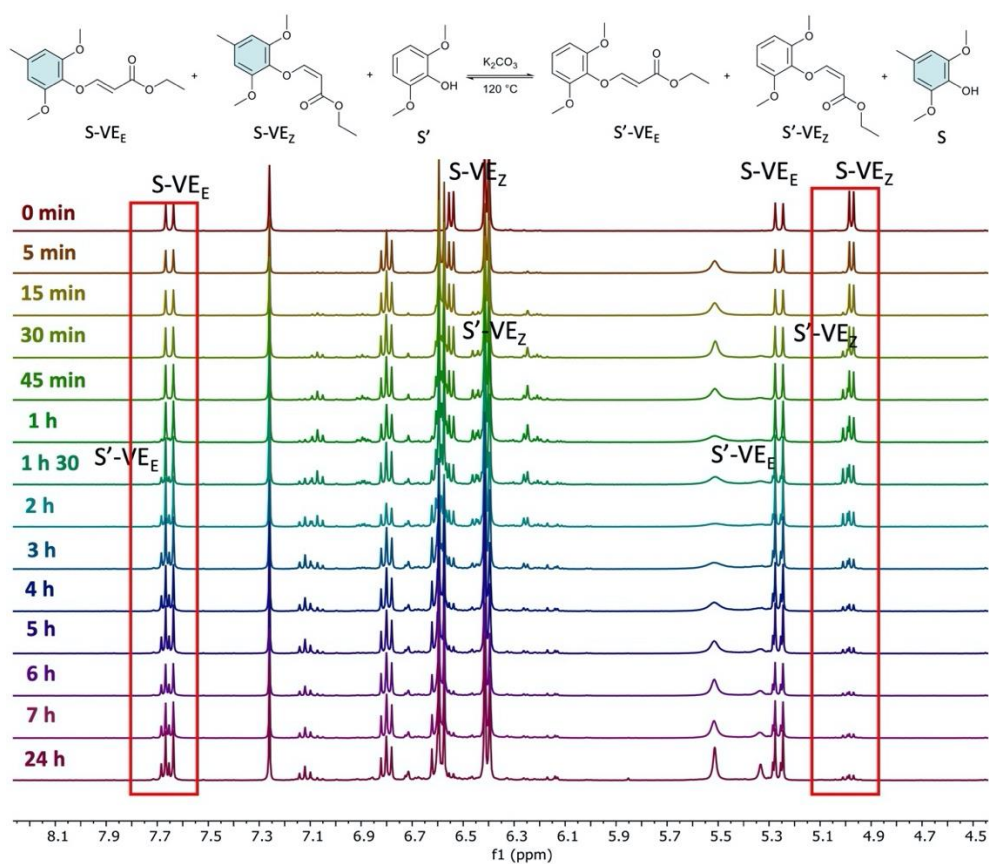


Figure S4-40. ¹H NMR sequence of SS' exchange reaction between S-VE and S' in CDCl₃.

CHAPITRE 4

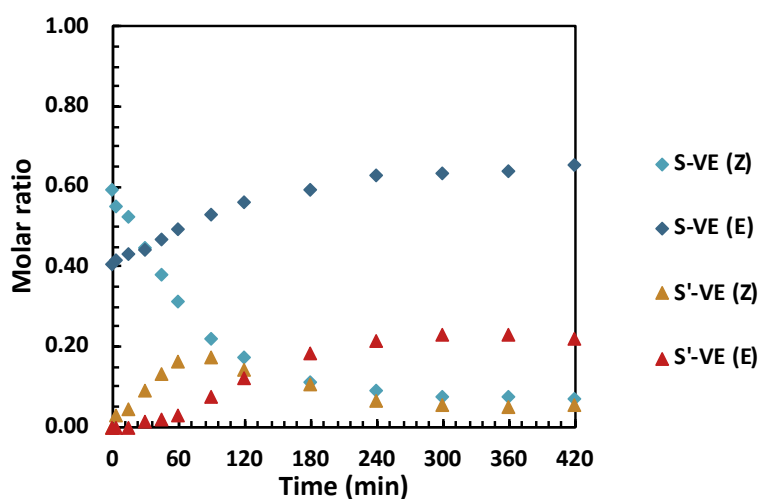


Figure S4-41. Kinetics of SS' exchange reaction between S-VE and S' at 120 °C.

$$K_{SS'} = \frac{[S' - VE][S]}{[S - VE][S']} = 0.18$$

Table S4-13. Parameters used for $K_{SS'}$ calculation.

Compound	ppm	Area	Relative area	Molar fraction
S-VE ^a	4.97-4.99 (Z) 7.64-7.67 (E)	39383	39383	0.31
S'	3.89	292905	48817	0.39
S'-VE ^a	4.99-5.01 (Z) 7.65-7.68 (E)	15351	15351	0.12
S	3.87	134776	22463	0.18

^aSum of *E* and *Z*-isomers.

System GS'

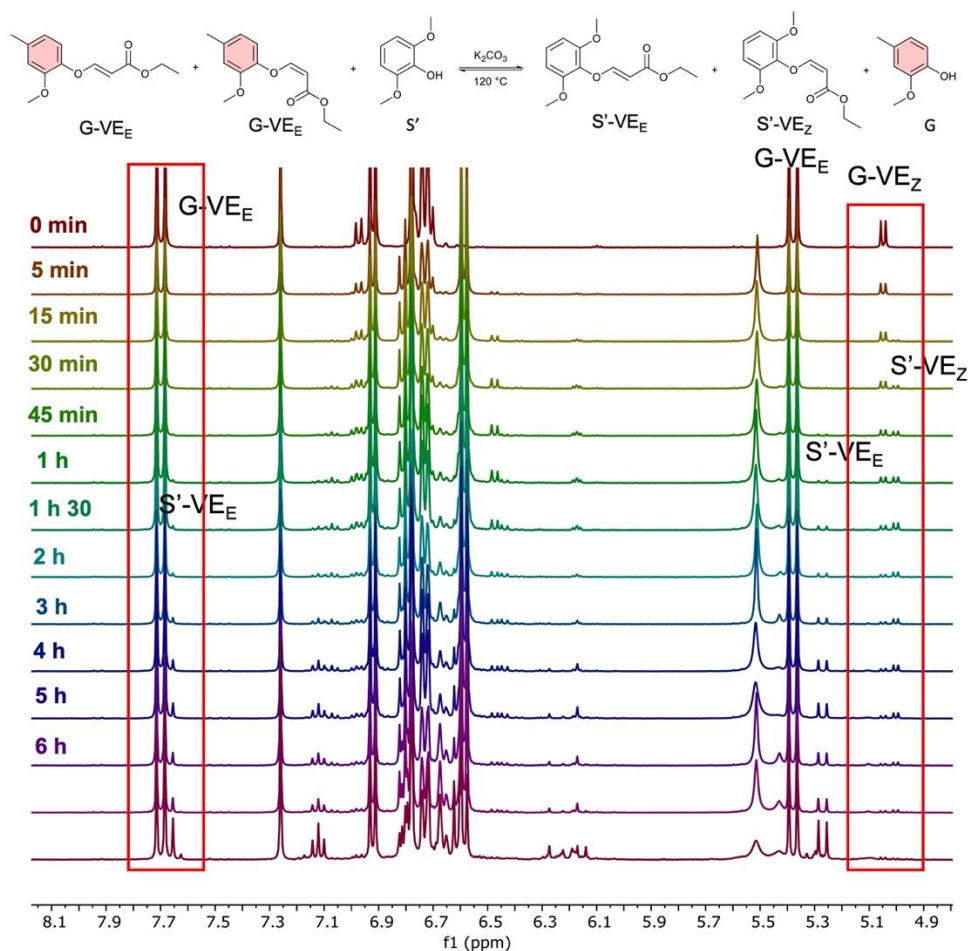


Figure S4-42. ¹H NMR sequence of GS' exchange reaction between G-VE and S' in CDCl₃.

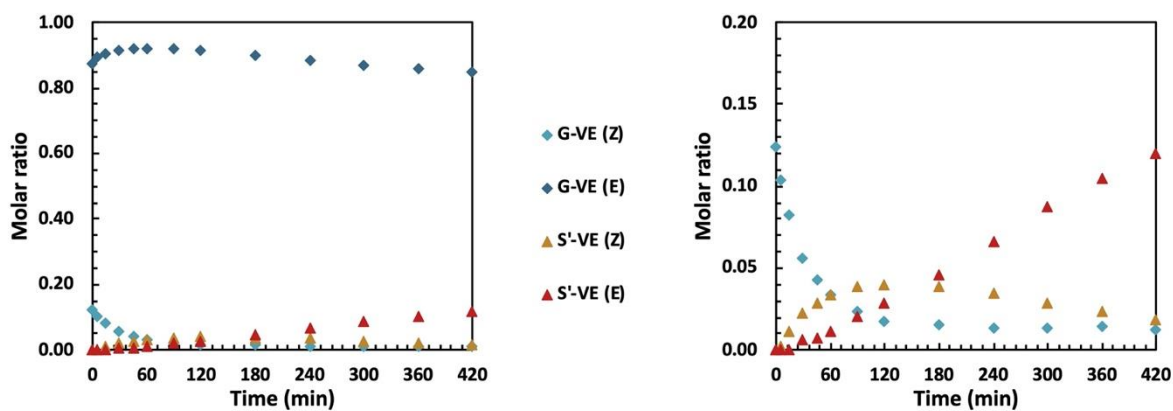


Figure S4-43. Kinetics of GS' exchange reaction between G-VE and S' at 120 °C, with zoom on molar ratios from 0 to 0.2.

$$K_{GS'} = \frac{[S' - VE][G]}{[G - VE][S']} = 0.27$$

CHAPITRE 4

Table S4-14. Parameters used for K_{GS} calculation.

Compound	ppm	Area	Relative area	Molar fraction
G-VE ^a	5.04-5.06 (<i>Z</i>) 5.36-5.39 (<i>E</i>)	44277	44277	0.45
S'	3.89	133929	22321	0.22
S'-VE ^a	4.99- 5.01 (<i>Z</i>) 5.26-5.29 (<i>E</i>)	14888	14888	0.15
G	3.87	54015	18005	0.18

^aSum of *E* and *Z*-isomers.

System SG'

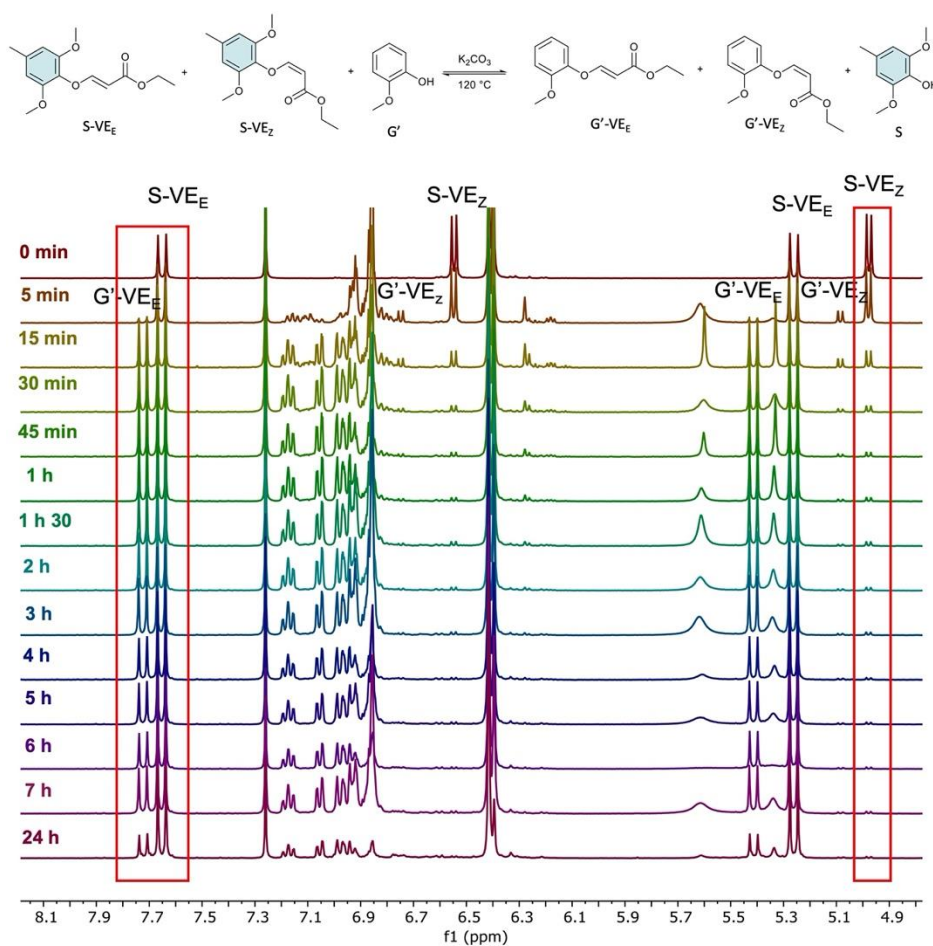


Figure S4-44. ¹H NMR sequence of SG' exchange reaction between S-VE and G' in CDCl₃.

CHAPITRE 4

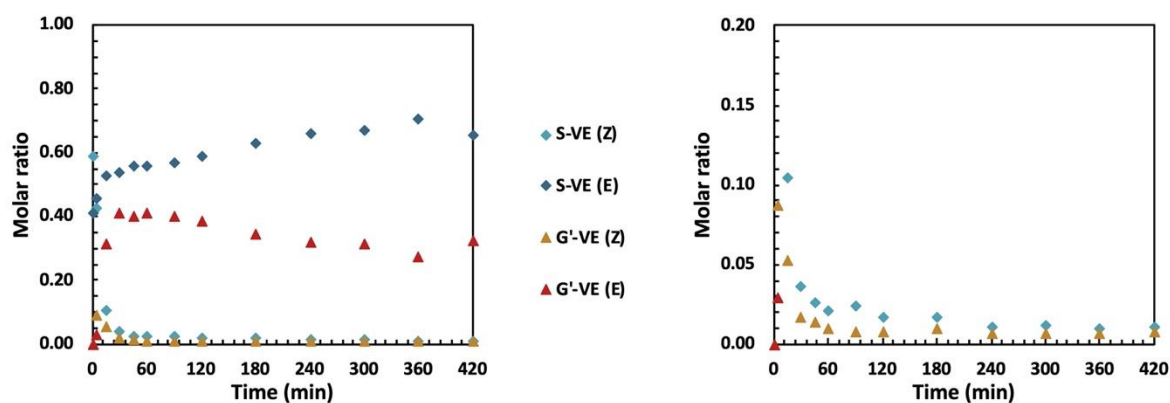


Figure S4-45. Kinetics of SG' exchange reaction between S-VE and G' at 120 °C, with zoom on molar ratios from 0 to 0.2.

$$K_{SG'} = \frac{[G' - VE][S]}{[S - VE][G']} = 0.37$$

Table S4-15. Parameters used for $K_{SG'}$ calculation.

Compound	ppm	Area	Relative area	Molar fraction
S-VE ^a	4.97-4.99 (Z) 7.64-7.67 (E)	38245	38245	0.34
G'	3.89	95568	31856	0.28
G'-VE ^a	5.08-5.09 (Z) 7.71-7.74 (E)	19049	19049	0.17
S	3.87	141778	23626	0.21

^aSum of *E* and *Z*-isomers.

System GSB

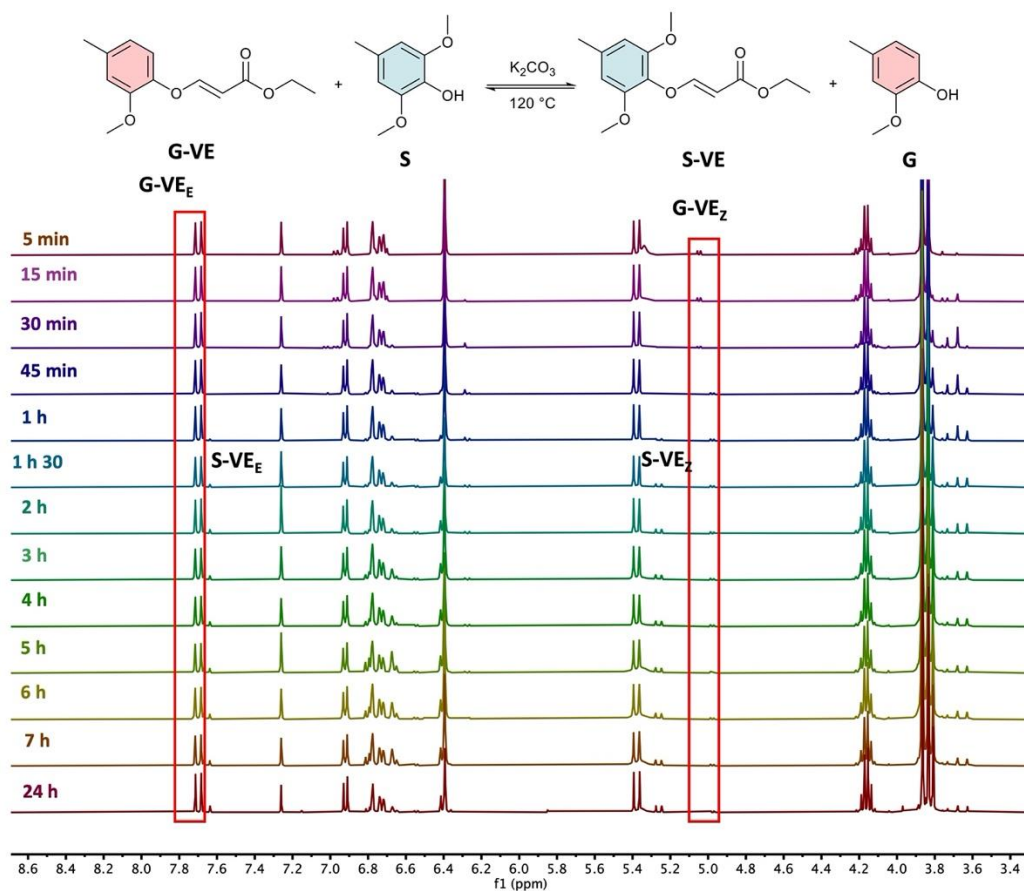


Figure S4-46. ¹H NMR sequence of GSB exchange reaction between G-VE and S in CDCl₃.

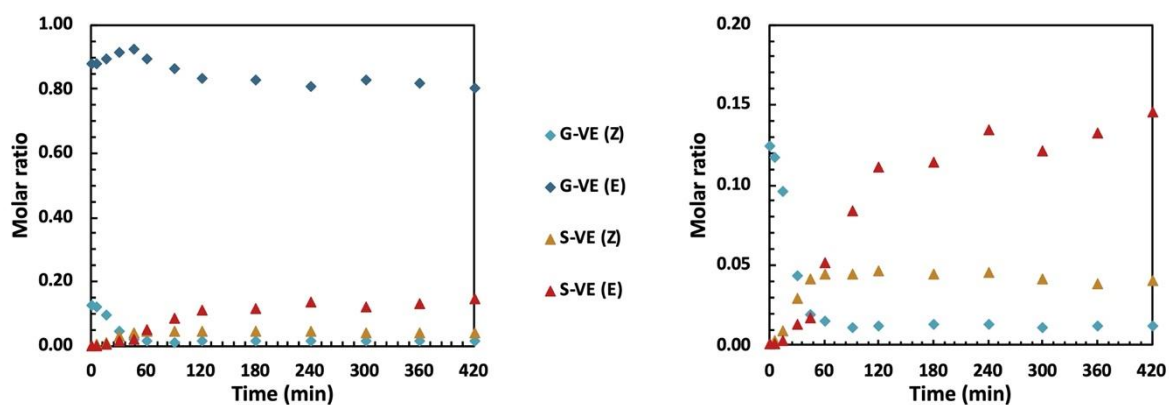


Figure S4-47. Kinetics of GSB exchange reaction between G-VE and S at 120 °C, with zoom on molar ratios from 0 to 0.2.

$$K_{GSB} = \frac{[S \cdot Me][G]}{[G \cdot Me][S]} = 0.05$$

CHAPITRE 4

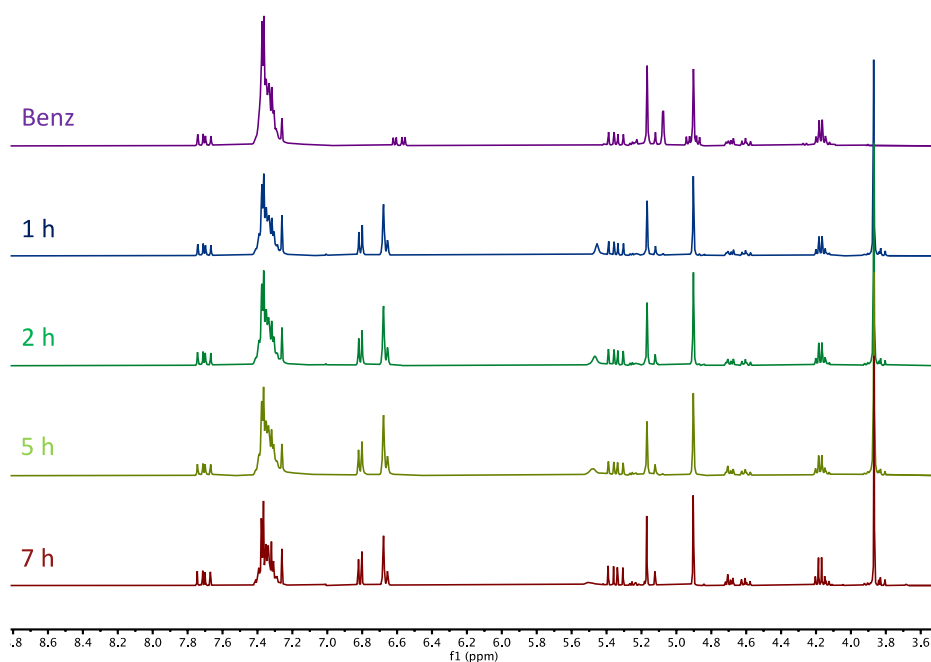


Figure S4-49. ^1H NMR sequence of Al-OH/G exchange reaction between Benz-VE and G in CDCl_3 .

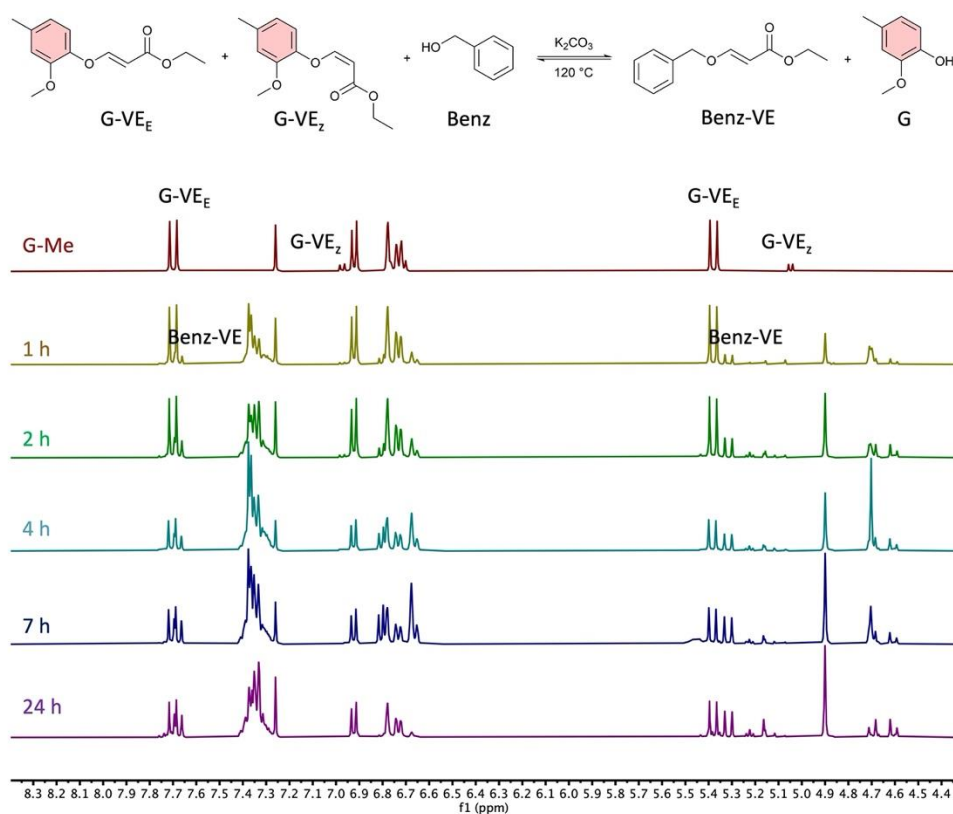


Figure S4-50. ^1H NMR sequence of G/Al-OH exchange reaction between G-VE and benzyl alcohol in CDCl_3 .

CHAPITRE 4

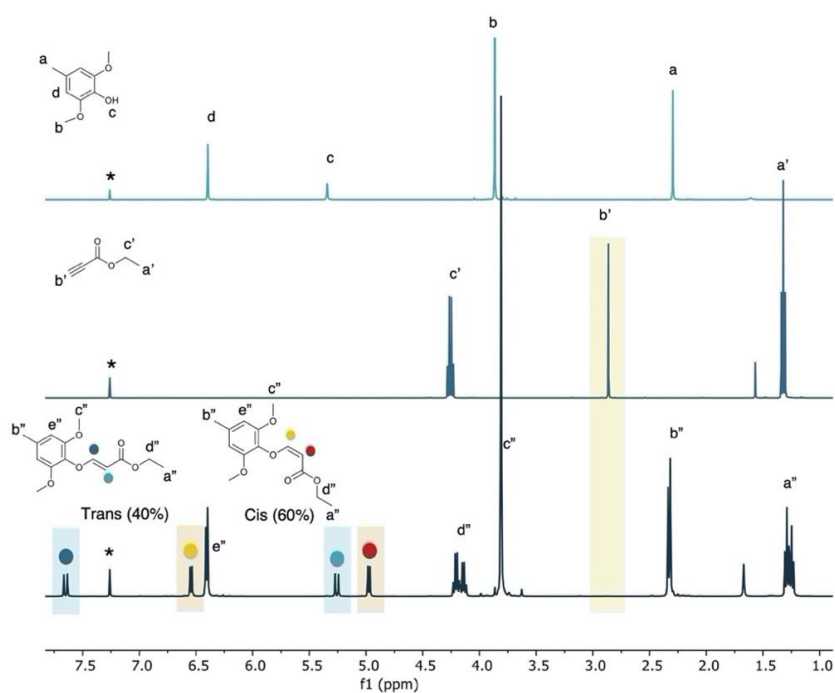


Figure S4-51. Stacked ^1H NMR spectra in CDCl_3 of S, ethyl propiolate and S-VE, from top to bottom. * = solvent.

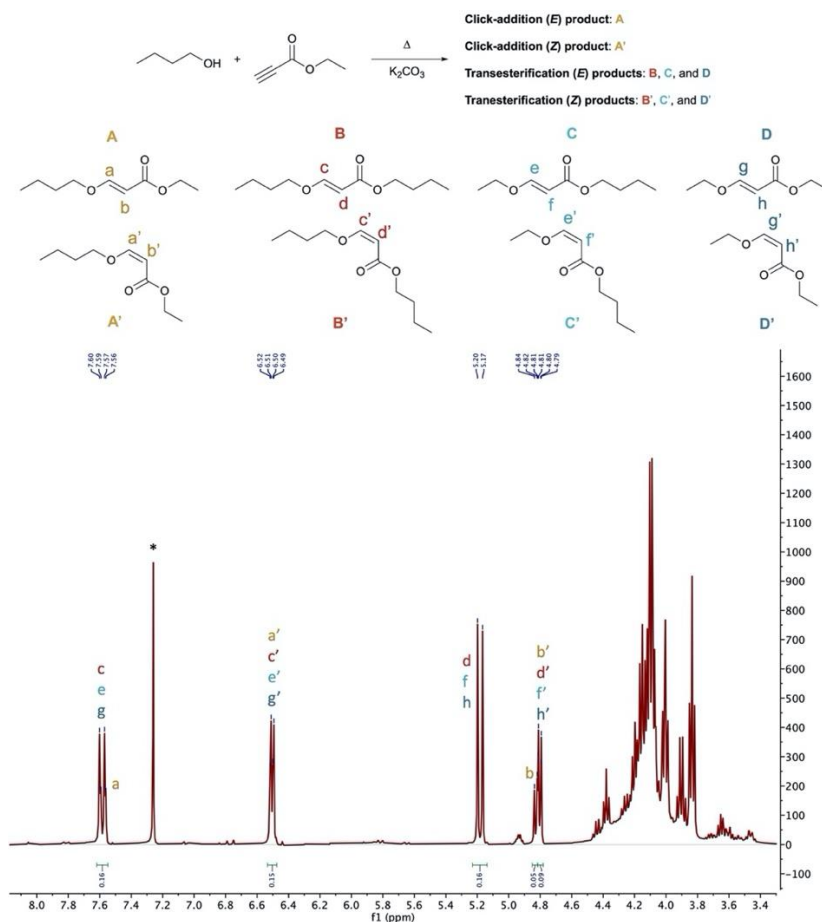


Figure S4-52. ^1H NMR of the reaction of 1-butanol with ethyl propiolate at $120\text{ }^\circ\text{C}$ in CDCl_3 and proposition for the attribution of possible product from click-addition and transesterification reactions.

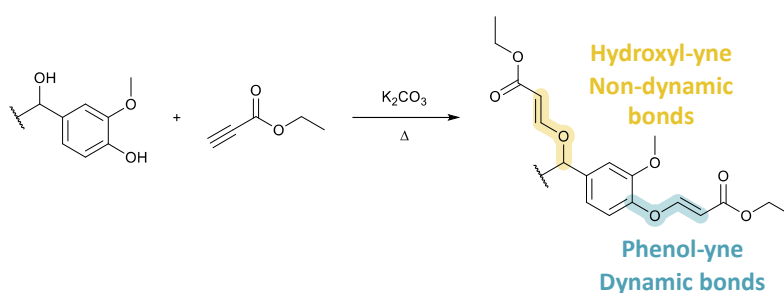


Figure S4-53. Representation of dynamic and non-dynamic vinyl ether adducts on lignin.

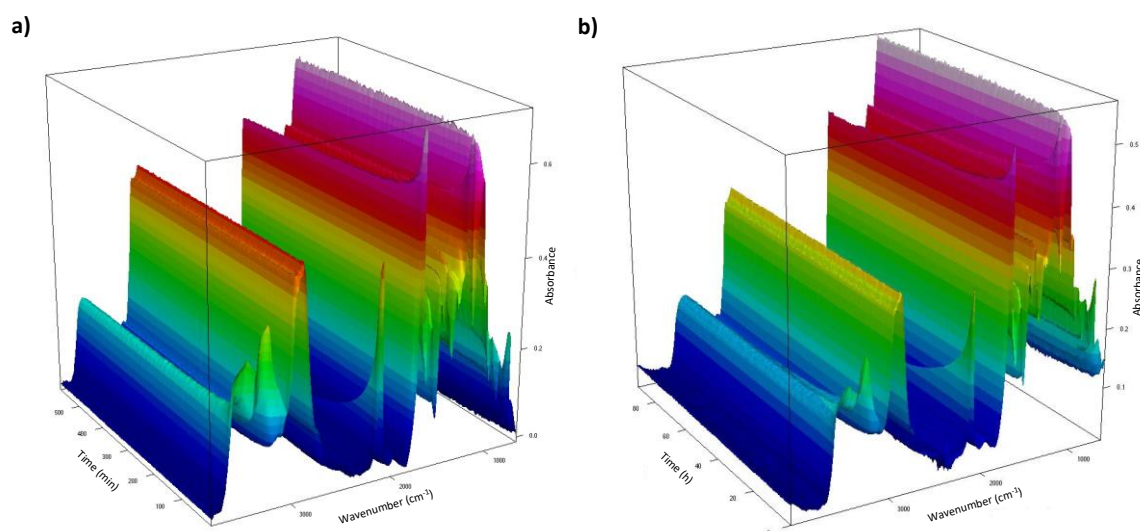


Figure S4-54. 3D view of the kinetic monitoring of the click addition by FT-IR at a) 120 °C and b) 80 °C.

Table S4-17. Relaxation parameters obtained at 190 °C varying the amount of free Ph-OH and the catalyst equivalents.

Entry	Free phenol equivalents	Catalyst equivalents	$\tau^*_{190\text{ °C}}$ (s)	β
1	0.05	0.3	3783	0.39
2	0.05	0.4	1688	0.45
3	0.2	0.3	1239	0.43
4	0.2	0.2	703	0.47

Table S4-18. Swelling, gel fraction and WCA values of the materials.

PY (Designations)	SR _{acetone}	SR _{water}	GF _{acetone}	GF _{water}	WCA (°)
KL-PY	30.6 ± 0.3	64.8 ± 0.8	98.0 ± 0.1	91.1 ± 0.1	81.0 ± 6.0
OSL-PY	29.5 ± 0.4	57.6 ± 2.0	100.0 ± 0.1	92.2 ± 0.4	49.1 ± 3.7
DOSL-PY	57.8 ± 0.7	61.4 ± 0.3	90.6 ± 0.3	90.1 ± 0.1	119.1 ± 5.4

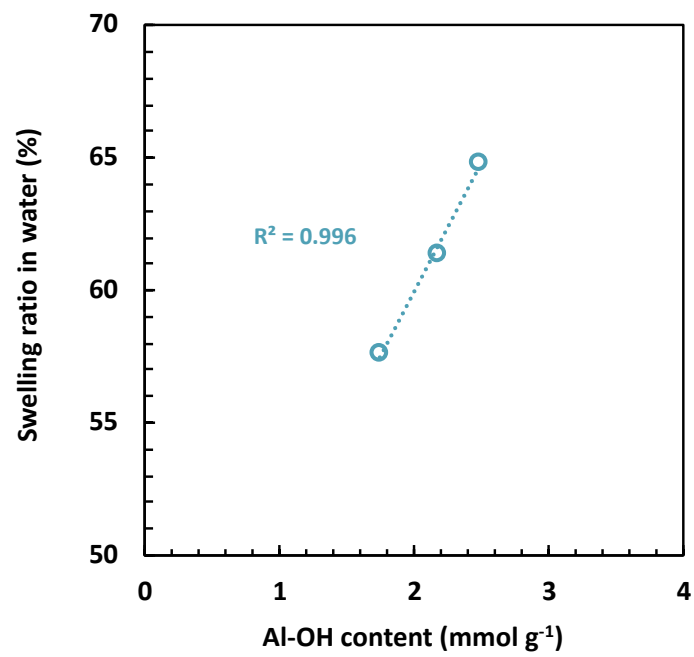


Figure S4-55. Evolution of swelling ratios in water with Al-OH content.

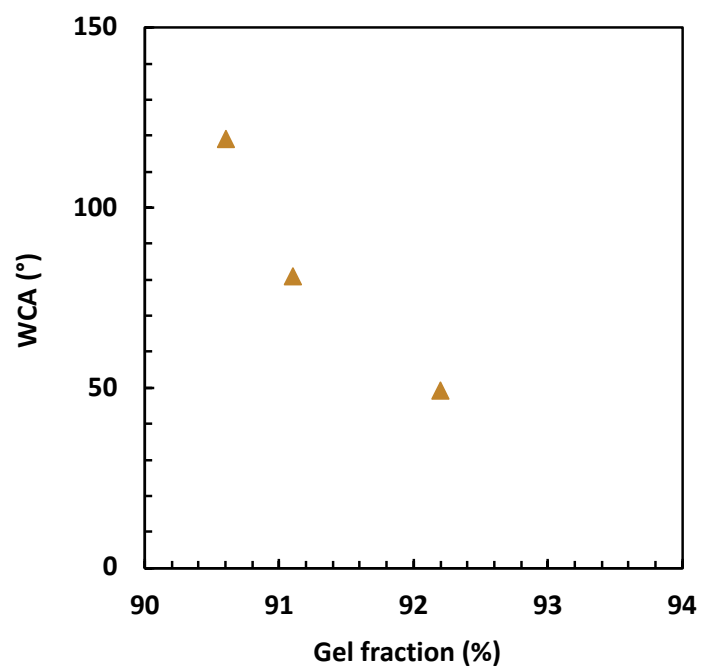


Figure S4-56. Evolution of the WCA with water GF.

CHAPITRE 4

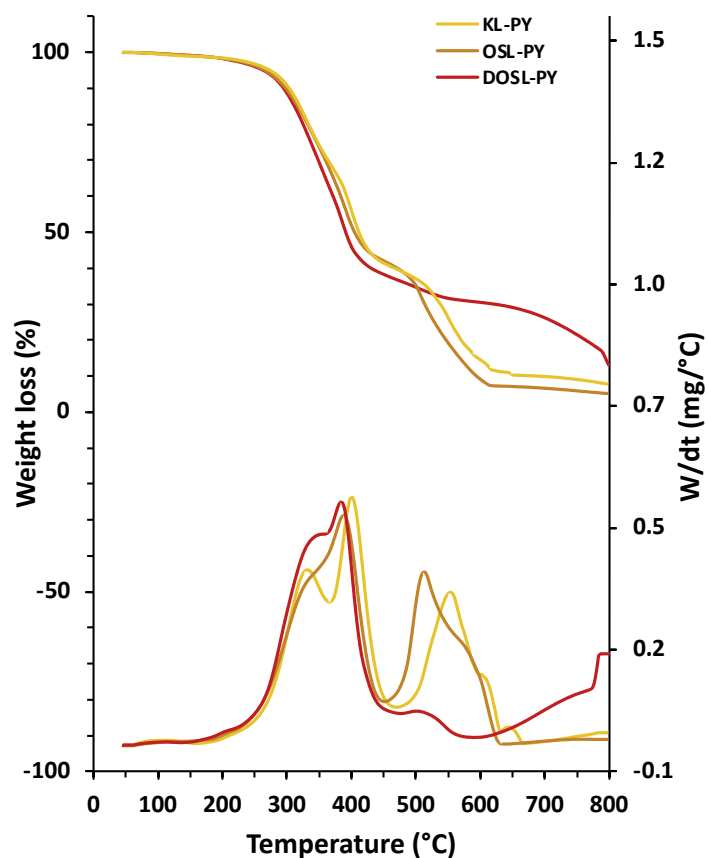


Figure S4-57. TGA curves of the materials.

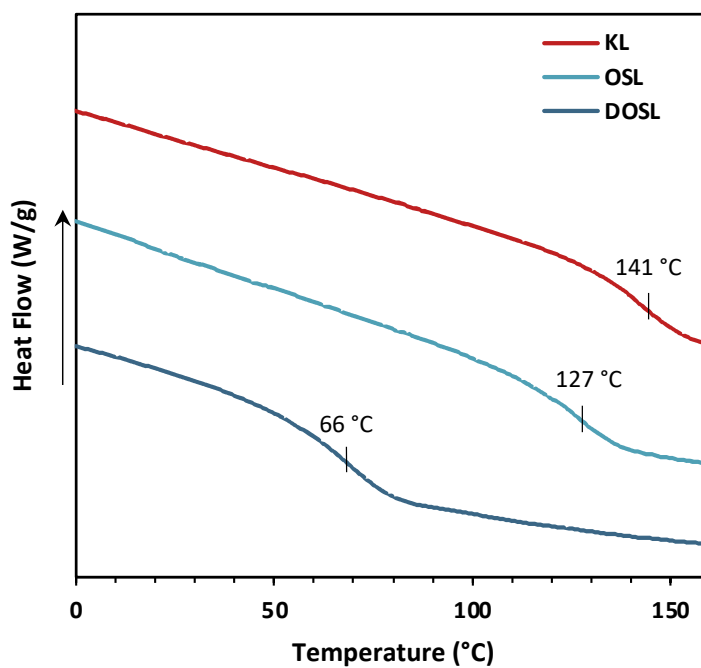


Figure S4-58. DSC curves of the different lignins: KL (red), OSL (light blue), and DOSL (dark blue).

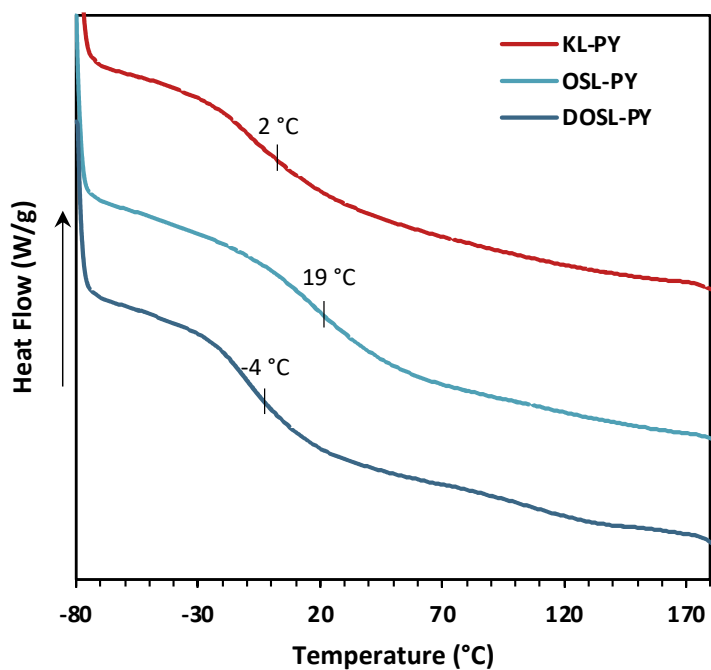


Figure S4-59. DSC curves of the series of materials.

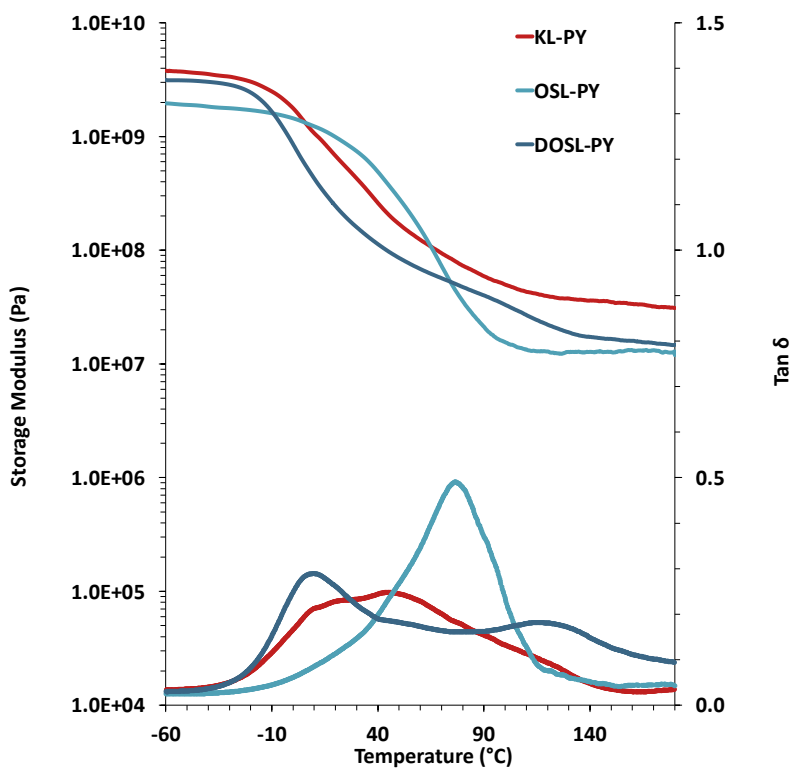


Figure S4-60. DMA curves of the materials.

CHAPITRE 4

Table S4-19. Parameters used for T_v calculation of each vitrimers.

PY (Designations)	G' (Pa)	τ^* (s)	A	B	T_v (°C)
KL-PY	3.50E+07	8.56E+04	10.979	-16.509	121
OSL-PY	1.27E+07	2.36E+05	9.351	-13.366	90
DOSL-PY	1.65E+07	1.82E+05	9.672	-15.593	76

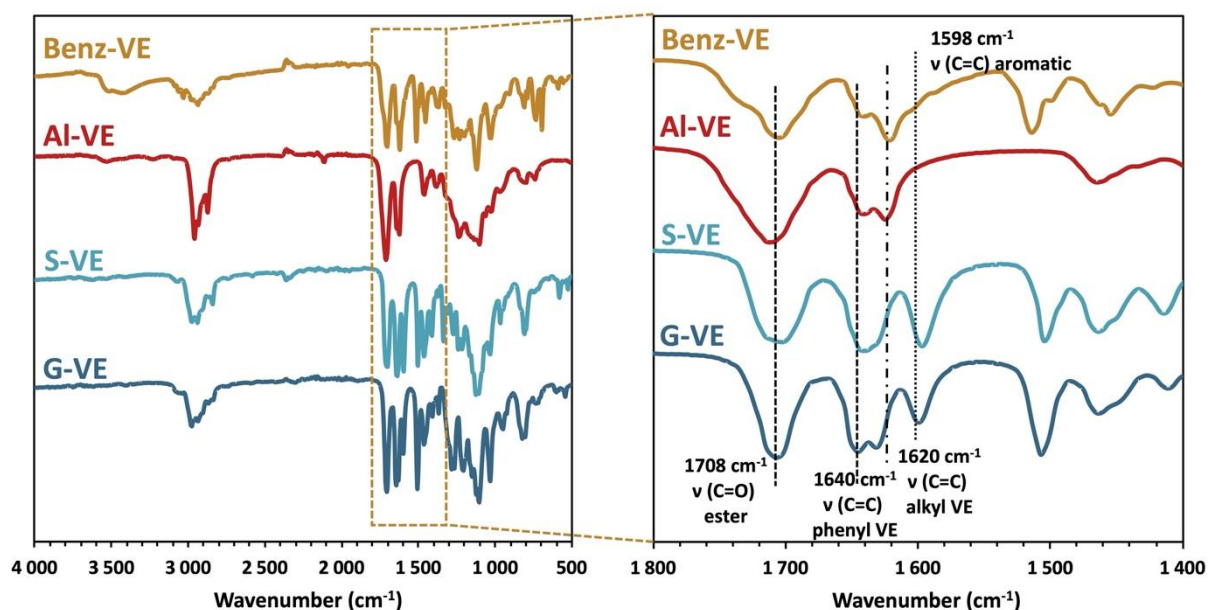


Figure S4-61. Stacked FT-IR spectra of aliphatic vinyl ethers (Benz-VE and Al-VE) and phenyl vinyl ethers (G-VE and S-VE).

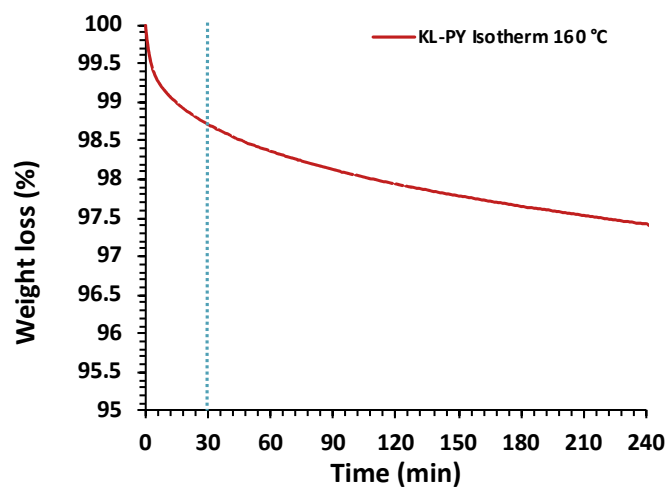


Figure S4-62. Curve of KL-PY thermal degradation under an isotherm at 160 °C for 4 h.

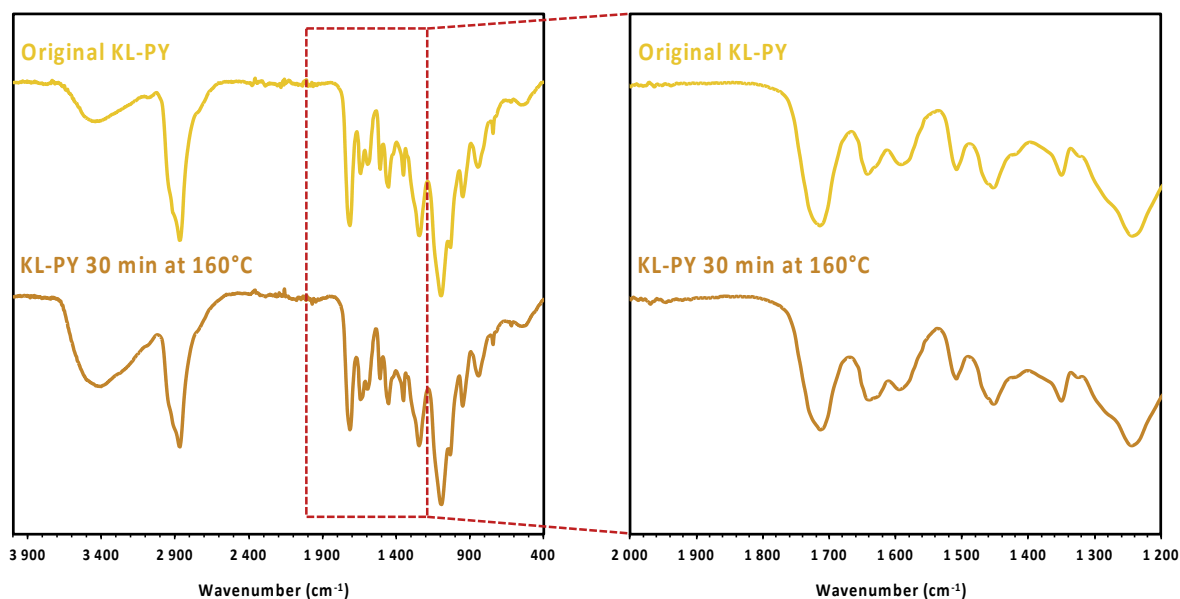


Figure S4-63. FT-IR spectra of pristine KL-PY and KL-PY after thermal treatment at 160 °C for 30 minutes.

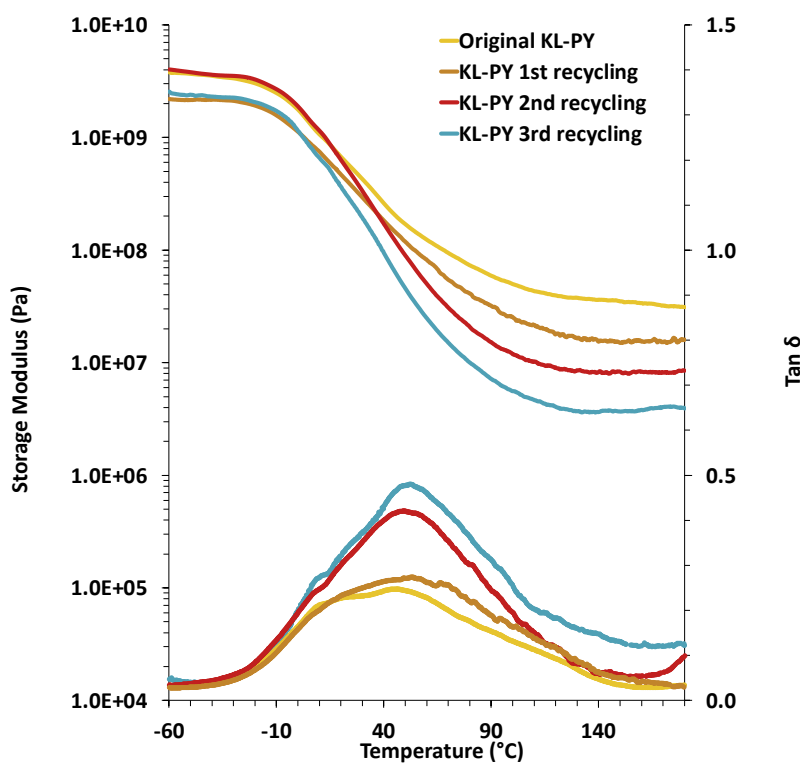


Figure S4-64. DMA curves of pristine and recycled KL-PY.

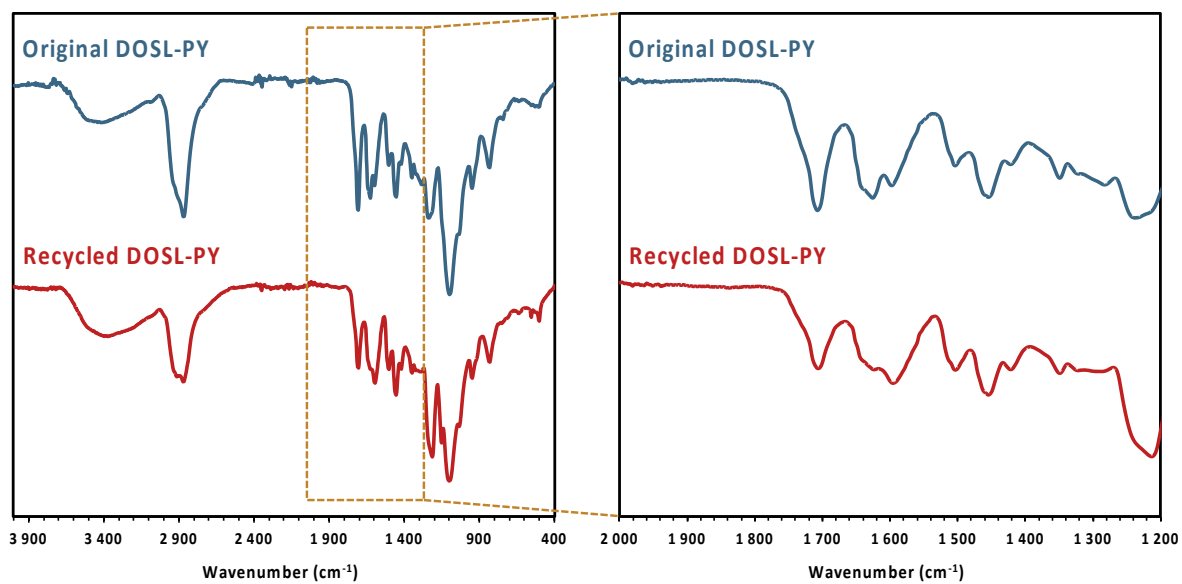


Figure S4-65. FT-IR spectra of pristine and recycled DOSL-PY.

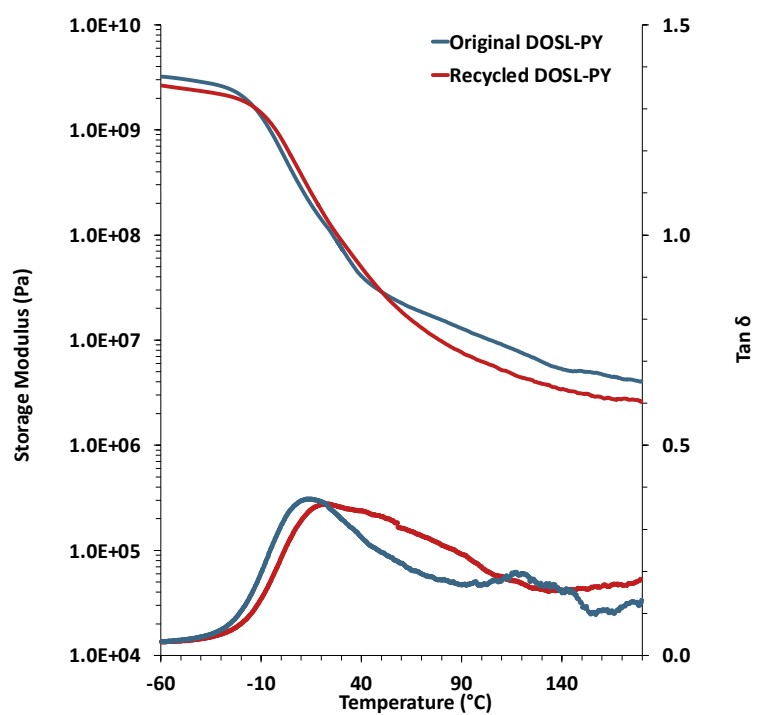


Figure S4-66. DMA curves of pristine and recycled DOSL-PY.

CHAPITRE 4

Table S4-20. Depolymerization tested conditions on OSL.

Entry	Sample concentration (mg mL ⁻¹)	Solvent	T (°C)	Observed solubilization?
1	10	HCl 2M	60	No
2	7.75	Acetone/HCl 2M (7:3)	60	No
3	7.75	Acetone/HCl 2M (7/3) + 2 drops HCl 37%	60	Yes
4	12	DMSO/HCl 1M (8:2)	70	Yes

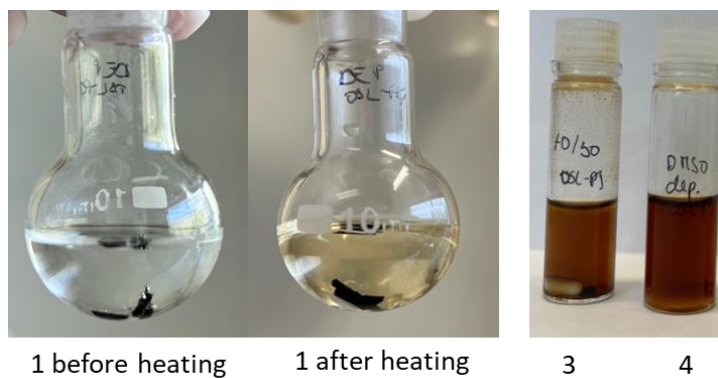


Figure S4-67. Pictures of the tested depolymerizations.

Table S4-21. Physicochemical properties of pristine and recovered KL.

Lignin (Designations)	Ph-OH content (mmol g ⁻¹)	M _n (g mol ⁻¹)	M _w (g mol ⁻¹)	Đ
Pristine KL	4.33	1580	5270	3.3
Recovered KL	1.62	1520	4040	2.7

CHAPITRE 4

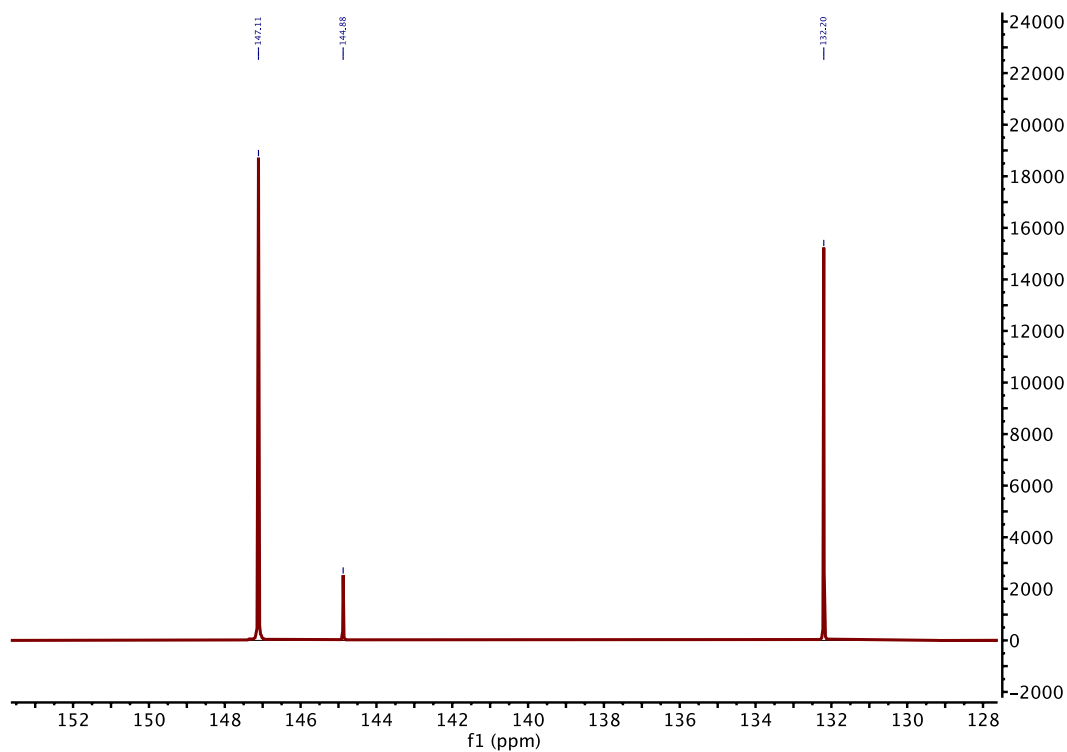


Figure S4-68. ^{31}P NMR of PEG₄₀₀.

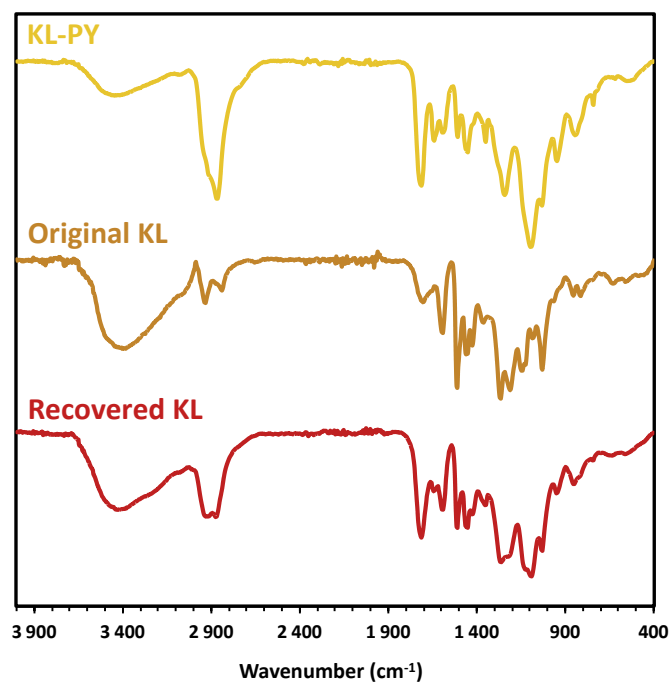


Figure S4-69. Stacked FT-IR spectra of KL-PY, pristine KL, and recovered KL.

CONCLUSION DU CHAPITRE 4

L'objectif de ce dernier chapitre était d'exploiter la chimie émergente phénol-yne pour le développement de nouveaux réseaux covalents adaptables aromatiques et biosourcés à partir de lignine.

Dans une première partie de ce chapitre d'ouverture, la dynamique des liaisons éthers d'énol a été mise en évidence sur des molécules modèles mono et di-substituées en position ortho, mimant les unités G et S de la lignine, démontrant ainsi que les réactions d'addition/éliminations sont possibles sur les groupements réactifs de la lignine. On a montré que la substitution des unités G et S influence la dynamique d'échange en raison de leurs encombrements stériques et leurs potentiels d'isomérisation respectifs. Les unités G peuvent plus facilement s'additionner sur les liaisons éther d'énol, alors que les unités S favorisant la formation d'isomères Z sont plus facilement sujet aux échanges de phénols grâce à une meilleure accessibilité du site d'addition. Une étude cinétique sur des composés modèles a par la suite démontré la meilleure réactivité des phénols avec les alcynes activés par rapports aux hydroxyles aliphatiques dans les conditions expérimentales de l'étude. Cette observation a également été faite sur des lignines kraft et organosolv, confirmant la formation favorisée de liaisons éthers d'énol aromatiques dynamiques. La synthèse d'une série de matériaux à haute teneur en lignine (jusqu'à 49%) a été réalisé avec succès à partir de différentes lignines techniques issus de différents procédés et fractionnements. Les morphologies et propriétés de ces matériaux ont été largement caractérisées.

Le comportement "vitrimère" des matériaux a été démontré via leur capacité à relaxer totalement les contraintes à température, montrant clairement les échanges entre les phénols libres des lignines et les liaisons éthers d'énol par addition/élimination. Les plus faibles masses molaires de la lignine dépolymérisée a montré une accélération des échanges de liaisons en raison d'une meilleure mobilité segmentaire nécessaire aux réarrangements. Le vitrimère issu de la lignine organosolv dépolymérisée a aussi montré une meilleure préservation de ses propriétés mécaniques après un recyclage physique, en comparaison aux autres matériaux. Le recyclage physique reste limité à cause de la formation successive de liaisons éthers d'énol aliphatiques non-dynamiques résultants de la réaction des hydroxyles aliphatiques libres de la lignine sur les éthers d'énol aromatiques dynamiques. Enfin, la dépolymérisation partielle par hydrolyse acide des matériaux a été observée via le clivage des liaisons éthers d'énol et esters. Une lignine de seconde génération a pu être récupérée et caractérisée, offrant un potentiel de recyclage en circuit fermé des vitrimères phénol-yne aromatiques à partir de lignines.

Cette dernière étude et chapitre a donc clairement montré le haut potentiel de l'approche développée basée sur la réaction click "phénol-yne" et augure de futurs et riches développements dans ce domaine innovant et dynamique (dans les différents sens de ce terme).

CONCLUSION GÉNÉRALE ET PERSPECTIVES

CONCLUSION GÉNÉRALE ET PERSPECTIVES

Cette thèse, dirigée par le Pr. Luc Avérous et co-encadrée par le Dr Antoine Duval, a été réalisée au sein de l'équipe BioTeam dans l'Institut de Chimie et procédés pour l'Énergie, l'Environnement et la Santé (ICPEES – UMR CNRS 7515) à Strasbourg. Ce travail a été financé par la fondation Jean-Marie Lehn dans le cadre du projet LigniCAN, suite à un appel à projets. L'objectif de cette thèse était de développer de nouveaux réseaux covalents adaptables aromatiques et biosourcés durables à partir de lignine en prenant en compte l'entièreté du cycle de vie du matériau, et adoptant une approche "du berceau au berceau" (cradle-to-cradle).

Ce travail de doctorat s'inscrit dans la continuité des travaux de recherche effectués dans la BioTeam portant sur la synthèse et le recyclage de polymères durables en combinant une double expertise : (i) dans le domaine de valorisation de la lignine (ii) dans la synthèse de matériaux performants tels que les CANs.

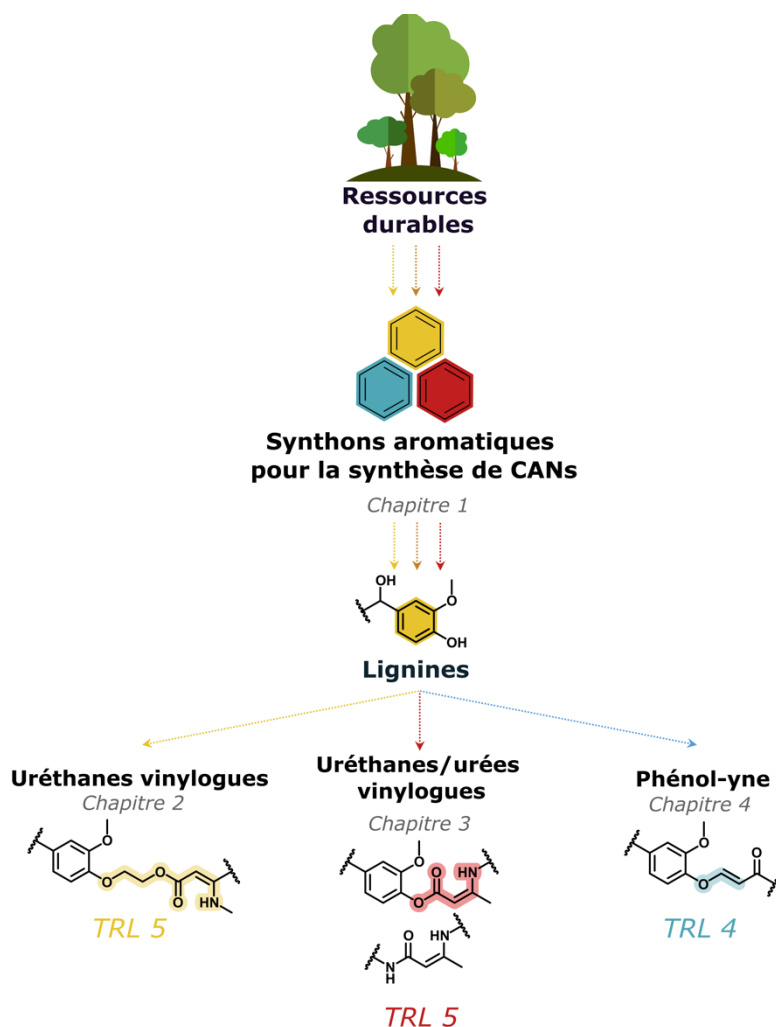


Figure 5-0-1. Structure globale de la thèse de doctorat et attribution de TRL à chaque chapitre.

Ce manuscrit a été structuré autour de 4 chapitres dont 3 expérimentaux (chapitres 2 à 4), en dehors de l'introduction et de la conclusion générale. La structure globale de la thèse est présentée dans la Figure 5-1. Le **chapitre 1** a présenté un état de l'art sur la synthèse et les applications des CANs aromatiques issus de ressources renouvelables. Cette revue de littérature a été soumise dans la revue *Materials Science and Engineering: R: Reports (Elsevier)*. Cet état de l'art a permis d'appréhender la richesse des chimies et des voies de synthèse de CANs à partir de synthons aromatiques biosourcés. Elle a mis en évidence la grande variété des composés aromatiques issus de ressources renouvelables tels

CONCLUSION GÉNÉRALE ET PERSPECTIVES

que la biomasse lignocellulosique ou les dérivés de polysaccharides. Les lignines, les tannins, le liquide de coque de noix de cajou et leurs dérivés ont montré être des molécules plateformes d'intérêt. Grâce à leurs multiples sites fonctionnels, ces synthons peuvent être facilement intégrés dans des réseaux dynamiques par des voies de synthèse simples, économes en atomes et innovantes. Ce premier chapitre a permis de mettre en exergue l'impact du choix des monomères sur les propriétés finales des matériaux, notamment induite par le choix de la chimie covalente dynamique utilisée. Au travers de l'empilement (stacking) π entre cycles aromatiques, l'utilisation de molécules aromatiques dans la synthèse de polymères a montré (i) le renforcement au travers des propriétés mécaniques des matériaux, (ii) être à l'origine de fonctionnalités dites avancées. Les polymères aromatiques possèdent notamment aussi une excellente résistance au feu et de bonnes propriétés d'adhésion. Associés à un large choix de chimies dynamiques, la dégradation contrôlée des CANs peut être réalisée dans divers environnements et peut ainsi répondre à diverses applications spécifiques. Le domaine biomédical tire particulièrement parti de cette caractéristique dans les systèmes d'administration de médicaments ou les implants résorbables. Des revêtements s'appuient également sur cela pour libérer des composés protecteurs tels que des agents anticorrosion. Bien que des défis à relever persistent dans le développement des CANs aromatiques et biosourcés, ce domaine constitue une solution prometteuse pour "concevoir" des matériaux robustes avec une fin de vie contrôlée pour un avenir plus durable.

Le **chapitre 2** amorce la partie expérimentale de cette thèse et est focalisé sur la synthèse de réseaux uréthane vinylogues recyclables et aromatiques à partir de lignine. L'objectif de cette étude a été de mettre au point une voie de modification chimique d'une lignine organosolv en macromonomère acétoacétate réactif pour la synthèse d'une gamme de CANs uréthane vinylogues. La teneur en lignine et la longueur de la chaîne de PEG ont montré être des paramètres clé influençant considérablement les propriétés thermiques, mécaniques et rhéologiques des diverses architectures macromoléculaires obtenus. Les matériaux ont démontré un comportement de vitrimères via la capacité de leurs réseaux à se réarranger par transamination en présence d'un excès d'amines. Les polymères ont montré leur aptitude à relaxer des contraintes rapidement à des températures relativement basses, leur permettant d'être remis en forme efficacement. Après deux cycles de recyclage physique, aucune perte majeure de propriétés n'a été observée. Ce chapitre a été publié sous la forme d'un article dans le journal *ChemSusChem* (Wiley) en 2023.

L'objectif du **chapitre 3** était de développer une nouvelle voie de synthèse de polymères uréthanes vinylogues dynamiques à partir de lignine en combinant un nombre d'étapes minimal avec une fonctionnalisation élevée. Pour cela, une réaction d'acétoacétylation permettant de greffer des groupements acétoacétates en une seule étape sur les alcools aliphatiques et aromatiques d'une lignine organosolv a été développée et ensuite optimisée. Les acétoacétates aromatiques de ce macromonomère ont montré être sujet à deux mécanismes de condensations formant des uréthanes et des urées vinylogues. L'équilibre de la condensation a pu être déplacé vers la formation d'uréthanes vinylogues de manière à limiter le "dé-greffage" de phénols. Une gamme de polymères a été synthétisée par condensation de la lignine acétoacétylée avec des diamines de longueur de chaînes différentes. Il a été constaté que la structure du squelette de la diamine influence fortement les propriétés morphologiques et mécaniques des matériaux. Ces polymères ont un comportement de vitrimère via des réarrangements de liaisons induits par des réactions de transamination en présence d'amines libres. Ces travaux ont montré l'excellent potentiel de recyclage physique des vitrimères sur plusieurs cycles de mise en forme. Enfin, la preuve de concept du recyclage chimique des polymères par dépolymérisation catalysée à l'acide a été démontrée.

Le **chapitre 4** avait pour objectif d'exploiter la chimie dynamique émergente de phénol-yne pour le développement de nouvelles architectures macromoléculaires recyclables à partir de lignine. Le potentiel de réarrangement par addition/élimination de phénols mono- et di-substitués a été dans un premier temps mis en évidence, démontrant que les échanges de phénols fonctionnent sur des structures que l'on trouve sur des lignines. Les isomères Z ont montré être plus facilement sujet à l'échange de phénols en raison d'une meilleure accessibilité du site d'addition. Par la suite, la réactivité supérieure

CONCLUSION GÉNÉRALE ET PERSPECTIVES

des alcools aromatiques vis-à-vis de l'addition avec des alcynes activés a été mise en évidence par rapport aux alcools aliphatiques sur des molécules modèles ainsi que sur la lignine. Des lignines issues de procédé à base ou non de soufre (Kraft et organosolv) et aussi partiellement ou non dépolymérisées ont été valorisées dans la préparation de réseaux via une réaction d'addition-click respectant des principes de chimie verte. Les matériaux relaxent complètement les contraintes en température, confirmant les échanges de phénols de la lignine sur les liaisons éthers d'énol. Les réarrangements de liaisons sont favorisés en présence de lignines de plus faible masses molaires. Le vitrimère issu de la lignine dépolymérisée a préservé ses propriétés mécaniques après un cycle de recyclage physique. Les fonctions ester et éther d'énol se sont révélées clivables en conditions acides, permettant la récupération d'un produit partiellement dépolymérisé dérivé de lignine. Cette preuve de concept de recyclage chimique offre un potentiel de revalorisation d'une lignine de seconde génération pour le développement de nouveaux polymères aromatiques durables.

Dans l'ensemble, ces divers résultats montrent le très haut potentiel de la lignine comme synton renouvelable pour la synthèse de polymères aromatiques à haute performance et respectueux de l'environnement avec une fin de vie contrôlée. Dans une approche de bioéconomie circulaire, l'amélioration des conditions de synthèses a fait l'objet d'une importante réflexion dans le but de suivre au maximum les principes de chimie verte (Tableau 5-1). Cela s'est traduit aussi par une augmentation successive de la teneur en lignine, de manière à augmenter la proportion de carbone renouvelable dans les polymères. Cela se reflète également dans la diminution consécutive du nombre d'étapes de modification chimique de lignine (de deux étapes à l'absence de modifications entre le chapitre 2 et 4) et dans la limitation de l'utilisation de solvants, jusqu'à son absence complète (dans le dernier chapitre).

Tableau 5-1. Évaluation des principes de chimie verte des différents chapitres.

Paramètre/Chapitre	2	3	4
Taux de lignine	14 à 20% massique	20 à 50% massique	39 à 49% massique
Nombre d'étapes de modifications de lignine	2	1	0
Nombre étapes de synthèse des matériaux	3	2	2
Solvant	CHCl ₃	DMF et CHCl ₃	Aucun
Composés dangereux (CMR ou toxiques)	CHCl ₃	DMF et CHCl ₃	Acide propiolique pour la synthèse de PEG-DA

Les différents travaux ont permis de développer des CANs ajustables. Un large éventail de propriétés mécaniques a ainsi été obtenu, permettant de répondre à diverses applications spécifiques (Figure 5-2). La plupart des polymères présentent des modules d'Young de l'ordre du MPa et d'importants allongements à la rupture, notamment les uréthanes vinylogues des chapitres 2 et 3. Ce comportement mécanique semblable au comportement d'élastomères est généralement plus marqué sur les matériaux développés dans ces travaux, par rapport aux CANs à base de lignine décrits dans la littérature utilisant d'autres liaisons covalentes dynamiques. En revanche, les matériaux aux propriétés les plus robustes du chapitre 2 ont un comportement mécanique similaires aux uréthanes vinylogues développés dans le groupe de Bernaerts (Liu et al., 2024).

Les vitrimères phénol-yne du chapitre 4 avec des liaison esters, présentent des modules d'Young plus importants (avoisinant parfois le GPa) et des allongements à la rupture plus modérés de l'ordre d'une dizaine de pourcents. Ces résultats sont comparables aux polyesters dynamiques déjà rapportés.

CONCLUSION GÉNÉRALE ET PERSPECTIVES

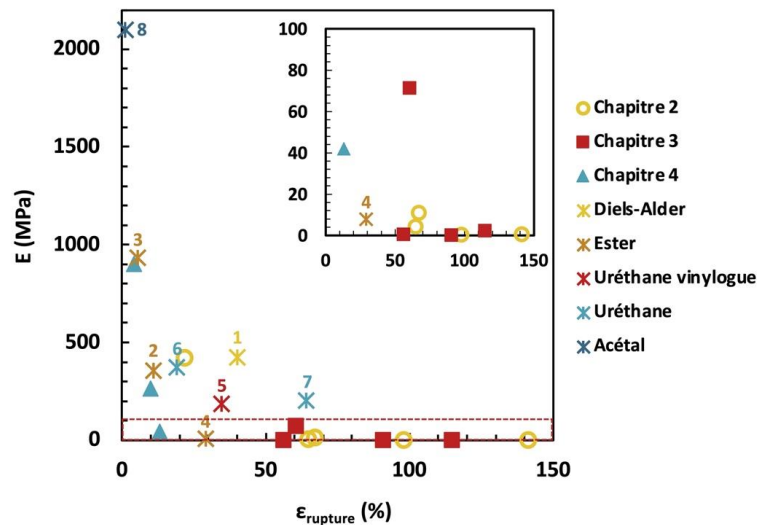


Figure 5-0-2. Récapitulatif des propriétés mécaniques obtenues dans les différents travaux de thèse et comparaison avec les CANs à partir de lignine rapportés dans la littérature. 1 = (Thys et al., 2021), 2 = (Zhang et al., 2018), 3 = (Xue et al., 2021), 4 = (Duval et al., 2024), 5 = (Liu et al., 2024), 6 = (Ma et al., 2023a), 7 = (Ma et al., 2023b), and 8 = (Moreno et al., 2021).

Différents comportements rhéologiques ont également été observés. Les polymères ont démontré un large panel de temps de relaxation dans différentes gammes de températures (Figure 5-3). Ces résultats ont mis en évidence l'adaptabilité des liaisons uréthanes vinylogues, dont la dynamique en absence de catalyseur peut être ajustée en utilisant des diamines possédant différentes réactivités. Les diamines les plus réactives permettent d'accélérer les échanges de liaisons. Au contraire, les diamines moins réactives ralentissent les réarrangements au sein des matériaux. Dans l'ensemble, les vitrimères du chapitre 2 se réarrangent à des températures plus faibles que la plupart des CANs rapportés précédemment (ester, uréthanes, uréthanes vinylogues et acétal).

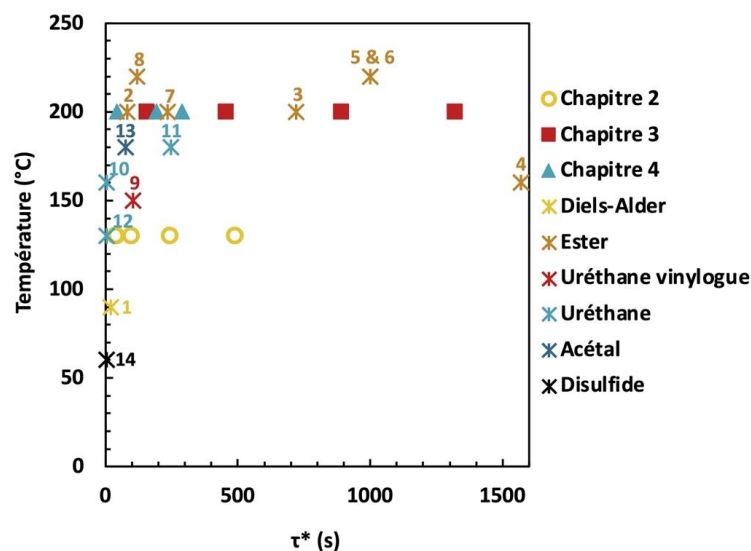


Figure 5-0-3. Récapitulatif des propriétés rhéologiques obtenues dans les différents travaux de thèse et comparaison avec les CANs à partir de lignines rapportés dans la littérature. 1 = (Thys et al., 2021), 2 = (Zhang et al., 2018), 3 = (Hao et al., 2019), 4 = (Xue et al., 2021), 5 = (Du et al., 2022), 6 = (Song et al., 2023), 7 = (Adjaoud et al., 2023), 8 = (Duval et al., 2024), 9 = (Liu et al., 2024), 10 = (Liu et al., 2019), 11 = (Ma et al., 2023a), 12 = (Ma et al., 2023b), 13 = (Moreno et al., 2021), and 14 = (Liu et al., 2020).

CONCLUSION GÉNÉRALE ET PERSPECTIVES

La chimie phénol-yne a quant à elle montré être compatible avec les phénols substitués et encombrés de la lignine en permettant une polymérisation rapide et économe en atomes, autorisant les échanges de phénols. Ces résultats ont mis en évidence des temps de relaxation dans l'ensemble plus courts que ceux des polyesters dynamiques à partir de lignines rapportées dans la littérature, traduisant des réarrangements de liaisons plus rapides. Bien qu'il reste encore quelques défis à relever pour obtenir une recyclabilité totale des polymères phénol-yne, cette chimie est très pertinente pour la valorisation de synthons phénoliques biosourcés.

Globalement, les résultats des divers travaux ont démontré l'ajustabilité des vitrimères à partir de lignine, leur permettant d'être compatible avec différents procédés de mise en œuvre et de répondre à diverses applications spécifiques.

Le niveau de maturation des différents travaux de cette thèse a été évalué à l'aide de l'échelle TRL (technology readiness level), initialement développée par la Nasa. Cette échelle constitue un outil essentiel et industriel pour identifier des défis et perspectives d'un nouveau concept ou d'une nouvelle technologie. Les différents niveaux de maturation sont décrits dans le Tableau 5-2.

Tableau 5-2. Description de l'échelle TRL. Adaptée de (Beims et al., 2019).

TRL	Échelle	Description
9	Industrielle	Production techniquement et économiquement viable
8	Industrielle	Système complet et validé
7	Industrielle	Démonstration du système à l'échelle du prototype en environnement opérationnel
6	Pilote	Démonstration d'un prototype en environnement représentatif
5	Laboratoire	Validation des composantes technologiques en environnement représentatif
4	Laboratoire	Validation de la technologie en laboratoire
3	Laboratoire	Preuve expérimentale de conception
2	Théorique	Formulation du concept technologique
1	Théorique	Observation des principes fondamentaux

Les TRL associés aux chapitres de ce mémoire de doctorat sont donnés sur la Figure 5-1. Un TRL de 5 semble être atteint pour les deux études portant sur la synthèse d'uréthanes vinylogues aromatiques à partir de lignines (chapitre 2 et 3). Les synthèses ont été effectuées avec succès sur plusieurs dizaines de grammes de lignine. Une vingtaine de grammes de matériaux ont été préparés et dûment caractérisés. Enfin, les polymères ont pu être soumis à trois cycles de recyclages physiques tout en conservant leurs propriétés mécaniques et rhéologiques. Un TRL de 4 a été attribué à l'étude portant sur les polymères phénol-yne à partir de lignine. Les synthèses sont performantes sur plusieurs dizaines de grammes. Une amélioration de la preuve de concept de recyclage physique et chimique pourrait augmenter le potentiel de cette étude, avec un gain en TRL.

Ce travail doctoral constitue une base solide pour le développement de nouveaux CANs biosourcés à partir de lignines. Il ouvre la voie à de nombreuses perspectives. Un premier axe potentiel de développement pourrait porter sur l'évaluation de la relation structure-propriété des vitrimères uréthanes vinylogues à base de lignine en utilisant d'autres types de lignines, provenant d'autres ressources et processus de fractionnement (kraft, sulfite, soda).

Conformément aux attentes sociétales pour un avenir plus durable, l'amélioration des conditions de recyclage chimique des CANs en fin de vie pourrait faire l'objet d'une étude complémentaire. En

CONCLUSION GÉNÉRALE ET PERSPECTIVES

effet, les uréthanes vinylogues préparés dans le chapitre 2 et 3 ont montré pouvoir être dépolymérisés par catalyse acide (chapitre 3). Cette approche, encore trop peu étudiée, présente une alternative sans danger pour la santé et l'environnement à la dépolymérisation à l'aide de monoamines courtes et toxiques. Elle permettrait de pouvoir récupérer d'une part les polyacétoacétates liquides et la lignine acétoacétylée, mais également les diamines utilisées. Ceci apporterait de nouvelles opportunités de recyclage pour la préparation de matériaux à la structure chimique identique et de surcyclage pour le développement de polymères à la structure chimique nouvelle.

Le chapitre d'ouverture (chapitre 4) offre de nombreuses perspectives, notamment sur la préparation de matériaux durables et recyclable à la demande. La photo-isomérisation des vitrimères phénol-yne pourrait s'avérer être une voie extrêmement pertinente pour obtenir une recyclabilité des matériaux à la demande. En déplaçant les configurations vers l'isomère *E* avec des longueurs d'onde appropriées, les matériaux pourraient présenter une dynamique inhibée et donc une résistance au fluage améliorée, tandis que le déplacement vers la configuration *Z* pourrait accélérer les réarrangements lors du recyclage physique. De plus, dans le but d'améliorer l'impact environnemental et sur la santé des matériaux phénol-yne, le greffage de fonctions alcyne pourrait être adapté pour se passer de l'acide propiolique, qui est le seul réactif CMR utilisé dans ce chapitre. Le propiolate d'éthyle, composé sans danger pour la santé, pourrait être par exemple employé pour modifier les alcools du polyéthylène glycol par transestérification.

La résistance insuffisante des CANs au fluage est de plus en plus reconnue comme étant l'un de leur inconvénient. Il serait pertinent d'étudier la résistance au fluage des différents matériaux synthétisés, de manière à appréhender leur vieillissement et leur stabilité dimensionnelle dans le temps. Dans l'éventualité d'un comportement altéré par le fluage, des stratégies spécifiques pourraient être mises en place pour renforcer leur résistance. Par exemple, il serait envisageable par exemple de piéger de manière réversible les amines libres des réseaux uréthanes vinylogues, d'incorporer une fraction considérable mais sous-critique de liaisons non-dynamiques, ou de combiner des liaisons dynamiques répondant à différents stimuli.

Plus généralement, pour améliorer la durabilité des vitrimères développés, il serait également pertinent d'essayer d'augmenter la proportion de carbone renouvelables au sein des matériaux. Pour cela, une teneur en lignine plus importante pourrait être intégrée dans les matériaux.

Afin de développer la production industrielle des CANs biosourcés et aromatiques à plus long terme, le changement d'échelle de production des matériaux constituerait un nouvel axe d'étude pertinent dans un contexte global de génie chimique et d'ingénierie des polymères.

Enfin, l'analyse du cycle de vie (ACV) des CANs synthétisés à partir de lignine dans les différents travaux doctoraux devrait être absolument menée pour évaluer précisément l'impact environnemental des principaux systèmes développés et optimisés. Ceci permettra de valider le potentiel et l'intérêt de CANs biosourcés et aromatiques à partir de lignine comme alternative haute performance et recyclable aux polymères conventionnels, pour un futur plus durable.

REFERENCES ASSOCIEES A LA CONCLUSION GENERALE

- Adjaoud, A., Puchot, L., Federico, C.E., Das, R., Verge, P., 2023. Lignin-based benzoxazines: A tunable key-precursor for the design of hydrophobic coatings, fire resistant materials and catalyst-free vitrimers. *Chem. Eng. J.* 453, 139895. <https://doi.org/10.1016/j.cej.2022.139895>
- Beims, R.F., Simonato, C.L., Wiggers, V.R., 2019. Technology readiness level assessment of pyrolysis of trygliceride biomass to fuels and chemicals. *Renew. Sustain. Energy Rev.* 112, 521–529. <https://doi.org/10.1016/j.rser.2019.06.017>
- Du, L., Jin, X., Qian, G., Yang, W., Su, L., Ma, Y., Ren, S., Li, S., 2022. Lignin-based vitrimer for circulation in plastics, coatings, and adhesives with tough mechanical properties, catalyst-free and good chemical solvent resistance. *Ind. Crops Prod.* 187, 115439. <https://doi.org/10.1016/j.indcrop.2022.115439>
- Duval, A., Benali, W., Avérous, L., 2024. Turning lignin into a recyclable bioresource: transesterification vitrimers from lignins modified with ethylene carbonate. *Green Chem.* <https://doi.org/10.1039/D4GC00567H>
- Hao, C., Liu, T., Zhang, S., Brown, L., Li, R., Xin, J., Zhong, T., Jiang, L., Zhang, J., 2019. A High-Lignin-Content, Removable, and Glycol-Assisted Repairable Coating Based on Dynamic Covalent Bonds. *ChemSusChem* 12, 1049–1058. <https://doi.org/10.1002/cssc.201802615>
- Liu, J., Pich, A., Bernaerts, K.V., 2024. Preparation of lignin-based vinylogous urethane vitrimer materials and their potential use as on-demand removable adhesives. *Green Chem.* <https://doi.org/10.1039/D3GC02799F>
- Liu, W., Fang, C., Chen, F., Qiu, X., 2020. Strong, Reusable, and Self-Healing Lignin-Containing Polyurea Adhesives. *ChemSusChem* 13, 4691–4701. <https://doi.org/10.1002/cssc.202001602>
- Liu, W., Fang, C., Wang, S., Huang, J., Qiu, X., 2019. High-Performance Lignin-Containing Polyurethane Elastomers with Dynamic Covalent Polymer Networks. *Macromolecules* 52, 6474–6484. <https://doi.org/10.1021/acs.macromol.9b01413>
- Ma, X., Li, S., Wang, F., Wu, J., Chao, Y., Chen, X., Chen, P., Zhu, J., Yan, N., Chen, J., 2023a. Catalyst-Free Synthesis of Covalent Adaptable Network (CAN) Polyurethanes from Lignin with Editable Shape Memory Properties. *ChemSusChem* 16, e202202071. <https://doi.org/10.1002/cssc.202202071>
- Ma, X., Wang, X., Zhao, H., Xu, X., Cui, M., Stott, N.E., Chen, P., Zhu, J., Yan, N., Chen, J., 2023b. High-Performance, Light-Stimulation Healable, and Closed-Loop Recyclable Lignin-Based Covalent Adaptable Networks. *Small* 19, 2303215. <https://doi.org/10.1002/sml.202303215>
- Moreno, A., Morsali, M., Sipponen, M.H., 2021. Catalyst-Free Synthesis of Lignin Vitrimers with Tunable Mechanical Properties: Circular Polymers and Recoverable Adhesives. *ACS Appl. Mater. Interfaces* 13, 57952–57961. <https://doi.org/10.1021/acsami.1c17412>
- Song, P., Du, L., Pang, J., Jiang, G., Shen, J., Ma, Y., Ren, S., Li, S., 2023. Preparation and properties of lignin-based vitrimer system containing dynamic covalent bonds for reusable and recyclable epoxy asphalt. *Ind. Crops Prod.* 197, 116498. <https://doi.org/10.1016/j.indcrop.2023.116498>
- Thys, M., Brancart, J., Van Assche, G., Vendamme, R., Van den Brande, N., 2021. Reversible Lignin-Containing Networks Using Diels–Alder Chemistry. *Macromolecules* 54, 9750–9760. <https://doi.org/10.1021/acs.macromol.1c01693>
- Xue, B., Tang, R., Xue, D., Guan, Y., Sun, Y., Zhao, W., Tan, J., Li, X., 2021. Sustainable alternative for bisphenol A epoxy resin high-performance and recyclable lignin-based epoxy vitrimers. *Ind. Crops Prod.* 168, 113583. <https://doi.org/10.1016/j.indcrop.2021.113583>
- Zhang, S., Liu, T., Hao, C., Wang, L., Han, J., Liu, H., Zhang, J., 2018. Preparation of a lignin-based vitrimer material and its potential use for recoverable adhesives. *Green Chem.* 20, 2995–3000. <https://doi.org/10.1039/C8GC01299G>

LISTE COMPLÈTE DES RÉFÉRENCES BIBLIOGRAPHIQUES

LISTE COMPLÈTE DES RÉFÉRENCES BIBLIOGRAPHIQUES

- ADEME, 2016. Plastiques biosourcés (Les). Libr. ADEME. URL <https://bibliothèque.ademe.fr/produire-autrement/3063-plastiques-biosources-les.html> (accessed 4.29.24).
- Adisakwattana, S., Moonsan, P., Yibchok-anun, S., 2008. Insulin-Releasing Properties of a Series of Cinnamic Acid Derivatives in Vitro and in Vivo. *J. Agric. Food Chem.* 56, 7838–7844. <https://doi.org/10.1021/jf801208t>
- Adjaoud, A., Puchot, L., Federico, C.E., Das, R., Verge, P., 2023. Lignin-based benzoxazines: A tunable key-precursor for the design of hydrophobic coatings, fire resistant materials and catalyst-free vitrimers. *Chem. Eng. J.* 453, 139895. <https://doi.org/10.1016/j.cej.2022.139895>
- Adjaoud, A., Puchot, L., Verge, P., 2022. High-Tg and Degradable Isosorbide-Based Polybenzoxazine Vitriimer. *ACS Sustain. Chem. Eng.* 10, 594–602. <https://doi.org/10.1021/acssuschemeng.1c07093>
- Ahmadi, M., Hanifpour, A., Ghiassinejad, S., van Ruymbeke, E., 2022. Polyolefins Vitrimers: Design Principles and Applications. *Chem. Mater.* 34, 10249–10271. <https://doi.org/10.1021/acs.chemmater.2c02853>
- Ahmed Khalil, A., ur Rahman, U., Rafiq Khan, M., Sahar, A., Mehmood, T., Khan, M., 2017. Essential oil eugenol: sources, extraction techniques and nutraceutical perspectives. *RSC Adv.* 7, 32669–32681. <https://doi.org/10.1039/C7RA04803C>
- Aladejana, J.T., Zeng, G., Zhang, F., Li, K., Li, X., Dong, Y., Li, J., 2023. Tough, waterproof, and mildew-resistant fully biobased soybean protein adhesives enhanced by furfuryl alcohol with dynamic covalent linkages. *Ind. Crops Prod.* 198, 116759. <https://doi.org/10.1016/j.indcrop.2023.116759>
- Allen, C.F.H., Fournier, J.O., Humphlett, W.J., 1964. THE THERMAL REVERSIBILITY OF THE MICHAEL REACTION: IV. THIOL ADDUCTS. *Can. J. Chem.* 42, 2616–2620. <https://doi.org/10.1139/v64-383>
- Altuna, F.I., Hoppe, C.E., Williams, R.J.J., 2019. Epoxy vitrimers with a covalently bonded tertiary amine as catalyst of the transesterification reaction. *Eur. Polym. J.* 113, 297–304. <https://doi.org/10.1016/j.eurpolymj.2019.01.045>
- Altuna, F.I., Pettarin, V., Williams, R.J.J., 2013. Self-healable polymer networks based on the cross-linking of epoxidised soybean oil by an aqueous citric acid solution. *Green Chem.* 15, 3360–3366. <https://doi.org/10.1039/C3GC41384E>
- Amornkitbamrung, L., Leungpuangkaew, S., Panklang, T., Jubsilp, C., Ekgasit, S., Um, S.H., Rimdusit, S., 2022. Effects of glutaric anhydride functionalization on filler-free benzoxazine/epoxy copolymers with shape memory and self-healing properties under near-infrared light actuation. *J. Sci. Adv. Mater. Devices* 7, 100446.
- Anastas, P., Eghbali, N., 2010. Green Chemistry: Principles and Practice. *Chem. Soc. Rev.* 39, 301–312. <https://doi.org/10.1039/B918763B>
- Andrew, J.J., Dhakal, H.N., 2022. Sustainable biobased composites for advanced applications: recent trends and future opportunities – A critical review. *Compos. Part C Open Access* 7, 100220. <https://doi.org/10.1016/j.jcomc.2021.100220>
- Arbenz, A., Avérous, L., 2015. Chemical modification of tannins to elaborate aromatic biobased macromolecular architectures. *Green Chem.* 17, 2626–2646. <https://doi.org/10.1039/C5GC00282F>
- Archipov, Y., Argyropoulos, D.S., Bolker, H.I., Heitner, C., 1991. 31P NMR Spectroscopy in Wood Chemistry. I. Model Compounds. *J. Wood Chem. Technol.* 11, 137–157. <https://doi.org/10.1080/02773819108050267>
- Asemani, M., Rabbani, A.R., 2020. Detailed FTIR spectroscopy characterization of crude oil extracted asphaltenes: Curve resolve of overlapping bands. *J. Pet. Sci. Eng.* 185, 106618. <https://doi.org/10.1016/j.petrol.2019.106618>
- A. Stewart, K., J. Lessard, J., J. Cantor, A., F. Rynk, J., S. Bailey, L., S. Sumerlin, B., 2023. High-performance polyimine vitrimers from an aromatic bio-based scaffold. *RSC Appl. Polym.* 1, 10–18. <https://doi.org/10.1039/D3LP00019B>
- Babra, T.S., Wood, M., Godleman, J.S., Salimi, S., Warriner, C., Bazin, N., Siviour, C.R., Hamley, I.W., Hayes, W., Greenland, B.W., 2019. Fluoride-responsive debond on demand adhesives: Manipulating polymer crystallinity and hydrogen bonding to optimise adhesion strength at low bonding temperatures. *Eur. Polym. J.* 119, 260–271. <https://doi.org/10.1016/j.eurpolymj.2019.07.038>
- Backfolk, K., Holmes, R., Ihalainen, P., Sirviö, P., Triantafillopoulos, N., Peltonen, J., 2007. Determination of the glass transition temperature of latex films: Comparison of various methods. *Polym. Test.* 26, 1031–1040. <https://doi.org/10.1016/j.polymertesting.2007.07.007>
- Bajwa, D.S., Pourhashem, G., Ullah, A.H., Bajwa, S.G., 2019. A concise review of current lignin production, applications, products and their environmental impact. *Ind. Crops Prod.* 139, 111526. <https://doi.org/10.1016/j.indcrop.2019.111526>
- Bakkali-Hassani, C., Edera, P., Langenbach, J., Poutrel, Q.-A., Norvez, S., Gresil, M., Tournilhac, F., 2023. Epoxy Vitriimer Materials by Lipase-Catalyzed Network Formation and Exchange Reactions. *ACS Macro Lett.* 12, 338–343. <https://doi.org/10.1021/acsmacrolett.2c00715>

LISTE COMPLÈTE DES RÉFÉRENCES BIBLIOGRAPHIQUES

- Bakkali-Hassani, C., Poutrel, Q.-A., Langenbach, J., Chappuis, S., Blaker, J.J., Gresil, M., Tournilhac, F., 2021. Lipase-Catalyzed Epoxy–Acid Addition and Transesterification: from Model Molecule Studies to Network Build-Up. *Biomacromolecules* 22, 4544–4551. <https://doi.org/10.1021/acs.biomac.1c00820>
- Banchereau, E., Lacombe, S., Ollivier, J., 1995. Solution reactivity of thiyl radicals with molecular oxygen: Unsensitized photooxidation of dimethyldisulfide. *Tetrahedron Lett.* 36, 8197–8200. [https://doi.org/10.1016/0040-4039\(95\)01698-H](https://doi.org/10.1016/0040-4039(95)01698-H)
- Bapat, A.P., Roy, D., Ray, J.G., Savin, D.A., Sumerlin, B.S., 2011. Dynamic-Covalent Macromolecular Stars with Boronic Ester Linkages. *J. Am. Chem. Soc.* 133, 19832–19838. <https://doi.org/10.1021/ja207005z>
- Bazin, A., Duval, A., Avérous, L., Pollet, E., 2022. Synthesis of Bio-Based Photo-Cross-Linkable Polyesters Based on Caffeic Acid through Selective Lipase-Catalyzed Polymerization. *Macromolecules* 55, 4256–4267. <https://doi.org/10.1021/acs.macromol.2c00499>
- Beller, H.R., Lee, T.S., Katz, L., 2015. Natural products as biofuels and bio-based chemicals: fatty acids and isoprenoids. *Nat. Prod. Rep.* 32, 1508–1526. <https://doi.org/10.1039/C5NP00068H>
- Belowich, M.E., Stoddart, J.F., 2012. Dynamic imine chemistry. *Chem. Soc. Rev.* 41, 2003–2024. <https://doi.org/10.1039/C2CS15305J>
- Berne, D., Coste, G., Morales-Cerrada, R., Boursier, M., Pinaud, J., Ladmiraal, V., Caillol, S., 2022a. Taking advantage of β -hydroxy amine enhanced reactivity and functionality for the synthesis of dual covalent adaptable networks. *Polym. Chem.* 13, 3806–3814. <https://doi.org/10.1039/D2PY00274D>
- Berne, D., Ladmiraal, V., Leclerc, E., Caillol, S., 2022b. Thia-Michael Reaction: The Route to Promising Covalent Adaptable Networks. *Polymers* 14, 4457. <https://doi.org/10.3390/polym14204457>
- Berne, D., Quienne, B., Caillol, S., Leclerc, E., Ladmiraal, V., 2022c. Biobased catalyst-free covalent adaptable networks based on CF 3 -activated synergistic aza-Michael exchange and transesterification. *J. Mater. Chem. A* 10, 25085–25097. <https://doi.org/10.1039/D2TA05067F>
- Biron, M., 2018. Thermoplastics and thermoplastic composites. William Andrew.
- Black, S.P., Sanders, J.K.M., Stefankiewicz, A.R., 2014. Disulfide exchange: exposing supramolecular reactivity through dynamic covalent chemistry. *Chem. Soc. Rev.* 43, 1861–1872. <https://doi.org/10.1039/C3CS60326A>
- Bo, C., Sha, Y., Song, F., Zhang, M., Hu, L., Jia, P., Zhou, Y., 2022. Renewable benzoxazine-based thermosets from cashew nut: Investigating the self-healing, shape memory, recyclability and antibacterial activity. *J. Clean. Prod.* 341, 130898. <https://doi.org/10.1016/j.jclepro.2022.130898>
- Boul, P.J., Reutenauer, P., Lehn, J.-M., 2005. Reversible Diels–Alder Reactions for the Generation of Dynamic Combinatorial Libraries. *Org. Lett.* 7, 15–18. <https://doi.org/10.1021/ol048065k>
- Bowman, C.N., Kloxin, C.J., 2012. Covalent Adaptable Networks: Reversible Bond Structures Incorporated in Polymer Networks. *Angew. Chem. Int. Ed.* 51, 4272–4274. <https://doi.org/10.1002/anie.201200708>
- Boyer, C., Hoogenboom, R., 2015. Multi-responsive polymers. *Eur. Polym. J.* 69, 438–440. <https://doi.org/10.1016/j.eurpolymj.2015.06.032>
- Brachvogel, R.-C., von Delius, M., 2016. The Dynamic Covalent Chemistry of Esters, Acetals and Orthoesters. *Eur. J. Org. Chem.* 2016, 3662–3670. <https://doi.org/10.1002/ejoc.201600388>
- Breuilac, A., Kassalias, A., Nicolaÿ, R., 2019. Polybutadiene Vitrimers Based on Dioxaborolane Chemistry and Dual Networks with Static and Dynamic Cross-links. *Macromolecules* 52, 7102–7113. <https://doi.org/10.1021/acs.macromol.9b01288>
- Briou, B., Améduri, B., Boutevin, B., 2021. Trends in the Diels–Alder reaction in polymer chemistry. *Chem. Soc. Rev.* 50, 11055–11097. <https://doi.org/10.1039/D0CS01382J>
- Britt, P.F., Coates, G.W., Winey, K.I., Byers, J., Chen, E., Coughlin, B., Ellison, C., Garcia, J., Goldman, A., Guzman, J., Hartwig, J., Helms, B., Huber, G., Jenks, C., Martin, J., McCann, M., Miller, S., O’Neill, H., Sadow, A., Scott, S., Sita, L., Vlachos, D., Waymouth, R., 2019. Report of the Basic Energy Sciences Roundtable on Chemical Upcycling of Polymers. USDOE Office of Science (SC) (United States). <https://doi.org/10.2172/1616517>
- Brutman, J.P., Delgado, P.A., Hillmyer, M.A., 2014. Polylactide Vitrimers. *ACS Macro Lett.* 3, 607–610. <https://doi.org/10.1021/mz500269w>
- Bueno-Ferrer, C., Hablot, E., Perrin-Sarazin, F., Garrigós, M.C., Jiménez, A., Averous, L., 2012. Structure and Morphology of New Bio-Based Thermoplastic Polyurethanes Obtained From Dimeric Fatty Acids. *Macromol. Mater. Eng.* 297, 777–784. <https://doi.org/10.1002/mame.201100278>
- Buono, P., Duval, A., Avérous, L., Habibi, Y., 2018. Clicking Biobased Polyphenols: A Sustainable Platform for Aromatic Polymeric Materials. *ChemSusChem* 11, 2472–2491. <https://doi.org/10.1002/cssc.201800595>
- Buono, P., Duval, A., Averous, L., Habibi, Y., 2017. Thermally healable and remendable lignin-based materials through Diels – Alder click polymerization. *Polymer* 133, 78–88. <https://doi.org/10.1016/j.polymer.2017.11.022>

LISTE COMPLÈTE DES RÉFÉRENCES BIBLIOGRAPHIQUES

- Cacciapaglia, R., Di Stefano, S., Mandolini, L., 2005. Metathesis Reaction of Formaldehyde Acetals: An Easy Entry into the Dynamic Covalent Chemistry of Cyclophane Formation. *J. Am. Chem. Soc.* 127, 13666–13671. <https://doi.org/10.1021/ja054362o>
- Caffy, F., Nicolaj, R., 2019. Transformation of polyethylene into a vitrimer by nitroxide radical coupling of a bis-dioxaborolane. *Polym. Chem.* 10, 3107–3115. <https://doi.org/10.1039/C9PY00253G>
- Caillol, S., 2023. The future of cardanol as small giant for biobased aromatic polymers and additives. *Eur. Polym. J.* 193, 112096. <https://doi.org/10.1016/j.eurpolymj.2023.112096>
- Caillol, S., 2018. Cardanol: A promising building block for biobased polymers and additives. *Curr. Opin. Green Sustain. Chem., Bioresources and Biochemicals / Biofuels and Bioenergy* 14, 26–32. <https://doi.org/10.1016/j.cogsc.2018.05.002>
- Candolle, A. de, 1885. *Origin of Cultivated Plants*. D. Appleton.
- Cao, Q., Li, J., Liu, B., Zhao, Y., Zhao, J., Gu, H., Wei, Z., Li, F., Jian, X., Weng, Z., 2023. Toward versatile biobased epoxy vitrimers by introducing aromatic N-heterocycles with stiff and flexible segments. *Chem. Eng. J.* 469, 143702. <https://doi.org/10.1016/j.cej.2023.143702>
- Cao, Y., He, J., Wu, J., Wang, X., Lu, W., Lin, J., Xu, Y., Chen, G., Zeng, B., Dai, L., 2022. A Smart Anticorrosive Epoxy Coating Based on Environmental-Stimuli-Responsive Copolymer Assemblies for Controlled Release of Corrosion Inhibitors. *Macromol. Mater. Eng.* 307, 2100983. <https://doi.org/10.1002/mame.202100983>
- Capelot, M., Montarnal, D., Tournilhac, F., Leibler, L., 2012a. Metal-Catalyzed Transesterification for Healing and Assembling of Thermosets. *J. Am. Chem. Soc.* 134, 7664–7667. <https://doi.org/10.1021/ja302894k>
- Capelot, M., Unterlass, M.M., Tournilhac, F., Leibler, L., 2012b. Catalytic Control of the Vitrimer Glass Transition. *ACS Macro Lett.* 1, 789–792. <https://doi.org/10.1021/mz300239f>
- Cash, J.J., Kubo, T., Bapat, A.P., Sumerlin, B.S., 2015. Room-Temperature Self-Healing Polymers Based on Dynamic-Covalent Boronic Esters. *Macromolecules* 48, 2098–2106. <https://doi.org/10.1021/acs.macromol.5b00210>
- Celotti, E., Ferrarini, R., Zironi, R., Conte, L.S., 1996. Resveratrol content of some wines obtained from dried Valpolicella grapes: Recioto and Amarone. *J. Chromatogr. A, 19th International Symposium on Column Liquid Chromatography* 730, 47–52. [https://doi.org/10.1016/0021-9673\(95\)00962-0](https://doi.org/10.1016/0021-9673(95)00962-0)
- Chakma, P., Konkolewicz, D., 2019. Dynamic Covalent Bonds in Polymeric Materials. *Angew. Chem. Int. Ed.* 58, 9682–9695. <https://doi.org/10.1002/anie.201813525>
- Chandel, A.K., Garlapati, V.K., Jeevan Kumar, S.P., Hans, M., Singh, A.K., Kumar, S., 2020. The role of renewable chemicals and biofuels in building a bioeconomy. *Biofuels Bioprod. Biorefining* 14, 830–844. <https://doi.org/10.1002/bbb.2104>
- Chatterjee, M., Ishizaka, T., Chatterjee, A., Kawanami, H., 2017. Dehydrogenation of 5-hydroxymethylfurfural to diformylfuran in compressed carbon dioxide: an oxidant free approach. *Green Chem.* 19, 1315–1326. <https://doi.org/10.1039/C6GC02977A>
- Chen, B.-B., Chang, S., Jiang, L., Lv, J., Gao, Y.-T., Wang, Y., Qian, R.-C., Li, D.-W., Hafez, M.E., 2022. Reversible polymerization of carbon dots based on dynamic covalent imine bond. *J. Colloid Interface Sci.* 621, 464–469. <https://doi.org/10.1016/j.jcis.2022.04.089>
- Chen, F., Cheng, Q., Gao, F., Zhong, J., Shen, L., Lin, C., Lin, Y., 2021. The effect of latent plasticity on the shape recovery of a shape memory vitrimer. *Eur. Polym. J.* 147, 110304. <https://doi.org/10.1016/j.eurpolymj.2021.110304>
- Chen, F., Gao, F., Zhong, J., Shen, L., Lin, Y., 2020. Fusion of biobased vinylogous urethane vitrimers with distinct mechanical properties. *Mater. Chem. Front.* 4, 2723–2730. <https://doi.org/10.1039/D0QM00302F>
- Chen, F., Xiao, H., Peng, Z.Q., Zhang, Z.P., Rong, M.Z., Zhang, M.Q., 2021. Thermally conductive glass fiber reinforced epoxy composites with intrinsic self-healing capability. *Adv. Compos. Hybrid Mater.* 4, 1048–1058. <https://doi.org/10.1007/s42114-021-00303-3>
- Chen, J., Lu, X., Xin, Z., 2023. A bio-based reprocessable and degradable polybenzoxazine with acetal structures. *React. Funct. Polym.* 191, 105653. <https://doi.org/10.1016/j.reactfunctpolym.2023.105653>
- Chen, M., Si, H., Zhang, H., Zhou, L., Wu, Y., Song, L., Kang, M., Zhao, X.-L., 2021. The Crucial Role in Controlling the Dynamic Properties of Polyester-Based Epoxy Vitrimers: The Density of Exchangeable Ester Bonds (ν). *Macromolecules* 54, 10110–10117. <https://doi.org/10.1021/acs.macromol.1c01289>
- Chen, M., Wu, Y., Chen, B., Tucker, A.M., Jagota, A., Yang, S., 2022. Fast, strong, and reversible adhesives with dynamic covalent bonds for potential use in wound dressing. *Proc. Natl. Acad. Sci.* 119, e2203074119. <https://doi.org/10.1073/pnas.2203074119>
- Chen, X., Dam, M.A., Ono, K., Mal, A., Shen, H., Nutt, S.R., Sheran, K., Wudl, F., 2002. A Thermally Remendable Cross-Linked Polymeric Material. *Science* 295, 1698–1702. <https://doi.org/10.1126/science.1065879>

LISTE COMPLÈTE DES RÉFÉRENCES BIBLIOGRAPHIQUES

- Chen, X., Li, L., Jin, K., Torkelson, J.M., 2017. Reprocessable polyhydroxyurethane networks exhibiting full property recovery and concurrent associative and dissociative dynamic chemistry via transcarbamoylation and reversible cyclic carbonate aminolysis. *Polym. Chem.* 8, 6349–6355. <https://doi.org/10.1039/C7PY01160A>
- Chen, Yixuan, Chen, B., Torkelson, J.M., 2023. Biobased, Reprocessable Non-isocyanate Polythiourethane Networks with Thionourethane and Disulfide Cross-Links: Comparison with Polyhydroxyurethane Network Analogues. *Macromolecules* 56, 3687–3702. <https://doi.org/10.1021/acs.macromol.3c00220>
- Chen, Yizhen, Zeng, Y., Wu, Y., Chen, T., Qiu, R., Liu, W., 2023. Flame-Retardant and Recyclable Soybean Oil-Based Thermosets Enabled by the Dynamic Phosphate Ester and Tannic Acid. *ACS Appl. Mater. Interfaces* 15, 5963–5973. <https://doi.org/10.1021/acsami.2c21279>
- Chen, Z., Wang, J., Qi, H.J., Wang, T., Naguib, H.E., 2020. Green and Sustainable Layered Chitin–Vitriimer Composite with Enhanced Modulus, Reprocessability, and Smart Actuator Function. *ACS Sustain. Chem. Eng.* 8, 15168–15178. <https://doi.org/10.1021/acssuschemeng.0c04235>
- Chenal, J.-M., Chazeau, L., Guy, L., Bomal, Y., Gauthier, C., 2007. Molecular weight between physical entanglements in natural rubber: A critical parameter during strain-induced crystallization. *Polymer* 48, 1042–1046. <https://doi.org/10.1016/j.polymer.2006.12.031>
- Cheng, C., Zhang, X., Chen, X., Li, J., Huang, Q., Hu, Z., Tu, Y., 2016. Self-healing polymers based on eugenol via combination of thiol-ene and thiol oxidation reactions. *J. Polym. Res.* 23, 110. <https://doi.org/10.1007/s10965-016-1001-x>
- Cheng, X., Li, L., Yang, L., Huang, Q., Li, Y., Cheng, Y., 2022. All-Small-Molecule Dynamic Covalent Hydrogels with Heat-Triggered Release Behavior for the Treatment of Bacterial Infections. *Adv. Funct. Mater.* 32, 2206201. <https://doi.org/10.1002/adfm.202206201>
- Cheng, X., Li, M., Wang, H., Cheng, Y., 2020. All-small-molecule dynamic covalent gels with antibacterial activity by boronate-tannic acid gelation. *Chin. Chem. Lett.* 31, 869–874. <https://doi.org/10.1016/j.ccllet.2019.07.013>
- Chiang, Y., Kresge, A.J., Young, C.I., 1978. Vinyl ether hydrolysis. XII. Use of *cis* – *trans* isomerism to probe the reaction mechanism. *Can. J. Chem.* 56, 461–464. <https://doi.org/10.1139/v78-074>
- Choi, Y., Park, K., Choi, H., Son, D., Shin, M., 2021. Self-Healing, Stretchable, Biocompatible, and Conductive Alginate Hydrogels through Dynamic Covalent Bonds for Implantable Electronics. *Polymers* 13, 1133. <https://doi.org/10.3390/polym13071133>
- Chung, C.-M., Roh, Y.-S., Cho, S.-Y., Kim, J.-G., 2004. Crack Healing in Polymeric Materials via Photochemical [2+2] Cycloaddition. *Chem. Mater.* 16, 3982–3984. <https://doi.org/10.1021/cm049394+>
- Chung, K.-T., Lu, Z., Chou, M.W., 1998. Mechanism of inhibition of tannic acid and related compounds on the growth of intestinal bacteria. *Food Chem. Toxicol.* 36, 1053–1060. [https://doi.org/10.1016/S0278-6915\(98\)00086-6](https://doi.org/10.1016/S0278-6915(98)00086-6)
- Ciaccia, M., Stefano, S.D., 2014. Mechanisms of imine exchange reactions in organic solvents. *Org. Biomol. Chem.* 13, 646–654. <https://doi.org/10.1039/C4OB02110J>
- Citarella, A., Amenta, A., Passarella, D., Micale, N., 2022. Cyrene: A Green Solvent for the Synthesis of Bioactive Molecules and Functional Biomaterials. *Int. J. Mol. Sci.* 23, 15960. <https://doi.org/10.3390/ijms232415960>
- Citeo, 2020. Citeo Prospective - Note réglementation plastiques compostables et biosourcés. URL <https://bo.citeo.com/sites/default/files/2020-06/Citeo%20Prospective%20-%20Note%20r%C3%A9glementation%20plastiques%20compostables%20et%20biosourc%C3%A9s.pdf> (accessed 4.29.24).
- Clark, T., Murray, J.S., Lane, P., Politzer, P., 2008. Why are dimethyl sulfoxide and dimethyl sulfone such good solvents? *J. Mol. Model.* 14, 689–697. <https://doi.org/10.1007/s00894-008-0279-y>
- Clemens, R.J., Hyatt, J.A., 1985. Acetoacetylation with 2,2,6-trimethyl-4H-1,3-dioxin-4-one: a convenient alternative to diketene. *J. Org. Chem.* 50, 2431–2435. <https://doi.org/10.1021/jo00214a006>
- Clemens, R.J., Witzeman, J.S., 1989. Kinetic and spectroscopic studies on the thermal decomposition of 2,2,6-trimethyl-4H-1,3-dioxin-4-one. Generation of acetylketene. *J. Am. Chem. Soc.* 111, 2186–2193. <https://doi.org/10.1021/ja00188a037>
- Collins, J., Nadgorny, M., Xiao, Z., Connal, L.A., 2017. Doubly Dynamic Self-Healing Materials Based on Oxime Click Chemistry and Boronic Acids. *Macromol. Rapid Commun.* 38, 1600760. <https://doi.org/10.1002/marc.201600760>
- Constant, S., Wienk, H.L.J., Frissen, A.E., Peinder, P. de, Boelens, R., Es, D.S. van, Grisel, R.J.H., Weckhuysen, B.M., Huijgen, W.J.J., Gosselink, R.J.A., Bruijninx, P.C.A., 2016. New insights into the structure and composition of technical lignins: a comparative characterisation study. *Green Chem.* 18, 2651–2665. <https://doi.org/10.1039/C5GC03043A>

LISTE COMPLÈTE DES RÉFÉRENCES BIBLIOGRAPHIQUES

- Cordes, E.H., Bull, H.G., 1974. Mechanism and catalysis for hydrolysis of acetals, ketals, and ortho esters. *Chem. Rev.* 74, 581–603. <https://doi.org/10.1021/cr60291a004>
- Costes, L., Laoutid, F., Brohez, S., Dubois, P., 2017. Bio-based flame retardants: When nature meets fire protection. *Mater. Sci. Eng. R Rep.* 117, 1–25. <https://doi.org/10.1016/j.mser.2017.04.001>
- Cromwell, O.R., Chung, J., Guan, Z., 2015. Malleable and Self-Healing Covalent Polymer Networks through Tunable Dynamic Boronic Ester Bonds. *J. Am. Chem. Soc.* 137, 6492–6495. <https://doi.org/10.1021/jacs.5b03551>
- Cui, C.-Y., Chen, W., Wang, H.-R., Ren, W.-M., Lu, X.-B., Zhou, H., 2024. Degradable sugar-derived poly(vinyl ether ester)s by hydroxyl-yne click polymerization. *Eur. Polym. J.* 211, 112997. <https://doi.org/10.1016/j.eurpolymj.2024.112997>
- Cui, G., Bi, Z., Wang, S., Liu, J., Xing, X., Li, Z., Wang, B., 2020. A comprehensive review on smart anti-corrosive coatings. *Prog. Org. Coat.* 148, 105821. <https://doi.org/10.1016/j.porgcoat.2020.105821>
- Cuminet, F., Berne, D., Lemouzy, S., Dantras, É., Joly-Duhamel, C., Caillol, S., Leclerc, É., Ladmiral, V., 2022. Catalyst-free transesterification vitrimers: activation via α -difluoroesters. *Polym. Chem.* 13, 2651–2658. <https://doi.org/10.1039/D2PY00124A>
- Cuminet, F., Caillol, S., Dantras, É., Leclerc, É., Ladmiral, V., 2021. Neighboring Group Participation and Internal Catalysis Effects on Exchangeable Covalent Bonds: Application to the Thriving Field of Vitriimer Chemistry. *Macromolecules* 54, 3927–3961. <https://doi.org/10.1021/acs.macromol.0c02706>
- Cuminet, F., Lemouzy, S., Dantras, É., Leclerc, É., Ladmiral, V., Caillol, S., 2023. From vineyards to reshapable materials: α -CF₂ activation in 100% resveratrol-based catalyst-free vitrimers. *Polym. Chem.* 14, 1387–1395. <https://doi.org/10.1039/D3PY00017F>
- Czarny-Krzywińska, K., Krawczyk, B., Szczukocki, D., 2023. Bisphenol A and its substitutes in the aquatic environment: Occurrence and toxicity assessment. *Chemosphere* 315, 137763. <https://doi.org/10.1016/j.chemosphere.2023.137763>
- D’Adamo, I., Gastaldi, M., Morone, P., Rosa, P., Sassanelli, C., Settembre-Blundo, D., Shen, Y., 2022. Bioeconomy of Sustainability: Drivers, Opportunities and Policy Implications. *Sustainability* 14, 200. <https://doi.org/10.3390/su14010200>
- Danthu, P., Simanjuntak, R., Fawbush, F., Leong Pock Tsy, J.M., Razafimamonjison, G., Abdillahi, M.M., Jahiel, M., Penot, E., 2020. The clove tree and its products (clove bud, clove oil, eugenol): prosperous today but what of tomorrow’s restrictions? *Fruits* 75, 224–242. <https://doi.org/10.17660/th2020/75.5.5>
- Davidson, E.R., Eichinger, B.E., Robinson, B.H., 2006. Hyperpolarizability: Calibration of theoretical methods for chloroform, water, acetonitrile, and *p*-nitroaniline. *Opt. Mater.* 29, 360–364. <https://doi.org/10.1016/j.optmat.2006.03.031>
- de Hoyos-Martínez, P.L., Merle, J., Labidi, J., Charrier – El Bouhtoury, F., 2019. Tannins extraction: A key point for their valorization and cleaner production. *J. Clean. Prod.* 206, 1138–1155. <https://doi.org/10.1016/j.jclepro.2018.09.243>
- Debnath, S., Kaushal, S., Ojha, U., 2020. Catalyst-Free Partially Bio-Based Polyester Vitrimers. *ACS Appl. Polym. Mater.* 2, 1006–1013. <https://doi.org/10.1021/acsapm.0c00016>
- Debnath, S., Tiwary, S.K., Ojha, U., 2021. Dynamic Carboxylate Linkage Based Reprocessable and Self-Healable Segmented Polyurethane Vitrimers Displaying Creep Resistance Behavior and Triple Shape Memory Ability. *ACS Appl. Polym. Mater.* 3, 2166–2177. <https://doi.org/10.1021/acsapm.1c00199>
- Debsharma, T., Engelen, S., De Baere, I., Van Paepegem, W., Du Prez, F., 2023. Resorcinol-Derived Vitrimers and Their Flax Fiber-Reinforced Composites Based on Fast Siloxane Exchange. *Macromol. Rapid Commun.* 44, 2300020. <https://doi.org/10.1002/marc.202300020>
- Decostanzi, M., Auvergne, R., Boutevin, B., Caillol, S., 2019. Biobased phenol and furan derivatives coupling for the synthesis of functional monomers. *Green Chem.* 21, 724–747. <https://doi.org/10.1039/C8GC03541E>
- del Río, J.C., Rencoret, J., Gutiérrez, A., Elder, T., Kim, H., Ralph, J., 2020. Lignin Monomers from beyond the Canonical Monolignol Biosynthetic Pathway: Another Brick in the Wall. *ACS Sustain. Chem. Eng.* 8, 4997–5012. <https://doi.org/10.1021/acssuschemeng.0c01109>
- Delavarde, A., Savin, G., Derkenne, P., Boursier, M., Morales-Cerrada, R., Nottelet, B., Pinaud, J., Caillol, S., 2024. Sustainable polyurethanes: toward new cutting-edge opportunities. *Prog. Polym. Sci.* 151, 101805. <https://doi.org/10.1016/j.progpolymsci.2024.101805>
- Demongeot, A., Groote, R., Goossens, H., Hoeks, T., Tournilhac, F., Leibler, L., 2017. Cross-Linking of Poly(butylene terephthalate) by Reactive Extrusion Using Zn(II) Epoxy-Vitriimer Chemistry. *Macromolecules* 50, 6117–6127. <https://doi.org/10.1021/acs.macromol.7b01141>
- Denissen, W., De Baere, I., Van Paepegem, W., Leibler, L., Winne, J., Du Prez, F.E., 2018. Vinylogous Urea Vitrimers and Their Application in Fiber Reinforced Composites. *Macromolecules* 51, 2054–2064. <https://doi.org/10.1021/acs.macromol.7b02407>

LISTE COMPLÈTE DES RÉFÉRENCES BIBLIOGRAPHIQUES

- Denissen, W., Droesbeke, M., Nicolaÿ, R., Leibler, L., Winne, J.M., Du Prez, F.E., 2017. Chemical control of the viscoelastic properties of vinylogous urethane vitrimers. *Nat. Commun.* 8, 14857. <https://doi.org/10.1038/ncomms14857>
- Denissen, W., M. Winne, J., Prez, F.E.D., 2016. Vitrimers: permanent organic networks with glass-like fluidity. *Chem. Sci.* 7, 30–38. <https://doi.org/10.1039/C5SC02223A>
- Denissen, W., Rivero, G., Nicolaÿ, R., Leibler, L., Winne, J.M., Du Prez, F.E., 2015. Vinylogous Urethane Vitrimers. *Adv. Funct. Mater.* 25, 2451–2457. <https://doi.org/10.1002/adfm.201404553>
- Dessbesell, L., Paleologou, M., Leitch, M., Pulkki, R., Xu, C. (Charles), 2020. Global lignin supply overview and kraft lignin potential as an alternative for petroleum-based polymers. *Renew. Sustain. Energy Rev.* 123, 109768. <https://doi.org/10.1016/j.rser.2020.109768>
- Dhers, S., Vantomme, G., Avérous, L., 2019. A fully bio-based polyimine vitrimer derived from fructose. *Green Chem.* 21, 1596–1601. <https://doi.org/10.1039/C9GC00540D>
- Dhinojwala, A., Hooker, J.C., Torkelson, J.M., 1994. Retardation of rotational reorientation dynamics in polymers near the glass transition: a novel study over eleven decades in time using second-order non-linear optics. *J. Non-Cryst. Solids, Relaxations in Complex Systems* 172–174, 286–296. [https://doi.org/10.1016/0022-3093\(94\)90447-2](https://doi.org/10.1016/0022-3093(94)90447-2)
- Ding, X.-M., Chen, L., Luo, X., He, F.-M., Xiao, Y.-F., Wang, Y.-Z., 2022. Biomass-derived dynamic covalent epoxy thermoset with robust mechanical properties and facile malleability. *Chin. Chem. Lett.* 33, 3245–3248. <https://doi.org/10.1016/j.cclet.2021.10.079>
- Dong, L., Wang, Y., Dong, Y., Zhang, Y., Pan, M., Liu, X., Gu, X., Antonietti, M., Chen, Z., 2023. Sustainable production of dopamine hydrochloride from softwood lignin. *Nat. Commun.* 14, 4996. <https://doi.org/10.1038/s41467-023-40702-2>
- Dorigato, A., 2021. Recycling of polymer blends. *Adv. Ind. Eng. Polym. Res., Recycling of Polymer Blends and Composites* 4, 53–69. <https://doi.org/10.1016/j.aiepr.2021.02.005>
- Du, L., Jin, X., Qian, G., Yang, W., Su, L., Ma, Y., Ren, S., Li, S., 2022. Lignin-based vitrimer for circulation in plastics, coatings, and adhesives with tough mechanical properties, catalyst-free and good chemical solvent resistance. *Ind. Crops Prod.* 187, 115439. <https://doi.org/10.1016/j.indcrop.2022.115439>
- Dusek, K., Matejka, L., 1984. Transesterification and Gelation of Polyhydroxy Esters Formed from Diepoxides and Dicarboxylic Acids, in: *Rubber-Modified Thermoset Resins, Advances in Chemistry*. American Chemical Society, pp. 15–26. <https://doi.org/10.1021/ba-1984-0208.ch002>
- Duval, A., Avérous, L., 2023. From thermoplastic polyurethane to covalent adaptable network via reversible photo-crosslinking of a biobased chain extender synthesized from caffeic acid. *Polym. Chem.* 14, 2685–2696. <https://doi.org/10.1039/D3PY00162H>
- Duval, A., Avérous, L., 2022. Dihydrolevoglucosenone (Cyrene™) as a versatile biobased solvent for lignin fractionation, processing, and chemistry. *Green Chem.* 24, 338–349. <https://doi.org/10.1039/D1GC03395F>
- Duval, A., Avérous, L., 2020. Mild and controlled lignin methylation with trimethyl phosphate: towards a precise control of lignin functionality. *Green Chem.* 22, 1671–1680. <https://doi.org/10.1039/C9GC03890F>
- Duval, A., Avérous, L., 2017a. Solvent- and Halogen-Free Modification of Biobased Polyphenols to Introduce Vinyl Groups: Versatile Aromatic Building Blocks for Polymer Synthesis. *ChemSusChem* 10, 1813–1822. <https://doi.org/10.1002/cssc.201700066>
- Duval, A., Avérous, L., 2017b. Cyclic Carbonates as Safe and Versatile Etherifying Reagents for the Functionalization of Lignins and Tannins. *ACS Sustain. Chem. Eng.* 5, 7334–7343. <https://doi.org/10.1021/acssuschemeng.7b01502>
- Duval, A., Benali, W., Avérous, L., 2024. Turning lignin into a recyclable bioresource: transesterification vitrimers from lignins modified with ethylene carbonate. *Green Chem.* <https://doi.org/10.1039/D4GC00567H>
- Duval, A., Couture, G., Caillol, S., Avérous, L., 2017. Biobased and Aromatic Reversible Thermoset Networks from Condensed Tannins via the Diels–Alder Reaction. *ACS Sustain. Chem. Eng.* 5, 1199–1207. <https://doi.org/10.1021/acssuschemeng.6b02596>
- Duval, A., Lange, H., Lawoko, M., Crestini, C., 2015. Reversible crosslinking of lignin via the furan–maleimide Diels–Alder reaction. *Green Chem.* 17, 4991–5000. <https://doi.org/10.1039/C5GC01319D>
- Duval, A., Lawoko, M., 2014. A review on lignin-based polymeric, micro- and nano-structured materials. *React. Funct. Polym.* 85, 78–96. <https://doi.org/10.1016/j.reactfunctpolym.2014.09.017>
- Duval, A., Layrac, G., van Zomeren, A., Smit, A.T., Pollet, E., Avérous, L., 2021. Isolation of Low Dispersity Fractions of Acetone Organosolv Lignins to Understand their Reactivity: Towards Aromatic Building Blocks for Polymers Synthesis. *ChemSusChem* 14, 387–397. <https://doi.org/10.1002/cssc.202001976>
- Duval, A., Vidal, D., Sarbu, A., René, W., Avérous, L., 2022. Scalable single-step synthesis of lignin-based liquid polyols with ethylene carbonate for polyurethane foams. *Mater. Today Chem.* 24, 100793. <https://doi.org/10.1016/j.mtchem.2022.100793>

LISTE COMPLÈTE DES RÉFÉRENCES BIBLIOGRAPHIQUES

- Elling, B.R., Dichtel, W.R., 2020. Reprocessable Cross-Linked Polymer Networks: Are Associative Exchange Mechanisms Desirable? *ACS Cent. Sci.* 6, 1488–1496. <https://doi.org/10.1021/acscentsci.0c00567>
- Emblem, A., 2012. 13 - Plastics properties for packaging materials, in: Emblem, Anne, Emblem, H. (Eds.), *Packaging Technology*. Woodhead Publishing, pp. 287–309. <https://doi.org/10.1533/9780857095701.2.287>
- Emiliani, G., Fondi, M., Fani, R., Gribaldo, S., 2009. A horizontal gene transfer at the origin of phenylpropanoid metabolism: a key adaptation of plants to land. *Biol. Direct* 4, 7. <https://doi.org/10.1186/1745-6150-4-7>
- Engelen, S., Dolinski, N.D., Chen, C., Ghimire, E., Lindberg, C.A., Crolais, A.E., Nitta, N., Winne, J.M., Rowan, S.J., Du Prez, F.E., 2024. Vinylogous Urea—Urethane Vitrimers: Accelerating and Inhibiting Network Dynamics through Hydrogen Bonding. *Angew. Chem.* 136, e202318412. <https://doi.org/10.1002/ange.202318412>
- Engelen, S., Wróblewska, A.A., Bruycker, K.D., Aksakal, R., Admiral, V., Caillol, S., Du Prez, F.E., 2022. Sustainable design of vanillin-based vitrimers using vinylogous urethane chemistry. *Polym. Chem.* <https://doi.org/10.1039/D2PY00351A>
- Eraghi Kazzaz, A., Fatehi, P., 2020. Technical lignin and its potential modification routes: A mini-review. *Ind. Crops Prod.* 154, 112732. <https://doi.org/10.1016/j.indcrop.2020.112732>
- European Commission, 2011. Règlement (UE) no 10/2011 de la Commission du 14 janvier 2011 concernant les matériaux et objets en matière plastique destinés à entrer en contact avec des denrées alimentaires. URL <https://eur-lex.europa.eu/LexUriServ/LexUriServ.do?uri=OJ:L:2011:012:0001:0089:fr:PDF> (accessed 5.2.24).
- Fache, M., Boutevin, B., Caillol, S., 2016. Vanillin Production from Lignin and Its Use as a Renewable Chemical. *ACS Sustain. Chem. Eng.* 4, 35–46. <https://doi.org/10.1021/acssuschemeng.5b01344>
- Fache, M., Boutevin, B., Caillol, S., 2015. Vanillin, a key-intermediate of biobased polymers. *Eur. Polym. J.* 68, 488–502. <https://doi.org/10.1016/j.eurpolymj.2015.03.050>
- Fairbanks, B.D., Singh, S.P., Bowman, C.N., Anseth, K.S., 2011. Photodegradable, Photoadaptable Hydrogels via Radical-Mediated Disulfide Fragmentation Reaction. *Macromolecules* 44, 2444–2450. <https://doi.org/10.1021/ma200202w>
- Fan, X., Zhou, W., Chen, Y., Yan, L., Fang, Y., Liu, H., 2020. An Antifreezing/Antiheating Hydrogel Containing Catechol Derivative Urushiol for Strong Wet Adhesion to Various Substrates. *ACS Appl. Mater. Interfaces* 12, 32031–32040. <https://doi.org/10.1021/acsami.0c09917>
- Feng, X., Fan, J., Li, A., Li, G., 2020. Biobased Tannic Acid Cross-Linked Epoxy Thermosets with Hierarchical Molecular Structure and Tunable Properties: Damping, Shape Memory, and Recyclability. *ACS Sustain. Chem. Eng.* 8, 874–883. <https://doi.org/10.1021/acssuschemeng.9b05198>
- Ferry, J.D., 1980. *Viscoelastic Properties of Polymers*. John Wiley & Sons.
- Feula, A., Tang, X., Giannakopoulos, I., M. Chippindale, A., W. Hamley, I., Greco, F., Buckley, C.P., R. Siviour, C., Hayes, W., 2016. An adhesive elastomeric supramolecular polyurethane healable at body temperature. *Chem. Sci.* 7, 4291–4300. <https://doi.org/10.1039/C5SC04864H>
- Flourat, A.L., Combes, J., Bailly-Maitre-Grand, C., Magnien, K., Haudrechy, A., Renault, J.-H., Allais, F., 2021. Accessing p-Hydroxycinnamic Acids: Chemical Synthesis, Biomass Recovery, or Engineered Microbial Production? *ChemSusChem* 14, 118–129. <https://doi.org/10.1002/cssc.202002141>
- Ford, L., Theodoridou, K., Sheldrake, G.N., Walsh, P.J., 2019. A critical review of analytical methods used for the chemical characterisation and quantification of phlorotannin compounds in brown seaweeds. *Phytochem. Anal.* 30, 587–599. <https://doi.org/10.1002/pca.2851>
- Fortman, D.J., Brutman, J.P., Cramer, C.J., Hillmyer, M.A., Dichtel, W.R., 2015. Mechanically Activated, Catalyst-Free Polyhydroxyurethane Vitrimers. *J. Am. Chem. Soc.* 137, 14019–14022. <https://doi.org/10.1021/jacs.5b08084>
- Fortman, D.J., Brutman, J.P., De Hoe, G.X., Snyder, R.L., Dichtel, W.R., Hillmyer, M.A., 2018. Approaches to Sustainable and Continually Recyclable Cross-Linked Polymers. *ACS Sustain. Chem. Eng.* 6, 11145–11159. <https://doi.org/10.1021/acssuschemeng.8b02355>
- Froidevaux, V., Negrell, C., Caillol, S., Pascault, J.-P., Boutevin, B., 2016. Biobased Amines: From Synthesis to Polymers; Present and Future. *Chem. Rev.* 116, 14181–14224. <https://doi.org/10.1021/acs.chemrev.6b00486>
- Frutos, P., Hervás, G., Giráldez, F.J., Mantecón, A.R., 2004. Review. Tannins and ruminant nutrition. *Span. J. Agric. Res.* 2, 191–202. <https://doi.org/10.5424/sjar/2004022-73>
- Fu, X., Qin, A., Tang, B.Z., 2024. Dynamic covalent polymers generated from X-yne click polymerization. *J. Polym. Sci.* 62. <https://doi.org/10.1002/pol.20230383>
- Galkin, K.I., Ananikov, V.P., 2019. When Will 5-Hydroxymethylfurfural, the “Sleeping Giant” of Sustainable Chemistry, Awaken? *ChemSusChem* 12, 2976–2982. <https://doi.org/10.1002/cssc.201900592>

LISTE COMPLÈTE DES RÉFÉRENCES BIBLIOGRAPHIQUES

- Gamardella, F., De la Flor, S., Ramis, X., Serra, A., 2020. Recyclable poly(thiourethane) vitrimers with high Tg. Influence of the isocyanate structure. *React. Funct. Polym.* 151, 104574. <https://doi.org/10.1016/j.reactfunctpolym.2020.104574>
- Gandini, A., 2013. The furan/maleimide Diels–Alder reaction: A versatile click–unclick tool in macromolecular synthesis. *Prog. Polym. Sci., Topical Issue on Polymer Chemistry* 38, 1–29. <https://doi.org/10.1016/j.progpolymsci.2012.04.002>
- Gandini, A., Belgacem, M.N., 1997. Furans in polymer chemistry. *Prog. Polym. Sci.* 22, 1203–1379. [https://doi.org/10.1016/S0079-6700\(97\)00004-X](https://doi.org/10.1016/S0079-6700(97)00004-X)
- Gandini, A., Lacerda, T.M., Carvalho, A.J.F., Trovatti, E., 2016. Progress of Polymers from Renewable Resources: Furans, Vegetable Oils, and Polysaccharides. *Chem. Rev.* 116, 1637–1669. <https://doi.org/10.1021/acs.chemrev.5b00264>
- Gao, S., Cheng, Z., Zhou, X., Liu, Y., Wang, J., Wang, C., Chu, F., Xu, F., Zhang, D., 2020. Fabrication of lignin based renewable dynamic networks and its applications as self-healing, antifungal and conductive adhesives. *Chem. Eng. J.* 394, 124896. <https://doi.org/10.1016/j.cej.2020.124896>
- García-Astrain, C., Gandini, A., Coelho, D., Mondragon, I., Retegi, A., Eceiza, A., Corcuera, M.A., Gabilondo, N., 2013. Green chemistry for the synthesis of methacrylate-based hydrogels crosslinked through Diels–Alder reaction. *Eur. Polym. J.* 49, 3998–4007. <https://doi.org/10.1016/j.eurpolymj.2013.09.004>
- Gedam, P.H., Sampathkumaran, P.S., 1986. Cashew nut shell liquid: Extraction, chemistry and applications. *Prog. Org. Coat.* 14, 115–157. [https://doi.org/10.1016/0033-0655\(86\)80009-7](https://doi.org/10.1016/0033-0655(86)80009-7)
- Genua, A., Montes, S., Azcune, I., Rekondo, A., Malburet, S., Daydé-Cazals, B., Graillot, A., 2020. Build-To-Specification Vanillin and Phloroglucinol Derived Biobased Epoxy-Amine Vitrimers. *Polymers* 12, 2645. <https://doi.org/10.3390/polym12112645>
- Gevrek, T.N., Sanyal, A., 2021. Furan-containing polymeric Materials: Harnessing the Diels-Alder chemistry for biomedical applications. *Eur. Polym. J.* 153, 110514. <https://doi.org/10.1016/j.eurpolymj.2021.110514>
- Glasser, W.G., 2019. About Making Lignin Great Again—Some Lessons From the Past. *Front. Chem.* 7. <https://doi.org/10.3389/fchem.2019.00565>
- Gong, X., Cheng, Z., Gao, S., Zhang, D., Ma, Y., Wang, J., Wang, C., Chu, F., 2020. Ethyl cellulose based self-healing adhesives synthesized via RAFT and aromatic schiff-base chemistry. *Carbohydr. Polym.* 250, 116846. <https://doi.org/10.1016/j.carbpol.2020.116846>
- Granata, A., Argyropoulos, D.S., 1995. 2-Chloro-4,4,5,5-tetramethyl-1,3,2-dioxaphospholane, a Reagent for the Accurate Determination of the Uncondensed and Condensed Phenolic Moieties in Lignins. *J. Agric. Food Chem.* 43, 1538–1544. <https://doi.org/10.1021/jf00054a023>
- Guerre, M., Taplan, C., Nicolaÿ, R., Winne, J.M., Du Prez, F.E., 2018. Fluorinated Vitriimer Elastomers with a Dual Temperature Response. *J. Am. Chem. Soc.* 140, 13272–13284. <https://doi.org/10.1021/jacs.8b07094>
- Guo, X., Gao, F., Chen, F., Zhong, J., Shen, L., Lin, C., Lin, Y., 2021. Dynamic Enamine-one Bond Based Vitriimer via Amino-yne Click Reaction. *ACS Macro Lett.* 10, 1186–1190. <https://doi.org/10.1021/acsmacrolett.1c00550>
- Haida, P., Abetz, V., 2020. Acid-Mediated Autocatalysis in Vinylogous Urethane Vitrimers. *Macromol. Rapid Commun.* 41, 2000273. <https://doi.org/10.1002/marc.202000273>
- Haida, P., Chirachanchai, S., Abetz, V., 2023. Starch-Reinforced Vinylogous Urethane Vitriimer Composites: An Approach to Biobased, Reprocessable, and Biodegradable Materials. *ACS Sustain. Chem. Eng.* 11, 8350–8361. <https://doi.org/10.1021/acssuschemeng.3c01340>
- Haida, P., Signorato, G., Abetz, V., 2022. Blended vinylogous urethane/urea vitrimers derived from aromatic alcohols. *Polym. Chem.* 13, 946–958. <https://doi.org/10.1039/D1PY01237A>
- Hajj, R., Duval, A., Dhers, S., Avérous, L., 2020. Network Design to Control Polyimine Vitriimer Properties: Physical Versus Chemical Approach. *Macromolecules* 53, 3796–3805. <https://doi.org/10.1021/acs.macromol.0c00453>
- Hamernik, L.J., Guzman, W., Wiggins, J.S., 2023. Solvent-free preparation of imine vitrimers: leveraging benzoxazine crosslinking for melt processability and tunable mechanical performance. *J. Mater. Chem. A* 11, 20568–20582. <https://doi.org/10.1039/D3TA04351G>
- Hammer, L., Van Zee, N.J., Nicolaÿ, R., 2021. Dually Crosslinked Polymer Networks Incorporating Dynamic Covalent Bonds. *Polymers* 13, 396. <https://doi.org/10.3390/polym13030396>
- Hao, C., Liu, T., Zhang, S., Brown, L., Li, R., Xin, J., Zhong, T., Jiang, L., Zhang, J., 2019. A High-Lignin-Content, Removable, and Glycol-Assisted Repairable Coating Based on Dynamic Covalent Bonds. *ChemSusChem* 12, 1049–1058. <https://doi.org/10.1002/cssc.201802615>
- Hassanian-Moghaddam, D., Asghari, N., Ahmadi, M., 2023. Circular Polyolefins: Advances toward a Sustainable Future. *Macromolecules* 56, 5679–5697. <https://doi.org/10.1021/acs.macromol.3c00872>

LISTE COMPLÈTE DES RÉFÉRENCES BIBLIOGRAPHIQUES

- Hatano, T., Shida, S., Han, L., Okuda, T., 1991. Tannins of Theaceous Plants. III. Camelliatannins A and B, Two New Complex Tannins from *Camellia japonica* L. *Chem. Pharm. Bull. (Tokyo)* 39, 876–880. <https://doi.org/10.1248/cpb.39.876>
- Hobbs, C.E., 2019. Recent Advances in Bio-Based Flame Retardant Additives for Synthetic Polymeric Materials. *Polymers* 11, 224. <https://doi.org/10.3390/polym11020224>
- Hocking, M.B., 1997. Vanillin: Synthetic Flavoring from Spent Sulfite Liquor. *J. Chem. Educ.* 74, 1055. <https://doi.org/10.1021/ed074p1055>
- Holloway, J.O., Taplan, C., Prez, F.E.D., 2022. Combining vinylogous urethane and β -amino ester chemistry for dynamic material design. *Polym. Chem.* 13, 2008–2018. <https://doi.org/10.1039/D2PY00026A>
- Hong, J., Hong, Y., Jeong, J., Oh, D., Goh, M., 2023. Robust Biobased Vitrimers and Its Application to Closed-Loop Recyclable Carbon Fiber-Reinforced Composites. *ACS Sustain. Chem. Eng.* 11, 14112–14123. <https://doi.org/10.1021/acssuschemeng.3c03468>
- Hong, K., Sun, Q., Zhang, X., Fan, L., Wu, T., Du, J., Zhu, Y., 2022. Fully Bio-Based High-Performance Thermosets with Closed-Loop Recyclability. *ACS Sustain. Chem. Eng.* 10, 1036–1046. <https://doi.org/10.1021/acssuschemeng.1c07523>
- Hopewell, J., Dvorak, R., Kosior, E., 2009. Plastics recycling: challenges and opportunities. *Philos. Trans. R. Soc. B Biol. Sci.* 364, 2115–2126. <https://doi.org/10.1098/rstb.2008.0311>
- Hoppe, C.E., Galante, M.J., Oyanguren, P.A., Williams, R.J.J., 2005. Epoxies Modified by Palmitic Acid: From Hot-Melt Adhesives to Plasticized Networks. *Macromol. Mater. Eng.* 290, 456–462. <https://doi.org/10.1002/mame.200400348>
- Howell, B.A., Daniel, Y.G., 2018. The impact of sulfur oxidation level on flame retardancy. *J. Fire Sci.* 36, 518–534. <https://doi.org/10.1177/0734904118806155>
- Huang, J., Jiang, X., 2018. Injectable and Degradable pH-Responsive Hydrogels via Spontaneous Amino–Yne Click Reaction. *ACS Appl. Mater. Interfaces* 10, 361–370. <https://doi.org/10.1021/acsami.7b18141>
- Huang, S., Kong, X., Xiong, Y., Zhang, X., Chen, H., Jiang, W., Niu, Y., Xu, W., Ren, C., 2020. An overview of dynamic covalent bonds in polymer material and their applications. *Eur. Polym. J.* 141, 110094. <https://doi.org/10.1016/j.eurpolymj.2020.110094>
- Hubbard, A.M., Ren, Y., Papaioannou, P., Sarvestani, A., Picu, C.R., Konkolewicz, D., Roy, A.K., Varshney, V., Nepal, D., 2022a. Vitriimer Composites: Understanding the Role of Filler in Vitriimer Applicability. *ACS Appl. Polym. Mater.* 4, 6374–6385. <https://doi.org/10.1021/acsapm.2c00770>
- Hubbard, A.M., Ren, Y., Picu, C.R., Sarvestani, A., Konkolewicz, D., Roy, A.K., Varshney, V., Nepal, D., 2022b. Creep Mechanics of Epoxy Vitriimer Materials. *ACS Appl. Polym. Mater.* 4, 4254–4263. <https://doi.org/10.1021/acsapm.2c00230>
- Hyatt, J.A., Feldman, P.L., Clemens, R.J., 1984. Ketenes. 20. Thermal decomposition of 2,2,6-trimethyl-4H-1,3-dioxin-4-one and 1-ethoxybutyn-3-one. *Acetylketene. J. Org. Chem.* 49, 5105–5108. <https://doi.org/10.1021/jo00200a018>
- Imbernon, L., Norvez, S., Leibler, L., 2016. Stress Relaxation and Self-Adhesion of Rubbers with Exchangeable Links. *Macromolecules* 49, 2172–2178. <https://doi.org/10.1021/acs.macromol.5b02751>
- ISO 15270, 2008. ISO 15270:2008(en), Plastics — Guidelines for the recovery and recycling of plastics waste [WWW Document]. URL <https://www.iso.org/obp/ui/en/#iso:std:iso:15270:ed-2:v1:en> (accessed 1.10.24).
- Jarach, N., Zuckerman, R., Naveh, N., Dodiuk, H., Kenig, S., 2021. Bio- and Water-Based Reversible Covalent Bonds Containing Polymers (Vitrimers) and Their Relevance to Adhesives – A Critical Review, in: *Progress in Adhesion and Adhesives*. John Wiley & Sons, Ltd, pp. 587–619. <https://doi.org/10.1002/9781119846703.ch13>
- Jehanno, C., Alty, J.W., Roosen, M., De Meester, S., Dove, A.P., Chen, E.Y.-X., Leibfarth, F.A., Sardon, H., 2022. Critical advances and future opportunities in upcycling commodity polymers. *Nature* 603, 803–814. <https://doi.org/10.1038/s41586-021-04350-0>
- Jia, P., Shi, Y., Song, F., Bei, Y., Huang, C., Zhang, M., Hu, L., Zhou, Y., 2022. Bio-based and degradable vitriimer-graphene/graphene oxide composites with self-healing ability stimulated by heat, electricity and microwave as temperature and fire warning sensors. *Compos. Sci. Technol.* 227, 109573. <https://doi.org/10.1016/j.compscitech.2022.109573>
- Jiang, L., Tian, Y., Wang, X., Zhang, J., Cheng, J., Gao, F., 2023. A fully bio-based Schiff base vitriimer with self-healing ability at room temperature. *Polym. Chem.* 14, 862–871. <https://doi.org/10.1039/D2PY00900E>
- Jiang, Q., Zhang, H., Jiang, Qilin, Zhang, S., Guan, S., Huang, W., Xue, X., Yang, H., Jiang, L., Jiang, B., Komarneni, S., 2023. Hydroxyl–yne click polymerization: a facile strategy toward poly(vinyl amino ether ester)s with color-tunable luminescence. *Polym. Chem.* 14, 1232–1240. <https://doi.org/10.1039/D2PY01581A>

LISTE COMPLÈTE DES RÉFÉRENCES BIBLIOGRAPHIQUES

- Jiang, Z., Bhaskaran, A., Aitken, H.M., Shackelford, I.C.G., Connal, L.A., 2019. Using Synergistic Multiple Dynamic Bonds to Construct Polymers with Engineered Properties. *Macromol. Rapid Commun.* 40, 1900038. <https://doi.org/10.1002/marc.201900038>
- Jin, D., Dai, J., Zhao, W., Liu, X., 2023. Biobased Epoxy Resin with Inherently Deep-UV Photodegradability for a Positive Photoresist and Anticounterfeiting. *ACS Appl. Polym. Mater.* 5, 3138–3147. <https://doi.org/10.1021/acsapm.3c00291>
- Jin, X., Li, X., Liu, X., Du, L., Su, L., Ma, Y., Ren, S., 2023. Simple lignin-based, light-driven shape memory polymers with excellent mechanical properties and wide range of glass transition temperatures. *Int. J. Biol. Macromol.* 228, 528–536. <https://doi.org/10.1016/j.ijbiomac.2022.12.098>
- J. Kloxin, C., N. Bowman, C., 2013. Covalent adaptable networks: smart, reconfigurable and responsive network systems. *Chem. Soc. Rev.* 42, 7161–7173. <https://doi.org/10.1039/C3CS60046G>
- John, G., Nagarajan, S., Vemula, P.K., Silverman, J.R., Pillai, C.K.S., 2019. Natural monomers: A mine for functional and sustainable materials – Occurrence, chemical modification and polymerization. *Prog. Polym. Sci.* 92, 158–209. <https://doi.org/10.1016/j.progpolymsci.2019.02.008>
- Johnson, R.M., Cortés-Guzmán, K.P., Perera, S.D., Parikh, A.R., Ganesh, V., Voit, W.E., Smaldone, R.A., 2023. Lignin-based covalent adaptable network resins for digital light projection 3D printing. *J. Polym. Sci.* n/a. <https://doi.org/10.1002/pol.20230026>
- Jourdain, A., Asbai, R., Anaya, O., Chehimi, M.M., Drockenmuller, E., Montarnal, D., 2020. Rheological Properties of Covalent Adaptable Networks with 1,2,3-Triazolium Cross-Links: The Missing Link between Vitrimers and Dissociative Networks. *Macromolecules* 53, 1884–1900. <https://doi.org/10.1021/acs.macromol.9b02204>
- Kaczmarek, B., 2020. Tannic Acid with Antiviral and Antibacterial Activity as A Promising Component of Biomaterials—A Minireview. *Materials* 13, 3224. <https://doi.org/10.3390/ma13143224>
- Karlinskii, B.Y., Ananikov, V.P., 2023. Recent advances in the development of green furan ring-containing polymeric materials based on renewable plant biomass. *Chem. Soc. Rev.* 52, 836–862. <https://doi.org/10.1039/D2CS00773H>
- Kasemsiri, P., Lorwanishpaisarn, N., Pongsa, U., Ando, S., 2018. Reconfigurable Shape Memory and Self-Welding Properties of Epoxy Phenolic Novolac/Cashew Nut Shell Liquid Composites Reinforced with Carbon Nanotubes. *Polymers* 10, 482. <https://doi.org/10.3390/polym10050482>
- Katritzky, A.R., Singh, S.K., Meher, N.K., Doskocz, J., Suzuki, K., Jiang, R., Sommen, G.L., Ciaramitaro, D.A., Steel, P.J., 2006. Triazole-oligomers by 1,3-dipolar cycloaddition. *Arkivoc* 2006, 43–62. <https://doi.org/10.3998/ark.5550190.0007.505>
- Kaur, G., Johnston, P., Saito, K., 2014. Photo-reversible dimerisation reactions and their applications in polymeric systems. *Polym. Chem.* 5, 2171–2186. <https://doi.org/10.1039/C3PY01234D>
- Ke, Y., Yang, X., Chen, Q., Xue, J., Song, Z., Zhang, Y., Madbouly, S.A., Luo, Y., Li, M., Wang, Q., Zhang, C., 2021. Recyclable and Fluorescent Epoxy Polymer Networks from Cardanol Via Solvent-Free Epoxy-Thiol Chemistry. *ACS Appl. Polym. Mater.* 3, 3082–3092. <https://doi.org/10.1021/acsapm.1c00284>
- Kim, H., Cha, I., Yoon, Y., Cha, B.J., Yang, J., Kim, Y.D., Song, C., 2021. Facile Mechanochemical Synthesis of Malleable Biomass-Derived Network Polyurethanes and Their Shape-Memory Applications. *ACS Sustain. Chem. Eng.* 9, 6952–6961. <https://doi.org/10.1021/acssuschemeng.1c00390>
- Kim, N.K., Cha, E.J., Jung, M., Kim, J., Jeong, G.-J., Kim, Y.S., Choi, W.J., Kim, B.-S., Kim, D.-G., Lee, J.-C., 2019. 3D hierarchical scaffolds enabled by a post-patternable, reconfigurable, and biocompatible 2D vitrimer film for tissue engineering applications. *J. Mater. Chem. B* 7, 3341–3345. <https://doi.org/10.1039/C9TB00221A>
- Kimura, K., Kohama, S., Yamazaki, S., 2006. Morphology Control of Aromatic Polymers in Concert with Polymerization. *Polym. J.* 38, 1005–1022. <https://doi.org/10.1295/polymj.PJ2006083>
- Kisszekelyi, P., Hardian, R., Vovusha, H., Chen, B., Zeng, X., Schwingenschlögl, U., Kupai, J., Szekely, G., 2020. Selective Electrocatalytic Oxidation of Biomass-Derived 5-Hydroxymethylfurfural to 2,5-Diformylfuran: from Mechanistic Investigations to Catalyst Recovery. *ChemSusChem* 13, 3127–3136. <https://doi.org/10.1002/cssc.202000453>
- Klein, F.C., Vogt, M., Abetz, V., 2023. Reprocessable Vanillin-Based Schiff Base Vitrimers: Tuning Mechanical and Thermomechanical Properties by Network Design. *Macromol. Mater. Eng.* n/a, 2300187. <https://doi.org/10.1002/mame.202300187>
- Kloxin, C.J., Scott, T.F., Adzima, B.J., Bowman, C.N., 2010. Covalent Adaptable Networks (CANs): A Unique Paradigm in Cross-Linked Polymers. *Macromolecules* 43, 2643–2653. <https://doi.org/10.1021/ma902596s>
- Konieczynska, M.D., Villa-Camacho, J.C., Ghobril, C., Perez-Viloria, M., Tevis, K.M., Blessing, W.A., Nazarian, A., Rodriguez, E.K., Grinstaff, M.W., 2016. On-Demand Dissolution of a Dendritic Hydrogel-based

LISTE COMPLÈTE DES RÉFÉRENCES BIBLIOGRAPHIQUES

- Dressing for Second-Degree Burn Wounds through Thiol–Thioester Exchange Reaction. *Angew. Chem. Int. Ed.* 55, 9984–9987. <https://doi.org/10.1002/anie.201604827>
- Konuray, O., Fernández-Francos, X., Ramis, X., 2023. Structural Design of CANs with Fine-Tunable Relaxation Properties: A Theoretical Framework Based on Network Structure and Kinetics Modeling. *Macromolecules* 56, 4855–4873. <https://doi.org/10.1021/acs.macromol.3c00482>
- Korley, L.T.J., Epps, T.H., Helms, B.A., Ryan, A.J., 2021. Toward polymer upcycling—adding value and tackling circularity. *Science* 373, 66–69. <https://doi.org/10.1126/science.abg4503>
- Košir, T., Slavič, J., 2023. Manufacturing of single-process 3D-printed piezoelectric sensors with electromagnetic protection using thermoplastic material extrusion. *Addit. Manuf.* 73, 103699. <https://doi.org/10.1016/j.addma.2023.103699>
- Kou, Z., Hu, Y., Ma, Y., Yuan, L., Hu, L., Zhou, Y., Jia, P., 2023. Bio-based dynamically crosslinked networks/Fe₃O₄ nanoparticles composites with self-healing ability driven by multiple stimuli for non-contact welding. *Ind. Crops Prod.* 195, 116401. <https://doi.org/10.1016/j.indcrop.2023.116401>
- Krall, E.M., Serum, E.M., Sibi, M.P., Webster, D.C., 2018. Catalyst-free lignin valorization by acetoacetylation. Structural elucidation by comparison with model compounds. *Green Chem.* 20, 2959–2966. <https://doi.org/10.1039/C8GC01071D>
- Krishnakumar, B., Pucci, A., Wadgaonkar, P.P., Kumar, I., Binder, W.H., Rana, S., 2022. Vitrimers based on bio-derived chemicals: Overview and future prospects. *Chem. Eng. J.* 433, 133261. <https://doi.org/10.1016/j.cej.2021.133261>
- Krishnakumar, B., Sanka, R.V.S.P., Binder, W.H., Parthasarthy, V., Rana, S., Karak, N., 2020. Vitrimers: Associative dynamic covalent adaptive networks in thermoset polymers. *Chem. Eng. J.* 385, 123820. <https://doi.org/10.1016/j.cej.2019.123820>
- K. Schoustra, S., Groeneveld, T., J. Smulders, M.M., 2021. The effect of polarity on the molecular exchange dynamics in imine-based covalent adaptable networks. *Polym. Chem.* 12, 1635–1642. <https://doi.org/10.1039/D0PY01555E>
- Kuhl, N., Bode, S., Hager, M.D., Schubert, U.S., 2015. Self-Healing Polymers Based on Reversible Covalent Bonds, in: Hager, M.D., van der Zwaag, S., Schubert, U.S. (Eds.), *Self-Healing Materials, Advances in Polymer Science*. Springer International Publishing, Cham, pp. 1–58. https://doi.org/10.1007/12_2015_336
- Kumar, A., Connal, L.A., 2023. Biobased Transesterification Vitrimers. *Macromol. Rapid Commun.* 44, 2200892. <https://doi.org/10.1002/marc.202200892>
- Lalanne, L., Nyanhongo, G.S., Guebitz, G.M., Pellis, A., 2021. Biotechnological production and high potential of furan-based renewable monomers and polymers. *Biotechnol. Adv.* 48, 107707. <https://doi.org/10.1016/j.biotechadv.2021.107707>
- Laoutid, F., Bonnaud, L., Alexandre, M., Lopez-Cuesta, J.-M., Dubois, Ph., 2009. New prospects in flame retardant polymer materials: From fundamentals to nanocomposites. *Mater. Sci. Eng. R Rep.* 63, 100–125. <https://doi.org/10.1016/j.mser.2008.09.002>
- Laurichesse, S., Avérous, L., 2014. Chemical modification of lignins: Towards biobased polymers. *Prog. Polym. Sci.* 39, 1266–1290. <https://doi.org/10.1016/j.progpolymsci.2013.11.004>
- Laurichesse, S., Huillet, C., Avérous, L., 2014. Original polyols based on organosolv lignin and fatty acids: new bio-based building blocks for segmented polyurethane synthesis. *Green Chem.* 16, 3958–3970. <https://doi.org/10.1039/C4GC00596A>
- Lawoko, M., Samec, J.S.M., 2023. Kraft lignin valorization: Biofuels and thermoset materials in focus. *Curr. Opin. Green Sustain. Chem.* 40, 100738. <https://doi.org/10.1016/j.cogsc.2022.100738>
- Lei, Z., Xing, W., Wu, J., Huang, G., Wang, X., Zhao, L., 2014. The proper glass transition temperature of amorphous polymers on dynamic mechanical spectra. *J. Therm. Anal. Calorim.* 116, 447–453. <https://doi.org/10.1007/s10973-013-3526-0>
- Leibler, L., Rubinstein, M., Colby, R.H., 1991. Dynamics of reversible networks. *Macromolecules* 24, 4701–4707. <https://doi.org/10.1021/ma00016a034>
- Lendlein, A., Jiang, H., Jünger, O., Langer, R., 2005. Light-induced shape-memory polymers. *Nature* 434, 879–882. <https://doi.org/10.1038/nature03496>
- Lessard, J.J., Garcia, L.F., Easterling, C.P., Sims, M.B., Bentz, K.C., Arencibia, S., Savin, D.A., Sumerlin, B.S., 2019a. Catalyst-Free Vitrimers from Vinyl Polymers. *Macromolecules* 52, 2105–2111. <https://doi.org/10.1021/acs.macromol.8b02477>
- Lessard, J.J., Garcia, L.F., Easterling, C.P., Sims, M.B., Bentz, K.C., Arencibia, S., Savin, D.A., Sumerlin, B.S., 2019b. Catalyst-Free Vitrimers from Vinyl Polymers. *Macromolecules* 52, 2105–2111. <https://doi.org/10.1021/acs.macromol.8b02477>

LISTE COMPLÈTE DES RÉFÉRENCES BIBLIOGRAPHIQUES

- Li, H., Zhang, B., Wang, R., Yang, X., He, X., Ye, H., Cheng, J., Yuan, C., Zhang, Y.-F., Ge, Q., 2022. Solvent-Free Upcycling Vitrimers through Digital Light Processing-Based 3D Printing and Bond Exchange Reaction. *Adv. Funct. Mater.* 32, 2111030. <https://doi.org/10.1002/adfm.202111030>
- Li, J., Weng, Z., Cao, Q., Qi, Y., Lu, B., Zhang, S., Wang, J., Jian, X., 2022. Synthesis of an aromatic amine derived from biomass and its use as a feedstock for versatile epoxy thermoset. *Chem. Eng. J.* 433, 134512. <https://doi.org/10.1016/j.cej.2022.134512>
- Li, L., Chen, X., Jin, K., Torkelson, J.M., 2018. Vitrimers Designed Both To Strongly Suppress Creep and To Recover Original Cross-Link Density after Reprocessing: Quantitative Theory and Experiments. *Macromolecules* 51, 5537–5546. <https://doi.org/10.1021/acs.macromol.8b00922>
- Li, L., Chen, X., Torkelson, J.M., 2020. Covalent Adaptive Networks for Enhanced Adhesion: Exploiting Disulfide Dynamic Chemistry and Annealing during Application. *ACS Appl. Polym. Mater.* 2, 4658–4665. <https://doi.org/10.1021/acsapm.0c00720>
- Li, Q., Ma, S., Li, P., Wang, B., Feng, H., Lu, N., Wang, S., Liu, Y., Xu, X., Zhu, J., 2021a. Biosourced Acetal and Diels–Alder Adduct Concurrent Polyurethane Covalent Adaptable Network. *Macromolecules* 54, 1742–1753. <https://doi.org/10.1021/acs.macromol.0c02699>
- Li, Q., Ma, S., Li, P., Wang, B., Yu, Z., Feng, H., Liu, Y., Zhu, J., 2021b. Fast Reprocessing of Acetal Covalent Adaptable Networks with High Performance Enabled by Neighboring Group Participation. *Macromolecules* 54, 8423–8434. <https://doi.org/10.1021/acs.macromol.1c01046>
- Li, Q., Ma, S., Wang, S., Liu, Y., Taher, M.A., Wang, B., Huang, K., Xu, X., Han, Y., Zhu, J., 2020. Green and Facile Preparation of Readily Dual-Recyclable Thermosetting Polymers with Superior Stability Based on Asymmetric Acetal. *Macromolecules* 53, 1474–1485. <https://doi.org/10.1021/acs.macromol.9b02386>
- Li, Q., Ma, S., Wang, S., Yuan, W., Xu, X., Wang, B., Huang, K., Zhu, J., 2019. Facile catalyst-free synthesis, exchanging, and hydrolysis of an acetal motif for dynamic covalent networks. *J. Mater. Chem. A* 7, 18039–18049. <https://doi.org/10.1039/C9TA04073K>
- Li, S., Li, W., Khashab, N.M., 2012. Stimuli responsive nanomaterials for controlled release applications. *Nanotechnol. Rev.* 1, 493–513. <https://doi.org/10.1515/ntrev-2012-0033>
- Li, W., Xiao, L., Wang, Y., Chen, J., Nie, X., 2021. Self-healing silicon-containing eugenol-based epoxy resin based on disulfide bond exchange: Synthesis and structure-property relationships. *Polymer* 229, 123967. <https://doi.org/10.1016/j.polymer.2021.123967>
- Li, W., Xiao, L., Wang, Y., Huang, J., Liu, Z., Chen, J., Nie, X., 2022. Thermal-induced self-healing bio-based vitrimers: Shape memory, recyclability, degradation, and intrinsic flame retardancy. *Polym. Degrad. Stab.* 202, 110039. <https://doi.org/10.1016/j.polymdegradstab.2022.110039>
- Liang, J.-Y., Shin, S.-R., Lee, S.-H., Lee, D.-S., 2019. Characteristics of Self-Healable Copolymers of Styrene and Eugenol Terminated Polyurethane Prepolymer. *Polymers* 11, 1674. <https://doi.org/10.3390/polym11101674>
- Liang, Y., Li, Z., Huang, Y., Yu, R., Guo, B., 2021. Dual-Dynamic-Bond Cross-Linked Antibacterial Adhesive Hydrogel Sealants with On-Demand Removability for Post-Wound-Closure and Infected Wound Healing. *ACS Nano* 15, 7078–7093. <https://doi.org/10.1021/acs.nano.1c00204>
- Liguori, A., Hakkarainen, M., 2022. Designed from Biobased Materials for Recycling: Imine-Based Covalent Adaptable Networks. *Macromol. Rapid Commun.* 43, 2100816. <https://doi.org/10.1002/marc.202100816>
- Lijsebetten, F.V., Bruycker, K.D., Ruymbeke, E.V., M. Winne, J., Prez, F.E.D., 2022. Characterising different molecular landscapes in dynamic covalent networks. *Chem. Sci.* 13, 12865–12875. <https://doi.org/10.1039/D2SC05528G>
- Lin, X., Gablier, A., Terentjev, E.M., 2022. Imine-Based Reactive Mesogen and Its Corresponding Exchangeable Liquid Crystal Elastomer. *Macromolecules* 55, 821–830. <https://doi.org/10.1021/acs.macromol.1c02432>
- Lin, Y., Yan, R., Zhang, Y., Yang, X., Ding, H., Xu, L., Li, S., Li, M., 2022. Synthesis of biobased polyphenols for preparing phenolic polyurethanes with self-healing properties. *Polym. Test.* 112, 107644. <https://doi.org/10.1016/j.polymertesting.2022.107644>
- Liu, H., Cheng, T., Xian, M., Cao, Y., Fang, F., Zou, H., 2014. Fatty acid from the renewable sources: A promising feedstock for the production of biofuels and biobased chemicals. *Biotechnol. Adv.* 32, 382–389. <https://doi.org/10.1016/j.biotechadv.2013.12.003>
- Liu, H., Sui, X., Xu, H., Zhang, L., Zhong, Y., Mao, Z., 2016. Self-Healing Polysaccharide Hydrogel Based on Dynamic Covalent Enamine Bonds. *Macromol. Mater. Eng.* 301, 725–732. <https://doi.org/10.1002/mame.201600042>
- Liu, J., Li, J.-J., Luo, Z.-H., Zhou, Y.-N., 2022. Mapping crosslinking reaction–structure–property relationship in polyether-based vinylogous urethane vitrimers. *AIChE J.* 68, e17587. <https://doi.org/10.1002/aic.17587>
- Liu, J., Miao, P., Leng, X., Che, J., Wei, Z., Li, Y., 2023. Chemically Recyclable Biobased Non-Isocyanate Polyurethane Networks from CO₂-Derived Six-membered Cyclic Carbonates. *Macromol. Rapid Commun.* 44, 2300263. <https://doi.org/10.1002/marc.202300263>

LISTE COMPLÈTE DES RÉFÉRENCES BIBLIOGRAPHIQUES

- Liu, J., Pich, A., Bernaerts, K.V., 2024. Preparation of lignin-based vinylogous urethane vitrimer materials and their potential use as on-demand removable adhesives. *Green Chem.* <https://doi.org/10.1039/D3GC02799F>
- Liu, T., Hao, C., Wang, L., Li, Y., Liu, W., Xin, J., Zhang, J., 2017. Eugenol-Derived Biobased Epoxy: Shape Memory, Repairing, and Recyclability. *Macromolecules* 50, 8588–8597. <https://doi.org/10.1021/acs.macromol.7b01889>
- Liu, T., Hao, C., Zhang, S., Yang, X., Wang, L., Han, J., Li, Y., Xin, J., Zhang, J., 2018. A Self-Healable High Glass Transition Temperature Bioepoxy Material Based on Vitrimer Chemistry. *Macromolecules* 51, 5577–5585. <https://doi.org/10.1021/acs.macromol.8b01010>
- Liu, T., Peng, J., Liu, J., Hao, X., Guo, C., Ou, R., Liu, Z., Wang, Q., 2021. Fully recyclable, flame-retardant and high-performance carbon fiber composites based on vanillin-terminated cyclophosphazene polyimine thermosets. *Compos. Part B Eng.* 224, 109188. <https://doi.org/10.1016/j.compositesb.2021.109188>
- Liu, W., Fang, C., Chen, F., Qiu, X., 2020. Strong, Reusable, and Self-Healing Lignin-Containing Polyurea Adhesives. *ChemSusChem* 13, 4691–4701. <https://doi.org/10.1002/cssc.202001602>
- Liu, W., Fang, C., Wang, S., Huang, J., Qiu, X., 2019. High-Performance Lignin-Containing Polyurethane Elastomers with Dynamic Covalent Polymer Networks. *Macromolecules* 52, 6474–6484. <https://doi.org/10.1021/acs.macromol.9b01413>
- Liu, W., Yang, S., Huang, L., Xu, J., Zhao, N., 2022. Dynamic covalent polymers enabled by reversible isocyanate chemistry. *Chem. Commun.* 58, 12399–12417. <https://doi.org/10.1039/D2CC04747K>
- Liu, W.-X., Zhang, C., Zhang, H., Zhao, N., Yu, Z.-X., Xu, J., 2017. Oxime-Based and Catalyst-Free Dynamic Covalent Polyurethanes. *J. Am. Chem. Soc.* 139, 8678–8684. <https://doi.org/10.1021/jacs.7b03967>
- Liu, X., Zhang, E., Feng, Z., Liu, J., Chen, B., Liang, L., 2021. Degradable bio-based epoxy vitrimers based on imine chemistry and their application in recyclable carbon fiber composites. *J. Mater. Sci.* 56, 15733–15751. <https://doi.org/10.1007/s10853-021-06291-5>
- Liu, Y., Yu, Z., Wang, B., Li, P., Zhu, J., Ma, S., 2022. Closed-loop chemical recycling of thermosetting polymers and their applications: a review. *Green Chem.* 24, 5691–5708. <https://doi.org/10.1039/D2GC00368F>
- Liu, Y., Zhang, Z., Fan, W., Yang, K., Li, Z., 2022. Preparation of renewable gallic acid-based self-healing waterborne polyurethane with dynamic phenol–carbamate network: toward superior mechanical properties and shape memory function. *J. Mater. Sci.* 57, 5679–5696. <https://doi.org/10.1007/s10853-022-07000-6>
- Liu, Y., Zhang, Z., Wang, J., Xie, T., Sun, L., Yang, K., Li, Z., 2021. Renewable tannic acid based self-healing polyurethane with dynamic phenol-carbamate network: Simultaneously showing robust mechanical properties, reprocessing ability and shape memory. *Polymer* 228, 123860. <https://doi.org/10.1016/j.polymer.2021.123860>
- Liu, Y.-L., Chuo, T.-W., 2013. Self-healing polymers based on thermally reversible Diels–Alder chemistry. *Polym. Chem.* 4, 2194–2205. <https://doi.org/10.1039/C2PY20957H>
- Liu, Y.-Y., He, J., Li, Y.-D., Zhao, X.-L., Zeng, J.-B., 2020. Biobased epoxy vitrimer from epoxidized soybean oil for reprocessable and recyclable carbon fiber reinforced composite. *Compos. Commun.* 22, 100445. <https://doi.org/10.1016/j.coco.2020.100445>
- Liu, Y.-Y., Liu, G.-L., Li, Y.-D., Weng, Y., Zeng, J.-B., 2021. Biobased High-Performance Epoxy Vitrimer with UV Shielding for Recyclable Carbon Fiber Reinforced Composites. *ACS Sustain. Chem. Eng.* 9, 4638–4647. <https://doi.org/10.1021/acssuschemeng.1c00231>
- Liu, Z., Zhang, C., Shi, Z., Yin, J., Tian, M., 2018. Tailoring vinylogous urethane chemistry for the cross-linked polybutadiene: Wide freedom design, multiple recycling methods, good shape memory behavior. *Polymer* 148, 202–210. <https://doi.org/10.1016/j.polymer.2018.06.042>
- Llevot, A., Grau, E., Carlotti, S., Grelier, S., Cramail, H., 2016. From Lignin-derived Aromatic Compounds to Novel Biobased Polymers. *Macromol. Rapid Commun.* 37, 9–28. <https://doi.org/10.1002/marc.201500474>
- Lochab, B., Shukla, S., Varma, I.K., 2014. Naturally occurring phenolic sources: monomers and polymers. *RSC Adv.* 4, 21712–21752. <https://doi.org/10.1039/C4RA00181H>
- Lora, J.H., Glasser, W.G., 2002. Recent industrial applications of lignin: a sustainable alternative to nonrenewable materials. *J. Polym. Environ.* 10, 39–48.
- Lorwanishpaisarn, N., Kasemsiri, P., Srikhao, N., Son, C., Kim, S., Theerakulpisut, S., Chindaprasirt, P., 2021. Carbon fiber/epoxy vitrimer composite patch cured with bio-based curing agents for one-step repair metallic sheet and its recyclability. *J. Appl. Polym. Sci.* 138, 51406. <https://doi.org/10.1002/app.51406>
- Lorwanishpaisarn, N., Srikhao, N., Jetsrisuparb, K., Knijnenburg, J.T.N., Theerakulpisut, S., Okhawilai, M., Kasemsiri, P., 2022. Self-healing Ability of Epoxy Vitrimer Nanocomposites Containing Bio-Based Curing Agents and Carbon Nanotubes for Corrosion Protection. *J. Polym. Environ.* 30, 472–482. <https://doi.org/10.1007/s10924-021-02213-3>

LISTE COMPLÈTE DES RÉFÉRENCES BIBLIOGRAPHIQUES

- Lucherelli, M.A., Duval, A., Averous, L., 2023. Combining Associative and Dissociative Dynamic Linkages in Covalent Adaptable Networks from Biobased 2,5-Furandicarboxaldehyde. *ACS Sustain. Chem. Eng.* 11, 2334–2344. <https://doi.org/10.1021/acssuschemeng.2c05956>
- Lucherelli, M.A., Duval, A., Avérous, L., 2022. Biobased vitrimers: Towards sustainable and adaptable performing polymer materials. *Prog. Polym. Sci.* 127, 101515. <https://doi.org/10.1016/j.progpolymsci.2022.101515>
- Lucintel, 2021. Management Consulting, Market Research Company, Market Research Firms [WWW Document], 2021. URL <https://www.lucintel.com/press/eugenol-market.aspx> (accessed 7.21.23).
- Ludmila, H., Michal, J., Andrea, Š., Aleš, H., 2015. LIGNIN, POTENTIAL PRODUCTS AND THEIR MARKET. *Wood Res.* 60, 973–986.
- Luo, W., Yu, H., Liu, Z., Ou, R., Guo, C., Tao liu, Zhang, J., 2022. Construction and application of hybrid covalent adaptive network with non-conjugated fluorescence, self-healing and Fe³⁺ ion sensing. *J. Mater. Res. Technol.* 19, 1699–1710. <https://doi.org/10.1016/j.jmrt.2022.05.157>
- Ma, X., Li, S., Wang, F., Wu, J., Chao, Y., Chen, X., Chen, P., Zhu, J., Yan, N., Chen, J., 2023a. Catalyst-Free Synthesis of Covalent Adaptable Network (CAN) Polyurethanes from Lignin with Editable Shape Memory Properties. *ChemSusChem* 16, e202202071. <https://doi.org/10.1002/cssc.202202071>
- Ma, X., Wang, X., Zhao, H., Xu, X., Cui, M., Stott, N.E., Chen, P., Zhu, J., Yan, N., Chen, J., 2023b. High-Performance, Light-Stimulation Healable, and Closed-Loop Recyclable Lignin-Based Covalent Adaptable Networks. *Small* 19, 2303215. <https://doi.org/10.1002/smll.202303215>
- Ma, Y., Jiang, X., Shi, Z., Berrocal, J.A., Weder, C., 2023. Closed-Loop Recycling of Vinylogous Urethane Vitrimers. *Angew. Chem. Int. Ed.* 62, e202306188. <https://doi.org/10.1002/anie.202306188>
- Mahajan, J.S., O’Dea, R.M., Norris, J.B., Korley, L.T.J., Epps, T.H., 2020. Aromatics from Lignocellulosic Biomass: A Platform for High-Performance Thermosets. *ACS Sustain. Chem. Eng.* 8, 15072–15096. <https://doi.org/10.1021/acssuschemeng.0c04817>
- Maity, A., Chen, J., Wilson-Faubert, N., Laventure, A., Nazemi, A., 2024. Harnessing Activated Alkyne-Hydroxyl “Click” Chemistry for Degradable and Self-Healing Poly(urea vinyl ether ester)s. *Macromolecules* 57, 305–316. <https://doi.org/10.1021/acs.macromol.3c01574>
- Manarin, E., Da Via, F., Rigatelli, B., Turri, S., Griffini, G., 2023. Bio-Based Vitrimers from 2,5-Furandicarboxylic Acid as Repairable, Reusable, and Recyclable Epoxy Systems. *ACS Appl. Polym. Mater.* 5, 828–838. <https://doi.org/10.1021/acscam.2c01774>
- Mao Png, Z., Zheng, J., Kamarulzaman, S., Wang, S., Li, Z., S. Goh, S., 2023. Correction: Fully biomass-derived vitrimeric material with water-mediated recyclability and monomer recovery. *Green Chem.* 25, 789–790. <https://doi.org/10.1039/D2GC90119F>
- Marcos Celada, L., Martín, J., Dvinskikh, S.V., Olsén, P., 2024. Fully Bio-Based Ionic Liquids for Green Chemical Modification of Cellulose in the Activated-State. *ChemSusChem* 17, e202301233. <https://doi.org/10.1002/cssc.202301233>
- Martins, M.L., Zhao, X., Demchuk, Z., Luo, J., Carden, G.P., Toletay, G., Sokolov, A.P., 2023. Viscoelasticity of Polymers with Dynamic Covalent Bonds: Concepts and Misconceptions. *Macromolecules* 56, 8688–8696. <https://doi.org/10.1021/acs.macromol.3c01545>
- Mather, B.D., Viswanathan, K., Miller, K.M., Long, T.E., 2006. Michael addition reactions in macromolecular design for emerging technologies. *Prog. Polym. Sci.* 31, 487–531. <https://doi.org/10.1016/j.progpolymsci.2006.03.001>
- Mauro, C.D., Genua, A., Mija, A., 2020. Building thermally and chemically reversible covalent bonds in vegetable oil based epoxy thermosets. Influence of epoxy-hardener ratio in promoting recyclability. *Mater. Adv.* 1, 1788–1798. <https://doi.org/10.1039/D0MA00370K>
- McBride, M.K., Worrell, B.T., Brown, T., Cox, L.M., Sowan, N., Wang, C., Podgorski, M., Martinez, A.M., Bowman, C.N., 2019. Enabling Applications of Covalent Adaptable Networks. *Annu. Rev. Chem. Biomol. Eng.* 10, 175–198. <https://doi.org/10.1146/annurev-chembioeng-060718-030217>
- Memon, H., Wei, Y., Zhang, L., Jiang, Q., Liu, W., 2020. An imine-containing epoxy vitrimer with versatile recyclability and its application in fully recyclable carbon fiber reinforced composites. *Compos. Sci. Technol.* 199, 108314. <https://doi.org/10.1016/j.compscitech.2020.108314>
- Meng, X., Crestini, C., Ben, H., Hao, N., Pu, Y., Ragauskas, A.J., Argyropoulos, D.S., 2019. Determination of hydroxyl groups in biorefinery resources via quantitative ³¹P NMR spectroscopy. *Nat. Protoc.* 14, 2627–2647. <https://doi.org/10.1038/s41596-019-0191-1>
- Merino, D.H., Feula, A., Melia, K., Slark, A.T., Giannakopoulos, I., Siviour, C.R., Buckley, C.P., Greenland, B.W., Liu, D., Gan, Y., Harris, P.J., Chippindale, A.M., Hamley, I.W., Hayes, W., 2016. A systematic study of the effect of the hard end-group composition on the microphase separation, thermal and mechanical

LISTE COMPLÈTE DES RÉFÉRENCES BIBLIOGRAPHIQUES

- properties of supramolecular polyurethanes. *Polymer, Self-Assembly* 107, 368–378. <https://doi.org/10.1016/j.polymer.2016.07.029>
- Meunier, F.C., Domokos, L., Seshan, K., Lercher, J.A., 2002. *In Situ* IR Study of the Nature and Mobility of Sorbed Species on H-FER during But-1-ene Isomerization. *J. Catal.* 211, 366–378. <https://doi.org/10.1006/jcat.2002.3703>
- Mgaya, J., Shombe, G.B., Masikane, S.C., Mlowe, S., Mubofu, E.B., Revaprasadu, N., 2019. Cashew nut shell: a potential bio-resource for the production of bio-sourced chemicals, materials and fuels. *Green Chem.* 21, 1186–1201. <https://doi.org/10.1039/C8GC02972E>
- Miao, J.-T., Ge, M., Wu, Y., Chou, T.Y., Wang, H., Zheng, L., Wu, L., 2020. Eugenol-derived reconfigurable high-performance epoxy resin for self-deployable smart 3D structures. *Eur. Polym. J.* 134, 109805. <https://doi.org/10.1016/j.eurpolymj.2020.109805>
- Mo, J., Dai, Y., Zhang, C., Zhou, Y., Li, W., Song, Y., Wu, C., Wang, Z., 2021. Design of ultra-stretchable, highly adhesive and self-healable hydrogels via tannic acid-enabled dynamic interactions. *Mater. Horiz.* 8, 3409–3416. <https://doi.org/10.1039/D1MH01324F>
- Molina-Gutiérrez, S., Ladmiral, V., Bongiovanni, R., Caillol, S., Lacroix-Desmazes, P., 2019. Emulsion Polymerization of Dihydroeugenol-, Eugenol-, and Isoeugenol-Derived Methacrylates. *Ind. Eng. Chem. Res.* 58, 21155–21164. <https://doi.org/10.1021/acs.iecr.9b02338>
- Montanari, E., Gennari, A., Pelliccia, M., Gourmel, C., Lallana, E., Matricardi, P., McBain, A.J., Tirelli, N., 2016. Hyaluronan/Tannic Acid Nanoparticles Via Catechol/Boronate Complexation as a Smart Antibacterial System. *Macromol. Biosci.* 16, 1815–1823. <https://doi.org/10.1002/mabi.201600311>
- Montarnal, D., Capelot, M., Tournilhac, F., Leibler, L., 2011a. Silica-Like Malleable Materials from Permanent Organic Networks. *Science* 334, 965–968. <https://doi.org/10.1126/science.1212648>
- Montarnal, D., Capelot, M., Tournilhac, F., Leibler, L., 2011b. Silica-Like Malleable Materials from Permanent Organic Networks. *Science* 334, 965–968. <https://doi.org/10.1126/science.1212648>
- Mora, A.-S., Tayouo, R., Boutevin, B., David, G., Caillol, S., 2020. A perspective approach on the amine reactivity and the hydrogen bonds effect on epoxy-amine systems. *Eur. Polym. J.* 123, 109460. <https://doi.org/10.1016/j.eurpolymj.2019.109460>
- Morales-Cerrada, R., Molina-Gutierrez, S., Lacroix-Desmazes, P., Caillol, S., 2021. Eugenol, a Promising Building Block for Biobased Polymers with Cutting-Edge Properties. *Biomacromolecules* 22, 3625–3648. <https://doi.org/10.1021/acs.biomac.1c00837>
- More, A., Elder, T., Pajer, N., Argyropoulos, D.S., Jiang, Z., 2023. Novel and Integrated Process for the Valorization of Kraft Lignin to Produce Lignin-Containing Vitrimers. *ACS Omega* 8, 1097–1108. <https://doi.org/10.1021/acsomega.2c06445>
- Moreau, C., Belgacem, M.N., Gandini, A., 2004. Recent Catalytic Advances in the Chemistry of Substituted Furans from Carbohydrates and in the Ensuing Polymers. *Top. Catal.* 27, 11–30. <https://doi.org/10.1023/B:TOCA.0000013537.13540.0e>
- Moreno, A., Morsali, M., Sipponen, M.H., 2021. Catalyst-Free Synthesis of Lignin Vitrimers with Tunable Mechanical Properties: Circular Polymers and Recoverable Adhesives. *ACS Appl. Mater. Interfaces* 13, 57952–57961. <https://doi.org/10.1021/acsami.1c17412>
- Morinval, A., Averous, L., 2022. Systems Based on Biobased Thermoplastics: From Bioresources to Biodegradable Packaging Applications. *Polym. Rev.* 62, 653–721. <https://doi.org/10.1080/15583724.2021.2012802>
- Mouren, A., Avérous, L., 2023. Sustainable cycloaliphatic polyurethanes: from synthesis to applications. *Chem. Soc. Rev.* 52, 277–317. <https://doi.org/10.1039/D2CS00509C>
- M. Sridhar, L., O. Oster, M., E. Herr, D., D. Gregg, J.B., A. Wilson, J., T. Slark, A., 2020. Re-usable thermally reversible crosslinked adhesives from robust polyester and poly(ester urethane) Diels–Alder networks. *Green Chem.* 22, 8669–8679. <https://doi.org/10.1039/D0GC02938F>
- Mubofu, E.B., Mgaya, J.E., 2018. Chemical Valorization of Cashew Nut Shell Waste. *Top. Curr. Chem.* 376, 8. <https://doi.org/10.1007/s41061-017-0177-9>
- Murphy, J.C., Watson, E.S., Harland, E.C., 1983. Toxicology evaluation of poison oak urushiol and its esterified derivative. *Toxicology* 26, 135–142. [https://doi.org/10.1016/0300-483X\(83\)90064-1](https://doi.org/10.1016/0300-483X(83)90064-1)
- Nabipour, H., Wang, X., Kandola, B., Song, L., Kan, Y., Chen, J., Hu, Y., 2023. A bio-based intrinsically flame-retardant epoxy vitrimer from furan derivatives and its application in recyclable carbon fiber composites. *Polym. Degrad. Stab.* 207, 110206. <https://doi.org/10.1016/j.polymdegradstab.2022.110206>
- Naderi Kalali, E., Lotfian, S., Entezar Shabestari, M., Khayatzaeh, S., Zhao, C., Yazdani Nezhad, H., 2023. A critical review of the current progress of plastic waste recycling technology in structural materials. *Curr. Opin. Green Sustain. Chem.* 40, 100763. <https://doi.org/10.1016/j.cogsc.2023.100763>

LISTE COMPLÈTE DES RÉFÉRENCES BIBLIOGRAPHIQUES

- Nagane, S.S., Kuhire, S.S., Mane, S.R., Wadgaonkar, P.P., 2019. Partially bio-based aromatic poly(ether sulfone)s bearing pendant furyl groups: synthesis, characterization and thermo-reversible cross-linking with a bismaleimide. *Polym. Chem.* 10, 1089–1098. <https://doi.org/10.1039/C8PY01477A>
- Nagasaka, R., Chotimarkorn, C., Shafiqul, I.Md., Hori, M., Ozaki, H., Ushio, H., 2007. Anti-inflammatory effects of hydroxycinnamic acid derivatives. *Biochem. Biophys. Res. Commun.* 358, 615–619. <https://doi.org/10.1016/j.bbrc.2007.04.178>
- Nasar, A.S., Shrinivas, V., Shanmugam, T., Raghavan, A., 2004. Synthesis and deblocking of cardanol- and anacardate-blocked toluene diisocyanates. *J. Polym. Sci. Part Polym. Chem.* 42, 4047–4055. <https://doi.org/10.1002/pola.20211>
- Nicolaÿ, R., Kamada, J., Van Wassen, A., Matyjaszewski, K., 2010. Responsive Gels Based on a Dynamic Covalent Trithiocarbonate Cross-Linker. *Macromolecules* 43, 4355–4361. <https://doi.org/10.1021/ma100378r>
- Nie, J., Xie, J., Liu, H., 2013. Activated carbon-supported ruthenium as an efficient catalyst for selective aerobic oxidation of 5-hydroxymethylfurfural to 2,5-diformylfuran. *Chin. J. Catal.* 34, 871–875. [https://doi.org/10.1016/S1872-2067\(12\)60551-8](https://doi.org/10.1016/S1872-2067(12)60551-8)
- Nishimura, Y., Chung, J., Muradyan, H., Guan, Z., 2017. Silyl Ether as a Robust and Thermally Stable Dynamic Covalent Motif for Malleable Polymer Design. *J. Am. Chem. Soc.* 139, 14881–14884. <https://doi.org/10.1021/jacs.7b08826>
- Nishiyabu, R., Kubo, Y., James, T.D., Fossey, J.S., 2011. Boronic acid building blocks: tools for self assembly. *Chem. Commun.* 47, 1124–1150. <https://doi.org/10.1039/C0CC02921A>
- Ocando, C., Ecochard, Y., Decostanzi, M., Caillol, S., Avérous, L., 2020. Dynamic network based on eugenol-derived epoxy as promising sustainable thermoset materials. *Eur. Polym. J.* 135, 109860. <https://doi.org/10.1016/j.eurpolymj.2020.109860>
- Ochoa-Gómez, J.R., Gómez-Jiménez-Aberasturi, O., Maestro-Madurga, B., Pesquera-Rodríguez, A., Ramírez-López, C., Lorenzo-Ibarreta, L., Torrecilla-Soria, J., Villarán-Velasco, M.C., 2009. Synthesis of glycerol carbonate from glycerol and dimethyl carbonate by transesterification: Catalyst screening and reaction optimization. *Appl. Catal. Gen.* 366, 315–324. <https://doi.org/10.1016/j.apcata.2009.07.020>
- Offenbach, J.A., Tobolsky, A.V., 1956. Chemical relaxation of stress in polyurethane elastomers. *J. Colloid Sci.* 11, 39–47. [https://doi.org/10.1016/0095-8522\(56\)90017-4](https://doi.org/10.1016/0095-8522(56)90017-4)
- Oh, Y., Lee, K.M., Jung, D., Chae, J.A., Kim, H.J., Chang, M., Park, J.-J., Kim, H., 2019. Sustainable, Naringenin-Based Thermosets Show Reversible Macroscopic Shape Changes and Enable Modular Recycling. *ACS Macro Lett.* 8, 239–244. <https://doi.org/10.1021/acsmacrolett.9b00008>
- Organization for Economic Co-operation and Development, 2022. Global plastics outlook: economic drivers, environmental impacts and policy options. OECD publishing.
- Osthoﬀ, R.C., Bueche, A.M., Grubb, W.T., 1954. Chemical Stress-Relaxation of Polydimethylsiloxane Elastomers ¹. *J. Am. Chem. Soc.* 76, 4659–4663. <https://doi.org/10.1021/ja01647a052>
- Pagliari, M., Albanese, L., Scurria, A., Zabini, F., Meneguzzo, F., Ciriminna, R., 2021. Tannin: a new insight into a key product for the bioeconomy in forest regions. *Biofuels Bioprod. Biorefining* 15, 973–979. <https://doi.org/10.1002/bbb.2217>
- Palmese, G.R., McCullough, R.L., 1992. Effect of epoxy–amine stoichiometry on cured resin material properties. *J. Appl. Polym. Sci.* 46, 1863–1873. <https://doi.org/10.1002/app.1992.070461018>
- Pan, X., Sengupta, P., Webster, D.C., 2011. High Biobased Content Epoxy–Anhydride Thermosets from Epoxidized Sucrose Esters of Fatty Acids. *Biomacromolecules* 12, 2416–2428. <https://doi.org/10.1021/bm200549c>
- Pascault, J.-P., Williams, R.J.J., 2018. Chapter 1 - Overview of thermosets: Present and future, in: Guo, Q. (Ed.), *Thermosets (Second Edition)*. Elsevier, pp. 3–34. <https://doi.org/10.1016/B978-0-08-101021-1.00001-0>
- Patel, V.R., Dumancas, G.G., Viswanath, L.C.K., Maples, R., Subong, B.J.J., 2016. Castor Oil: Properties, Uses, and Optimization of Processing Parameters in Commercial Production. *Lipid Insights* 9, LPI.S40233. <https://doi.org/10.4137/LPI.S40233>
- Pelckmans, M., Renders, T., Vyver, S.V. de, Sels, B.F., 2017. Bio-based amines through sustainable heterogeneous catalysis. *Green Chem.* 19, 5303–5331. <https://doi.org/10.1039/C7GC02299A>
- Pemba, A.G., Miller, S.A., 2019. Acetal Metathesis: Mechanistic Insight. *Synlett* 30, 1971–1976. <https://doi.org/10.1055/s-0037-1611833>
- Peng, J., Xie, S., Liu, T., Wang, D., Ou, R., Guo, C., Wang, Q., Liu, Z., 2022. High-performance epoxy vitrimer with superior self-healing, shape-memory, flame retardancy, and antibacterial properties based on multifunctional curing agent. *Compos. Part B Eng.* 242, 110109. <https://doi.org/10.1016/j.compositesb.2022.110109>

LISTE COMPLÈTE DES RÉFÉRENCES BIBLIOGRAPHIQUES

- Perego, A., Lazarenko, D., Cloitre, M., Khabaz, F., 2022. Microscopic Dynamics and Viscoelasticity of Vitrimers. *Macromolecules* 55, 7605–7613. <https://doi.org/10.1021/acs.macromol.2c00588>
- Peters, E.N., 2017. 1 - Engineering Thermoplastics—Materials, Properties, Trends, in: Kutz, M. (Ed.), *Applied Plastics Engineering Handbook (Second Edition)*, Plastics Design Library. William Andrew Publishing, pp. 3–26. <https://doi.org/10.1016/B978-0-323-39040-8.00001-8>
- Phani Kumar, P., Paramashivappa, R., Vithayathil, P.J., Subba Rao, P.V., Srinivasa Rao, A., 2002. Process for Isolation of Cardanol from Technical Cashew (*Anacardium occidentale* L.) Nut Shell Liquid. *J. Agric. Food Chem.* 50, 4705–4708. <https://doi.org/10.1021/jf020224w>
- Picinelli, A., Dapena, E., Mangas, J.J., 1995. Polyphenolic Pattern in Apple Tree Leaves in Relation to Scab Resistance. A Preliminary Study. *J. Agric. Food Chem.* 43, 2273–2278. <https://doi.org/10.1021/jf00056a057>
- Pickering, S.J., 2006. Recycling technologies for thermoset composite materials—current status. *Compos. Part Appl. Sci. Manuf.*, The 2nd International Conference: Advanced Polymer Composites for Structural Applications in Construction 37, 1206–1215. <https://doi.org/10.1016/j.compositesa.2005.05.030>
- Pinto, O., Romero, R., Carrier, M., Appelt, J., Segura, C., 2018. Fast pyrolysis of tannins from pine bark as a renewable source of catechols. *J. Anal. Appl. Pyrolysis* 136, 69–76. <https://doi.org/10.1016/j.jaap.2018.10.022>
- Pire, M., Norvez, S., Iliopoulos, I., Le Rossignol, B., Leibler, L., 2010. Epoxidized natural rubber/dicarboxylic acid self-vulcanized blends. *Polymer* 51, 5903–5909. <https://doi.org/10.1016/j.polymer.2010.10.023>
- Pizzi, A., 2019. Tannins: Prospectives and Actual Industrial Applications. *Biomolecules* 9, 344. <https://doi.org/10.3390/biom9080344>
- Pizzi, A., Daling, G.M.E., 1980. Laminating wood adhesives by generation of resorcinol from tannin extracts. *J. Appl. Polym. Sci.* 25, 1039–1048. <https://doi.org/10.1002/app.1980.070250606>
- Plastics Europe, 2022. *Plastics - the facts 2022*. Plast. Eur. FR. URL <https://plasticseurope.org/fr/knowledge-hub/plastics-the-facts-2022/> (accessed 4.23.24).
- Png, Z.M., Zheng, J., Kamarulzaman, S., Wang, S., Li, Z., Goh, S.S., 2022. Fully biomass-derived vitrimeric material with water-mediated recyclability and monomer recovery. *Green Chem.* 24, 5978–5986. <https://doi.org/10.1039/D2GC01556K>
- Poplata, S., Tröster, A., Zou, Y.-Q., Bach, T., 2016. Recent Advances in the Synthesis of Cyclobutanes by Olefin [2 + 2] Photocycloaddition Reactions. *Chem. Rev.* 116, 9748–9815. <https://doi.org/10.1021/acs.chemrev.5b00723>
- Popp, J., Kovács, S., Oláh, J., Divéki, Z., Balázs, E., 2021. Bioeconomy: Biomass and biomass-based energy supply and demand. *New Biotechnol.* 60, 76–84. <https://doi.org/10.1016/j.nbt.2020.10.004>
- Porath, L., Huang, J., Ramlawi, N., Derkaloustian, M., Ewoldt, R.H., Evans, C.M., 2022. Relaxation of Vitrimers with Kinetically Distinct Mixed Dynamic Bonds. *Macromolecules* 55, 4450–4458. <https://doi.org/10.1021/acs.macromol.1c02613>
- Porath, L.E., Evans, C.M., 2021. Importance of Broad Temperature Windows and Multiple Rheological Approaches for Probing Viscoelasticity and Entropic Elasticity in Vitrimers. *Macromolecules* 54, 4782–4791. <https://doi.org/10.1021/acs.macromol.0c02800>
- Post, W., Susa, A., Blaauw, R., Molenveld, K., Knoop, R.J.I., 2020. A Review on the Potential and Limitations of Recyclable Thermosets for Structural Applications. *Polym. Rev.* 60, 359–388. <https://doi.org/10.1080/15583724.2019.1673406>
- Pu, Y., Cao, S., Ragauskas, A.J., 2011. Application of quantitative ³¹P NMR in biomass lignin and biofuel precursors characterization. *Energy Environ. Sci.* 4, 3154–3166. <https://doi.org/10.1039/C1EE01201K>
- Purwanto, N.S., Chen, Y., Torkelson, J.M., 2023. Reprocessable, Bio-Based, Self-Blowing Non-Isocyanate Polyurethane Network Foams from Cashew Nutshell Liquid. *ACS Appl. Polym. Mater.* 5, 6651–6661. <https://doi.org/10.1021/acsapm.3c01196>
- Qiu, J., Ma, S., Wang, S., Tang, Z., Li, Q., Tian, A., Xu, X., Wang, B., Lu, N., Zhu, J., 2021. Upcycling of Polyethylene Terephthalate to Continuously Reprocessable Vitrimers through Reactive Extrusion. *Macromolecules* 54, 703–712. <https://doi.org/10.1021/acs.macromol.0c02359>
- Quienne, B., Kasmi, N., Dieden, R., Caillol, S., Habibi, Y., 2020. Isocyanate-Free Fully Biobased Star Polyester-Urethanes: Synthesis and Thermal Properties. *Biomacromolecules* 21, 1943–1951. <https://doi.org/10.1021/acs.biomac.0c00156>
- Ragaert, K., Ragot, C., Van Geem, K.M., Kersten, S., Shiran, Y., De Meester, S., 2023. Clarifying European terminology in plastics recycling. *Curr. Opin. Green Sustain. Chem.* 44, 100871. <https://doi.org/10.1016/j.cogsc.2023.100871>
- Ralph, J., Lundquist, K., Brunow, G., Lu, F., Kim, H., Schatz, P.F., Marita, J.M., Hatfield, R.D., Ralph, S.A., Christensen, J.H., Boerjan, W., 2004. Lignins: Natural polymers from oxidative coupling of 4-

LISTE COMPLÈTE DES RÉFÉRENCES BIBLIOGRAPHIQUES

- hydroxyphenyl- propanoids. *Phytochem. Rev.* 3, 29–60. <https://doi.org/10.1023/B:PHYT.0000047809.65444.a4>
- Raquez, J.-M., Deléglise, M., Lacrampe, M.-F., Krawczak, P., 2010. Thermosetting (bio)materials derived from renewable resources: A critical review. *Prog. Polym. Sci., Topical Issue on Biomaterials* 35, 487–509. <https://doi.org/10.1016/j.progpolymsci.2010.01.001>
- Rashid, M.A., Dayan, Md.A.R., Jiang, Q., Wei, Y., Liu, W., 2023. Optimizing mechanical and thermomechanical properties of the self-healable and recyclable biobased epoxy thermosets. *J. Polym. Res.* 30, 70. <https://doi.org/10.1007/s10965-023-03456-5>
- Rashid, M.A., Hasan, M.N., Dayan, M.A.R., Ibna Jamal, M.S., Patoary, M.K., 2023. A Critical Review of Sustainable Vanillin-modified Vitrimers: Synthesis, Challenge and Prospects. *Reactions* 4, 66–91. <https://doi.org/10.3390/reactions4010003>
- Rashid, M.A., Zhu, S., Jiang, Q., Wei, Y., Liu, W., 2023. Developing Easy Processable, Recyclable, and Self-Healable Biobased Epoxy Resin through Dynamic Covalent Imine Bonds. *ACS Appl. Polym. Mater.* 5, 279–289. <https://doi.org/10.1021/acsapm.2c01501>
- Rashid, M.A., Zhu, S., Jiang, Q., Zhang, L., Wei, Y., Liu, W., 2022. A Quercetin-Derived Polybasic Acid Hardener for Reprocessable and Degradable Epoxy Resins Based on Transesterification. *ACS Appl. Polym. Mater.* 4, 5708–5716. <https://doi.org/10.1021/acsapm.2c00674>
- Rashid, M.A., Zhu, S., Zhang, L., Jin, K., Liu, W., 2023. High-performance and fully recyclable epoxy resins cured by imine-containing hardeners derived from vanillin and syringaldehyde. *Eur. Polym. J.* 187, 111878. <https://doi.org/10.1016/j.eurpolymj.2023.111878>
- Reddy, K.S.K., Chen, Y.-C., Jeng, R.-J., Abu-Omar, M.M., Lin, C.-H., 2023. Upcycling Waste Polycarbonate to Poly(carbonate imine) Vitrimers with High Thermal Properties and Unprecedented Hydrolytic Stability. *ACS Sustain. Chem. Eng.* 11, 8580–8591. <https://doi.org/10.1021/acsschemeng.3c01454>
- Reinitz, S.D., Carlson, E.M., Levine, R.A.C., Franklin, K.J., Van Citters, D.W., 2015. Dynamical mechanical analysis as an assay of cross-link density of orthopaedic ultra high molecular weight polyethylene. *Polym. Test.* 45, 174–178. <https://doi.org/10.1016/j.polymertesting.2015.06.008>
- Rekondo, A., Martin, R., Luzuriaga, A.R. de, Cabañero, G., Grande, H.J., Odriozola, I., 2014. Catalyst-free room-temperature self-healing elastomers based on aromatic disulfide metathesis. *Mater. Horiz.* 1, 237–240. <https://doi.org/10.1039/C3MH00061C>
- Ren, J., Yang, H., Wu, Y., Liu, S., Ni, K., Ran, X., Zhou, X., Gao, W., Du, G., Yang, L., 2022. Dynamic reversible adhesives based on crosslinking network via Schiff base and Michael addition. *RSC Adv.* 12, 15241–15250. <https://doi.org/10.1039/D2RA02299K>
- Renders, T., Bosch, S.V. den, Koelewijn, S.-F., Schutyser, W., Sels, B.F., 2017. Lignin-first biomass fractionation: the advent of active stabilisation strategies. *Energy Environ. Sci.* 10, 1551–1557. <https://doi.org/10.1039/C7EE01298E>
- Ricarte, R.G., Tourmilhac, F., Cloître, M., Leibler, L., 2020. Linear Viscoelasticity and Flow of Self-Assembled Vitrimers: The Case of a Polyethylene/Dioxaborolane System. *Macromolecules* 53, 1852–1866. <https://doi.org/10.1021/acs.macromol.9b02415>
- Rinaldi, R., Jastrzebski, R., Clough, M.T., Ralph, J., Kennema, M., Bruijninx, P.C.A., Weckhuysen, B.M., 2016. Paving the Way for Lignin Valorisation: Recent Advances in Bioengineering, Biorefining and Catalysis. *Angew. Chem. Int. Ed.* 55, 8164–8215. <https://doi.org/10.1002/anie.201510351>
- Rocha, L.D., Monteiro, M.C., Teodoro, A.J., 2012. Anticancer Properties of Hydroxycinnamic Acids -A Review. *Cancer Clin. Oncol.* 1, 109–121. <https://doi.org/10.5539/cc.v1n2p109>
- Rochette, J.M., Ashby, V.S., 2013. Photoresponsive Polyesters for Tailorable Shape Memory Biomaterials. *Macromolecules* 46, 2134–2140. <https://doi.org/10.1021/ma302354a>
- Rodrigues Pinto, P.C., Borges da Silva, E.A., Rodrigues, A.E., 2012. Lignin as Source of Fine Chemicals: Vanillin and Syringaldehyde, in: Baskar, C., Baskar, S., Dhillon, R.S. (Eds.), *Biomass Conversion: The Interface of Biotechnology, Chemistry and Materials Science*. Springer, Berlin, Heidelberg, pp. 381–420. https://doi.org/10.1007/978-3-642-28418-2_12
- Roig, A., Hidalgo, P., Ramis, X., De la Flor, S., Serra, À., 2022a. Vitrimeric Epoxy-Amine Polyimine Networks Based on a Renewable Vanillin Derivative. *ACS Appl. Polym. Mater.* 4, 9341–9350. <https://doi.org/10.1021/acsapm.2c01604>
- Roig, A., Petrauskaitė, A., Ramis, X., Flor, S.D. la, Serra, À., 2022b. Synthesis and characterization of new bio-based poly(acylhydrazone) vanillin vitrimers. *Polym. Chem.* 13, 1510–1519. <https://doi.org/10.1039/D1PY01694F>
- Romero, C., Brenes, M., 2012. Analysis of Total Contents of Hydroxytyrosol and Tyrosol in Olive Oils. *J. Agric. Food Chem.* 60, 9017–9022. <https://doi.org/10.1021/jf3026666>
- Rosato, D.V., Rosato, M.G., 2012. *Injection molding handbook*. Springer Science & Business Media.

LISTE COMPLÈTE DES RÉFÉRENCES BIBLIOGRAPHIQUES

- Röttger, M., Domenech, T., van der Weegen, R., Breuillac, A., Nicolay, R., Leibler, L., 2017. High-performance vitrimers from commodity thermoplastics through dioxaborolane metathesis. *Science* 356, 62–65. <https://doi.org/10.1126/science.aah5281>
- Rowe, M.D., Eyler, E., Walters, K.B., 2016. Hydrolytic degradation of bio-based polyesters: Effect of pH and time. *Polym. Test.* 52, 192–199. <https://doi.org/10.1016/j.polymertesting.2016.04.015>
- Roy, P.S., Mention, M.M., Patti, A.F., Garnier, G., Allais, F., Saito, K., 2023. Photo-responsive lignin fragment-based polymers as switchable adhesives. *Polym. Chem.* 14, 913–924. <https://doi.org/10.1039/D2PY01474B>
- Rubinstein, M., Semenov, A.N., 1998. Thermoreversible Gelation in Solutions of Associating Polymers. 2. Linear Dynamics. *Macromolecules* 31, 1386–1397. <https://doi.org/10.1021/ma970617+>
- Ruiz, E., Romero-García, J.M., Romero, I., Manzanares, P., Negro, M.J., Castro, E., 2017. Olive-derived biomass as a source of energy and chemicals. *Biofuels Bioprod. Biorefining* 11, 1077–1094. <https://doi.org/10.1002/bbb.1812>
- Saito, K., Eisenreich, F., Türel, T., Tomović, Ž., 2022. Closed-Loop Recycling of Poly(Imine-Carbonate) Derived from Plastic Waste and Bio-based Resources. *Angew. Chem. Int. Ed.* 61, e202211806. <https://doi.org/10.1002/anie.202211806>
- Saito, K., Türel, T., Eisenreich, F., Tomović, Ž., 2023. Closed-Loop Recyclable Poly(imine-acetal)s with Dual-Cleavable Bonds for Primary Building Block Recovery. *ChemSusChem* 16, e202301017. <https://doi.org/10.1002/cssc.202301017>
- Santos, T., Pérez-Pérez, Y., Rivero, D.S., Diana-Rivero, R., García-Tellado, F., Tejedor, D., Carrillo, R., 2022. Dynamic Hydroxyl–Yne Reaction with Phenols. *Org. Lett.* 24, 8401–8405. <https://doi.org/10.1021/acs.orglett.2c03518>
- Sardon, H., Mecerreyes, D., Basterretxea, A., Avérous, L., Jehanno, C., 2021. From Lab to Market: Current Strategies for the Production of Biobased Polyols. *ACS Sustain. Chem. Eng.* 9, 10664–10677. <https://doi.org/10.1021/acsschemeng.1c02361>
- Sarika, P.R., Nancarrow, P., Khansaheb, A., Ibrahim, T., 2020. Bio-Based Alternatives to Phenol and Formaldehyde for the Production of Resins. *Polymers* 12, 2237. <https://doi.org/10.3390/polym12102237>
- Sastri, V.R., Tesoro, G.C., 1990. Reversible crosslinking in epoxy resins. II. New approaches. *J. Appl. Polym. Sci.* 39, 1439–1457. <https://doi.org/10.1002/app.1990.070390703>
- Schenk, V., Labastie, K., Destarac, M., Olivier, P., Guerre, M., 2022. Vitriemer composites: current status and future challenges. *Mater. Adv.* 3, 8012–8029. <https://doi.org/10.1039/D2MA00654E>
- Scheutz, G.M., Lessard, J.J., Sims, M.B., Sumerlin, B.S., 2019. Adaptable Crosslinks in Polymeric Materials: Resolving the Intersection of Thermoplastics and Thermosets. *J. Am. Chem. Soc.* 141, 16181–16196. <https://doi.org/10.1021/jacs.9b07922>
- Schmolke, W., Perner, N., Seiffert, S., 2015. Dynamically Cross-Linked Polydimethylsiloxane Networks with Ambient-Temperature Self-Healing. *Macromolecules* 48, 8781–8788. <https://doi.org/10.1021/acs.macromol.5b01666>
- Schoustra, S.K., Dijkstra, J.A., Zuilhof, H., Smulders, M.M.J., 2021. Molecular control over vitriemer-like mechanics – tuneable dynamic motifs based on the Hammett equation in polyimine materials. *Chem. Sci.* 12, 293–302. <https://doi.org/10.1039/D0SC05458E>
- Schutyser, W., Renders, T., Bosch, S.V. den, Koelewijn, S.-F., Beckham, G.T., Sels, B.F., 2018. Chemicals from lignin: an interplay of lignocellulose fractionation, depolymerisation, and upgrading. *Chem. Soc. Rev.* 47, 852–908. <https://doi.org/10.1039/C7CS00566K>
- Scott, T.F., Schneider, A.D., Cook, W.D., Bowman, C.N., 2005. Photoinduced Plasticity in Cross-Linked Polymers. *Science* 308, 1615–1617. <https://doi.org/10.1126/science.1110505>
- Semenov, A.N., Rubinstein, M., 1998. Thermoreversible Gelation in Solutions of Associative Polymers. 1. Statics. *Macromolecules* 31, 1373–1385. <https://doi.org/10.1021/ma970616h>
- Shameli, K., Bin Ahmad, M., Jazayeri, S.D., Sedaghat, S., Shabanzadeh, P., Jahangirian, H., Mahdavi, M., Abdollahi, Y., 2012. Synthesis and Characterization of Polyethylene Glycol Mediated Silver Nanoparticles by the Green Method. *Int. J. Mol. Sci.* 13, 6639–6650. <https://doi.org/10.3390/ijms13066639>
- Sharma, H., Rana, S., Singh, P., Hayashi, M., Binder, W.H., Rossegger, E., Kumar, A., Schlögl, S., 2022. Self-healable fiber-reinforced vitriemer composites: overview and future prospects. *RSC Adv.* 12, 32569–32582. <https://doi.org/10.1039/D2RA05103F>
- Shen, H., Qiao, H., Zhang, H., 2022. Sulfur-urushiol copolymer: A material synthesized through inverse vulcanization from renewable resources and its latent application as self-repairable and antimicrobial adhesive. *Chem. Eng. J.* 450, 137905. <https://doi.org/10.1016/j.cej.2022.137905>
- Shi, B., Greaney, M.F., 2005. Reversible Michael addition of thiols as a new tool for dynamic combinatorial chemistry. *Chem. Commun.* 7, 886–888. <https://doi.org/10.1039/B414300K>

LISTE COMPLÈTE DES RÉFÉRENCES BIBLIOGRAPHIQUES

- Shi, J., Zheng, T., Guo, B., Xu, J., 2019. Solvent-free thermo-reversible and self-healable crosslinked polyurethane with dynamic covalent networks based on phenol-carbamate bonds. *Polymer* 181, 121788. <https://doi.org/10.1016/j.polymer.2019.121788>
- Shi, Q., Jin, C., Chen, Z., An, L., Wang, T., 2023. On the Welding of Vitrimers: Chemistry, Mechanics and Applications. *Adv. Funct. Mater.* 33, 2300288. <https://doi.org/10.1002/adfm.202300288>
- Shi, Y., Bai, T., Bai, W., Wang, Z., Chen, M., Yao, B., Sun, J.Z., Qin, A., Ling, J., Tang, B.Z., 2017. Phenol-yne Click Polymerization: An Efficient Technique to Facilely Access Regio- and Stereoregular Poly(vinylene ether ketone)s. *Chem. – Eur. J.* 23, 10725–10731. <https://doi.org/10.1002/chem.201702966>
- Shrestha, S., Zhang, W., Smid, S.D., 2021. Phlorotannins: A review on biosynthesis, chemistry and bioactivity. *Food Biosci.* 39, 100832. <https://doi.org/10.1016/j.fbio.2020.100832>
- Si, H., Wang, K., Song, B., Qin, A., Tang, B.Z., 2020. Organobase-catalysed hydroxyl-yne click polymerization. *Polym. Chem.* 11, 2568–2575. <https://doi.org/10.1039/D0PY00095G>
- Simon, J., Barla, F., Kelemen-Haller, A., Farkas, F., Kraxner, M., 1988. Thermal stability of polyurethanes. *Chromatographia* 25, 99–106. <https://doi.org/10.1007/BF02259024>
- Smit, A.T., Dezaire, T., Riddell, L.A., Bruijninx, P.C.A., 2023. Reductive Partial Depolymerization of Acetone Organosolv Lignin to Tailor Lignin Molar Mass, Dispersity, and Reactivity for Polymer Applications. *ACS Sustain. Chem. Eng.* 11, 6070–6080. <https://doi.org/10.1021/acssuschemeng.3c00617>
- Smit, A.T., Verges, M., Schulze, P., van Zomeren, A., Lorenz, H., 2022. Laboratory- to Pilot-Scale Fractionation of Lignocellulosic Biomass Using an Acetone Organosolv Process. *ACS Sustain. Chem. Eng.* 10, 10503–10513. <https://doi.org/10.1021/acssuschemeng.2c01425>
- Solanki, A., Thakore, S., 2015. Cellulose crosslinked pH-responsive polyurethanes for drug delivery: α -hydroxy acids as drug release modifiers. *Int. J. Biol. Macromol.* 80, 683–691. <https://doi.org/10.1016/j.ijbiomac.2015.07.003>
- Soleimani, A., Sadeghi, G.M.M., 2022. Synthesis, Characterization and Thermal Properties of Intrinsic Self-Healing Polyurethane Nanocomposites. *ChemistrySelect* 7, e202103978. <https://doi.org/10.1002/slct.202103978>
- Song, B., Lu, D., Qin, A., Tang, B.Z., 2022. Combining Hydroxyl-Yne and Thiol-Ene Click Reactions to Facilely Access Sequence-Defined Macromolecules for High-Density Data Storage. *J. Am. Chem. Soc.* 144, 1672–1680. <https://doi.org/10.1021/jacs.1c10612>
- Song, P., Du, L., Pang, J., Jiang, G., Shen, J., Ma, Y., Ren, S., Li, S., 2023. Preparation and properties of lignin-based vitrimer system containing dynamic covalent bonds for reusable and recyclable epoxy asphalt. *Ind. Crops Prod.* 197, 116498. <https://doi.org/10.1016/j.indcrop.2023.116498>
- Sonnier, R., Taguet, A., Ferry, L., Lopez-Cuesta, J.-M., 2018. Towards Bio-based Flame Retardant Polymers, *SpringerBriefs in Molecular Science*. Springer International Publishing, Cham. <https://doi.org/10.1007/978-3-319-67083-6>
- Sougrati, L., Duval, A., Avérous, L., 2023a. From Lignins to Renewable Aromatic Vitrimers based on Vinylogous Urethane. *ChemSusChem* 16, e202300792. <https://doi.org/10.1002/cssc.202300792>
- Sougrati, L., Wendels, S., Dinescu, S., Balahura, L.-R., Sleiman, L., Avérous, L., 2023b. Renewable adhesives based on oleo-chemistry: From green synthesis to biomedical applications. *Sustain. Mater. Technol.* 37, e00656. <https://doi.org/10.1016/j.susmat.2023.e00656>
- Souto, F., Calado, V., 2022. Mystifications and misconceptions of lignin: revisiting understandings. *Green Chem.* 24, 8172–8192. <https://doi.org/10.1039/D2GC01914K>
- Spiesschaert, Y., Danneels, J., Van Herck, N., Guerre, M., Acke, G., Winne, J., Du Prez, F., 2021. Polyaddition Synthesis Using Alkyne Esters for the Design of Vinylogous Urethane Vitrimers. *Macromolecules* 54, 7931–7942. <https://doi.org/10.1021/acs.macromol.1c01049>
- Spiesschaert, Y., Guerre, M., De Baere, I., Van Paepegem, W., Winne, J.M., Du Prez, F.E., 2020. Dynamic Curing Agents for Amine-Hardened Epoxy Vitrimers with Short (Re)processing Times. *Macromolecules* 53, 2485–2495. <https://doi.org/10.1021/acs.macromol.9b02526>
- Sriharshitha, S., Krishnadevi, K., Prasanna, D., 2022. Vitrimers trigger covalent bonded bio-silica fused composite materials for recycling, reshaping, and self-healing applications. *RSC Adv.* 12, 26934–26944. <https://doi.org/10.1039/D2RA03794G>
- Stadler, R., 1988. Association phenomena in macromolecular systems - influence of macromolecular constraints on the complex formation. *Macromolecules* 21, 121–126. <https://doi.org/10.1021/ma00179a025>
- Statista, 2021. Cashew nut: global production. URL <https://www.statista.com/statistics/967702/global-cashew-nut-production/> (accessed 7.13.23).
- Stouten, J., de Roy, M.K.N., Bernaerts, K.V., 2023. Synthesis and characterization of water-borne vanillin derived copolymers containing dynamic imine cross-links. *Mater. Today Sustain.* 22, 100396. <https://doi.org/10.1016/j.mtsust.2023.100396>

LISTE COMPLÈTE DES RÉFÉRENCES BIBLIOGRAPHIQUES

- Stricker, L., Taplan, C., Du Prez, F.E., 2022. Biobased, Creep-Resistant Covalent Adaptable Networks Based on β -Amino Ester Chemistry. *ACS Sustain. Chem. Eng.* 10, 14045–14052. <https://doi.org/10.1021/acssuschemeng.2c04822>
- Sultania, M., Rai, J.S.P., Srivastava, D., 2011. Process modeling, optimization and analysis of esterification reaction of cashew nut shell liquid (CNSL)-derived epoxy resin using response surface methodology. *J. Hazard. Mater.* 185, 1198–1204. <https://doi.org/10.1016/j.jhazmat.2010.10.031>
- Sun, Y., Tian, X., Xie, H., Shi, B., Zhong, J., Liu, X., Yang, Y., 2022. Reprocessable and degradable bio-based polyurethane by molecular design engineering with extraordinary mechanical properties for recycling carbon fiber. *Polymer* 258, 125313. <https://doi.org/10.1016/j.polymer.2022.125313>
- Sun, Z., Fridrich, B., de Santi, A., Elangovan, S., Barta, K., 2018. Bright Side of Lignin Depolymerization: Toward New Platform Chemicals. *Chem. Rev.* 118, 614–678. <https://doi.org/10.1021/acs.chemrev.7b00588>
- Sung, C.S.P., Schneider, N.S., 1977. Temperature Dependence of Hydrogen Bonding in Toluene Diisocyanate Based Polyurethanes. *Macromolecules* 10, 452–458. <https://doi.org/10.1021/ma60056a041>
- Symes, W.F., Dawson, C.R., 1954. Poison Ivy “Urushiol.” *J. Am. Chem. Soc.* 76, 2959–2963. <https://doi.org/10.1021/ja01640a030>
- Symes, W.F., Dawson, C.R., 1953. Separation and Structural Determination of the Olefinic Components of Poison Ivy Urushiol, Cardanol and Cardol. *Nature* 171, 841–842. <https://doi.org/10.1038/171841b0>
- Takahashi, Y., Tobolsky, A.V., 1971. Chemorheological Study on Natural Rubber Vulcanizates. *Polym. J.* 2, 457–467. <https://doi.org/10.1295/polymj.2.457>
- Tang, R., Xue, B., Tan, J., Guan, Y., Wen, J., Li, X., Zhao, W., 2022. Regulating Lignin-Based Epoxy Vitrimer Performance by Fine-Tuning the Lignin Structure. *ACS Appl. Polym. Mater.* 4, 1117–1125. <https://doi.org/10.1021/acsapm.1c01541>
- Tang, S., Lin, H., Dong, K., Zhang, J., Zhao, C., 2023. Closed-loop recycling and degradation of guaiacol-based epoxy resin and its carbon fiber reinforced composites with S-S exchangeable bonds. *Polym. Degrad. Stab.* 210, 110298. <https://doi.org/10.1016/j.polymdegradstab.2023.110298>
- Tannert, R., Taubert, A., Weber, J., 2023. Biobased Epoxy Eugenol Vitrimers: Influence of Impurities of Technical Grade Monomers on the Network Characteristics. *Macromol. Mater. Eng.* n/a, 2300236. <https://doi.org/10.1002/mame.202300236>
- Tao, Y., Fang, L., Dai, M., Wang, C., Sun, J., Fang, Q., 2020. Sustainable alternative to bisphenol A epoxy resin: high-performance recyclable epoxy vitrimers derived from protocatechuic acid. *Polym. Chem.* 11, 4500–4506. <https://doi.org/10.1039/D0PY00545B>
- Tao, Y., Liang, X., Zhang, J., Lei, I.M., Liu, J., 2023a. Polyurethane vitrimers: Chemistry, properties and applications. *J. Polym. Sci.* 61, 2233–2253. <https://doi.org/10.1002/pol.20220625>
- Tao, Y., Liang, X., Zhang, J., Lei, I.M., Liu, J., 2023b. Polyurethane vitrimers: Chemistry, properties and applications. *J. Polym. Sci.* 61, 2233–2253. <https://doi.org/10.1002/pol.20220625>
- Taofiq, O., González-Paramás, A.M., Barreiro, M.F., Ferreira, I.C.F.R., 2017. Hydroxycinnamic Acids and Their Derivatives: Cosmeceutical Significance, Challenges and Future Perspectives, a Review. *Molecules* 22, 281. <https://doi.org/10.3390/molecules22020281>
- Taplan, C., Guerre, M., Du Prez, F.E., 2021. Covalent Adaptable Networks Using β -Amino Esters as Thermally Reversible Building Blocks. *J. Am. Chem. Soc.* 143, 9140–9150. <https://doi.org/10.1021/jacs.1c03316>
- Taplan, C., Guerre, M., Winne, J.M., Du Prez, F.E., 2020. Fast processing of highly crosslinked, low-viscosity vitrimers. *Mater. Horiz.* 7, 104–110. <https://doi.org/10.1039/C9MH01062A>
- Tellers, J., Pinalli, R., Soliman, M., Vachon, J., Dalcanale, E., 2019. Reprocessable vinylogous urethane cross-linked polyethylene via reactive extrusion. *Polym. Chem.* 10, 5534–5542. <https://doi.org/10.1039/C9PY01194C>
- Tesoro, G.C., Sastri, V., 1990. Reversible crosslinking in epoxy resins. I. Feasibility studies. *J. Appl. Polym. Sci.* 39, 1425–1437. <https://doi.org/10.1002/app.1990.070390702>
- Thomas, S., Yang, W., 2009. *Advances in polymer processing: from macro- to nano-scales.* Elsevier.
- Thys, M., Brancart, J., Van Assche, G., Van den Brande, N., Vendamme, R., 2023a. LignoSwitch: A Robust Yet Reversible Bioaromatic Superglue for Enhanced Materials Circularity and Ecodesign. *ACS Sustain. Chem. Eng.* 11, 17941–17950. <https://doi.org/10.1021/acssuschemeng.3c04477>
- Thys, M., Brancart, J., Van Assche, G., Vendamme, R., Van den Brande, N., 2021. Reversible Lignin-Containing Networks Using Diels–Alder Chemistry. *Macromolecules* 54, 9750–9760. <https://doi.org/10.1021/acs.macromol.1c01693>
- Thys, M., Kaya, G.E., Soetemans, L., Van Assche, G., Bourbigot, S., Baytekin, B., Vendamme, R., Van den Brande, N., 2023b. Bioaromatic-Associated Multifunctionality in Lignin-Containing Reversible Elastomers. *ACS Appl. Polym. Mater.* 5, 5846–5856. <https://doi.org/10.1021/acsapm.3c00491>

LISTE COMPLÈTE DES RÉFÉRENCES BIBLIOGRAPHIQUES

- Tian, P.-X., Li, Y.-D., Weng, Y., Hu, Z., Zeng, J.-B., 2023. Reprocessable, chemically recyclable, and flame-retardant biobased epoxy vitrimers. *Eur. Polym. J.* 193, 112078. <https://doi.org/10.1016/j.eurpolymj.2023.112078>
- Tiz, D.B., Vicente, F.A., Kroflič, A., Likozar, B., 2023. Lignin-Based Covalent Adaptable Network Polymers—When Bio-Based Thermosets Meet Recyclable by Design. *ACS Sustain. Chem. Eng.* 11, 13836–13867. <https://doi.org/10.1021/acssuschemeng.3c03248>
- Tobolsky, A.V., MacKnight, W.J., Takahashi, M., 1964. Relaxation of Disulfide and Tetrasulfide Polymers. *J. Phys. Chem.* 68, 787–790. <https://doi.org/10.1021/j100786a013>
- Tong, X., Ma, Y., Li, Y., 2010. Biomass into chemicals: Conversion of sugars to furan derivatives by catalytic processes. *Appl. Catal. Gen.* 385, 1–13. <https://doi.org/10.1016/j.apcata.2010.06.049>
- Trejo-Machin, A., Puchot, L., Verge, P., 2020. A cardanol-based polybenzoxazine vitrimer: recycling, reshaping and reversible adhesion. *Polym. Chem.* 11, 7026–7034. <https://doi.org/10.1039/D0PY01239D>
- Tremblay-Parrado, K.-K., Avérous, L., 2020. Renewable Responsive Systems Based on Original Click and Polyurethane Cross-Linked Architectures with Advanced Properties. *ChemSusChem* 13, 238–251. <https://doi.org/10.1002/cssc.201901991>
- Tremblay-Parrado, K.-K., Avérous, L., 2020. Synthesis and behavior of responsive biobased polyurethane networks cross-linked by click chemistry: Effect of the cross-linkers and backbone structures. *Eur. Polym. J.* 135, 109840. <https://doi.org/10.1016/j.eurpolymj.2020.109840>
- Tremblay-Parrado, K.-K., Bordin, C., Nicholls, S., Heinrich, B., Donnio, B., Avérous, L., 2020. Renewable and Responsive Cross-Linked Systems Based on Polyurethane Backbones from Clickable Biobased Bismaleimide Architecture. *Macromolecules* 53, 5869–5880. <https://doi.org/10.1021/acs.macromol.0c01115>
- Tremblay-Parrado, K.-K., García-Astrain, C., Avérous, L., 2021. Click chemistry for the synthesis of biobased polymers and networks derived from vegetable oils. *Green Chem.* 23, 4296–4327. <https://doi.org/10.1039/D1GC00445J>
- Tretbar, C.A., Neal, J.A., Guan, Z., 2019. Direct Silyl Ether Metathesis for Vitrimers with Exceptional Thermal Stability. *J. Am. Chem. Soc.* 141, 16595–16599. <https://doi.org/10.1021/jacs.9b08876>
- Tribot, A., Amer, G., Abdou Alio, M., De Baynast, H., Delattre, C., Pons, A., Mathias, J.-D., Callois, J.-M., Vial, C., Michaud, P., Dussap, C.-G., 2019. Wood-lignin: Supply, extraction processes and use as bio-based material. *Eur. Polym. J.* 112, 228–240. <https://doi.org/10.1016/j.eurpolymj.2019.01.007>
- Trinh, T.E., Ku, K., Yeo, H., 2023. Reprocessable and Chemically Recyclable Hard Vitrimers Based on Liquid-Crystalline Epoxides. *Adv. Mater.* 35, 2209912. <https://doi.org/10.1002/adma.202209912>
- Truong, V.X., Dove, A.P., 2013. Organocatalytic, Regioselective Nucleophilic “Click” Addition of Thiols to Propiolic Acid Esters for Polymer–Polymer Coupling. *Angew. Chem.* 125, 4226–4230. <https://doi.org/10.1002/ange.201209239>
- Türel, T., Saito, K., Glišić, I., Middelhoek, T., Tomović, Ž., 2024. Closing the loop: polyimine thermosets from furfural derived bioresources. *RSC Appl. Polym.* 2, 395–402. <https://doi.org/10.1039/D3LP00268C>
- Türel, T., Tomović, Ž., 2023. Chemically Recyclable and Upcyclable Epoxy Resins Derived from Vanillin. *ACS Sustain. Chem. Eng.* 11, 8308–8316. <https://doi.org/10.1021/acssuschemeng.3c00761>
- Upton, B.M., Kasko, A.M., 2016. Strategies for the Conversion of Lignin to High-Value Polymeric Materials: Review and Perspective. *Chem. Rev.* 116, 2275–2306. <https://doi.org/10.1021/acs.chemrev.5b00345>
- Van den Tempel, P., Picchioni, F., Bose, R.K., 2022. Designing End-of-Life Recyclable Polymers via Diels–Alder Chemistry: A Review on the Kinetics of Reversible Reactions. *Macromol. Rapid Commun.* 43, 2200023. <https://doi.org/10.1002/marc.202200023>
- Van Es, D.S., 2013. Rigid Biobased Building Blocks. *J. Renew. Mater.* 1, 61–72. <https://doi.org/10.7569/JRM.2012.634108>
- Van Lijsebetten, F., De Bruycker, K., Spiesschaert, Y., Winne, J.M., Du Prez, F.E., 2022a. Suppressing Creep and Promoting Fast Reprocessing of Vitrimers with Reversibly Trapped Amines. *Angew. Chem. Int. Ed.* 61, e202113872. <https://doi.org/10.1002/anie.202113872>
- Van Lijsebetten, F., De Bruycker, K., Winne, J.M., Du Prez, F.E., 2022b. Masked Primary Amines for a Controlled Plastic Flow of Vitrimers. *ACS Macro Lett.* 11, 919–924. <https://doi.org/10.1021/acsmacrolett.2c00255>
- Van Lijsebetten, F., Holloway, J.O., Winne, J.M., Prez, F.E.D., 2020. Internal catalysis for dynamic covalent chemistry applications and polymer science. *Chem. Soc. Rev.* 49, 8425–8438. <https://doi.org/10.1039/D0CS00452A>
- Van Putten, R.-J., van der Waal, J.C., de Jong, E., Rasrendra, C.B., Heeres, H.J., de Vries, J.G., 2013. Hydroxymethylfurfural, A Versatile Platform Chemical Made from Renewable Resources. *Chem. Rev.* 113, 1499–1597. <https://doi.org/10.1021/cr300182k>

LISTE COMPLÈTE DES RÉFÉRENCES BIBLIOGRAPHIQUES

- Van Zee, N.J., Nicolay, R., 2020. Vitrimers: Permanently crosslinked polymers with dynamic network topology. *Prog. Polym. Sci.* 104, 101233. <https://doi.org/10.1016/j.progpolymsci.2020.101233>
- Vanholme, R., Demedts, B., Morreel, K., Ralph, J., Boerjan, W., 2010. Lignin Biosynthesis and Structure. *Plant Physiol.* 153, 895–905. <https://doi.org/10.1104/pp.110.155119>
- Vantomme, G., Lehn, J.-M., 2014. Reversible Adaptation to Photoinduced Shape Switching by Oligomer–Macrocycle Interconversion with Component Selection in a Three-State Constitutional Dynamic System. *Chem. – Eur. J.* 20, 16188–16193. <https://doi.org/10.1002/chem.201404561>
- Vidil, T., Llevot, A., 2022. Fully Biobased Vitrimers: Future Direction toward Sustainable Cross-Linked Polymers. *Macromol. Chem. Phys.* 223, 2100494. <https://doi.org/10.1002/macp.202100494>
- Wahyudiono, Sasaki, M., Goto, M., 2008. Recovery of phenolic compounds through the decomposition of lignin in near and supercritical water. *Chem. Eng. Process. Process Intensif.* 47, 1609–1619. <https://doi.org/10.1016/j.cep.2007.09.001>
- Wang, C., Kelley, S.S., Venditti, R.A., 2016. Lignin-Based Thermoplastic Materials. *ChemSusChem* 9, 770–783. <https://doi.org/10.1002/cssc.201501531>
- Wang, H., Fu, Y., Liu, Y., Li, J., Sun, X., Liu, T., 2023. Synthesis of facilely healable and recyclable imine vitrimers using biobased branched diamine and vanillin. *Eur. Polym. J.* 196, 112309. <https://doi.org/10.1016/j.eurpolymj.2023.112309>
- Wang, L., Yang, X., Chen, H., Gong, T., Li, W., Yang, G., Zhou, S., 2013. Design of Triple-Shape Memory Polyurethane with Photo-cross-linking of Cinnamon Groups. *ACS Appl. Mater. Interfaces* 5, 10520–10528. <https://doi.org/10.1021/am402091m>
- Wang, M., Yin, G.-Z., Yang, Y., Fu, W., Díaz Palencia, J.L., Zhao, J., Wang, N., Jiang, Y., Wang, D.-Y., 2023. Bio-based flame retardants to polymers: A review. *Adv. Ind. Eng. Polym. Res., Advances in Flame Retardant Materials and Technologies* 6, 132–155. <https://doi.org/10.1016/j.aiepr.2022.07.003>
- Wang, S., Ma, S., Li, Q., Xu, X., Wang, B., Huang, K., Liu, Y., Zhu, J., 2020. Facile Preparation of Polyimine Vitrimers with Enhanced Creep Resistance and Thermal and Mechanical Properties via Metal Coordination. *Macromolecules* 53, 2919–2931. <https://doi.org/10.1021/acs.macromol.0c00036>
- Wang, S., Ma, S., Li, Q., Xu, X., Wang, B., Yuan, W., Zhou, S., You, S., Zhu, J., 2019. Facile in situ preparation of high-performance epoxy vitrimer from renewable resources and its application in nondestructive recyclable carbon fiber composite. *Green Chem.* 21, 1484–1497. <https://doi.org/10.1039/C8GC03477J>
- Wang, X., Zhang, S., He, Y., Guo, W., Lu, Z., 2022. Reprocessable Polybenzoxazine Thermosets with High T_gs and Mechanical Strength Retentions Using Boronic Ester Bonds as Crosslinkages. *Polymers* 14, 2234. <https://doi.org/10.3390/polym14112234>
- Wang, Y., Jin, B., Ye, D., Liu, Z., 2022a. Fully recyclable carbon fiber reinforced vanillin-based epoxy vitrimers. *Eur. Polym. J.* 162, 110927. <https://doi.org/10.1016/j.eurpolymj.2021.110927>
- Wang, Y., Xu, A., Zhang, L., Chen, Z., Qin, R., Liu, Y., Jiang, X., Ye, D., Liu, Z., 2022b. Recyclable Carbon Fiber Reinforced Vanillin-Based Polyimine Vitrimers: Degradation and Mechanical Properties Study. *Macromol. Mater. Eng.* 307, 2100893. <https://doi.org/10.1002/mame.202100893>
- Wang, Z., Zhang, X., Cai, J., Xie, J., 2023. Plant-derived p-hydroxyphenylacrylic acid-derived epoxy resins exhibit excellent flame retardancy, hydrophobicity, degradability, and low dielectric loss after curing with bio-based fluorinated Schiff bases. *Polym. Degrad. Stab.* 209, 110270. <https://doi.org/10.1016/j.polymdegradstab.2023.110270>
- Wegelin, S., Meier, M.A.R., 2024. Biobased aromatics for chemicals and materials: Advances in renewable drop-in and functional alternatives. *Curr. Opin. Green Sustain. Chem.* 100931. <https://doi.org/10.1016/j.cogsc.2024.100931>
- Wei, X., Ge, J., Gao, F., Chen, F., Zhang, W., Zhong, J., Lin, C., Shen, L., 2021. Bio-based self-healing coating material derived from renewable castor oil and multifunctional alamine. *Eur. Polym. J.* 160, 110804. <https://doi.org/10.1016/j.eurpolymj.2021.110804>
- Wen, Z., Bonnaud, L., Dubois, P., Raquez, J.-M., 2022. Catalyst-free reprocessable crosslinked biobased polybenzoxazine-polyurethane based on dynamic carbamate chemistry. *J. Appl. Polym. Sci.* 139, 52120. <https://doi.org/10.1002/app.52120>
- Wendels, S., Avérous, L., 2021. Biobased polyurethanes for biomedical applications. *Bioact. Mater.* 6, 1083–1106. <https://doi.org/10.1016/j.bioactmat.2020.10.002>
- Williams, G., Watts, D.C., 1970. Non-symmetrical dielectric relaxation behaviour arising from a simple empirical decay function. *Trans. Faraday Soc.* 66, 80–85. <https://doi.org/10.1039/TF9706600080>
- Winne, J.M., Leibler, L., Prez, F.E.D., 2019. Dynamic covalent chemistry in polymer networks: a mechanistic perspective. *Polym. Chem.* 10, 6091–6108. <https://doi.org/10.1039/C9PY01260E>
- Witzeman, J.S., Nottingham, W.D., 1991. Transacetoacetylation with tert-butyl acetoacetate: synthetic applications. *J. Org. Chem.* 56, 1713–1718. <https://doi.org/10.1021/jo00005a013>

LISTE COMPLÈTE DES RÉFÉRENCES BIBLIOGRAPHIQUES

- Worch, J.C., Stubbs, C.J., Price, M.J., Dove, A.P., 2021. Click Nucleophilic Conjugate Additions to Activated Alkynes: Exploring Thiol-yne, Amino-yne, and Hydroxyl-yne Reactions from (Bio)Organic to Polymer Chemistry. *Chem. Rev.* 121, 6744–6776. <https://doi.org/10.1021/acs.chemrev.0c01076>
- Xie, W., Huang, S., Liu, S., Zhao, J., 2021. Imine-functionalized biomass-derived dynamic covalent thermosets enabled by heat-induced self-crosslinking and reversible structures. *Chem. Eng. J.* 404, 126598. <https://doi.org/10.1016/j.cej.2020.126598>
- Xing, P., Chen, H., Xiang, H., Zhao, Y., 2018. Selective Coassembly of Aromatic Amino Acids to Fabricate Hydrogels with Light Irradiation-Induced Emission for Fluorescent Imprint. *Adv. Mater.* 30, 1705633. <https://doi.org/10.1002/adma.201705633>
- Xu, J., Liu, Y., Hsu, S., 2019. Hydrogels Based on Schiff Base Linkages for Biomedical Applications. *Molecules* 24, 3005. <https://doi.org/10.3390/molecules24163005>
- Xu, N., Gong, J., Huang, Z., 2016. Review on the production methods and fundamental combustion characteristics of furan derivatives. *Renew. Sustain. Energy Rev.* 54, 1189–1211. <https://doi.org/10.1016/j.rser.2015.10.118>
- Xu, X., Ma, S., Feng, H., Qiu, J., Wang, S., Yu, Z., Zhu, J., 2021. Dissociate transfer exchange of tandem dynamic bonds endows covalent adaptable networks with fast reprocessability and high performance. *Polym. Chem.* 12, 5217–5228. <https://doi.org/10.1039/D1PY01045J>
- Xue, B., Tang, R., Xue, D., Guan, Y., Sun, Y., Zhao, W., Tan, J., Li, X., 2021. Sustainable alternative for bisphenol A epoxy resin high-performance and recyclable lignin-based epoxy vitrimers. *Ind. Crops Prod.* 168, 113583. <https://doi.org/10.1016/j.indcrop.2021.113583>
- Yan, P., Zhao, W., Fu, X., Liu, Z., Kong, W., Zhou, C., Lei, J., 2017. Multifunctional polyurethane-vitrimers completely based on transcarbamoylation of carbamates: thermally-induced dual-shape memory effect and self-welding. *RSC Adv.* 7, 26858–26866. <https://doi.org/10.1039/C7RA01711A>
- Yang, H., Yu, B., Xu, X., Bourbigot, S., Wang, H., Song, P., 2020. Lignin-derived bio-based flame retardants toward high-performance sustainable polymeric materials. *Green Chem.* 22, 2129–2161. <https://doi.org/10.1039/D0GC00449A>
- Yang, R., Li, W., Mo, R., Zhang, X., 2023. Recyclable and Degradable Vinylogous Urethane Epoxy Thermosets with Tunable Mechanical Properties from Isosorbide and Vanillic Acid. *ACS Appl. Polym. Mater.* 5, 2553–2561. <https://doi.org/10.1021/acsapm.2c02186>
- Yang, W., Ding, H., Zhou, W., Liu, T., Xu, P., Puglia, D., Kenny, J.M., Ma, P., 2022. Design of inherent fire retarding and degradable bio-based epoxy vitrimer with excellent self-healing and mechanical reprocessability. *Compos. Sci. Technol.* 109776. <https://doi.org/10.1016/j.compscitech.2022.109776>
- Yang, X., Ke, Y., Chen, Q., Shen, L., Xue, J., Quirino, R.L., Yan, Z., Luo, Y., Zhang, C., 2022. Efficient transformation of renewable vanillin into reprocessable, acid-degradable and flame retardant polyimide vitrimers. *J. Clean. Prod.* 333, 130043. <https://doi.org/10.1016/j.jclepro.2021.130043>
- Yang, Y., Du, F.-S., Li, Z.-C., 2020. Highly Stretchable, Self-Healable, and Adhesive Polyurethane Elastomers Based on Boronic Ester Bonds. *ACS Appl. Polym. Mater.* 2, 5630–5640. <https://doi.org/10.1021/acsapm.0c00941>
- Yang, Y., Zhou, H., Chen, X., Liu, T., Zheng, Y., Dai, L., Si, C., 2023. Green and ultrastrong polyphenol lignin-based vitrimer adhesive with photothermal conversion property, wide temperature adaptability, and solvent resistance. *Chem. Eng. J.* 477, 147216. <https://doi.org/10.1016/j.cej.2023.147216>
- Yao, B., Mei, J., Li, J., Wang, J., Wu, H., Sun, J.Z., Qin, A., Tang, B.Z., 2014. Catalyst-Free Thiol–Yne Click Polymerization: A Powerful and Facile Tool for Preparation of Functional Poly(vinylene sulfide)s. *Macromolecules* 47, 1325–1333. <https://doi.org/10.1021/ma402559a>
- Yasar, M., Oktay, B., Dal Yontem, F., Haciosmanoglu Aldogan, E., Kayaman Apohan, N., 2023. Development of self-healing vanillin/PEI hydrogels for tissue engineering. *Eur. Polym. J.* 188, 111933. <https://doi.org/10.1016/j.eurpolymj.2023.111933>
- Yazaki, Y., 2015. Utilization of Flavonoid Compounds from Bark and Wood: A Review. *Nat. Prod. Commun.* 10, 513–520. <https://doi.org/10.1177/1934578X1501000333>
- Ye, C., Voet, V.S.D., Folkersma, R., Loos, K., 2021. Robust Superamphiphilic Membrane with a Closed-Loop Life Cycle. *Adv. Mater.* 33, 2008460. <https://doi.org/10.1002/adma.202008460>
- Yu, S., Wu, S., Zhang, C., Tang, Z., Luo, Y., Guo, B., Zhang, L., 2020. Catalyst-Free Metathesis of Cyclic Acetals and Spirocyclic Acetal Covalent Adaptable Networks. *ACS Macro Lett.* 9, 1143–1148. <https://doi.org/10.1021/acsmacrolett.0c00527>
- Yuan, Y., Chen, H., Jia, L., Lu, X., Yan, S., Zhao, J., Liu, S., 2023. Aromatic polyimine covalent adaptable networks with superior water and heat resistances. *Eur. Polym. J.* 187, 111912. <https://doi.org/10.1016/j.eurpolymj.2023.111912>

LISTE COMPLÈTE DES RÉFÉRENCES BIBLIOGRAPHIQUES

- Yue, L., Ke, K., Amirkhosravi, M., Gray, T.G., Manas-Zloczower, I., 2021. Catalyst-Free Mechanochemical Recycling of Biobased Epoxy with Cellulose Nanocrystals. *ACS Appl. Bio Mater.* 4, 4176–4183. <https://doi.org/10.1021/acsabm.0c01670>
- Zamani, P., Zabihi, O., Ahmadi, M., Mahmoodi, R., Kannangara, T., Joseph, P., Naebe, M., 2022. Biobased Carbon Fiber Composites with Enhanced Flame Retardancy: A Cradle-to-Cradle Approach. *ACS Sustain. Chem. Eng.* 10, 1059–1069. <https://doi.org/10.1021/acssuschemeng.1c07859>
- Zeng, C., Seino, H., Ren, J., Hatanaka, K., Yoshie, N., 2013. Self-healing bio-based furan polymers cross-linked with various bis-maleimides. *Polymer* 54, 5351–5357. <https://doi.org/10.1016/j.polymer.2013.07.059>
- Zhang, C., Xue, J., Yang, X., Ke, Y., Ou, R., Wang, Y., Madbouly, S.A., Wang, Q., 2022. From plant phenols to novel bio-based polymers. *Prog. Polym. Sci.* 125, 101473. <https://doi.org/10.1016/j.progpolymsci.2021.101473>
- Zhang, D., Dumont, M.-J., 2018. Reprocessable 5-hydroxymethylfurfural derivative-based thermoset elastomers synthesized through the thiol-Michael and Diels–Alder reactions. *J. Mater. Sci.* 53, 11116–11129. <https://doi.org/10.1007/s10853-018-2375-4>
- Zhang, D., Dumont, M.-J., 2017. Advances in polymer precursors and bio-based polymers synthesized from 5-hydroxymethylfurfural. *J. Polym. Sci. Part Polym. Chem.* 55, 1478–1492. <https://doi.org/10.1002/pola.28527>
- Zhang, D., Dumont, M.-J., Cherestes, A., 2016. An efficient strategy for the synthesis of 5-hydroxymethylfurfural derivative based poly(β -thioether ester) via thiol-Michael addition polymerization. *RSC Adv.* 6, 83466–83470. <https://doi.org/10.1039/C6RA17532E>
- Zhang, H., Cui, J., Hu, G., Zhang, B., 2022. Recycling strategies for vitrimers. *Int. J. Smart Nano Mater.* 13, 367–390. <https://doi.org/10.1080/19475411.2022.2087785>
- Zhang, L., Rowan, S.J., 2017. Effect of Sterics and Degree of Cross-Linking on the Mechanical Properties of Dynamic Poly(alkylurea–urethane) Networks. *Macromolecules* 50, 5051–5060. <https://doi.org/10.1021/acs.macromol.7b01016>
- Zhang, S., Liu, T., Hao, C., Wang, L., Han, J., Liu, H., Zhang, J., 2018. Preparation of a lignin-based vitrimer material and its potential use for recoverable adhesives. *Green Chem.* 20, 2995–3000. <https://doi.org/10.1039/C8GC01299G>
- Zhang, W., Gao, F., Chen, X., Shen, L., Chen, Y., Lin, Y., 2023. Recyclable, Degradable, and Fully Bio-Based Covalent Adaptable Polymer Networks Enabled by a Dynamic Diacetal Motif. *ACS Sustain. Chem. Eng.* 11, 3065–3073. <https://doi.org/10.1021/acssuschemeng.2c06870>
- Zhang, W., Gao, F., Shen, L., Chen, Y., Lin, Y., 2022. Unexploited Design and Application of Dynamic Covalent Networks: Phenol-yne Click Reaction and Porous Film Generation. *ACS Mater. Lett.* 4, 2090–2096. <https://doi.org/10.1021/acsmaterialslett.2c00633>
- Zhang, X., Wang, S., Jiang, Z., Li, Y., Jing, X., 2020. Boronic Ester Based Vitrimers with Enhanced Stability via Internal Boron–Nitrogen Coordination. *J. Am. Chem. Soc.* 142, 21852–21860. <https://doi.org/10.1021/jacs.0c10244>
- Zhang, Yajie, Yuan, L., Liang, G., Gu, A., 2023. Bio-based Tetrafunctional Epoxy Monomer Containing a Dicyclo Diacetal Structure and Its Medium-Temperature-Cured Epoxy Vitrimer System with Excellent Mechanical and Multifunctional Properties. *ACS Sustain. Chem. Eng.* 11, 9264–9280. <https://doi.org/10.1021/acssuschemeng.3c02568>
- Zhang, Y., Yukiko, E., Tadahisa, I., 2023. Bio-based vitrimers from divanillic acid and epoxidized soybean oil. *RSC Sustain.* 1, 543–553. <https://doi.org/10.1039/D2SU00140C>
- Zhao, F., Lian, W.-Q., Li, Y.-D., Weng, Y., Zeng, J.-B., 2022. Synthesis of epoxidized soybean oil-derived covalent adaptable networks through melt Schiff base condensation. *Ind. Crops Prod.* 187, 115499. <https://doi.org/10.1016/j.indcrop.2022.115499>
- Zhao, S., Abu-Omar, M.M., 2019. Catechol-Mediated Glycidylation toward Epoxy Vitrimers/Polymers with Tunable Properties. *Macromolecules* 52, 3646–3654. <https://doi.org/10.1021/acs.macromol.9b00334>
- Zhao, W., Feng, Z., Liang, Z., Lv, Y., Xiang, F., Xiong, C., Duan, C., Dai, L., Ni, Y., 2019. Vitrimer-Cellulose Paper Composites: A New Class of Strong, Smart, Green, and Sustainable Materials. *ACS Appl. Mater. Interfaces* 11, 36090–36099. <https://doi.org/10.1021/acsmi.9b11991>
- Zhao, X.-L., Li, Y.-D., Weng, Y., Zeng, J.-B., 2023. Biobased epoxy covalent adaptable networks for high-performance recoverable adhesives. *Ind. Crops Prod.* 192, 116016. <https://doi.org/10.1016/j.indcrop.2022.116016>
- Zhao, X.-L., Li, Y.-D., Zeng, J.-B., 2022a. Progress in the design and synthesis of biobased epoxy covalent adaptable networks. *Polym. Chem.* 13, 6573–6588. <https://doi.org/10.1039/D2PY01167K>
- Zhao, X.-L., Tian, P.-X., Li, Y.-D., Zeng, J.-B., 2022b. Biobased covalent adaptable networks: towards better sustainability of thermosets. *Green Chem.* 24, 4363–4387. <https://doi.org/10.1039/D2GC01325H>

LISTE COMPLÈTE DES RÉFÉRENCES BIBLIOGRAPHIQUES

- Zhao, Z.-H., Wang, D.-P., Zuo, J.-L., Li, C.-H., 2021. A Tough and Self-Healing Polymer Enabled by Promoting Bond Exchange in Boronic Esters with Neighboring Hydroxyl Groups. *ACS Mater. Lett.* 3, 1328–1338. <https://doi.org/10.1021/acsmaterialslett.1c00314>
- Zheng, H., Zhang, W., Li, B., Zhu, J., Wang, C., Song, G., Wu, G., Yang, X., Huang, Y., Ma, L., 2022. Recent advances of interphases in carbon fiber-reinforced polymer composites: A review. *Compos. Part B Eng.* 233, 109639. <https://doi.org/10.1016/j.compositesb.2022.109639>
- Zheng, J., Png, Z.M., Ng, S.H., Tham, G.X., Ye, E., Goh, S.S., Loh, X.J., Li, Z., 2021. Vitrimers: Current research trends and their emerging applications. *Mater. Today* 51, 586–625. <https://doi.org/d>
- Zheng, P., McCarthy, T.J., 2012. A Surprise from 1954: Siloxane Equilibration Is a Simple, Robust, and Obvious Polymer Self-Healing Mechanism. *J. Am. Chem. Soc.* 134, 2024–2027. <https://doi.org/10.1021/ja2113257>
- Zheng, Y., Liu, T., He, H., Lv, Z., Xu, J., Ding, D., Dai, L., Huang, Z., Si, C., 2023. Lignin-based epoxy composite vitrimers with light-controlled remoldability. *Adv. Compos. Hybrid Mater.* 6, 53. <https://doi.org/10.1007/s42114-023-00633-4>
- Zhong, L., Hao, Y., Zhang, J., Wei, F., Li, T., Miao, M., Zhang, D., 2022. Closed-Loop Recyclable Fully Bio-Based Epoxy Vitrimers from Ferulic Acid-Derived Hyperbranched Epoxy Resin. *Macromolecules* 55, 595–607. <https://doi.org/10.1021/acs.macromol.1c02247>
- Zhou, S., Huang, K., Xu, X., Wang, B., Zhang, W., Su, Y., Hu, K., Zhang, C., Zhu, J., Weng, G., Ma, S., 2023. Rigid-and-Flexible, Degradable, Fully Biobased Thermosets from Lignin and Soybean Oil: Synthesis and Properties. *ACS Sustain. Chem. Eng.* 11, 3466–3473. <https://doi.org/10.1021/acssuschemeng.2c06990>
- Zhou, Y., Goossens, J.G.P., Sijbesma, R.P., Heuts, J.P.A., 2017. Poly(butylene terephthalate)/Glycerol-based Vitrimers via Solid-State Polymerization. *Macromolecules* 50, 6742–6751. <https://doi.org/10.1021/acs.macromol.7b01142>
- Zhou, Y., Zeng, G., Zhang, F., Li, K., Li, X., Luo, J., Li, Jiongjiong, Li, Jianzhang, 2023. Design of tough, strong and recyclable plant protein-based adhesive via dynamic covalent crosslinking chemistry. *Chem. Eng. J.* 460, 141774. <https://doi.org/10.1016/j.cej.2023.141774>
- Zhou, Z., Su, X., Liu, J., Liu, R., 2020. Synthesis of Vanillin-Based Polyimine Vitrimers with Excellent Reprocessability, Fast Chemical Degradability, and Adhesion. *ACS Appl. Polym. Mater.* 2, 5716–5725. <https://doi.org/10.1021/acsapm.0c01008>
- Zhu, L., Xu, L., Jie, S., Li, B.-G., 2023. Preparation of Styrene–Butadiene Rubber Vitrimers with High Strength and Toughness through Imine and Hydrogen Bonds. *Ind. Eng. Chem. Res.* 62, 2299–2308. <https://doi.org/10.1021/acs.iecr.2c03133>
- Zia, K.M., Noreen, A., Zuber, M., Tabasum, S., Mujahid, M., 2016. Recent developments and future prospects on bio-based polyesters derived from renewable resources: A review. *Int. J. Biol. Macromol.* 82, 1028–1040. <https://doi.org/10.1016/j.ijbiomac.2015.10.040>
- Zou, J., Duan, H., Chen, Y., Ji, S., Cao, J., Ma, H., 2020. A P/N/S-containing high-efficiency flame retardant endowing epoxy resin with excellent flame retardance, mechanical properties and heat resistance. *Compos. Part B Eng.* 199, 108228. <https://doi.org/10.1016/j.compositesb.2020.108228>
- Zou, W., Dong, J., Luo, Y., Zhao, Q., Xie, T., 2017. Dynamic Covalent Polymer Networks: from Old Chemistry to Modern Day Innovations. *Adv. Mater.* 29, 1606100. <https://doi.org/10.1002/adma.201606100>

Développement de nouveaux réseaux covalents adaptables biosourcés et aromatiques à partir de lignines

Résumé

La biomasse lignocellulosique représente la plus grande source de structures aromatiques renouvelables sur Terre. Parmi les nombreux composés issus de cette matière première, la lignine s'impose comme une source intéressante de phénols pour la synthèse de polymères durables. En raison de son importante fonctionnalité, la lignine est très largement utilisée pour préparer des thermodurcissables dont la structure réticulée limite considérablement le potentiel de recyclabilité. Les réseaux covalents adaptables (CANs) se sont révélés être une stratégie élégante pour remédier aux problématiques de recyclabilité des polymères réticulés traditionnels sans compromettre leurs propriétés. Dans ce contexte, de nouvelles architectures macromoléculaires à la fin de vie contrôlée ont été élaborées à partir de lignine, en adoptant une philosophie de bioéconomie circulaire. De nouvelles modifications chimiques de lignine ont été développées et caractérisées. Des chimies dynamiques innovantes ont été utilisées pour synthétiser de nouveaux polymères. Les propriétés thermiques et mécaniques de ces nouvelles architectures ont été caractérisées. Le comportement rhéologique des différentes chimies dynamiques utilisés a été investigué de manière à déterminer des conditions optimales de remise en forme des polymères. Leur potentiel de recyclabilité a été mis en évidence via des études de recyclage physique et chimique. Les systèmes conçus présentent des propriétés modulables leur permettant de convenir à un large domaine d'applications, révélant leur potentiel en tant que matériaux innovants pour un avenir plus durable.

Mots clés : lignine, réseaux covalents adaptables, vitrimère, durabilité, circularité

Résumé en anglais

Lignocellulosic biomass represents the largest source of renewable aromatic compounds on Earth. Among the various compounds derived from this feedstock, lignin emerged as an attractive source of phenols for the synthesis of sustainable polymers. Because of its high functionality, lignin is widely used for the preparation of thermosets, whose crosslinked structure considerably limits their recyclability potential. Covalent adaptable networks (CANs) have revealed to be an elegant strategy to address the recyclability issues of traditional thermosets without compromising on properties. In this context, new macromolecular architectures with controlled end-of-life were designed from lignin, embracing a circular bioeconomy philosophy. New lignin chemical modifications were developed and characterized. Innovative dynamic chemistries were used to synthesize new polymers. Thermal and mechanical properties of these architectures were characterized. Rheological behaviors of the different dynamic chemistries employed was investigated to determinate the polymers optimal thermo-mechanical recycling conditions. Their recyclability potential was highlighted through physical and chemical recycling studies. The designed systems present tunable properties making them suitable for a wide range of applications, revealing their potential as innovative materials for a more sustainable future.

Keywords: lignin, covalent adaptable networks, vitrimer, sustainability, circularity

